

NINTH INTERNATIONAL CONFERENCE ON NUCLEAR AND RADIOCHEMISTRY - NRC9



HELSINKI, FINLAND
AUGUST 29 - SEPTEMBER 2, 2016
ABSTRACTS

INTERNATIONAL ADVISORY BOARD:

Prof. Jukka Lehto, chairman
University of Helsinki,
Finland

Dr. Stéphane Bourg
CEA, France

Prof. Sue Clark
Washington State University, USA

Prof. Melissa Denecke
University of Manchester,
UK

Prof. Xiaolin Hou
Technical University of Denmark,
Denmark

Prof. Jan John
Czech Technical University in
Prague, Czech Republic

Prof. Stepan Kalmykov
Moscow State University, Russia

Prof. Frank Rösch
University of Mainz, Germany

Prof. Thorsten Stumpf
Helmholz Zentrum Dresden-
Rossendorf, Germany

Prof. Andreas Tuerler
University of Bern /PSI,
Switzerland

ORGANIZING COMMITTEE:

Jukka Lehto, chairman

Risto Koivula, coordinator

Anu Airaksinen

Risto Harjula

Kerttuli Helariutta

Pirkko Hölttä

Teija Koivula

Jukka Kuva

Marja Siitari-Kauppi

Valtteri Suorsa (layout)

SUPPORT



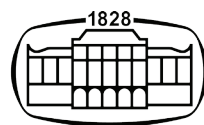
FEDERATION OF FINNISH LEARNED SOCIETIES
Delegation of the Finnish Academies of Science and Letters



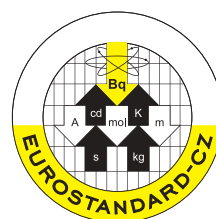
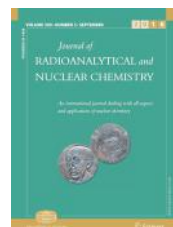
MAP MEDICAL
TECHNOLOGIES

HIDEX

DOCTORAL PROGRAMME IN
CHEMS
CHEMISTRY AND MOLECULAR SCIENCES



AKADÉMIAI KIADÓ



CONTENTS

MONDAY 29TH AUGUST

OPENING LECTURE 48

Thomas Fanghänel (*Belgium*)

Closing the nuclear fuel cycle for future sustainable nuclear energy

CHEMISTRY OF THE NUCLEAR FUEL CYCLE I 51

Palladium behavior in the presence of irradiated diluent in the PUREX process

S. De Sio, I. Klur, E. Tison, C. Bouyer, D. Lebeau, F. Goutelard, L. Séjourné, C. Eysseric and N. Vigier (*France*)

Selected non-pertechetate species relevant to Hanford tank waste

T.G. Levitskaia, S. Chatterjee, G.B. Hall, A. Andresen, N.M. Washton, E.D. Walter (*USA*)

Controls on iron oxyhydroxide formation in the Enhanced Actinide Removal Plant (EARP), Sellafield, UK

J. Weatherill, K. Morris, P. Bots, T. Stawski, A. Janssen, L. Abrahamsen, R. Blackham, S. Shaw (*UK*)

ENVIRONMENTAL RADIOACTIVITY I 58

Fukushima accident: Environmental impact on land and ocean

M. Ayoama (*Invited lecture*) (*Japan*)

Determination of plutonium and americium in snow on Mt Zugspitze

K. Gückel, M. Christl, T. Shinonaga (*Germany, Switzerland*)

Radionuclides distribution among biotic and abiotic components in artificial reservoirs

N.V. Kuzmenkova, I.E. Vlasova, A.K. Rozhkova, E.A. Pryakhin, Yu.G. Mokrov, S.N. Kalmykov (*Russia*)

Study of Cs, Pu and Am sorption to natural clay and bottom sediments

G. Lujaniene, L. Levinskaite, R. Juškeenas, K. Štamberg, A. Kačergius, I. Kulakauskaite, S. Šemčuk, D. Vopalka (*Lithuania, Czech Republic*)

Devaluation of Rhinoceros horn through nuclear techniques

J.R. Zeevaart, C. Krös, D. Kotze, D. Hudson-Lamb, J. van Rooyen, A. Buffler, A. Faanhof (*South Africa*)

ACTINIDE CHEMISTRY

63

Progress of the actinide separation research in China

G. Ye (*Invited lecture*)

Uranium(VI) solubility and hydrolysis in NaCl solutions at elevated temperatures

F. Endrizzi, X. Gaona, M.M. Fernandes, B. Baeyens, M. Altmaier (*Germany, Switzerland*)

Actinide Hybrid Materials: Supramolecular assembly and periodic trends

R.G. Surbella III, K.L. Pellegrini, B.K. McNamara, L. Ducati, J. Autschbach, G. Simon, P.C. Burns, J.M. Schwantes, C.L. Cahill (*USA, Brazil*)

Measurements of electrode reaction kinetics for uranium and rare-earths in LiCl-KCl eutectic electrolyte, and its application to modeling of electrochemical polarization

K.R. Kim, S.K. Kim, C.S. Seo, W.I. Goh, G.I. Park (*Korea*)

Novel highly selective ligand for separation of actinides and lanthanides. Experimental verification of the theoretical prediction

G. Lavrov, N. Ustynyuk, I. Gloriov, Yu. Ustynyuk, M. Alyapyshev, L. Tkachenko, V. Babain (*Russia*)

Water adsorption on actinide oxide surfaces

J.P.W. Wellington, A. Kerridge, N. Kaltsoyannis (*Invited lecture*) (*UK*)

TRANSACTINIDE CHEMISTRY

74

Developments in the chemistry of the heaviest elements

C. Düllmann (*Invited lecture*) (*Germany*)

Chemistry of the heaviest actinides and early transactinides – Experimental achievements and perspectives

Y. Nagame (*Invited lecture*) (*Japan*)

Experimentally assessing the metal-carbon bond stability in $\text{Sg}(\text{CO})_6$

R. Eichler, M. Asai, H. Brand, N.M. Chiera, A. Di Nitto, R. Dressler, Ch.E. Düllmann, J. Even, R. Eichler, F. Fangli, M. Goetz, H. Haba, W. Hartmann, E. Jäger, D. Kaji, J. Kanaya, Y. Kaneya, J. Khuyagbaatar, B. Kindler, Y. Komori, B. Kraus, J.V. Kratz, J. Krier, Y. Kudou, N. Kurz, S. Miyashita, K. Morimoto, K. Morita, M. Murakami, Y. Nagame, K. Ooe, D. Piguet, N. Sato, T.K. Sato, J. Steiner, P. Steinegger, T. Sumita, M. Takeyama, K. Tanaka, T. Tomitsuka, A. Toyoshima, K. Tsukada, A. Türlér, I. Usoltsev, Y. Wakabayashi, Y. Wang, N. Wiehl, A. Yakushev, S. Yamaki, S. Yano, S. Yamaki, Z. Qin (*Switzerland, Japan, Germany, China*)

Laser spectroscopy on nobelium isotopes at GSI

M. Block, M. Laatiaoui, H. Backe, W. Lauth, D. Ackermann, B. Cheal, P. Chhetri, C. Droese, Ch.E. Düllmann P. Van Duppen, J. Even, R. Ferrer, F. Giacoppo, S. Götz, F.P. Heßberger, M. Huyse, O. Kaleja, J. Khuyagbaatar, P. Kunz, F. Lautenschlaeger, A.K. Mistry, S. Raeder, E. Minaya Ramirez, Th. Walther, C. Wraith, A. Yakushev (*Germany, UK, Belgium, Canada*)

First ionization potentials of heavy actinides

T.K. Sato, M. Asai, Y. Kaneya, K. Tsukada, A. Toyoshima, A. Mitsukai, S. Takeda, A. Vascon, M. Sakama, D. Sato, K. Ooe, S. Miyashita, Y. Shigekawa, A. Borschevsky, H. Makii, A. Osa, S. Ichikawa, Y. Nagame, M. Schädel, K. Eberhardt, J. Runke, P. Thörle-Pospiech, D. Renisch, E. Eliav, U. Kaldor, J. V. Kratz, T. Stora, Ch. E. Düllmann, N. Trautmann (*Japan, Netherlands, Germany, Israel, Switzerland*)

First on-line vacuum chromatography experiments with single atoms of Tl on SiO₂

P. Steinegger, M. Asai, R. Dressler, R. Eichler, Y. Kaneya, A. Mitsukai, Y. Nagame, D. Piguet, T. K. Sato, M. Schädel, S. Takeda, A. Toyoshima, K. Tsukada, A. Türlér, A. Vascon (*Switzerland, Japan, Russia*)

TUESDAY 30TH AUGUST

RADIOANALYTICAL CHEMISTRY I

83

Radiochemical analysis for decommissioning nuclear facilities

X. Hou (*Invited lecture*) (*Denmark*)

Development of robust automated techniques for radionuclide separation

F.M. Burrell, P.E. Warwick, I.W. Croudace, W.S. Walters (*UK*)

A new plastic scintillation resin for single-step separation, concentration and measurement of ^{99}Tc

J. Barreda, A. Tarancón, H. Bagán, J. F. García (*Spain*)

Precipitation of titanium dioxide with simultaneous uranium sorption and its application in Accelerator Mass Spectrometry

I. Špendlíková, M. Němec, P. Steier (*Czech Republic, Austria*)

Advanced approaches of compound-specific radiocarbon analysis (CSRA) of environmental and radiolabeled materials

S. Szidat, G. Salazar, K. Agrios, C. Espic, C. Uglietti, B. Z. Cvetcović, E. Wieland (*Switzerland*)

RADIONUCLIDE SPECIATION I

92

Speciation of actinides by time-resolved laser fluorescence spectroscopy

P. Panak (*Invited lecture*) (*Germany*)

A multi-approach technique to unravel the molecular speciation of tetravalent actinide-diethylenetriaminepentaacetate complex

J. Aupiais, L. Bonin, C. Den Auwer, P. Moisy, B. Siberchicot, S. Topin (*France*)

Cooperative effects of adsorption, reduction, and polymerization observed for hexavalent actinides on the muscovite basal plane

S. Hellebrandt, K. E. Knope, S. S. Lee, A. J. Lussier, J. E. Stubbs, P.J. Eng, L. Soderholm, P. Fenter, M. Schmidt (*Germany*)

Actinide speciation in sea water and possible in vivo accumulation

M. Maloubier, M. R. Beccia, M. Matara Aho, M. Monfort, P.L. Solari, D.K. Shuh, S. Minasian, H. Michel, M.Y. Dechraoui Bottein, P. Moisy, C. Moulin, C. Den Auwer (*Invited lecture*) (*France, Finland, USA, Monaco*)

POSTER SESSION I

CHEMISTRY OF THE NUCLEAR FUEL CYCLE 101

- P1-1** **Reactive diffusive transport of strontium in Czech compacted bentonite**
L. Baborová, D. Vopálka, A. Vetešník (*Czech Republic*)
- P1-2** **Chemistry of technetium under repository-relevant conditions: solubility and carbonate complexation of Tc(IV)**
A. Baumann, E. Yalcintas, X. Gaona, R. Polly, M. Altmaier, H. Geckeis (*Germany*)
- P1-3** **Neptunium(V) uptake by granitic rock and bentonite colloids and the influence of colloids on Np(V)**
O. Elo, N. Huittinen, P. Hölttä (*Finland*)
- P1-4** **Trace element variation in concrete coarse aggregate - implications to the decommissioning waste inventory, case Loviisa nuclear power plant**
T. Eurajoki (*Finland*)
- P1-5** **Effects of bentonite colloids on the radionuclide migration in granitic rock**

P. Hölttä, O. Elo, V. Suorsa, E. Honkaniemi, S. Niemiaho (*Finland*)
- P1-6** **The diffusion of tritiated water and chloride through granodiorite**
J. Ikonen, M. Voutilainen, M. Matara-aho, M. Siitari-Kauppi, A. Martin (*Finland, Switzerland*)
- P1-7** **Tomographic investigation of caesium migration in Olkiluoto veined gneiss and Grimsel granodiorite**
J. Kuva, M. Voutilainen, J. Parkkonen, T. Turpeinen, M. Siitari-Kauppi, J. Timonen (*Finland*)

- P1-8 Sorption of dissolved inorganic radiocarbon on goethite, hematite and magnetite**
J. Lempinen, J. Lehto (*Finland*)
- P1-9 On redox sensitive radionuclide immobilization by rock matrix with large pieces using electromigration method**
X. Li, H. Yang, P. Hu, L. Liu, D. Cui, B. Gylling, M. Lofgren, I. Puigdomenech (*China, Finland, Sweden*)
- P1-10 Selenite sorption on main minerals of crystalline rock**
X. Li, J. Ikonen, A. Lindberg, M. Siitari-Kauppi (*Finland*)
- P1-11 The sorption and diffusion of ^{133}Ba in granitic rocks**
E. Muuri, J. Ikonen, M. Matara-aho, A. Lindberg, M. Siitari-Kauppi (*Finland*)
- P1-12 Effect of cation exchange on ion migration in bentonite**
N.M. Nagy, J. Kónya (*Hungary*)
- P1-13 Batch and in-situ K_d-values in Lastensuo and Pesänsuo peat samples: comparison between different methods**
L. Parviainen, A.-M. Lahdenperä, M. Lusa (*Finland*)
- P1-14 Sorption of tin on fracture minerals in granitic groundwater simulant**
E. Puukko, J. Lehto (*Finland*)
- P1-15 Eu(III)/Cm(III), Np(V), and U(VI) sorption onto clay minerals: from low to high ionic strength conditions**
A. Schnurr, R. Marsac, M. Marques, Th. Rabung, J. Lützenkirchen, X. Gaona, B. Baeyens, H. Geckeis (*Germany, Switzerland*)
- P1-16 Block-scale experiment on bentonite colloid – radionuclide interaction**
V. Suorsa, P. Hölttä (*Finland*)
- P1-17 Laboratory scale advection-matrix diffusion experiment in Olkiluoto veined gneiss using H-3 and Cl-36 as tracers**
M. Voutilainen, P. Kekäläinen, J. Kuva, M. Siitari-Kauppi, L. Koskinen (*Finland*)

- P1-18 Indigenous solid/liquid partitioning of Cs, Sr and U in some soil and sediment samples from the Olkiluoto site and its surroundings**
A.T.K. Ikonen, A.-M. Lahdenperä (*Finland*)
- P1-19 Uptake of nickel by bacteria and fungus isolated from a nutrient-poor boreal bog**
J. Knuutinen, M. Bomberg, J. Lehto, M. Lusa (*Finland*)
- P1-20 Speciation and sorption of iodine on boreal forest soil**
M. Söderlund, J. Virkanen, H. Aromaa, N. Gracheva, J. Lehto (*Finland, Russia*)
- P1-21 Effect of interlayer species charge on the swelling of Na⁺, K⁺ and Ca²⁺ montmorillonites: DFT and molecular dynamics studies**
E. Puhakka, A. Seppälä, M. Olin (*Finland*)
- P1-22 Cm³⁺ incorporation in La_{1-x}Gd_xPO₄ monazites: a TRLS and XAFS study**
N. Huittinen, A. C. Scheinost, A. Wilden, Y. Arinicheva (*Germany*)
- P1-23 Evidence of a new Incorporation species of Eu(III) in Calcite and its dependence of the background electrolyte**
S.E. Hellebrandt, S. Hofmann, N. Jordan, A. Barkleit, M. Schmidt (*Germany*)
- P1-24 Retardation and release of uranium on phlogopite mica at the absence and presence of humic acid: A batch and TRLS study**
D. Pan, W. Wu (*China*)
- P1-25 Spectroscopic and microcalorimetric investigations on An(III)/Ln(III) complexes formed by the cement additive malate**
F. Taube, M. Acker, S. Taut, T. Stumpf (*Germany*)
- P1-26 Radionuclide inventory of KAERI R&D radwastes**
H.J. Ahn, K.-S. Choi, B. Kang, K. Seo, J. Kim, K.Y. Jee, J.-W. Yeon (*Korea*)

- P1-27 Sorption properties of ^{60}Co and ^{137}Cs on nanocomposite material GO-TiO_2**
V. Brynych, J. Pospěchová, K. Kolomá, M. Kolářová, V. Štengl, J. Tolasz
(Czech Republic)
- P1-28 Study on volatility of ^{99}Tc and ^{137}Cs for the dry ashing of DAW**
K.-S. Choi, H.-J. Im, K.W. Suh, J. Hwang, H.-J. Ahn (Korea)
- P1-29 Separation of radionuclides from the organic complexants using ionic liquids**
K. Cubova, B. Basarabova, M. Nemec, M. Florianova (Czech Republic)
- P1-30 Modeling of the efficient ^{137}Cs decontamination of fresh and saline waters by a new cyanoferrate mesoporous material**
C. Michel, L. De Windt, Y. Barré, C. de Dieuleveult, A. Grandjean
(France)
- P1-31 The flotation separation of rare earth elements – a contribution to reprocessing of the spent nuclear fuel**
F.-L. Fan, Z. Qin, J.-R. Wang, F. Yang (China)
- P1-32 The recycling of radioactive concrete resulted from the decommissioning of the VVR-S nuclear research reactor**
D. Gurau, R. Deju, M. Dragusin (Romania)
- P1-33 Back-extraction in a Grouped ActiNide EXtraction system based on 1-octanol**
J. Halleröd, M. Lin (Sweden)
- P1-34 Recyclable superparamagnetic adsorbent based on mesoporous carbon for sequestration of radioactive cesium**
S.M. Husnain, W. Um, Y.-Y. Chang, Y.-S. Chang (Korea)
- P1-35 Synthesis of phosphonate modified magnetic mesoporous carbon for removal of uranium**
S.M. Husnain, W. Um, Y.-S. Chang (Korea)
- P1-36 Ashing characteristics of dry active wastes in nuclear power plants**
J. Hwang, S. Oh, K.-S. Choi, H.J.Ahn, J.M. Park (Korea)

- P1-37 Solubility model for ferrous iron hydroxide in sodium chloride solutions spiked with sodium EDTA: a Pitzer approach**
J.-H. Jang, M. Nemer (*USA*)
- P1-38 Korean scaling factor for LILWs from nuclear power plants**
K.Y. Jee, H.J. Ahn, S.H. Han, Y.J. Park, J.-W. Yeon, H.H. Lee (*Korea*)
- P1-39 Removal of cobalt and nickel from aqueous solutions with manganese dioxide sorbent produced by in-situ precipitation**
M. Kaipainen, R. Koivula, R. Harjula (*Finland*)
- P1-40 An effect of bismuth ion on the reduction of lanthanum ion in molten LiCl-KCl eutectic salt**
B.K. Kim, H.J. Han, B.G. Park (*Korea*)
- P1-41 Bismuth-based inorganic sorbents for the removal of iodine from subsurface plumes**
T. Levitskaia, M. Leonard, J. Romero, S. Chatterjee, T. Varga, B. Schwenzer, T. Kaspar (*USA*)
- P1-42 The effect of initial solution pH on the removal of trace amounts of Co-60 from NPP waste water using UV-C irradiation, TiO₂ P25 and ion exchange material CoTreat**
L. Malinen, J.-M. Mäki (*Finland*)
- P1-43 Adsorption properties of actinoids (U, Am, Np) for various zeolites**
H. Mimura, M. Matsukura, N. Fujita, H. Kanda, A. Kirishima, N. Sato (*Japan*)
- P1-44 Radiochemistry related to ADS at IMP**
Z. Qin, F.-L. Fan, W. Tian, X.-L. Wu, C.-M. Tan, J. R. Wang, S. Li, Y. Wang, J. Bai, X.-J. Yin (*China*)
- P1-45 Sorption of Cs, Pu and Am sorption to graphene oxide based nanosorbents**
S. Šemčuk, G. Lujanienė, A. Leščinskytė, S. Tautkus, I. Kulakauskaitė, R. Juškėnas (*Lithuania*)
- P1-46 Removal of cesium by heteropolyacid salts from radioactive waste in HCl system**
T. Suzuki, Y. Tachibana, Y. Sakate, Son Nguyen An, Lanh Dang (*Japan*)

- P1-47 Sorption of uranium from aqueous solutions by TiO₂-graphen oxide composite materials**
Z. Tomášová, V. Brynych, J. Pospěchová, P. Ecorchard, J. Tolasz
(Czech Republic)
- P1-48 Effects of synthesis conditions on trace level ion exchange properties of α-zirconium phosphate variants for ¹⁵²Eu³⁺ and ²⁴¹Am³⁺**
E.W. Wiikinkoski, R. Koivula, R. Harjula (Finland)
- P1-49 Uranium uptake during iron (oxyhydr)oxide formation: application to radioactive waste effluent treatment**
E. Winstanley, K. Morris, L. Abrahamsen, S. Shaw (UK)
- P1-50 Development and testing of new technetium selective media TcTreat**
I. Välimaa, R. Harjula, B. Salo, R. Koivula, E. Tusa, P. Kelokaski
(Finland)
- P1-52 Application of extraction express-method for radwaste characterization before hot chamber montejus dismantling**
A. Stepanov, I. Simirskii, S. Smirnov, A. Safronov, I. Semin, V. Stepanov
(Russia)
- P1-53 Modeling molten-salt separation of radionuclides in spent nuclear fuel**
S. Choi, D. Kang, B. Park (Korea)
- P1-54 Quantifying TBP dimers and trimers in alkane solutions via simulations and experiments**
Q. Vo, J. Unangst, L. Dang, M. Nilsson, H. Nguyen (USA)
- P1-55 Sorption of toxic metals by magnetic nanocomposites**
I. Kulakauskaite, G. Lujaniene, K. Mažeika, V. Darius, S. Sergej, P. Vidas, S. Martynas, T. Saulius (Lithuania)

- P1-56 Degradation mechanism of a novel carboxamide ligand and its impact on actinide and lanthanide co-extraction efficiency**
A. Ossola, E. Macerata, W. Panzeri, A. Mele, M. Giola, M. Mariani, A. Casnati (*Italy*)
- P1-57 New method for alpha dose rate profile determination at HLW matrix/water interfaces**
M. Tribet, S. Mougnaud, C. Jégou (*France*)
- P1-58 Complexation studies of modified calix[4]arenes with uranium in non-aqueous solution**
A. Bauer, K. Schmeide, J. März, A. Jäschke, F. Glasneck, B. Kersting (*Germany*)
- P1-59 Local environment of Gd doped actinide oxides ($U_{1-x}Gd_x$)O₂ and (Th_{1-x}Gd_x)O₂ measured by X-ray absorption spectrometry**
R. Bès, J. Pakarinen, S. Conradson, A. Baena, M. Verwerft, I. Makkonen, F. Tuomisto (*Finland, Belgium, France*)
- P1-60 Thermochemistry of reactor materials: actinide and fission product compounds**
E.E. Moore, R.J.M. Konings (*Germany*)
- P1-61 Gen IV reactors: fuel, coolant and their interactions**
T. Retegan, F. Espegren, E. Karlsson (*Sweden*)
- P1-62 Accident tolerant fuel: uranium microspheres doped with chromium prepared by modified internal sol gel**
A. Sajdova, M. Hedberg, T. Retegan, C. Ekberg (*Sweden*)

ENVIRONMENTAL RADIOACTIVITY

197

- P1-63 Evaluation of radioactive contamination of alfa emitters in tundra of Western Greenland**
A. Cwanek, J.W. Mietelski, E. Łokas, M.A. Olech (*Poland*)
- P1-64 Assessment of ²¹⁰Pb-contamination in soil**
D.Ø. Eriksen, K. Haarstad (*Norway*)

- P1-65 Seasonal variation and chemical property of radioactive cesium released by the FDNPP accident**
N. Fujita, K. Ninomiya, Z. Zhang, S. Kakitani, T. Yoshimura, Y. Yamaguchi, K. Kita, H. Tsuruta, A. Watanabe, H. Yamamoto, A. Shinohara (*Japan*)
- P1-66 Radiation contamination factor (RCF) in marine sediments from Cuba north and south coasts**
M. García Batlle, J.M. Navarrete (*Mexico*)
- P1-67 Measuring the NORM in the Oil Fields & Oil Ports in Libya (2)**
E. Hamida (*Libya*)
- P1-68 Radon emanation from fresh, altered and disturbed granitic rock characterized by ^{14}C -PMMA impregnation and autoradiography**
K-H. Hellmuth, M. Siitari-Kauppi, H. Arvela, A. Lindberg (*Finland*)
- P1-69 Cs-137 source identification and its use as geochronometer in a sediment of the water reservoir Klingnau, Switzerland**
M. Jäggi, J. Eikenberg (*Switzerland*)
- P1-70 Transuranic elements in soil samples from Fukushima Prefecture collected in March 2011**
R. Kierepko, S.K. Sahoo (*Japan, Poland*)
- P1-71 Concentrations of radiocesium in wild mushrooms collected in Miyagi prefecture, Japan**
Y. Kino, A. Irisawa, T. Sekine (*Japan*)
- P1-72 Detection of ^{90}Sr in the teeth of cattle contaminated by environmental pollution from the Fukushima-Daiichi Nuclear Power Plant accident**
K. Koarai, Y. Kino, A. Takahashi, T. Suzuki, Y. Shimizu, M. Chiba, K. Osaka, K. Sasaki, T. Fukuda, E. Isogai, H. Yamashiro, T. Oka, T. T. Sekine, M. Fukumoto, H. Shinoda (*Japan*)
- P1-73 Diagnostic possibility of digital autoradiography in a study of ^{137}Cs behavior in “soil-plant” system, model experiment**
N. Kuzmenkova, T. Paramonova, M. Godjaeva (*Russia*)

- P1-74 Radionuclide extraction from aqueous solutions by ionic liquids**
R. Leyma, S. Platzer, M. Habibi, W. Kandoller, R. Krachler, G. Wallner
(*Austria*)
- P1-75 The study on sorption process in geological materials of long-lived radioactive isotopes Sr-90 and Cs-137 in model systems with the use of short-lived isotopes Sr-85 and Cs-134**
M. Miecznik, J.W. Mietelski, E. Łokas (*Poland*)
- P1-76 Variation of ^{210}Pb , ^{210}Po , ^{238}U and ^{232}Th concentrations in atmospheric deposition and aerosol samples collected in Rokkasho, Aomori, Japan**
Y. Ohtsuka, Y. Takaku, S. Hisamatsu (*Japan*)
- P1-77 Ionizing radiation in the upper atmosphere over Finland**
J. Paatero, J. Hatakka, R. Kivi (*Finland*)
- P1-78 Interaction of radio-metals with microorganisms**
J. Raff, M. Vogel, A. Günther, B. Drobot, C. Schmoock, H. Moll, H. Börnick, E. Worch, T. Stumpf (*Germany*)
- P1-79 Scavenging processes of natural and anthropogenic radionuclides on the continental margin of the East China Sea**
M. Yamada, J. Zheng (*Japan*)
- P1-80 Development of aerosol generation system for simulating dry deposition process of radioactive nuclides released from the Fukushima accident**
Z. Zhang, K. Ninomiya, A. Shinohara (*Japan*)
- P1-81 Atmospheric $^{90}\text{Sr}/^{137}\text{Cs}$ activity ratio in eastern Japan after the FDNPP accident**
Z. Zhang, K. Ninomiya, Y. Yamaguchi, T. Saito, K. Kita, H. Tsuruta, Y. Igarashi, A. Shinohara (*Japan*)
- P1-82 $^{239+240}\text{Pu}$ and heavy metals (Zn, As, V, Cu, Co, Ni, U, Pb, and Cr) in archived human samples from Finland**
S. Salminen-Paatero, J. Paatero (*Finland*)

- P1-83 Simulation of the Occupational Radiation Dose Caused by Contamination of Primary Circuit Media in Pressurized Water Reactor**
A. Artmann, G. Bruhn, S. Schneider, E. Strub (*Germany*)
- P1-84 Effect of air radiolysis products on the chemistry of ruthenium during a severe nuclear accident**
I. Kajan, T. Kärkelä, A. Auvinen, C. Ekberg (*Sweden, Finland*)
- P1-85 Retention of organic iodides on charcoal filter material**
E. Aneheim, M. Foreman (*Sweden*)
- P1-86 Indoor radon (^{222}Rn) concentration level study in child care centers and kindergartens using nuclear track methodology (NTM)**
G. Espinosa, J.I. Golzarri (*Mexico*)
- P1-87 Natural radionuclides in infant formulae (powder milk)**
M. Trdin, L. Benedik (*Slovenia*)
- P1-88 An experimental study on in situ gamma spectrometry using room model**
C.-J. Kim, Y.-Y. Ji, M. JANG, K.H. Chung (*Korea*)

EDUCATION

236

- P1-89 Beta-ray spectrometry for radiation education**
E. Furuta, K. Kusama, Y. Watanabe (*Japan*)
- P1-90 Undergraduate summer school in radiochemistry at OSU**
A. Paulenova (*USA*)
- P1-91 Remote controlled radiochemical experiments developed at the Institute for Radioecology and Radiation Protection, Hanover**
W. Schulz (*Germany*)
- P1-92 Remote controlled radiochemical experiments developed at the University of Oslo**
J.P. Omtvedt, C. Fournier, H.V. Lerum, T. Grønås, J.Ø. Matsdal, C. Walther (*Norway, Germany*)

- P1-93 Development of self-glowing ceramics based on cubic stabilized zirconia**
O. Bogdanova, B. Burakov, Y. Kuznetsova (*Russia*)
- P1-94 Seleted major, minor and trace elements study of Precambrian outcrops from the south of Eastern Paraguay by XRF and NAA**
P. Kump, J. Cabello, J.F. Facetti-Masulli (*Paraguay*)
- P1-95 Determination of proton beam energy with target activation method**
V. Jakovlev, S. Makkonen-Craig, E. Honkaniemi, V. Jallinoja, J. Järvenpää, M. Keskitalo, M. Matara-aho, S. Muje, A.-E. Pasi, V. Suorsa, K. Helariutta (*Russia, Finland*)
- P1-96 On the identification of titanium-tantalum niobates in «wiikites» from Karelia**
M.H. Khanmiri, D.K. Goldwirt, N.V. Platonova, S.Y. Janson, Y.S. Polekhovski, R.V. Bogdanov (*Russia*)
- P1-97 Volume reduction technology for treatment of spent uranium catalyst used for production of acrylonitrile**
K.-W. Kim, K.-Y. Lee, M.-J. Kim, M.-K. Oh, J. Kim, D.-Y. Chung, J.-K. Moon, J.-W. Choi (*Korea*)
- P1-98 Apatite rock digestion with sulfuric acid and phosphoric acid**
P. Laukkanen, R. Harjula (*Finland*)
- P1-99 On the solubility of radium sulfate and carbonate in sodium chloride media**
A.V. Matyskin, P.L. Brown, C. Ekberg (*Sweden, Australia*)
- P1-100 K concentration in peel and seeds of coffee and cacao by ^{40}K radioactive detection.**
J.M. Navarrete, K. Lüchinger (*Mexico*)
- P1-101 The force dependent of time and quantity with applications in the Uranium's extraction**
M. Răileanu (*Romania*)

- P1-102 C-14-PMMA porosity analysis of andesite from Petite Anse, Martinique**
J. Sammaljärvi, C. Delayre, P. Sardini, K. Kallonen, M. Voutilainen, M. Siitari-Kauppi (*Finland*)
- P1-103 The investigation of heterogeneous equilibria in the saturated aqueous solutions of rare earth elements uranyl silicates and uranyl germinates**
N. Zakharycheva (*Russia*)
- P1-104 Modelling an Iso-Breeder Nuclear Programme: Determining optimum cooling time and generating waste inventories**
K. Dungan, (*UK*)

Highly selective inorganic ion exchangers in Fukushima cleanup

J. Lehto (*Invited lecture*) (*Finland*)

Development of a selective americium separation process using TPAEN as a water-soluble stripping agent

C. Marie, V. Vanel, M.-T. Duchesne, E. Russello, P. Kaufholz, A. Wilden, G. Modolo, M. Miguirditchian (*France, Germany*)

Application of Aliquat-336 nitrate ionic liquid based extractants for minor actinide separation

P. Zsabka, M. Van de Voorde, K. Van Hecke, T. Cardinaels, M. Verwerft, G. Modolo, K. Binnemans (*Belgium, Germany*)

Polonium evaporation from liquid lead-bismuth eutectic coolant and its capture for accelerator driven systems

B.G. Prieto, A. Aerts, J. Neuhausen, E.A. Maugeri, R. Eichler (*Belgium, Switzerland*)

Carbon-11 chemistry - Why fighting 20 minutes half-life really makes sense

A. Windhorst (*Invited lecture*) (*Netherlands*)

Bifunctional tetraamine chelator ^{99m}Tc -SpmTrien (^{99m}Tc -1, 12-diamino-3, 6, 9-triazadodecane) for renal function imaging

B. Barrios-Lopez, T.R. Hayes, E. Witthuhn, J. Vepsäläinen, K. Bergström, P.D. Benny, A.J. Airaksinen (*Finland*)

Labelling of DOTA-Girentuximab conjugates with therapeutic radionuclides

T.B. Bernabeu, S. Pektor, J. Moreno, M. Miederer, A. Türlér (*Switzerland, Germany*)

Macrocyclic bisphosphonates for diagnosis and therapy of bone metastases: Chemistry, in vivo evaluation and human application

N. Pfannkuchen, M. Meckel, R. Bergmann, J. Pietzsch, J. Steinbach, M. Miederer, W. Mohnike, C.S. Bal, M. Sathekge, F. Rösch (*Germany, India, South Africa*)

WEDNESDAY 31ST AUGUST

CHEMISTRY OF THE NUCLEAR FUEL CYCLE III 272

Study of actinide chemistry in big scientific facilities

Z. Chai (*Invited lecture*)

Interfacial mass transfer studies of selected Pu(IV), Am(III), and Pm(III) liquid-liquid extraction systems by microfluidic technique

P. Bartl, A.V. Gelis, C.A. Launiere, P. Distler, M. Nemec, J. John
(*Czech Republic, USA*)

Recent results on the U-Pu-Pb-Bi-O phase relation

K. Popa, D. Prieur, P.M. Martin, J.-F. Vigier, O. Beneš, P.E. Raison, R.J.M. Konings, J. Somers (*Germany, France*)

Recent process in pyroprocessing technology development for spent fuel recycling at KAERI

G. Park, W. I. Ko, D. Ahn, J. Ku, K.C. Song (*Republic of Korea*)

Reversibility of $^{241}\text{Am}^{3+}/^{152}\text{Eu}^{3+}$ during alteration and ageing of 2-line ferrihydrite: implications for radionuclide mobility

G. Kenyon, S. Shaw, N. Bryan, K. Morris (*UK*)

ENVIRONMENTAL RADIOACTIVITY II 280

Chernobyl lava and radioactive particles: 30 years of existence

I. Vlasova, A. Shiryaev, V. Yapaskurt, A. Averin, Y. Zubavichus, O. Batuk, S. Conradson, B. Ogorodnikov, B. Burakov, S. Kalmykov
(*Invited lecture*) (*Russia*)

Marine dispersion of ^{236}U in Danish Straits

J. Qiao, P. Steier, S. Nielsen, X. Hou, R. Roos, R. Golser
(*Denmark, Austria*)

^{137}Cs , ^{90}Sr , $^{238,239+240}\text{Pu}$ and ^{241}Am in terrestrial Antarctic ecosystem

K.M. Szufa, J.W. Mietelski, M.A. Olech (*Poland*)

Environmental ^{129}I : level, distribution and source in Northwestern China

D. Zhang, X. Hou (*China, Denmark*)

Chemical effects on production mechanism of fission product aerosols

K. Takamiya, T. Tanaka, S. Nitta, S. Sekimoto, Y. Oki, T. Ohtsuki (*Japan*)

RADIOPHARMACEUTICAL CHEMISTRY II 288

Radiolabeling with novel ^{18}F -labeled electrophilic agents

O. Solin (*Invited lecture*) (*Finland*)

Preparation of n.c.a. 6- ^{18}F fluoro-L-tryptophan using copper-mediated radiofluorination

D. Schäfer, P. Weiß, J. Ermert, J.C. Meleán, B. Neumaier (*Germany*)

Synthesis of ^{18}F -DPA, a novel ^{18}F -DPA-714 analogue for PET imaging of neuroinflammation

T. Keller, A. Krzyczmonik, S. Forsback, A. Kirjavainen, P.F. Lopez, R. Almajidi, J. Takkinen, J. Rajander, F. Cacheux, A. Damont, F. Dollé, J.O. Rinne, M. Haaparanta-Solin, O. Solin (*Finland, France*)

Synthesis of a tetrazine-based prosthetic group for synthesis of ^{111}In and ^{68}Ga radiopharmaceuticals via biorthogonal click reactions

D. Lumen, O. Keinänen, B. Barrios-Lopez, K.A. Bergström, A.J. Airaksinen (*Finland*)

AAZTA-5: a new theranostic chelator with kit-type labeling abilities for ^{68}Ga , ^{44}Sc and ^{177}Lu

J-P. Sinnes, D. Wiebe, S. Böhland, A. Fuente, F. Roesch
(Germany)

CHEMISTRY OF THE NUCLEAR FUEL CYCLE IV 297

Recycling the actinides, a promising pathway for improving the nuclear environmental footprint, and sustainability

C. Poinssot (*Invited lecture*) (France)

Sorption of Cs(I), Ra(II), Eu(III), Am(III), Pu(IV), Np(V), U(VI) and Se(-II) on the rocks of the exocontact zone of Nizhnekansky granitoid massif

V. Petrov, I. Vlasova, N. Kuzmenkova, A. Kashtanov, T. Kuchinskaya, V. Petrov, V. Poluektov, S. Kalmykov, J. Hammer
(Russia, Germany)

Sorption competition of trivalent metals on corundum ($\alpha\text{-Al}_2\text{O}_3$) studied on the macro- and microscopic scale

S. Virtanen, M. Eibl, S. Meriläinen, A. Rossberg, J. Lehto, T. Rabung, N. Huittinen (*Finland, Germany*)

Comparative study of 3-H, 36-Cl, Se, 99-Tc, and 125-I diffusion through Grimsel rock samples

E. Hofmanová, K. Kolomá, V. Havlová (*Czech Republic*)

Selective complexation and separation of pentavalent and hexavalent actinides for nuclear processes

M. Nilsson, C.G. Bustillos, R. Copping, C. Hawkins, I. May (*Invited lecture*) (USA)

The incorporation of uranium into Fe(II)/Fe(III) (oxyhydr)oxide phases

H.E. Roberts, K. Morris, G.T.W. Law, P. Bots, J.F.W. Mosselmans, S. Shaw (*UK*)

THURSDAY 1ST SEPTEMBER

ENVIRONMENTAL RADIOACTIVITY III

307

The characterisation, treatment and disposal of NORM

D. Read (*Invited lecture*) (*UK*)

The uptake of Se by two strains of *Pseudomonas* sp. isolated from a nutrient-poor boreal bog

M. Lusa, J. Knuutinen, J. Lehto, M. Bomberg (*Finland*)

Organically Bound Tritium (OBT) activity determination in environmental samples. How monitoring labs are dealing with it? Feedback of the international OBT working group.

N. Baglan, S.B. Kim, C. Cossonnet, I.W. Croudace
(*France, Canada, UK*)

Challenges with naturally occurring radioactive material (NORM) in road- and tunnel construction

L. Skipperud (*Invited lecture*) (*Norway*)

RADIOANALYTICAL CHEMISTRY II

315

In-beam neutron activation analysis at Heinz Maier-Leibnitz Zentrum

Z. Revay, P. Kudejová, K. Kleszcz, C. Stieghorst (*Invited lecture*)
(*Germany*)

Ultra-low level determination of actinides in large-volume urine samples using compact accelerator mass spectrometry

X. Dai, M. Christl, S. Kramer-Tremblay, H.-A. Synal
(*China, Canada, Switzerland*)

Resonant Laser-SNMS on actinides for spatially resolved ultra-trace analysis

C. Walther, H. Bosco, M. Franzmann, L. Hamann, M. Tanha, K. Wendt (*Germany*)

⁴¹Ca in concrete by liquid scintillation and inductively coupled plasma mass spectrometry

M. Garcia Miranda, B. Russell, S. Woods, A. Arinc, P. Ivanov (*UK*)

A novel approach for analyzing element composition of large aqueous solution samples with a PGNA setup

D. Hei, C. Cheng, W. Jia (*China*)

POSTER SESSION II

ACTINIDE CHEMISTRY

324

P2-1 New extraction systems on the base of polar fluorinated diluent

I. Voronaev, V. Babain, M. Alyapyshev, M. Logunov (*Russia*)

P2-2 Interaction and effect of the complexation of actinides by a protein: the Calmodulin

F. Brulfert, S. Safi, A. Jeanson, C. Berthomieu, J. Roques, S. Sauge-Merle, E. Simoni (*France*)

P2-3 The role of mixed solvents on the solvation and complexation of trivalent f-elements

H.M. Felmy, Z. Wang, S.B. Clark (*USA*)

P2-4 Adsorption behavior of Lr on a Ta surface at high temperature

Y. Kaneya, M. Asai, Ch. E. Düllmann, K. Eberhardt, R. Eichler, S. Goto, J. Grund, K. Hirose, H. Kamada, Y. Kasamatsu, J. V. Kratz, H. Makii, A. Mitsukai, S. Miyashita, Y. Nagame, R. Naguwa, K. Nishio, K. Ooe, A. Osa, V. Pershina, J. Runke, M. Sakama, D. Sato, T. K. Sato, M. Schädel, M. Shibata, Y. Shigekawa, K. Shingu, K. Shirai, P. Steinegger, P. Thörler-Pospiech, T. Tomitsuka, A. Toyoshima, N. Trautmann, K. Tsukada, A. Yakushev (*Japan, Germany, Switzerland*)

P2-5 Derivatives of phenantroline- and pyridine-dicarboxylic acids as selective extractants for separation of Am(III), Cm(III) and lanthanides(III)

P. Matveev, V. Petrov, G. Lavrov, I. Soglasov, S. Kalmykov, N. Ustynyuk, Y. Ustynyuk (*Russia*)

P2-6 Uranyl polyrotaxanes involving cucurbituril: Diversity of topologic structures and uranyl secondary building units

L. Mei, W.-Q. Shi, Z.-F. Chai (*China*)

P2-7 Solid phase alpha spectrometry – application of leached ThO₂ pellets

E. Myllykylä, L. Koivula, T. Lavonen, K. Ollila, K. Helariutta, M. Siitari-Kauppi (*Finland*)

P2-8 THERMAC – a joint project on aquatic actinide chemistry and thermodynamics at elevated temperature conditions

P.J. Panak, M. Altmaier, F. Brandt, V. Brendler, I. Chiorescu, E. Colàs, H. Curtius, F. Endrizzi, C. Franzen, X. Gaona, M. Grivé, S. Hagemann, C. Koke, D.A. Kulik, S. Krüger, J.-Y. Lee, M. Maiwald, A. Skerencak-Frech, R. Steudtner, T. Thoenen, S. Tsushima (*Germany, Spain, Switzerland*)

P2-9 Is the chemistry of lawrencium peculiar?

W.-H. Xu, P. Pyykkö (*China, Finland*)

P2-10 Silica-salophen hybrid material for uranium sequestration

J. Unangst, K.J. Shea, M. Nilsson (*USA*)

P2-11 Theoretical insights into the bonding nature and stabilities of a series of low-oxidation actinide complexes

Q.-Y. Wu, C.-Z. Wang, J.-H. Lan, Z.-F. Chai, W.-Q. Shi (*China*)

TRANSACTINIDE CHEMISTRY

340

P2-12 Chemical identification and chemistry of transactinide elements at FLNR

N.V. Aksenov, S.N. Dmitriev (*Russia*)

- P2-13 The challenge of target preparation for superheavy element research**
G. Bozhikov, A.V. Sabel'nikov, N.V. Aksenov, G.K. Vostokin, S.N. Dmitriev (*Russia*)
- P2-14 Towards selenides of the SHE Copernicium and Flerovium: Unexpected Cn-Se bond formation**
N.M. Chiera, N.V. Aksenov, Y.V. Albin, G.A. Bozhikov, V.I. Chepigin, S.N. Dmitriev, R. Dressler, R. Eichler, V.Ya. Lebedev, A. Madumarov, O.N. Malyshev, D. Piguet, Y.A. Popov, A.V. Sabel'nikov, P. Steinegger, A.I. Svirikhin, A. Türlér, G.K. Vostokin, A. Vögele, A.V. Yeremin (*Switzerland, Russia*)
- P2-15 Radiochemical investigation of the kinematics of multi-nucleon transfer reactions in $^{48}\text{Ca} + ^{248}\text{Cm}$ collisions 10% above the Coulomb barrier**
M. Götz, S. Götz, J.V. Kratz, Ch.E. Düllmann, J. Ballof, H. Dorrer, J. Grund, D. Huber, E. Jäger, O. Keller, J. Krier, J. Khuyagbaatar, L. Lens, B. Lommel, M. Mendel, Ch. Mokry, K.J. Moody, J. Runke, M. Schädel, P. Scharrer, B. Schausten, D. Shaughnessy, M. Schmitt, J. Steiner, P. Thörle-Pospiech, N. Trautmann, N. Wiehl, A. Yakushev, V. Yakusheva (*Germany, Japan, USA*)
- P2-16 Speeding up gas-phase chemistry to access elements beyond Fl**
S. Götz, M. Block, Ch.E. Düllmann, M. Götz, E. Jäger, O. Kaleja, J. Krier, L. Lens, A.K. Mistry, S. Raeder, A. Yakushev (*Germany*)
- P2-17 Production and decay studies of ^{261}Rf , ^{262}Db , ^{265}Sg , and ^{266}Bh for superheavy element chemistry**
H. Haba, F. Fan, D. Kaji, Y. Kasamatsu, H. Kikunaga, Y. Komori, N. Kondo, H. Kudo, K. Morimoto, K. Morita, M. Murakami, K. Nishio, K. Ooe, Z. Qin, N. Sato, A. Shinohara, M. Takeyama, T. Tanaka, A. Toyoshima, K. Tsukada, Y. Wakabayashi, Y. Wang, S. Yamaki, S. Yano, Y. Yasuda, T. Yokokita, A. Yoneda (*Japan*)
- P2-18 Development of a rapid solvent extraction apparatus for aqueous chemistry of the heaviest elements**
Y. Komori, H. Haba, K. Ooe, A. Toyoshima, A. Mitsukai, M. Murakami, D. Sato, R. Motoyama, S. Yano, K. Watanabe, A. Sakaguchi, J. Inagaki, H. Kikunaga, S. Wulff, J.P. Omtvedt (*Japan*)

P2-19 Single-atom flerovium chemistry at TASCA

L. Lens, A. Yakushev, Ch.E. Düllmann, M. Asai, M. Block, H.M. David, J. Despotopulos, A. Di Nitto, K. Eberhardt, M. Götz, S. Götz, H. Haba, L. Harkness-Brennan, F.P. Heßberger, R.-D. Herzberg, D. Hinde, J. Hoffmann, A. Hübner, E. Jäger, D. Judson, J. Khuyagbaatar, B. Kindler, Y. Komori, J. Konki, J.V. Kratz, J. Krier, N. Kurz, M. Laatiaoui, S. Lahiri, B. Lommel, M. Maiti, A.K. Mistry, C. Mokry, K. Moody, Y. Nagame, J.P. Omtvedt, P. Papadakis, V. Pershina, D. Rudolph, J. Runke, M. Schädel, P. Scharrer, T. Sato, D. Shaughnessy, B. Schausten, J. Steiner, P. Thörle-Pospiech, N. Trautmann, K. Tsukada, J. Uusitalo, A. Ward, M. Wegrzecki, E. Williams, N. Wiehl, V. Yakusheva, (*Germany, USA, Japan, UK, Australia, Finland, India, Norway, Sweden, Poland*)

P2-20 Kinetic studies on the mercury – selenium interaction using inverse thermochromatography

A. Madumarov, N.M. Chiera, N. Aksenov, R. Eichler, D. Piguet, A. Türlér, A. Vögele (*Russia, Switzerland*)

P2-22 Extraction behavior of rutherfordium as a cationic fluoride complex with a TTA chelate extractant from HF/HNO₃ acidic solutions

A. Yokoyama, Y. Kitayama, Y. Fukuda, H. Kikunaga, M. Murakami, Y. Komori, S. Yano, H. Haba, K. Tsukada, and A. Toyoshima (*Japan*)

RADIONUCLIDE SPECIATION

358

P2-23 Thermodynamics of An^{IV}DTPA complexes in biological medium: new brand values and prediction for unknown chemical systems

L. Bonin, J. Aupiais, M. Kerbaa, P. Moisy, S. Topin, B. Siberchicot (*France*)

P2-24 Speciation of trivalent actinides and lanthanides in body fluids

A. Barkleit, C. Wilke, A. Heller, A. Ikeda-Ohno, T. Stumpf (*Germany*)

P2-25 Uranium(VI) speciation in seawater : precision on the role of earth alkali cations

M.R. Beccia, M. Matara-Aho, M. Maloubier, P.L. Solari, J. Roques, M. Monfort, C. Moulin, C. Den Auwer (*France*)

- P2-26 Actinide's valence states determination in materials: benefits and perspectives of high energy resolution fluorescence detected X-ray absorption spectrometry**
R. Bès, K. Kvashnina, P. Martin, J. Rothe, A.C. Scheinost, P.L. Solari, T. Vitova (*Finland*)
- P2-27 Speciation of ruthenium in TBP/TPH organic phases (structure and reactivity)**
C. Lefebvre, T. Dumas, M.-C. Charbonnel, P.L. Solari (*France*)
- P2-28 X-ray absorption spectroscopy study the chemical states of U, Th and Cs absorbed in montmorillonite and MX-80**
W.-T. Liu, C.-H. Lee, S.-C. Tsai, T.-L. Tsai (*Taiwan*)
- P2-29 Speciation of U in systems relevant for safety assessment of nuclear waste repositories by high-energy resolution X-ray absorption spectroscopy**
I. Pidchenko, K.O. Kvashnina, T. Yokosawa, N. Finck, D. Schild, J. Göttlicher, T. Schäfer, J. Rothe, H. Geckeis, T. Vitova (*Germany, France*)
- P2-30 X-ray absorption fine structure spectroscopy study of technetium halides and metal-metal bonded complexes: a review**
F. Poineau (*USA*)
- P2-31 Stability of selenate and selenite and their separation using anion exchange chromatography**
K. Shi, R. Li, J. Yang, W. Wu (*China*)

RADIOANALYTICAL CHEMISTRY

371

- P2-32 Determination of ^{126}Sn in intermediate level radioactive waste emerging from the decommissioning of the NPP A1 Jaslovske Bohunice**
B. Andris, J. Bena (*Slovakia*)
- P2-33 Determination of ^3H , ^{36}Cl , ^{22}Na , ^{134}Cs and ^{133}Ba by means of precipitation and distillation**
H. Aromaa, K. Helariutta, M. Siitari-Kauppi, L. Koskinen (*Finland*)

- P2-34 Determination of Zr and Mo isotopes in spent nuclear fuel solution by isotope dilution inductively coupled plasma mass spectrometry for validation of calculated values**
S. Asai, Y. Hanzawa, M. Konda, D. Suzuki, M. Magara, T. Kimura
(*Japan*)
- P2-35 Ra-226 determination in a certain types of mineral water**
N.D. Betenekov, M. Saidzoda, T.I. Mikhailova, D.V. Beresneva (*Russia*)
- P2-36 Validation of three laboratory-developed test methods for determination of ^{90}Sr in aqueous samples and milk and ^{99}Tc in aqueous samples**
G. Bilancia, M. Ferreira, L. Fornara, A. Ravazzani, M. Roveri, R. Vasselli, N. Bianco, G. Cornara, I. Cydzyk, M. Merlo, L. Paolemili, D. Rossi (*Italy*)
- P2-37 The separation of Th, Ac and Ra using extraction chromatographic material with HDEHP on polyacrylonitrile (PAN)**
Y. Buchatskaya, M. Nemec (*Czech Republic*)
- P2-39 Evaluation of ion-exchange and extraction chromatography techniques for the separation of ^{227}Th from its decay products**

P.I. Ivanov, E.M. van Es, M.G. Miranda, S.M. Collins, B.C. Russell, S.M. Jerome (*UK*)
- P2-40 Development of strontium-90 pine needle reference material and the labs intercomparison radiochemical analysis**
Y. Ji, F. Chen, X. Shao, L. Yin (*China*)
- P2-41 Chemical separation of cadmium and silver from fission products**
J. Jiang, C. Gilligan, R. Barfoot (*UK*)
- P2-42 A rapid method for the determination of radiostrontium in seawater using automated separation system**
Y. Jung, H. Kim, J.-M. Lim (*Korea*)
- P2-43 Radiochemical approaches to the measurement of tritium in metallic components**
B. Kang, K.Y. Jee, H.-J. Ahn (*Korea*)

- P2-44 Determination of Cs-137, Sr-90 and plutonium in fish using ion chromatography and extraction chromatography**
C. Landstetter, V. Damberger, E.-M. Lindner, C. Katzlberger (*Austria*)
- P2-45 Study of cadmium extraction from aqueous solutions with high chloride concentration using radiotracer and NMR**
H.V. Lerum, A.M. Bouzga, S. Jørgensen, D. Petersen, D.Ø. Eriksen, E.W. Hansen, J.P. Omtvedt, G. Wibetoe (*Norway*)
- P2-46 Improvement of chemical treatments for ^{32}P analysis in radioisotope wastes**
S.H. Lim, D.J. Lee, S.C. Sohn, K.Y. Jee, H.J. Ahn (*Korea*)
- P2-47 Behavior of rare-earth elements and Ac in system UTEVA- acid solution**
G. Marinov, A. Marinova, M. Milanova, S. Happel, D. Filosofov (*Russia, Bulgaria, France*)
- P2-48 Comparison between two methods of sequential determination of Am, Pu, U isotopes in metallic radioactive waste**
A. Șandru, L. Toro, A. Mușat, G. Teodorov (*Romania*)
- P2-49 Rapid determination of Radium-224/226 in seawater sample**
L. Song, X. Dai, M. Luo, Y. Yang (*China*)
- P2-50 Preparation of anhydrous uranium tetrafluoride as a possible matrix material for Accelerator Mass Spectrometry**
I. Špendlíková, M. Němec, T. Prášek (*Czech Republic*)
- P2-51 The evaluation of Ca contents on a radiochemical separation of Sr, Fe, Nb, and Ni in DAW**
K. Suh, K.S. Choi, H.J. Lee, H.J. Oh, H.J. Ahn (*Korea*)
- P2-52 Method development for the analysis of very low-activity ^{226}Ra contaminated environmental water samples by alpha-spectrometry**
E.M. van Es, P. Ivanov, D. Read (*UK*)
- P2-53 Optimization of isolation and mass spectrometric analysis of lanthanides from spent nuclear fuel**
K. Van Hoecke, J. Bussé, M. Gysemans, L. Adriaensen, A. Dobney, T. Cardinaels (*Belgium*)

- P2-54 Determination of polonium-210 in Lebanese tobacco**
A. Younes, G. Montavon, M. Mokili, C. Alliot (*USA*)
- P2-55 Assessment and comparison of methods for the fast analysis of alpha and beta emitters in air filters**
D. Zapata-Garcia, H. Wershofen, M. Seferinoğlu, A. Dirican, N. Aslan, G. Kahraman, Ü. Yucel (*Germany, Turkey*)

NUCLEAR ANALYTICAL METHODS

401

- P2-56 Emission mossbauer spectroscopy applied for studies on the structure and behavior of amorphous materials under critical conditions**
I. Alekseev (*Russia*)
- P2-57 Numerical efficiency calibration for environmental gamma spectrometry using a medical imaging software**
T. Alrefae (*Kuwait*)
- P2-58 Study of the disequilibrium of ^{238}U and ^{232}Th decay chains by mapping approach**
A. Angileri, P. Sardini, M. Descostes, S. Duval, M. Fialin, T. Oger, P. Patrier, M. Siitari-Kauppi, H. Toubon, J. Donnard (*France, Finland*)
- P2-59 Studies of organohalogen species in lipid extracts of northern pink shrimp by neutron activation, chromatographic, nuclear magnetic resonance and mass spectrometric techniques**
C.S. Bottaro, J.W. Kiceniuk, A. Chatt (*Canada*)
- P2-60 Analytical applications of nuclear methods at NIST**
P.M. Chu, R.G. Downing, R. Oflaz, R.L. Paul, D. Turkoglu, R. Zeisler (*USA*)
- P2-61 Comparison of two autoradiography techniques: Phosphoimager versus The Beaver PIM device on hydrothermally altered andesites from Petite Anse, Martinique.**
C. Delayre, P. Sardini, P. Patrier, J. Sammaljärvi, T. Oger, J. Donnard, M. Siitari-Kauppi (*France, Finland*)

- P2-62 Hair-selenium concentration in Algerian psoriatics using instrumental neutron activation analysis: relation to gender and age**
A. Mansouri, B. Beladel, L.Baba Ahmed, L. Hamidatou Alghem, A. Bendaas, M. Chohra, M.E.A. Benamar (*Algeria*)
- P2-63 Impurity measurements in ^{99}Mo solution by means of high resolution gamma spectrometer**
M.Fallone Koskinas, D.S. Moreira, Jamille da Silveira Almeida, Mauro da Silva Dias (*Brazil*)
- P2-64 Inter-comparison between ML-EM and gold deconvolution algorithms to suppress compton backgrounds in gamma-rays spectroscopy**
S.M.T. Hoang, G.M. Sun, K. Lee, J. Kim, H. Baek (*Korea*)
- P2-65 Self-absorption correction for gamma spectrometry of radioactive environmental reference materials in Taiwan**
P.J. Huang, P.F. Lee, Y.-H. Lin, Lee, Hsiu-Wei (*Taiwan*)
- P2-66 The simultaneous determination of ^{235}U and ^{239}Pu using delayed neutron activation analysis**
R. Kapsimalis, D. Glasgow, B. Anderson, S. Landsberger (*USA*)
- P2-67 Determination of ultra-low levels of radium and radon by LSC with pulse shape analysis and delayed coincidence technique**
H.J. Kim, S.J. Song, S. Pandey (*Korea*)
- P2-68 Calibration of new RAD-air-water exchanger system for continuous monitoring of radon in water**
K.Y. Lee, S.Y. Cho, Y.Y. Yoon, K. Ha, K.-S. Ko (*Korea*)
- P2-69 Development of radon generator and radon standards for radon in air and radon in water**
K.Y. Lee, M.-J. Kim, S.Y. Cho, Kyoochul Ha Kyung-Seok Ko (*Korea*)
- P2-70 Simulation of prompt gamma activation analysis for detecting fake tungsten gold bar by using the MCNPX code**
K. Lee, G. Sun (*Korea*)

- P2-71 High-resolution alpha-particle spectrometry of ^{226}Ra**
M. Marouli, S. Pommé, R. Van Ammel, E. García-Toraño, T. Crespo, S. Pierre (*Belgium, Spain, France*)
- P2-72 Quantitative autoradiography of alpha particle emission in geo-materials using the Beaver™ system**
P. Sardini, A. Angileri, M. Descostes, S. Duval, T. Oger, P. Patrier, N. Rividi, M. Siitari-Kauppi, H. Toubon, J. Donnard (*France, Finland*)
- P2-73 Zinc and tellurium contents in tellurite glass materials**
S. Sekimoto, K. Shikano, S. Fukutani, T. Ohtsuki (*Japan*)
- P2-74 Artificial neural networks in spectroscopy of ionizing radiations: current state**
R.K. Spirau, A.N. Nikitin (*Belarus*)
- P2-75 Investigation on Fire Gilding using XRF and NAA**
R. Margreiter, K. Eberhardt, B. Niemeyer, M. Radtke, E. Strub (*Germany*)
- P2-76 Nondestructive analysis of difficult-to-measure radionuclides by TOF-PGA**
Y. Toh, M. Ebihara, M. Huang, A. Kimura, S. Nakamura, H. Harada (*Japan*)
- P2-77 Characterisation of activity content of ^{226}Ra in spiked metallurgical slag using an interlaboratory comparison**
F. Tzika, E. Garcia-Toraño, M. Hult, D. Arnold, O. Burda, T. Branger, P. Carconi, B. Caro, P. Dryak, A. Fazio, L. Ferreux, S. Klemola, A. Luca, V. Peyrés, M. Reis, M. Sahagia, M. Santos, J. Šolc, Z. Tyminski, B. Vodenik (*Belgium, Spain, Germany, Italy, France, Finland, Romania, Portugal, Czech Republic, Poland, Slovenia*)
- P2-78 Activation analysis methods - an analytical toolkit for silicon solar cell developments**
B. Karches, C. Stieghorst, K. Welter, H. Gerstenberg, G. Hampel, J.V. Kratz, P. Krenckel, P. Kudejova, C. Plonka, B. Ponsard, T. Reich, S. Riepe, J. Schön, N. Wiehl (*Germany, Belgium*)

P2-79 Clearance-level radioactive waste measurement comparisons of two gamma-ray counting systems

C.-H. Yeh, M.-C. Yuan, P.-J. Huang (*Taiwan*)

P2-80 Calibration of elemental sensitivities in PGAA of hydrogen-containing samples

R. Zeisler, M.V. Martinez, R. Paul, D. Turkoglu (*USA, Brazil*)

RADIOPHARMACEUTICAL CHEMISTRY

438

P2-81 Automatic production of astatinated radiopharmaceuticals – from target material to labeled product

E. Aneheim, S. Lindegren, H. Jensen (*Sweden, Denmark*)

P2-82 Study of the dissociation kinetics of DOTA derivatives by immobilization on solid supports

R. Bhardwaj, J. Gascon, H. T. Wolterbeek, A. G. Denkova, P. Serra-Crespo (*Netherlands*)

P2-83 3D cell culture evaluation of polymer vesicles designed for alpha radionuclide therapy

R.M. De Kruijff, A. van der Meer, K.G.A. Drost, D. Lathouwers, A. Morgenstern, F. Bruchertseifer, P. Sminia, H.T. Wolterbeek, A.G. Denkova (*Netherlands, Germany*)

P2-84 Pyridine containing azacrown ligands as possible chelators for Bi³⁺, Y³⁺, Pb²⁺ and Cu²⁺ in aqueous solutions

Bayirta Egorova (*Russia*)

P2-85 Bulk production and evaluation of high specific activity ¹⁸⁶Re for cancer therapy using enriched ¹⁸⁶WO₃ targets in a proton beam

M.E. Fassbender, V. Radchenko, H.T. Bach, E. Balkin, E.R. Birnbaum, M. Brugh, J.W. Engle, M. D. Gott, J. Guthrie, H.M. Hennkens, K.D. John, A.R. Ketrang, M. Kuchuk, J.R. Maassen, C.M. Naranjo, F.M. Nortier, T.E. Phelps, D.S. Wilbur, S.S. Jurisson (*USA*)

P2-86 Radiochemistry of short-lived positron emitters at Turku PET Centre

S. Forsback, A. Kirjavainen, S. Lahdenpohja, S. Helin, C. Bin-Yim, O. Solin (*Finland*)

- P2-87 Metal-implanted mesoporous silicon nanoparticles as a novel drug carrier for radiation theranostics**
U. Jakobsson, A. Airaksinen, A. Etile, J. Ikonen, E. Mäkilä, J. Salonen, K. Helariutta (*Finland*)
- P2-88 Efficient method for locating nanoparticles with pretargeted PET imaging**
O. Keinänen, E. Mäkilä, R. Lindgren, H. Virtanen, H. Liljenbäck, M. Sarparanta, C. Molthoff, A.D. Windhorst, A. Roivainen, J. Salonen, A.J. Airaksinen (*Finland*)
- P2-89 Fully automated synthesis of [^{18}F]FTHA**
A. Kirjavainen, N. Sarja, O. Solin (*Finland*)
- P2-90 ^{90}Y microspheres prepared by sol-gel method, promising material for medical application**
M. Konior, E. Iller, W. Łada, D. Wawszczak (*Poland*)
- P2-91 Utilization of VUV-photons for synthesis of high specific activity [^{18}F]F₂ gas**
A. Krzyczmonik, T. Keller, A. Kirjavainen, S. Forsback, O. Solin (*Finland*)
- P2-92 The use of [^{18}F]selectfluor bis(triflate) in electrophilic fluorination**
S. Lahdenpohja, A. Kirjavainen, S. Forsback, O. Solin, (*Finland*)
- P2-93 Complex of europium with azacrown-ether: stability in aqueous solutions and fetal bovine serum**
E.V. Matazova, B.V. Egorova, M.S. Oshchepkov, A.D. Zubenko, Yu.V. Fedorov, O.A. Fedorova,, S.N. Kalmykov (*Russia*)
- P2-94 Synthesis of ^{177}Lu DOTATATE in a microchannel**
E. Oehlke (*Netherlands*)
- P2-95 Evaluation of ^{111}In -labelled peptide functionalized silicon nanoparticles in a rat model of myocardial infarction**
S. Ranjan, M.P.A. Ferreira, S.M. Kinnunen, V. Balasubramanian, B. Barrios-Lopez, A.M. Correia, E. Mäkilä, V. Talman, J. Salonen, J.T. Hirvonen, H.J. Ruskoaho, H.A. Santos, A.J. Airaksinen (*Finland*)

P2-96 Production and separation of platinum-191 and astatine-211 and their medical applications

A. Kanda, A. Toyoshima,, Y. Hayashi, N. Takahashi, Y. Manabe, A. Shimoyama, K. Kabayama K. Ogawa, H. Ikeda, S. Watanabe, E. Shimosegawa, T. Kamiya, G. Horitsugi, A. Odani, T. Yoshimura, K. Fukase, J. Hatazawa, A. Shinohara(*Japan*)

P2-97 Production and application of copper-64 at Turku PET Centre

C.-B. Yim, V.-V. Elomaa, K. Mikkola, L. van Dijk, J. Rajander, P. Nuutila, O. Solin (*Finland, Netherlands*)

RADIONUCLIDE PRODUCTION

469

P2-98 Complexation studies of Po(IV) with a novel hexadentate chelating agent “N₂S₂O₂/N₄O₂”

A. Younes, D. Deniaud, S. Gouin, G. Montavon, C. Alliot,, M. Mokili, J. Champion (*France*)

P2-99 Comparison of microfluidic and conventional extraction for ⁹⁹Mo produced by Szilard-Chalmers reaction

I. Dalmázio, J.W. van Dorp, E. Oehlke (*Brazil, Netherlands*)

P2-100 Production of radiochemically pure ¹⁶³Ho for the ECHo experiment

H. Dorrer, K. Chrysalidis, T.D. Goodacre, C.E. Düllmann, K. Eberhardt, C. Enss, L. Gastaldo, R. Haas, C. Hassel, K. Johnston, T. Kieck, U. Köster, B. Marsh, C. Mokry, S. Rothe, J. Runke, F. Schneider, T. Stora, A. Türlér, K. Wendt for the ECHo collaboration (*Germany, Switzerland, France*)

P2-101 ⁴⁷Sc separation from ^{nat}Ti irradiated by 55 MeV photons

E.B. Furkina, R.A. Aliev, G.Yu. Aleshin, A.B. Priselkova, S.N. Kalmykov (*Russia*)

P2-102 ⁹⁹Mo generation by accelerator-driven neutrons and thermo-separation of ^{99m}Tc

M. Kawabata, S. Motoishi, K. Hashimoto, Y. Hatsukawa, A. Ohta, T. Shiina, H. Saeki, N. Takeuchi, Y. Nagai (*Japan*)

- P2-103 Separation of terbium radionuclides from europium target irradiated by alpha particles**
A.G. Kazakov, R.A. Aliev, A.Yu. Bodrov, A.B. Priselkova, S.N. Kalmykov
(Russia)
- P2-104 ^{37}Ar production via two photonuclear based methods**
T.K. Mathew, K.H. Robert (USA)
- P2-105 Measurement of production cross sections of Tc isotopes in deuteron-induced reactions on $^{\text{nat}}\text{Mo}$ up to 24 MeV**
Y. Komori, M. Murakami, H. Haba (Japan)
- P2-106 Production of $^{223}\text{RaCl}_2$ and $^{224}\text{RaCl}_2$ preparations from neutron irradiated ^{226}Ra**
R. Kuznetsov, P. Butkalyuk, V. Tarasov, E. Romanov, A. Baranov, I. Butkalyuk (Russia)
- P2-107 Production and purification of no-carrier-added ^{139}Ce at the Leipzig cyclotron CYCLONE® 18/9**
A. Mansel, K. Franke (Germany)
- P2-108 Preparation of enriched nickel-63 for nuclear β -voltaic batteries and coatings on its base**
A. Kostylev, V. Mazgunova, M. Alyapyshev (Russia)
- P2-109 Evaluation a radionuclide purity of ^{226}Th formed from the decay of ^{230}U for Targeted Alpha Therapy**
R. Misiak, M. Bartyzel, B. Wąs, J.W. Mietelski, A. Bilewicz (Poland)
- P2-110 Cross section measurements for cosmochemical important elements with 80-400 MeV monoenergetic neutrons**
A. Nanbu, K. Ninomiya, K. Fujihara, R. Yasui, T. Omoto, S. Sekimoto, H. Yashima, T. Shima, Y. Iwamoto, D. Satoh, M. Hagiwara, H. Matsumura, S. Shibata, Y. Kasamatsu, N. Takahashi, A. Shinohara, M. W. Caffee, K. Nishiizumi (Japan, USA)
- P2-111 Measurements of production cross sections of Be-10 and Al-26 by 120 GeV proton bombardment of Ni-nat., Co-59, and Au-197 targets**
S. Sekimoto, S. Okumura, H. Yashima, T. Ohtsuki (Japan)
- P2-112 Quality of accelerator produced $^{99\text{m}}\text{Tc}$ based on $^{100}\text{Mo}(\text{p},2\text{n})$ reaction**
S. Takács (Hungary)

- P2-113 R&D on $^{99}\text{Mo}/^{99\text{m}}\text{Tc}$ separation-concentration apparatus based on solvent extraction and column chromatography**
K. Tsuchiya, Y. Suzuki, K. Nishikata, A. Shibata, N. Nakamura, M. Tanase, T. Shiina, A. Ohta, M. Kawabata, N. Takeuchi (*Japan*)
- P2-114 Separation of the samarium-europium radiolanthanide couple for the production of medical samarium-153 using radiation-resistant supported ionic liquid phases**
M. Van de Voorde, P. Zsabka, K. Van Hecke, S. Cagno, T. Cardinaels, K. Binnemans (*Belgium*)
- P2-115 Synthesis and evaluation of inorganic ion-exchangers for separation of medically relevant radioisotopes**
A. Younes, J. Fitzsimmons, A. Abraham, L. Bonich, D. Medvedev (*USA*)
- P2-116 Radiometric determination of thyrotoxic effects of exogenous bromide**
S. Pavelka (*Czech Republic*)
- P2-117 Improved radiometric enzyme assays for extremely sensitive determination of iodothyronine deiodinases**
S. Pavelka (*Czech Republic*)
- P2-118 The influence of foodstuff grouping on doses in safety assessments**
J. Pohjola, J. Turunen, T. Lipping, A.T.K. Ikonen (*Finland*)
- P2-119 Preliminary investigation of radioactive emissions from incinerators of municipal solid waste**
F.P. Carvalho, J.M. Oliveira, M. Malta (*Portugal*)
- P2-120 Distribution of radionuclides in a uranium mine pond**
Fernando P. Carvalho, J. M. Oliveira, M. Malta (*Portugal*)
- P2-121 Radon removal from groundwater using an aeration-ventilation system in a small community water supply system**
K.Y. Lee, K.-S. Ko, S.Y. Cho, D.-H. Kim, K. Ha (*Korea*)

- P2-122 Study of radium nitrate solubility in nitric acid solution**
P. Butkalyuk, I. Butkalyuk, A. Baranov, A. Kuprianov, R. Abdullov, R. Kuznetsov (*Russia*)
- P2-123 Radiolytic decomposition of zinc stearate in presence of PuO₂ powders**
J. Gracia, L. Venault, J. Vermeulen, M. Guigue, J. Maurin, F. Audubert, X. Colin (*France*)
- P2-124 Optimization of Hauser-Feshback statistical calculation and evolution of p nuclei with mass numbers of 130–150 in stellar environments**
N. Kinoshita (*Japan*)
- P2-125 Atmosphere dependence of formation process of oxygen vacancy in zinc oxide**
S. Komatsuda, W. Sato, Y. Ohkubo (*Japan*)
- P2-126 New experimental methods for light ion track etched pores in polymer films**
S. Makkonen-Craig, A. Bhandari, K. Yashina, N. Bassein, K. Helariutta (*Finland*)
- P2-127 Development of muonic atom beam extraction system for chemical reaction studies of muonic atoms**
G. Yoshida, K. Ninomiya, M. Inagaki, J. Aoki, M. Toyoda, N. Kawamura, A. Shinohara (*Japan*)
- P2-128 On the development of a method for the isolation of molybdenum**
A. Bombard, C. Dirks, S. Happel (*Japan*)
- P2-129 Comparative study for determination of naturally occurring radioactive materials by ED-XRF, ICP-MS, and gamma spectrometry**
J.-M. Lim, Y.-Y. Ji, J.-Y. Park, C.-J. Kim, K.-H. Chung, M.-J. Kang (*Korea*)

RADIONUCLIDE SPECIATION II

516

Actinide isotopic analysis in nuclear materials without chemical preparation by resonance ionization mass spectrometry

B.H. Isselhardt, M.R. Savina, A. Kucher (*Invited lecture*) (USA)

Speciation of tetravalent uranium with inorganic ligands in aqueous solution investigated by UV/vis and time-resolved laser-fluorescence measurements.

S. Lehmann, R. Steudtner, V. Brendler (*Germany*)

Impact of electrospray ionization on trivalent f-element: ligand solution equilibria

M.P. Kelley, A.E. Clark, S.B. Clark (USA)

The composition and stability of uranium (IV)-silicate colloids in alkaline systems

T.S. Neill, K. Morris, C.I. Pearce, N.K. Sherriff, S. Shaw (*UK, USA*)

EDUCATION SESSION

524

Outcome of CINCH EU projects

J. John (*Czech Republic*)

Educational opportunities within the UNLV radiochemistry program

W. Johns (USA)

Webinar-based education and training

A. Paulenova (USA)

FRIDAY 2ND SEPTEMBER

PRODUCTION OF RADIONUCLIDES

528

Non-conventional radionuclides for therapy: looking for new production routes

R. Aliev (*Invited lecture*) (*Russia*)

^{43}Sc production development by cyclotron irradiation of ^{43}Ca and ^{46}Ti

K.A. Domnanich, C. Müller, A. Türler, N.P. van der Meulen
(*Switzerland*)

Why proton or deuteron induced reactions are not relevant for clinically used ^{201}Tl production

A. Hermanne, F. Tárkányi, S. Takács, F. Ditrói, Z. Szücs, K. Brezovcsik (*Belgium, Hungary*)

Medical use radioisotope production with accelerator neutrons by deuterons

K. Tsukada, S. Watanabe, N. S. Ishioka, Y. Hatsukawa, K. Hashimoto, Y. Sugo, N. Sato, T. Kin, M. Kawabata, H. Saeki, Y. Nagai (*Japan*)

Nano-structured materials as possible sorbents for radionuclide generators

J.L.T.M. Moret, J. Alkemade, E. Oehlke, H.T. Wolterbeek, J.R. van Ommen, A.G. Denkova (*Netherlands*)

RADIATION CHEMISTRY

536

Irradiation effects of extraction agents used for An/Ln partitioning

C. Ekberg, B. Gruner, J. Halleröd, G. Modolo, H. Schmidt, J. Svehla (*Invited lecture*) (*Sweden, Germany, Czech Republic*)

Electronic irradiation stability of alteration layer formed during nuclear glass leaching by water: comparison with initial glass behavior

S. Mougnaud, M. Tribet, J.-P. Renault, C. Jegou, B. Boizot, G. Panczer, T. Charpentier (*France*)

Evaluation of the impacts of gamma radiolysis on an i-SANEX process solvent

D.R. Peterman (*USA*)

CLOSING LECTURE

542

Olli Heinonen (*USA*)

Nuclear and radiochemical methods in nuclear non-proliferation

ABSTRACTS BOOK

MONDAY 29TH AUGUST
OPENING LECTURE

Closing the Nuclear fuel Cycle for Future Sustainable Nuclear Energy

Th. Fanghänel

*European Commission,
Joint Research Centre
Rue du Champs de Mars 21, 1050 Brussels, Belgium*

For more than a decade, the Generation IV International Forum (GIF) has led international collaborative efforts to develop next generation nuclear energy systems. The GEN IV initiative focuses on sustainability, economy, safety and proliferation resistance as key parameters for the use of nuclear systems to meet energy demands for the next decades. Six reactor technologies have been selected for further research and development, these include the: Gas – cooled Fast Reactor (GFR), Lead – cooled Fast Reactor (LFR), Sodium – cooled Fast Reactor (SFR), Molten Salt Reactor (MSR), Supercritical Water – cooled Reactor (SCWR) and Very High Temperature Reactor (VHTR).

Closing the nuclear fuel cycle and the deployment of fast reactors is central to four of the six selected systems, namely the GFR, LFR, SFR and MSR. The deployment of fast reactors paves the way for improved radioactive waste management. The fuel cycle must be closed and valuable fissile material recovered for irradiation in the next reactor cycles. Thus the fuel must be dissolved and the U and Pu recovered in partitioning steps. Furthermore, the minor actinides (MA) can be recovered also and converted into a suitable fuel form for irradiation in the reactor system. The transmutation of these actinides into fission products can in theory at least reduce the long-term radiotoxicity of the spent fuel from some 100,000 years down to 300 years. Depending on the efficiency of the partitioning and separation processes it seems likely that a reduction to 1000 years can be achieved (see figure 1). A further benefit is also accomplished. Namely, the heat load of the spent fuel is decreased, which will increase the effective capacity of a repository by a factor 10 and indeed more if high heat load elements such as strontium and caesium are separated and stored separately in appropriate forms.

The deployment of partitioning and transmutation strategies requires the use of a fast neutron system. This can be the classical fast reactor, or can be a dedicated system, such as the accelerator driven system (ADS). The latter device can yield improved safety as it uses a proton accelerator to generate neutrons by spallation following their collision with a suitable target.

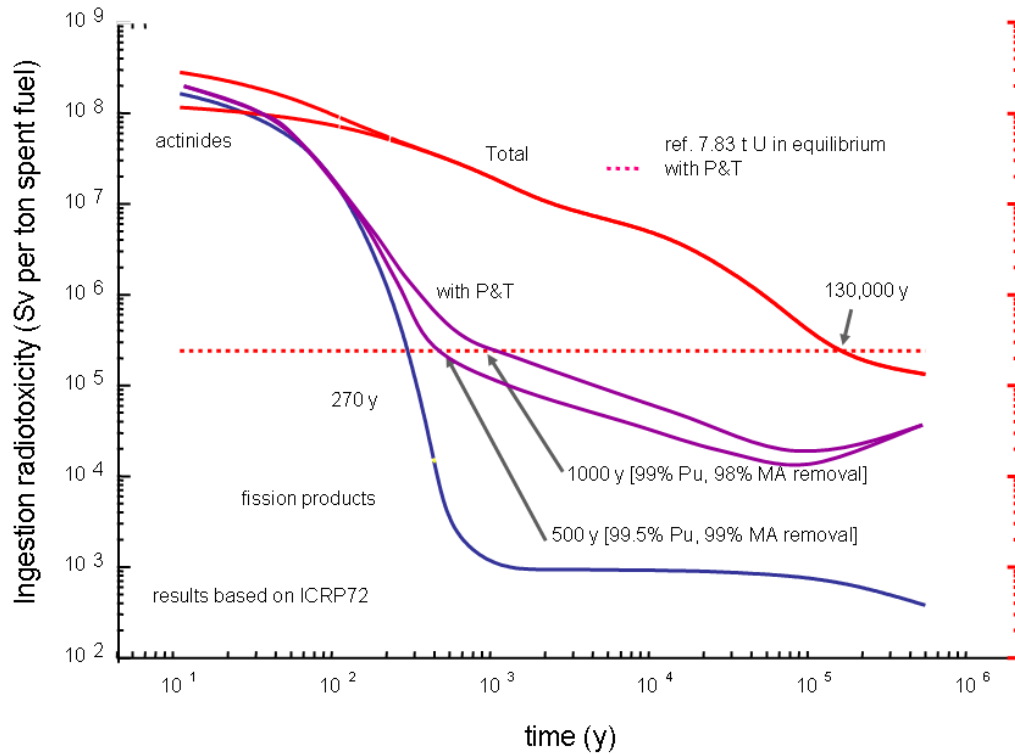


Figure 1 - Radiotoxicity of spent nuclear fuel as a function of time.

The research and development required to enable the deployment of such minor actinide management systems is significant. Recycling processes are required to go beyond today's capabilities, which are largely based on the recovery of Pu and U by the PUREX process. New extractants capable of separating minor actinides from the lanthanides are required. Indeed, a single grouped extraction step for all actinides is attractive from a proliferation point of view. Pyrometallurgical processing is also considered as a promising alternative to aqueous reprocessing of spent fuel. The conversion step from the reprocessing solutions to solid fuel and its subsequent shaping into suitable form for irradiation is a demanding step. Finally, fuel qualification must be achieved through dedicated irradiation testing in normal and transient conditions, and subsequent post irradiation examination (PIE). Modelling and simulation of the entire fuel cycle will gain an increasing importance in the coming years both at engineering and atomistic levels.

Several international large-scale partitioning and transmutation experiments have been carried out or are still on-going. Two of them – the so-called SUPERFACT and METHAFIX experiments – are discussed. For both experiments various minor actinide fuels have been fabricated, characterized, irradiated by fast neutrons, analysed by post irradiation examination and reprocessed either by aqueous or by pyro-reprocessing. Transmutation rates achieved are up to 30 %. The results of these experiments clearly demonstrate the feasibility of closing the nuclear fuel cycle.

CHEMISTRY OF THE NUCLEAR FUEL CYCLE I

Palladium behavior in the presence of irradiated diluent in the PUREX process

S. De Sio^a, I. Klur^a, E. Tison^a, C. Bouyer^b, D. Lebeau^b, F. Goutelard^b, L. Séjourné^b, C. Eysseric^b and N. Vigier^a

^aAREVA NC, France

^bCommissariat à l'Energie Atomique et aux Energies Alternatives (CEA), France

Most reprocessing operations today use the well-proven hydrometallurgical PUREX process. Uranium and plutonium are separated from fission products and minor actinides using solvent extraction – the extractant being 30% tri-n-butylphosphate (TBP) diluted into hydrogenated tetrapropylene (TPH). France has a long history of reprocessing irradiated nuclear fuel using the PUREX process. At La Hague facility, UP3 plant and UP2-800 started operations respectively in 1990 and 1994 and are operated now by AREVA NC. In 2012, some columns in UP3-T4 plutonium purification facility showed significant dysfunctions and had to be replaced consequently. After their replacement, inspection of the damaged equipment revealed the presence of precipitate inside the columns (Figure 1).



Figure 1 – Precipitate found in T4 column.

Experiments were conducted both by AREVA and the CEA to understand what caused such precipitation inside T4 columns. Microprobe analysis revealed high proportions of palladium (>50%w.) and carbon (>25%w.) in the precipitates (Figure 2).

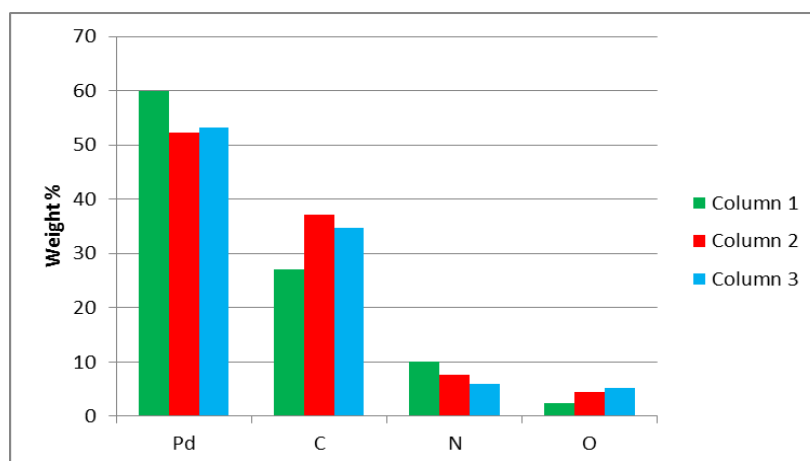


Figure 2 – Microprobe analysis results.

The significant amount of carbon is characteristic of aliphatic compounds and suggests the presence of TPH or its derivatives. In order to confirm this hypothesis, the impact of TPH degradation products on palladium extraction and precipitation was studied: TPH was contacted with Pd nitrate solutions and samples were irradiated at 500 kGy using ⁶⁰Co gamma-rays. A precipitate was formed and analyzed by XRD and IRTF. Both XRD diagrams and IRTF spectra of synthetic precipitate and UP3-T4 precipitate showed similarity, hence indicating that TPH degradation products could be responsible for precipitating palladium compounds (Figure 3).

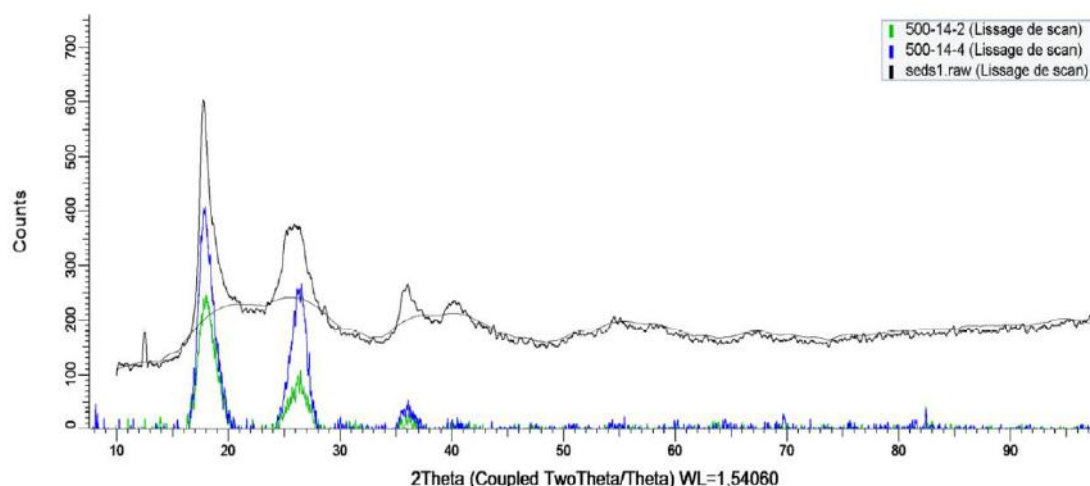


Figure 3 – XRD diagrams of T4 (black) and synthetic (blue, green) precipitates.

Pd behavior was compared in the presence of commercial TPH and regenerated TPH from La Hague: fission products raffinate solution containing Pd was contacted with TPH without stirring and Pd concentration was measured in the aqueous phase using ICP-AES after 8, 27, 52, 98 and 111 days. Results showed that Pd concentration in the aqueous phase decreases almost linearly with time and that the kinetics is very similar for commercial TPH and regenerated TPH from La Hague. In both cases, after 111 days, the aqueous phase contains no more Pd.

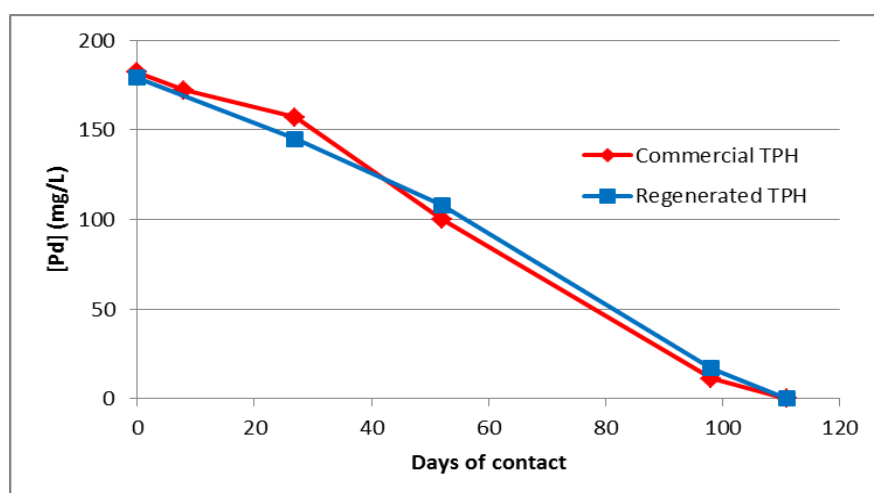


Figure 4 – Pd concentration decrease in aqueous phase after contact with commercial TPH (red) or regenerated TPH from La Hague (blue).

From an industrial point of view, in order to avoid further clogging and to dissolve current precipitates that may be present in other columns at La Hague, dissolution of the precipitate was studied in various media (HNO_3 , 1 M NaOH, isopropanol). Pd concentration was measured in the different solutions after 1 day and 28 days. 1 M NaOH solutions proved to be the most efficient to dissolve the precipitate after 1 day, with no significant change of Pd aqueous concentration after 28 days. Therefore, several columns in La Hague are from now on washed periodically with 1 M NaOH.

Additional experiments are still in progress to improve our knowledge on the palladium behavior in the different steps of the PUREX process in the presence of irradiated diluent and to determine the speciation of the Pd complexes and precipitates.

Selected non-pertechnetate species relevant to Hanford tank waste

T.G. Levitskaia ⁽¹⁾, S. Chatterjee ⁽¹⁾, GB Hall ⁽¹⁾, A. Andresen ⁽²⁾, N.M. Washton ⁽²⁾, E.D. Walter ⁽²⁾

¹ Radiochemical Processing Laboratory, Pacific Northwest National Laboratory, Richland, WA, USA

² Environmental Molecular Sciences Laboratory, Pacific Northwest National Laboratory, Richland, WA, USA

Among radioactive constituents present in the Hanford tank waste technetium-99 (Tc) poses a multitude of problems associated with its radiotoxicity, unique and relatively poorly understood chemistry, and high mobility in the environment. Technetium is one of the most difficult contaminants to be addressed at the U.S. Department of Energy (DOE) Hanford Site because of its complex chemical behavior in tank waste and limited incorporation in the glass waste forms during mid- to high-temperature immobilization processes. The majority of Tc exists in the supernatant and salt cake fractions of both single- and double-shell tanks as pertechnetate TcO_4^- (oxidation state +7) and in the reduced forms (oxidation state < +7) collectively known as non-pertechnetate (non- TcO_4^-) species. There is no definitive information on the origin of the non-pertechnetate species, nor is there a comprehensive description of their composition and behavior. One report indicates that the low-valent Tc species can be derivatives of Tc(I) carbonyl compounds [1]. The objective of this work is to investigate aspects of the nature and chemistry of the non-pertechnetate species derived from the $\text{Tc}(\text{CO})_3^+$ coordination center, specifically under the conditions typical for the alkaline liquid fraction of the tank waste and to gain better understanding and control over their redox behavior.

Oxidative stability and hydrolytic speciation of $[\text{Tc}(\text{CO})_3(\text{H}_2\text{O})_3]^+$ in a pseudo-Hanford tank supernatant simulant solution at variable nitrate and hydroxide concentrations was investigated. The method used for these studies was primarily ^{99}Tc NMR spectroscopy. The triaqua $[\text{Tc}(\text{CO})_3(\text{H}_2\text{O})_3]^+$ ion exists only in acidic aqueous solutions and undergoes extensive hydrolysis starting at near-neutral pH. Consistent with literature reports [2,3] the mono-hydrolyzed $[\text{Tc}(\text{CO})_3(\text{OH})(\text{H}_2\text{O})_2]$ species was observed to undergo oligomerization readily and form the neutral, tetrameric $[\text{Tc}(\text{CO})_3(\text{OH})]_4$ species. One avenue being pursued in order to understand the rich chemistry of Tc complexes is the development of a spectral library, including ^{99}Tc NMR, to aid in the assignment of novel Tc compounds, as well as any presently unidentified components/reactants present in nuclear wastes. However, interpretation of the ^{99}Tc NMR data is hindered by the lack of reference compounds. Density Functional Theory (DFT) calculations can help to fill this gap, but to date few computational studies have focused on ^{99}Tc NMR of compounds and complexes. Theoretical DFT calculations resulted in excellent agreement of the predicted and experimental ^{99}Tc NMR chemical shifts of these Tc(I) $[\text{Tc}(\text{CO})_3]^+$ aqua complexes.

It was demonstrated that in the solutions with the high hydroxide concentrations, the $[\text{Tc}(\text{CO})_3]^+$ species undergo fast oxidative decomposition most likely due to the hydrolytic destruction of the Tc-CO backbone via OH^- nucleophilic attack at the carbonyl carbon. However it was observed that presence of the high salt and small organic chelators in the solutions simulating alkaline nuclear wastes increases the stability of non-pertechnetate species. Stable non-pertechnetate species were generated *ex situ* by a laboratory synthetic route include Tc(I) $[\text{Tc}(\text{CO})_3]^+ \bullet \text{IDA}$ complex (where IDA is iminodiacetate), which accounted for about 70% of total Tc present in the sample 4 months after sample preparation. In comparison, the oxidation rate of the $[\text{Tc}(\text{CO})_3]^+ \bullet \text{Gluconate}$ complex was considerably faster than the $[\text{Tc}(\text{CO})_3]^+ \bullet \text{IDA}$ complex. Complex $[\text{Tc}(\text{CO})_3]^+ \bullet \text{Ligand}$ species, where ligand is a polyaminocarboxylate chelator, were found to easily oxidize to TcO_4^- .

Stable non-pertechnetate species were also generated *in situ* from TcO_4^- using CO/H_2 reductant at elevated pressure and temperature in pseudo-Hanford tank supernatant simulant with and without gluconate and/or catalytic noble metals. Interestingly, stable non-pertechnetate products included both $[\text{Tc}(\text{CO})_3]^+$ -based species as well as Tc(IV/VI) species in intermediate oxidation states. The nature of these intermediate Tc

oxidation species was largely dependent on the presence of the catalytic noble metals in the simulant, which promoted formation of the $[\text{Tc}(\text{CO})_3]^+$ reduction products. With time $[\text{Tc}(\text{CO})_3]^+$ either converted to other non-pertechnetate species or oxidized to TcO_4^- . Intriguingly, Tc(VI) non-pertechnetate species in the intermediate oxidation state were found to be resistant to further oxidation. Overall, significant fractions of *in situ* generated non-pertechnetate persisted in three out of four simulant samples. To our knowledge this is the first identification of stable inorganic Tc(VI) species, and additional experimentation is warranted for elucidation of their structure and chemical composition.

- [1] W. W. Lukens, D. K. Shuh, N. C. Schroeder, K. R. Ashley. *Env. Sci. Tech.* 38, 229 (2004).
- [2] N. I. Gorshkov, A. A. Lumpov, A. E. Miroslovov, D. N. Suglovov. *Radiochemistry*, 45, 116 (2000).
- [3] R. Alberto, R. Schibli, A. Egli, U. Abram, S. Abram, T. A. Kaden, P. A. Schubiger. *Polyhedron* 17, 1133 (1998).

Controls on iron oxyhydroxide formation in the Enhanced Actinide Removal Plant (EARP), Sellafield, UK

Joshua Weatherill¹, Katherine Morris¹, Pieter Bots¹, Tomasz Stawski², Arne Janssen³, Liam Abrahamsen⁴, Richard Blackham⁵ and Samuel Shaw^{1*}

¹Research Centre for Radwaste Disposal and Williamson Research Centre, School of Earth, Atmospheric and Environmental Sciences, University of Manchester, Oxford Road, Manchester, , ²School of Earth and Environment, University of Leeds, Leeds, ³School of Materials, University of Manchester, Oxford Road, Manchester, ⁴National Nuclear Laboratory, Chadwick House, Warrington Road, Birchwood Park, Warrington, ⁵Sellafield Ltd, Seascale, Cumbria
*sam.shaw@manchester.ac.uk

Iron (oxyhydr)oxide (FeOOH) floc treatment processes are utilised for clean-up of industrial effluents. They remove a variety of contaminants, including radionuclides, by reaction with FeOOH particles. One crucial treatment facility of this type is the Enhanced Actinide Removal Plant (EARP) at Sellafield, UK which removes alpha/beta activity from highly radioactive and acidic effluent streams by inducing FeOOH precipitation via NaOH addition¹. EARP is very efficient, but with Sellafield due to transition from fuel reprocessing activities to decommissioning in the next few years, EARP feeds are set to significantly change to post operational clean out (POCO) effluents. Since solution composition is known to affect the FeOOH formation pathways, as well as the composition, size and charge of the formed particles, it is crucial to have a thorough understanding of FeOOH formation in EARP under a range of conditions to underpin future utility of EARP.

In the current work, the EARP treatment process was replicated in the lab using an automated small volume reactor. Here, a 1 M nitric acid ferric nitrate solution (400 ppm Fe) was raised from pH 0.10 to pH 9.0 by the addition of NaOH over approximately 45 mins. In addition to this baseline system, further experiments with added sulfate (1000 ppm), phosphate (100 ppm) or boron (150 ppm) were performed to investigate their effect on particle formation. To characterise these processes, *in situ* and time resolved Small Angle X-ray Scattering (SAXS) measurements were performed at the Diamond Light Source, in conjunction with infrared spectroscopy (ATR-FTIR) and transmission electron microscopy (TEM).

Results show that 2-line ferrihydrite was precipitated as the end product, with SAXS indicating formation proceeded via a pre-nucleation cluster aggregation pathway in all systems. At pH > 0.15, ~ 1 nm diameter colloidal particles/clusters form when the solution is undersaturated with respect to ferrihydrite. Comparison of SAXS data with simulated scattering curves suggests that these clusters are Fe₁₃ Keggin clusters (Sadeghi *et al.*, 2015)². The clusters are initially persistent at low pH for periods of at least 18 days, but when base addition is continued they aggregate to form ferrihydrite. Aggregation commences from ~ pH 1.0 in the baseline ferric nitrate system (Fig.1), but is shifted to lower pH in the phosphate system (~ pH 0.5) and higher pH in the sulfate (pH ~ 1.8) and boron (pH ~ 2.0) systems, indicating that these additional species perturb the formation pathway.

The results of ATR-FTIR analysis provide further insight into the mechanisms of phosphate, borate and sulfate interactions during the hydrolysis process, with both inner and outer sphere complexation observed for different anions. These results highlight the complexity of particle formation in this system and will directly inform EARP effluent management in the future.

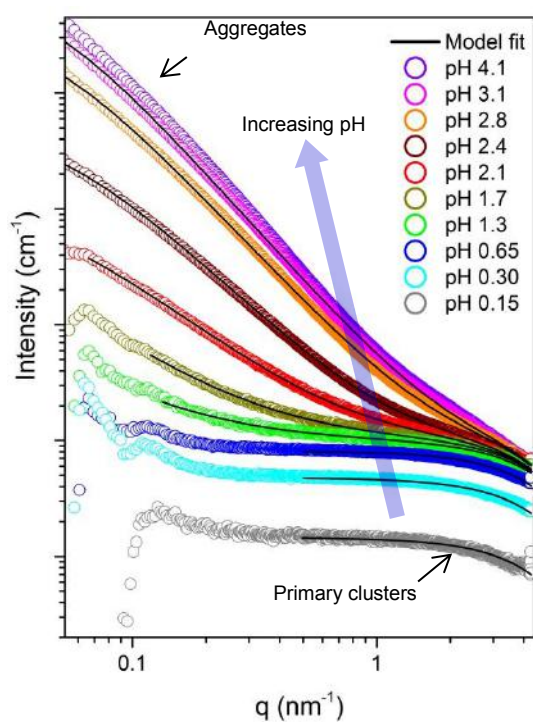


Fig.1: *In situ* SAXS patterns collected at different pHs for the baseline ferric nitrate system. Increasing scattering intensity in the low-q region indicates aggregation of the primary clusters.

References

- (1) <http://www.sellafielddisposal.com/solution/waste-management/effluent-management/>
- (2) Sadeghi *et al. Science*, 347, 6228 (2015)

We gratefully acknowledge Sellafield Ltd and The University of Manchester who co-funded this work via the Effluents and Decontamination Centre of Excellence.

ENVIRONMENTAL RADIOACTIVITY I

Fukushima accident: Environmental impact on land and ocean

Michio Aoyama

Fukushima University, Fukushima, Japan

^{134}Cs and ^{137}Cs , hereafter radiocaesium, were released to the North Pacific Ocean by two major likely pathways, direct discharge from the Fukushima NPP1 accident site and atmospheric deposition off Honshu Islands of Japan, east and northeast of the site. Activities of radiocaesium released by the Fukushima Dai-ichi Nuclear Power Plant (FNPP1) accident were measured by surface sampling at 408 stations in 2011-2013 and in vertical profiles at 24 stations in 2011 and 2012, at 13 station in 2015 in the North Pacific Ocean, and time-series samples were collected at two coastal stations. TEPCO and Japanese government also continue to monitor radiocaesium in seawaters close to the site. After July 2012, ^{137}Cs activity in the surface water near FNPP1 remained around 1000 Bq m⁻³ until the end of 2014, which corresponds to a discharge rate of about 10 GBq day⁻¹. FNPP1-derived radiocaesium spread eastward in surface water across the mid-latitude North Pacific with a speed of 7 km day⁻¹ (8 cm s⁻¹) until March 2012, and of 3 km day⁻¹ (3.5 cm s⁻¹) from March 2012 through August 2014. And Fukushima derived radiocaesium had detected trace amount at western coast of Canada in February 2015. Our model simulation results show good agreement with the observed radiocaesium activities at western coast of Canada, while in the Mexican coast our model projection shows that it will reach in 2016 not in 2015.

In June 2012, ^{134}Cs activity reached a maximum of 6.12 ± 0.50 Bq m⁻³ at a 151-m depth (potential density, 25.3 kg m⁻³) at 29°N, 165°E. This subsurface maximum, which was also observed along 149°E, might reflect the southward transport of FNPP1-derived radiocaesium in association with the formation and subduction of subtropical mode water (STMW). In June 2012 at 34°N–39°N along 165°E, ^{134}Cs activity showed a maximum at around potential density= 26.3 kg m⁻³, which corresponds to central mode water (CMW). ^{134}Cs activity was higher in CMW than in any of the surrounding waters, including STMW. These observations also indicate that the most effective pathway by which FNPP1-derived radiocaesium is introduced into the ocean interior on a 1-year time scale is CMW formation and subduction. In June-July 2015 at 36°N–44°N along 165°E, there are only very weak signal of subduction of Fukushima derived radiocaesium which mean subducted radiocaesium might move eastward from this region.

We also estimated the inventories of radiocaesium released by the Tokyo Electric Power Company Fukushima Dai-ichi Nuclear Power Plant (FNPP1) accident to the North Pacific Ocean by using compiled data and model simulations. By comparing the observed inventories with model-simulated results, we obtained 12–15 PBq of ^{137}Cs for the atmospheric deposition released by the FNPP1 accident in the North Pacific Ocean. Before the Fukushima accident, ^{137}Cs activity in the North Pacific Ocean was about 69 PBq. Therefore, the 12–15 PBq of ^{137}Cs newly added by atmospheric deposition together with the 3.5 ± 0.7 PBq added by direct discharge increased the total ^{137}Cs inventory in the North Pacific Ocean by 22 - 27%. We also estimated the total amount of ^{137}Cs released to the atmosphere to be 15 - 20 PBq, and the total amount of ^{137}Cs released to the environment to be 19 - 24 PBq, respectively. Observed ^{134}Cs to ^{137}Cs activity ratio at the time of accident was close to 1 and extremely uniform, therefore, the total amount of ^{134}Cs deposition in the North Pacific Ocean, that of released to the atmosphere, that of direct discharge to the ocean and that of released to the environment were the same amounts as those of ^{137}Cs .

Comparison of estimates of radiocaesium (^{137}Cs or ^{134}Cs) amount released to the environment:
unit PBq

Source of estimate	Direct ¹	Atmosphere ²	From atmosphere to the ocean ³	Total ⁴
Aoyama et al., 2016	3.6 ± 0.7	15 - 20	12 - 15	15 – 18
UNSCEAR 2013	3 - 6	6 - 20	5 - 8	8 -14*
Tsumune et al., 2013	3.6 ± 0.7			
Bailly du Bois et al., 2012	27 ± 15			
Charette et al., 2013	11 - 16			
Rypina et al., 2013	16.2±1.6			
Miyazawa et al., 2013	5.5 - 5.9			
Kawamura et al.,2011	4		5	9*
Estounel et al., 2012	4.1 - 4.5		5.7 - 5.9	9.8 - 10.4*
Kobayashi et al., 2013	3.5	13	7.6	11.1*
Stohl et al., 2012		37 ± 50% (19 - 56)*		
Terada et al., 2012		8.8		
Mathieu et al., 2012		20.6		
Katata et al., 2012		11		
Saunier et al., 2013		15.5		
Winiarek et al., 2014		19.3		
Katata et al., 2015		14.5		
Inomata et al., 2015			15.3±2.6	
Tsubono et al., accepted.			16.1±1.4	

*: Numbers in italics (calculated by us) shown for reference

1 Direct release to the ocean or Direct release to the ocean + atmospheric deposition at near FNPP1 site, 2 Total release to the atmosphere, 3 Total deposition from the atmosphere on ocean surface, 4 Total amount in the North Pacific Ocean

Devaluation of Rhinoceros horn through nuclear techniques

JR Zeevaart^{1,2}, C Krös¹, D Kotze¹, D Hudson-Lamb¹, J van Rooyen¹, A Buffler³, A Faanhof^{1,2}

¹South African Nuclear Energy Corporation SOC, Pretoria, South Africa

²North-West University, Mahikeng, South Africa

³University of Cape Town, Cape Town, South Africa

Introduction

South Africa is home to 83% of Africa's rhinoceroses and 73% of all wild rhinoceroses worldwide and an important country for rhinoceros conservation. However, the poaching of rhinoceroses has reached a crisis point, and if the killing continues at this rate, population decline could be expected in 2016-2018, meaning rhinoceroses could go extinct in the very near future^[1]. The total number of rhinoceroses poached in South Africa last year was 1,175 - 40 fewer than in 2014 but still significantly higher than the 13 killed in 2007^[2]. Several attempts have been made to stem poaching, ranging from implants of electronic signal devices to possible colouring impregnation or even poisoning of horns. This abstract reports on a research project currently being undertaken at Necsa to investigate the use of in situ labelling of rhinoceros horn through neutron activation. The primary purpose of radioactive labelling techniques is to enable the detection of poached rhinoceros horn at border control points through radiation monitoring.

Methods

One Rhino Horn (white rhino) was cut/sawed into "discs" of about 20 mm thick. Accordingly, 11 "discs" and 11 "saw dust" samples were obtained.

A) The individual disks were analysed for the natural nuclides emitting gamma-rays using a state of the art broad-energy germanium detector mounted in an ultra-low background shield.

B) The "saw dust" samples were analysed for their elemental composition using Inductively Coupled Plasma Mass Spectrometry (ICP-MS), Inductively Coupled Plasma Optical Emission Spectrometry (ICP- OES), Atomic Absorption Spectrometry (AAS), Instrumental Neutron Activation Analysis (INAA) and Combustion Analysis. This resulted in 48 elements found.

C) Based on the elemental composition a theoretical model was developed (using FISPACT-II) to simulate an in situ irradiation of a rhino horn for 5 minutes with a portable neutron generator producing 14 MeV neutrons at a rate of 10^{15} neutrons per second.

D) Experimental irradiations at 2.5MeV (DD) and 14 MeV (DT) of the re-assembled horn were performed. High-density polyethylene $[(C_2H_4)_n]$ that will contribute little in a activation experiment) was used as spacers to replace the cut/sawed sections of the horn and plastic straps to tie the sections together.

Results

A) As radium is chemically similar to calcium, which forms part of the composition of rhino horn, elephant ivory and other species of horn as e.g. warthog and hippopotamus^[3], one can expect all types of horn to have elevated levels of radium and their daughters. The radiation doses are mainly (75-90%) due to ^{228}Ra , ^{226}Ra , ^{210}Pb and ^{210}Po ^[4]. Accordingly, the postulated /modelled/calculated/estimated yearly dose for the public will be close to and even above the allowed 0,250 mSv/a by legislation in South Africa, for both the horn of white and black rhino.

B) Initial neutron activation and ICP-analysis confirmed the existence of calcium and phosphorus, but at substantial lower concentrations as originally anticipated from available literature. It was found that C, O, N, H and S made up for the major elements in rhino horn (~ 99,2%), the minor elements in the horn material

were Ca, Al, P, Fe, Cl, K, Na, Si, Mg and Zn totalling to around 0,8%, while the other 33 trace elements made up for < 0,01% of the material.

C) From the irradiation model the following activities are expected to be generated in the horn which will still be prevalent after one year and should be easily detected due to the relatively high gamma energies and emission rates from a series of radionuclides, i.e. ^{54}Mn with a 835 keV gamma at an emission rate of 2350 gammas per second per kilogram horn and ^{22}Na and ^{65}Zn emitting 511, 1116 and 1274 keV gammas with respective emission rates of 1825, 350 and 1000 gammas per second per kilogram horn. 2 years after irradiation these values have dropped to 1050, 1380, 125 and 765 gammas per second per kilogram horn respectively, which will still be detectable.

D) The DD neutron flux attainable during the experiment was about three (3) orders of magnitude lower than the theoretical first order evaluation, leaving the induced activity on a relatively small sample of the horn (13.38 gram) below the detection limits obtained from the gamma-spectrometric measurements done on average 12 hours and 3 weeks after the irradiation. The first measurement showed that the induced activity of ^{42}K compared well with the predicted value, while the induced activity of ^{24}Na was lower than predicted by a factor 10. For ^{56}Mn , ^{65}Zn , ^{51}Cr , ^{59}Fe , ^{122}Sb , ^{54}Mn and ^{40}K the sensitivity of the gamma-measurements was too low to be quantified although the nuclides could be identified in the spectra. These irradiations will be repeated using 14MeV neutrons, larger sample sizes and longer irradiation periods. In the same experiment the induced dose on the skull of the rhino will also be monitored to determine the radiation safety of the experiment.

Conclusion

The in situ irradiation of Rhino horn is feasible and activation of long-lived nuclides ^{54}Mn , ^{22}Na and ^{65}Zn allows detection of the horn material (by airport scanners) up to 2 years after irradiation. The practical application in terms of irradiation time required as well as radiation safety for the animal has still to be determined.

References

- [1] Assessment of Rhino Horn as a Traditional Medicine. A report prepared for the CITES Secretariat by Kristin Nowell on behalf of TRAFFIC, SC62 Doc. 47.2 Annex (Rev. 2), Species trade and conservation Rhinoceroses, April 2012.
- [2] National Geographic wild life watch. <http://news.nationalgeographic.com/2016/01/160121-rhino-poaching-statistics-South-Africa-trade-lawsuit/>
- [3] F. J. Fouché, D. Kotze, I. Louw. Fingerprinting of ivory and horn through the application of nuclear analytical techniques, Journal of Radioanalytical and Nuclear Chemistry, July 2003, Volume 257, Issue 1, pp 109-112.
- [4] C Krös, D Kotze, B Poole, JR Zeevaart, D Hudson-Lamb, A Faanhof. Natural Radioactivity in Some Species of South African Rhinoceros Horn and Elephant Ivory and the Radiological Exposure Due to Intake. Manuscript in preparation.

Acknowledgement

The authors gratefully acknowledge the financial support received from the Peace Park Foundation for the funding of this research.

ACTINIDE CHEMISTRY

Status and progress of actinides separation in China

Guoan Ye

China Institute of Atomic Energy, Beijing 201413, China

In the nuclear fuel cycle, actinides should be recovered from the used fuel for reused to generate electricity and improving the efficient of uranium resource, as well as for transmutation of produced actinides because of their high toxicity and long half-life. In the past 20 years, a great effort has been made in separation of actinides from the used fuel of PWR in China.

A pilot reprocessing plant of used nuclear fuel has been established, and a hot test has been successfully carried out in the end of 2010. The flow-sheet called improved PUREX process and key self-developed equipment has been verified.

To minimize the volume of solid waste produced during operation of the reprocessing plant, and to reprocess high burnup fuel, a new flowsheet aimed to simplify the process has been developed in CIAE, APOR process, i.e. advanced process base on the organic salt-free reagents. The reaction thermodynamics and kinetics of series organic reagents with Pu(IV), Np(VI) and Np(V) has been investigated, along with Fe^{2+} , U^{4+} and HAN. Here are some examples:

DMHAN with Pu(IV):

$$-\frac{d[\text{Pu(IV)}]}{dt} = \frac{k[\text{Pu(IV)}]^2[\text{DMHAN}]^{1.18}}{(8.12[\text{Pu(III)}] + 95.9[\text{Pu(IV)}])[H^+]^{2.22}} \quad k = 10^3 \text{ s}^{-1}$$

HU with Pu(IV):

$$-\frac{d[\text{Pu(IV)}]}{dt} = k[\text{Pu(IV)}]^2[\text{HU}][H^+]^{-0.9}, \quad k = 5.83 \times 10^3 \text{ s}^{-1}$$

HSC with Pu(IV):

$$-\frac{d[\text{Pu(IV)}]}{dt} = k_o[\text{Pu(IV)}][\text{HSC}]^{1.06}[H^+]^{-0.43}[\text{NO}_3^-]^{-0.58} \quad k = 11.8 \text{ s}^{-1}$$

For separation of minor actinides (MA) from the used fuel, the hot test of TRPO process has been carried out in Tsinghua University. Meanwhile, a process based on TOGDA/DHOA has also been developed in CIAE. Directly following APOR process, a new completed separation flowsheet has been proposed, which can separate and recover U, Pu and MA in the entire process.

The China Reprocessing and Radiochemistry Laboratory has been designed in 2004, the construction was finished in 2014. The hot test of APOR process was carried out in this facility in 2015 using used UO_2 fuel, series experiment equipment and analytical methods were verified. The recovery, separation efficiency and decontamination factors for U and Pu meet the requirement.

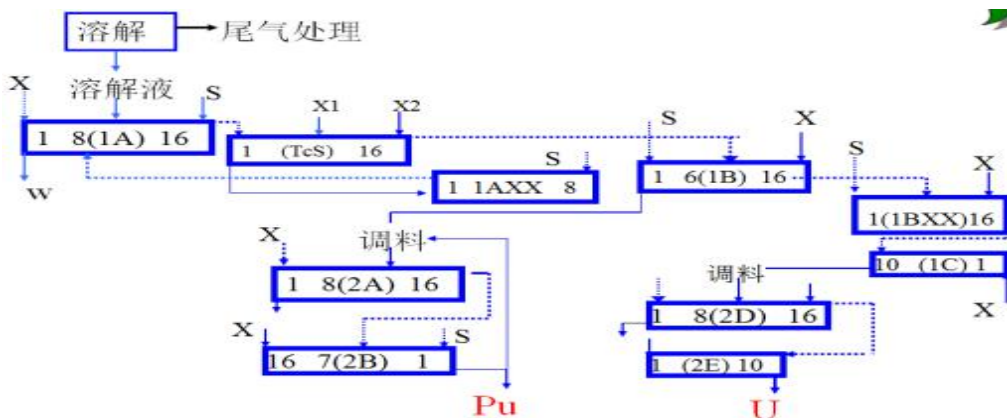


Fig. 1 APOR flowsheet

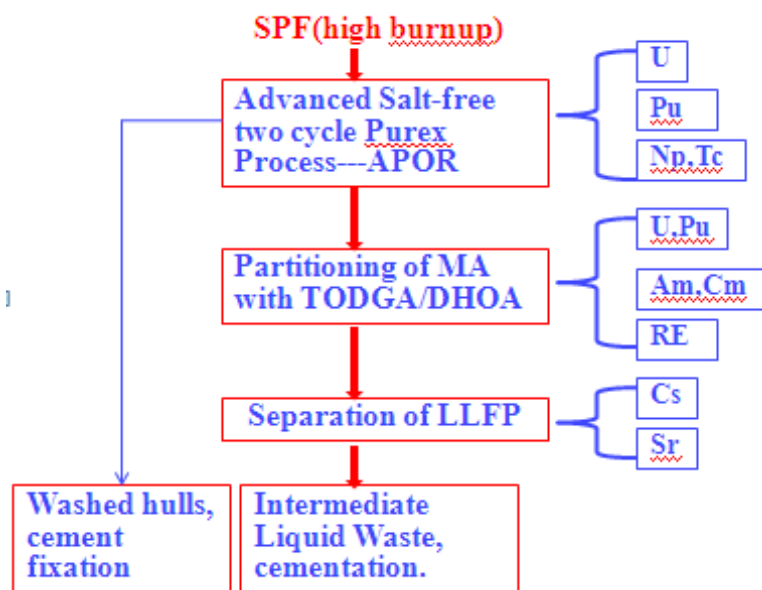


Fig.2 Process of recover U, Pu and MA



Fig.3 Outside view of CRARL



Fig.4 Hot cell and warm cell zone of CRARL

Uranium(VI) solubility and hydrolysis in NaCl solutions at elevated temperatures

Francesco Endrizzi¹, Xavier Gaona¹, Maria Marques Fernandes², Bart Baeyens², Marcus Altmaier¹

¹Karlsruhe Institute of Technology, Institute for Nuclear Waste Disposal, Germany

²Paul Scherrer Institute, Laboratory for Waste Management, Switzerland

francesco.endrizzi@kit.edu

Repositories for high-level radioactive waste are expected to feature elevated temperature conditions over a significant period of time during early stages of operation. In scenarios involving early canister failure, radionuclides may then contact aquatic systems at relatively high temperatures (up to 200°C depending on hostrock system and repository concept, *e.g.* [1]). Adequate scientific tools must therefore be provided in order to model the chemical and physical reactions of radionuclides at elevated temperatures and predict their fate under realistic repository in-situ conditions. Uranium chemistry is relevant in the context of nuclear waste disposal. Uranium has the largest inventory in the radioactive waste, with U(VI) being the most stable oxidation state, under anoxic and oxidising conditions [2]. The present work is integrated into the German research project (ThermAc) which aims to improve the scientific understanding and implement the available thermodynamic database for modelling the chemistry of actinides at elevated temperatures.

Undersaturation solubility experiments with U(VI) were conducted in 0.10, 0.51 and 5.15 mol/kg NaCl solutions in the pH range $4 \leq \text{pH}_m \leq 14$ (with $\text{pH}_m = -\log m_{\text{H}^+}$). Solutions in the acidic pH range ($4 \leq \text{pH}_m \leq 7$) were equilibrated with metaschoepite, $\text{UO}_3 \cdot 2\text{H}_2\text{O}(\text{cr})$, whereas solutions prepared in the alkaline pH range ($7 \leq \text{pH}_m \leq 14$) were equilibrated with sodium uranate, $\text{Na}_2\text{U}_2\text{O}_7 \cdot \text{H}_2\text{O}(\text{cr})$. Batch samples were prepared in screw-cap, gastight and chemically inert Teflon bottles. Leaching tests carried out on these bottles confirmed that no release of organic content (as quantified by TOC) into solution occurred during the solubility experiments at elevated temperature. Solubility experiments were conducted at $T = 25, 55$ and 80°C , in all cases with solid phases previously equilibrated at $T = 80^\circ\text{C}$. Samples were stored in compact ovens located in an Ar glovebox, allowing to work strictly under inert gas atmosphere. The U(VI) concentration in the equilibrium solution was periodically sampled and determined by ICP-MS after filtration with tempered syringe filters (Teflon membrane, $0.2\ \mu\text{m}$ pore size, *Acrodisc*, Pall Co.); pH_m was measured at the same temperature of equilibration, using a glass electrode (ROSS, Orion) and keeping the samples in a customized dry-block heater. After attaining equilibrium conditions, solid phases were characterized by XRD, quantitative chemical analysis and SEM-EDS.

The results indicate that $\text{UO}_3 \cdot 2\text{H}_2\text{O}(\text{cr})$, equilibrated in 0.1 mol/kg NaCl solutions at $T = 80^\circ\text{C}$, is transformed into a Na-U(VI) phase, even in the acidic pH range. Experiments carried out in 0.51 mol/kg NaCl at $T = 80^\circ\text{C}$ show that the solubility of $\text{Na}_2\text{U}_2\text{O}_7 \cdot \text{H}_2\text{O}(\text{cr})$ significantly increases, up to two orders of magnitude at $\text{pH}_m > 9$, compared to room temperature conditions (Figure 1). This effect is mainly due to the enhanced hydrolysis of U(VI) at higher temperatures, as a result of the increased $\log K'_w$. The solubility of $\text{Na}_2\text{U}_2\text{O}_7 \cdot \text{H}_2\text{O}(\text{cr})$ at $T = 25^\circ\text{C}$, previously tempered at $T = 80^\circ\text{C}$ is noticeably decreased (0.5 log units), compared to previous solubility data measured at $T = 25^\circ\text{C}$ for non-tempered $\text{Na}_2\text{U}_2\text{O}_7 \cdot \text{H}_2\text{O}(\text{cr})$ [3]. Thermodynamic modelling of the data collected at $T = 25$ and 80°C yield reasonable estimates of the enthalpies of solubility and hydrolysis of U(VI) in the alkaline range (Figure 1). Forthcoming results from solubility experiments at $T = 55^\circ\text{C}$ and new results from experiments at $T = 80^\circ\text{C}$ will provide a reliable set of data for modelling the chemical behavior of U(VI) in both the acidic and the alkaline range at different temperatures and NaCl concentrations.

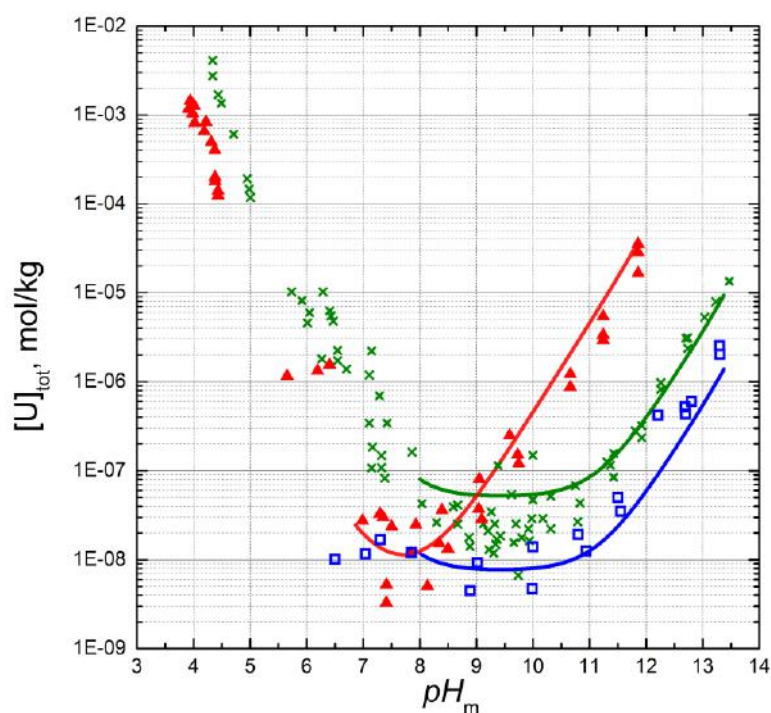


**Figure 5 Solubility of $\text{Na}_2\text{U}_2\text{O}_7 \cdot \text{H}_2\text{O}(\text{cr})$ as a function of pH_m in 0.5 mol/kg NaCl. Symbols: experimental data.
 ✕ Data at 25 °C from ref. [3]; \blacksquare Current data at 25 °C, $\text{Na}_2\text{U}_2\text{O}_7 \cdot \text{H}_2\text{O}(\text{s})$ preliminarily equilibrated at 80 °C;
 ▲ Data at 80 °C; Continuous lines are the calculated solubility curves.**

References

- [1] Nagra, 2002. Project Opalinus Clay – safety report: demonstration of disposal feasibility for spent fuel, vitrified high-level waste and long-lived intermediate-level waste (Entsorgungsnachweis). Nagra Technical Report NTB 02-05
- [2] R. Guillaumont, T. Fanghanel, J. Fuger, I. Grenthe, V. Neck, D. A. Palmer, M. H. Rand, (2003) “Update on the chemical thermodynamics of uranium, neptunium, plutonium, americium and technetium” (F. J. Mompean, M. Illemassene, C. Domenech-Orti, Ben K. Said, Eds.), Amsterdam: Elsevier B. V., 2003, p. 964.
- [3] Altmaier, M., Neck, V., Metz, V., Müller, R., Schlieker, M., Fanghanel, Th. (2003). Solubility of U(VI) in NaCl and MgCl_2 solution. Migration Conference 2003, Gyeongju (Korea)

Acknowledgement:

This work was partially funded by the German Federal Ministry for Education and Research (BMBF). KIT-INE is working in ThermAc under the contract 02NUK039A.

Actinide hybrid materials: Supramolecular assembly and periodic trends

Robert G. Surbella III¹, Kristi L. Pellegrini², Bruce K. McNamara², Lucas Ducati³, Jochen Autschbach⁴, Ginger Simon⁵, Peter C. Burns⁵, Jon M. Schwantes² and Christopher L. Cahill¹

¹Department of Chemistry, The George Washington University, 800 22nd St NW, Washington, D.C. 20052.

²Pacific Northwest National Laboratories, 902 Battelle Blvd, Richland, WA 99354.

³Fundamental Chemistry Department, The University of São Paulo, São Paulo, Brazil.

⁴Department of Chemistry, University at Buffalo, State University of New York, 312 Natural Sciences Complex, Buffalo, New York 14260.

⁵Department of Civil & Environmental Engineering & Earth Sciences, The University of Notre Dame, Notre Dame, Indiana 46556.

The synthesis, crystal structures, and spectroscopic properties of a series of uranium, neptunium, plutonium and americium anions, e.g., $[\text{MO}_2\text{Cl}_4]^{2-}$ and $[\text{MCl}_6]^{2-}$ ($\text{M} = \text{U}, \text{Np}, \text{Pu}, \text{Am}$), assembled via charge balancing pyridinium cations are presented. The compounds were prepared utilizing supramolecular assembly, a strategy based upon the use of non-covalent interactions (NCIs) to assemble discrete molecular building units or *tectons* into extended topologies. The single crystal X-ray diffraction data show that these compounds contain hydrogen and halogen bonding interaction motifs that ultimately facilitate and direct assembly. We have recently demonstrated in uranyl, $[\text{UO}_2]^{2+}$, containing systems that the strengths and quantity of the NCIs may influence material properties, namely, luminescence and thermochromism. Whereas our efforts to prepare transuranic containing hybrid materials are admittedly less-mature compared to analogous UO_2^{2+} containing systems, we have preliminarily observed a number of structural motifs and assembly principles that uniformly transverse the actinide series ($\text{U}, \text{Np}, \text{Pu}$ and Am). Presented will be an overview of assembly criteria, along with strategies and methods to influence material properties and topologies.

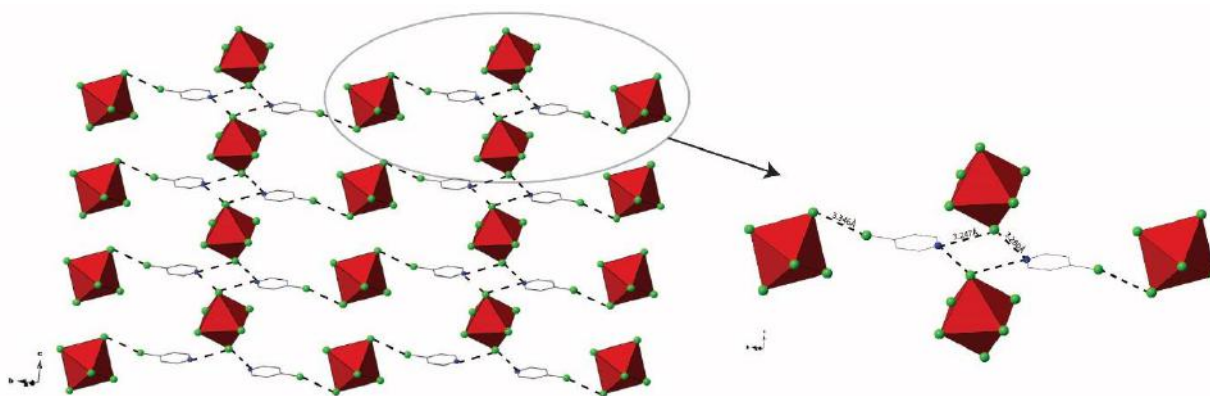


Figure 1. Hydrogen and halogen bonding interactions (dashed lines) stitch the $[\text{PuCl}_6]^{2-}$ and 4-chloropyridinium building units into supramolecular sheets. The plutonium metal centers are represented as red polyhedra whereas the chlorine atoms are depicted as green spheres.

Measurements of electrode reaction kinetics for uranium and rare-earths in LiCl-KCl eutectic electrolyte, and its application to modeling of electrochemical polarization

Kim, K.R., Kim, S.K., Seo, C.S., Goh, W.I., Park, G.I

Korea Atomic Energy Research Institute, Korea

Pyrochemical treatment of nuclear spent fuel has been receiving an attention because the technology has advantages over aqueous process such as less proliferation risk and compact equipment. A pyrometallurgical process employing molten-salt electrochemical technology is now considered as one of the most alternative options in an innovative nuclear fuel cycle. Thus, this promising technology has led to the demonstration tests to assess the feasibility of integrated pyroprocessing development in Korea.

Electrorefining and electrowinning steps are configured as the key processes in which the actinides are separated from the bulk of the fission products in a molten-salt electrolyte by electrotransport. The properties of the electrode reaction rate of uranium and fission products in molten-salt media are essential to be understood for electrochemical polarization. This information may be necessary to model and design the future electrochemical systems.

The investigation of kinetics of the relevant electrode reaction is a significant experimental challenge, because only limited data of kinetics for spent fuel elements has been available in the molten-salt electrochemical system. For this reason, the assessment of electrochemical kinetic data of actinides as well as those of rare-earths is of high importance.

A few investigations to relate electrochemical properties of an electrode reaction rate have been described in the literature. Most of the measurements for the electrode reaction kinetics have been performed by using the solid metal cathode in the molten salt electrolyte. This study attempts to investigate the determination of the exchange current densities using the liquid metal electrode of cadmium which is immiscible in the molten salt electrolyte. The molten cadmium electrodes in contact with a molten salt electrolyte are known to take an electrolytic condition of low chemical activities of transuranic (TRU) elements for the group separation.

In this study, measurements of current-potential relations under carefully controlled conditions could yield information on the electrode reaction rates. Polarization measurements are an important research tool in investigations of a variety of electrochemical phenomena. Such measurements permit studies of the reaction mechanism and kinetics of electrode reaction in an oxidation-reduction system. The exchange current densities of some rare-earth elements and uranium were quantified by applying a linear polarization resistance technique in the cell with a molten cadmium electrode and LiCl-KCl eutectic electrolyte at 500°C. These kinetic constants were obtained from linear slope of the current-overpotential polarization plots. Through the potentiodynamic polarization technique, it provided a reasonable and rapid method for quantitatively predicting the electrode reaction kinetics in the molten-salt system.

In addition to these measurements, computational fluid dynamics (CFD) is a very useful tool for characterizing the electrochemical polarization in a cell at a very low cost. CFD can be effectively applied to scale-up any type of the cell in the design work. A sophisticated approach based on the underlying equations of electrochemical kinetics for the estimation of the spatial polarization in an electrochemical winner is presented. The kinetic parameters obtained from above measurements were applied to the modeling for the polarization characteristics of electrode. A CFD platform linked together electrode reaction kinetics was used to simulate the 3-dimensional electric potential and current density as part of an evaluation of the electrodeposition quality on the liquid cadmium electrode.

It was seen from the CFD analysis coupled with a tertiary electrochemical model helped in finding out polarization characteristics inside the electrowinning process. The effects of the geometry of the system, the kinetic parameters of the cathode reactions and the resistivity of the electrolyte are also discussed to explore a novel design that aims at increased efficiency. This modeling approach could lead to the need for expected electrochemical performance in designing practical cell geometries together with information on operational guidance for product quality.

A novel selective N-heterocyclic ligands for extraction separation of actinides and lanthanides

G. Lavrov,^a N. Ustynyuk,^a I. Gloriov,^b Yu. Ustynyuk,^b M. Alyapyshev,^{c,d} L. Tkachenko,^{c,d} and V. Babain^e

^a A. N. Nesmeyanov Institute of Organoelement Compounds, Russian Academy of Sciences, 28, Vavilova st., Moscow, 119991 Russia.

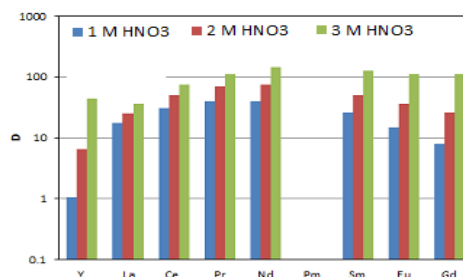
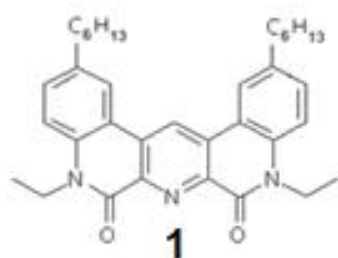
^b Lomonosov Moscow State University, 1/3, Leninskie Gory Moscow, 119991 Russia.

^c V. G. Khlopin Radium Institute, 28, 2-nd Murinskiy pr., Saint Petersburg, 194021 Russia.

^d ITMO University, 49, Kronverkskii pr., Saint Petersburg, 197101 Russia.

^e ThreeArc Mining Ltd., 5, Staryi Tolmachevskii pr., Moscow, 115184 Russia

The development of efficient extraction processes for the separation of minor actinides (Am, Np, Cm) and lanthanides upon spent nuclear fuel processing in the nuclear fuel cycle and the separation of rare-earth elements in order to obtain their high-purity substances is among high-priority problems. The design of highly selective extractants for such processes is complicated due to the fact that the properties of these 4f- and 5f-elements are very close. In the present work, the structures and properties of several pyridine-2,6-dicarboxylic acid diamides and related compounds having different substituents at the amide nitrogen atoms were simulated using DFT, first-principles gradient-corrected PBE functional and relativistic all-electron TZ basis set). Based on the calculation data, dilactams **1** were shown to be a promising ligand for the separation of actinides and lanthanides ($SF_{Am/Eu} \approx 20$) and, therefore, its synthesis was carried out.



The extraction experiments in the systems aqueous HNO₃/*m*-nitrobenzotrifluoride (F3), aqueous HNO₃/CHCl₃ and aqueous HNO₃/dichloroethane confirmed the theoretical predictions. The ligands of this class showed unprecedented values of distribution coefficients ($D \geq 100$ for a 0.01 M solution of ligand **1** in F3), as well as high selectivity factors $SF_{Am/Eu} \approx 30$ and $SF_{Ln1/Ln2} \geq 2$ for adjacent lanthanides. The optimum strategies for the design of highly selective ligands are discussed.

Water adsorption on actinide oxide surfaces

Joseph P. W. Wellington,¹ Andrew Kerridge² and Nikolas Kaltsoyannis³

¹ *Department of Chemistry, University College London, 20 Gordon Street, London WC1H 0AJ, UK*

² *Department of Chemistry, Lancaster University, Bailrigg, Lancaster LA1 4YP, UK*

³ *School of Chemistry, The University of Manchester, Oxford Road, Manchester, M13 9PL, UK*

Of the world's c. 250 tonnes of separated Plutonium, more than 100 tonnes are stored at Sellafield in the UK as PuO₂ powder in sealed steel cans. Under certain circumstances, gas generation may occur in these cans, with consequent pressurization. Many routes to gas production have been suggested, including:

- (i) Helium accumulation from α decay
- (ii) Decomposition of polymeric packing material
- (iii) Steam produced by H₂O desorption from hygroscopic PuO₂ due to self-heating
- (iv) Radiolysis of adsorbed water, and
- (v) Generation of H₂ by chemical reaction of PuO₂ with H₂O, producing a postulated PuO_{2+x} phase.

The last 3 mechanisms, all involving PuO₂/H₂O interactions, are complex, inter-connected and poorly understood.

In light of this, we are studying quantum mechanically the interactions of AnO₂ (An = U, Pu) surfaces with water. Typically, such calculations are performed using density functional theory (DFT) in conjunction with periodic boundary conditions (PBC). However, it is well known that standard PBC implementations of DFT using generalized gradient approximation (GGA) functionals often fail to reproduce key features of actinide solids, *e.g.* predicting metallic properties in systems known to be insulating. This failure stems from incorrect description of the strongly correlated 5f electrons, which are overly delocalized by the GGA, and the standard solution to this problem is to correct the GGA functionals with an onsite Coulomb repulsion term known as the Hubbard *U*.

A more elegant solution is to employ hybrid DFT, in which a certain amount of the exact exchange energy of Hartree-Fock theory is incorporated into the Hamiltonian. Such functionals typically produce more localized 5f electrons, and recover insulator behavior. They are, however, extremely expensive to employ in PBC calculations, and are very rarely used in the calculation of actinide solids. We have therefore sought a computational model which allows the routine use of hybrid DFT in AnO₂/water systems, and in this presentation I will report our development of the periodic electrostatic embedded cluster method (PEECM) [1], in which a quantum mechanically treated cluster is embedded in an infinite 2- or 3-dimensional array of point charges (for surface or bulk studies respectively), to AnO₂/water interactions. This approach allows us to treat a cluster of AnO₂ and adsorbing water molecules using hybrid DFT (PBE0) whilst the long-range electrostatic interactions with the bulk are modelled *via* the embedding of charges.

In our hands, the PEECM correctly predicts the electronic structure of bulk UO₂, NpO₂ and PuO₂, including the change from Mott-Hubbard insulator to charge transfer insulator behaviour as the actinide series is crossed. The adsorptions of water – both molecular and dissociative – are also found to compare well with previous theory and with experiment. For example, Figure 1 shows ball and stick images of a single water molecule adsorbing either molecularly or dissociatively on a cluster representation of the (111) surface of UO₂, and Table 1 summarises the energies of these processes in comparison with very recent PBC DFT results. I will discuss these data in my presentation, and report analogous results for the UO₂ (110) surface. Equivalent adsorptions for the (111) and (110) surfaces of PuO₂ will also be presented. I will conclude with a discussion of the future directions for the project.

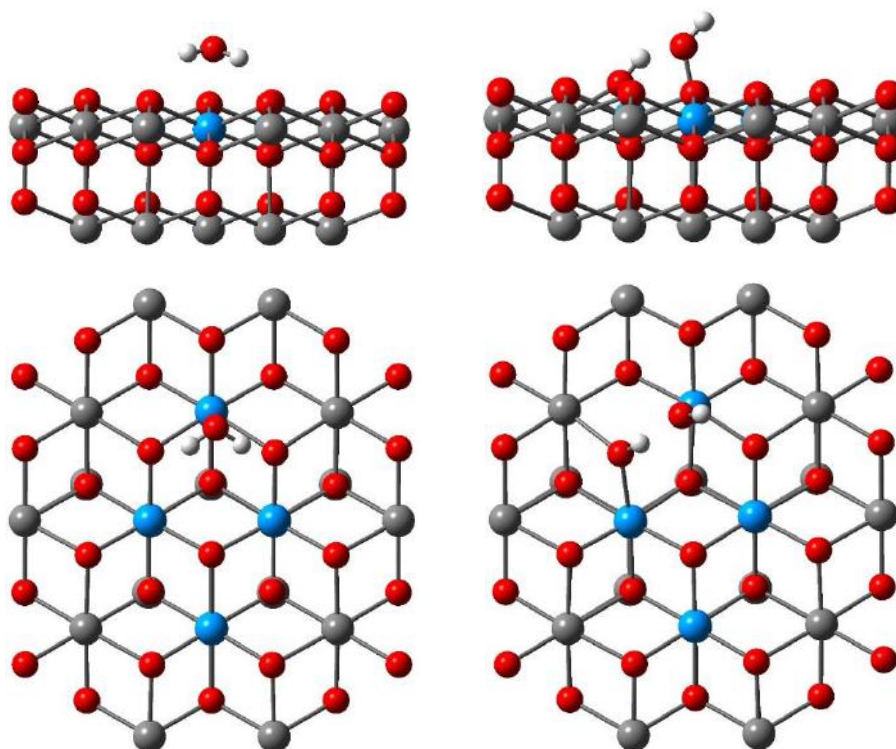


Figure 1: Molecular (left) and dissociative (right) adsorption of a single water molecule on the (111) surface of a $\text{U}_{19}\text{O}_{38}$ cluster. Top view shows the cluster in the plane of the surface, whilst the bottom view is perpendicular to the surface. Hydrogen atoms are shown in white, oxygen atoms in red and uranium atoms in blue and grey. Embedding point charges not shown.

Number of adsorbing water molecules	1		2		3			4			
Type of adsorption	1m	1d	1m, 1d	2d	3m	2m, 1d	1m, 2d	3d	3m, 1d	2m, 2d	1m, 3d
Our work	-0.66	-0.66	-0.78	-0.56	-0.64	-0.76	-0.68	-0.53	-0.71	-0.74	-0.68
GGA+ U [2]	-0.61	-0.68							-0.60	-0.65	-0.53

Table 1: Adsorption energies (eV) of water on a $\text{U}_{19}\text{O}_{38}$ cluster representation of the (111) surface of UO_2 within the PEECM. Type of adsorption is denoted by m for molecular or d for dissociative. 1 to 4 water molecules correspond to approximately 25% to 100% surface coverage respectively

[1] A. M. Burow et al. *J. Chem. Phys.* **130** 174710 (2009)

[2] T. Bo et al. *J. Nucl. Mater.*, **454**, 446 (2014)

TRANSACTINIDE CHEMISTRY

Developments in the chemistry of the heaviest elements

Christoph E. Düllmann^{1,2,3}

¹*Institut für Kernchemie, Johannes Gutenberg-Universität Mainz, 55128 Mainz, Germany*

²*GSI Helmholtzzentrum für Schwerionenforschung, 64291 Darmstadt, Germany*

³*Helmholtz-Institut Mainz, 55099 Mainz, Germany*

Studies of the heaviest currently known elements are interdisciplinary, bridging fields including nuclear physics, atomic physics as well as nuclear- and radiochemistry. Challenges encountered in any studies of the heaviest elements are similar across the various disciplines and mainly include small production rates and short nuclear lifetimes. Chemical elements beyond fermium (atomic number $Z=100$) are only available in atom-at-a-time quantities. Nevertheless, all elements up to $Z=118$ are reported to date, with the last four most recently being officially acknowledged by the IUPAC [1], completing the 7th row of the Periodic Table of the Elements. A comprehensive overview including i) these element's synthesis – artificially as well as potentially in nature –, ii) their nuclear structure – knowledge of which also derives from nuclear chemical studies –, iii) atomic physics aspects, as well as iv) their chemical properties has recently been compiled [2]. Their chemical properties have been reviewed recently in [3,4].

Chemical studies of transactinide elements, i.e., with $Z \geq 104$, allow studying the influence of relativistic effects on the atomic shell under the influence of very high nuclear charge. All elements up to hassium ($Z = 108$) as well as copernicium ($Z = 112$) have been studied in several experiments and reproducible results were obtained [3,4]. Based on these, the evolution of properties down the respective groups was traced and these elements generally conform to the behavior of the homologs in their groups. In more detailed studies, deviations from expectations based on trends established in the respective groups were found. These typically become well understood once the growing influence of relativity is accounted for.

Beyond copernicium, experimental data is scarce. While just a first attempt to study element 113 was performed to date, significant effort was devoted to elucidating volatility and reactivity of flerovium ($Z = 114$), with barely consistent results achieved.

In my presentation, I will give a current overview on the status and on recent advances in the experimental studies of the chemistry of the heaviest elements and briefly touch on some theoretical aspects. In more detail, I will then focus on single-atom studies of the volatility and reactivity of copernicium and flerovium, and obtained results will be compared to state-of-the-art theoretical results. A second emphasis will be on developments towards significantly broadening the range of experimentally accessible compounds for transactinide elements, becoming possible thanks to new experimental capabilities. A first highlight was the recent synthesis of a first carbonyl complex, $\text{Sg}(\text{CO})_6$.

[1] P.J. Karol *et al.*, Pure Appl. Chem. 88 (2016) 139-155; Pure Appl. Chem. 88 (2016) 155-160.

[2] Ch.E. Düllmann, R.-D. Herzberg, W. Nazarewicz, Yu.Ts. Oganessian (Eds.) *Special Issue on Superheavy Elements*, Nucl. Phys. A vol. 944, 2015.

[3] M. Schädel & D. Shaughnessy (Eds.) *The Chemistry of Superheavy Elements*, Springer-Verlag Berlin Heidelberg, 2014.

[4] A. Türler & V. Pershina, *Advances in the Production and Chemistry of the Heaviest Elements*, Chem. Rev., vol. 113, 1237ff, 2013.

Chemistry of the heaviest actinides and early transactinides – Experimental achievements and perspectives

Yuichiro Nagame

Advanced Science Research Center, Japan Atomic Energy Agency, Tokai, Ibaraki 319-1195, Japan

Chemical characterization of the heaviest elements at the farthest reach of the Periodic Table is a challenging and fascinating subject not only in nuclear and radiochemistry but also chemistry as a whole [1, 2]. One of the most important and interesting aspects here is to clarify basic chemical properties of these newly synthesized elements, such as ionic radii, redox potentials, or their ability to form chemical compounds as well as to elucidate the influence of relativistic effects on valence electrons of the heaviest elements and the impact on chemical properties of these elements. The heaviest elements with atomic numbers $Z \geq 101$, however, are all man-made elements synthesized at accelerators using nuclear reactions of heavy-ion beams with heavy element target materials. They can only be identified through measurement of their characteristic nuclear decay or that of their known daughter nuclei using sensitive detection techniques. As both half-lives and cross sections of these nuclides are rapidly decreasing, they are usually available in quantities of only a few atoms or often one atom at a time. Here, we demonstrate recent highlighted studies of the chemical separation and characterization experiments with the heaviest actinides and early transactinides, in liquid-phase chemistry and in studies of atomic properties.

The liquid-phase experiments have been accomplished by partition methods with single atoms, e.g., liquid-liquid extraction, ion-exchange chromatography, and reversed-phase extraction chromatography. The recent studies of the early transactinides, rutherfordium (Rf) and dubnium (Db) are briefly reviewed [3]. Redox studies of the heaviest elements are expected to offer valuable information on valence electronic states influenced by strong relativistic effects, such as oxidation states and redox potentials. Well established electrochemical approaches like cyclic voltammetry are, however, not available for the one atom-at-a-time chemistry of the heaviest elements. Thus, one needs to investigate redox properties of the heaviest elements based on the partition behavior of single atoms between two phases instead of measurements of electric currents generated by redox reactions. A newly developed experimental approach to investigate single atoms of the heaviest elements with an electrochemical method has been developed based on a flow electrolytic cell combined with column chromatography [4]. The successful redox experiments with nobelium (No) and mendelevium (Md) are reported.

Study of atomic properties of the heaviest elements is indispensable to understand electronic ground state configurations. The first ionization energy (IP_1) is an atomic property which most sensitively reflects the outermost electronic configuration. Precise and accurate determination of IP_1 provides significant information on the binding energy of the valence electrons and, thus, on increasingly strong relativistic effects. Recently, the IP_1 value of the heaviest actinide element lawrencium (Lr) was successfully measured using a surface ionization technique coupled to a mass separator [5]. We will outline the experimental method and a result obtained from it. Prospects for future studies of chemical properties of the heaviest elements will be briefly discussed.

- [1] M. Schädel & D. Shaughnessy (eds.), *Chemistry of Superheavy Elements*, 2nd ed., Springer (2014).
- [2] A. Türler & V. Pershina, *Chem. Rev.* **113**, 1237 (2013).
- [3] Y. Nagame, J.V. Kratz & M. Schädel, *Nucl. Phys. A* **944**, 614 (2015).
- [4] A. Toyoshima *et al.* *J. Am. Chem. Soc.* **131**, 9180 (2009).
- [5] T.K. Sato *et al.* *Nature* **520**, 209 (2015).

Experimentally assessing the metal-carbon bond stability in $\text{Sg}(\text{CO})_6$

Robert Eichler^{1,2}, M. Asai³, H. Brand⁴, N.M. Chiera^{1,2}, A. Di Nitto^{4,5}, R. Dressler¹, Ch.E. Düllmann^{4,5,6}, J. Even^{4,6}, R. Eichler^{1,2}, F. Fangli⁷, M. Goetz^{4,5,6}, H. Haba⁸, W. Hartmann⁴, E. Jäger⁴, D. Kaji⁸, J. Kanaya⁸, Y. Kaneya³, J. Khuyagbaatar^{4,6}, B. Kindler⁴, Y. Komori⁸, B. Kraus^{1,2}, J.V. Kratz⁵, J.Krier⁴, Y. Kudou⁸, N. Kurz⁴, S. Miyashita^{3,9}, K. Morimoto⁸, K. Morita^{8,10}, M. Murakami^{8,11}, Y. Nagame³, K. Ooe¹¹, D. Piguet¹, N. Sato⁸, T.K. Sato³, J. Steiner⁴, P. Steinegger^{1,2}, T. Sumita⁸, M. Takeyama⁸, K. Tanaka⁸, T. Tomitsuka¹¹, A. Toyoshima³, K. Tsukada³, A. Türler^{1,2}, I. Usoltsev^{1,2}, Y. Wakabayashi⁸, Y. Wang⁷, N. Wiehl^{5,6}, A. Yakushev^{4,6}, S. Yamaki⁸, S. Yano⁸, S. Yamaki⁸, Z. Qin⁷

¹Paul Scherrer Institute, 5232 Villigen, Switzerland.

²University of Bern, 3012 Bern, Switzerland.

³Advanced Science Research Center, Japan Atomic Energy Agency, Tokai, Ibaraki 319-1195, Japan.

⁴GSI Helmholtzzentrum für Schwerionenforschung GmbH, 64291 Darmstadt, Germany.

⁵Johannes Gutenberg-Universität Mainz, 55099 Mainz, Germany.

⁶Helmholtz-Institut Mainz, 55099 Mainz, Germany.

⁷Institute of Modern Physics Lanzhou; Chinese Academy of Sciences, 730000 Lanzhou, China.

⁸Nishina Center for Accelerator-Based Science, RIKEN, Wako, Saitama 351-0198, Japan.

⁹Hiroshima University, Kagamiyama, Higashi-Hiroshima 739-8526, Japan.

¹⁰Kyushu University, Higashi-Ku, Fukuoka, 812-8581, Japan.

¹¹Niigata University, Niigata, Niigata 950-2181, Japan.

Advances in using physical pre-separation methods [1-3] for chemical investigations of transactinides allowed for the first time to produce and chemically identify fragile gas phase carbonyl complexes of transition metals [4-8]. This work culminated recently in an experiment where the $\text{Sg}(\text{CO})_6$ carbonyl complex was produced and its adsorption interaction with silica surfaces was determined quantitatively [9]. The result was in line with relativistic density functional calculations predicting a similar adsorption interaction for hexacarbonyl complexes of the group 6 elements [10], bolstering the chemical speciation of these single molecular species. Here we describe the development of a second generation experiment intending to assess the thermodynamic metal-carbon bond stability within the $\text{Sg}(\text{CO})_6$ complex. $\text{Sg}(\text{CO})_6$ was predicted to be slightly more stable than the same complex of its lighter homologues $\text{W}(\text{CO})_6$ and $\text{Mo}(\text{CO})_6$ [11]. These calculations included the relativistic effects governing the electron structure of the heavy atoms promoting both the σ -donation from CO into the molecular e_g orbital and the contribution of the π -back-bonding, involving the t_{2g} molecular orbitals in the case of $\text{Sg}(\text{CO})_6$. Thus, the first carbonyl bond dissociation enthalpy (FBDE) was suggested as 204 ± 8 kJ/mol, which is about 12 kJ/mol higher compared to the FBDE of the corresponding tungsten complex [11]. We developed a thermal decomposition experiment for carbonyl complexes on silver surfaces which are inert towards CO and the carbonyl complex up to elevated temperatures [12]. The result of the described experiments yields a decomposition survival curve as depicted in Fig. 1.

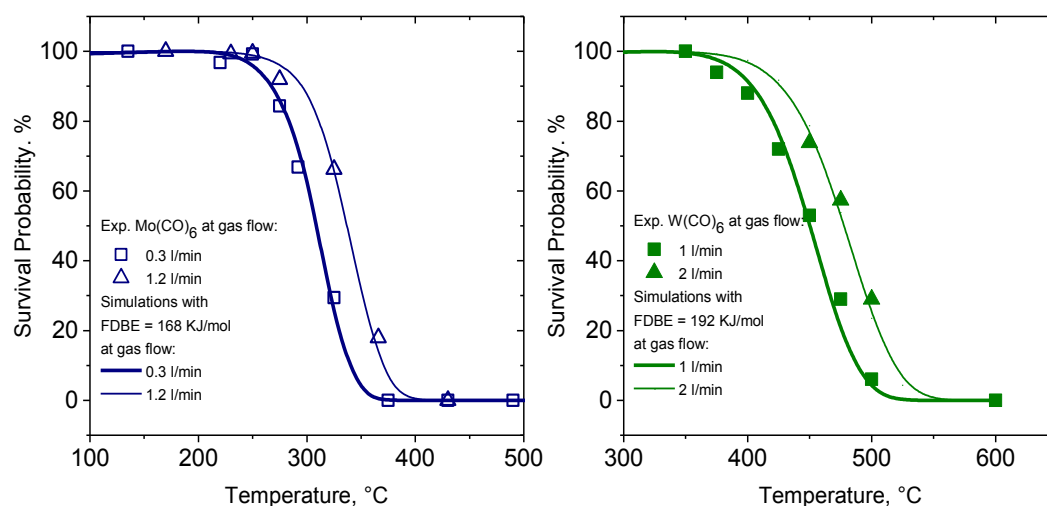


Fig.1 Decomposition survival curves measured for group 6 carbonyl complexes (symbols) [12] together with results of a simulation model (lines) using available data for Mo and W hexacarbonyls [13].

A kinetic adsorption-decomposition model was developed to link the observed survival curves to thermodynamic bond stability [13]. This model well describes the experimental observations with Mo and W at various experimental conditions and it was used to suggest an experimental campaign with Sg. A first experiment is scheduled for April-May 2016 at the RIKEN facilities, Wako, Japan. Experimental details and first results will be included in this presentation.

References:

- [1] Ch. E. Düllmann et al., Nucl. Instrum. Methods A 551, 528 (2005).
- [2] H. Haba et al., J. Nucl. Radiochem. Sci. 8, 55 (2007).
- [3] H. Haba et al., Phys. Rev. C 85, 024611 (2012).
- [4] J. Even et al., Inorg. Chem. 51, 6431 (2012).
- [5] J. Even et al., Radiochim. Acta 102, 1093 (2014).
- [6] J. Even et al., J. Radioanal. Nucl. Chem. 303, 2457 (2015).
- [7] Y. Wang et al. Radiochim. Acta 102(1-2), 69-76, 2015.
- [8] Y. Wang et al. Phys. Chem. Chem. Phys. 17, 13228-13234 (2015).
- [9] J. Even et al., Science 345, 1491 (2014).
- [10] V. Pershina, J. Anton, J. Chem. Phys. 138, 174301 (2013).
- [11] C. S. Nash, B. E. Bursten, J. Am. Chem. Soc. 121, 10830 (1999).
- [12] I. Usoltsev et al., Radiochim. Acta, 104, (3), 141–151 (2015).
- [13] I. Usoltsev et al., Radiochim. Acta, in press (2016).

Laser spectroscopy on nobelium isotopes at GSI

M. Block^{1,2,3}, M. Laatiaoui^{1,2}, H. Backe³, W. Lauth³, D. Ackermann¹, B. Cheal⁴, P. Chhetri⁵, C. Droese⁶, Ch.E. Düllmann^{1,2,3}, P. Van Duppen⁷, J. Even¹, R. Ferrer⁷, F. Giacoppo^{1,2}, S. Götz^{1,2,3}, F.P. Heßberger^{1,2}, M. Huyse⁷, O. Kaleja⁵, J. Khuyagbaatar^{1,2}, P. Kunz⁸, F. Lautenschlaeger⁵, A.K. Mistry^{1,2}, S. Raeder^{1,2}, E. Minaya Ramirez^{1,2}, Th. Walther⁵, C. Wraith⁴, A. Yakushev^{1,2}

¹GSI Helmholtzzentrum, Darmstadt, Germany

²Helmholtz-Institut Mainz, Germany

³Univ. Mainz, Germany

⁴Univ. Liverpool, UK

⁵TU Darmstadt, Germany

⁶Univ. Greifswald, Germany

⁷KU Leuven, Belgium

⁸TRIUMF Vancouver, Canada

Precision measurements of atomic properties by laser spectroscopy allow probing an element's electronic structure. This is of particular importance for the heaviest elements whose electronic structure is strongly affected by relativistic effects, quantum electrodynamics, and electron correlations [1,2]. Despite significant progress in laser spectroscopy of radionuclides in recent years no experimental data on atomic levels of any element beyond fermium are available to date [3,4]. Isotopes of these elements can be produced in complete fusion-evaporation reactions at accelerator facilities on-line, however, only at rates of at most a few particles per second.

A very sensitive method based on a two-step laser-ionization scheme has been developed for optical spectroscopy of nobelium [5]. In this approach nobelium ions are separated from the primary beam by the velocity filter SHIP at GSI Darmstadt. Subsequently, they are slowed down in high-purity argon gas, accumulated on a filament, thermally evaporated from the filament, and eventually laser ionized and detected by their characteristic decay.

In an experiment in 2015 for the first time atomic transitions in nobelium atoms were identified. Besides the strong 1S_0 - 1P_1 transition from the atomic ground state of nobelium several high-lying Rydberg-states were found in ^{254}No . In addition, the frequency shift for the 1S_0 - 1P_1 transition in the isotopes $^{252,253}\text{No}$ was studied. The lowest yield available at the experimental setup was on the order of one particle every ten seconds in the case of ^{252}No . In this contribution, the experimental results will be presented and compared to predictions by state-of-the-art atomic theories. Perspectives for future measurements in heavier elements will be addressed.

References

- [1] E. Eliav, S. Fritzsche, U. Kaldor, Nucl. Phys. A 944, 518 (2015)
- [2] P. Schwerdtfeger, L. F. Pasteka, A. Punnett, P. O. Bowman, Nucl. Phys. A 944, 551 (2015)
- [3] H. Backe, W. Lauth, M. Block, M. Laatiaoui, Nucl. Phys. A 944, 492 (2015)
- [4] P. Campbell, I. Moore, M. Pearson, Progress in Part. and Nucl. Phys. 86 (2016) 127
- [5] M. Laatiaoui, H. Backe, M. Block et al., Eur. Phys. J. D 68, 71 (2014)

First ionization potentials of heavy actinides

T. K. Sato¹, M. Asai¹, Y. Kaneya^{1,2}, K. Tsukada¹, A. Toyoshima¹, A. Mitsukai^{1,2}, S. Takeda^{1,3}, A. Vascon¹, M. Sakama³, D. Sato⁴, K. Ooe⁴, S. Miyashita⁵, Y. Shigekawa⁶, A. Borschevsky⁷, H. Makii¹, A. Osa¹, S. Ichikawa⁸, Y. Nagame¹, M. Schädel¹, K. Eberhardt^{9,10}, J. Runke^{10,11}, P. Thörle-Pospiech^{9,10}, D. Renisch¹⁰, E. Eliav¹², U. Kaldor¹², J. V. Kratz¹⁰, T. Stora¹³, Ch. E. Düllmann^{9, 10, 11}, and N. Trautmann¹⁰

¹Japan Atomic Energy Agency, Tokai, Japan;

²Ibaraki University, Japan; ³Tokushima University, Japan; ⁴Niigata University, Japan; ⁵Hiroshima University, Japan; ⁶Osaka University, Japan; ⁷University of Groningen, Netherlands; ⁸RIKEN, Wako, Japan; ⁹Helmholtz-Institut Mainz, Germany; ¹⁰University of Mainz, Germany; ¹¹GSI Helmholtz Centre for Heavy Ion Research, Darmstadt, Germany; ¹²Tel aviv University, Israel; ¹³CERN, Geneva, Switzerland

The first ionization potential (IP₁) yields information on the valence electronic structure of an atom. IP₁ values of heavy actinides beyond einsteinium (Es, Z = 99), however, have not been determined experimentally so far due to the difficulty in obtaining these elements on scales of more than one atom at a time.

Recently, we successfully measured the IP₁ of lawrencium (Lr, Z = 103) using a surface ionization method [1]. The result suggests that Lr has a loosely-bound electron in the outermost orbital. In contrast to Lr, nobelium (No, Z = 102) is expected to have the highest IP₁ among the actinide elements owing to its fully-filled 5f and the 7s orbitals [2]; due to the similarity of heavy actinides to heavy lanthanides, it is expected that the IP₁ value of heavy actinoids would increase monotonically with filling electrons up in the 5f orbital like heavy lanthanoids.

In the present study, we have determined IP₁ values of No as well as of fermium (Fm, Z = 100) and mendelevium (Md, Z = 101) using a surface ionization method as described in [1]. Surface ionization takes place on a solid surface in a small cavity which is kept at a high temperature. The ionization efficiency I_{eff} of an element can be described based on the Saha-Langmuir equation [3, 4] as follows,

$$I_{\text{eff}} = \frac{N \exp((\phi - \text{IP}^*)/kT)}{1 + N \exp((\phi - \text{IP}^*)/kT)}, \quad \dots (1)$$

where ϕ and T are a work function and temperature of the surface, respectively. N is the effective number of collisions of an atom with the surface. IP^* is the effective ionization potential of an atom, defined as $\text{IP}^* = \text{IP}_1 - kT \ln(Q_i/Q_o)$ (Q_i and Q_o are partition functions of electrons in an atom and an ion, respectively), k the Boltzmann constant. The IP₁ value of the element of interest is determined by exploiting the dependence of I_{eff} on IP^* [1].

The surface ion-source installed in JAEA-ISOL (Isotope Separator On-Line) [5] was applied for measuring the ionization of short-lived isotopes produced in the following nuclear reactions: ²⁵⁶Lr ($T_{1/2} = 27$ s), ²⁵⁷No ($T_{1/2} = 24.5$ s), ²⁵¹Md ($T_{1/2} = 4.27$ min), and ²⁴⁹Fm ($T_{1/2} = 2.6$ min) were produced in the ²⁴⁹Cf + ¹¹B, ²⁴⁸Cm + ¹³C, ²⁴³Am + ¹²C, and ²⁴³Am + ¹¹B reactions, respectively, at the JAEA tandem accelerator. The number of ions collected after mass-separation with the ISOL system was determined by α -particle or γ -ray energy measurements to evaluate I_{eff} values. In order to obtain a relationship between I_{eff} and IP^* in the present system, I_{eff} values of various short-lived isotopes were also measured as outlined in [1].

We successfully ionized and mass-separated ²⁵⁶Lr, ²⁵⁷No, ²⁵¹Md, and ²⁴⁹Fm with ionization efficiencies of approximately 36%, 0.5%, 1.2%, and 1.1% at 2800 K, respectively. From the I_{eff} value of each element, IP₁ values were determined. The obtained experimental results are in good agreement with the relativistic coupled cluster calculations carried out as part of this work, as well as with earlier predictions [1, 2, 6]. Details of the experiments and results will be given in the presentation.

- [1] T. K. Sato, et al., Nature **520** (2015) 209-211.
- [2] A. Borschevsky, et al., Phys. Rev. A **75** (2007) 042514.
- [3] E'. Y. Zandberg & N. I. Ionov, Sov. Phys. Usp. **2** (1959) 255-281.
- [4] R. Kirchner, Nucl. Instrum. Method. A **292** (1990) 203-208.
- [5] T. K. Sato, et al., Rev. Sci. Instrum. **84** (2013) 023304.
- [6] J. Sugar, J. Chem. Phys. **60** (1974) 4103.

First on-line vacuum chromatography experiments with single atoms of Tl on SiO₂

P. Steinegger^{1,2*}, M. Asai³, R. Dressler¹, R. Eichler^{1,2}, Y. Kaneya³, A. Mitsukai³, Y. Nagame³, D. Piguet¹, T. K. Sato³, M. Schädel³, S. Takeda³, A. Toyoshima³, K. Tsukada³, A. Türlér^{1,2} and A. Vascon³

¹ Paul Scherrer Institut, 5232 Villigen PSI, Switzerland

² Department of Chemistry and Biochemistry, Universität Bern, 3012 Bern, Switzerland

³ Advanced Science Research Center, Japan Atomic Energy Agency, Tokai, Ibaraki 319-1195, Japan

* Current affiliation: Joint Institute for Nuclear Research, 141980 Dubna, Russia

A first on-line isothermal vacuum chromatography experiment has been conducted with thallium on quartz at the one-atom-at-a-time level, yielding an adsorption enthalpy of $-\Delta H_{ads}^{SiO_2}(Tl) = 158 \pm 3 \text{ kJ} \cdot \text{mol}^{-1}$ [1]. The presented experiments act as a proof of principle, ultimately aiming at a first unambiguous chemical characterization of E113. The determined adsorption energy differs significantly from earlier measurements of the same physicochemical system [2] and from the adsorption enthalpy for TlOH on quartz [3]. The experimental approach is presented and the outcome is briefly discussed in the light of the mentioned discrepancies. Additionally, the successful vacuum chromatography experiment included a first-ever on-line β -spectroscopy detection stage using diamond-based solid state detectors. This novel sensor material allows for being employed in high-temperature environments [4], making it perfectly suitable for future chemistry experiments with transactinide elements, such as e.g., E113.

References

- [1] P. Steinegger et al., *Physical Chemistry C*, **120**, 13 (2016), pp. 7122-7132
- [2] B. Eichler, ZfK-Report 346 (1977)
- [3] A. Serov et al., *Radiochimica Acta*, **101**, 7 (2013), pp. 421-426
- [4] P. Steinegger et al., to be submitted to *Nuclear Instruments and Methods in Physics Research A*

TUESDAY 30TH AUGUST
RADIOANALYTICAL CHEMISTRY I

Radiochemical analysis for decommissioning of nuclear facilities

Xiaolin Hou

*Technical University of Denmark, Center for Nuclear Technologies (DTU Nutech), Risø Campus,
DK-4000 Roskilde, Denmark
xiho@dtu.dk*

With increasing numbers of nuclear facilities, especially nuclear power reactors, being closed in recent years and from now on, a considerable work is going to be carried out all over the world for decommissioning these nuclear facilities. For this purpose, characterization of various types of materials from the nuclear facilities is required for evaluation of the radioactivity inventory and distribution in various materials and decision making for management of the produced waste. This is implemented by quantitative determination of various radionuclides presenting in these materials.

The neutron activation products of components and impurity in the materials used in the nuclear facilities, such as ^3H , ^{14}C , ^{36}Cl , ^{41}Ca , ^{60}Co , ^{55}Fe , ^{63}Ni , ^{79}Se , ^{93}Mo , ^{93}Zr , ^{94}Nb , ^{126}Sn , ^{133}Ba , ^{152}Eu , ^{154}Eu and some transuranics (isotopes of Pu, Np, Am and Cm) are the main contributors to the total radioactivity, especially in the construction materials. While the long-lived fission products, such as ^{90}Sr , ^{99}Tc , ^{129}I , ^{135}Cs and ^{137}Cs , are the major concern for materials contaminated by leaked spent nuclear fuel. Of these radionuclides, the gamma emitting radionuclides, such as ^{60}Co , ^{133}Ba , ^{152}Eu , ^{154}Eu and ^{137}Cs , are easily measured by gamma spectrometry. While the determination of pure beta and alpha emitters including ^3H , ^{14}C , ^{36}Cl , ^{41}Ca , ^{55}Fe , ^{63}Ni , ^{90}Sr , ^{99}Tc , ^{129}I and some transuranics is the major challenges, because they could not be measured without separation from the matrix of the samples and from all other radionuclides, this entitles them as the radionuclides of hard to measure.

Radiochemical analysis is the only way to implement determination of these hard to measure radionuclides by including a separation of individual radionuclides from matrix and other radionuclides before measurement. Although plenty of analytical methods have been reported for the determination of these radionuclides since the discovery of radioactivity, the suitable methods are not always available for the purpose of characterization of various materials from decommissioning. This is attributed to a few reasons including complicate and various components of the sample matrix, some orders of magnitude lower concentration of some target radionuclides comparing to the major radionuclides which needs a high decontamination factors, complicated and active chemical properties of some important target radionuclides, and a large number of samples required to be analyzed during the decommissioning, which needs simple and rapid methods to provide a good analytical capacity. In particular, the sample matrix varies very much from concrete, graphite, exchange resin, to various metals, which requires different radiochemical methods for different sample matrix and target radionuclides.

Besides the conventional radiometric methods for the measurement of radionuclides, such as liquid scintillation counting, low level beta counting, and alpha spectrometry for these hard to measure radionuclides, some new methods have been proposed and applied. Among them, mass spectrometry especially ICP-MS and accelerator mass spectrometry (AMS) has been widely used for the measurement of long-lived radionuclides, such as ^{41}Ca , ^{36}Cl , ^{99}Tc , ^{129}I , ^{135}Cs and transuranics. With these techniques, the measurement time can be significantly reduced from few days to some minutes, enabling to rapid measurement of large number of samples.

In the past few years, a large numbers of radiochemical analytical methods aiming to characterize various decommissioning waste by determination of various radionuclides of hard to measure have been developed in many laboratories. This work aims to present the state of the art analytical methods for characterization of nuclear waste from the decommissioning of nuclear facilities, not only the updated chemical separation

procedure, but also advanced measurement techniques. Meanwhile, some examples of analytical methods will be also presented, including (1) rapid determination of ^3H and ^{14}C in solid materials; (2) determination of ^{36}Cl and ^{129}I in graphite, concrete and metals (3) Simultaneously determination of multi-nuclides such as ^{41}Ca , ^{55}Fe , ^{63}Ni , ^{90}Sr and transuranics; (4) Challenge on the determination of low level ^{93}Mo , ^{93}Zr , ^{135}Cs , ^{79}Se and ^{126}Sn in decommissioning waste.

References:

- Hou X.L., Frøsig Østergaard L.; Nielsen S.P., Determination of Ni-63 and Fe-55 in nuclear waste and environmental samples, *Anal. Chim. Acta*, 2005, 535:297-307
- Hou X.L. Determination of C-14 and H-3 in Reactor Graphite and Concrete for Decommission, *Applied Radiation and Isotopes*, 2005, 62:871-882.
- Hou X.L., Radiochemical determination of ^{41}Ca in reactor concrete for decommissioning, *Radiochim., Acta*, 2005, 93:611-617.
- Hou X.L., Østergaard L.F., Nielsen S.P., Determination of ^{36}Cl in Nuclear Waste from Reactor Decommissioning, *Anal. Chem.*, 2007, 79, 3126-3134.
- Hou X.L, Radiochemical analysis of radionuclides difficult to measure, *J. Radioanal. Nucl. Chem.*, 2007, 273, 43-48.
- Hou X.L., Roos P., Critical Comparison of Radiometric and Mass Spectrometric Methods for the Determination of Radionuclides in Environmental, Biological and Nuclear Waste samples, *Anal. Chim. Acta*, 2008, 608, 105-139.
- Hou X.L. Determination of long-lived radionuclides in the environment using ICP-MS and AMS, *J. Anal. Sci. Technol.* 2011, 2(Suppl A) A120-124.
- Qiao J.X., Shi K.L., Hou X.L., Nielsen S.P., Roos P., Rapid multi-sample analysis for simultaneous determination of anthropogenic radionuclides in marine environment, *Environment. Sci. Technol.* 2014, 48:3935-3942.
- Shi K., Hou X.L., Roos P., Wu W.S. Stability of technetium and decontamination of Ru and Mo in determination of ^{99}Tc in environmental solid samples by ICP-MS, *Anal. Chem.*, 2012, 84:2009-2016.
- Zheng J., Bu W.T., Tagami K., Shikamori Y., Nakano K., Uchida S., Ishii N. Determination of ^{135}Cs and $^{135}\text{Cs}/^{137}\text{Cs}$ atomic ratio in environmental samples by combining ammonium molybdophosphate (AMP)-selective Cs adsorption and ion-exchange chromatographic separation to triple-quadrupole inductively coupled plasma-mass spectrometry, *Anal. Chem.*, 2014, 86:7103-7110.

Development of robust automated techniques for radionuclide separation

Burrell F.M.¹, Warwick P.E.¹, Croudace I.W.¹, Walters W.S.²

¹(GAU-Radioanalytical) University of Southampton, ²National Nuclear Laboratory, UK

Radioanalytical characterisation underpins extensive environmental monitoring, geochemical research, health physics and decommissioning programmes worldwide. This demand and the increased pressure to develop emergency-response techniques have led to advancements in rapid radioanalytical techniques ranging from the use of vacuum boxes to speed up the flow of solutions through chromatographic separation columns to fully-automated pumped fluid handling systems (Fig. 1).

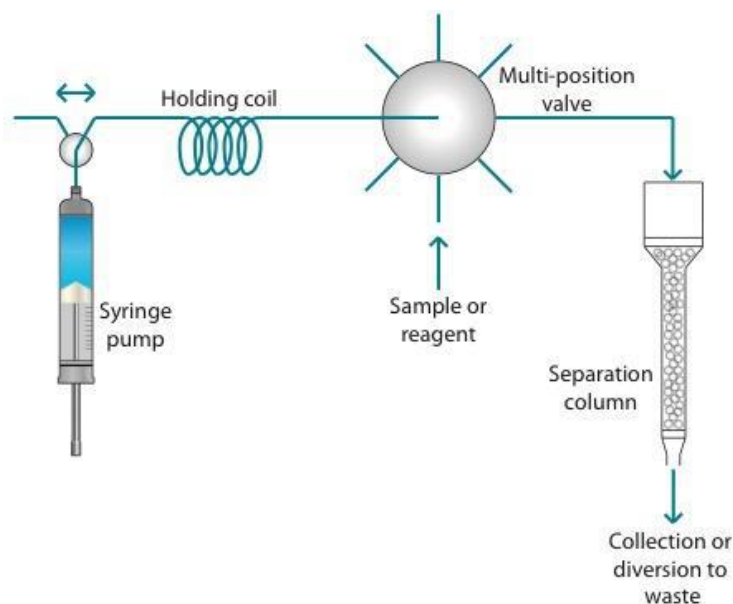


Figure 1

Sequential injection fluid handling system.

A syringe pump is used to draw sample and reagent solutions into the holding coil via a multi-position valve.

The flow is then reversed and the solutions pass through the chromatographic separation column to be collected or diverted to waste. There is also the potential for online detection by solid scintillation or ICP-MS.

Currently, a knowledge gap exists between new chromatographic separation technologies and the traditional methods they derive from. In particular, chromatographic techniques were initially developed and characterised under gravity-driven flow rates; consequentially, there is limited understanding regarding the effect of elevated flow rates on analyte yields and decontamination from interferents. Existing automated systems often choose flow rates based on basic empirical findings or other practical considerations.

The current research presented is focussing on reducing the 'knowledge gap' using a combination of experimental data and mechanistic modelling. The response of the analyte breakthrough peak in terms of position, width and symmetry has been investigated for a range of column parameters including flow rate, bed length, particle size, distribution constant and sorption kinetics.

An assessment of the Gaussian-shaped theoretical plate model in describing breakthrough curves has also been carried out. This model was found to have limited applicability for predicting the behaviour of systems exhibiting increased tailing due to slow sorption kinetics or elevated flow rates. Additionally, an over-estimation of the time of peak elution may be generated by the Gaussian model if local concentrations approach the maximum value of the Langmuir sorption isotherm.

Mechanistic computer simulations have been explored to provide an explanation for the limitations of simple equation-based models and provide a more robust prediction of elution profiles for a wide range of analytes, matrices and sorptive materials.

The ultimate aim of this project is the development and validation of user-friendly graphical software that can be applied to any radioanalytical separation system provided the required input parameters are known. Recommendations on the tests needed to derive input parameters for an uncharacterised material or analyte will also be made. By predicting and implementing the appropriate flow rate, column length and reagent volumes the analyst can meet the required decontamination levels whilst maintaining a high throughput. This easy adjustment of column and reagent parameters will also support the future use of the system as a method development tool.

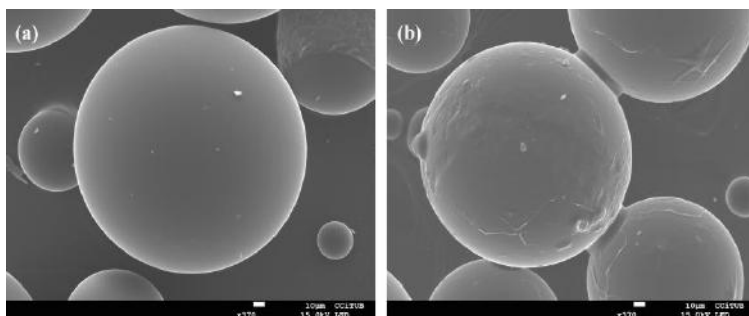
A new plastic scintillation resin for single-step separation, concentration and measurement of ^{99}Tc

Barreda, J.; Tarancón, A.; Bagán, H.; García, J.F.

Department of Analytical Chemistry, Universitat de Barcelona, Martí i Franqués, 1-11, Barcelona, Spain

^{99}Tc is a long-lived radionuclide ($T_{1/2} = 2.13 \cdot 10^5$ years); most of which is produced in the fission of ^{235}U in nuclear power plants (NPP), where its concentration in high-level radioactive waste is relatively important. Thus, interest in ^{99}Tc is related, on the one hand, to representing future doses of one of the major contributions to the inventory of radioactive waste; and on the other hand, to its high mobility in the solid/water system and the potential contamination of the environment. As a long-lived, pure beta emitter ($E_{\text{max}} = 291$ keV), ^{99}Tc can be detected by ICP-MS or by scintillation counting; although both methods should be preceded by chemical separation to remove interferences. In spite of large variety of method for its separation, concentration and measurement, no single procedure presents high recovery values, high decontamination factors, low consumption of reagents and low waste production; consequently, there is a need for more efficient methods of ^{99}Tc analysis. Recently, plastic scintillation resins (PS resin) have been developed as a new material for the selective separation and detection of alpha and beta emitting radionuclides. PS resins are based on plastic scintillation microspheres (PSm) coated with an extractant which is selective for the radionuclide under analysis. The use of PS resins permits unification of the extraction chromatography and scintillation measurement steps within the use of just one material. This presents the advantages of simplifying the analytical procedure, and reducing the processing time and man power and also the amounts of reagents required, as well as the waste generated. In the case of TcO_4^- , Aliquat-336 has been reported to be an optimal extractant, due to its selective extraction from other radionuclides or chemical interferences. Therefore, the objective of this study was to prepare and characterise a PSresin for the analysis of ^{99}Tc in seawater and urine.

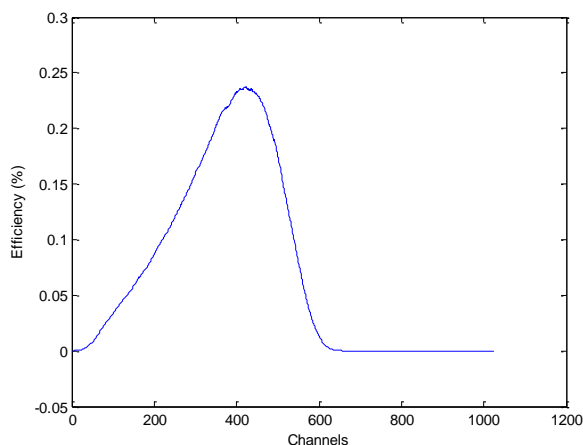
The PSresins were prepared by impregnating the PSm with Aliquat-336. The columns were prepared by packing 3 g of the PSresin into a modification of the 6 mL scintillation vials including caps at the top and the bottom. In this configuration the vial can be connected to a pump to perform the separation, but also close by both sides and to place it directly into the LS counter for measurement. Figure shows the change in the morphology of the PSm's (a) when they are coated (b)).



First, the ^{99}Tc (in the form of TcO_4^-) separation and measurement reproducibility was determined via triplicate analysis of distilled water samples containing a known amount of ^{99}Tc using four different batches of PS resin. Separation procedure consists on four steps: conditioning with 5 mL of HCl 0.1M; loading of 10 mL of sample in HCl 0.1M medium; cleaning with 20 mL of water; removal of the solution in the column-vial.

Values of detection efficiency and mean spectrum are shown next.

Batch	⁹⁹ Tc Detection Efficiency (%)
1	71.9 ± 1.3
2	69.3 ± 1.5
3	68.3 ± 1.1
4	69.8 ± 1.9



The relative standard deviation of the detection efficiency was lower than 3% in all cases, proving good reproducibility in each batch. Between the different immobilisation batches, the values of detection efficiency were statistically equivalent, showing good reproducibility between batches. Finally, the retention of technetium in the column was quantitative in all the analyses performed. The mean values of the blank and detection efficiency were 1.62 ± 0.16 cpm, and $70.0\% \pm 1.9\%$ respectively. From these values, detection limit obtained were comparable to those reported in the literature (375 mBq L^{-1} for a 10 mL sample and 24 h counting time). Detection limits could be improved if sample is previously pre-concentrated by evaporation.

Next the influence of several anionic and radioactive interferences was studied. Results obtained showed that nitrates and sulphates do not affect the retention and detection efficiency. In the case of chlorides, retention is quantitative although a small decrease on the detection efficiency (67.6 %) was observed. In the case of the radioactive interferences, retention of ³⁶Cl can be avoided by adding a cleaning step with HCl 0.5 M. In the case of uranium (and daughters) the cleaning with a HNO₃ 0.1 M and HF 0.1 M avoids the retention of ²³⁴Th in the resin.

Finally, seawater and urine samples spiked with ⁹⁹Tc were analysed for method validation. Quantification was performed with errors lower than 10% in all cases showing the viability of the method.

Precipitation of titanium dioxide with simultaneous uranium sorption and its application in Accelerator Mass Spectrometry

Irena Špendlíková¹, Mojmír Němec¹, Peter Steier²,

¹ *Department of Nuclear Chemistry, Faculty of Nuclear Sciences and Physical Engineering, Czech Technical University, 115 19 Prague, Czech Republic*

² *VERA Laboratory, Faculty of Physics, Universität Wien, 1090 Vienna, Austria*

In the environmental studies the determination of low concentrations has always been a key issue and therefore, the concentration step is usually a crucial part of the sample processing, regardless the employed detection techniques. Another key step is the final sample modification to meet the special requirements of the detection techniques.

Accelerator Mass Spectrometry (AMS) has recently become one of the leading detection techniques for the determination of ultra-trace concentrations in the environmental samples and its development is inseparably connected to the continuous development of sample preparation procedures. The advantages of Accelerator Mass Spectrometry which is based on single atom counting are microgram amount of sample needed for the measurements or high interference suppression which enable to measure such radionuclides as Be-10, Al-26, Ca-41 or U-236. The applications have widely broadened from dating materials, through forensic studies to supernovae remnants on Earth.

This paper focuses on the improvements of the existing sample preparation method for the determination of U-236 using Accelerator Mass Spectrometry and at the same time it proposes a new matrix based on titanium dioxide for AMS measurements. One of the drawbacks of the existing sample preparation method is the so often used iron coprecipitation which was recognised as a source of anthropogenic uranium contamination input. Our proposed method is based on unique properties of fresh hydrous titanium oxide prepared by hydrolysis of its organic precursor - tetra-n-butylorthotitanate which shows relatively high uranium uptake also from real aqueous samples. The advantages of this new method are the minimization of possible contamination inputs and the suitability of titanium dioxide as AMS matrix. Both conclusions were confirmed via AMS measurements at VERA facility, Vienna, Austria. Titanium dioxide as a new AMS matrix showed its high potential for the application in AMS research field mainly due to providing up to 4 times higher negative ion yields in caesium sputter source than standard uranium oxide matrix. Mass scans showed that this new matrix does not add any molecular interferences and the stability allows long and stable measurements. Overall, this new matrix is suitable for U-236 AMS measurements and could improve the statistics of the final results.

Advanced approaches of compound-specific radiocarbon analysis (CSRA) of environmental and radiolabeled materials

Sönke Szidat¹, Gary Salazar¹, Konstantinos Agrios^{1,2}, Christophe Espic¹, Chiara Uglietti^{1,3}, Benjamin Z. Cvetcović⁴,
Erich Wieland⁴

¹ University of Bern, Department of Chemistry and Biochemistry & Oeschger Centre for Climate Change Research,
3012 Bern, Switzerland

² Paul Scherrer Institute, Laboratory for Radiochemistry, 5232 Villigen-PSI, Switzerland

³ Paul Scherrer Institute, Laboratory for Environmental Chemistry, 5232 Villigen-PSI, Switzerland

⁴ Paul Scherrer Institute, Laboratory for Waste Management, 5232 Villigen-PSI, Switzerland

szidat@dcb.unibe.ch

Radiocarbon (¹⁴C, half-life 5730 yr) is an important radionuclide for dating of archeologic finds and environmental materials based on the natural ¹⁴C production. Furthermore, artificial activities of ¹⁴C are widely studied in radiolabeling experiments or radioecologic studies. For all of these applications, analytical methods with increasing chemical specificity have been employed, from bulk procedures to fraction separation, isolation of compound classes and compound-specific radiocarbon analysis (CSRA). Due to the complexity of organic chemistry, separation methods often involve chromatographic isolation, which is very powerful in specificity on the one hand, but often only provide small amounts of analytes on the other hand. Therefore, the more specific isolation is intended, the more sensitive ¹⁴C detection is required. Accelerator mass spectrometry (AMS) is a very sensitive method of radiocarbon detection [1], especially in combination with a gas ion source, which allows direct injection of CO₂ instead of production of solid graphite targets for measurement [2]. The direct gas injection into the ion source of the AMS provides two advantages for the analysis of carbon fractions and CSRA: on the one hand, it allows the measurement of small sample amounts down to a few µg C; on the other hand, it makes possible the connection of instruments dedicated to chemical separation with the AMS device. In a first step, we have applied such hyphenation by combination of an elemental analyzer with the AMS [2,3], which performs total combustion of organic materials and online ¹⁴C measurement. This is a helpful tool for automated radiocarbon analysis with high throughput of fractions extracted by offline separation with different chromatographic techniques (e.g. gas, liquid or ion chromatography). Furthermore, we connected a specialized instrument for temperature-controlled oxidation with AMS for the separation of different carbon fractions from atmospheric particulate matter filters with online radiocarbon determination [4]. Whereas this connection employs intermediate trapping which limits the separation of near-by peaks, even real-time online radiocarbon analysis becomes possible, if specified interfaces are used enriching CO₂ by chemical [4] or physical [5] removing of the carrier gas.

In this work, we present an overview of such advanced approaches of fraction-selective, compound-class-selective and compound-specific radiocarbon analysis using hyphenated systems of separation instruments with the gas ion source of an AMS. Three applications of these approaches will be discussed: a) fraction-selective and compound-specific ¹⁴C analysis of atmospheric particulate matter for apportionment of fossil and contemporary emission sources of carbonaceous aerosols, b) compound-specific identification of ¹⁴C released during anoxic corrosion of activated steel in a cementitious repository for radioactive waste and c) prospects of real-time online hyphenation of gas chromatography with AMS.

[1] Szidat et al., *Radiocarbon* **56**, 561-566, 2014.

[2] Wacker et al., *Nucl. Instr. Meth. Phys. Res. B* **294**, 315-319, 2013.

[3] Salazar et al., *Nucl. Instr. Meth. Phys. Res. B* **361**, 163-167, 2015.

[4] Agrios et al., *Nucl. Instr. Meth. Phys. Res. B* **361**, 288-293, 2015.

[5] Salazar et al., *Anal. Chem.* **88**, 1647-1653, 2016.

RADIONUCLIDE SPECIATION I

Speciation of actinides by time-resolved laser fluorescence spectroscopy

Petra J. Panak

*Institute of Physical Chemistry, University of Heidelberg, 69120 Heidelberg, Germany
petra.panak@kit.edu*

Spectroscopic actinide speciation, providing fundamental information on processes on a molecular scale, is essential for various fields of nuclear chemistry (e.g. performance assessment of nuclear waste repositories, the development of partitioning strategies or toxicology of actinide ions in the human body). Time-resolved laser fluorescence spectroscopy (TRLFS) is a very sensitive speciation technique, which allows actinide characterization and quantification without disturbing the chemical equilibrium. Cm(III) has excellent fluorescence properties and thus can be used as a valuable representative of the trivalent actinides in speciation studies down to the nano-molar concentration range [1]. TRLFS provides information on the structure of An(III) complexes and allows the determination of thermodynamic data ($\log K$, ΔH and ΔS) of different complexation reactions with various inorganic, organic and bio-ligands. TRLFS can be applied not only to solutions but also to solids and suspensions. In this presentation the basic principles of TRLFS are explained and an example of application from the field of toxicology of trivalent actinides is given.

If actinides are accidentally released into the environment, they can cause a serious health risk upon incorporation into bodily tissues. Since they have no essential function in the human body little is known about the biochemistry of actinides in man. To allow the development of potential decontamination therapies, a detailed understanding of the mechanisms of relevant biochemical reactions is required [2]. The chemistry of actinides in aqueous systems at physiological conditions ($\text{pH} \sim 7.4$) is dominated by the formation of complexes with available organic and inorganic ligands (OH^- , CO_3^{2-} etc.). Blood serum proteins have a high affinity towards various metal ions and thus might have a significant impact on the biochemical behavior of incorporated actinides [3]. One representative of utmost importance is the human serum protein “transferrin”. Transferrin is an iron carrier protein in blood with a molecular mass of 79570 Da consisting of a glycopolypeptide of 679 amino acids. The ternary structure of transferrin is characterized by folding into two similar lobes which are joined by a short peptide chain. Each lobe consists of two domains separated by a cleft housing the metal binding site for Fe(III). In both lobes Fe(III) is coordinated by two tyrosines, one aspartate, one histidine and the synergistic anion carbonate in a distorted octahedral geometry [4].

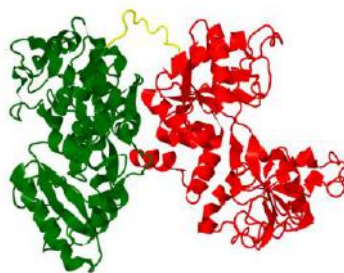


Fig. 1: 3D structure of human serum transferrin with N-lobe (green) and C-lobe (red). Each lobe houses one metal binding site.

Coordination of Fe(III) at the binding site leads to a conformational change of transferrin from an open to a closed form. This structural change stabilizes the transferrin metal ion complex and is important for the recognition of the metal ion transferrin complex by the receptor. In blood, transferrin is about 30% saturated with iron. Consequently, non-saturated transferrin is available for the complexation of other metal ions including actinides in different oxidation states. In the present work we study the complexation of Cm(III) with human serum transferrin in the pH range from 3.5 to 11.0 using time-resolved laser fluorescence spectroscopy (TRLFS). The fluorescence spectra are shown in Fig. 2 a. At $\text{pH} \geq 7.4$ Cm(III) is incorporated at the Fe(III) binding site of transferrin (see Fig 2 b), whereas at lower pH a nonspecific Cm(III) transferrin species

is formed. These results are confirmed by fluorescence life time measurements of the Cm(III) transferrin species and EXAFS investigations using Am(III) [5].

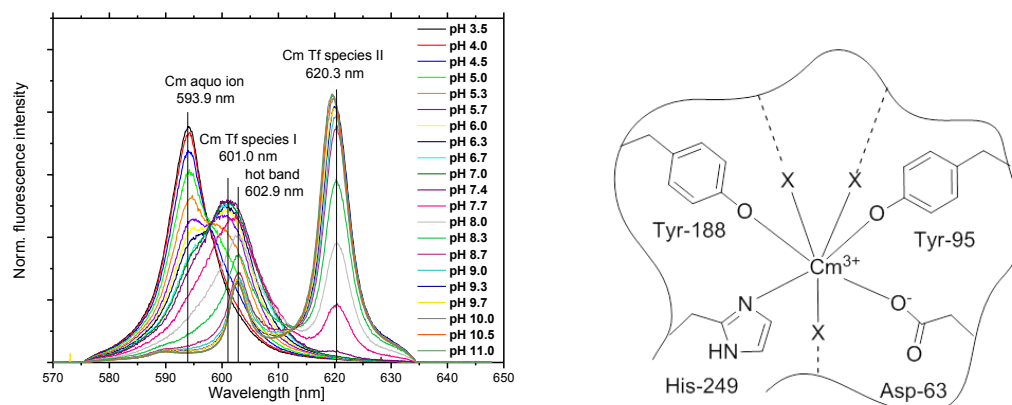


Fig 2: a) Normalized fluorescence emission spectra of the Cm(III) transferrin complexation in the pH range between 3.5 and 11.0 at room temperature. $c(\text{Cm}) = 1 \cdot 10^{-7} \text{ M}$, $c(\text{Tf}) = 5.1 \cdot 10^{-6} \text{ M}$, **b)** Proposed structure of the Cm(III) transferrin species with Cm(III) incorporated at the binding site; X represents additional ligands such as carbonate, bicarbonate and/or hydroxide (the two coordinating water molecules are not shown).

At physiological conditions carbonate acts as a synergistic anion [4]. Carbonate coordinates to Fe(III) in a bidentate mode and is linked to the protein by hydrogen bonding which leads to the formation of a very stable metal Fe(III)–carbonate–transferrin ternary complex. Furthermore, complexation of the synergistic anion reduces the positive charge of the protein which originates from an arginine sidechain and a helix N-terminus directed towards the binding site. This facilitates the coordination of a positively charged metal ion. Thus, we investigate the impact of carbonate concentration on the Cm(III) transferrin complexation using TRLFS. The results show that carbonate complexation of Cm(III) is an important competition reaction repressing Cm(III) transferrin complexation but favors the incorporation of Cm(III) at the Fe(III) binding site at significantly lower pH values [6]. Another important issue discussed in the literature is the difference in complexation strength of the C- and N- lobe of human transferrin. Though the coordinating amino acids are the same for both binding sites, the sites are thermodynamically not equivalent. The stability constants for the N- and C-lobe of Fe_2Tf differ significantly ($\log K_C = 21.4$ and $\log K_N = 20.3$) [7]. Thus, we perform spectroscopic speciation studies of Cm(III) complexation at the N-Lobe using recombinant N-lobe of human serum transferrin und compare them to our previous results obtained for the C-lobe [8]. Furthermore, pH independent stability constants are determined for Cm(III) complexes with both binding sites.

With the presented results we want to illustrate that time-resolved laser fluorescence spectroscopy is a powerful tool to obtain information on the structure of actinide coordination compounds and to quantify complexation reactions even with highly complex ligand systems, such as human serum proteins.

- [1] Edelstein, N.M., Klenze, R., Fanghänel, Th., Hubert, S. 2006 Coord. Chem. Rev., 250, 948-973.
- [2] A. E. V. Gorden, J. D. Xu, K. N. Raymond and P. Durbin, Chem. Rev., 2003, 103, 4207.
- [3] D. M. Taylor, J. Alloys Compd., 1998, 271, 6.
- [4] R. T. A. MacGillivray, S. A. Moore, J. Chen, B. F. Anderson, H. Baker, Y. G. Luo, M. Bewley, C. A. Smith, M. E. P. Murphy, Y. Wang, A. B. Mason, R. C. Woodworth, G. D. Brayer, E. N. Baker, Biochemistry, 1998, 37, 7919.
- [5] Bauer, N., Fröhlich, D. R., Panak, P. J., Dalton Trans. 2014, 43, 6689.
- [6] Bauer, N., Panak, P. J., New J. Chem. 2015, 39, 1375.
- [7] P. Aisen, A. Leibman and J. Zweier, J. Biol. Chem., 1978, 253, 1930
- [8] Bauer, N., Smith, V. C., MacGillivray, R. T. A., Panak, P. J., Dalton Trans. 2015, 44, 1850.

A multi-approach technique to unravel the molecular speciation of tetravalent actinide-diethylenetriaminepentaacetate complex

J. Aupiais ^{*(1)}, L. Bonin ⁽²⁾, C. Den Auwer ⁽³⁾, P. Moisy ⁽²⁾, B. Siberchicot ⁽¹⁾, S. Topin ⁽¹⁾

1) CEA, DAM, DIF, F-91297 Arpajon cedex, (2) CEA, DEN, DRCP, F-30207 Bagnols sur Cèze, (3) Université Nice Sophia Antipolis, Institut de Chimie de Nice, UMR7272, 06108 Nice, France

In case of an accidental nuclear event, contamination of humans by actinide elements may occur. These elements exhibit both a radiological and chemical toxicity that may induce severe damages in target organs (bones, liver, and kidneys). In order to eliminate the actinide elements before they are stored in target organs sequestering agents must be quickly injected. However to date, DTPA (diethylenetriamine-pentaacetic acid) raises current interests for an oral or alternative self-administrable form. Although mostly biokinetics data are available, molecular scale characterization of the actinide-DTPA complexes is still scarce. There is a strong interest for the characterization of An^{IV} -DTPA complexes at the molecular level because it opens the way for predicting stability constants of unknown systems or even for developing new analytical strategies aimed at better and more selective decorporation. For that purpose, investigations by Extended X-ray Absorption Fine Structure (EXAFS) and Ab Initio Molecular Dynamics (AIMD) were undertaken and compared with capillary electrophoresis (CE) used in a very unusual way. It is surprising that the affinity constants reported in the literature for the tetravalent actinides with DTPA are scarce, impeding to emphasize any useful trend. As examples, variation up to 3 orders of magnitude is observed for the same element at $I = 1.0$ M: from 28.8 to 31.8 for U^{IV} -DTPA, from 30.3 to 32.3 for Np^{IV} -DTPA and from 31.4 to 33.67 for Pu^{IV} -DTPA. These differences are too large for properly assessing the behavior of tetravalent actinides in blood. It is therefore crucial to refine data either by determining new brand and more precise values or to accurately evaluate them with an appropriate model. According to the ionic model of chemical bonding (chemical forces are largely of electrostatic type), the bond energy between is governed by the size and charge of the reactant. In the particular case where the same ligand is studied with various metal (e.g. tetravalent actinides), it is expected a relationship in $\frac{Z_M}{d_{M-L}}$, where Z_M is the effective charge of the metal and d_{M-L} the bond distance between the metal M and the ligand L. An example of the separation of An^{IV} -DTPA species is depicted in the Figure 1. Their detection by CE-ICPMS has always shown one peak which results in a fast equilibrium between the formation and the dissociation of the complex. As expected, their migration times are close (but not identical) due to similar charge and size. It is qualitatively observed in all experiments the order of migration $\mu_{PuDTPA} > \mu_{NpDTPA} > \mu_{ThDTPA}$ which follows the decrease of the ionic radius: $r_{Pu} < r_{Np} < r_{Th}$. Under our conditions, U^{IV} DTPA was rarely detected due to almost complete re-oxidation. It resulted in a very small signal for a few experiments with the impossibility to precisely determine the migration time.

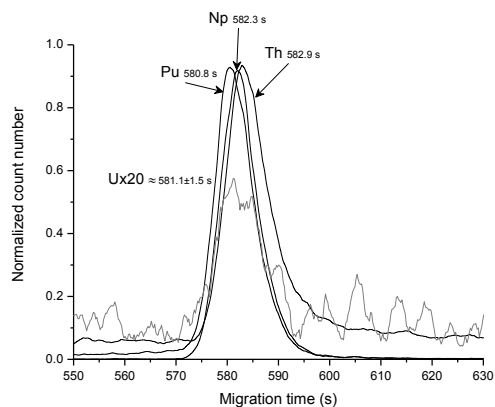


Figure 1 : Electropherograms of An^{IV} -DTPA species. Conditions of separation: $[DTPA] = 10^{-2}$ M, $[An^{4+}] = 10^{-7}$ M, electrolyte support $NaClO_4$ 0.1 M, pH 6.045, $V = 10$ kV, $L = 59.6$ cm, $T = 25$ °C, injection 0.5 psi for 3 s. The signal relative to the U^{IV} has been increased by a factor of 20 due to an almost complete reoxidation and a small affinity of DTPA for U^{VI} .

Due to the hardness character of tetravalent actinide a linear trend is observed between the stability constant and the distance oxygen-metal. The distance An-O can be obtained either by experience (EXAFS) or by simulation (AIMD). The An-O distances agree quite well in both techniques, as depicted in Figure 2.

Cooperative effects of adsorption, reduction, and polymerization observed for hexavalent actinides on the muscovite basal plane

Stefan Hellebrandt^a, Karah E. Knope^{b, †}, Sang Soo Lee^b, Aaron J. Lussier^c, Joanne E. Stubbs^d, Peter J. Eng^d, L. Soderholm^b, Paul Fenter^b, Moritz Schmidt^{*,a}

^aHelmholtz-Zentrum Dresden - Rossendorf, Institute of Resource Ecology, Dresden, Germany

^bChemical Sciences and Engineering Division, Argonne National Laboratory, Argonne, IL, USA

^cDepartment of Civil & Environmental Engineering & Earth Sciences, University of Notre Dame, Notre Dame, IN, USA

^dCenter for Advanced Radiation Sources, University of Chicago, Chicago, IL, USA

[†]Current address: Department of Chemistry, Georgetown University, Washington, DC, USA.

Reliable long-term predictions about the safety of a potential nuclear waste repository must be based on a sound, molecular-level comprehension of the geochemical behavior of the radionuclides. Especially, their reactivity at the water/mineral interface will control their mobility and thus hazard potential.¹ Understanding the geochemical behavior of plutonium has been particularly challenging, due to its multitude of accessible oxidation states and its capability to form nanoparticles or *eigencolloids*. Despite the generally accepted importance of Pu(IV)-nanoparticles for Pu's chemical⁴⁻⁶ and environmental behavior,^{2, 3, 7, 8} the mechanism of their formation is still the subject of ongoing research.⁹ Several previous studies have identified Pu(IV) nanoparticles to be the final state of adsorbed Pu, starting from both higher¹⁰⁻¹² and lower oxidation states,¹³ on both redox active^{10, 12} and redox inactive substrates.^{11, 13} In our own previous work we suggested a mechanism, in which the enhanced concentration of Pu(III) at the interface, in combination with the presence of minor quantities of Pu(IV) in equilibrium, drives the formation of these nanoparticles in an effectively surface-catalyzed reaction.¹³ This mechanism would be independent of Pu's initial oxidation state assuming there is adequate amounts of Pu(IV) present in equilibrium. In order to be able to understand these processes analytical techniques that allow selectively probing the mineral/water interface and elucidating processes at the interface under *in situ* conditions are required. X-ray reflectivity techniques, such as crystal truncation rod (CTR) measurements and resonant anomalous x-ray reflectivity (RAXR) have proven to be valuable tools for geochemical studies concerning reactions in the interfacial regime¹⁴, especially for complex reactions of the actinides.^{13, 15}

To further elucidate the interfacial reactivity of Pu in its various oxidation states, and to test the viability of the mechanisms discussed above for Pu(III), we study the reactivity of hexavalent PuO₂²⁺ at the muscovite (001) basal plane and compare it to the behavior of ostensibly analogous UO₂²⁺ ([Pu] = 0.1 mmol L⁻¹, [U] = 1 mmol L⁻¹, pH = 3.2 ± 0.2, I(NaCl) = 0.1 mol L⁻¹) using resonant anomalous X-ray reflectivity (RAXR) and crystal truncation rods (CTR), as well as grazing-incidence X-ray adsorption near-edge structure (GI-XANES) spectroscopy and alpha spectrometry. The RAXR data indicate that adsorbed Pu has a broad distribution that extends up to 60 Å from the surface. Independent quantification of the adsorption of Pu by alpha spectrometry finds a coverage of 8.3 Pu/A_{UC} (where A_{UC} = 46.72 Å² is the surface unit cell area). The observed broad structure and large coverage cannot be explained by ionic adsorption of PuO₂²⁺, indicating adsorption of Pu(IV)-oxo-nanoparticles. GI-XANES confirms that most Pu at the interface was tetravalent. These observations corroborate a redox-partner independent mechanism for the interfacial formation of Pu(IV)-oxo-nanoparticles put forward previously. Uranium exhibits clearly different behavior. No discernible RAXR signal was detected, indicating no adsorption of UO₂²⁺. GI-XANES and alpha spectrometry also showed very weak signal, in agreement with the RAXR findings, and in the case of GI-XANES indicating predominantly hexavalent U. Our results reveal significant differences between Pu and U in terms of mineral uptake, greatly impacting their geochemical mobility and potentially useful for predicting the fate of these contaminants' in the aqueous environment.

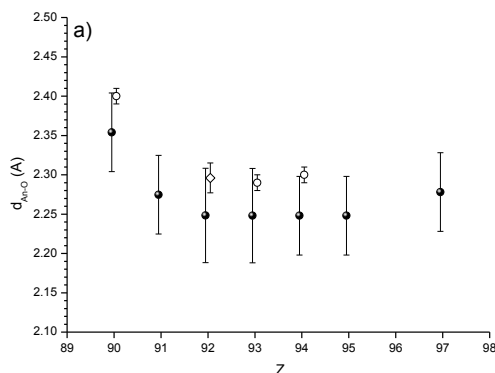


Figure 2: distances An^{IV}-oxygen (a) and An-nitrogen (b) by theoretical method (Ab initio molecular dynamics – AIMD) [●] and experiments (EXAFS [○], and average from thermodynamic+ CE-ICPMS values [◇]).

Since UDTPA was not often detected in several experiments (EXAFS, CE-ICPMS) due to unstable conditions, it was interesting to predict the structure of such complex by calculating the distance U-O in UDTPA⁻ based on calibration between AIMD and experimental parameters (stability constants, electrophoretic mobilities, ionic radii). Results are gathered in the Table 1 that show a good agreement between all independent techniques.

Table 1: distance Uranium – Oxygen interpolated by 3 calibrated methods and ab initio calculation. The distances d_{Th-O} , d_{Np-O} , and d_{Pu-O} used for the linear regressions are obtained by *ab initio* molecular dynamics (AIMD).

Method / linear regression (An=Th, Np, Pu)	d_{U-O} (Å)
Thermodynamic / $\log K = f(d_{An-O})$	
I = 0.5 M	2.28 ± 0.03
I = 1 M	2.29 ± 0.02
I = 1 M	≈ 2.30
EXAFS / $d_{An-O} = f(r_{An}^{4+})^*$	2.33 ± 0.02
CE-ICPMS / $\Delta\mu = f(d_{An-O})$	
I = 0.05 M	2.32 ± 0.05
I = 0.1 M	2.29 ± 0.02
AIMD / no calibration	2.30 ± 0.06

*Coordination Number = 8

The validation of the calibrated methods opens the way to a predictive capability for unknown systems like PaDTPA, AmDTPA and even BkDTPA. The interpolation for Pa has an obvious interest for the future Th-based nuclear power plant developed by India where protactinium chemistry could play an important role in the reprocessing. The extrapolation above Pu may be subject to discussion since Am^{IV}- and Bk^{IV} DTPA compounds are unstable in aqueous solution. However, such calculation may be helpful to extend the observed trend to other solvents like ionic liquids which present larger chemical stability areas. Using data at I = 1.0 M (including U^{IV}), the stability constants can be evaluated for Pa⁴⁺, Am⁴⁺, Bk⁴⁺: $\log K_{PaDTPA} = 31.7$, $\log K_{AmDTPA} = 33.7$, and $\log K_{BkDTPA} = 33.1$.

1. H. Geckeis, J. Lützenkirchen, R. Polly, T. Rabung and M. Schmidt, *Chemical Reviews*, 2013, **113**, 1016-1062.
2. A. B. Kersting, D. W. Efur, D. L. Finnegan, D. J. Rokop, D. K. Smith and J. L. Thompson, *Nature*, 1999, **397**, 56-59.
3. A. P. Novikov, S. N. Kalmykov, S. Utsunomiya, R. C. Ewing, F. Horreard, A. Merkulov, S. B. Clark, V. V. Tkachev and B. F. Myasoedov, *Science*, 2006, **314**, 638-641.
4. L. Soderholm, P. M. Almond, S. Skanthakumar, R. E. Wilson and P. C. Burns, *Angewandte Chemie-International Edition*, 2008, **47**, 298-302.
5. K. E. Knope and L. Soderholm, *Chemical Reviews*, 2012, **113**, 944-994.
6. V. Neck, M. Altmaier and T. Fanghänel, *Comptes Rendus Chimie*, 2007, **10**, 959-977.
7. R. J. Silva and H. Nitsche, *Radiochimica Acta*, 1995, **70/71**, 377-396.
8. A. B. Kersting, *Inorganic Chemistry*, 2013, **52**, 3533-3546.
9. C. Walther and M. A. Denecke, *Chemical Reviews*, 2013, **113**, 995-1015.
10. R. Kirsch, D. Fellhauer, M. Altmaier, V. Neck, A. Rossberg, T. Fanghänel, L. Charlet and A. C. Scheinost, *Environmental Science & Technology*, 2011, **45**, 7267-7274.
11. A. E. Hixon, Y. Arai and B. A. Powell, *Journal of Colloid and Interface Science*, 2013, **403**, 105-112.
12. A. E. Hixon and B. A. Powell, *Environmental Science & Technology*, 2014, **48**, 9255-9262.
13. M. Schmidt, S. S. Lee, R. E. Wilson, K. E. Knope, F. Bellucci, P. J. Eng, J. E. Stubbs, L. Soderholm and P. Fenter, *Environmental Science & Technology*, 2013, **47**, 14178-14184.
14. P. Fenter, *Reviews in Mineralogy and Geochemistry*, 2002, **49**, 149-220.
15. M. Schmidt, S. Hellebrandt, K. E. Knope, S. S. Lee, J. E. Stubbs, P. J. Eng, L. Soderholm and P. Fenter, *Geochimica et Cosmochimica Acta*, 2015, **165**, 280-293.

**Spectroscopy of actinides in natural seawater and further uptake by model marine specimen
*Aplysina cavernicola***

M. Maloubier¹, M. R. Beccia¹, M. Matara Aho^{1,2}, M. Monfort³, P. L. Solari⁴, D. K. Shuh⁵, S. Minasian⁵, H. Michel¹, M. Y. Dechraoui Bottein⁶, P. Moisy⁷, C. Moulin³, C. Den Auwer¹

¹University Nice Sophia Antipolis, Institut de Chimie de Nice UMR7272, 06108 Nice, France

²Laboratory of Radiochemistry, University of Helsinki, Finland

³Commissariat à l'Energie Atomique, DAM/DIF/DASE 91297 Arpajon, France

⁴Synchrotron SOLEIL, MARS beam line, 91192 Gif sur Yvette, France

⁵Chemical Sciences Division, Lawrence Berkeley National Laboratory, Berkeley, CA, USA

⁶IAEA, Environment Laboratory, 4 Quai Antoine 1er, MC-98000, Monaco

⁷Commissariat à l'Energie Atomique, DEN/DRCP 30207 Bagnols sur Cèze, France

What happens to natural radionuclides or those resulting from nuclear activity in the environment, particularly in sea water, is a social and scientific issue.¹ The magnitude 9.0 Tohoku-oki earthquake and subsequent tsunami forced the shutdown of the Fukushima Daiichi Nuclear Power Plant, leading to accidents in three reactors and resulting in release of radionuclides into the environment is one of the latest examples.² Hence, the need in managing the risk, controlling environmental fate and transport, and preventing human exposure through direct contact and indirectly through the food chain is essential. Among the different environmental matrices, seawater has not been extensively studied although it contains traces of radionuclides from previous atmospheric nuclear tests or accidental releases. It is also the ultimate receptacle of rivers containing radionuclides at trace levels. The latest event of the Fukushima accident has dramatically demonstrated that seawater might be of first major concern due to the potential impact of numerous radionuclides present within the reactors. This question is even more crucial given that very few studies have been carried out on this subject. It is therefore of crucial importance to attempt to perform direct determination of the physico-chemical species or speciation of these elements in the various compartments of the biosphere and especially in seawater.³

We will address in the first part of this presentation the speciation of uranium (under the $\{U(VI)O_2^{2+}\}$ form), neptunium (under the $\{Np(V)O_2^+\}$ form), thorium (under the form Th^{4+}) and americium (under the Am^{3+} form) together with Eu^{3+} (as a non radioactive surrogate) with a combination of Extended X-ray Absorption Fine Structure (EXAFS), Time-Resolved Laser-Induced Fluorescence (TRLIF) and speciation modeling using the JCHESS code. Given the available sensitivities of both TRLIF and EXAFS spectroscopic probes we have decided to work at a doping concentration of $[Th, U, Np, Am, Eu] = 5 \cdot 10^{-5} M$ ($10^{-5} M$ was also performed).^{4,5} This value is most probably not representative of the amount, which can be released, in accidental cases but it is a compromise between our lowest workable concentration for EXAFS acquisition and the less intrusive doping concentration. Indeed, at $5 \cdot 10^{-5} M$ actinide concentrations are still below the main ion concentrations (in particular carbonates). Figure 1 shows the adjusted EXAFS spectra at the L_{III} and L_{II} edges of uranium and neptunium respectively (for Np, the presence of bromine in seawater precludes the use of L_{III} edge). For uranium(VI), comparison between the theoretical speciation using JCHESS and the spectroscopic data (TRLIF and EXAFS) lead to unambiguously identify the $Ca_2UO_2(CO_3)_3$ complex as the main uranium species in doped seawater at $[U(VI)] = 5 \cdot 10^{-5} M$. Interestingly, the spectroscopic data on doped seawater obtained in this work are in very good agreement with previous work on natural water from a different matrix for which the predominant species was determined to be the $Ca_2UO_2(CO_3)_3$ complex, although the presence of the ternary $Mg-UO_2-CO_3$ complex has also been reported lately.⁶ For neptunium(V), EXAFS data indicate the presence of at least one carbonate ligand but a mixing cannot be precluded. Indeed according to the speciation calculation, neptunium should be present in two forms in approximately equal amounts : the $Np(V)$ aquo ion and the monocarbonato complex. Using a specific design for diluted samples, EXAFS data have been obtained at $10^{-5} M$ (which is only three order of magnitude higher than uranium

natural concentration) and similar results have been obtained. For americium, the theoretical speciation predicts a monocarbonato species and the analysis of the EXAFS data confirms this speciation with a monodentate carbonate ligand. Similar work has been performed on neptunyl and uranyl cations at the same doping concentration ($5 \cdot 10^{-5}$ M) but also at a lower concentration (10^{-5} M). An attempt at concentration 10^{-6} M for a doped neptunium seawater solution has also been performed and a XANES spectrum has been obtained.

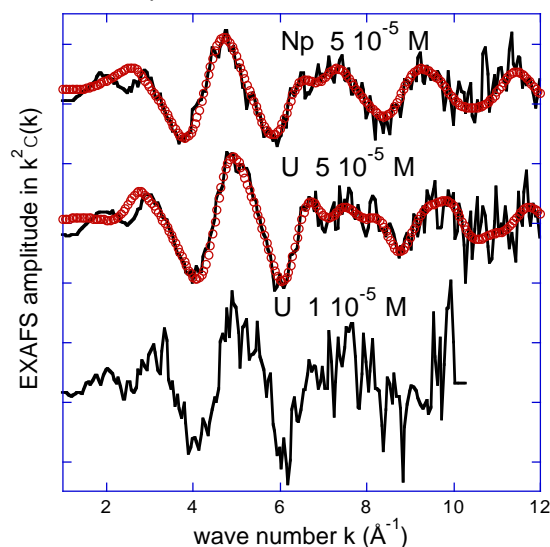


Figure 1 : Experimental and adjusted EXAFS spectra at the L_{III} and L_{II} edges of uranium and neptunium respectively in doped seawater at two different concentrations.

These data confirm the role of carbonates in seawater and the importance of the speciation to understand the behavior of radionuclides in complex natural media, in particular seawater.

The bioaccumulation of stable inorganic contaminants (often referred to as "heavy metals") has already been described in occurrence with organisms from all trophic levels such as algae, mussels, fish and sponges. Some studies have also shown that actinides present in seawater can be strongly accumulated by some marine organisms without knowing their speciation.⁷ Among these organisms, sponges are immobile active filter feeders and have been identified as hyper accumulators of many heavy metals. We will report in the second part of the presentation on the accumulation mechanism of Eu^{3+} and Am^{3+} in the Mediterranean sponge *Aplysina cavernicola*. Europium(III) was targeted for this study as a representative of the trivalent actinides such as americium or curium, as well as plutonium(III) which is poorly understood but an important chemical form of plutonium under strong reducing conditions. Lanthanides are often taken as non-radioactive surrogates of the heavier actinide elements that are easier to manipulate, while retaining many of the same physico-chemical properties observed for actinides in the second half of the actinide series. First, the uptake curve of sponge *A. cavernicola* with a cocktail of radiotracer ^{152}Eu and stable $^{151,153}\text{Eu}$ in seawater was recorded, reaching concentration factors between 1600 and 2100. Second, the global speciation of europium within the sponge was investigated using both TRLIFS and XANES (Eu L_{III} edge) probes.

¹ Maher, K. et al., G., et al., Inorg. Chem. (2013) **52**, 3510 .

² Le Petit, G., et al., Pure and Applied Geophysics, (2014) **171**, 629.

³ Choppin, G.R., Marine Chemistry, (2006) **99**, 83.

⁴ Maloubier M. et al., Dalton Trans. (2015) **44**, 20584.

⁵ Maloubier M. et al., Dalton Trans. (2015), **44**, 5417.

⁶ Endrizzi, F. et al., Chemistry, a European Journal (2014) **20**, 14499

⁷ Stewart, G.M., et al., U-Th series nuclides in aquatic systems (2008) **13**, 269

POSTER SESSION I
CHEMISTRY OF THE NUCLEAR FUEL CYCLE

Reactive diffusive transport of strontium in Czech compacted bentonite

*Lucie Baborová, Dušan Vopálka, Aleš Vetešník

¹Czech Technical University in Prague, Faculty of Nuclear Sciences and Physical Engineering, Dpt. of Nuclear Chemistry, Břehová 7, Prague, 16000

*Email address: Lucie.Baborova@jfifi.cvut.cz

This work is aimed at the reactive transport of radionuclides in the compacted bentonite that is considered as a barrier material in the Czech concept of geological repository of radioactive waste. The material selected was non-activated bentonite of Czech origin, in which the diffusion of interacting Sr was studied with the use of ^{85}Sr as a tracer. Diffusion experiments were carried out on plugs of compacted bentonite in diffusion cells, described by Gondolli and Vecernik [1]. During the diffusion experiments, in which relatively small volumes of working reservoirs were used (160 mL), it was not necessary to correct the concentration in reservoirs, as own code for evaluation of experimental results respects the time dependant change of radionuclide concentration in the inlet and outlet reservoirs. The code *Diffnelin2* prepared in the GoldSim environment [2], outputs of which are time dependent concentrations in both inlet and outlet reservoirs and the concentration profile in the layer of compacted bentonite in the time of termination of an experiment, is further able to eliminate the concentration drops in separating filters and to take into account linear and non-linear (Freundlich and Langmuir) form of sorption isotherm. The great precedence of the use of the code for the evaluation of diffusion experiments is its ability to obtain necessary characteristics of the diffusion transport also for experiments in which the stationary state was not reached.

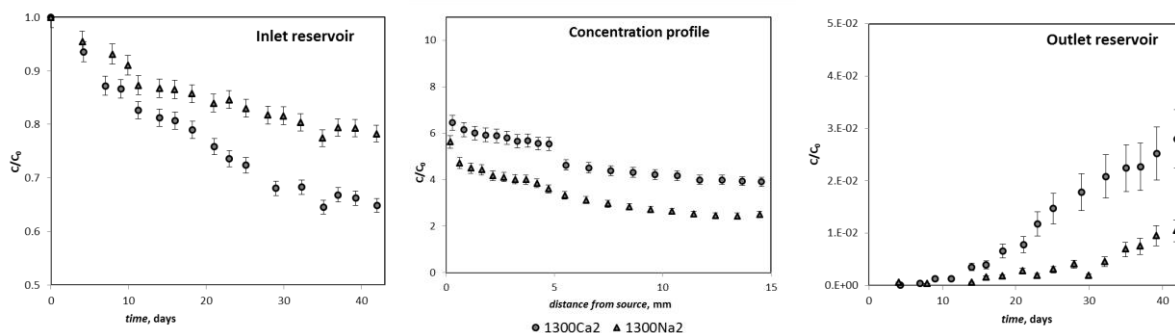


Figure 3: Relative concentration change of Sr in the inlet reservoir (left) and outlet reservoir (right) of diffusion cell and Sr concentration profile in bentonite plug after 42 days (center) for experiments with bentonite BaM in the bulk density of 1300 kg/m^3 , Sr initial concentration $10^{-3} \text{ mol}\cdot\text{L}^{-1}$ and two types of background electrolyte (CaCl_2 $0.033 \text{ mol}\cdot\text{L}^{-1}$ and NaCl $0.1 \text{ mol}\cdot\text{L}^{-1}$)

In our experimental study with plugs of compacted bentonite BaM of the width of 15 mm, duration of diffusion experiments was from 21 up to 42 days and the initial concentration of Sr (non-active SrCl_2 spiked with ^{85}Sr as a radioactive tracer) was from 10^{-5} to $10^{-3} \text{ mol}\cdot\text{L}^{-1}$. It was found out that for both compactions used (1300 and 1600 $\text{kg}\cdot\text{m}^{-3}$) steady state was not reached. During the contact time, liquid samples of 2 mL were withdrawn from both working reservoirs in regular intervals, activity of ^{85}Sr was measured and samples were returned into the reservoirs. After the experiment termination, bentonite plug was pushed out of the diffusion cell and cut into thin slices, which were dried and measured with 3 mL of distilled water in the same manner as liquid samples. Data from two selected experiments which lasted 42 days are shown in Figure 1. Obtained experimental data were evaluated by multiparametric regression of two parameters of transport equation in *Diffnelin2* module, in which distribution coefficient K_d and geometric factor G were determined. Based on these values, apparent diffusion coefficient D_a and effective diffusion coefficient D_e were calculated according to equations used in this field (i.e. by Shackelford and Moore [3]). Obtained sorption and diffusion parameters are summarized in Table 1. The results

indicate that the diffusion transport is slower and the sorption in the layer of compacted bentonite is lower when NaCl ($0.1 \text{ mol}\cdot\text{L}^{-1}$) is used as the background electrolyte, in comparison with CaCl_2 ($0.033 \text{ mol}\cdot\text{L}^{-1}$) as the background electrolyte. This difference may be caused by higher swelling of Na bentonite which closes a part of pores. Supplementary batch sorption experiments were simultaneously performed which did not predict such behaviour. Preliminary results further indicate concentration dependence of Sr migration in compacted bentonite in the selected concentration range ($10^{-3} - 10^{-5} \text{ mol}\cdot\text{L}^{-1}$).

Table 1: Summary of diffusion experiments conditions and resulting diffusion parameters

Cell code	Background electrolyte	Sr initial concentration [$\text{mol}\cdot\text{L}^{-1}$]	Contact time [days]	Bulk density [$\text{kg}\cdot\text{m}^{-3}$]	Porosity ϵ [-]	Geometric factor G [-]	K_d [$\text{L}\cdot\text{kg}^{-1}$]	D_a [$10^{-11} \text{ m}^2\cdot\text{s}^{-1}$]	D_e [$10^{-10} \text{ m}^2\cdot\text{s}^{-1}$]
1300Ca1	CaCl_2	1E-03	21	1287	0.561	0.568	7.7	4.82	5.04
1600Ca1	CaCl_2	1E-03	21	1586	0.459	0.328	5.5	2.60	2.38
1300Ca2	CaCl_2	1E-03	42	1293	0.559	1.061	10.9	6.38	9.38
1300Ca3	CaCl_2	1E-05	21	1286	0.561	0.335	4.7	4.50	2.97
1600Ca3	CaCl_2	1E-05	21	1583	0.460	0.226	4.9	2.01	1.65
1300Na1	NaCl	1E-03	21	1292	0.559	0.156	2.9	3.20	1.38
1600Na1	NaCl	1E-03	21	1596	0.455	0.129	2.9	1.81	0.93
1300Na2	NaCl	1E-03	42	1288	0.560	0.578	6.1	6.11	5.12
1300Na3	NaCl	1E-05	21	1287	0.561	0.143	4.0	2.20	1.27
1600Na3	NaCl	1E-05	21	1585	0.459	0.209	6.4	1.43	1.52

However, it must be noted that the uncertainty of diffusion parameters resulting from this type of experiment is relatively high ($>10\%$) and it is given by material heterogeneity, experimental uncertainty and by uncertainty connected with the multiparametric regression during the data evaluation. Despite this fact, this method is a valuable tool which significantly reduces time required for diffusion data acquisition. In general, this work contributes to the understanding of transport processes in bentonite barrier of geological repository with respect to the conditions of Czech concept and helps to evaluate local materials. Development of experimental and modelling methodologies is an important part of the scientific support for the geological repository concept advancement.

- [1] Gondolli, J. and Vecernik, P. The uncertainties associated with the application of through-diffusion, the steady-state method: a case study of strontium diffusion. *Geological Society, London, Special Publications*. 2014. Pp. 603-612.
- [2] Golder Associates. GoldSim Contaminant Transport Module, Manual, Version 1.30. *GoldSim Technology Group, Redmond, Washington*. 2002. 285 p.
- [3] Shackelford, C.D. and Moore, S.M. Fickian diffusion of radionuclides for engineered containment barriers: Diffusion coefficients, porosities, and complicating issues. *Engineering Geology* 152. 2013. Pp. 133–147.

Chemistry of technetium under repository-relevant conditions:
solubility and carbonate complexation of Tc(IV)

A. Baumann*, E. Yalcintas, X. Gaona, R. Polly, M. Altmaier, H. Geckeis

Institute for Nuclear Waste Disposal (INE), Karlsruhe Institute of Technology (KIT), Karlsruhe, Germany

Technetium-99 is one of the main fission products of ^{235}U and ^{239}Pu in nuclear reactors. Due to its long half-life ($2.1 \cdot 10^5$ a) and redox-sensitive character, ^{99}Tc is a very relevant radionuclide in the safety assessment of repositories for radioactive waste disposal. Tc(VII) is the prevailing oxidation state under oxidizing and redox-neutral conditions and exists as soluble and mobile TcO_4^- . On the contrary, Tc(IV) forms sparingly soluble hydrous oxides ($\text{TcO}_2 \cdot x\text{H}_2\text{O}(\text{s})$) under reducing conditions as those expected in deep underground repositories. Carbonate on the other hand is a relevant component in the pore water of clay and crystalline systems and is known to form strong complexes with metal cations, potentially contributing to the mobilization of radionuclides into the biosphere. In this context, an appropriate understanding of the Tc(IV) solubility and aqueous speciation in alkaline carbonate-containing solutions will provide key inputs for assessing the behaviour of Tc in underground repositories for radioactive waste disposal. The solubility and carbonate complexation of Tc(IV) was investigated in carbonate-containing solutions of varying ionic strength ($I = 0.5 - 5.0$ M) and at different pH_m ($-\log[\text{H}^+] = 8.5 - 14.5$). The experiments were split in three independent series. One series at constant ionic strength $I = 5.0$ M ($\text{NaCl}-\text{NaHCO}_3-\text{Na}_2\text{CO}_3$) with total carbonate concentration ($C_\text{tot} = [\text{HCO}_3^-] + [\text{CO}_3^{2-}]$) $0.01 \text{ M} \leq C_\text{tot} \leq 0.5 \text{ M}$ and $8.5 \leq \text{pH}_\text{m} \leq 12.0$, one series at constant $C_\text{tot} = 0.1 \text{ M}$, $0.5 \text{ M} \leq I \leq 5.0 \text{ M}$ ($\text{NaCl}-\text{NaHCO}_3-\text{Na}_2\text{CO}_3$) and $8.5 \leq \text{pH}_\text{m} \leq 12.0$, and one final series at constant $C_\text{tot} = 0.1, 0.5$ and 1.0 M with $0.01 \text{ M} \leq [\text{NaOH}] \leq 0.6 \text{ M}$ (in the absence of NaCl). SnCl_2 was used as reducing agent to ensure that Tc both as solid and in solution remains in oxidation state +IV. $[\text{Tc}]$, pH_m and E_h were monitored at regular time intervals. After attaining equilibrium conditions, solid phase characterization of selected batch experiments was performed by XRD, SEM-EDS and quantitative chemical analysis. Redox speciation of Tc in the aqueous phase was quantified for selected samples using solvent extraction with TPPC. In all investigated samples, a strong effect of carbonate was observed, leading to up to 2 orders of magnitude greater solubility than in carbonate-free systems. This increase can be explained by the formation of the $\text{TcCO}_3(\text{OH})_2(\text{aq})$ and $\text{TcCO}_3(\text{OH})_3^-$ species reported in literature, although thermodynamic calculations based on the available data for these species significantly underestimates the experimental data obtained in the present study^{[1][2][3]}. The increase of ionic strength has a minor impact on Tc(IV) solubility in the presence of carbonate. This observation is attributed to the low charge of the ternary species forming in solution ($\text{TcCO}_3(\text{OH})_2(\text{aq})$ and $\text{TcCO}_3(\text{OH})_3^-$) and consequently rather weak ion-interaction processes. Strong kinetics are observed in the experimental data obtained in the hyper alkaline pH region, although equilibrium data hint towards the formation of a new carbonate species not reported so far ($\text{TcCO}_3(\text{OH})_4^{2-}$). The formation and stability of this species is further investigated and supported by DFT calculations performed in the gas phase, with the Conductor-like Screening Model (COSMO) as a continuum solvation model and a simulated aqueous system consisting of a water cluster with 100 water molecules. The systematic and very comprehensive solubility dataset obtained for Tc(IV) in alkaline carbonate-containing solutions allows deriving accurate chemical, thermodynamic and activity (SIT) models for the system $\text{Tc}^{4+}-\text{H}^+-\text{Na}^+-\text{CO}_3^{2-}-\text{HCO}_3^--\text{OH}^--\text{Cl}^--\text{H}_2\text{O}(\text{l})$. These models are highly relevant in geochemical calculations and for the estimation of reliable Tc(IV) source term concentrations in the context of safety assessments for nuclear waste repositories.

1. T.E. Eriksen, P. Ndalamba, J. Bruno, M. Caceci, *The Solubility of $\text{TcO}_2 \cdot n\text{H}_2\text{O}$ in Neutral to Alkaline Solutions under Constant p_{CO_2}* , *Radiochimica Acta* **58/59**, **1992**, 67-70.
2. I. Alliot, C. Alliot, P. Vitorge, M. Fattahi, *Speciation of Technetium(IV) in Bicarbonate Media*, *Environ. Sci. Technol.* **43**, **2009**, 9174-9182.
3. R. Guillaumont, T. Fanghänel, J. Fuger, I. Grenthe, V. Neck, D.A. Palmer, M.H. Rand, *Update on the Chemical Thermodynamics of U, Np, Pu, Am and Tc*, Vol.5 of *Chemical Thermodynamics*, Elsevier, Amsterdam, **2003**.

Neptunium(V) uptake by granitic rock and bentonite colloids and the influence of colloids on Np(V) transport

O. Elo¹, N. Huittinen² and P. Hölttä¹

[1] Laboratory of Radiochemistry, Department of Chemistry, 00014 University of Helsinki, Finland

[2] Helmholtz Zentrum Dresden-Rossendorf, 01328 Dresden, Germany

In Finland, the spent nuclear fuel (SNF) is going to be buried 500 meters beneath the surface in the crystalline granitic bedrock in Olkiluoto following the SKB-3V concept. The natural geological barrier, the bedrock itself, and the engineered barrier systems (EBS), consisting of a solid fuel capsule, a copper container and the bentonite buffer should prevent the migration of radionuclides to the biosphere. As other aluminosilicates, the bentonite buffer is known to retain radionuclides, thus, preventing them from migrating from the repository with the groundwater. Stable and mobile bentonite colloids can, however, form from the EBS when the meltwater dilutes the ground water after a possible glacial period. In these mildly oxidic conditions neptunium is in its pentavalent state as NpO_2^+ , which is a highly mobile and poorly sorbing cation. Due to the long half-life of neptunium-237 (2.144×10^6 a), it will be a major dose contributor after 100 000 years in the SNF repository. By batch sorption and column experiments, this study aimed at investigating the two processes: retardation of Np(V) on the bentonite colloids and granitic rock under stagnant conditions, and the effect of the stable and mobile bentonite colloids on the migration of Np(V) in intact and crushed granitic rock columns under flowing water conditions.

The materials used in this study were bentonite colloids prepared from MX-80 bentonite, and Kuru Gray granitic rock. Np(V) sorption on these materials under stagnant conditions was studied as a function of pH, solid concentration, time and Np(V) concentration. The sorption experiments as a function of pH (5 – 11), were performed at a constant Np(V) concentration of 10^{-6} M. The sorption isotherms, as a function of Np(V) concentration, were conducted at concentration from 10^{-9} to 5×10^{-6} M at pH 8, 9 and 10. All the batch sorption studies were conducted in 10 mM NaClO_4 either in N_2 -atmosphere (bentonite colloids) or in normal atmosphere (granitic rock). The batch sorption results for Np(V) sorption on colloids and crushed granite as a function of pH are presented in Fig 1.

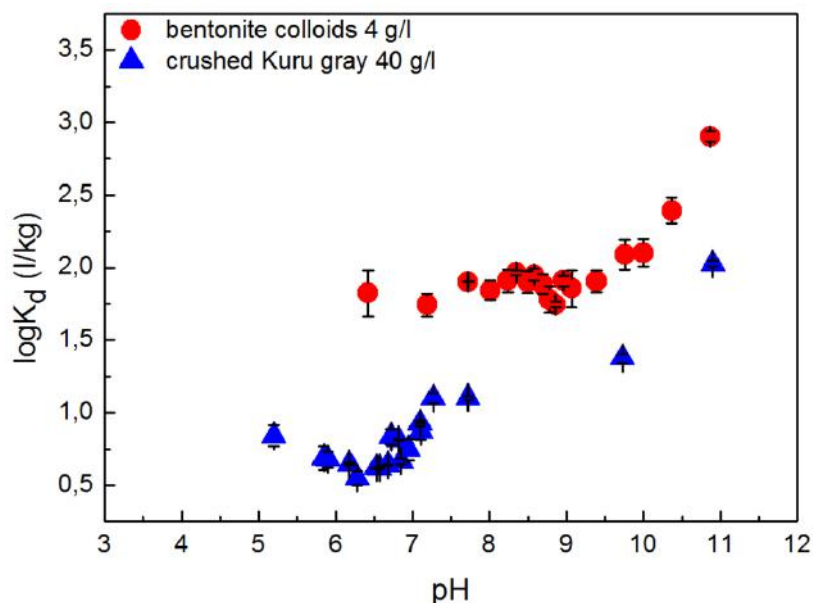


Figure 1. Np(V) ($c = 10^{-6}$ M) sorption onto bentonite colloids (red symbols) and crushed granite (blue symbols) in 10 mM NaClO_4 as a function of pH.

The effect of bentonite colloids on Np(V) migration was studied under flowing water conditions in column experiments^[1], where the solid column material was either crushed granite or an intact drill core of the Kuru Gray granite. For both columns two different flow rates were used: 1.5 ml/h and 0.3 ml/h for drill core column, and 0.8 ml/h and 0.3 ml/h for crushed granite column. The tracer was injected into the flow through an injection loop of known volume. The colloid concentration was determined by photon correlation spectroscopy (PCS) and standard series, and the Np(V) concentration was determined after PCS measurements by a liquid scintillation counter. The Np(V) and colloid break-through curves are presented in Fig 2.

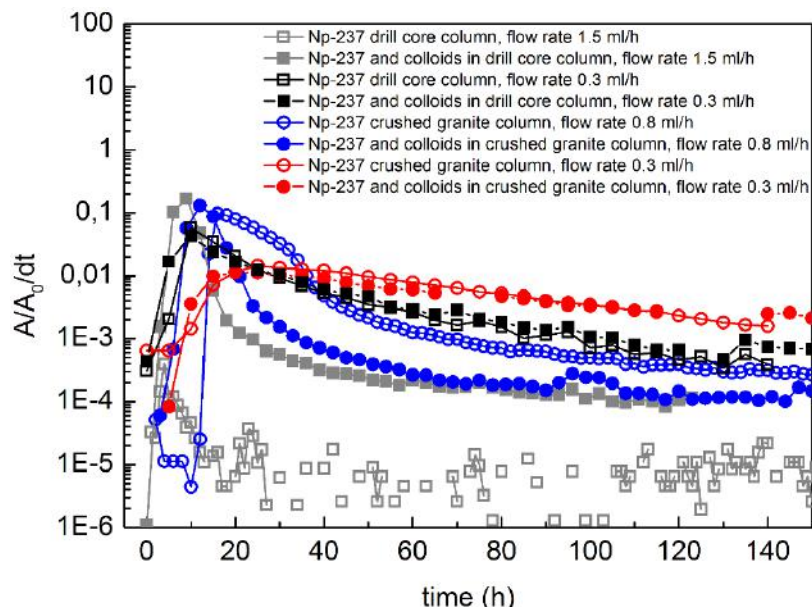


Figure 2. The break through curves of Np(V) through drill core (grey and black symbols) and crushed granite (blue and red symbols) columns with flow rates 1.5 ml/h and 0.3 ml/h for drill core and 0.8 ml/h and 0.3 ml/h for crushed column. Open symbols in the absence and closed symbols in the presence of colloids.

At pH 8, which is expected to be the prevailing pH in the deep geosphere in Olkiluoto, bentonite colloids show a rather poor uptake of Np(V) (Fig 1). In addition, Np(V) is not retained on the crushed granite (Fig 1) indicating that Np(V) will be mobilized as a neptunyl cation in the solution. The weak sorption capacity of the bentonite colloids could indicate that the mobility of them does not enhance the migration of Np(V). However, the obtained results from crushed granite Kuru gray columns under fast flow conditions (Fig 2, blue symbols) show that Np(V) is eluted from the column faster in the presence of colloids. Thus, the results under these flow conditions are not in agreement with the observation under slower flow conditions where the results indicate that the bentonite colloids are not affecting the migration of Np(V) (Fig 2, red and black symbols). These results are not sufficient to verify whether the bentonite colloids are enhancing the migration of Np(V). Therefore, column experiments at higher pH and slower flow rates in combination with additional batch sorption studies are required.

[1] P. Hölttä, A. Poteri, M. Siitari-Kauppi and N. Huittinen (2008). Phys. Chem. Earth 33, 983 – 990.

Trace element variation in concrete coarse aggregate - implications to the decommissioning waste inventory, case Loviisa nuclear power plant

Tapani Eurajoki

Fortum Power and Heat Oy, PL 100, FI-00048 FORTUM, Finland

Introduction

Due to the gamma and neutron radiation from the reactor core, the reactor pressure vessels of nuclear power plants (NPPs) are surrounded with massive concrete structures. The concrete around the pressure vessel is exposed to neutron radiation, resulting in activation of concrete aggregate and cement. The Loviisa NPP with two VVER-440 units was constructed in the 1970s. For the concrete structures, aggregate was taken from local gravel extraction sites in the Wiborg rapakivi granite batholith. According to the decommissioning plan of the Loviisa NPP [1], the waste resulting from activated concrete is estimated to amount over 600 tonnes. The trace element concentrations in the concrete were not measured during construction. Those parts of the concrete structure which are exposed to the highest neutron fluence, are not practically accessible for sampling or activity measurements. Trace element contents in concrete specimens have been determined at a different location of the same structure [2]. In this paper, the study focuses on the distribution of the trace elements in different rocks types found in the coarse aggregate in sample taken from another location.

Factors affecting the neutron flux and activation of concrete

The majority of the activity in concrete under neutron irradiation is induced by thermal or epithermal neutrons. Inside a concrete structure the neutron flux depends on the fast flux entering the concrete as well as the thermalization and absorption properties of the concrete. Hydrogen content in concrete is a key issue in thermalization of fast neutrons, due to its large scattering cross section. In concrete, hydrogen can exist in some aggregates, but in case of many typical aggregates, including granite, it is found in the cement paste, mostly as chemically bound water. In addition to the hydrogen content, the thermal neutron flux density is determined by the thermal absorption cross section of concrete. Typically aggregates and cements contain a few trace elements with exceptionally high thermal absorption cross sections. Even though representing only a minor fraction of the mass, they have a significant contribution to the neutron absorption. Some of these elements, such as Eu, Cs, and Co, generate activation products with strong gamma radiation and relatively long half-lives. These activation products determine, how concrete is to be handled and disposed of in the decommissioning of the power plant. On the other hand, not all the isotopes with large absorption cross sections, present in concrete, form such activation products, but may even have a favorable effect to neutron activation, reducing the thermal flux density and thus the inducing activity of the long-lived strong gamma-emitters.

Coarse aggregate in the Loviisa structure

According to a sample taken from the structure of the Loviisa NPP, the coarse aggregate (here defined over 6 mm) consists of three clearly different rock types: wiborgite, red, fine-grained granitic rock, and light grey metamorphic rock. The trace element concentrations for these rock types have been analyzed by Geological Survey of Finland, and the analysis shows clear differences between the rock types. For example the Eu concentration in wiborgite is 30 ppm, whereas in red granite it is only 9 ppm. On the other hand, the concentration of an effective neutron absorber, Gd, is in red granite almost twice the corresponding value in wiborgite (1020 ppm and 590 ppm, respectively). Table 1 presents the products of concentrations and thermal cross sections of a few elements in the three coarse aggregate types. Based on the equations describing the activation reactions, it is possible to derive that assuming the activation induced by thermal neutrons only the resulting activity of an activation

product inside a large concrete structure is proportional to the product given in Table 1 for the target element, and inversely proportional to the sum of the products (the "total" in the table) over all elements in concrete. Hence, if the aggregate consisted only of metamorphic rock, the inducing Co-60 activity would be over tenfold compared to the case of red granite. For Cs and Eu the difference is lower. However, not all the activity is induced by thermal neutrons, but a part of it is due to epithermal neutrons, and that may reduce the difference. Another issue, not discussed in detail here, which may affect the induced activity is the distribution of the trace elements between distinct minerals in the aggregate rock. For example Cs has higher concentrations in biotite than in the rest of the minerals of the analysed rock types.

Table 1. Thermal absorption cross sections (b) multiplied with element concentrations (%) in the main constituents of concrete and in a few elements with high cross sections found in coarse aggregate.

	Wiborgite	Red granite	Grey metamorphic rock
Main constituents of concrete: Si, O, Ca, Al, K, Na, Fe, Mg, C	21	21	21
Co	0.2	0.1	0.5
Cs	1.9	1.1	0.6
Eu	30	9.0	20
B	17	23	43
Sm	72	85	46
Gd	593	1023	206
Total (incl. elements not given in the table)	800	1243	381

Conclusions

As all the three coarse aggregate types originate in the same gravel extraction site, and as their fractions may vary within that site (in fact a comparison with [2] indicates to that), the induced activity inventory of structural concrete remains uncertain, unless the trace element contents of the concrete at the location exposed to neutron radiation are known. In case of the Loviisa NPP, this emphasizes the significance of sampling at the decommissioning phase to validate the calculated results. Regarding new build NPPs, attention should be paid on the aggregate and its trace element contents.

References

1. Kisanlahti, M., Eurajoki, T., Mayer, E., Rämä, T. & Nummi, O. (2012) Decommissioning of the Loviisa NPP, Edition 2012. Fortum Power and Heat Ltd.
2. Ervanne, H., Hakanen, M., Lehto, J., Kvarnström, R. & Eurajoki, T. (2009) Determination of Ca and γ -emitting radionuclides in concrete from a nuclear power plant. *Radiochimica Acta*. 97, p. 631-636.

Effects of bentonite colloids on the radionuclide migration in granitic rock

Pirkko Hölttä, Outi Elo, Valtteri Suorsa, Elina Honkaniemi and Suvi Niemiahö

Laboratory of Radiochemistry, Department of Chemistry, University of Helsinki, Finland

In Finland, the repository for spent nuclear fuel (SNF) will be excavated at a depth of about 500 meters in the fractured crystalline bedrock in Olkiluoto at Eurajoki implemented by Posiva Oy. The bentonite erosion resulting in the formation of colloids may have a direct impact on the overall performance of the bentonite buffer used in the Engineered Barrier System (EBS). The potential relevance of colloids for radionuclide transport is highly dependent on the colloid formation, the stability and mobility of colloids in different chemical environments and their interaction with radionuclides. If colloids are sufficiently stable and mobile, irreversible sorption on colloids may increase radionuclide transport. In this work bentonite colloid stability, radionuclide sorption on bentonite colloids and clay suspension, colloid mobility and the effect of colloids on radionuclide migration were studied.

The materials were MX-80 Volclay type bentonite (76 % montmorillonite), Nanocor PGN Montmorillonite (98 %) and colloid dispersion solutions separated ultrasonically from bentonite powder. Solutions of different ionic strength and pH used in the experiments were low salinity granitic Allard ($I = 4.2 \cdot 10^{-3}$ M) and saline OLSO ($I = 0.517$ M) reference groundwater, diluted OLSO, NaCl and CaCl_2 electrolytes. OLSO simulated the current saline groundwater in Olkiluoto in oxic conditions. In batch type colloid erosion experiments, 1 g of bentonite powder or two pellets were placed in a sample tube where 50 mL of solution was added. The samples were stored for the sampling with and without agitation and the colloidal particle fraction was separated by centrifugation. The colloid generation and stability were followed as a function of time by analysing particle size distribution applying the photon correlation spectroscopy (PCS) and Zeta potential applying the dynamic electrophoretic mobility (Malvern Zetasizer Nano ZS). Colloid concentration was estimated using a standard series made from bentonite colloids and a count rate obtained PCS measurements or by analyzing the aluminum content of montmorillonite using ICP-MS.

The interaction of Sr-85 and Eu-152 with bentonite colloids and clay suspension was investigated as a function of ionic strength and pH. The sorption parameters were determined by conducting batch experiments in a clove box under CO_2 free conditions. In the sorption experiments, mineral or colloid suspension was added to the solution spiked with a tracer, 4.7 mL aliquot were taken after 2 h, 1, 2 and 7 days and solid colloid fraction was separated by ultracentrifugation (90000 rpm/60 min). Sorption was quantified by the determination of the distribution ratio of radionuclide activity between solid and liquid phase. Desorption experiments were done to investigate the reversibility of europium sorption reaction on colloids and montmorillonite. The colloid mobility and radionuclide-colloid migration was studied in the crushed rock, drill core and rock fracture columns.

The bentonite erosion and stability of bentonite colloids depended strongly on the ionic strength of the medium and the valence of the cation. Gentle agitation increased the bentonite erosion significantly. In a long-term erosion experiment, the colloidal dispersion has remained stable in low salinity solutions so far for over five years. Noticeable colloid generation occurred only in the most diluted (1 and 5 mM) solutions and the colloid concentration reached the level where no more colloids were released. Strontium and europium adsorption onto the bentonite colloids and montmorillonite was highly pH dependent, adsorption increasing with increasing pH. K_d -values of Eu-152 for Nanocor PGN Montmorillonite colloids in Allard reference groundwater are shown in Figure 1. In desorption experiments at constant pH 8, almost 60 % of Eu-152 was removed from the Nanocor PGN Montmorillonite colloid solution and suspension after two weeks when the solution was changed every second day (Figure 2).

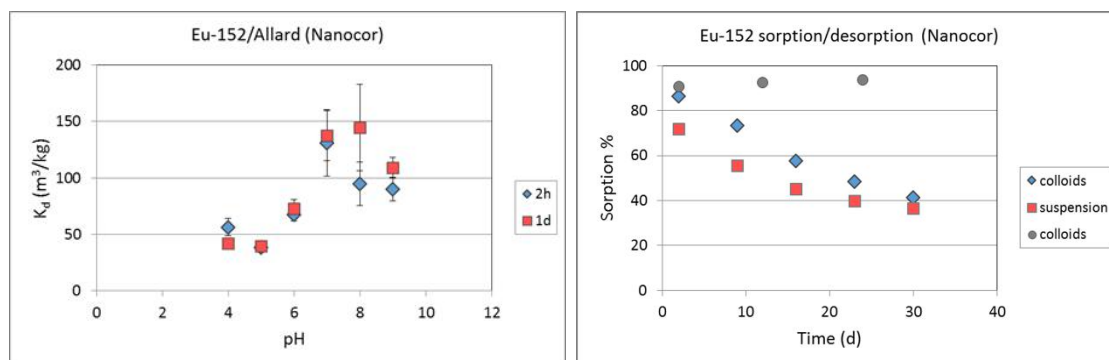


Figure 1. (Left) K_d -values of Eu-152 for Nanocor PGN Montmorillonite (right) colloids in Allard water.

Figure 2. (Right) Eu-152 desorption in Nanocor colloid solution and suspension in Allard water.

Migration of colloids was affected by the rock alteration, the type and length of column, water flow rate and colloid size. The recovery of bentonite colloids shown in Figure 3 was low. Slowing down the water flow rate, the recovery was decreased. In all columns, particularly Eu-152 was strongly retarded but also Sr-85 was retarded without colloids. In the presence of bentonite colloids, the faster elution of Sr-85 was obtained (Figure 4).

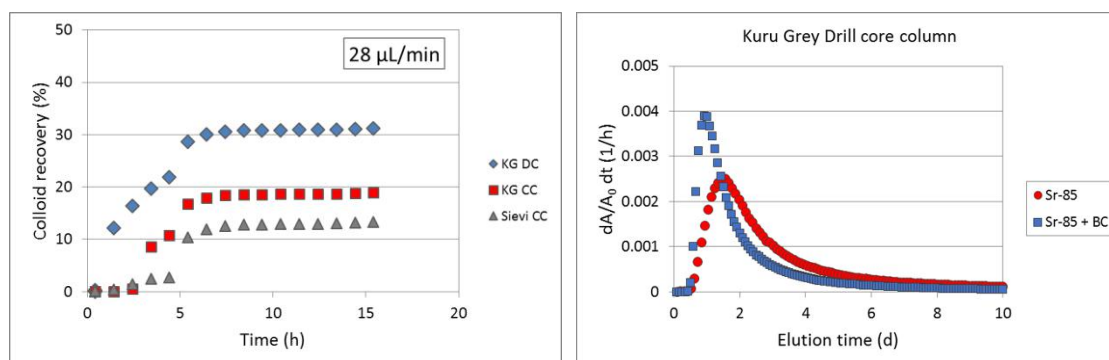


Figure 3. (Left) The colloid recovery in Kuru grey granite drill core column (28 cm) (blue), crushed rock columns (15 cm): Kuru grey (red) and Sievi altered tonalite (grey).

Figure 4. (Right) The elution of Sr-85 through Kuru grey granite drill core column in the absence (red) and presence (blue) of MX-80 bentonite colloids. Allard water flow rate was 10 µL/min.

pH had a great influence on the chemical form of the radionuclides (Eu-152) and thus on their sorption onto colloids. Europium speciation calculations are needed to explain its sorption behaviour. Desorption experiments showed reversible europium sorption on bentonite colloids and mineral surfaces. However, fully reversible sorption was not obtained. Colloid mobility and radionuclide-colloid migration experiments performed in a small laboratory scale, showed that colloids had an effect on radionuclide transport. However, the flow rates in these experiments were orders of magnitudes faster than the groundwater flow. The main uncertainties remain still in the quantification of colloids under realistic repository conditions and how mobile colloids are.

The research leading to these results has received funding from the European Atomic Energy Community's Seventh Framework Programme (FP7/2007-2011) under grant agreement n° 295487. Research has received funding also from Finnish Research Programme on Nuclear Waste Management financed by The State Nuclear Waste Management Fund

The diffusion of tritiated water and chloride through granodiorite

Jussi Ikonen*, Mikko Voutilainen*, Minja Matara-aho*, Marja Siitari-Kauppi*, Andrew Martin**

* *University of Helsinki, Laboratory of Radiochemistry, Department of Chemistry, Helsinki, Finland*

** *Nagra (National Cooperative for the Disposal of Radioactive Waste), Wettingen, Switzerland*

Spent nuclear fuel from Finnish power plants will be disposed of deep in the crystalline bedrock in western Finland. When they are eventually released into the bedrock, radionuclides will be transported by advection along water conducting fractures. Retardation can occur by molecular diffusion from the fractures into the stagnant pore water and/or by immobilisation onto mineral surfaces in the rock matrix. Estimating the transport behaviour of radionuclides in groundwater is important in assessing the risk to health due to radionuclide release at the waste disposal site.

The Swiss National Cooperative for Disposal of Radioactive Waste (Nagra) has been conducting extensive in-situ experiments at the Grimsel test site (GTS) in the field of radionuclide migration and retention in the rock matrix. A second Long Term Diffusion (LTD) experiment executed as an in- and through diffusion test started in spring 2014 using radionuclides HTO, Na-22, Cs-134, Cl-36 and Ba-133 and a nonradioactive selenium isotope.

The aim of this work was to study the diffusion of HTO and Cl-36 in granitic rock in the laboratory to provide data for modelling and to compare the results with those from the in-situ experiment. Grimsel Granodiorite (GG) is homogeneous, medium grained and slightly foliated granodiorite. Porosity is 0.65 % and permeability $(1.3 \pm 0.3) \times 10^{-17} \text{ m}^2$. The effective diffusion coefficients of HTO and Cl-36, which do not interact significantly with the matrix pore walls, were obtained by in- and through diffusion experiments in a GG rock block (length 20 cm and diameter 30 cm, see Fig 1). These kind of block scale experiments are useful for comparing the laboratory results to in-situ experiments because of the similar measurement geometry.



Figure 1. Grimsel Granodiorite rock block used in in- and through diffusion experiment.

The results of block scale diffusion experiments may be challenging to analyse using existing analytical tools since the initial and boundary conditions are not easy to handle due to the geometry of the experimental system and irregularity of the sampling. One possibility to deal with such complexity is to apply Time Domain Diffusion (TDD) method which has been developed for simulating diffusion in heterogeneous media. The method is a time-domain

execution of the random walker and it is a rapid particle-tracking method that makes possible to simulate diffusion in heterogeneous media when the local porosities and diffusion coefficients are set.

The results obtained during over four months experiment in a GG rock block show that 40 % of HTO and 20 % of Cl-36 had diffused into the rock from the injection bore holes. Significant breakthrough of the tracers was detected in the observation hole at 3 cm distance from the injection hole (Fig 2). It was observed that HTO diffuses significantly faster than chloride within the permeable GG matrix. More detailed results with numerical analyses will be provided in the conference presentation.

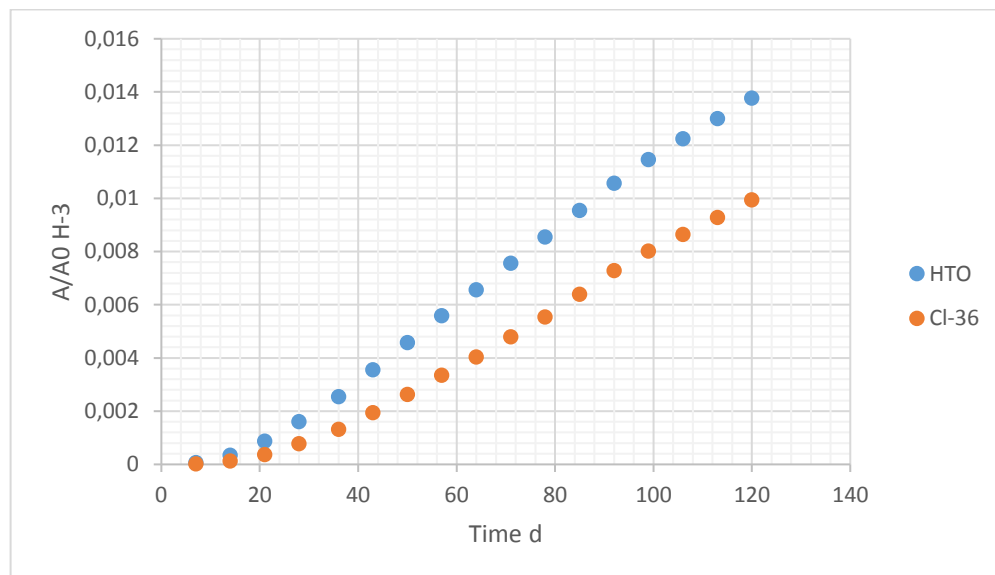


Figure 2. HTO and Cl-36 breakthrough into the observation hole at 3 cm distance from the injection hole in GG rock block.

Tomographic investigation of caesium migration in Olkiluoto veined gneiss and Grimsel granodiorite

J. Kuva⁽¹⁾, M. Voutilainen⁽²⁾, J. Parkkonen⁽¹⁾, T. Turpeinen⁽¹⁾, M. Siitari-Kauppi⁽²⁾, J. Timonen⁽¹⁾

⁽¹⁾ *Department of Physics, University of Jyväskylä, P.O. Box 35, 40014 University of Jyväskylä, Finland*

⁽²⁾ *Laboratory of Radiochemistry, Department of Chemistry, University of Helsinki, Finland*

The Finnish plan for the final disposal of nuclear waste is an underground repository in crystalline bedrock in Olkiluoto. In the safety analysis of the repository, capacity of the bedrock to retard radionuclides if they leak into the groundwater is an important factor. There are still many uncertainties concerning e.g. groundwater transport routes and bedrock porosity, which have caused the present safety analyses to consciously underestimate the retarding capacity of the bedrock. To gain more information on how the heterogeneous microscopic structure affects retardation, we set out to study element intrusion into rock samples with X-Ray microtomography (X μ CT).

For the tracer we wanted to choose an element that is relevant to the safety case, and has a high enough atomic number and density compared to the most common elements in rock minerals to be distinguishable from XCT images. In the safety assessment of the spent nuclear fuel on a long-term basis ¹³⁵Cs is classified as a second (high) priority radionuclide. After the closure of the repository anionic highly mobile elements are expected to be a major dose source for humans. However the importance of ¹³⁵Cs arises from its high content in the spent nuclear fuel and a long physical half-life of 2.3×10^6 years, even though it is considered relatively immobile. Furthermore, caesium has a highly mineral-dependent sorption coefficient, which makes the rock matrix heterogeneous with respect to caesium retardation. The high aqueous solubility of caesium as CsCl also allowed for a high enough concentration for the experiment. There are two on-going in-situ transport experiments (Olkiluoto, Finland and Grimsel, Switzerland) using caesium as one of the tracers. The main rock types selected for these studies are the same as in the in-situ experiments: veined gneiss from Olkiluoto and granodiorite from Grimsel. This way this study also serves as a supporting experiment for the in-situ experiments.

Three cubic samples, about $1 \times 1 \times 1$ cm³ in size, of both rock types, were manufactured and imaged with a SkyScan 1172 XCT scanner with a pixel size of 6.1 μ m at the University of Jyväskylä. Five of the six faces of the samples were sealed with epoxy resin, thus caesium would only diffuse from one face of the samples into the rock matrix. First scanning was done before immersion of the samples, then the samples were immersed into supersaturated aqueous CsCl solution. Second scanning was done after 141 days for first samples and after 249 days for second samples. The third samples will be in CsCl for one year. Migration velocity of caesium was thus followed by rescanning the samples after different amounts of contact time.

The post-immersion XCT images showed intrusion of caesium in the samples. By finding three corresponding points from the two scans of the same sample, and calculating a translation vector, images could be aligned since the scannings were done using the same exact parameters. Difference of the aligned images then showed exactly where caesium had migrated. It had migrated to the open pore space within highly porous mineral clusters and to biotite veins. In the Olkiluoto sample, caesium was migrated through the whole sample, also filling a microfracture in the sample, and there were areas of high caesium concentration corresponding to areas of high local porosity (see Figure 1). In the Grimsel sample caesium had migrated only a few mm into the sample. A few openings within biotite grains surrounding feldspars and quartz were filled with CsCl. There were no areas of high caesium concentration, as there are no high porosity areas in Grimsel granodiorite (see Figure 2). The results indicate that there is a highly connected pore network in the Olkiluoto sample forming fast migration paths for the diffusion of nuclides. In Grimsel sample the connectivity of the migration paths was less pronounced and highly porous patches behaving as sinks along transport pathway of elements did not appear.

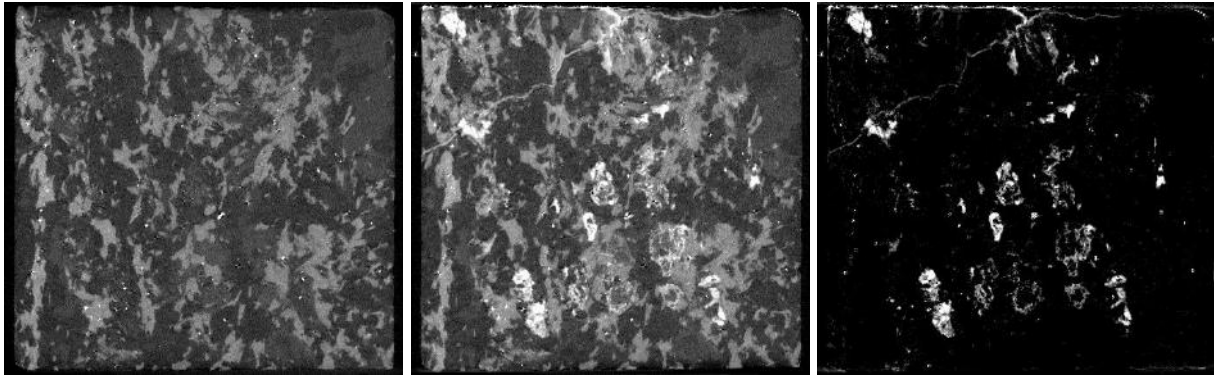


Figure1. Olkiluoto sample before CsCl immersion (left panel) and after 249 days contact time (middle panel). The difference of the two images (right panel) shows caesium intrusion throughout the sample. Caesium has infiltrated the sample from above. Sample size is $1 \times 1 \times 1 \text{ cm}^3$.

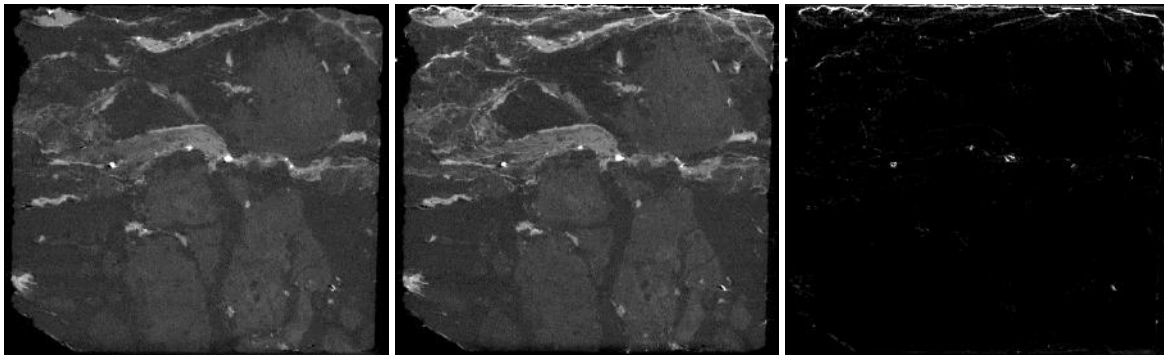


Figure 2. Grimsel sample before CsCl immersion (left panel) and after 249 days contact time (middle panel). The difference of the two images (right panel) shows caesium intrusion only a few mm deep into the sample. Caesium has infiltrated the sample from above. Sample size is $1 \times 1 \times 1 \text{ cm}^3$.

Sorption of dissolved inorganic radiocarbon on goethite, hematite and magnetite

J. Lempinen, J. Lehto

Laboratory of Radiochemistry, Department of Chemistry, University of Helsinki, Finland

Radiocarbon is a top priority class radionuclide with respect to the disposal of spent nuclear fuel. Due to its long half-life of 5730 years and great mobility, it is one of the radionuclides that can migrate through the bedrock into the biosphere. Radiocarbon can migrate along the groundwater flow as dissolved inorganic radiocarbon or small organic molecules such as methane. Methane or other hydrocarbons do not sorb onto minerals, whereas sorption mechanisms for dissolved inorganic radiocarbon can be considered. Radiocarbon can be retained from groundwater onto calcite by isotope exchange and on iron oxide and hydroxide minerals by electrostatic adsorption.

The adsorption on iron minerals can be attributed to electrostatic attraction. Sorption is expected if the groundwater pH is lower than the isoelectric point (IEP) of the mineral but greater than the first dissociation constant of carbonic acid (6.3). In such conditions the net surface charge on the mineral is positive and the predominant form of dissolved inorganic carbon is bicarbonate ion. The aim of the present study is to quantify the adsorption of bicarbonate ions on synthetic goethite, hematite and magnetite. The IEPs of goethite, hematite and magnetite are approximately 8.8 [1], 8.5 [2] and 7 [3]. Therefore sorption in the pH range of groundwaters (7-9) sorption of dissolved inorganic radiocarbon is expected on goethite and hematite but not magnetite. The aim of the present study is to quantify the sorption on these minerals and its dependence on pH.

Experiments have been carried out to determine the sorption isotherms of dissolved inorganic radiocarbon on goethite and hematite. In these batch experiments solutions of varying DIC concentrations were prepared and labelled with $^{14}\text{HCO}_3^-$ tracer. 10 mM tris(hydroxymethyl)aminomethane buffer was used to achieve a pH of 8.2. The minerals were added into the solutions as suspensions to achieve a solid to solution ratio of 5 g/L. The solutions were then allowed to equilibrate for one week, after which they were centrifuged and the activity of the solution was measured to determine the amount of bicarbonate ions sorbed onto the mineral surface. Similar experiment is ongoing to study the sorption on magnetite.

The sorption isotherms of bicarbonate on goethite and magnetite are shown in Figure 1. It can be seen that the amount of bicarbonate sorbed onto these minerals rapidly increases up to DIC concentration of 1 mM, after which the increase levels. This is typical of Langmuir adsorption isotherm that describes sorption in monomolecular layer. These results show that radiocarbon dissolved in inorganic form can be sorbed on goethite and magnetite and thus be retained in bedrock. In addition to goethite and hematite, sorption on magnetite will also be discussed in the conference contribution along with the effect of pH on the sorption.

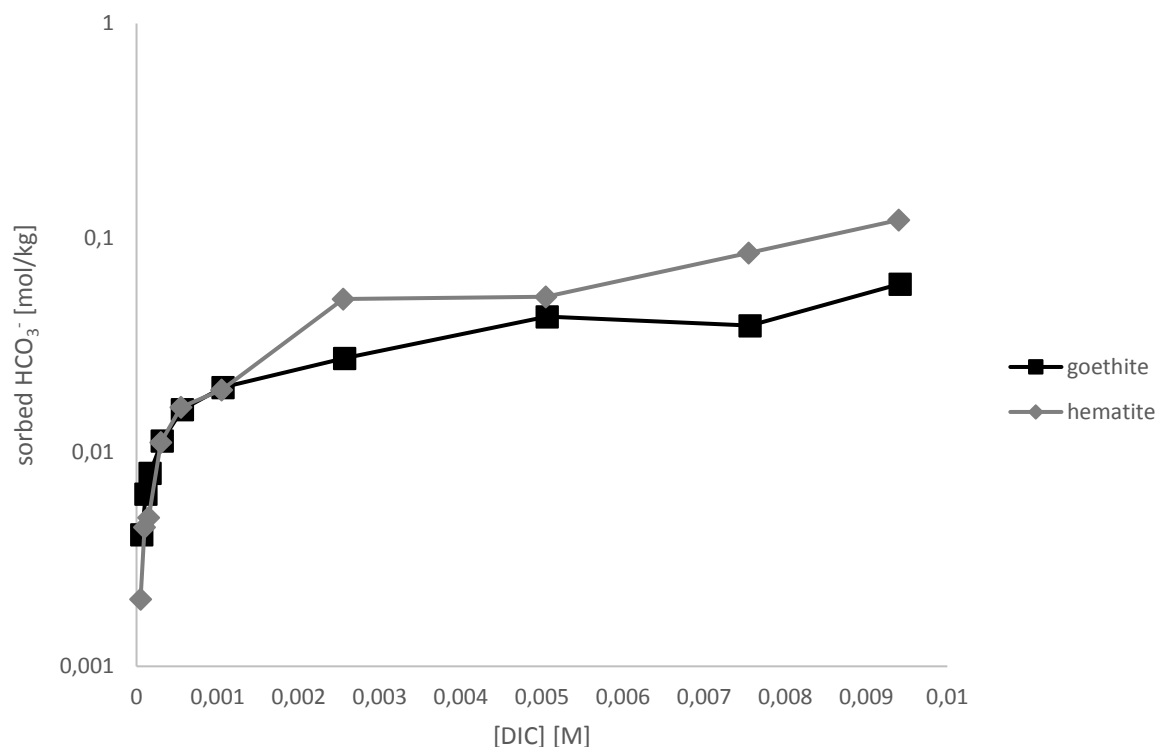


Figure 4. The amount of bicarbonate ions sorbed onto calcite as a function of the dissolved inorganic carbon concentration of the solution at pH 8.2.

References

- [1] Kosmulski M, Maczka E, Jartych E, Rosenholm JB. Synthesis and characterization of goethite and goethite-hematite composite: experimental study and literature survey, *Advances in Colloid and Interface Science* 19;103(1):57-76, 2003
- [2] Y. Thomas He, Jiamin Wan, Tetsu Tokunaga. Kinetic stability of hematite nanoparticles: the effect of particle sizes, *Journal of Nanoparticle Research* 10:321–332, 2008
- [3] Gomez-Lopera SA, Plaza RC, Delgado AV. Synthesis and Characterization of Spherical Magnetite/Biodegradable Polymer Composite Particles, *Journal of Colloid and Interface Science* 240:40–47, 2001

On redox sensitive radionuclide immobilization by rock matrix with large pieces using electromigration method

Xiaodong Li^{1,2,3}, Hui Yang¹, Peizhuo Hu⁴, Longcheng Liu⁵, Daqing Cui^{1,3*}, Bjorn Gylling⁶, Martin Lofgren⁶ and Ignasi Puigdomenech⁶

¹Department of Radiochemistry, China Institute of Atomic Energy, Beijing, China

²Laboratory of Radiochemistry, Department of Chemistry, University of Helsinki, Helsinki, Finland

³Department of materials and Chemistry, Stockholm University, Stockholm, Sweden

⁴Department of Radiochemistry, Lanzhou University, Lanzhou, China

⁵Chemical Engineering and Technology, Royal Institute of Technology KTH, Stockholm, Sweden

⁶SKB, Stockholm, Sweden

Introduction

The sorption coefficients in large rock pieces can be nearly an order of magnitude lower than that measured from crushed rocks. The results of experiment on immobilization of radionuclides on the crushed rock particles, therefore, can't be directly used in the safety assessment of nuclear waste repository. The information of the specific surface areas of the reducing minerals in the rock and the immobilization rates of redox sensitive radionuclides in the pore system of the rock are not well known. The measurements of radionuclide immobilization on large rock pieces take very long time. André et al. developed a method to speed up the intrusion of charged species into large rock pieces by applying an electric field. This speeds up the intrusion immensely and has been successfully used for cesium, which is not redox sensitive.

With the efforts on avoiding contacting of redox sensitive nuclides with electrodes and oxygen in air, the immobilization of redox sensitives U(VI), Se(IV), Se(VI) in synthetic groundwater in large rock pieces were investigated in a glove box with lower oxygen content. The immobilization of redox stable elements, cations Sr^{2+} , Cs^+ , Co^{2+} and anions I^- , simulating fission products, were comparatively investigated simultaneously.

Experimental steps

In the first test, Cs^+ is first added in the chamber named as "source" in Fig 1. Afterwards, a more complexed cocktail of cations should be used, i.e., reversible absorbable cation Sr^{2+} , irreversible absorbable Cs^+ , and surface complexing Co^{2+} are added in the chamber named as "source" in Fig 1, and simultaneously anions would be added, inert I^- , carbonate complexing and reducible U(VI) (as $\text{UO}_2(\text{CO}_3)_3^{4-}$) and reducible Se(IV) (as SeO_3^{2-}) and Se(VI) (as SeO_4^{2-}) in the chamber named as "recipient" in Fig 1.

The advantages of using cocktail solution containing different species in this electro-migration/immobilization experiment are:

a) Simplicity. To investigate several species at the same experiment can save a lot time. It is assumed that the surface sites of the rock that can sorb or reduce radionuclides are much more exceeding than those accessible by the aqueous species under study. ICP-MS offers the technical possibility of measuring many species at the same time.

b) Comparison. The immobilization process of redox sensitive U(VI) and Se(VI)/(IV) and stable fission product ions, cations Sr^{2+} , Cs^+ and anions I^- , on the rock sample can be compared. This information is useful for understanding the immobilization mechanisms of radionuclides.

The rock samples are collected from Äspö underground laboratory. All rock samples will be shaped and loaded with synthetic groundwater and being vacuumed in a tight vessel to get all surfaces in pores being saturated with water. The reaction chamber with the electrical potential gradient have been made according to the previous work of Magnus André and Magnus Sidborn [1] as shown in Fig. 1.

The experiment is still under conducting, the information obtained will be useful for the safety assessment.

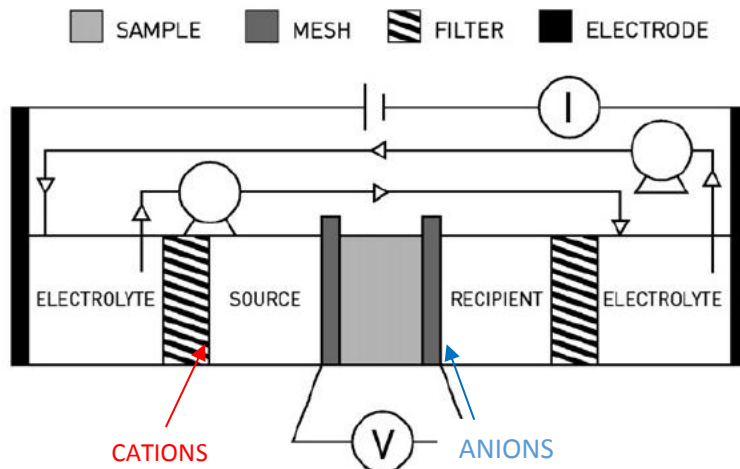


Fig 1. Setup for the through-migration experiments, modified from a figure in reference [2]. The tracer migrates through the sample between two solution containers driven by an electrical gradient. The solutions in the containers are mixed drop-wise.

References

1. André, M., Malmström, M. E., Neretnieks, I., 2008. Measuring sorption coefficients and BET surface areas on intact drillcore and crushed granite samples, *Radiochimica Acta* 96, 673–677.
2. André, M., Malmström, M. E., Neretnieks, I., 2009. Determination of sorption properties of intact rock samples: New methods based on electromigration, *Journal of Contaminant Hydrology* 103, 71–81.

Selenite sorption on main minerals of crystalline rock

Xiaodong Li¹, Jussi Ikonen¹, Antero Lindberg² and Marja Siitari-Kauppi¹

¹*Laboratory of Radiochemistry, Department of Chemistry, University of Helsinki, Helsinki, Finland*

²*Geological Survey of Finland, Espoo, Finland*

Spent nuclear fuel from Finnish and Swedish power plants will be disposed of deep in the crystalline bedrock. Estimating migration of radioactive elements in groundwater is important for assessing the risk at the waste disposal site. It is relatively easy to gain confidence in the performance assessment of a nuclear waste repository if we could have a deep understanding of the behavior of the elements at the near and far field of the repository. In particular, selenium as ⁷⁹Se, is an element that needs special concern because of the long half-life ($\sim 6.5 \times 10^4$ years) and potentially high impact on the cumulative radioactive dose in a high level nuclear waste repository.

The objective of this work was to examine sorption behavior of selenite (SeO_3^{2-} , Se(IV)) on the crystalline rock granodiorite and its main minerals. Firstly, the pH changes were studied during equilibration of Grimsel groundwater simulant (GGWS) which resembles the groundwater in Grimsel test site with crushed granodiorite rock and its main minerals, muscovite, plagioclase and biotite and two common fracture filling minerals, kaolinite and calcite. Secondly, the distribution coefficients (K_d) of selenite for granodiorite and the main minerals listed above were determined by batch sorption method carried out as a function of initial concentrations.

The composition of the granodiorite rock and different minerals were determined by XRD and SEM methods. The pH was followed during the equilibration of 0.5 g crushed rock and minerals with 10 mL of GGWS (Figure 1). After two weeks shaking of different minerals and GGWS, variable concentrations of Na_2SeO_3 solutions were added into the vials, resulting in the initial Se(IV) concentrations from 1×10^{-8} to 1×10^{-3} mol/L. The vials were shaken for another 2 weeks continuously and after that the concentrations of remaining Se(IV) in the solutions were measured by ICP-MS. The K_d values of Se(IV) for granodiorite and the main minerals were calculated (Figure 2).

The XRD results showed that minerals muscovite, biotite and calcite in the experiment were pure, but granodiorite and plagioclase were mixtures of the main minerals and kaolinite used was only 45% pure. From Figure 1 we can see that after equilibration the pH values of GGWS solution varied between the different samples equilibrated. The initial pH value of GGWS was 7.68 while the pH value changes after equilibration followed the order of calcite (8.70) > plagioclase (8.54) > granodiorite (8.03) > biotite (7.66) > muscovite (7.46) > kaolinite (7.00). Figure 2 shows that the K_d values of selenite on the studied minerals and granodiorite rock followed the order kaolinite > calcite > biotite > granodiorite > muscovite > plagioclase. The K_d values of kaolinite, calcite, biotite and granodiorite showed obvious increasing trend with decreasing Se(IV) initial concentration while the K_d values of muscovite just increased a little and the K_d values of plagioclase kept nearly constant. The K_d values from this experiment are within the limit of uncertainty in agreement with the ones determined previously by Söderlund et al. (2016) for typical Olkiluoto soil minerals and Ikonen et al. (2016) for Grimsel granodiorite.

Our results show that K_d values of Se(IV) are dependent on the minerals used as well as on the selenium concentrations, but no accurate data could be achieved in the low concentration region, because the detection limit of ICP-MS method is considerably high, 7.6×10^{-8} mol/L. Low Se(IV) concentration experiments can be done by using ⁷⁵Se which is radioactive and can be detected by using radiochemistry method.

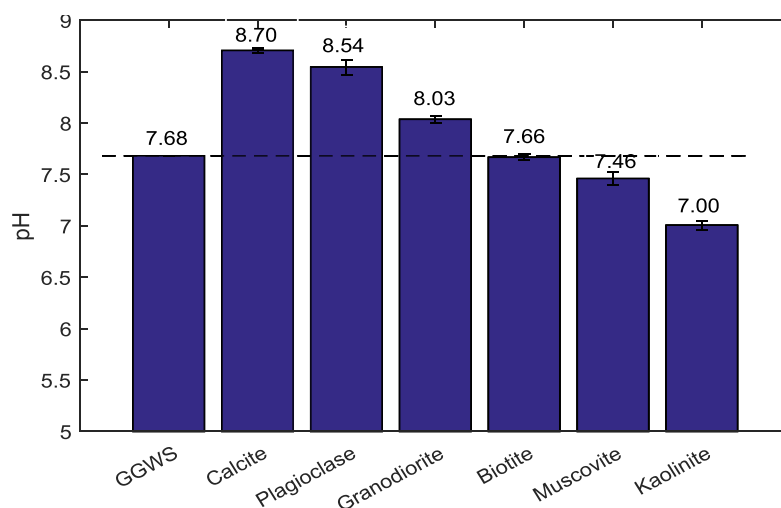


Figure 1 pH values of solutions with granodiorite and the main minerals with Grimsel groundwater simulant equilibrated for 2 weeks. (■) muscovite; (●) plagioclase; (◆) biotite; (▲) calcite; (×) granodiorite; (▼) kaolinite

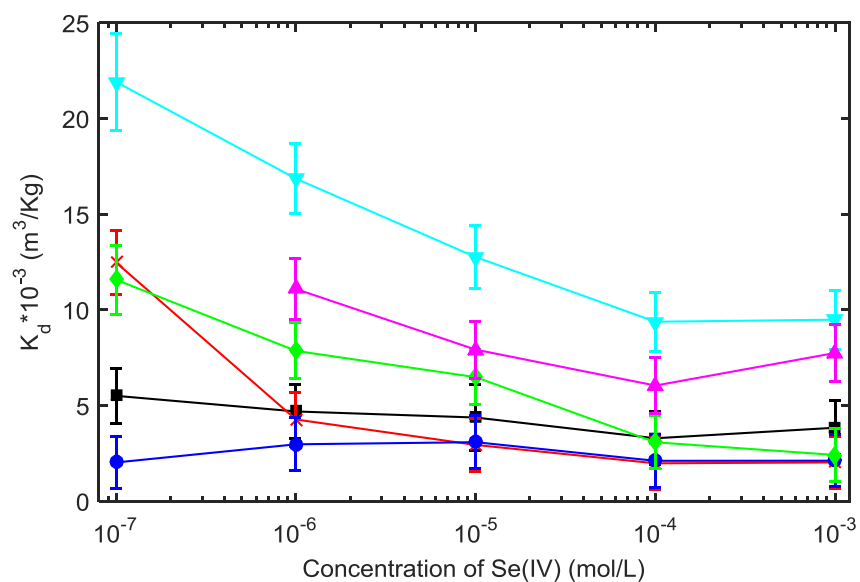


Figure 2 K_d values of minerals as a function of initial Se(IV) concentration. (■) muscovite; (●) plagioclase; (◆) biotite; (▲) calcite; (×) granodiorite; (▼) kaolinite

The sorption and diffusion of ^{133}Ba in granitic rocks

Eveliina Muuri, Jussi Ikonen, Minja Matara-aho, *Antero Lindberg, Marja Siitari-Kauppi

Laboratory of Radiochemistry, Department of Chemistry, University of Helsinki, P.O. Box 55, 00014 University of Helsinki, Finland

**Geological Survey of Finland, P.O.Box 96, Espoo, Finland*

The final disposal of spent nuclear fuel in the Olkiluoto site in Finland will take place in crystalline granitic rock, which is generally considered safe due to the multiple release barriers. However, the processes affecting the transport of the radionuclides from the nuclear fuel to the biosphere need to be considered when assessing the overall safety of the repository. As a result, it is necessary to study the sorption and diffusion properties of safety relevant radionuclides through both laboratory and in-situ experiments to assess the physical and chemical processes affecting the transport of radionuclides in the release barriers of the repository, for instance in the bedrock. In this study the sorption and diffusion behaviour of barium was investigated in pegmatitic granite and veined gneiss obtained from the Olkiluoto test site, granodiorite obtained from the Grimsel test site and their main minerals. The tests were carried out in the presence of the groundwater simulants made to resemble the groundwater in the Olkiluoto and Grimsel test sites.

The distribution coefficients of barium in the Olkiluoto pegmatite and veined gneiss, Grimsel granodiorite and their main minerals (quartz, plagioclase, potassium feldspar and biotite) were obtained by batch sorption experiments carried out as a function of concentration. The sorption results were also modelled with the PHREEQC calculation code. The specific surface areas of the rocks and minerals were measured with the BET method and the effect of the specific surface area to the sorption results was studied. The composition of the rocks and minerals was also analysed with the XRD method. Additionally, the diffusion of barium into rock cubes obtained from the test sites was also studied both experimentally and computationally and the rock cubes from the diffusion experiments were studied with autoradiography and scanning electron microscopy to study the spatial distribution of barium.

The batch sorption results showed that the distribution coefficients followed roughly the specific surface area results. In addition, the distribution coefficients of barium were found to be largest on veined gneiss and biotite and the sorption of barium on all the investigated minerals followed a similar decreasing trend with changing concentration. It was discovered in the experiments that the distribution coefficients in saline water were considerably smaller than the results in low salinity water, which confirms that competing ions play a significant role in the sorption of barium. In addition, the concentration decrease of barium in the diffusion experiments was largest in granodiorite which can also be explained with the lack of competing ions. It was discovered with autoradiography and scanning electron microscopy that the barium was mainly sorbed in the dark minerals of the rocks, but that the barium sorption on plagioclase was also significant. The sorption data obtained from this study will be utilised in the heterogeneous diffusion modelling and in the interpretation of the results from the in situ through diffusion experiments.

Effect of cation exchange on ion migration in bentonite

Noémi M Nagy and József Kónya

Imre Lajos Isotope Laboratory, Department of Colloid and Environmental Chemistry, University of Debrecen, Hungary

Bentonite clay rock is supposed as barrier material for the deep geological disposal of high activity nuclear waste. The main mineral component in bentonite rocks is montmorillonite, a swelling clay mineral having exchangeable cations. The swelling as well as the isolation properties are influenced by the entities of the exchangeable cations.

The radionuclide species, depending on their charges, migrate in the different water spaces of bentonite, namely in the free pore water, water of the electrostatic double layer, and in the montmorillonite interlayer water. The migration pathways of the cations and anions are different: the cations can be present in all water types, the anions, however, are excluded from the interlayer water and their quantity is less in the water of the electrostatic double layer than that of cations. It is important to note that the electro neutrality must be fulfilled at molecular level: the sum of the positive and negative charges (cations, anions, layer charges, edge charges) must be zero in all small volumes of the systems. Moreover, the cations can be sorbed in the interlayer of montmorillonite, inhibiting the migration.

Since the interlayer cations have a great effect on the swelling properties of montmorillonite, and as a result on the ratio of the water spaces. In the literature, the factors influencing the water types and the differences between the anion and cation migrations are extensively studied both by experimentally and theoretically in sodium-bentonite. The migration models use the porosity and density of dry bentonite, as well as the distribution coefficients of the migrating cation.

In the real systems, however, the bentonites are wet and the interlayer sodium cations can exchange with cations in groundwater. As well-known from the natural transformation of the sodium-bentonites with marine origin to calcium-bentonite when contacting to groundwater with calcium content, the bivalent and trivalent cations bind stronger to the layer charge of montmorillonite, and modify the swelling properties as well as the ratio of water types. Obviously, other cation exchange bentonites also take place in exchange processes with cations in the environment.

In this work, the migration of chloride anion and cesium cation is studied in different cation exchanged (sodium, calcium, iron(III) , and rare earth bentonite). The migration coefficients (Table 1) are compared and some conclusions are drawn for the effect of cation exchange on the anion and cation migration.

Table 1: Migration coefficients of chloride and cesium ions (^{137}Cl and ^{137}Cs) in different cation exchanged bentonites

	D_a (m ² /s)	
	Cl^-	Cs^+
Na-bentonite	1.15E-11	3.07E-13
Ca-bentonite	6.32E-12	3.07E-13
Fe(III)-bentonite	4.30E-12	9.27E-13
Mean of seven rare earth bentonites	5.34E-12	2.28E-13

Batch and in-situ K_d -values in Lastensuo and Pesänsuo peat samples: comparison between different methods

Lauri Parviainen¹, Anne-Maj Lahdenperä², Merja Lusa³

¹Posiva Oy, Olkiluoto, 27160 Eurajoki, Finland, lauri.parviainen@posiva.fi

²Saario & Riekkola Oy, 00420 Helsinki, Finland

³Laboratory of Radiochemistry, Department of Chemistry, 00014 University of Helsinki, Finland

Posiva Oy was granted construction license for final disposal facility of spent nuclear fuel and is doing safety case for the operating license application. For the safety case, radionuclide transport (RNT) and dose calculations are needed in order to evaluate the safety of the selected disposal method and the fulfillment of the long term safety requirements. In this study, two methods to determine distribution coefficients (K_d -values), which are used in the RNT model, of peat have been compared. In the so called **batch** method radioactive tracers are used and in **in-situ** method concentrations of indigenous elements are measured.

I. Methods

Peat samples were collected from Lastensuo and Pesänsuo mires using peat corer with a core length of 50 cm and a diameter of 15 cm or 5 cm [1]. Lastensuo (Fig. 1) is a 5300-year-old mire with maximum peat thickness of approximately 6.5 meters and it is open from the center and surrounded by trees. Pesänsuo (Fig. 2) is a 9200-year-old mire, with maximum peat thickness of 6.7 meters and it is fully forested [2].



Figure 1. Lastensuo mire (left) and Pesänsuo mire (right) (Lentokuva Vallas Oy, 2010).

I.A. Batch sorption experiments

Batch sorption experiments were conducted using radioactive tracers (^{63}Ni , $^{110\text{m}}\text{Ag}$, ^{135}Cs , ^{125}I , ^{99}Mo and ^{85}Sr) for peat samples from Lastensuo mire. First 0.5 g of fresh or dried peat was incubated for one week in 25 mL of synthetic bog water in the dark [1], which after a known amount of selected tracer was added and the sample was further incubated for 7 days. For experiments with ^{99}Mo an incubation time of four days, without preconditioning was used. After incubation, samples were centrifuged at 20 000 rpm for 20 minutes and filtered through a 0.2 μm syringe filter. The activity of the solution was measured and the difference between initial and final activity was expressed as distribution coefficient (K_d).

I.B. *In-situ* distribution coefficients

In the *in-situ* method fresh peat samples from Lastensuo mire and Pesänsuo mire were saturated with MQ-water and incubated for one week (for more detailed method, see [3]). Pore water was extracted by centrifugation and the concentrations of nickel (Ni), silver (Ag), strontium (Sr), molybdenum (Mo), cesium (Cs) and iodine (I) were analyzed using ICP-SFMS. The remaining solid fraction was leached with 1 M ammonium acetate for bioavailable elements and with HNO₃/HF and LiBO₂ for the total dissolution. K_d-values, both for bioavailable fraction and total fraction, were obtained by dividing the concentrations in the solid sample by the concentrations found in the pore water.

III. RESULTS

The obtained K_d-values for Ni, Ag, Sr, Mo, Cs and I varied depending on the used method and highest average values were obtained using either total dissolution or batch method (Table 1). For Ni (15300 L/kg DW, Lastensuo), Sr (2640 L/kg DW, Lastensuo), Cs (1510 L/kg DW, Pesänsuo) and I (3650 L/kg DW, Lastensuo) the highest K_d-values were obtained using HNO₃/HF/LiBO₂ extraction and for Ag and Mo the highest values, 14700 L/kg DW and 15800 L/kg DW respectively, were obtained using batch method. In both studied mires, the K_d-values of the bioavailable fractions were on average only 10 % of the maximum values obtained either using HNO₃/HF/ LiBO₂ extraction or batch method.

Table 2. K_d-values of peat samples from Lastensuo and Pesänsuo. The values are arithmetic means of all determined values in different layers from surface to the bottom clay. For the batch values, incubation time of 7 days, except for Mo 4 days, was used.

K _d (L/kg DW)	Ni	Ag	Sr	Mo	Cs	I
Batch	10600 ^a	14700 ^a	2570 ^a	15800 ^a	45 ^{b*}	540 ^{a**} and 180 ^b
Lastensuo bioavailable	3290	240	1660	11	119	2.0
Lastensuo total	15300	8550	2640	4330	1470	3650
Pesänsuo bioavailable	227	116	916	51	69	12
Pesänsuo total	1600	345	1650	3190	1510	2470

a) Fresh peat samples, b) Dried peat samples, * From [1], **From [4]

IV. CONCLUSIONS

For Ni, Ag and Sr, the batch K_d-values obtained using fresh samples corresponded closely to the values determined using the HNO₃/HF/LiBO₂ extraction. The difference in the values between these two methods was only on average 5 percentage points. For Mo, considerably higher, 3-fold, values were obtained using batch method, compared to the HNO₃/HF/LiBO₂ extraction. However, it should be noted, that for Mo only short, four days incubation in the batch experiments could be used, due to the short (66 h) half-life of ⁹⁹Mo and therefore the equilibrium between the sample and Mo is probably not obtained. For Cs and I, the batch values more closely corresponded to the values obtained from the bioavailable fraction. For Cs the batch values were on average 40 % of the values obtained from the 1 M ammonium acetate extraction, but for I considerably higher values were obtained from the batch experiments compared to the values for the bioavailable fraction (see Table 1.). In addition, the batch K_d-values of I obtained using fresh samples and aseptic methods, were on average 3-fold compared to the values obtained using dried samples. It has been previously reported, that increase in the incubation time, increases the retention of I in the fresh peat samples and after 84 days of incubation the average batch K_d-value was reported to be 6500 L/kg DW in the Lastensuo peat samples [4]. It was also reported, that sterilization of fresh peat decreases the retention in the Lastensuo samples [4, 5]. Non-aseptic handling and drying of the sample changes the pristine microbial population of the sample, which in turn can affect the obtained K_d-values. Because of the limited amount of samples and significant variation found in the K_d-values obtained using tracers, ammonium acetate or HNO₃/HF/LiBO₂, more comparative research between *in situ* and batch methods is still needed to fully understand their effect on the resulting K_d-values.

Sorption of tin on fracture minerals in granitic groundwater simulant

Esa Puukko and Jukka Lehto

Laboratory of Radiochemistry, Department of Chemistry, University of Helsinki

The sorption of tin on fracture minerals was determined in fresh slightly reducing granitic groundwater simulant ALLMR. The minerals were chlorite, illite, kaolinite and quartz. Chlorite and illite were obtained from American Clay Minerals Society Source Clays Repository. Kaolinite belongs to the reference clays of American Clay Minerals Society. The quartz is fine ground alpha quartz Min-U-Sil 5 from US Silica Company (www.u-s-silica.com). Illite and chlorite were ground in agate mortar and sieved to smaller than 0.149 μm grain size. Kaolinite was already in fine ground form when obtained. Illite was pretreated according to the method of Tournassat et al. (2007). Finally the pretreated illite was freeze-dried by Alpha 1-4 LSC. Chlorite and kaolinite were used without pre-treatment. Due to the very fine grain size of chlorite, there was a possibility of its dissolution during pre-treatment. Min-U-Sil 5 was leached with hydrochloric acid for removal of iron, leached with water to neutral pH and air-dried. Surface areas of the minerals were measured by nitrogen adsorption (BET/N₂) method at the Tampere University of Technology (TUT) using Micromeritics Flowsorb instrument.

Table 1. Minerals for sorption experiments with tin.

Mineral	Origin	Surface area (g/cm ²)
Chlorite	CCa-2 Ripidolite El Dorado County, California, USA	2.6
Illite	IMt-1 Cambrianshale, Silver Hill Montana, USA	6.4
Kaolinite	KGa-1b Washington County, Georgia; USA	11.1
Quartz	Quartz Min-U-Sil 5	4.9

The sorption of tin on minerals was determined with batch sorption experiments. The fresh slightly reducing granitic groundwater simulant ALLMR was prepared in deionized water (Milli-Q) and pro analysis grade reagents under argon atmosphere. All experiments were performed inside a glove box under argon to prevent interference of atmospheric carbon dioxide. In addition to reference pH of the ALLMR solution, the pH of solutions was adjusted to between 7- 10. Organic buffers of MES, MOPS, TRIS and CHES were used to buffer the solutions. In the solutions the buffer concentration was $1 \cdot 10^{-3}$ M and pH was adjusted with 0.1 M HCl or NaOH (Merck, Titrisol) according to Perrin & Dempsey (1974).

The solid to solution ratio was 20 mg / 20 mL for the minerals and experimental time was one week. The Sn tracer nuclide was Sn-113 ($T_{1/2} = 115$ d) (Eckert & Ziegler), which contained stable tin. In the beginning of the experiment the concentration of Sn was $8 \cdot 10^{-7}$ M. The amount of tracer was optimized so that Sn(OH)₄ will not be saturated with respect to SnO₂ (am) after sorption. The solid material was separated by filtration (Millipore GW 0.22 μm). From the solution Sn-113 was radio assayed with Perkin Elmer 1480 Wizard automatic gamma counter.

The speciation of tin and the modelling of the sorption of tin on kaolinite KGa-1b and illite IMt-1 was calculated with PHREEQC program (Parkhurst & Appelo 2003) using ThermoChimie (ANDRA 2009) data base. The speciation of tin in fresh ALLMR solution is presented in Figure 1. The modelled results of sorption are presented in Figures 2 and 3.

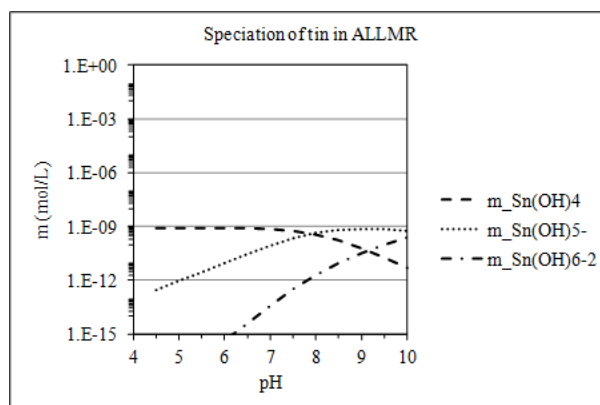


Figure 1. Speciation of tin in fresh ALLMR solution.

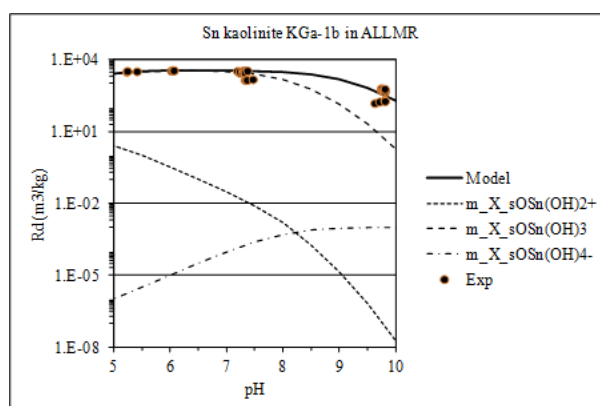


Figure 2. The calculated (Model) and the experimental (Exp) sorption of tin on kaolinite KGa 1b in ALLMR solution including the sorbed species of Sn.

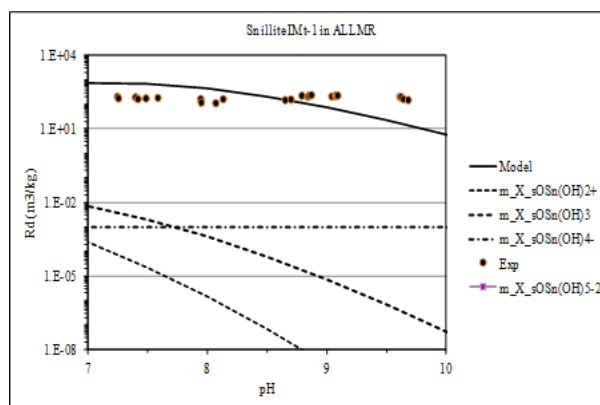


Figure 3. The calculated (Model) and the experimental (Exp) sorption of tin on illite IMt-1 in ALLMR solution including the sorbed species of Sn.

Eu(III)/Cm(III), Np(V), and U(VI) sorption onto clay minerals: from low to high ionic strength conditions

A. Schnurr¹, R. Marsac¹, M. Marques², Th. Rabung¹, J. Lützenkirchen¹, X. Gaona¹, B. Baeyens², H. Geckeis¹

¹*Institute for Nuclear Waste Disposal (INE), Karlsruhe Institute of Technology (KIT), Karlsruhe, Germany*

²*Laboratory for Waste Management (LES), Paul Scherrer Institute (PSI), Villigen, Switzerland*

In the context of nuclear waste disposal actinide retention at clay mineral surfaces is a well-established process, which has been intensely investigated (e.g. [1], [2], [3]). However, at present no mechanistic sorption model exists that reliably describes actinide uptake at elevated ionic strength (> 1 M). Such conditions are to be expected e.g. in the vicinity of a repository in rock salt formations, in the Jurassic and lower Cretaceous clay rock layers in Northern Germany [4] or in sedimentary rocks in Canada [5], all identified as potential host rocks for the disposal of high level nuclear waste.

Within the present study, the uptake of actinide/lanthanide (Eu(III) (^{152}Eu quantification by γ -counting), Cm(III), Np(V) (^{237}Np quantification by LSC and HR-ICP-MS), and U(VI) (^{238}U quantification by ICP-MS) by illite (IdP), montmorillonite (SWy), and a synthetic iron free montmorillonite (IfM) was investigated in dilute to concentrated saline systems (0.1 – 4.0 M NaCl; 0.06 – 2.0 M MgCl_2 and CaCl_2) in the absence of carbonate (Ar glovebox). Eu(III), Np(V), U(VI) batch sorption studies and Cm(III) time-resolved laser fluorescence spectroscopy (TRLFS) experiments were carried out for $3 < \text{pH}_c < 12$ (for MgCl_2 solutions up to $\text{pH}_c = 9$).

In case of Eu(III) ionic strength has a small impact on $\log K_D$ values in NaCl systems under near-neutral to hyperalkaline pH conditions (Fig. 1, (a)). Only under acidic pH conditions where cation exchange is the dominating binding mechanism a significant decrease of Eu(III) sorption is observed with increasing NaCl concentration. Unlike in the NaCl system, a significant decrease in the extent of uptake is observed in all solutions with elevated Mg/CaCl₂ concentrations ($[\text{Mg}/\text{CaCl}_2]_{\text{max}} = 2.0$ M; Fig. 1, (b)). Even so, $\log K_D$ (expressed in $\text{L}\cdot\text{kg}^{-1}$) values remain high ($\log K_D \geq 4.5$) for all systems in the pH_c range 8 - 11. TRLFS studies in NaCl systems do not indicate any significant change in the first coordination sphere of Cm(III) at a given pH_c if ionic strength is increased. As a consequence, we do not expect any change in the surface speciation of Cm(III) at elevated ionic strength compared to a previous study at low background electrolyte concentration [6]. Identical surface species are assumed and Eu(III) uptake data are sufficiently well described using the 2SPNE SC/CE approach [1] calibrated at lower ionic strength. The impact of elevated ionic strength on the activity coefficients of solutes and the activity of water is taken into account by applying the Pitzer approach. In the CaCl_2 system and especially at higher ionic strengths different spectral features are observed compared to the NaCl system pointing to some changes in Cm(III) surface speciation. In addition the assumption of an additional mixed Ca-Eu-OH surface species was necessary to accurately describe the experimental data at very high pH_c (> 11).

Sorption data for Np(V) and U(VI) is shown in figure 1 (c) and (d) respectively. The actinyl-cations exhibit no significant ionic strength dependency over the whole pH range. As expected Np(V) sorption is relatively low compared to the other systems starting at $\text{pH}_c \sim 8$ ($> 20\%$) and approaching quasi quantitative retention ($> 95\%$) at $\text{pH}_c > 10$. Nevertheless, the sorption data does not change between 0.1 and 4.0 M NaCl background electrolyte concentration and/or due to the variation of the metal concentration of about two orders of magnitude. The model description is in agreement with the experimental data (Fig.1 (c)).

The shape of the sorption edge for U(VI) uptake is very similar to the one for Eu(III), but it is slightly shifted towards more acidic conditions as a result of the stronger hydrolysis of U(VI). Notably, under the experimental conditions no significant outer-sphere complexation (ion-exchange) of U(VI) at low pH occurs. A pronounced uptake ($> 20\%$) can be observed at $\text{pH}_c > 4$. The retention of U(VI) onto the clay minerals is quasi quantitative ($> 99.5\%$) within the pH range ($7 < \text{pH}_c < 11$), where the aqueous speciation of uranium is mostly dominated by $\text{UO}_2(\text{OH})_3^-$. At $\text{pH}_c > 11$, the sorption of U(VI) decreases steadily as a result of the

increasing predominance of the species $\text{UO}_2(\text{OH})_4^{2-}$. Calculations applying the 2SPNE SC/CE approach for U(VI) sorption are in accordance with experimental data when introducing a new chlorine containing surface complex (Fig.1 (d)).

It can be concluded that even under high ionic strength conditions clay minerals exhibit a strong retardation for tri-, penta-, and hexavalent radionuclides in absence of carbonate. The predictive modeling generally is in good agreement with experimental findings.

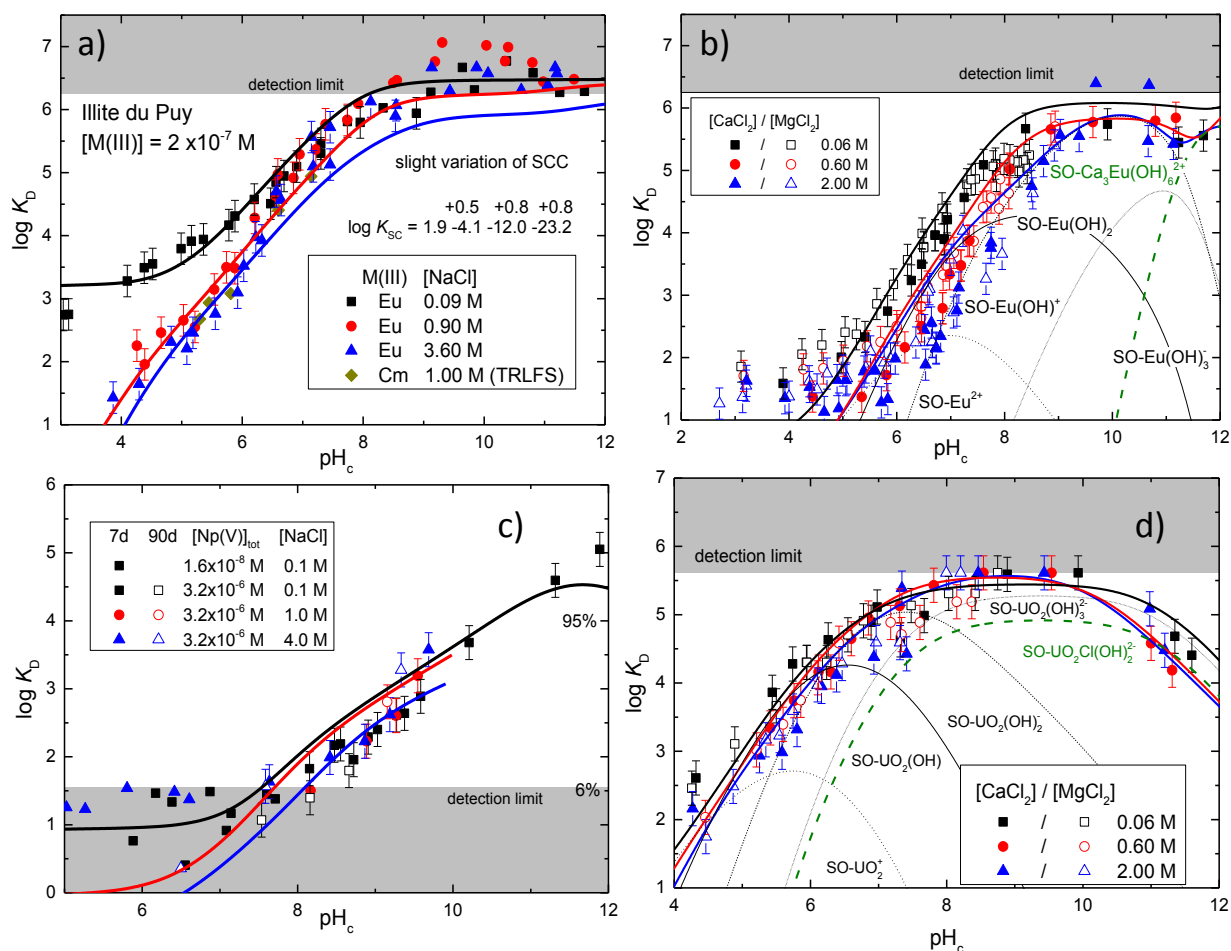


Figure 1: Sorption edges of Eu(III) ($[\text{Eu}]_{\text{tot}} = 2 \cdot 10^{-7} \text{ M}$) onto IdP, (a) + (b); of Np(V) ($[\text{Np}]_{\text{tot}} = 1.6 \cdot 10^{-8}$ and $3.2 \cdot 10^{-6} \text{ M}$) onto IdP (c); and of U(VI) ($[\text{U}]_{\text{tot}} = 4 \cdot 10^{-7} \text{ M}$ and $1 \cdot 10^{-6} \text{ M}$) onto IdP (d) in saline media. Solid lines corresponding to model calculations using 2 SPNE SC/CE with K_D values expressed in $\text{L} \cdot \text{kg}^{-1}$.

References

- [1] M. H. Bradbury, B. Baeyens, *Geochim. Cosmochim. Acta* 66, 2325 (2002).
- [2] X. Tan, et al., *Molecules* 15, 8431 (2010).
- [3] H. Geckeis, et al., *Chem. Rev.* 113, 1016 (2013).
- [4] W. Brewitz, *Zusammenfassender Zwischenbericht*, GSF T 114 (1980).
- [5] P. Fritz, S. K. Frape, *Chem. Geol.* 36, 179 (1982).
- [6] Th. Rabung, et al., *Geochim. Cosmochim. Acta* 69, 5393 (2005).

Acknowledgement

This work is partially funded by the German Federal Ministry for Economic Affairs and Energy (BMWi) under contract no. 02 E 10961.

Block-scale experiment on bentonite colloid – radionuclide interaction

Valtteri Suorsa, Pirkko Hölttä

*Laboratory of Radiochemistry, Department of Chemistry, University of Helsinki,, Finland.
valtteri.suorsa@helsinki.fi*

In Finland, the repository for spent nuclear fuel (SNF) will be excavated at a depth of about 500 meters in the fractured crystalline bedrock in Olkiluoto implemented by Posiva Oy. The spent uranium fuel placed in the final disposal tunnels in copper iron canisters will be surrounded with bentonite clay, which is assumed to be a potential source of colloids due to bentonite erosion. Colloids may affect the migration of radionuclides and the colloid-facilitated transport may be significant to the long-term performance of a spent nuclear fuel repository. The collective processes of the rock matrix, bentonite colloids and radionuclides are important to investigate to assess the relevance of bentonite colloids regarding the safety disposal of the spent nuclear fuel. The bentonite colloid – radionuclide interaction have been studied in a block scale experiment, which provides an intermediate between conventional laboratory and in-situ experiments. In addition supportive colloid stability and batch sorption studies have been performed.

The block scale experiments were performed in Kuru Grey granite block with a horizontal natural water conducting fracture (Fig. 1.). [1, 2] A drill holes drilled orthogonally to the fracture were equipped with sealing packers and an injection packer in the farthest corner. Synthetic groundwater was injected to the fracture and the samples were collected from the opposite side of the block. The reference groundwater used was low salinity granitic Allard ($I = 4.2$ mM) or Grimsel groundwater ($I = 1.2$ mM). The bentonite material investigated in the experiments was synthetic Ni-labeled montmorillonite synthesised in Karlsruhe Institute of Technology, Germany (Fig. 2.). At the beginning, the locations of flow-channels (Fig. 1) were investigated with an uranine dye. The flow conditions in the fracture were determined with ^3H , ^{36}Cl and Amino-G coloring agent, which were considered as conservative tracers. The colloid – radionuclide interaction experiments were carried with ^{152}Eu , which act as an analog for trivalent actinides like Cm^{3+} and Am^{3+} .

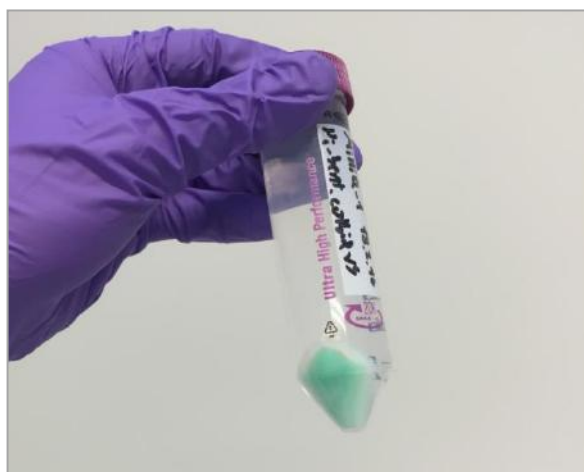
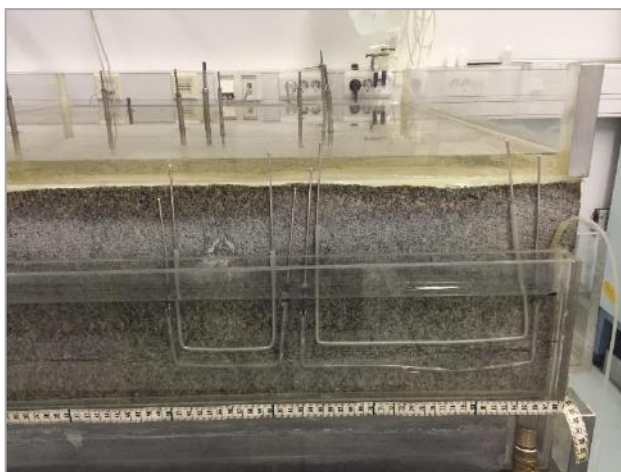


Figure 1. (left) The block fracture with the sample collection pools. The pools are limited with rods inside the hoses. The hose on the right side of the picture is used for preventing the water level from flooding.
Figure 2. (right) The colloid suspension prepared from the Ni-labeled montmorillonite after the separation of excess solid matter from the suspension with a centrifuge.

The initial colloid concentration used was 100 mg/l, the total europium concentration 1×10^{-4} mol/l and the flow rate 50 μ l/min. The concentration of Amino-G was determined with UV-VIS, ^3H and ^{36}Cl were detected by liquid-scintillation counting and ^{152}Eu by gamma-spectroscopy. As an indicator of the stability, the colloid size as a function of time was determined with Photon Correlation Spectroscopy (PCS). Colloid concentration was determined with Inductive Coupled Plasma Mass Spectrometer (ICP-MS) and Laser Induced Breakdown Detection (LIBD). The Europium speciation was investigated with Time Resolved Laser Fluorescence (TRLFS). The TRLFS and LIBD measurements were done in KIT-INE in Karlsruhe, Germany.

Ionic strength and pH had a great influence on the stability of colloids. Ni-montmorillonite colloids were found to be stable in Grimsel groundwater (GGW) but not in Allard (Fig. 3.). The particle size remained quite stable at least for a week in GGW but the particles aggregated in Allard. In the block fracture, repeatable breakthrough curves were obtained with ^3H , ^{36}Cl and Amino-G (Fig. 4.). The effect of bentonite colloids on ^{152}Eu transport was found in the block fracture experiments. No breakthrough of ^{152}Eu activity was detected during two-week experiment without the presence of bentonite colloids. The results from the batch sorption and block fracture experiments will be presented and the importance of bentonite colloids to the migration of radionuclides in environmentally relevant conditions for SNF repository is discussed.

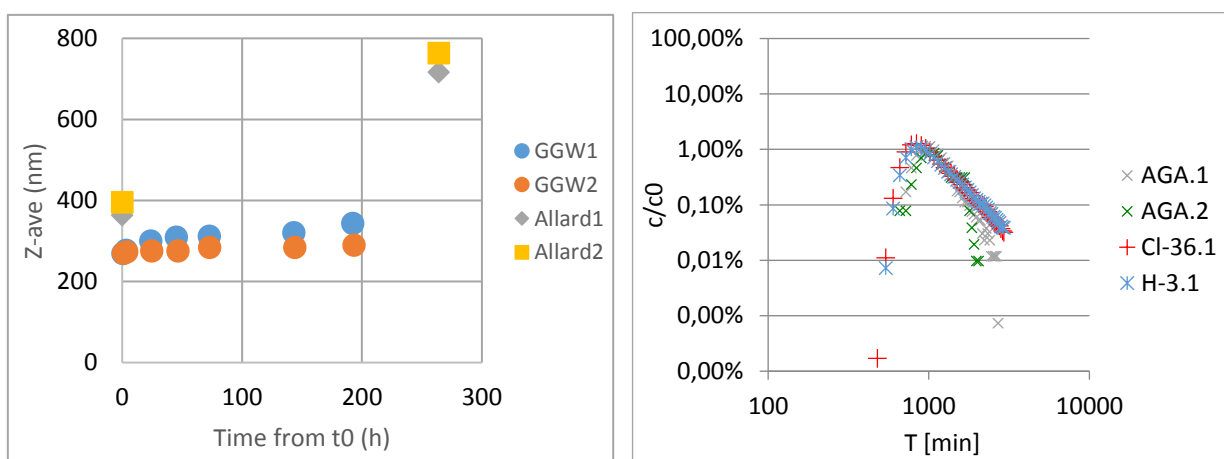


Figure 3. (left) The colloid size was followed as indicator of the stability in the Allard and Grimsel Ground Water simulants. The average size of the particles risen in a week almost to 800 nm in Allard. In Grimsel Groundwater the average size remained quite constant.

Figure 2. (right) Similar breakthrough curves were obtained with AGA, ^3H and ^{36}Cl . A slight drop can be seen in the curve of AGA. This is probably because of the uncertainty of the detection method with low concentration compared to liquid scintillation used with radiotracers.

[1] Hölttä, P.; Poteri, A.; Siitari-Kauppi, M.; Huittinen, N. Retardation of mobile radionuclides in granitic rock fractures by matrix diffusion. *Physics and Chemistry of the Earth* 33 (2008) 983–990.

[2] Hölttä, P.; Poteri, A.; Hakanen, M.; Hautajärvi, A. Fracture flow and radionuclide transport in block-scale laboratory experiments. *Radiochim. Acta* 92, (2004) 775–779.

Laboratory scale advection-matrix diffusion experiment in Olkiluoto veined gneiss using H-3 and Cl-36 as tracers

Mikko Voutilainen¹, Pekka Kekäläinen¹, Jukka Kuva², Marja Siitari-Kauppi¹, Lasse Koskinen³

¹*Department of Chemistry, University of Helsinki, Helsinki, Finland.*

²*Department of Physics, University of Jyväskylä, Jyväskylä, Finland.*

³*Posiva Oy, Olkiluoto, Finland.*

Spent nuclear fuel from nuclear power plants owned by TVO and Fortum is planned to be deposited to a repository at a depth of more than 400 meters in the bedrock of Olkiluoto (Eurajoki, Finland). The repository system of multiple release barriers consists of the vitrified nuclear fuel, a copper canister with a cast iron insert, a bentonite buffer around the canister and backfilling of the tunnels. Furthermore, the surrounding rock is the last barrier if the manmade barriers fail during passage of the millennia. Therefore, safe disposal of spent nuclear fuel requires information on the radionuclide transport (i.e., advection and matrix diffusion) and retention (i.e., diffusion and distribution coefficients) properties within the porous and water-containing rock matrix along the water conducting flow paths. To this end, various laboratory and in-situ experiments have been performed as a part of a project rock matrix REtention PROperties (REPRO) [1-2]. The research site is located in ONKALO, the underground rock characterization facility in Olkiluoto, at a depth of 420 meters close to the planned repository site. The aim of the REPRO project is to study matrix diffusion and sorption of radionuclides in the surrounding bedrock in laboratory and in-situ conditions and demonstrate how the conditions affect the results. More importantly, the results are utilized to investigate if the assumptions applied in the safety case are in line with the site evidence. Furthermore, the laboratory experiments are used to produce parameters for analyzing in-situ experiments and to test analysis tools used for in-situ experiments.

In currently running Water Phase Diffusion Experiment in laboratory (WPDElab) a short concentrated pulse of H-3 and Cl-36 was injected to a synthetic ground water flow through an artificial fracture in contact with a veined gneiss sample from the REPRO site. The 2 mm thick fracture is formed between a 0.8 m long plastic tube (inner diameter 46 mm) and a drill core sample (outer diameter 42 mm) placed in the center of the tube. It is assumed here that due to diffusion radionuclides migrate at a lower speed than that of the advective flow of water. In this experiment synthetic ground water was pumped through the fracture with a constant flow rate of 20 µl/min and a mixture of H-3 and Cl-36 tracers was injected into the advective flow. Concentrations of the radionuclides as a function of time, i.e. breakthrough curves, were measured from collected water samples with a liquid scintillation counter (Tri-Carb 2910 TR). The activities were determined using double labelling and manual quench correction. Preliminary results of the experiment show that the heterogeneity of the advection field affects the early part of the breakthrough curve. Late part of the curve shows that the transport of Cl-36 is retarded less than that of H-3 due to anion exclusion. Currently the experiment is still running and more detailed results with numerical analyses [3] will be provided in the conference presentation. A similar experiment has been performed in in-situ conditions also and a discussion on possible differences will be included.

[1] Voutilainen, M., Poteri, A., Helariutta, K., Siitari-Kauppi, M., Nilsson, K., Andersson, P., Byegård, J., Skålberg, M., Kekäläinen, P., Timonen, J., Lindberg, A., Pitkänen, P., Kemppainen, K., Liimatainen, J., Hautajärvi, A., Lasse Koskinen, L., (2014), Insitu experiments for investigating the retention properties of rock matrix in ONKALO, Olkiluoto, Finland, in WM2014 Conference Proceedings, 14258.

[2] Kuva, J., Voutilainen, M., Kekäläinen, P., Siitari-Kauppi, M., Timonen, J., Koskinen, L., (2015), Gas phase measurements of porosity, diffusion coefficient, and permeability in rock samples from Olkiluoto bedrock, Finland, Transport Porous Med. 107(1), 187-204.

[3] Kekäläinen, P., (2014), Analytical solutions to matrix diffusion problems, AIP Conference Proceedings 1618(1), 513-516.

Indigenous solid/liquid partitioning of Cs, Sr and U in some soil and sediment samples from the Olkiluoto site and its surroundings

Ari T. K. Ikonen ¹ & Anne-Maj Lahdenperä ²

¹ EnviroCase Ltd., Hallituskatu 1 D 4, 28100 Pori, Finland
ari.ikonen@envirocase.fi

² Saanio & Riekkola Oy, Laulukuja 4, 00420 Helsinki, Finland
anne-maj.lahdenpera@sroy.fi

INTRODUCTION

The Olkiluoto Island on the western coast of Finland has been selected as a repository site for nuclear waste. At this site, the post-glacial crustal rebound shapes the landscape from a coastal to an inland type within a few millennia in the future (*i.e.*, in the time frame in which releases from the waste repositories could reach the biosphere). The land uplift and the shoreline displacement will change the local biosphere conditions and influence soil and sediment properties and the groundwater flow pattern. As these effects are important for the long-term safety and biosphere assessments that address the radiation exposure of people and biota in scenarios of radionuclide releases, a broad range of hydrogeochemical conditions in various types of soils and sediments needs to be duly considered. The sorption of the radionuclides released from the waste in soils and sediments is an integral part of such modelling, the solid/liquid partition coefficient (K_d) is a key parameter, and often the indigenous stable isotopes of the same elements are used as analogues to the long-lived radioisotopes. In this contribution, a dataset of so-called *in situ* K_d data for Cs, Sr and U is studied for relationships between the K_d values and other soil and sediment properties.

MATERIALS AND METHODS

For the field data, samples of forest, mire and agricultural soils, lake sediments, and coastal gyttja analysed within Posiva's Olkiluoto repository programme (Haapanen *et al.* 2012; Lahdenperä 2013; Lahdenperä in prep.) are utilised here. In addition to the K_d data, pH, C concentration and fraction of fines (clay and silt, *i.e.*, grain size <0.06 mm) in the same samples are considered. For the *in situ* K_d values, fresh soil samples were incubated for one week at room temperature and afterwards centrifuged (5000 rpm, 15 min.). The extracted pore solution was aspirated through a 0.45 µm filter and acidified using de-ionised HNO₃ to pH <2 before the determination of element concentrations. The element concentrations in the solids fraction were determined after drying at 50°C, homogenisation by grinding, and HNO₃-HF(trace) digestion or LiBO₂ fusion. An ICP-SFMS equipment was used to determine the element concentrations. The K_d values ((µg/kg dry)/(µg/l)) were calculated as the ratio of the element concentration in the dried solids (µg/kg_{dw}) to that in the extracted pore solution (µg/l), subtracted with the residual moisture content of the solids after the extraction (l/kg) (as by Sheppard *et al.* 2009). pH (SFS-ISO 1090), grain size distribution and C concentration (DIN ISO 10694) were determined from the bulk material. The observed K_d values are here also compared with respective values predicted with the regressions (Sheppard *et al.* 2009) of K_d with pH and contents of fines.

RESULTS AND CONCLUSIONS

In the dataset, the peat samples represent, as typical, a high carbon content, low pH and undetermined but at most marginal amount of fines. The samples most rich in fines are forest soils and lake sediments. Otherwise there are no clear relationships between these properties except for the general tendency of increase in pH with increasing fines fraction (Figure 1A).

The K_d of Cs exhibits a tendency of increasing with pH, a weak tendency of decreasing with C content for the organic soil layers but not for the mineral soils and sediments, and K_d very weakly increasing with the content of fines. The observed K_d values agree very well with those predicted with the regressions (*i.e.*, the observed and the predicted values are within an order of magnitude from each other, except for few samples). With the K_d for Sr, there is a trend of increase with pH for the mineral soil/sediment layers but no clear trend for the organic ones, whereas there is an increase with C content for the organic but not for the mineral layers. Comparison of the K_d with the fines content does not add much to the previous. Again there is a fairly good agreement between the observed and the predicted values, but less so than for Cs. The K_d for U exhibits the typical increase with pH for lower and decrease for higher pH values (with a peak around 4–5; Figure 1B), although with a considerable spread of the data points. Also, a very clear increase in K_d with the C content is observed for the mineral layers, with a drop towards the high C content of the organic layers. However, there is a large variability in the K_d values of the peat samples. No clear trends in respect of the fines content is seen. The observed and the predicted K_d values for U agree reasonably well, except for the lake sediments. This implies that some relevant co-factors are not included in the regression used for the predictions (the source, Sheppard *et al.* 2009, considered only forest, mire and agricultural soils in Sweden). It is to be noted, also, that the predicted values could not be calculated for peat, humus and gyttja samples due to lacking grain size data, and that the original regressions used the clay fraction as opposed to equating it here with the fines fraction reported in the dataset studied here. Also, due to the limited scope of this study and the limitations of the dataset at hand, not all soil and sediment properties and conditions possibly affecting the K_d values (*e.g.*, other indicators of redox conditions or competing elements, depending on the element addressed) could be included.

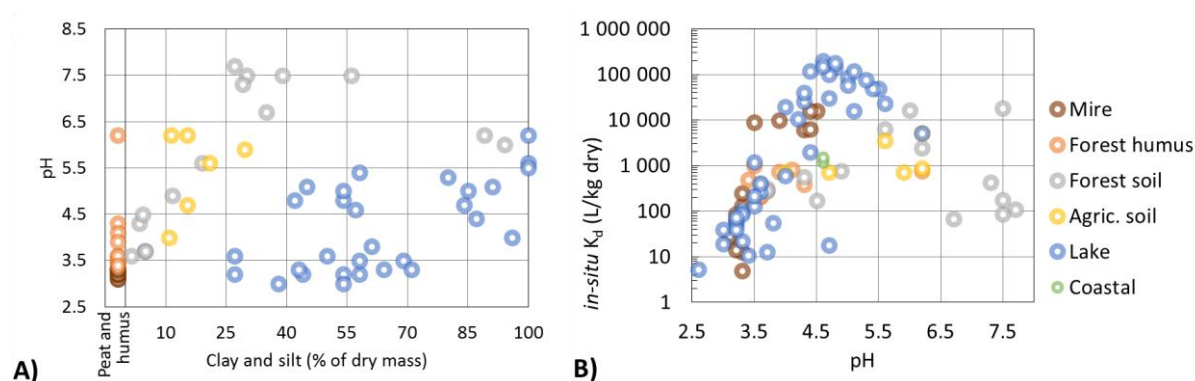


Figure 1. Example results: **A)** pH vs. fines content, **B)** in situ K_d for U vs. pH in the samples.

As a conclusion, it seems feasible to credibly use regression models to fill in data gaps in K_d data for modelling, provided that the data basis to establish the regressions is representative enough to the purpose. However, some caveats remain, and also sorption experiments with tracers are needed anyway especially for sufficient process understanding hard to gain through direct analysis of field samples alone.

REFERENCES

- Haapanen, R., Aro, L., Helin, J. Ikonen, A.T.K. & Lahdenperä, A-M. 2012. Studies on Reference mires: 1. Lastensuo and Pesänsuo in 2011–2012. Working Report 2012-102. Posiva Oy, Eurajoki, Finland. 84 pp.
- Lahdenperä, A-M. 2013. Geochemical and physical properties, distribution coefficients of soils and sediments at the Olkiluoto Island and the Reference Area in 2010-2011. Working Report 2013-66. Posiva Oy, Eurajoki, Finland. 84 pp.
- Sheppard, S., Long, J., Sanipelli, B. & Sohlenius, G. 2009. Solid/liquid partition coefficients (K_d) for selected soils and sediments at Forsmark and Laxemar-Simpevarp. Report R-09-27. Swedish Nuclear Fuel and Waste Management Co. (SKB), Stockholm. 78 pp.

Uptake of nickel by bacteria and fungus isolated from a nutrient-poor boreal bog

Jenna Knuutinen¹, Malin Bomberg², Jukka Lehto¹, Merja Lusa¹

¹ Laboratory of Radiochemistry, Department of Chemistry, University of Helsinki, Helsinki, Finland.

² VTT Technical Research Center of Finland, Espoo, Finland
jenna.knuutinen@helsinki.fi

In nuclear power reactors, activation of the corrosion products results in the formation of radioactive nickel (⁵⁹Ni). In addition to nuclear energy production, Ni mining and industrial use also result in environmental Ni pollution. Many environmental microbes have an ability to bind nickel, and various Ni uptake mechanisms, including biosorption on cell wall structures and active bioaccumulation, have been presented. In the boreal region, nutrient-poor bogs represent unique ecological niches, with distinct microbial populations. However, so far there is only limited knowledge about the metabolism of the microbes inhabiting northern bogs. Previously we isolated six bacterial strains belonging to genera *Pseudomonas* (PS-0-L, T5-6-L), *Burkholderia* (K5-6-SY), *Rhodococcus* (B6-7-CB) and *Paenibacillus* (V0-1-LW, B6-7-W) (Figure 1.) from the boreal nutrient-poor Lastensuo bog, and all of these bacteria were able to remove Ni from nutrient broths [4]. The previously isolated bacteria represented only a minority of the bacterial population of the studied bog. Here, we aimed to isolate new bacterial and fungal strains from the same bog, identify them by 16S and 18S rRNA gene sequencing and to investigate the Ni uptake of these microbial strains using batch experiments with ⁶³Ni²⁺. In addition, the morphology of the isolated fungus before and after incubation with 9·10⁻⁴ M Ni²⁺ was examined using transmission electron microscopy (TEM).

Bacteria and fungi were isolated from peat samples using a serial dilution method and Tryptone Soya Agar¹, R2A Agar¹, Plate Count Agar¹, Potato Dextrose Agar¹ or Malt Extract Agar¹ plates. The plates were incubated at 20°C for 1 week in the dark. Pure cultures were prepared on corresponding agar plates by consecutive streak dilutions. Bacterial cells from each pure culture were Gram stained and examined using a light microscope (Nikon ECLIPSE E200) with 1000-fold magnification and eight bacterial strains (2 Gram⁺ and 6 Gram⁻) and one fungus were selected for further studies.

For identification of the microbial isolates, DNA was first extracted using NucleoSpin Soil DNA extraction kit (Macherey-Nagel) where after the DNA samples were sent for purification and sequencing of the 16S and 18S rRNA genes to Macrogen Inc., Belgium. The sequences were subjected to phylogenetic analysis using the Geneious Pro v. 6.1.6. (Biomatters Ltd.) software, based on which the isolated bacteria affiliated with genera *Paenibacillus* (KV-0-YR, IV-0-L and VV-0-L), *Bacillus* (VP-0-W and V6-7-LL), *Massilia* (K5-6-BS and P5-6-BD) and *Methylobacterium* (P4-5-LR) (Figure 1). The isolated fungus represented genus *Exophiala* (M4-5-BD).

Uptake of Ni by the isolated bacteria and fungus was studied using batch experiments in two different growth media, 1 % Tryptone and 1 % Yeast extract, at 20°C with incubation times of 7 and 14 days. The initial nickel (⁶³Ni) concentration was adjusted to 14 Bq/mL and 0.2-1.4 mg DW (dry weight)/mL of bacteria or fungus was added depending on the microbial strain used. After incubation, the microbial biomass was separated from the broth by filtration through a 0.2 µm syringe filter and the final ⁶³Ni activity of the remaining broth was determined using liquid scintillation counter (Quantulus, Perkin Elmer). The uptake of Ni by the cells was expressed as distribution coefficient (K_d, L/kg DW).

All studied isolates removed Ni from the solution, but the efficiency depended on the experimental conditions. Highest Ni uptake was shown by *Methylobacterium* P4-5-LR, with a maximum uptake of 400 L/kg DW after 14 days incubation in 1 % Tryptone. This bacterium also showed higher Ni retention (K_d values between 75 and 84 L/kg DW) than the other studied bacteria in 1 % Yeast extract. However, the maximum Ni uptake of this bacterium was significantly lower, than the uptake observed in the previously isolated bacteria, where *Pseudomonas* PS-0-L showed a maximum uptake of 1500 L/kg DW [4]. The highest uptake

by the *Paenibacillus* strains (KV-0-YR, IV-0-L and VV-0-L was observed in 1 % Yeast extract, with maximum K_d values of 44 L/kg DW, 11 L/kg DW and 90 L/kg DW for KV-0-YR, IV-0-L and VV-0-L, respectively. This is also significantly lower than previously observed for *Paenibacillus* strains V0-1-LW and B6-7-W (450 – 720 L/kg DW) [4]. The two *Bacillus* strains, VP-0-W and V6-7-LL, behaved quite differently and the highest uptake for strain VP-0-W was observed in 1 % Yeast extract (14 L/kg DW) and for V6-7-LL in 1 % Tryptone (15 L/kg DW). In addition, the highest nickel uptake for *Massilia* K5-6-SY occurred after 7 days incubation in 1 % Yeast extract (K_d 44 L/kg DW), while *Massilia* P5-6-BD showed Ni retention only in 1 % Tryptone (K_d 19 L/kg DW) (Figure 2A).

Based on the uptake experiments conducted with the new bacterial isolates (this study) and previously isolated bacterial strains, Ni uptake varies between different bacterial genera, depending on uptake conditions. Different species also appear to have variable Ni metabolism and significant variation in the ability to tolerate nickel between different species of the same bacterial genera exists.

In the morphological TEM images of *Exophiala* M4-5-BD after incubation with $9 \cdot 10^{-4}$ M Ni(II) solution, dense crystalline accumulates, suggesting that Ni affects the cellular processes and is probably accumulated into the cell, were observed (Figure 2 B and C). However, further analysis is still needed for more detailed elemental analysis of these accumulates.

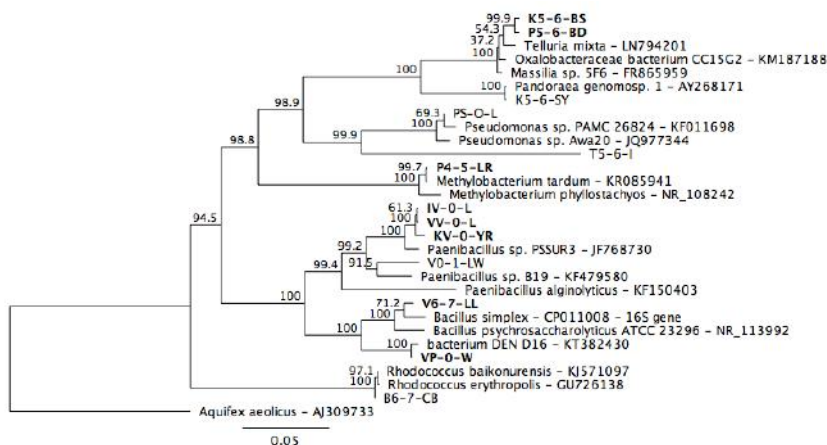


Figure 1. Phylogenetic tree constructed from the 16S rRNA gene sequences of bacterial isolates. Strain names in bold font represent new isolates of this study.

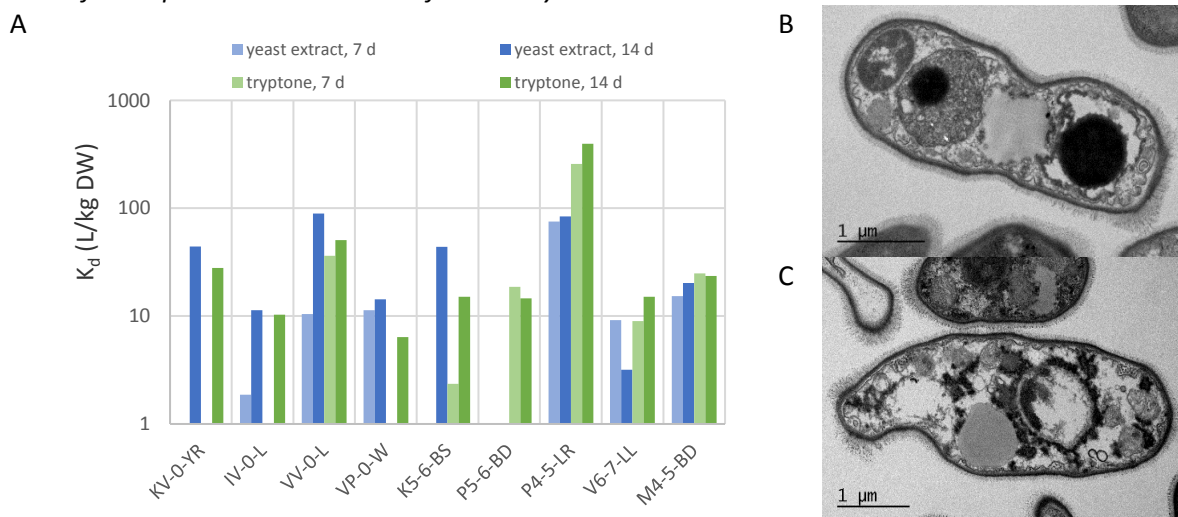


Figure 2. A) Uptake of nickel in 1% Tryptone and 1% Yeast extract by *Paenibacillus* KV-0-YR, IV-0-L and VV-0-L, *Bacillus* VP-0-W and V6-7-II, *Massilia* K5-6-BS and P5-6-BD, *Methylobacterium* P4-5-LR and *Exophiala* M4-5-BD. B) and C) TEM images of *Exophiala* M4-5-BD incubated without nickel (B) and with nickel ($9 \cdot 10^{-4}$ M)(C).

Speciation and sorption of iodine on boreal forest soil

Mervi Söderlund^a, Juhani Virkanen^b, Hanna Aromaa^a, Nadezda Gracheva^c, Jukka Lehto^a

^a*Laboratory of Radiochemistry, Department of Chemistry, P.O. BOX 55, FIN-00014 University of Helsinki, Finland, email: mervi.soderlund@helsinki.fi*

^b*Department of Geosciences and Geography, University of Helsinki, Finland*

^c*Radiochemistry Division, Chemistry Department, Lomonosov Moscow State University, Moscow, Russia*

¹²⁹I is one of the main concern radionuclides in the safety assessment of spent nuclear fuel in Finland. It has the potential to be one of the major dose inducing radionuclides for a man in the future due to its high content in the spent fuel (²³⁵U and ²³⁹Pu combined fission yield 2.2 %) long physical half-life of 15.7×10^6 years and presence as anionic moieties in a wide range of E_h-pH conditions in the final repository near-field and far-field environments. In the reducing repository conditions and surrounding near-field bedrock, iodine speciation is expected to be dominated by highly mobile and non-retaining iodide (I⁻). Upon further migration into far-field environments such as overburden and biosphere, oxidation to iodate (IO₃⁻) and formation of molecular iodine (I₂) and organo-iodine compounds is presumable.

Since iodine speciation has direct impact on its retention and migration behaviour in soil, it urged us to study the species transformation and sorption of iodide and iodate on humus and mineral soil samples of Olkiluoto, the site in southwestern Finland where the final disposal of Finnish spent nuclear fuel is to be executed in a deep underground cavity. For research purposes, a 4-metre deep boreal forest soil pit was excavated and samples were taken from five depths in addition to surface humus samples. These samples were used in batch experiments with stable iodide and iodate to determine iodine liquid phase speciation and concentration of the different species with HPLC-ICP-MS and to derive mass distribution coefficient (K_d) from the obtained results. The experimental conditions were varied in accordance with the oxidation-reduction status, pH, temperature, initial iodine concentration and microbial activity. Additional tests were done with pure minerals met in Olkiluoto soil.

Albeit iodide proved to be rather stable in the studied samples with the applied experimental conditions, significant transformation of iodate to iodide took place. The fraction of reduction of IO₃⁻ to I⁻ increased with time, anaerobic soil conditions, low pH, presence of microbes and temperature. For example, in humus the IO₃⁻ → I⁻ conversion increased from 25 % on day one to 41 % on day 21. In frozen soil only 0.47 % of iodate reduced to iodide upon soil thawing, whereas at a constant temperature of +22 °C vast reduction of 83 % was seen. In sterilised and non-sterilised soil samples the respective fraction was 0.24 % and 1.7 %. These results clearly indicate iodate to be unstable in the studied soil environment and its reduction to be dominated by soil microbial compartment.

Iodate conversion to unidentified organo-iodine species took place especially in organic matter rich humus samples and in pH 4–5 mineral soil samples (Figure 1). Small quantities of the unidentified species with retention time of 340 s (peak 3 in Figure 1) was also detected in aerobic samples. The formation of organo-iodine compounds in the same experimental conditions as for iodate was also seen for iodide but in a lesser extent. In the mineral background samples iodide was the species extracted from the soil, whereas in humus several different species occurred in addition to iodide. Thus, it is assumed that iodide can be stable in the mineral soil poor with organic matter, but in the soil layers enriched with organic matter significant change in the iodine speciation towards the dominance of organo-compounds occur. This change can be directly associated with soil microbes.

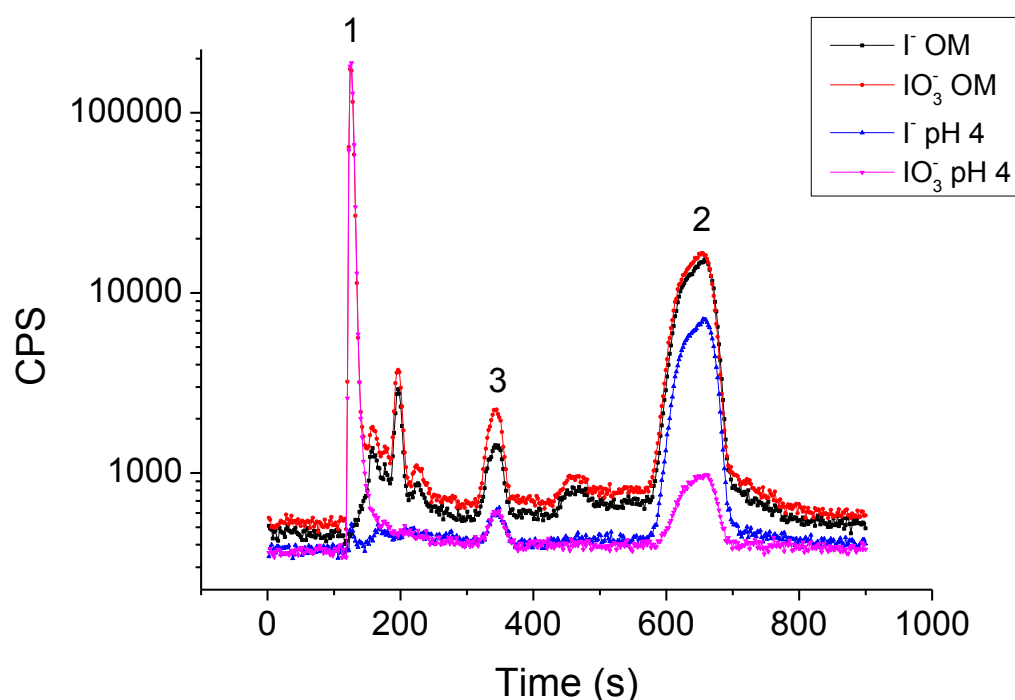


Figure 1. Chromatograms for iodide (I^-) and iodate (IO_3^-) in organic matter rich humus (OM) and in mineral soil at pH 4. Iodate (1), iodide (2) and organo-iodine (3) peaks can be distinguished from the chromatograms in addition to four unidentified iodine peaks in the chromatogram of iodine in humus.

The retention of iodine on Olkiluoto mineral soil was found to be very low as the highest K_d values were below 10 ml/g. Sorption increased with increasing organic matter content and weakly crystalline aluminium and iron oxide content, decreasing pH, rise in microbial activity and favourable aerobic soil conditions. Iodate was typically retained better than iodide probably caused by their different sorption mechanisms. Iodate tends to adhere by surface complexation like oxyanions selenite and phosphate, whereas iodide can be retained on mineral surfaces by anion exchange. It is likely that inorganic iodine species iodide and iodate exhibit considerable mobility in the mineral soil in lack of the retentive processes. Significant sorption of iodide and iodate took place in humus, as the K_d values reached 40 ml/g on day 21. The results suggest the importance of organic matter not only as a sorbent for anions, but also as a medium for microbially induced reduction processes and possible assimilation on organic compounds.

Effect of interlayer species charge on the swelling of Na⁺, K⁺ and Ca²⁺ montmorillonites: DFT and molecular dynamics studies

Eini Puhakka^a, Anniina Seppälä^b, Markus Olin^b

^a *Laboratory of Radiochemistry, Department of Chemistry, University of Helsinki, Finland*

^b *VTT Technical Research Centre of Finland Ltd, VTT, Finland*

The swelling and cation exchange properties of a smectite group mineral montmorillonite are fundamental in a wide range of applications such as fluid filtration, catalytic processes and the disposal of spent nuclear fuel. In the KBS-3 concept, a multi barrier system is planned to prevent/retard the release of radionuclides into biosphere. Montmorillonite is the main component of one barrier, bentonite clay. The retardation of radionuclides is based on diffusional transport and sorption on solid mineral surfaces; bentonite swells in contact with water thus blocking transport pathways and has a large specific surface area for effective retardation by sorption.

Montmorillonite is a very fine-grained and mechanically stable mineral which is characterized by the amount of layer charge (e/unit cell) and the location of the charge sites, tetrahedral and/or octahedral sheets. The sheets form negatively charged layers, the charge of which is compensating with cations between the layers and near the mineral surfaces. Montmorillonite has the ability to absorb water molecules into the interlayer space, which results in swelling of the mineral, and to change its cationic composition. Swelling and cation exchange properties also depend on solution properties like pH, ionic strength and ligands. Therefore the beneficial macroscopic properties of montmorillonites are based on the nano level structures and reactions.

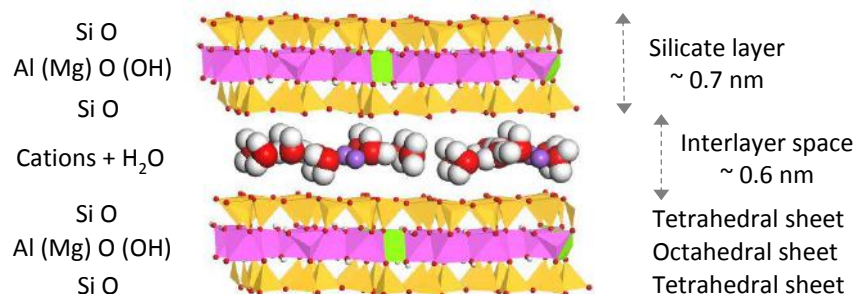


Figure 1. The layered structure of montmorillonite .

The swelling and cation exchange properties result from multiple factors and, though widely studied, data on the effects of charge (layer and interlayer charges) need additional clarification especially on the molecular level. In this study, quantum mechanics (QM) was used to obtain atomic level data on the swelling of montmorillonites, and interactions of chloride, hydroxide and phosphate salts on the edge surfaces of montmorillonites. In the QM calculations with CASTEP code (Materials Studio software), the total electronic energy and overall electronic density distribution were solved in order to define the energetically stable [1] montmorillonite-water structures in the presence of different salts. As a result, the sorption energies for salts on the montmorillonite edge surfaces were obtained.

The optimized montmorillonite structures defined by the QM methods were also utilized in MD simulations where swelling was studied by forcing water molecules into the interlayer and finding the equilibrium state of the system at a temperature of 298 K and pressure 1 bar. The MD method produces time evolution of a system, the trajectory, by solving Newton's equation of motion for the N-body system under the influence of specified forces. These calculations were used to evaluate equilibrium and transport properties that

cannot be calculated analytically. The studied systems were significantly larger than those in the QM calculations, and the calculations were done using the molecular dynamics software LAMMPS [2] with the CLAYFF [3] interaction potential.

Both the QM and MD calculations are based on the experimentally determined montmorillonite structures of Tsipursky and Drits [4]. In montmorillonites, the equivalent amount of exchangeable cations depends on the amount of Mg(II) atoms replacing Al(III) in the negatively charged octahedral sheets. In the structure by Tsipursky and Drits [4] for K-smectite, the Mg:Al ratio is 1:1. However, in montmorillonites, the typical Mg:Al ratio is 1:5, which was also used in this study. Further, typically the so-called dry montmorillonite contains about 8-10 wt-% water in its interlayer spaces. Based on the molecular mass of water and montmorillonite without interlayer water, the unit cell of the montmorillonite contains 2-4 water molecules. This means according to QM and MD simulations that only one water molecular layer exists in the interlayer space of the montmorillonite. When the water content is over 10 wt-%, the interlayer space between the negatively charged layers starts to increase causing the swelling of the montmorillonite.

According to the QM calculations, the increasing positive charge of the interlayer space has a retarding effect on the swelling. When considering sorption properties of sodium phosphate, sodium hydroxide and calcium chloride onto the edge surfaces of montmorillonites, it was detected that sorption of sodium phosphate strengthens when its amount increases. Otherwise the sorption of sodium hydroxide and calcium chloride decreases when their content increases on the edge surfaces.

The MD calculations were used successfully to determine the formation of water layer structure from one layer to three layers in the interlayer space of montmorillonites. Comparison with the QM results indicated that QM predicts larger d-values than MD. Further, the diffusion coefficients for water and different cations were defined based on MD results. Conclusion of the present work is that QM/MD techniques together are relevant methods to study nano level interactions which determine macroscopic phenomena related to montmorillonites.

Acknowledgements

The authors wish to acknowledge funding received from Posiva Oy.

References

- [1] A. R. Leach, Molecular Modelling, Principles and Applications, 2nd ed., Pearson Education Limited, Essex, (2001).
- [2] R. T. Cygan, J.-J. Liang, and A. G. Kalinichev, Molecular Models of Hydroxide, Oxyhydroxide, and Clay Phases and the Development of a General Force Field, J. Phys. Chem. B, 108, 1255-1266 (2004).
- [3] S. Plimpton, Fast Parallel Algorithms for Short-Range Molecular Dynamics, J. Comp. Phys., 117, 1-19 (1995). <http://lammps.sandia.gov>.
- [4] S. I. Tsipursky, and V. A. Drits, The distribution of octahedral cations in the 2:1 layers of dioctahedral smectites studied by oblique-texture electron diffraction, Clay Minerals, 19, 177-193, (1984).

Cm³⁺ incorporation in La_{1-x}Gd_xPO₄ monazites: a TRLFS and XAFS study

N. Huittinen¹, A. C. Scheinost^{1,2}, A. Wilden³, Y. Arinicheva³

¹Helmholtz-Zentrum Dresden-Rossendorf, Institute of Resource Ecology, Dresden, Germany

²The Rossendorf Beamline, The European Synchrotron Radiation Facility (ESRF), Grenoble, France

³Forschungszentrum Jülich, Institute of Energy and Climate Research, Nuclear Waste Management and Reactor Safety (IEK-6), Jülich, Germany

Crystalline ceramic materials show promise as potential waste forms for immobilization of high-level radioactive wastes. Especially for the immobilization of trivalent minor actinides (MA) and plutonium, some ceramic materials such as the lanthanide phosphates (LnPO₄) crystallizing in the monazite structure have been envisioned as host materials due to their thermal stability, high radiation tolerance, and chemical durability [1]. Thus, for a reliable long-term safety assessment of nuclear waste repositories for conditioned radioactive waste, a fundamental understanding of the MA incorporation process in these envisioned ceramic matrices is required. In the present study, the incorporation of the minor actinide Cm³⁺ in a series of La_{1-x}Gd_xPO₄ ($x = 0, 0.2, 0.5, 0.8, 1$) monazite solid solutions has been investigated using time-resolved laser fluorescence- (TRLFS) and Cm L₃-edge x-ray absorption fine-structure spectroscopy (XAFS). The Cm³⁺ excitation spectra obtained with the TRLFS method of the pure LaPO₄ and GdPO₄ end-members (Figure 1) show four well-resolved peaks corresponding to the 4-fold splitting of the Cm³⁺ ground state. The highly resolved ground-state splitting indicates the presence of only one, very well-defined, crystalline environment for the incorporated Cm³⁺ cation in the La and Gd monazite end-members. The situation changes when examining the solid solution compositions (La_{0.8}Gd_{0.2}PO₄, La_{0.5}Gd_{0.5}PO₄, and La_{0.2}Gd_{0.8}PO₄) where the complete loss of the splitting fine-structure and the broadening of the excitation peaks indicate a decrease of the short-range order in these solid solutions.

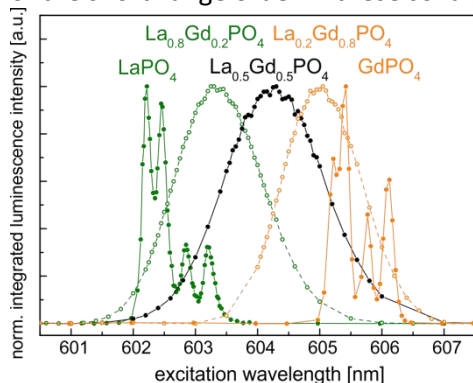


Figure 1. Excitation spectra of the synthetic La_{1-x}Gd_xPO₄ monazite solid solutions doped with 50 ppm Cm³⁺.

The fitting of the first coordination shell of our Cm L₃ XAFS data (Figure 2) for LaPO₄, La_{0.5}Gd_{0.5}PO₄, and GdPO₄, indicate a contraction of the Cm-O distance when going from the larger LaPO₄ monazite toward GdPO₄ (see Table 1). In addition the Debye-Waller (DW, σ^2) factor (which is an indicator for thermal and structural disorder) decreases substantially from 0.0079 Å² in LaPO₄ to 0.004 Å² in GdPO₄, while an increase is observed for the solid-solution composition (0.0112 Å²). The shortening of the Cm...O bond distance can be understood by the decreasing size of the monazite unit cell when going from the larger La³⁺-bearing host toward the smaller GdPO₄. The differences in the DW factors between the monazite end-members can be explained when examining our previously obtained results for Eu³⁺ incorporation in LnPO₄ monazites [2]. Here we could show that a larger mismatch between host and dopant radii causes a larger distortion of the monazite crystal lattice around the trivalent dopant. The cation radii of nine-fold coordinated La³⁺, Cm³⁺, and Gd³⁺ are 121.6 Å [3], 114.6 Å [4], and 110.7 Å [3], respectively. Thus, the larger mismatch of host and dopant radii in Cm³⁺-doped LaPO₄ could explain the larger DW factor than obtained for Cm³⁺ incorporation in GdPO₄. The large DW factor obtained for La_{0.5}Gd_{0.5}PO₄ in comparison to the monazite end-members is in concordance with the excitation line broadening observed for the monazite solid solutions in our Cm³⁺ excitation spectra (Figure

1), implying an increasing disordering of the monazite crystal structure. In our previous work investigating the incorporation of Eu^{3+} in $\text{La}_{1-x}\text{Gd}_x\text{PO}_4$ monazites [5], the systematic excitation line broadening could be attributed to an increasing broadening of the $\text{Eu}\cdots\text{O}$ bond distance distribution in the synthetic solid solution series when going from the pure end-members with very well-defined $\text{Eu}\cdots\text{O}$ distances toward the $\text{La}_{0.5}\text{Gd}_{0.5}\text{PO}_4$ composition.

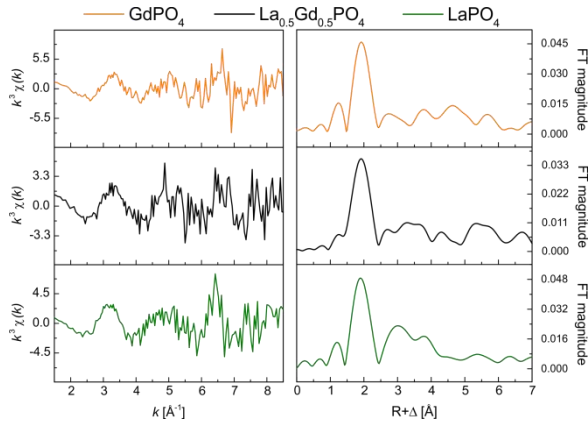


Figure 2: Cm L₃-edge XAFS spectra of the Cm-doped monazites.

Table 1. Cm-L₃ XAFS fit results of the Cm-doped monazites.

Sample	1 st Coordination shell				
	CN	R [Å]	σ^2 [Å ²]	ΔE_0 [eV]	χ^2_{res} %
LaPO ₄	6.4	2.46	0.0079	7.6	8.9
La _{0.5} Gd _{0.5} PO ₄	5.4	2.43	0.0112	8.8	10.5
GdPO ₄	4.2	2.42	0.0040	8.7	19.0

CN: coordination number, error $\pm 25\%$, R: Radial distance, error ± 0.01 Å, σ^2 : Debye-Waller factor, error ± 0.0005 Å², $S_0^2=0.7$, fit range $1.5 - 8.5$ Å⁻¹.

Our spectroscopic results obtained in the present study show that Cm^{3+} is substituted for the host cation sites in all investigated monazites. Although the spectroscopic data suggest a disordering of the monazite solid solution series due to less explicit $\text{Ln}\cdots\text{O}$ bond distances in the mixed solids, the spectroscopic investigations also imply that no preferential incorporation of dopants on host cation sites with similarly sized cation radii occurs, which is of great importance when considering the performance of monazite materials as immobilization matrices for highly radioactive actinide compounds.

- [1] G. R. Lumpkin (2006) "Ceramic waste forms for actinides." Elements 2: 365-372.
- [2] N. Huittinen et al. (submitted) Using Eu^{3+} as an atomic probe to investigate the local environment in LaPO_4 - GdPO_4 monazite end-members.
- [3] R. D. Shannon (1976) Revised effective ionic radii and systematic studies of interatomic distances in halides and chalcogenides. Acta Cryst. A32, 751-767.
- [4] F. H. David and V. Vokhmin (2003) Thermodynamic properties of some tri- and tetravalent actinide aquo ions. New J. Chem., 27, 1627-1632.
- [5] N. Huittinen et al. (submitted) Structural incorporation of Eu^{3+} in $\text{La}_{1-x}\text{Gd}_x\text{PO}_4$ monazite solid solutions: A combined spectroscopic and computational study.

Evidence of a new incorporation species of Eu(III) in calcite and its dependence of the background electrolyte

Hellebrandt, Sophia E.; Hofmann, Sascha; Jordan, Norbert; Barkleit, Astrid; Schmidt, Moritz

*Helmholtz-Zentrum Dresden-Rossendorf, Institute of Resource Ecology, Germany
sophia.hellebrandt@hzdr.de*

Calcite plays a significant role in nuclear waste disposal sites, both as a constituent of geological formations and as a secondary mineral, e.g. upon weathering of concrete. As such it has a direct impact on a repository's safety and performance. Geochemically, calcite has the potential to adsorb as well as incorporate guest ions with a similar ionic radius, e.g. Eu(III), Pu(III) and Am(III), for Ca(II) in the host lattice. For the safety assessment of nuclear waste disposal sites these trivalent actinides with long half-lives (especially Am) dominate its long-term radiotoxicity and are thus of particular interest.

Schmidt et al. investigated the influence of different dissolved cations on the incorporation process by [1] time-resolved laser fluorescence spectroscopy (TRLFS) with Eu(III)/Cm(III). They could show that there exists a coupled substitution mechanism $[Cm(III)/Eu(III) + Na(I) \leftrightarrow 2 Ca(II)]$. The experiments by Schmidt, et al. were performed under growth conditions, representative of the formation of a secondary phase. Calcite already present as a constituent of the host rock, however, would be more likely to interact with the contaminants at, or very close to equilibrium. Under these conditions its reactivity will be governed by its recrystallization rate, and different interaction mechanism – and consequently different contaminant speciation – may be expected.

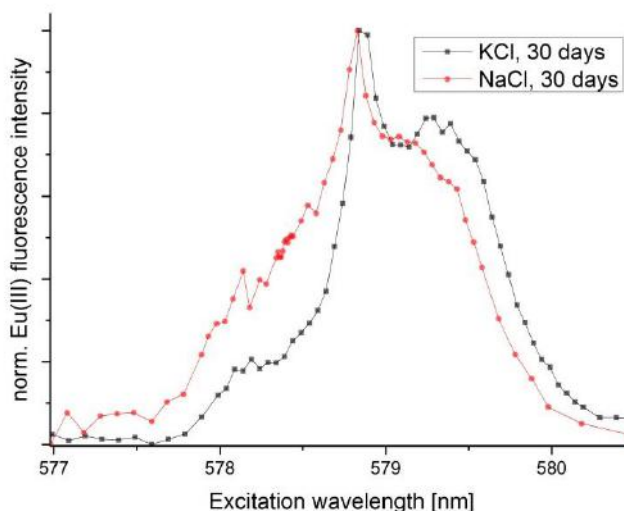


Fig. 1: ${}^7F_0 \rightarrow {}^5D_0$ Excitation spectra after a reaction time of 1 month with NaCl and KCl as background electrolyte, respectively. Spectra have been normalized to the intensity of the peak at 578.9 nm for easier comparison.

For our experiments we used Eu as homologue because of its similar ionic charge and radius, as well as its desirable luminescence properties [2]. We conducted batch studies with calcite powder in calcite saturated solutions with NaCl or KCl as background electrolyte. The speciation of the incorporated Eu(III) was then investigated by site-selective time-resolved laser fluorescence spectroscopy (TRLFS). The speciation of both systems is dominated by a species with its excitation maximum at 578.9 nm (Fig. 1), which had not been identified in previous investigations of this process under growth [1] and phase transformation conditions [3]. A long lifetime of $\sim 4000 \mu s$ demonstrates complete loss of hydration [4], consequently Eu must have

been incorporated into the bulk crystal. The corresponding emission spectrum shows the maximum splitting pattern implying a low symmetry of the ligand field surrounding Eu(III)[2]. After 1 month reaction time the excitation spectrum of the calcite in contact with NaCl shows a strongly blue-shifted excitation spectrum compared to the same calcite with KCl, demonstrating the effect of the background electrolyte on the Eu(III) speciation. As the peak at 579.3 nm belongs to a sorption species, this indicates enhanced incorporation in NaCl background relative to the KCl system. This may indicate that also under recrystallization conditions coupled substitution of Eu(III) and Na(I) for two Ca(II) is required for incorporation. Incorporation remains a significant interaction mechanism in the KCl system, likely due to a considerable amount of naturally occurring Na in the calcite .

The results show, that the speciation of Eu(III) in calcite depends on the conditions of its incorporation, i.e. growth *versus* recrystallization. A hitherto unknown incorporation has been identified, and our results strongly suggest incorporation under recrystallization conditions strongly depends on the availability of Na(I).

- [1] M. Schmidt, Angew. Chem., Int. Ed. 2008, 47, 5846-5850.
- [2] K.Binnemans, Coord. Chem. Rev. 2015,295, 1-45.
- [3] M. Schmidt, J. Colloid Interface Sci. 2010, 351, 50-56.
- [4] W. DeW. Horrocks, Jr., J. Am. Chem. Soc. 1979, 101, 334-340.

**Retardation and release of uranium on phlogopite mica at the absence and presence of humic acid:
A batch and TRLFS study**

Duoqiang Pan, Wangsuo Wu*

*Radiochemistry Laboratory, School of Nuclear Science & Technology, Lanzhou University, Lanzhou, Gansu
730000, China*

The batch experiments and cryogenic time-resolved laser-induced fluorescence spectroscopy (TRLFS) technique were applied to investigate uranium(VI) sorption/desorption on phlogopite at the absence and presence of humic acid (HA) in this work. The results showed that at the absence of HA, the uranium(VI) sorption on phlogopite was strongly dependent on pH while minimally affected by the ionic strength, multiple inner-sphere surface species (including $\equiv\text{SOUO}_2^+$, $\equiv\text{SO}(\text{UO}_2)_2(\text{OH})_2\text{CO}_3^-$ and $\equiv\text{SOUO}_2(\text{CO}_3)_x^{1-2x}$) were formed with their abundance varying as a function of pH, and a portion of uranium precipitated as uranyl oxyhydroxides at high pH (> 9). The presence of HA made little difference below pH 4 while inhibited uranium(VI) sorption above pH 4, and such effects became much more pronounced by increasing HA concentration from 20 mg/L to 50 mg/L. Fluorescence spectra indicated the formation of ternary surface complex at low pH, uranium-humate complex preferred binding directly on surface rather than via HA. Multiple aqueous uranium-humate complexes were responsible for the suppression of uranium sorption at high pH. The presence of HA enhanced uranium mobility without altering dominant surface species before and after desorption treatment.

Spectroscopic and microcalorimetric investigations on An(III)/Ln(III) complexes formed by the cement additive malate

F. Taube¹, M. Acker¹, S. Taut¹, T. Stumpf²

¹Dresden University of Technology, Central Radionuclide Laboratory, 01062 Dresden, Germany
email: franziska.taube1@tu-dresden.de

²Helmholtz-Zentrum Dresden-Rossendorf, Institute of Resource Ecology, Bautzner Landstraße 400, 01328 Dresden, Germany

High-level nuclear waste, whose long-term radiotoxicity is mainly determined by transuranium elements like americium, curium and plutonium [1], is going to be stored in canisters in deep geological formations. Cement is used for both conditioning of the waste and as backfill material or engineering barriers within the repository [2]. Due to the degradation of the concrete which might be caused by water intrusion in the waste repository, soluble components (sodium, potassium, calcium and cementitious admixtures) can be leached out from the cement matrix causing a highly alkaline medium (pH 9-13). The organic additives, which are used to improve the workability of fresh concrete after water contact, are potential complexation agents for radionuclides and might have an impact on the aqueous chemistry of actinides. There can be found a variety of additives like modified lignosulphonates, sulphonated melamines and poly(hydroxo)carboxylates. The α -hydroxydicarboxylic acid, malic acid is used in water-reducers or retarders. [3, 4] The understanding of the interactions of organic additives with radionuclides in solution is still very poor and only a few investigations on the effect of concrete admixtures on the aqueous speciation of actinides are available [3, 5].

This work describes the first experiments to generate a complete set of thermodynamic data for the complexation of Am(III) and Nd(III)/Eu(III) as chemical analogues for An(III) with the cement additive malate in order to be able to access the migration behaviour of An/Ln in a waste repository under cementitious influence. The complexation is first examined in the acidic pH range using different methods before extending the pH value into the alkaline range. EXAFS data with Am(III) are going to be presented to clarify the metal coordination and structural bindings.

Using UV/Vis measurements, two species were identified: NdMal^+ with $\log\beta_{110} = 4.88 \pm 0.61^*$ and NdMalH^{2+} with $\log\beta_{111} = 7.40 \pm 0.46^*$. A 1:2 complex also exists in solution but it could not be distinguished between NdMal_2H and $\text{Nd}(\text{MalH})_2^+$. A pH titration until pH 11 showed that an additional unknown mixed species $\text{NdMal}_2\text{OH}^{2-}$ might exist next to Nd-hydroxo complexes. With time-resolved laser-induced fluorescence spectroscopy (figure 1) two complex species, namely EuMal^+ with $\log\beta_{110} = 4.53 \pm 0.09^*$ and EuMal_2^- with $\log\beta_{120} = 7.72 \pm 0.50^*$ were determined. A ligand titration at pH 8 showed that the Eu-hydroxo complexes are suppressed by the complexation of Eu with malate so that malate complexation becomes dominant at this pH value. Microcalorimetric measurements with Nd and malate (table 1) prove that the reaction enthalpies are decreasing with increasing ionic strength like it was already expected considering other small organic ligands like lactat [6].

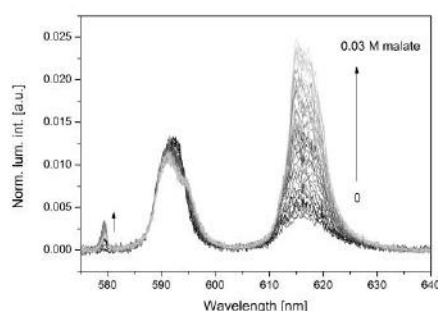


Figure 1: Fluorescence spectra of Eu malate titration at pH 6, $[\text{Eu}] = 5 \cdot 10^{-6} \text{ M}$

The datasets were used to calculate a proper speciation for the Nd(III) malate complexation in the acidic pH range at an ionic strength of 0.5 m NaCl including the protonation constants from literature [7–9] (figure 2).

Table 1: Stability constants and enthalpies of the Nd-malate complexation from microcalorimetric measurements at pH 6 and T=25°C, *...preliminary results

I=0.5		
n	$\log \beta_n [m]^*$	$\Delta H_n [kJ/mol]^*$
1	4.60±0.79	0.38±0.80
2	7.99±1.38	-1.07±0.21
3	11.08±1.29	-2.14±0.19
I=2		
n	$\log \beta_n [m]^*$	$\Delta H_n [kJ/mol]^*$
1	4.09±0.15	-0.86±0.11
2	6.96±2.24	-2.49±0.09
3	9.41±0.88	-5.90±0.31

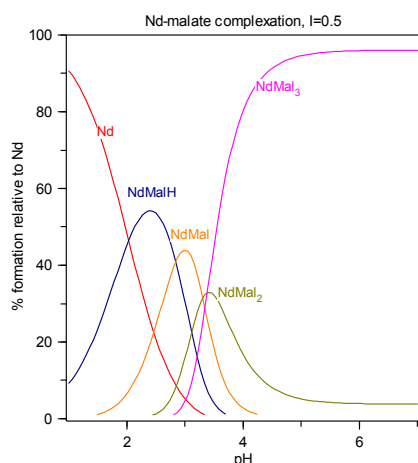


Figure 2: Resulting speciation using Nd-malate experiments

References

- [1] C. Poinssot and H. Geckeis, vol. 42. Woodhead Publishing Series in Energy, 2012.
- [2] A. Lommerzheim and M. Jobmann, DBE Technology, Peine, Technischer Bericht TEC-08-2014-Z, 2014.
- [3] M. A. Glaus and L. R. Van Loon, Paul Scherrer Institut, Technischer Bericht, 2004.
- [4] V. S. Ramachandran, National Research Council, Ontario, Canada: Noyes Publications, 1995.
- [5] E. Wieland, B. Lothenbach, M. A. Glaus, T. Thoenen, and B. Schwyn, *Appl. Geochem.*, vol. 49, pp. 126–142, Oct. 2014.
- [6] A. Barkleit, J. Kretzschmar, S. Tsushima, and M. Acker, *Dalton Trans.*, vol. 43, pp. 11221–11232, 2014.
- [7] I. V. Sukhno, V. Y. Buz'ko, V. T. Panushkin, and M. B. Gavriluk, *Russ. J. Coord. Chem.*, vol. 30, no. 8, pp. 591–598, 2004.
- [8] D. D. Perrin, IUPAC Chemical Data Series- No.22, Pergamon Press, pp. 168- 171, 1979.
- [9] H. Kitano, Y. Onishi, A. Kirishima, N. Sato, and O. Tochiyama, *Radiochim. Acta*, vol. 94, no. 9–11, pp. 541–547, Nov. 2006.

Radionuclide inventory of KAERI R&D radwastes

Hong Joo Ahn*, Kwang-Soon Choi, Byungman Kang, Kyungwon Seo, Junhyuck Kim, Kwang Yong Jee,
and Jei-Won Yeon

Nuclear Chemistry Research Division, KAERI, Daedeok-daero, Yuseong-gu, Daejeon, Republic of Korea

*[*ahjoo@kaeri.re.kr](mailto:ahjoo@kaeri.re.kr)*

Radioactive wastes in Korea have been widely divided into nuclear fuel cycle radwastes and non-nuclear fuel cycle radwastes. The nuclear fuel cycle radwastes are the waste arising in nuclear power plants (NPPs) and nuclear fuel fabrication facilities, and the non-nuclear fuel cycle radwastes are arising from educational settings, medical institutes, and various industries. As the non-nuclear fuel cycle radwastes, KAERI R&D radwastes are mostly arising in R&D activities and operation of a research reactor (HANARO), and approximately 10,000 drums are being temporarily stored in an interim site of KAERI. For a permanent disposal of the R&D radwastes, the evaluation of radionuclide inventories should be carried out based on the Korean Nuclear Safety and Security Commission (NSSC) Notice No. 2015-4, in which the acceptance criteria for LILWs is specified.

In this study, KAERI R&D wastes, such as spent air filters, metals and combustible wastes, were sampled at each R&D facility, and the activities of radionuclides were determined by radiochemical methods. The evaluations of radionuclide inventories were carried out by a representative sampling method and a scaling factor method. The analytical and estimated results of each drum were verified by using a statistical method with a reliability of within 2σ . Eventually, KAERI R&D waste drums including spent air filters and metals were permanently disposed on November 2015, and combustible wastes arising from HANARO research reactor will be evaluated by using the KAERI R&D scaling factor and transferred to a KORAD permanent disposal site.

Sorption properties of 60-Co and 137-Cs on nanocomposite material GO-TiO₂

Vojtěch Brynych^{*1}, Jana Pospěchová¹, Kateřina Kolomá¹, Markéta Kolářová¹, Václav Štengl², Jakub Tolasz²

¹ÚJV Řež, a. s., Waste Management & Fuel Cycle Chemistry Division, Husinec-Řež, Czech Republic

²Department of Materials Chemistry, Institute of Inorganic Chemistry, Husinec-Řež, Czech Republic

*vojtech.brynych@ujv.cz

The nuclear and radiation industry produces large volumes of waste with radionuclides. Cobalt and cesium have various applications in medical and industrial fields. Moreover, the spent nuclear fuel also contains cobalt and especially significant amount of cesium. 60-Co and 137-Cs with half-life 5.3 years and 31 years respectively are one of the key isotopes in terms of radiation safety. Both of these isotopes produce high intensity gamma-ray radiation and they pose risk for the environment, especially Cs(I) due to chemically similarity to K(I) and possible incorporation into living organisms.

Until now, composites of graphene oxide (GO) and TiO₂ were predominantly utilized as photocatalysts (Štengl, Bakardjieva, et al. 2013). The nanocomposite materials may be effective sorbent of radionuclide, e.g. (Chen et al. 2015) synthesized titanate/graphene oxide composite for sorption of radiocobalt.

The composite material GO-TiO₂ was synthesized according (Štengl, Henych, et al. 2013). Graphene was produced from natural graphite utilizing high-intensity cavitation field in a pressurized batch-ultrasonic reactor. GO was synthesized by modified Hummers method (Štengl 2012). The composite material GO-TiO₂ was prepared by homogeneous precipitation of Titanium(IV) Oxysulfate with urea in presence of GO. The final product was characterized by using X-ray diffraction, scanning electron microscopy (SEM) (Fig. 1) and transmission electron microscopy (TEM).

The radionuclide sorption on GO-TiO₂ was studied by two types of experimental setup - batch and dynamic method. The batch method is based on the contact of solid material with tracer solution. The volume of the solution was 1.5 ml and the mass of the sorbent was 0.01 g. The contact time was 24 hours. Sorption experiments were carried out at 24 °C under atmospheric conditions. After the adsorption of radionuclides, the suspension was centrifuged and an aliquot of the supernatant was measured on the gamma spectrometer. The batch method was utilized for determination of kinetics (Fig. 2) and Langmuir and Freundlich isotherms of Cs(I) and Co(II). The sorption of both Cs(I) and Co(II) on GO-TiO₂ can be better fitted by Langmuir model compared to Freundlich model. The maximum sorption capacities calculated from Langmuir model were 0.1 and 0.12 mmol/g for Cs(I) and Co(II), respectively.

The dynamic method (Palágyi et al. 2009) was utilized only for sorption of Cs(I). The results are demonstrated in Fig. 3. The dimensions of column were as follows: height, 6.5 cm; diameter, 1.2 cm; volume, 6 ml; frit, glass S3; pores diameter, 16-40 μm. The GO-TiO₂ has density 2.85 g/cm³ and grain size <125 μm. The sorption material (5.45 g) was put in the column. The column was oriented vertically and solution was injected from top by peristaltic pump with the flow 0.1 ml/min. The 3-H tracer was utilized for determination of column hydrodynamic properties and behavior of GO-TiO₂ for conservative non-sorbing tracer. Solution of CsCl 10⁻³ mol/L was utilized for the sorption experiments with Cs(I). The concentration of Cs(I) on the column outlet was measured by atomic absorption spectroscopy. The following parameters were utilized for the evaluation of column experiments: pore volume (PV), relative concentration of sorbate (*c_{rel}*), number of pore volumes (*n_{PV}*), retardation coefficient (*R*) and distribution coefficient (*K_d*).

The retardation coefficient *R* of 3-H calculated from the breakthrough curve (Fig. 3) was 1.11 corresponding to negligible sorption. The breakthrough curve for Cs(I) (Fig. 3) demonstrates strong sorption of Cs(I) on GO-

TiO₂ – R was 107 and distribution coefficient K_d was 103.6 ml/g. The Cs(I) was detected on the column outlet after the in-flow of 100 pore volumes, representing 500 ml of solution and 5 days of experiment.

The batch experiments on nanocomposite material GO-TiO₂ prepared by homogeneous precipitation demonstrated high sorption capabilities for Cs(I) and Co(II). The dynamic experiments were carried out only for Cs(I) and they confirmed good sorption capabilities. Although similar material prepared by (Chen et al. 2015) demonstrated higher sorption capabilities, the synthesis method was not identical and final material was approximately 20x more expensive.

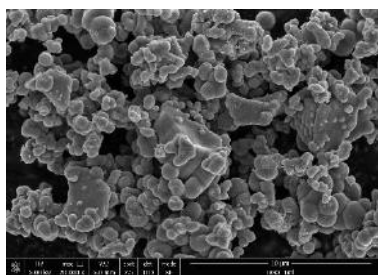


Fig. 1: SEM observations of GO-TiO₂

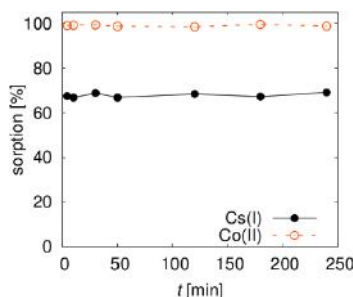


Fig. 2: Dependence of the sorption of Cs(I) and Co(II) on contact time

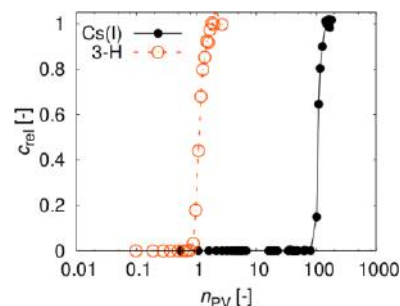


Fig. 3: The breakthrough curve of Cs(I) and 3-H in column filled with GO-TiO₂; the axis x is in logarithmic scale

The presentation/poster can be downloaded here: <https://goo.gl/IrMBwB>

Acknowledgments: We thank for support from TAČR project no. TA04020222 and NATO SfP project no. 984599.

References

- Chen, L.; Lu, S.; Wu, S.; Zhou, J.; Wang, X. J. Mol. Liq. **2015**, 209, 397–403.
 Štengl, V. Chem. - A Eur. J. **2012**, 18, 14047–14054.
 Štengl, V.; Bakardjieva, S.; Grygar, T. M.; Bludská, J.; Kormunda, M. Chem. Cent. J. **2013**, 7, 41 53.
 Štengl, V.; Henych, J.; Vomáčka, P.; Slušná, M. Photochem. Photobiol. **2013**, 89, 1038–1046.
 Palágyi, Š.; Vodičková, H.; Landa, J.; Palágyiová, J.; Laciok, A. J. Radioanal. Nucl. Chem. **2009**, 279, 431–441.

Study on volatility of ^{99}Tc and ^{137}Cs for the dry ashing of DAW

Kwang-Soon Choi*, Hee-Jung Im, Kyung Won Suh, Jaesik Hwang and Hong-Joo Ahn

Nuclear Chemistry Research Division, KAERI, Daedeok-daero, Yuseong-gu, Daejeon, Republic of Korea

**nkschoi@kaeri.re.kr*

The volatility of Tc_2O_7 and Cs_2O is temperature-dependent, so the heating temperature for the dry ashing of DAW (dry active waste) was examined from 200 to 500 °C using a paper towel as a simulated form of the DAW in a beaker and a SUS (stainless special use steel) planchet, respectively. The produced ash of the paper towel was completely dissolved in a mixture of 10 mL of HNO_3 , 4 mL of HCl , and 0.25 mL of HF on a hot plate. The amount of ^{99}Tc in the paper towel and the SUS planchet was determined by ICP-MS and gas proportional counter, respectively. ^{99}Tc on the SUS planchet and in the paper towel was quantitatively recovered upto 300 and 500 °C, respectively. While the recovery of ^{99}Tc on the SUS planchet decreased with increase of temperature from 350 to 500 °C. However, ^{137}Cs measured by gamma spectrometry was not volatile with a SUS planchet and a paper towel until 500 °C. In conclusion, the dry ashing temperature of DAW should be controlled below 500 °C.

Separation of radionuclides from the organic complexants using ionic liquids

Katerina Cubova, Barbara Basarabova, Mojmir Nemec, Marketa Florianova

Department of Nuclear Chemistry, Faculty of Nuclear Sciences and Physical Engineering, Czech Technical University, 115 19 Prague, Czech Republic

Before any adjustment, maintenance, control or decommissioning of the nuclear equipment, decontamination must be performed in order to reduce radiation fields and in this way to minimise the occupational radiation exposure. Many various mechanical, chemical or electrochemical methods have been proposed but all of them generate secondary waste containing the removed contaminants. The major volume of the secondary waste is usually represented by liquid waste that contains low activities of the radioactive substances (usually types of ILW or LLW). Technologies for the treatment of such liquid radioactive wastes are therefore focused to remove radionuclides from the bulk of the liquid and to concentrate the radioactivity into a small volume for subsequent conditioning and disposal. Resulting procedure will enable to significantly decrease the bulk of liquid radioactive waste which is generated during the current used processes of decontamination.

One of the possible ways could be the use of the ionic liquids. According to a commonly accepted definition, ionic liquids (ILs) are the salts with the melting point below 100°C, many of them are liquid even at room temperature (RTIL) [1]. ILs are composed of organic cations (including imidazolium, pyridinium, pyrrolidinium, ammonium and phosphonium) and anions (either organic or inorganic). The composition of ILs makes them unique system for studying the coordination chemistry and extraction mechanisms of metal ions. Due to the enhanced selectivity the use of ILs in liquid-liquid extraction seems to be very promising way for the separation of metals and radionuclides in the solutions resulting from the processes of decontamination and decommissioning or treatment of an industrial waste.

Liquid-liquid extraction of the metals and radionuclides of interest, screening of the optimum extraction parameters and the most suitable ionic liquids was tested. As an extraction phase, pure room temperature ionic liquids based on imidazolium cations and NTf₂ anions and solution of selected extraction agent in the IL were compared. For this purpose the CMPO was selected because of its extraction properties towards lanthanides and actinides. The selection of the particular metals and radionuclides was based on the common radionuclide inventory in the aqueous/liquid radioactive wastes coming from the solutions after decontamination and decommissioning, where Co-60 as the common activation product and Eu-152 as the representative of lanthanides were selected. The solution of these radionuclides in nitric acid was used as the aqueous phase, in addition two types of complexing agents – oxalic and citric acids as the representatives of the organic complexants usually present in decontamination solutions – were used. In the described system, the dependence of distribution ratios on pH, concentration of acids and composition of organic phase was tested. In the experiments, various ionic liquids were used as a pure solvent and diluent, for comparison and background extraction behaviour the organic phase consisting of CMPO solution in toluene was used.

Current results show that the used ionic liquids have significant influence and they are improving the extraction in the CMPO system compared to the CMPO solution in toluene. The distribution ratios are sufficiently high even at the presence of complexing agents allowing more than sufficient separation and the distribution ratios of Eu-152 are increasing with decreasing HNO₃ concentration. The results also showed that the structure and type of substituents of the ionic liquid are influencing extraction too. Direct extraction of

radionuclides into the ionic liquids showed that at the tested conditions the used hydrophobic ionic liquids do not extract the tested radionuclides at the moment.

References:

- [1] Mudring A.V., Tang S.: Eur. J. Inorg. Chem (2010), 2569-2581

Acknowledgement: This work was supported by grant project of the Technology Agency of the Czech Republic TH01020381

Modeling of the efficient ^{137}Cs decontamination of fresh and saline waters by a new cyanoferrate mesoporous material

Caroline Michel^{1,2}, Laurent De Windt³, Yves Barré¹, Caroline de Dieuleveult³, Agnès Grandjean¹

¹CEA, DEN, DTCD, SPDE, F-30207 Bagnols sur Cèze, France

²CEA, DEN, DTCD, SCDV, F-30207 Bagnols sur Cèze, France

³MINES ParisTech, PSL Research University, Centre de Géosciences, F-77305 Fontainebleau, France

The demand for effective and inexpensive treatment for decontamination of waters from radionuclides is high. In particular, ^{137}Cs is considered to be one of the most abundant and hazardous radionuclide due to its presence in many effluents and wastes. Furthermore, industrial and natural waters may contain a great variety of non-radioactive ions, such as alkaline and alkaline earth ions in concentrations several orders of magnitude greater than the levels reached by radionuclides. Thus the developed solid-phase extraction process must be highly selective for removing radionuclides in trace level from concentrated saline solutions. In this context the CEA (France) designed a selective adsorbent material for Cs (SORBMATECH® 202, S202), consisting of nanoparticles of potassium/copper ferrocyanide deposited in the mesoporosity of silica grains.

Several batch experiments (e.g. isotherms performed at different pH) were carried out in order to obtain kinetic and thermodynamic data of the cation exchange processes. Three water types of increasing salinity were considered: deionised water, Ca-bicarbonate fresh water and seawater. The S202 material proved to be an efficient decontaminating agent due to high sorption capacity (0.20 mmol/g) and distribution coefficients of ^{137}Cs ($K_d(\text{Cs}) = 10^5 - 10^6 \text{ mL/g}$), as well as fast kinetics of sorption. These experiences demonstrated the competitive effects of the cations naturally present in the natural waters (K^+ , Na^+ , Mg^{2+} and Ca^{2+}). Following a methodology previously developed for another ferrocyanide material [1], the chemical speciation code CHESS was used to determine the selectivity coefficients using the Vanselow's formalisms (Fig. 1A). CHESS was then applied to correctly modeled the cationic exchange population and $K_d(\text{Cs})$ over a wide range of Cs concentration for the different types of water (e.g. Fig. 1B in fresh water).

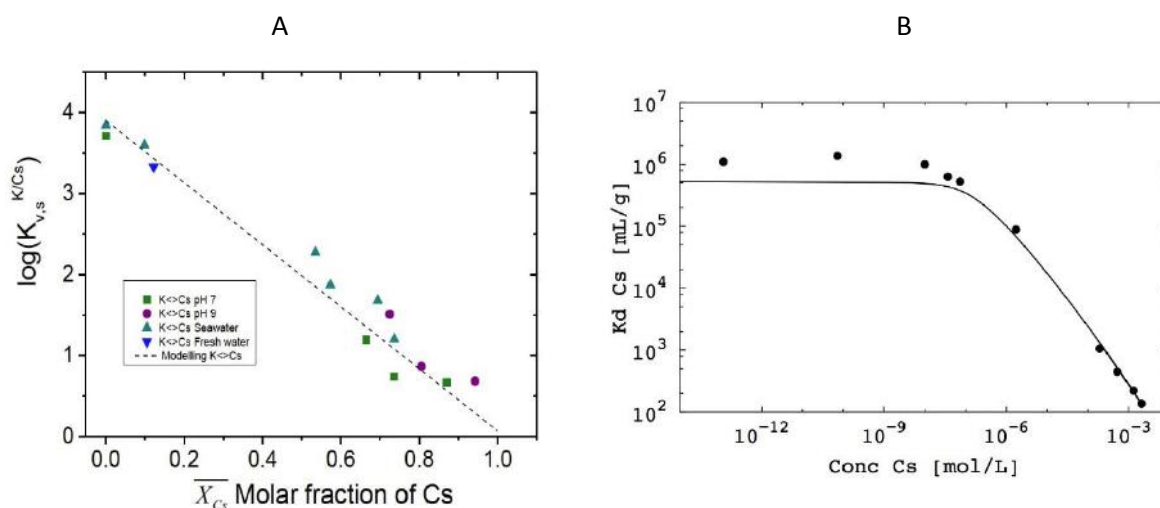


Figure 1. Properties of the S202 material. (A) Evolution of the selectivity coefficient with the molar fraction for a large range of Cs concentrations and different aqueous solutions (pure water, fresh water and seawater); (B) evolution of the ^{137}Cs distribution coefficient versus Cs concentration in fresh water.

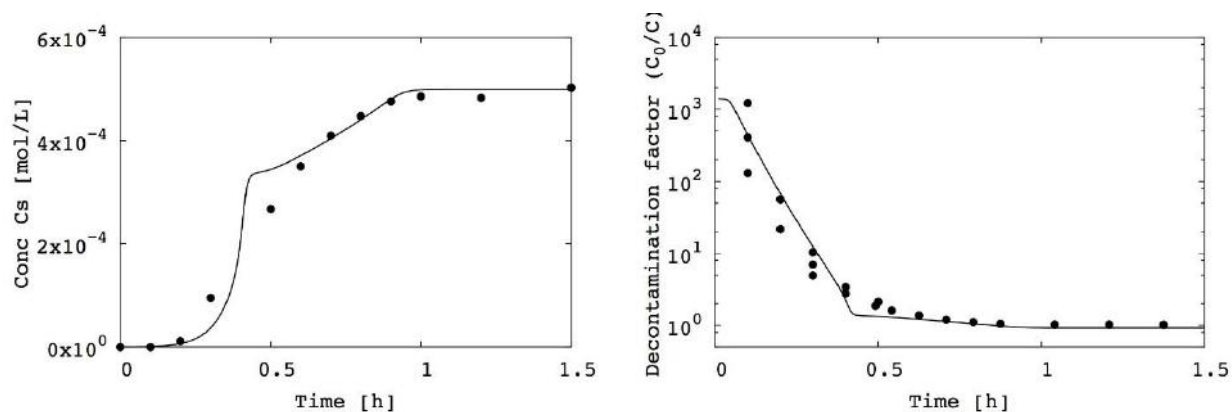


Figure 2. Experimental and modeling results of the breakthrough curve (A) and decontamination factor (B) of ^{137}Cs in fresh water and a S202 packed column at high flow rate.

The performance of the S202 material was tested in columns in a second stage of the study. Breakthrough curve experiments were carried out varying the flow rate and column geometry. The breakthrough curves and decontamination factors were modeled with the code OPTIPUR coupling water chemistry, ion exchange and reactive transport [2]. The experimental data were correctly modeled (e.g. Fig. 2 in fresh water) provided a dual diffusive transport within the S202 grains was taken into account in addition to convective/dispersive transport between the grains. The S202 material proved to be a promising candidate for application in the case of column decontamination processes since high flow-rates could be applied in column.

The present dataset can be extrapolated to other K-ferrocyanides and waters, eventually helping to support further designs of decontamination units.

- [1] Michel, C., Barré, Y., de Dieuleveult, C., Grandjean, A., De Windt, L. (2015). Cs ion exchange by a potassium nickel hexacyanoferrate loaded on a granular support. *Chemical Engineering Science* 137, 904-913.
- [2] Bachet, M., Jauberty, L., De Windt, L., Tevissen, E., de Dieuleveult, C., Schneider, H. (2014). Comparison of mass transfer coefficient approach and Nernst-Planck formulation in the reactive transport modeling of Co, Ni, and Ag removal by mixed-bed ion-exchange resins. *Industrial & Engineering Chemistry Research* 53, 11096-11106.

The flotation separation of rare earth elements – a contribution to reprocessing of the spent nuclear fuel

Fang-Li Fan¹, Zhi Qin^{1*}, Jie-Ru Wang¹, Fang Yang²

¹*Institute of Modern Physics, Chinese Academy of Sciences, 509 Nanchang Road, Lanzhou, 730000*

²*Xiamen Institute of Rare-earth Materials, Haixi Institute, Chinese Academy of Sciences, No.1300 Jimei Road, Xiamen, 361021*

Rare earth elements of the fission products generated during nuclear reactions, which have a large neutron absorption cross-section, such as Sm-149 ($\sigma=74500$ b), were called neutron poisons usually. Because these fission product poisons can absorb many neutrons in the nuclear reactors, they will have an impact on the continually running of nuclear reactors. Hence, it is necessary to separate these rare earth elements from spent nuclear fuel for advanced nuclear fuel cycling. Presently, solvent extraction is one of the most promising methods for the separation of rare earth metals during reprocessing of the spent nuclear fuel. But this method is complicated and must be repeated many times, resulting in energy and time consumption, high production costs and environmental pollution because of the large amount of organic solvents used. In order to increase the usage rate of spent fuel and decrease the disposition of nuclear waste, solid-solid separation is provided to remove rare earth elements from spent nuclear fuel. Flotation process was popularly used to separate rare earth elements from rare earth minerals. In this work, the feasibility of the flotation process was first investigated in the nuclear fuel reprocessing field.

In the experiment, the mixture of U_3O_8 and all kinds of rare earths oxide were regarded as simulate spent fuel. Flotation system was constituted by suitable ionic liquid, organic solvent and capture agents for rare earths oxide. U_3O_8 and rare earths oxide will not be dissolved in these liquids during the flotation experiment. Rare earths oxide will be removed from the mixture and the amount will be minimized after several flotation cycles. At the same time, the technological process experiments were also carried out using flotation machine. The amount of U and RE in the mixture was measured by XRF (X Ray Fluorescence spectroscopy) before and after separation. Figure 1 shows the separation results of U_3O_8 with all rare earths oxide. It can be concluded this simple flotation separation system can remove the rare earth elements from simulate spent fuel. The more detail experiments are ongoing in our laboratory.

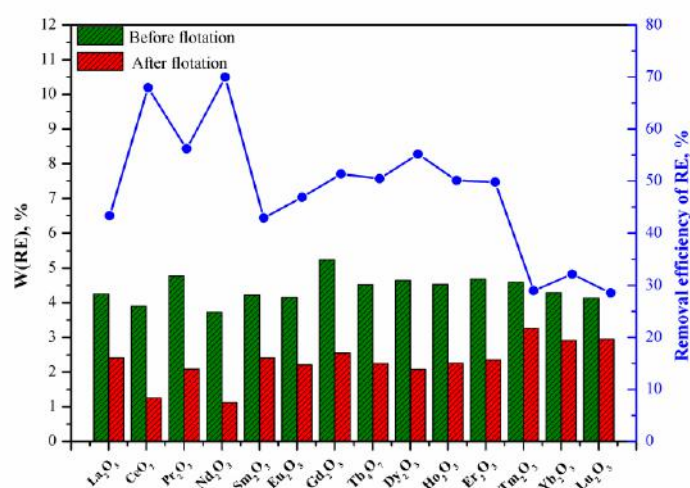


Figure 1. The separation results of U_3O_8 with all rare earths oxide

The recycling of radioactive concrete resulted from the decommissioning of the VVR-S nuclear research reactor

Daniela Gurau, Radu Deju, Mitica Dragusin

Horia Hulubei National Institute for R&D in Physics and Nuclear Engineering, Bucharest, Magurele, Romania

Within the nuclear industry, many installations or facilities that will start the decommissioning process, contain a large amount of structural or shielding concrete. This concrete is usually disposed as low-level radioactive waste (LLW) involving important economic and environmental consequences. Most often, the LLW is preplaced solidified with mortar (mixture of fine aggregate obtained from natural resources, cement and water) to provide adequate strength during disposal. The classic technology ensures a filling ratio of nearly 50% from the volume of each waste container, most of them being disposed in this final form. IFIN-HH, as the owner of the VVR-S nuclear research reactor and the manager of the decommissioning project, has the safe processing and disposal of the radioactive waste as a primary responsibility, respecting and applying the IAEA fundamental safety principles. All the practices that involve the recycling of the radioactive materials resulted from the decommissioning of the nuclear facilities are controlled based on the radiological protection principles that includes three main components: justification and optimization of the practice and the individual dose limitation. Usually, no practice involving exposure to ionizing radiation shall be adopted unless its application produces positive benefits. Considering this, IFIN-HH is the leader of a national research project that has as main purpose the minimization of the volume of the radioactive concrete (LLW) produced during the decommissioning project, taking into account all the applied legal requirements. Using the radioactive concrete as recycled fine aggregate in the mortar used to solidify the radioactive concrete rubble inside the disposal waste containers, it is intended to increase the fill ratio of radioactive concrete waste or to reduce the total LLW disposal volume. During this project, an innovative methodology has been developed, proposing a final waste disposal product (220 liter carbon steel drum) filled with a composite material containing radioactive concrete rubble immobilized in a mortar matrix made with fine aggregate obtained also from radioactive concrete. All technological processes must be executed preventing the spread of the radioactive contaminants in order to protect health of the workers, population and environment. In this paper is presented an international top issue regarding the minimization of the total amount of LLW that arise from the decommissioning of the nuclear facilities. Is presented the methodology for recycling the radioactive concrete, developed and implemented for the first time in Romania, in the same time innovative at international level. First, analyses were made using non-radioactive concrete in order to identify the proper mortar recipes which fit with the proposed specification for fluidity and allow obtaining the highest fill ratio for mortar. Two stages of crushing process were developed for producing recycled fine aggregate for mortar. The establishing of the concrete composition involves the evaluation of the components quantities necessary for preparing 1m³ of fresh concrete. Four types of mortar (R, P, DR and DP) were tested using recycled fine aggregate in composition with a particle size <2.5mm, obtained with C25/30 original concrete, crushed in the first stage with Jaw crusher and in the second with a hammer crusher. The results were compared with reference samples marked as N, obtained with natural river aggregates. The experiments were made both at laboratory level and on mock-ups in order to notice the most suitable parameters for the recycling of the radioactive concrete that will be in the end tested for validation in real conditions. The tests were performed to study the leaching behavior of ¹³⁷Cs, ⁶⁰Co and ¹⁵²Eu radionuclides from mortar made with natural aggregated and recycled radioactive concrete. Small cylindrical test samples (80 mm diameter and 15 mm height) with different composition and different curing time, were artificially contaminated and were marked as N, DR and DP for unique identification. The activity was evaluated using a dedicated gamma-ray spectrometry laboratory system consisting from a high purity germanium detector (model GEM60P4-95), a DSPEC jr. 2.0 Digital Gamma-Ray Spectrometer, a lead castle and a computer. Monte Carlo simulations based on GESPECOR code were used to evaluate the efficiencies. Glass jar with lid of 600 ml volume, placed on a

PVC pad were used to expose the entire surface of the cured mortar samples to 400 ml to leaching agent. After a period of time previously established, the water jar was transferred in cylindrical PE containers with sealing lids and then replaced with the same volume of fresh distilled water. Every time was checked if the water contain concrete residue. For the collected water samples, the pH was determined using a pH meter type WTW Inolab 720, the conductivity using a conductivity meter type WTW Inolab 720 and the activity using a gamma-ray spectrometry system. The leaching fraction value (λ_n/λ_i) (λ_n is the activity leached out of sample after the leaching time (Bq); λ_i is the initial sample activity at zero time (Bq)) was studied for concrete samples cured both for 28 days and for 56 days, comparing DR and DP samples with N samples. During the experiment, was observed that the high initial release of ^{137}Cs radionuclide which, however is quite short-lived, can be attributed to surface activities that are easily washed when the sample comes in contact with the leaching agent. To predict the leaching rate of ^{137}Cs , ^{60}Co and ^{152}Eu radionuclides of potential concern from immobilized waste matrix under continuously saturated condition that represent the worst case, the cumulative leach fraction (CLF) was evaluated with the following formula: $\text{CLF} = ((\lambda_n/\lambda_i)/(V/S))$, were: V is the sample volume (cm^3) and S is the sample surface (cm^2). Was observed that the leachate activity increased over 50%, for cement matrix made with recycled fine aggregates than cement matrix made with natural aggregates. To study the effect of natural and recycled aggregates concrete properties, mercury porosimetry was investigated. Was observed that the porosity appreciated through the specific pores volume (cm^3/g) present a higher value for DR mortar samples with recycled aggregates in composition, followed by DP samples with recycled aggregated and powder obtained by grinding. The mortar samples with natural aggregates present the lowest porosities. The proposed recycling technology is complex because a large number of technological variables of the process must be studied for the determination of the best conditions for fine aggregate fraction recycling. Also, high qualified workforce and dedicated scientific methods for radiological characterization of materials must be used. Regulatory requirements regarding nuclear field, environment, occupational health and safety should be respected. By carrying out these experiments, it is aimed to achieve, test and implement, for the first time at national level, a recycling technology that shows the use of radioactive concrete as fine aggregate for preparing the mortar that fills the empty space in the radioactive drums. The innovative method will be implemented to increase the filling ratio for radioactive concrete or to reduce the total volume of LLW.

Back-extraction in a Grouped ActiNide EXtraction system based on 1-octanol

Jenny Halleröd* and Mu Lin

*Nuclear Chemistry, Department of Chemistry and Chemical Engineering,
Chalmers University of Technology, Gothenburg, Sweden
hallerod@chalmers.se*

The electricity and electrical energy demand is very high, both in Sweden as well as in the other industrialised countries in the world. The overall amount of electrical energy required world-wide increases every day due to an expanding industrialisation together with a globally increasing population. One way to fulfil the energy demand is nuclear power. Modernisation of the nuclear power plants including recycling of the used nuclear fuel would make nuclear power a suitable option for sustainable energy.

A possible way to reuse used nuclear fuel is partitioning and transmutation of the present actinides. The partitioning and transmutation concept involves separation of the transuranic elements from the fission products present in the used nuclear fuel. The transuranic elements can then be transmuted using a fast neutron spectra. This technique reduces the radiotoxicity of the used nuclear fuel from over 100,000 years to around 1,000 years.

At Chalmers University of Technology, the main research focus within the partitioning and transmutation field has been the development of a Group ActiNide EXtraction (GANEX) process. The GANEX process is a liquid-liquid extraction process based on two cycles. The first cycle removes the uranium bulk from the used fuel dissolution liquor and the second cycle (the actual GANEX extraction) where the transuranic elements are separated from the fission products. The transuranic elements are extracted together as a group to avoid pure plutonium streams.

The GANEX process developed at Chalmers combines two extractants in a diluent. Several different combinations have during the years been examined. In this work, the back-extraction of a GANEX solvent based on the diluent 1-octanol containing CyMe₄-BTBP and TBP has been investigated.

Recyclable superparamagnetic adsorbent based on mesoporous carbon for sequestration of radioactive cesium

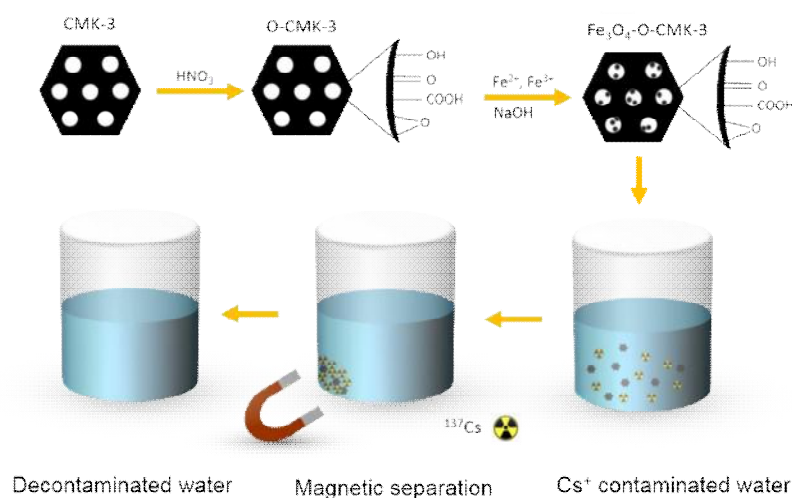
Syed M. Husnain ^a, Wooyong Um ^b, Yoon-Young Chang ^c and Yoon-Seok Chang ^{a*}

^a School of Environmental Science and Engineering

^b Division of Advanced Nuclear Engineering, Pohang University of Science and Technology (POSTECH),
Pohang 790-784, Republic of Korea

^c Department of Environmental Engineering, Kwangju University, Seoul 139-701, Republic of Korea

Novel and recyclable superparamagnetic adsorbent $\text{Fe}_3\text{O}_4\text{-O-CMK-3}$ was synthesized by *in situ* growth of nanometer sized magnetite particles (m-NPs) on the surface of mesoporous carbon at low temperature (70 °C) using ecologically-benign materials. Structural characterization by transmission electron microscopy (TEM) confirmed the formation of m-NPs surrounded by an oxidized mesoporous carbon layer ~20 nm thick. Thermogravimetric analysis (TGA) results revealed dense carboxylic groups and phenolic groups on the surface of $\text{Fe}_3\text{O}_4\text{-O-CMK-3}$. Because of these abundant polar groups the $\text{Fe}_3\text{O}_4\text{-O-CMK-3}$ had stronger adsorption affinity towards Cs than did magnetic mesoporous carbons O-Fe-CMK-3 synthesized by impregnation, and Fe-O-CMK-3 synthesized by co-casting, even in the presence of high concentrations of competing cations (K^+ , Na^+ , Li^+ , and Ca^{2+}). The $\text{Fe}_3\text{O}_4\text{-O-CMK-3}$ adsorbent reached a steady state quickly (< 5 min) with maximum adsorption capacity of 205 mg g^{-1} which is sufficiently higher than other magnetic adsorbents (usually lower than 110 mg g^{-1}) reported in the literature. The synthesized nanostructure adsorbent could be retrieved in a few seconds using an external magnet and reused several times for contaminant removal.



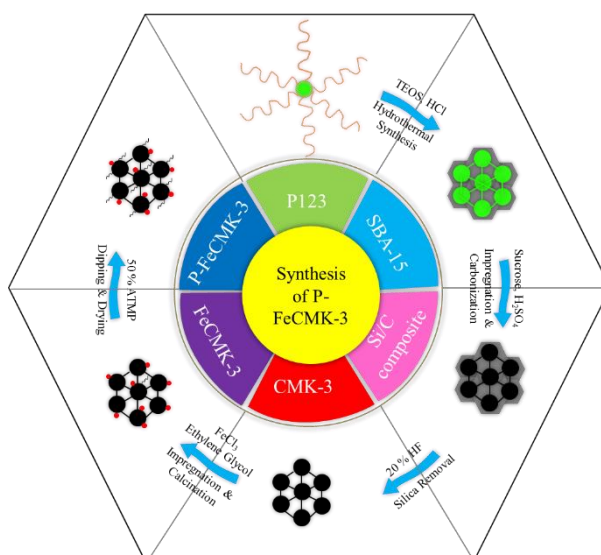
Synthesis of phosphonate modified magnetic mesoporous carbon for removal of uranium

Syed M. Husnain ^a, Wooyong Um ^b and Yoon-Seok Chang ^{a*}

^a School of Environmental Science and Engineering

^b Division of Advanced Nuclear Engineering, Pohang University of Science and Technology (POSTECH),
Pohang 790-784, Republic of Korea

Ordered mesoporous carbon functionalized with phosphonates groups and magnetic nanoparticles has been successfully synthesized by modifying the mesoporous carbon with amino trimethylenephosphonic acid (ATMP). Through the in-situ reduction of Fe^{3+} , magnetic nanoparticles were successfully incorporated into the mesopores, resulting in the multifunctional mesoporous carbon, P-Fe-CMK-3. The obtained composite carbon material possesses mesoporous structure, high Brunauer-Emmett-Teller (BET) surface area, large pore volume, phosphonate ligand on the surface, and excellent magnetic property. The functionalized hybrid inorganic-organic adsorbent also showed high efficiency for the removal of aqueous uranium from waste solutions.



Ashing characteristics of dry active wastes in nuclear power plants

Jaesik Hwang^{1*}, Simon Oh¹, Kwang-Soon Choi¹, Hong Joo Ahn¹, Jong Min Park²

¹*Nuclear Chemistry Research Division, Korea Atomic Energy Research Institute, 111 Daedeok-daero
989beon-gil, Yuseong-gu, Daejeon, Republic of Korea*

²*Korea Hydro & Nuclear Power Co., LTD, 1655, Bulguk-ro, Gyeongju-si, Gyeongsangbuk-do, Republic of
Korea*

* jaesikhwang@kaeri.re.kr

Dry active waste (DAW) is most common radioactive wastes in nuclear power plants. To dispose the DAW safely is accompanied of radionuclide analysis. A chemical analysis of DAW has technical difficulties due to its high volume, representatives of samples, and various decomposition characteristics. For that, it minimizes the volume by ashing and then dissolves using the various acids. However the ashing characteristics of DAW are different in the ashing time and temperature because of the various chemical compositions.

We investigated ashing characteristics for analytical samples arising from nuclear power plants. The analytical samples are prepared with three types of decontamination papers, polyurethane-coated gloves and cotton gloves. The weight of the each sample 50 g and cutting with the size of 10 by 10 mm. In order to ash the samples, the temperature of a furnace went from 673 to 473 K for four hours, and samples were ashed at 723 K for eight hours straight. After completely ashing, the ash amounts of samples were 0.49 g (1.04%), 0.3 g (0.6%) and 5.78 g (11.83%), respectively. In the ashing results, ashing ratio of the polyurethane-coated gloves was comparably very higher than other samples. For this reason, ashing with the polyurethane-coated gloves in the radiochemical analysis should be deeply considered because of representatives in the samples.

Solubility model for ferrous iron hydroxide in sodium chloride solutions spiked with sodium EDTA: a Pitzer approach

Je-Hun Jang^a and Martin Nemer^b

^a*Sandia National Laboratories¹, Defense Waste Management Programs, 4100 National Parks Highway,
Carlsbad NM 88220, U.S.A.*

^b*Sandia National Laboratories¹, Thermal and Fluid Sciences, 1515 Eubank Blvd SE, Albuquerque, NM 87123,
U.S.A.*

jjang@sandia.gov

The U.S. Department of Energy (DOE) Waste Isolation Pilot Plant (WIPP) is a deep underground repository for the permanent disposal of transuranic (TRU) radioactive waste. The WIPP is constructed in the embedded salt formation located in the Permian Delaware Basin near Carlsbad, New Mexico, U.S.A. The TRU waste includes, but is not limited to, iron-based alloys and organic complexing agents, such as ethylenediaminetetraacetic acid, H₄EDTA. Iron is also present from the steel used in the waste containers. The ferrous iron, Fe(+2), will be generated through anoxic corrosion of elemental iron, Fe(0), after closure of the WIPP. The dissolved ferrous iron, along with other dissolved metals such as calcium and magnesium, are expected to decrease the total dissolved concentration of EDTA(-4) by (a) forming solubility-limiting phases, and/or (b) competing with actinides for complexing with dissolved EDTA. The net result of dissolved metal - EDTA interactions is that there is less EDTA available for complexing with actinides, but the current WIPP model does not account for the Fe(+2) - EDTA(-4) interaction.

The objective of this analysis is to derive the Pitzer ion interaction parameters of pairs and/or triplets, the members of which are one of the aqueous complexes of Fe(+2) and EDTA(-4) and ion(s) of background electrolytes, in order to expand current WIPP thermodynamic database in a self-consistent manner under Pitzer formulation. The total dissolved Fe(+2) concentration was measured once the dissolution of ferrous iron hydroxide, Fe(OH)₂(s), reached equilibrium in sodium chloride solutions spiked with Na₂H₂EDTA. Anoxic gloveboxes were used to keep the oxygen level low (<1 ppm) throughout the experiments due to redox sensitivity of the experiments. An aqueous model for the Fe(+2) - Na(+1) - Cl(-1) - EDTA(-4) - H(+1) - H₂O system was fitted to the experimentally measured total dissolved Fe(+2) concentration. The aqueous model consists of several chemical reactions and uses the Pitzer activity coefficient equation to deal with the high ionic strength of the groundwater that could infiltrate the WIPP after closure.

EQ3NR, a computer program for geochemical aqueous speciation-solubility calculations, packaged in EQ3/6 v.8.0a, calculates the aqueous speciation using an aqueous model addressed in EQ3/6's database. The calculation of aqueous speciation was iterated by adjusting the Pitzer interaction parameters for the pairs/triplets of interest. The equilibrium constants of reactions (i.e., stability constants, solubility products) were adjusted if they were considered of low confidence. The iteration was performed until the parameter values were found that make the sum of squared difference between the 10-based logarithms of measured total dissolved Fe(+2) concentration and calculated total dissolved Fe(+2) concentration the smallest for the given number of experiments. Results will be presented at the time of conference.

Korean scaling factor for LILWs from nuclear power plants

Kwang Yong Jee¹⁾, Hong Joo Ahn¹⁾, Sun Ho Han¹⁾, Yong Jun Park¹⁾, Je-Won Yeon¹⁾, Hee Hwan Lee²⁾

¹⁾*Nuclear Chemistry Research Division, KAERI, Daedeok-daero, Yuseong-gu, Daejeon, Republic of Korea*

²⁾*Korea Hydro & Nuclear Power Co., LTD, Bulguk-ro, Gyeongju-si, Gyeongsangbuk-do, Republic of Korea*
nkyjee@kaeri.re.kr

According to the acceptance criteria for a low and intermediate level radioactive waste (LILW) listed in Notice No. 2015-4 of Korean Nuclear Safety and Security Commission (NSSC), specific concentrations of radionuclides in a drum has to be identified for a permanent disposition. To evaluate the radionuclide inventories in Korean NPP radwastes, dry active waste, spent resin and concentration bottom drums arising during 2004 ~ 2008 were destructively analyzed and eventually, Korean scaling factors were derived in 2009. Using the scaling factor, approximately 5,000 of LILWs drums from NPPs have been permanently disposed at an underground silo every year since it was first disposed of LILWs of Hanul NPP site in 2010. At present, 93,127 drums of the LILWs are stored in an interim storage facility of each nuclear power plant unit as of March 2016.

In Korea, new LILWs after 2008 are still analyzed radiochemically because the Notice clarifies that the Korean scaling factors should be verified biennially. To verify the scaling factor, some analytical samples in the dry active waste, spent resin and concentration bottom are being collected at each NPP units, and radionuclides concentrations were analyzed to compare with the established Korean scaling factors using statistical methods. In conclusions, the established scaling factors were verified with a reliability of within 2σ , and the Korean scaling factors will be applied to the new LILWs to evaluate the radionuclide inventories. Three times of periodic verification for the Korean scaling factor has been carried out up to now since 1st verification was carried out in 2010, and next verification is preparing this year.

Removal of cobalt and nickel from aqueous solutions with manganese dioxide sorbent produced by in-situ precipitation

M. Kaipainen, R. Koivula, R. Harjula

Laboratory of Radiochemistry, Department of Chemistry, University of Helsinki, Finland
maria.kaipainen@helsinki.fi

Numerous methods are used for the removal of heavy metals from industrial wastewaters, for example, ion exchange, adsorption, membrane filtration and electrochemical technologies, but it is still a challenge to remove metals effectively. Furthermore, the high content of alkali or alkaline earth metals in wastewater complicate a selective elimination of required metals. Selective ion exchangers, which demonstrate a high affinity for heavy metals, provide a possibility for their effective removal. Nowadays, conventional ion exchange materials are prepared from synthetic polymers, for example, polystyrene divinylbenzene, or inorganic compounds. Inorganic oxide, as ferric, aluminum, titanium and manganese oxides, based exchangers own such characteristic advantages as good chemical and thermal stability, high capacity and selectivity.

Manganese oxides that might be used as mineral or synthetic sorbents show ion-sieve properties, because of the layer or tunnel structures. Depending on structure of manganese oxide, the selectivity of cations changes. For example, todorokite minerals are effective for a wide range of radionuclides, due to the three-dimensional pore structure, the sequence of affinity in dilute nitric acid is $^{137}\text{Cs} > ^{57}\text{Co} > ^{63}\text{Ni} > ^{89}\text{Sr}$.¹ On the other hand, birnessite mineral has a layer structure and this type of manganese oxides demonstrates high affinity for cesium, as well for cobalt and nickel. However, Cs^+ ions adsorb on birnessite mineral mainly by the formation of outer sphere complexes, but nickel ions also sorb by structural incorporation into the vacancy site.^{2,3} Peacock and Sherman suggest that nickel sorption on birnessite mineral may be irreversible, because of the structural incorporation of nickel ions to the mineral.³ Based on the previously mentioned studies, birnessite might be suitable sorbent for nickel and cobalt removal.

The objective of this study was to remove cobalt and nickel from aqueous solution by manganese oxide. We synthesized manganese oxide by in-situ precipitation method in simulated alkaline wastewater solution. This simulated solution, consisting of 2.5 mol/l of sodium and 0.2 mol/l potassium, was used as a base for synthesis and birnessite manganese dioxide was synthesized. The characterization of synthesized material was done by XRD and scanning electron microscopy (SEM). The sorption efficiency of the material for two metal cations (Ni and Co) was measured in sodium nitrate solution as a function of solution pH and contact time by batch experiments.

The results of batch experiments indicate that nickel sorption on synthesized manganese oxide in sodium nitrate solution increases with increasing pH; however, the cobalt sorption is independent on solution pH. The sorption capacities of studied manganese oxide for nickel and cobalt in sodium nitrate solution at neutral pH were calculated. The sorption capacity for cobalt was 0.90 mmol/g, what is higher than for nickel (0.63 mmol/g). Under optimal conditions in sodium nitrate solution, the removal efficiency of manganese oxides for both cations achieved 99 %. Furthermore, sorption isotherms for Ni/Na and Co/Na ions exchange were determined at neutral pH. We described the sorption experimental data by using the Langmuir and Freundlich isotherm models. Correlation coefficients demonstrate the following order to fit isotherms: Langmuir > Freundlich for both metal cations. In addition, selectivity coefficients for Ni/Na and Co/Na ion exchange reactions were calculated using the isotherm data. Due to the selectivity coefficient dependence on the concentration of metal on sorbent, there are two different ion exchange sites on manganese oxide for cobalt and nickel. Figure 1 demonstrates the selectivity coefficients for cobalt, where average $k_{\text{Co/Na}}$ is

5200 g/ml and 5 g/ml in concentration range 0 – 0.5 mmol/g and 0.5 – 1 mmol/g respectively. The selectivity coefficients for nickel have the same trend as for cobalt.

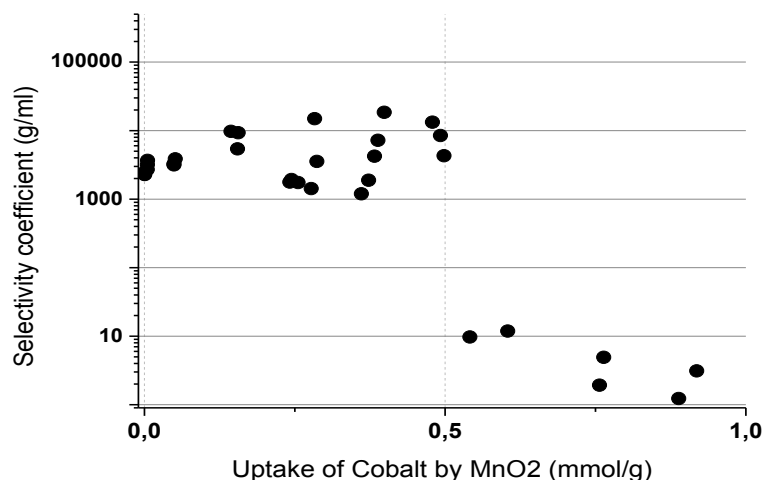


Figure 7. Dependence of selectivity coefficient $k_{\text{Co/Na}}$ on uptake of cobalt by manganese dioxide in neutral pH in 0.1 M NaNO₃ solution

The obtained capacity of manganese oxide and distribution coefficients for cobalt and nickel over sodium ions are promising for future applications in cobalt and nickel removal from aqua solutions with high sodium concentration. Next step in research is to investigate the in-situ precipitation of manganese oxide directly in industrial wastewater.

References

1. Dyer, A., Pillinger, M., Newton, J., Harjula, R., Möller, T. and Amin, S., Sorption Behavior of Radionuclides on Crystalline Synthetic Tunnel Manganese Oxides, *Chemistry of Materials* 2000, 12 (12), pp 3798-3804
2. Sasaki, K., Yu, Q., Momoki, T., Kaseyama, T., Adsorption characteristics of Cs⁺ on biogenic birnessite, *Applied Clay Science*, 2014, Vol 101, pp 23-29
3. Peacock, C.L. and Sherman, D. M., Sorption of Ni by birnessite: Equilibrium controls on Ni in seawater, *Chemical Geology*, 2007, Vol. 238, pp 94–106

An effect of bismuth ion on the reduction of lanthanum ion in molten LiCl-KCl eutectic salt

Beom Kyu Kim, Hwa Jeong Han and Byung Gi Park

*Department of Energy & Environmental Engineering, Soonchunhyang University, Soonchunhyangro 22,
Asan, Chungnam 336-745, Republic of Korea
krs@krs.or.kr*

The pyroprocess is an electrometallurgical process in the molten salt to recover uranium and transuranic elements from the used nuclear fuels (UNFs). [1] It is mainly envisaged for group separation of actinides from fission products for enhancing proliferation-resistance during reprocessing of UNFs. Radioactive wastes generated from the pyroprocess have various forms of metallic wastes, salt wastes, and so on. The salt wastes among them would be generated after recovery of uranium and transuranic elements with the electrometallurgical processes and be classified as a high-level radioactive waste by containing a residual actinide. Recovery and recycle of the residual actinide in the salt wastes allow radiotoxicity of the salt waste to be reduced to an intermediate-level radioactive waste. It will be beneficial to conditioning and disposing of radioactive wastes. PyroRedSox process was proposed to recover the residual actinide in the salt waste and to recycle into the electrometallurgical process. [1] It is a sequential process of electrolytic reduction and selectively oxidative extraction for recovery of residual actinide in the salt waste using molten salt-liquid metal extraction system. A combination of electrometallurgical process and molten salt-liquid metal extraction process would be expected to be the greater recovery efficiency of actinides in conditions of dilute concentration of actinides in comparison with lanthanides.

The electrolytic reduction can be achieved with liquid Bi metal electrode in the process. Reduction of metals into liquid Bi resulted in the formation of complex intermetallic compound with Bi metal. The co-reduction of rare-earth metals and bismuth would be occurred during electrolytic reductive extraction into liquid Bi metal in molten LiCl-KCl eutectic salt. The co-reduction consists of a simultaneous reduction of two or more metallic ions on an electrode to form an alloy of the two metals. Gibilaro et al.[2] have applied this process to remove lanthanides from the used salt and to recycle the purified salt and have investigated the Nd, Sm, and Ce extraction on inert electrode (W) in LiF-CaF₂-AlF₃ melts. Co-reduction by intermetallic compound formation would result in underpotential deposition in the electro-reduction process that is beneficial to the operation of unit processor for PyroRedSox process. Hence, it is necessary to understand the behavior of co-reduction under environment with and/or without bismuth chloride in the molten salt. In the present work, the effect of bismuth ion on the electro-reduction of lanthanum ion against liquid Bi electrode was investigated using electrochemical transient techniques. As shown in Figure 1, several peaks on pair of anodic and cathodic reaction were observed. Peak Cp1/Ap1 indicates redox reaction of lanthanum and other peaks indicate redox reactions of intermetallic compounds between lanthanum and bismuth. The addition of bismuth ion into the molten salt resulted in decrease of anodic peak Ap1 and increase of other anodic peaks. Randles-Sevick formula was used to estimate a concentration of lanthanum ion according to the addition of bismuth ion. Without bismuth ion, diffusion coefficient of lanthanum ion was estimated to be 8.18×10^{-5} cm²/s. If anodic peak Ap1 only depends on the lanthanum ion in the molten salt, co-reduction of lanthanum ion according to the addition of bismuth ion can be estimated with Randles-Sevick formula with the obtained diffusion coefficient. Figure 2 exhibits that lanthanum ion is reduced into liquid Bi metal as bismuth ion is increased. This indicates that bismuth ion affects the reduction of lanthanum ion by leading co-deposition.

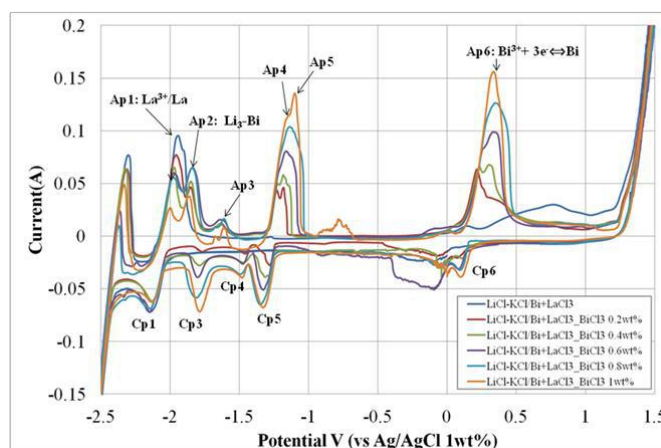


Figure 8. Cyclic voltammograms of LiCl-KCl-LaCl₃(1wt%) and at liquid Bi electrode with BiCl₃(0~1wt%)

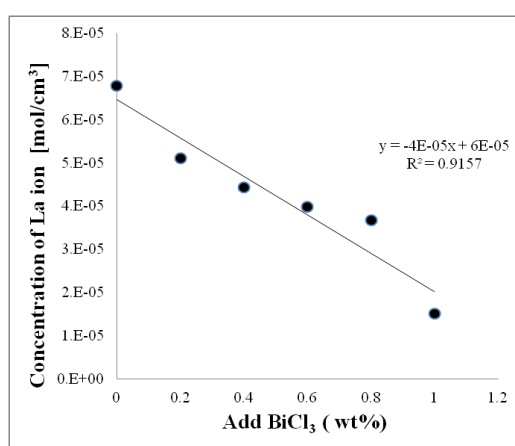


Figure 2. Reduction of the Lanthanum ion accompanied by increasing Bismuth ion

References

- [1] H. Lee, G. Park, K. Kang, J. Hur, J. Kim, D. Ahn, Y. Cho, E. Kim, "Pyroprocessing Technology Development at KAERI", Nuclear Science and Technology, 43(4), 2011, 317-328.
- [2] M. Gibilaro, L. Massot, P. Chamelot, P. Taxil, "Study of neodymium extraction in molten fluorides by electrochemical co-reduction with aluminum", Journal of Nuclear Materials, 382 (2008) 39.

Bismuth-based inorganic sorbents for the removal of iodine from subsurface plumes

T. Levitskaia ⁽¹⁾, M. Leonard ⁽¹⁾, J. Romero ⁽¹⁾, S. Chatterjee ⁽¹⁾, T. Varga ⁽²⁾, B. Schwenzer ⁽²⁾, T. Kaspar ⁽²⁾

Radiochemical Processing Laboratory, Pacific Northwest National Laboratory, Richland, WA, USA
Environmental Molecular Sciences Laboratory, Pacific Northwest National, Laboratory, Richland, WA, USA

Iodine-129 (¹²⁹I) is one of the most persistent radioactive isotopes present in subsurface plumes at the U.S. Department of Energy Hanford and Savannah River sites. It is of particular concern due to its long half-life ($t_{1/2} = 1.6 \times 10^7$ y), a high bioaccumulation factor (90% of all the body's iodine concentrates in the thyroid), a high inventory at source terms (due to its high fission yield), its ability to move rapidly in the environment, and its distribution over a large area. Currently there are very few approaches that effectively manage the risk that ¹²⁹I presents to human health and the environment, and removal of ¹²⁹I from the subsurface will substantially reduce these risks. In Hanford groundwater and vadose zone, ¹²⁹I exists in various chemical forms including iodate IO_3^- , iodide I^- , and organoiodine. It has been previously established that Hanford groundwater contains predominantly IO_3^- . Separation of iodate from groundwater via commercial ion exchange resins is limited in effectiveness. The objective of this study is to design inorganic sorbents that can effectively separate different species of iodine present in Hanford groundwater; specifically targeting the development of composite materials with high affinity for IO_3^- to enable direct removal of this contaminant from the groundwater in the pump and treat system without introducing the preconditioning steps such as reduction of IO_3^- to I^- .

Recent work at PNNL has focused on bismuth-based inorganic materials exhibiting high affinity for iodine in its various forms, with the aim of directly removing it from groundwater. A library of sorbents based on bismuth (III) has been synthesized and screened for iodine removal from deionized water and Hanford groundwater. Raman spectroscopy is used to monitor and quantify IO_3^- uptake, while inductively coupled plasma mass spectrometry (ICP/MS) is used to measure total iodine uptake in batch tests using Hanford groundwater. Several materials prepared at PNNL have demonstrated effective uptake of iodine.

The obtained materials were characterized by vibrational spectroscopy, x-ray diffraction (XRD), x-ray photoelectron spectroscopy (XPS), and scanning electron microscopy / energy dispersion spectroscopy (SEM/EDS) techniques before and after saturation with either KIO_3 or KI solution. It was observed that upon exposure to iodate both materials undergo molecular and crystalline structure reorganization generating nearly identical final mixed product containing IO_3^- and reduced I^- anions strongly bound to the Bi oxide layers. Exposure to iodide resulted in the formation of the bismuth oxiodide product, which can be interpreted as mixes of BiOI and $\text{Bi}_5\text{O}_7\text{I}$ phases.

[1] Zhang S, C Xu, D Creeley, Y-F Ho, H-P Li, R Grandbois, KA Schwehr, DI Kaplan, CM Yeager, D Wellman, and PH Santschi. 2013. Iodine-129 and Iodine-127 Speciation in Groundwater at the Hanford Site, U.S.: Iodate Incorporation into Calcite. *Environmental Science & Technology* 47:9635–9642.

The effect of initial solution pH on the removal of trace amounts of Co-60 from NPP waste water using UV-C irradiation, TiO₂ P25 and ion exchange material CoTreat

Leena Malinen*, Jussi-Matti Mäki**

**Laboratory of Radiochemistry, Department of Chemistry, University of Helsinki, Finland*

***Fortum Power and Heat Oy, Finland*

leena.k.malinen@helsinki.fi

One of the most problematic radionuclides in the liquid waste produced by nuclear power plants (NPPs) is Co-60 which has a relatively long half-life (5.2 a) and high gamma decay energy (1.3 and 1.2 MeV). In order to remove the radioactive metals, such as Co-60, from contaminated structures and equipment of NPPs, decontamination solutions are used. These solutions often contain complexing agents, such as ethylenediaminetetraacetic acid (EDTA). In addition, the liquid waste often contains high amounts of inactive metal ions and only low chemical concentration of Co-60. Therefore the method for its removal has to be highly selective and additional treatment methods such as advanced oxidation processes (AOPs) might be required to enable efficient cobalt removal [1].

The liquid waste used in this study was an evaporate concentrate from a boiling water reactor (BWR) NPP. It contained 14 g l⁻¹ Na, 1 g l⁻¹ K, 61 mg l⁻¹ Mg and 16 mg l⁻¹ Ca. The activity of Co-60 was 2,200 Bq l⁻¹ and solution pH was 8.4. The amount of TOC was approximately 119 mg l⁻¹. No exact information about the organic compounds in the solution was available. Assumptions were made that some organic complexing agents were the reason why there was 2,200 Bq l⁻¹ of Co-60 left in the solution after treating it with ion exchange resins. The experiments related to this liquid waste have been published earlier by the authors [2]. The purpose of the research presented now is to clarify the possible reasons why the specific results were obtained.

According to the results presented earlier [2], solution pH affected the efficiency of the two-step process (UV-C oxidation + ion-exchange) significantly. When the liquid waste was oxidized with UV-C light and photocatalyst, TiO₂ P25 Aeroxide (Evonik Industries), 900 Bq l⁻¹ Co-60 was left in the solution and the solution pH rose to 9.3. When the solution was further treated with CoTreat (Fortum), Co-60 activity decreased to 600 Bq l⁻¹ and the solution pH remained at the same level as prior to the batch experiment. When the solution pH was adjusted with HNO₃ to 3.5 prior to the UV-C oxidation, solution pH rose to 7.2 and 500 Bq l⁻¹ Co-60 was left in the solution. After batch treatment with CoTreat, the Co-60 activity in the solution decreased as low as 30 ± 10 Bq l⁻¹. These results have been collected in Figure 1. It has not been published earlier, that after the oxidation of the original solution TOC decreased to 87 ppm and after the oxidation of the pH adjusted solution TOC decreased to 19 ppm. This also highlights how strongly the oxidation effectivity was affected by the pH of the solution.

The point of zero charge (PZC) of TiO₂ Aeroxide P25 is approximately at pH 6.5 [3]. The surface of the material is therefore positively charged in an acidic medium (when pH < 6.5: TiOH + H⁺ ↔ TiOH₂⁺) and negatively charged in an alkaline medium (when pH > 6.5: TiOH + OH⁻ ↔ TiO⁻ + H₂O). To estimate the surface charge of possible cobalt species in the solution, the program Visual Minteq [4] was used. If an assumption was made that the solution would contain at least equimolar amounts of Co²⁺ and EDTA, mainly negatively charged complexes, CoHEDTA⁻ and CoEDTA²⁻, would be present in the solution at pH 3.5 and above pH 5 only CoEDTA²⁻ would be present in the solution. Below pH 6.5 the adsorption of the negatively charged complexes on the surface of the positively charged photocatalyst is possible. In addition to the formation of the electron-hole pairs in TiO₂ under UV-C irradiation, the oxidation of the substrates adsorbed onto the surface of the photocatalyst would be possible. However, it should be noted that even though the organic compounds in the solutions were known, the speciation in solution does not indicate the speciation on the surface of the photocatalyst.

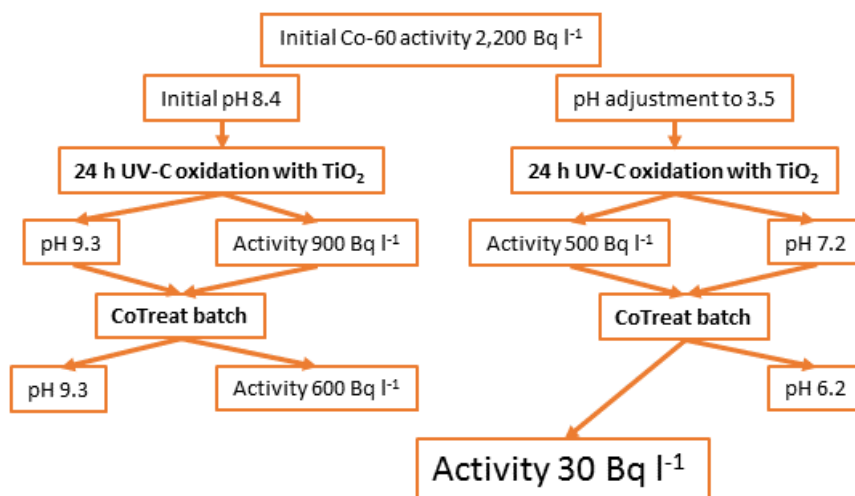


Figure 1. Co-60 activity and pH of a BWR NPP liquid waste prior to and after UV-C oxidation with TiO₂ P25 and CoTreat batch experiments.

As was seen from the results, TiO₂ P25 can also remove cobalt from the solution. Because the surface charge of TiO₂ P25 is positive below pH 6.5, the adsorption of the positively charged cobalt ions is hindered in acidic solutions. This can also partly explain why the photocatalytic efficiency of the material is higher when the solution pH was adjusted to 3.5 prior to the UV-C irradiation. In acidic solution, the adsorption of cobalt on the surface of the photocatalyst is insignificant and the surface of the photocatalyst remains “free” and available for photocatalysis. The progress of the oxidation of organic compounds causes the solution pH to rise and enables the change in the surface charge of the photocatalyst. When UV-C oxidation was done at pH 8.4, the negative surface charge of the photocatalyst made the adsorption of liberated cobalt ions possible. Thereby the surface of the material could have been blocked by cobalt and the photocatalytic efficiency of the material was lower. It should be taken into account that only a simplification of the oxidation process is presented here. The solid/solution system should be considered as a multiple ligand system, where EDTA and the surface compete for cationic cobalt.

References

- [1] L. K. Malinen, R. Koivula and R. Harjula, “Removal of Radiocobalt from EDTA-Complexes Using Oxidation and Selective Ion Exchange”, *Water Science & Technology*, 60.4, 1097 (2009).
- [2] L. Malinen, J.-M. Mäki, “Removal of Trace Amounts of Co-60 from NPP Waste Water Using UV-C Irradiation, TiO₂ and CoTreat Inorganic Ion Exchange Media”, *Proc. of the WM’16 Conference*, Phoenix, AZ, March 6-10, 2016.
- [3] M. Kosmulski, “Compilation of PZCs/IEPs” in *Surface Charging and Points of Zero Charge*, Surfactant Science Series 145, 454-459, CRC Press, Taylor and Francis Group (2009).
- [4] J. P. Gustafsson, Visual Minteq 3.0, a free equilibrium speciation model, <http://vminteq.lwr.kth.se/> (verified 22.3.2016).

Acknowledgements

Jenny and Antti Wihuri Foundation is highly appreciated for the financial support.

Adsorption properties of actinoids (U, Am, Np) for various zeolites

Hitoshi Mimura^{1*}, Minoru Matsukura¹, Natsuki Fujita², Hitoshi Kanda², Akira Kirishima³, Nobuaki Sato³

¹ UNION SHOWA K.K., 1-8-40 Kounan Minato-ku, Tokyo, 108-0075, JAPAN.

² Tohoku University, Graduate School of Engineering, Aramaki-Aza-Aoba, Aoba-ku, Sendai, JAPAN.

³ Tohoku University, Institute of Multidisciplinary Research for Advanced Materials, Katahira, Aoba-ku, Sendai, JAPAN.

*E-mail: hmimura@st.cat-v.ne.jp

Large amounts of highly contaminated water over 700,000 m³ accumulated in the reactor, turbine building and the trench in the facility were generated from the nuclear accident of Fukushima NPP-1 (BWR) caused by the Great East Japan Earthquake. At present, the cold shutdown is completed stably by the Circulating Injection Cooling System (SARRY, KURION) for the decontamination of radioactive nuclides such as ¹³⁴Cs and ¹³⁷Cs using zeolites and crystalline silicotitanates (CST), and the Advanced Liquid Processing System (ALPS) is operating for the decontamination of 62 nuclides such as ⁹⁰Sr, ¹²⁹I and ⁶⁰Co, etc. (Fig. 1). However, the adsorption behaviors of actinoids through the decontamination systems are complicated, and especially their adsorption properties for zeolites, a major adsorbent, are not yet clarified. This study deals with the distribution behaviors of actinoids (U, Am, Np) for various kinds of zeolites, and the adsorbability was clarified by batch adsorption method.

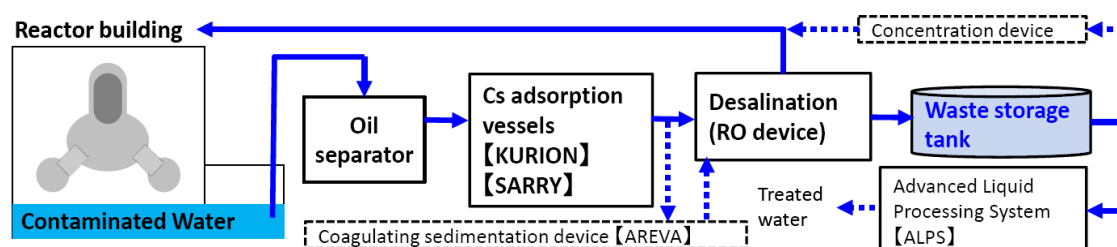


Fig. 1 Decontamination system in Fukushima NPP-1.

Zeolites used in this study are A, X, Y, L, chabazite, synthetic mordenite, natural mordenite, clinoptilolite, erionite and phillipsite. Actinoids solutions were prepared as follows. ²³⁷U was produced by (γ , n) reaction using bremsstrahlung at LINAC in Tohoku University, and separated and purified by TBP extraction method. As for ²⁴¹Am, AmO₂ was dissolved by HNO₃-HF and finally 0.1 M HClO₄ solution was used for the experiments. ²³⁹Np was prepared by milking of ²⁴³Am using TOA extraction (Sill method). By using the above zeolites and actinoids solutions, distribution coefficient (K_d , cm³/g) and uptake (%) were determined in a wide pH range (pH 1~10) by batch method. In the case of distribution experiments of ²³⁹Np, inorganic adsorbents other than zeolites were also used.

In general, the adsorption behavior of actinoids on zeolites is schematically shown by a distribution curve consisting of ion exchange, surface adsorption of hydrolysis species and sedimentation of colloids depending on equilibrium pH (Fig. 2). In the adsorption

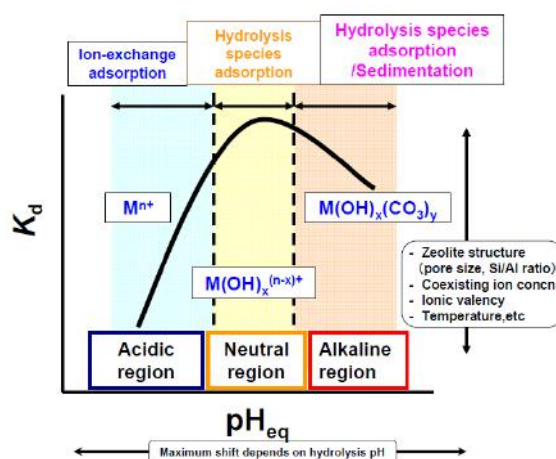


Fig. 2 Schematic distribution curve of actinoids for zeolites.

profile, the pH at the maximum varies depending on hydrolysis pH of each actinoids, and K_d value depends on pore size, Si/Al ratio, coexisting cation concentration, etc.

The distribution of UO_2^{2+} greatly depended on equilibrium pH; K_d value (K_U) markedly increased with equilibrium pH (pH_{eq}) and had a maximum around neutral region (pH 6~7), and then tended to decrease in the alkaline region (**Fig. 3**). The concentrated uranium adsorption layer was formed on the surface of the zeolite particle after treatment with 10^3 ppm $\text{UO}_2(\text{NO}_3)_2$ solution (equilibrium pH= 6.3). The K_U value roughly tended to increase with Al content of zeolite; zeolite A having the largest Al content has the largest K_U value.

As for Am^{3+} ions, the K_d value (K_{Am}) increased steeply with equilibrium pH and had a maximum around neutral region (pH 6~8), and then tended to decrease in the alkaline region (**Fig. 4**). The K_d value at pH 3 tended to increase with pore size of zeolites; zeolite L with a large pore size (7.1~7.8 Å) had the largest K_d value over 10^4 cm³/g at pH 3. Zeolite L had also a relatively large K_d value of 3.5×10^4 cm³/g for Eu^{3+} ions. The ion exchange of hydrated Am^{3+} ions in zeolites much depends on their pore sizes; that is, in the zeolites having a smaller pore size, ion-sieve effect may act more strongly on the hydrated Am^{3+} ions.

On the other hand, the K_d value of NpO_2^+ ions having a higher hydrolysis pH tended to increase with equilibrium pH up to 10; in the case of zeolite X, the K_d value was estimated to be over 10^2 cm³/g in the presence of 0.1 M NaCl- 10^{-3} M HCl (**Fig. 5**).

Thus the zeolites have relatively large K_d values of actinoids depending on equilibrium pH, and hence the accurate distribution behavior of actinoids in Fukushima decontamination systems should be evaluated by considering the equilibrium pH and characteristics of adsorbents.

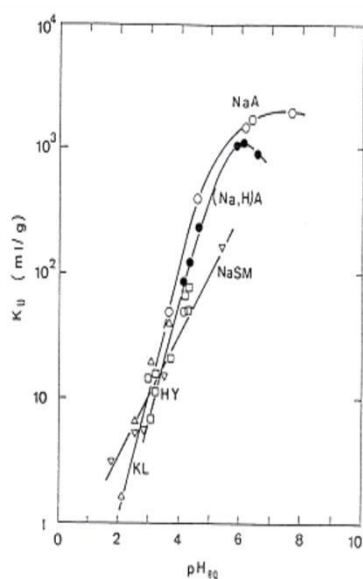


Fig. 3 K_d of UO_2^{2+} vs pH_{eq} .
 $V/m = 300$ cm³/g, $[\text{U}] = 10^{-5}$ M,
0.1 M (H,Na) NO_3 solution,
25°C, 1 d.

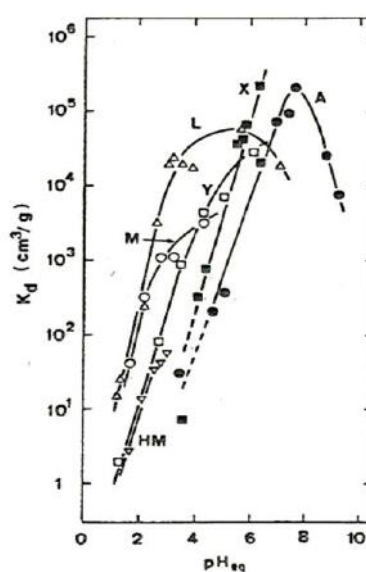


Fig. 4 K_d of Am^{3+} vs pH_{eq} .
 $V/m = 300$ cm³/g, 0.1 M
 HClO_4 - NaClO_4 - NaOH
solution, 25°C, 3 d.

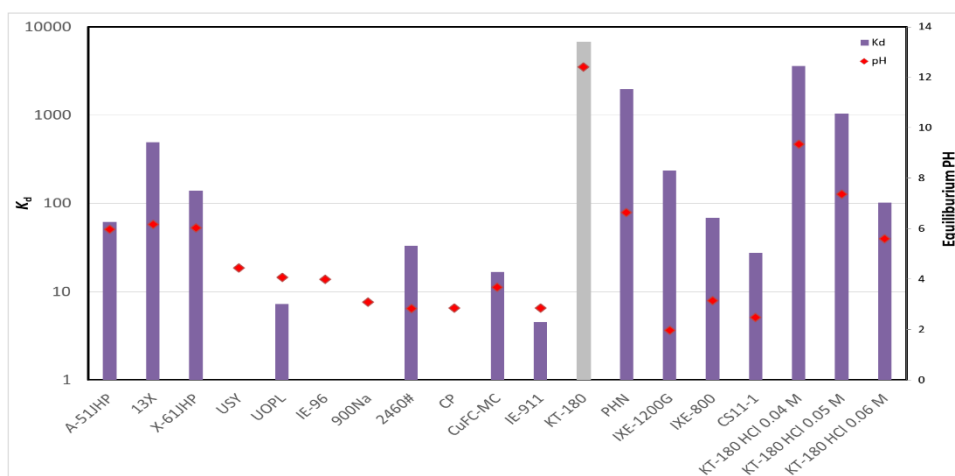


Fig. 5 K_d of NpO_2^+ vs pH_{eq} . $V/m = 100$ cm³/g, 0.1 M NaCl/0.001 M HCl solution, 25°C, 1 d.

Radiochemistry related to ADS at IMP

Z. Qin*, F.-L. Fan, W. Tian, X.-L. Wu, C.-M. Tan, J. R. Wang, S. Li, Y. Wang, J. Bai, X.-J. Yin

Institute of Modern Physics, Chinese Academy of Sciences, Lanzhou 730000, China

With growing of nuclear power in china, the safety management of spent fuel becomes most important issues. Accelerator Driven Sub-critical System (ADS) takes the spallation neutrons as external neutron source to drive the sub-critical blanket system, has the inherent safety. With the performance of hard and wide neutron spectra, large flux, powerful transmutation ability for long-lived fission products and minor actinides, Chinese Academy of Science started the “Strategic Priority Research program ---Future Advanced Nuclear Fission energy” at 2011.

This report will describe some efforts on the radiochemistry aspect to the close cycle of spent fuel based on the accelerator driven system at IMP.

Sorption of Cs, Pu and Am sorption to graphene oxide based nanosorbents

Sergej Šemčuk¹, Galina Lujanienė¹, Agnė Leščinskytė¹, Stasys Tautkus², Ieva Kulakauskaitė, Remigijus Juškėnas¹

1 SRI Center for Physical Sciences and Technology, Savanorių ave 231, Vilnius, LT-02300, Lithuania

2 VU Faculty of Chemistry, Naugarduko str. 24, LT-03225 Vilnius, Lithuania

The high requirements for the environmental protection resulted in the development of new low-cost and effective technologies based on the efficient and environmental friendly materials. Graphene oxide (GO) based nano-composites belong to the group of the most promising sorbents capable of efficiently removing heavy metals and radionuclides from contaminated solutions. GO has a large surface area and a variety of groups such as epoxy (COC), hydroxyl (-OH), carboxyl (-COOH) and carbonyl (-C = O), which can efficiently bind metal ions and radionuclides. In addition, recent studies have shown that graphene oxide is a precursor and a substrate for various chemical modifications. GO and its composites have been adapted to the waste water treatment and clean-up of contaminated areas from pollution. It is believed that GO is also suitable for the radioactive waste management. The aim of this work was to synthesize GO and Prussian blue magnetic graphene oxide (PBMGO) and apply them to the removal of radionuclides from contaminated solutions and for environmental application, e.g. for pre-concentration of Cs ions from seawater.

GO synthesis was performed from the graphite powder (<20 µm synthetic, Sigma-Aldrich, Switzerland) using the modified Hummer's method. MGO and PBMGO sorbent was synthesized by mixing together aqueous solutions of GO and magnetite. Then aqueous solution of FeCl₃ and K₄[Fe(CN)₆] was slowly introduced into the mixture. The obtained precipitate was washed with water and dried at 50° C. MGO and MPBGO were characterized by Mössbauer spectroscopy, X-ray diffraction (XRD) and Transmission electron microscopy (TEM). The batch technique was used to study the adsorption of elements and three sets were conducted for each experiment. In experiments with Cs, in addition to CsCl solutions, 100 mg L⁻¹ of CsCl in seawater (35‰) and natural seawater from the Baltic Sea was used. Pu(IV) and Am spikes were used to achieve initial concentrations of 1·10⁻⁹ mol·L⁻¹ and 3·10⁻¹¹ mol·L⁻¹ of the elements, respectively.

In addition, the effects of pH and coexisting ions on the adsorption of radionuclides to GO based composites were investigated. The maximum adsorption capacities of Cs were found to be 362 mg g⁻¹. The efficiency of MPBGO to pre-concentrate from natural sea water was about 100%. The maximum uptake of Pu and Am by GO was found at the initial pH values of 3-5, while an increase of Pu and Am adsorption from 60% to ≈100% was observed for MGO in the pH range from 3 to 9.

Removal of cesium by heteropolyacid salts from radioactive waste in HCl system

T. Suzuki^{1,*}, Y. Tachibana¹, Y. Sakate¹, Son Nguyen An², Lanh Dang²

1. Department of Nuclear System Safety Engineering, Nagaoka University of Technology, Japan

2. Nuclear engineering Department, Dalat University, Vietnam

*tasuzuki@vos.nagaokaut.ac.jp

We have proposed the novel reprocessing process with nuclide separation based on the chromatographic techniques in HCl solution system [1]. In this reprocessing system, we plan to use the pyridine resin for main process. The high radiation nuclides are desired to be removed before sending the spent fuel solution to main process, although the pyridine resin has the high radiation resistance. Radioactive cesium is one of the main radiation generators in the spent fuel. It is well-known that the heteropolyacid salts have a high cesium selectivity and a high cesium adsorption capacity [2,3]. In the present work, we used the ammonium molybdophosphate (AMP) and the ammonium tungstophosphate (AWP) as the heteropolyacid salts, and the fundamental study was carried out for the investigation on the feasibility of cesium removal from radioactive solution in HCl system.

First, the distribution coefficients of alkali metal ions and alkaline earth ions on AMP and AWP in HCl solution are evaluated by batch experiments using powder type AMP and AWP. The obtained distribution coefficients of alkali metal ions are shown in Fig. 1. It was confirmed that both AMP and AWP have a high cesium selectivity. We also confirmed that alkaline earth ions are not strongly adsorbed on AMP and AWP.

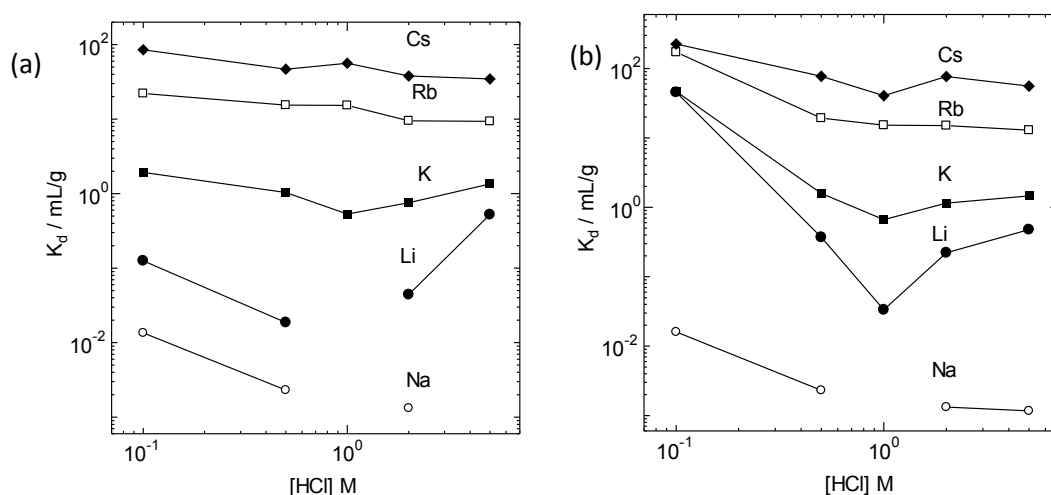


Fig. 1 Distribution coefficient of alkali metal ions on (a) AMP and (b) AWP in HCl.

The stabilities of AMP and AWP in HCl solution were also investigated. The dissolution of molybdenum and tungsten are confirmed. We confirmed that the AWP is more stable than AMP in HCl solution, and the dissolution of both the AMP and AWP are suppressed in the higher concentration of HCl.

[1] T. Suzuki, et al., Global 2013, Salt Lake City, Utah, USA (2013) No.8169, pp.578-581.

[2] Y. Wu, et al. Science China Chem.55(2012)1719.

[3] H. Mimura, et al. Nucl. Eng. Design, 241(2011)4750.

Sorption of uranium from aqueous solutions by TiO₂-graphen oxide composite materials

Z. Tomášová¹, V. Brynych¹, J. Pospěchová¹, P. Ecorchard², J. Tolasz²

¹ÚJV Řež, a. s. Waste Management & Fuel Cycle Chemistry Division
Hlavní 130, 250 68 Husinec-Řež, Czech Republic

²Department of Materials Chemistry, Institute of Inorganic Chemistry AS ČR v.v.i,
Husinec-Řež č.p. 1001, 250 68 Řež, Czech Republic

Introduction

Uranium mining and milling activities, followed by processing to nuclear fuel produce wastes, including the liquid ones. Commonly used methods for radionuclide removal from radioactive contaminated waters are membrane processes, solvent extraction, ion exchange, precipitation and adsorption. TiO₂ is considered to be a promising sorbent of heavy metals. The combination with graphen oxide could further enhance the potential for uranium removal (Comarmond et al., 2011; Bonato et al., 2012). In the presented study the composite nanomaterials TiO₂-graphen oxide (TiO₂-GO) were tested by batch sorption experiment to determine the influence of time and sorbate concentration on sorption behaviour.

Methods

The composite material was synthesized according to the protocol described in Štengl et al., 2013. The product was characterized by X-ray diffraction, scanning electron microscopy (HRSEM, Fig. 1), and transmission electron microscopy (HRTEM, Fig.2).

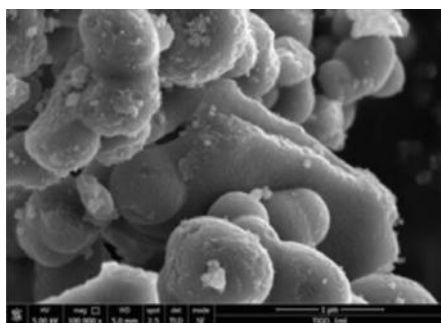


Figure 1: HRSEM image of TiO₂-GO.

The sorption properties of TiO₂-GO were examined using the batch sorption experiments. In order to determine the sorption kinetic, 1.5 mL of UO₂(NO₃)₂ solution was added to 0.01 g of sorbent. In order to avoid the precipitation of uranium complexes, the final pH value was set by addition of HClO₄ to pH 3.5. The experiment was carried out for various contact time, from 4 min to 24 hours. The sorption isotherm studies were carried out for defined period of time with solution concentration from 3.80·10⁻⁵ to 7.00·10⁻⁴ mol/L using the same solid/liquid ratio. The final UO₂²⁺ concentrations in the solution were determined by UV spectrophotometry, Arsenazo III method.

Measured data were fitted into Langmuir and Freundlich isotherm models. The Langmuir isotherm is expressed by formula:

$$q_e = \frac{K_L \cdot q_{\max} \cdot c_e}{1 + K_L \cdot c_e},$$

where q_{\max} means the maximum sorbate uptake [mg/g], K_L is the coefficient [L/mol], c_e is the equilibrium concentration of the solute [mg/L] and q_e is the adsorbed amount of the sorbate [mg/g].

Following equation describes the Freundlich isotherm:

$$q_e = K_F \cdot c_e^{\frac{1}{n}}, [\text{mg/g}],$$

where K_F and n are the characteristic constants.

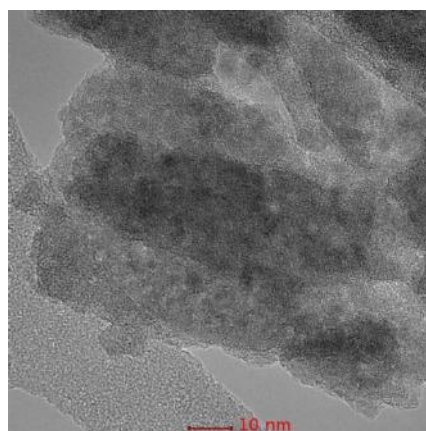


Figure 2: HRTEM image of TiO₂-GO.

Results

The dependence of adsorbed amount of U on reaction time is shown in Fig. 2(left). As possible to see from the graph, the sorption kinetic is fast and the equilibrium is reached during the first few minutes. The time of 24 hours was selected for the isotherm experiments.

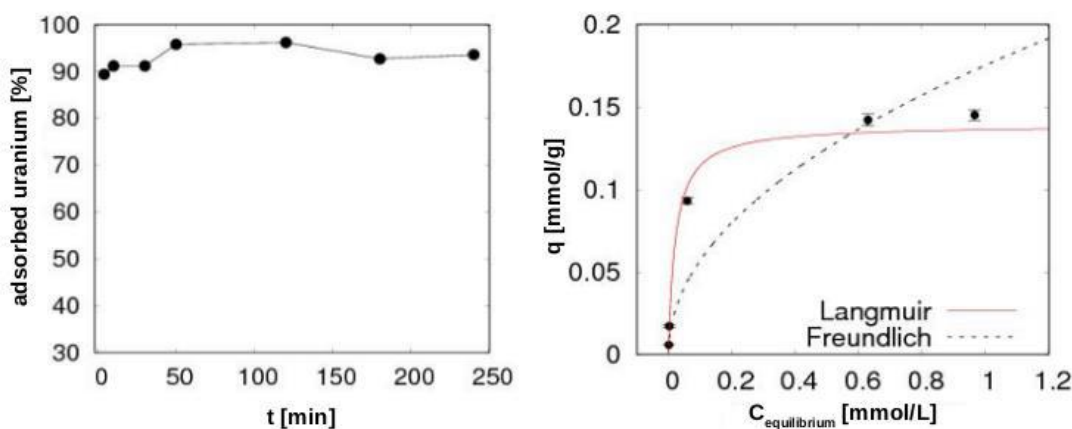


Figure 3: Uranium sorption onto TiO₂-GO, sorption kinetics (left), Langmuir and Freundlich isotherm models (right).

Fig. 3(right) presents the Langmuir and Freundlich isotherm models. The parameters of the models are listed in Tab. 1. The sorption isotherm is better represented by the Langmuir model with χ^2 corresponding to 77.8 and maximum sorbate uptake 37.5 mg/g.

Table 1: Parameters of isotherms.

Langmuir		Freundlich	
q_{\max} [mg/g]	37.5	n	2.5
K_L	0.139	K_F	0.175
χ^2	77.8	χ^2	1010

Conclusion

The batch sorption experiments were performed on a synthesised nanocomposite material TiO₂-GO in order to determine the sorption properties for uranium. The sorption kinetic is fast. The sorption isotherm corresponds to Langmuir model with maximum sorbate uptake 37.5 mg/g.

Acknowledgements

We thank for support from TAČR project no. TA04020222.

References

- Bonato M.; Ragnatsdottir K. V.; Allen G. C.: Removal of Uranium(VI), Lead(II) at the Surface of TiO₂ Nanotubes Studied by X-Ray Photoelectron Spectroscopy. *Water, Air and Soil Pollution*, 2012, 223(7), 3845-3857.
- Comarmond M. J.; Payne, T. E.; Harrison J. J.; Thiruvoth S.; Wong H. K.; Aughterson R. D.; Lumpkin G. R.; Müller K.; Foerstendor H.: Uranium Sorption on Various Forms of Titanium Dioxide – Influence of Surface Area, Surface Charge, and Impurities. *Environmental Science and Technology*, 2011, 45 (13), 5536-5542.
- Štengl V.: Preparation of Graphene by Using an Intense Cavitation Field in a Pressurized Ultrasonic Reactor. *Chemistry - A European Journal*, 2012, 18(44), 14047-14054.
- Štengl V.; Henych J.; Vomáčka P.; Slušná M.: Doping of TiO₂-GO and TiO₂-rGO with Noble Metals: Synthesis, Characterization and Photocatalytic Performance for Azo Dye Discoloration. *Photochemistry Photobiology*, 2013, 89(5), 1038–1046.

Effects of synthesis conditions on trace level ion exchange properties of α -zirconium phosphate variants for $^{152}\text{Eu}^{3+}$ and $^{241}\text{Am}^{3+}$

Elmo W. Wiikinkoski*, Risto Koivula, Risto Harjula

*Laboratory of Radiochemistry, Department of Chemistry, University of Helsinki
A.I. Virtasen aukio 1, P.O. Box 55, 00014 University of Helsinki, FINLAND*

*[*elmo.wiikinkoski@helsinki.fi](mailto:elmo.wiikinkoski@helsinki.fi)*

Worldwide ongoing research on partitioning and transmutation (P&T) is an attempt to advance nuclear energy industry by multiple means. The research aims to maximize fission energy gain from bulk nuclear fuel while minimizing long term radiotoxicity of nuclear fuel waste. New partitioning methods are essential in the development of closed fuel cycles. By the means of P&T, it is possible to recycle a fraction of used fuel and to lessen the radioactivity in nuclear waste final repositories. The time for fuel to cool down in temporary waste storages is shortened by addressing nuclides generating large amounts of heat.

The goal of this study is to develop hydrochemical separation method based on inorganic ion exchanger α -zirconium phosphate (ZrP) and its modifications. By looking at different synthesis parameters and their effect on lanthanide and actinide ion exchange properties, systematically, we aim to develop greater understanding on the effect of synthesis modifications on said properties. Different synthesis modifications include reaction time, phosphorous content during refluxation, reaction temperature, and reagent ratio. Finally, an optimal exchange material can be synthesized for trivalent actinide-lanthanide individual separations or ideally even group separations.

EXPERIMENTAL

ZrP is synthesized by precipitation reaction of zirconium oxychloride octahydrate and sodium dihydrogen phosphate in hydrochloric acid, followed by refluxation. In the presented work, effect of modifying reaction time is studied: three variants of ZrP, having 1 hour, 5 hours or 25 hours as reaction time, are synthesized. Resulting materials are characterized and studied for their trace level europium and americium ion exchange properties in nitric acid media.

The synthesized ZrPs are characterized by powder x-ray diffraction on their structure and crystallinity, by titration experiments on their acidity, and by sorption experiments on their selectivity (Eu and Am distribution coefficients and separation factor). Further experiments include Zr:P molar ratio and shape characterization by scanning electron microscopy, and infrared spectroscopy.

RESULTS

Trivalent lanthanide Eu-152 and trivalent actinide Am-241 are used as a model nuclides for separation study. Although they are very similar by ion size and by their chemistry, the studied α -zirconium phosphates exhibit far greater affinity for europium (Eu:Am separation factors of around 10 to 100 depending on pH and material in question). In Fig. 1, distribution coefficients of three ZrP variants are presented. The synthesis conditions of these three variants are identical, except for reaction time: 1 hour, 5 hours and 25 hours.

First major results present the effect of reaction time: as reaction time increases, the crystallinity increases but the materials acidity and its selectivity towards Eu and Am (Eu/H and Am/H) decreases. The materials first acid constants (pK_{a1} , determined graphically from titration curves) for 1 hour, 5 hours and 25 hours variants are 2.98, 3.12 and 3.28, respectively. These reaction time modified variants differ by their distribution coefficients in a way that two of the ZrP variants could be usable for Eu-Am separation in pH of around 0.5 where as one could be usable in pH of around 1.0 (low coefficient for the other but high for the

other). In general, α -Zirconium phosphates are chemically stable in acidic conditions (pH less than 3, up to 13 molar nitric acid) and have very high distribution coefficients ($> 10^6$ mL/g) at pH 2-3.

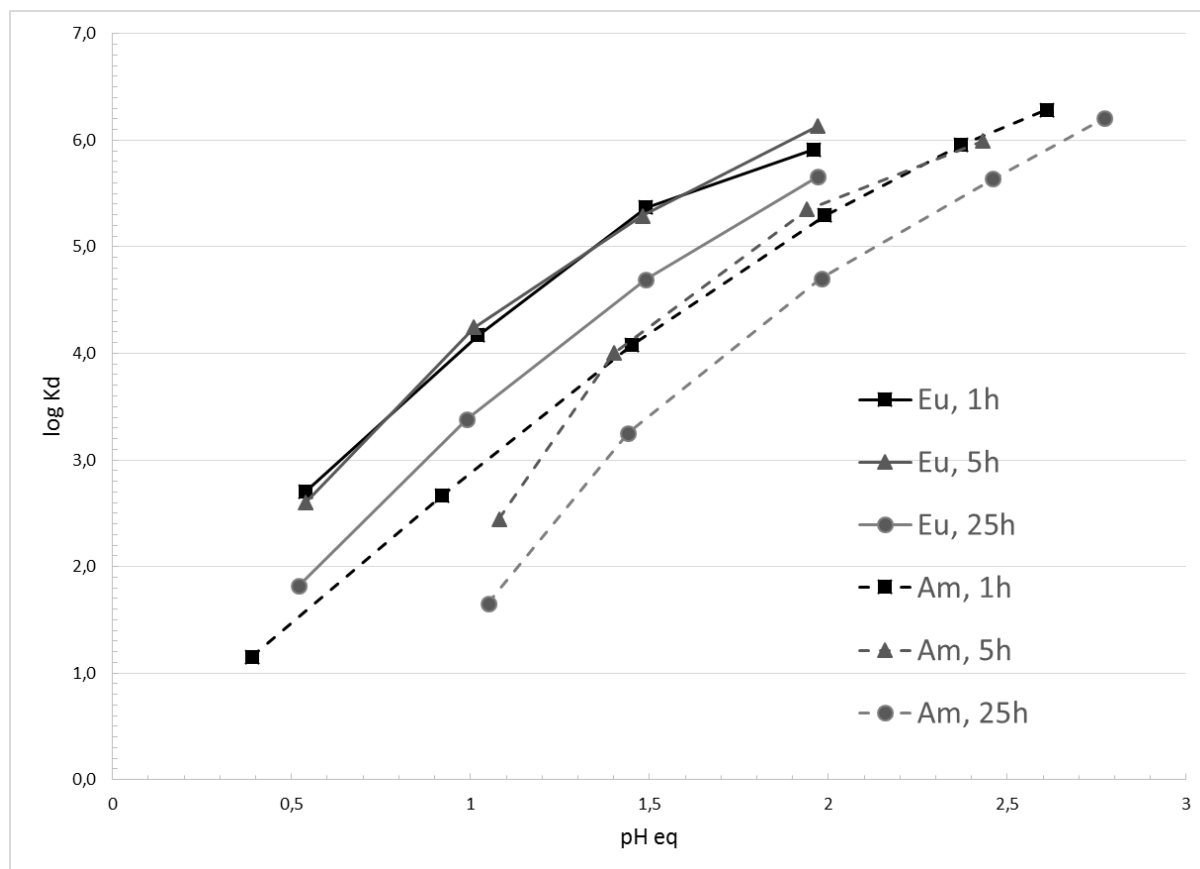


Figure 1. Distribution coefficients, K_d (mL/g), as function of pH in nitric acid including 0.1 molar NaNO_3 for trace level americium and europium of three α -zirconium phosphate variants, differing by reaction time during their synthesis: 1 hour (1h), 5 hours (5h) and 25 hours (25h).

ACKNOWLEDGEMENTS

The research is partly funded by State Nuclear Waste Management Fund (VYR), on the basis of proposals by the Ministry of Employment and Education. It is part of Finnish Research Programme on Nuclear Waste Management (KYT) 2015-2018 which is based on the Nuclear Energy Act (990/1987) and is continuation to preceding work done during the previous KYT programme.

Uranium uptake during iron (oxyhydr)oxide formation: application to radioactive waste effluent treatment

E. Winstanley^a, K. Morris^a, L. Abrahamsen^b, S. Shaw^a

^a *Research Centre for Radwaste and Disposal, Williamson Research Centre, School of Earth, Atmospheric and Environmental Science, University of Manchester, Manchester, United Kingdom*

^b *National Nuclear Laboratory, Chadwick House, Warrington, WA3 6AE, United Kingdom*

Nanoparticulate iron(III) (oxyhydr)oxides (e.g. ferrihydrite) have a high surface reactivity and specific surface area meaning they have the capacity to sorb large amounts of trace metals, including radionuclides, from aqueous solution. They are commonly used in industry to remove contaminant metal species from aqueous waste streams. One key example of this is the Enhanced Actinide Removal Plant (EARP) facility (Sellafield, UK) which decontaminates radioactive aqueous effluent using iron (oxyhydr)oxide formation. In EARP the pH of iron-rich effluent is increased via base addition, causing $\text{Fe(III)}_{(\text{aq})}$ hydrolysis and subsequent precipitation of an iron (oxyhydr)oxide floc composed of ferrihydrite nanoparticles. The vast majority of radioactive species are sequestered by the floc, however the pathway and the mechanism(s) by which the radionuclides are removed from solution are poorly constrained at a mechanistic level.

There are several possible mechanisms by which the radionuclides can be sequestered by the floc including: adsorption onto the floc surfaces, incorporation within the ferrihydrite particles, physical capture within the rapidly forming/aggregating floc or even precipitation of the radionuclide as a distinct phase. Any combination of these mechanisms may occur, with each having a different effect on the effluent decontamination process and on the active iron (oxyhydr)oxide product.

In this project small scale laboratory experiments were undertaken to mimic the EARP process. Our aims were to characterise the mechanism of uranium (U(VI)) removal from solution during the EARP process by observing the partitioning of U(VI) between the solution and iron oxyhydroxide phase, and probing the solid phase atomic-scale bonding environment of uranium via Extended X-ray Absorption Fine Structure (EXAFS) spectroscopy. PHREEQC modelling of this system was also completed using a CD-MUSIC based approach.

Analysis of the solid product using powder X Ray Diffraction (XRD) and Transmission Electron Microscopy (TEM) imaging showed 2-line ferrihydrite as the only solid product, with no indications of any iron-uranium or distinct uranium hydroxide phases within the concentration range investigated. Solution analysis indicated that 100% of iron had fully precipitated from solution by pH 4 with the majority of the uranium removed between pH 3 and 6. This is supported by the PHREEQC model, where the iron has fully precipitated from solution by pH 4 and the uranium is removed from solution between pH 3.5 and 5.5 (Figure 1). The slight differences occur because the PHREEQC model equilibrates at every step whereas the experimental system undergoes rapid hydrolysis with no chance to equilibrate. EXAFS spectroscopy of the solid floc taken at pH 9 indicated that uranium associated with the solid floc is uranyl U(VI) , and showed that this was present as a bidentate edge-sharing adsorbed species at the ferrihydrite surface. EXAFS data also showed that carbonate present in solution at ~pH 8 forms a ternary complex with the uranyl surface complex.

Results from solution and solid phase data, along with advanced synchrotron spectroscopic data and computer based modelling give a comprehensive insight into the fundamental mechanisms of radionuclide removal by iron hydrolysis within such a dynamic system. Overall our results show that during the EARP process the ferrihydrite particles initially form and precipitate from solution, after which uranium is removed from solution by adsorbing to the surface of the newly formed 2-line ferrihydrite floc as a bidentate, edge-sharing, inner sphere surface adsorbed species.

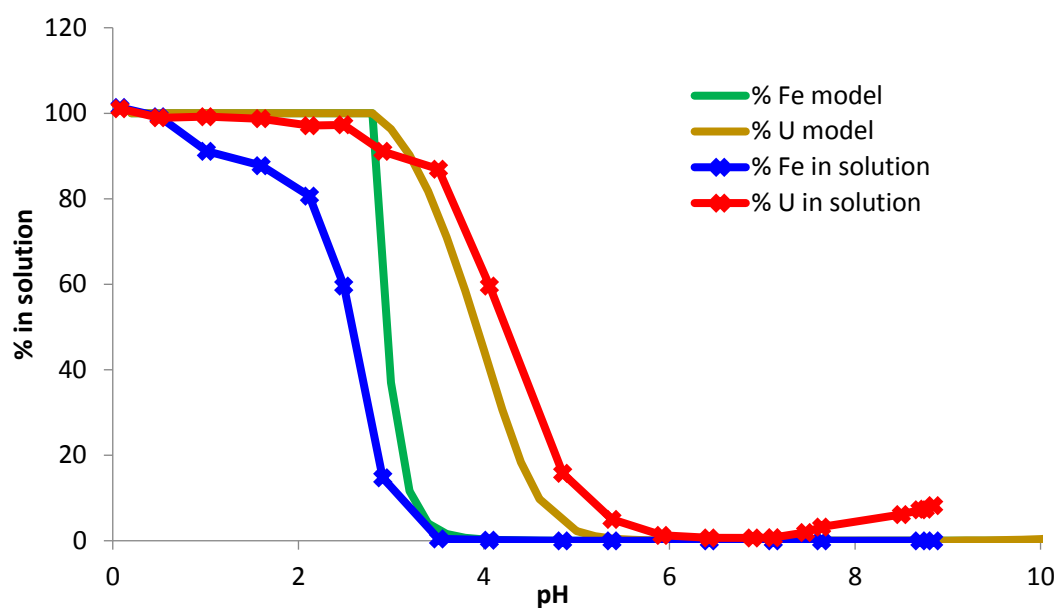


Figure 1: Comparison of experimental data of Fe(III) and U(VI) in solution (blue and red), with the PHREEQC modelled data predicting Fe(III) and U(VI) in solution (green and purple).

We would like to acknowledge Sellafield Ltd. and The University of Manchester for funding this PhD project.

Development and testing of new technetium selective media TcTreat

Ilkka Välimaa, Risto Harjula, Benjamin Salo, Risto Koivula, Esko Tusa**, Pasi Kelokaski**

Laboratory of Radiochemistry, Department of Chemistry, University of Helsinki, Finland

*** Fortum Power and Heat Oy, Finland*

e-mail: ilkka.valimaa@helsinki.fi

Technetium-99 (β^-_{max} : 293.7 keV; $t_{1/2}$: 2.1×10^5 years) is a byproduct of uranium-235 fission (6 % fission yield) and comprises a large component of radioactive waste. It is a challenging radionuclide from the perspective of radioactive waste management. The predominant form of technetium under oxic conditions is the pertechnetate anion (TcO_4^-), which is highly mobile in environment and difficult to separate from solution by most conventional methods.

A new zirconium oxide based material “TcTreat” is under development and testing for the removal of radioactive oxoanionic species ($^{99}\text{TcO}_4^-$ pertechnetate, ^{106}Ru ruthenate) from solutions. “TcTreat” has been tested for Tc uptake from common salt solutions.

Test

Static batch experiments were carried out to measure the distribution coefficients (k_d) of ^{99}Tc for TcTreat in NaNO_3 , NaCl , $\text{Ca}(\text{NO}_3)_2$, Na_2CO_3 and Na_2SO_4 solutions of different concentration (0.01-3.0 M) that were traced with ^{99}Tc . One set of experiments was carried out in 1.0 M NaNO_3 solutions adjusted to different pH-values (2-12) with NaOH .

Dynamic column experiments were carried out using small minicolumns (bed volume $\text{BV} = 1.0$ ml, packed with 0.7 g of “TcTreat”, grain size 0.25 – 0.8 mm). About 1.7 litres 1 M NaNO_3 solution was fed to the column using a peristaltic pump with flow rate about 20 ml /h (20 BV / h). The outlet solution was collected in fractions and counted for ^{99}Tc . The decontamination factor (DF) for the solution was calculated as the ratio of the activity in the outlet and feed solution, respectively.

Results

Static uptake tests showed a high uptake of ^{99}Tc by the TcTreat materials with the different salt solutions. With the exception of Na_2CO_3 solution, even in the 1.0 M salt concentrate uptake was high. The values of k_d being in the range of 100,000 ml/g and above. Regarding the pH of the solution, the uptake of ^{99}Tc from 1 M NaNO_3 had a very broad maximum between $\text{pH} = 4 - 10$. The level of uptake was very high, the values of k_d being in the range of 500,000 ml/g. In the carbonate solution (Na_2CO_3), the ^{99}Tc uptake was much lower than in other salt solutions. This is probably due to the complexation of technetium with carbonate ion in solution.

As it could expected from the high batch uptake k_d -values, the column packed with TcTreat materials was effective for ^{99}Tc removal from 1 M NaNO_3 solutions. Flowrate in the test was 20 BV/h and decontamination factor was between 2000 – 3000 during the experiment. There was seen some indication of exhaustion about after 1200 BV, where DF decrease slightly.

Application of extraction express-method for radwaste characterization before hot chamber montejus dismantling

Alexey Stepanov, Iurii Simirskii, Sergey Smirnov, Alexey Safronov, Ilia Semin, and Vyacheslav Stepanov

National Research Centre - Kurchatov Institute, Moscow, Russia

From 2011 specialists of the NRC "Kurchatov Institute" carry out the dismantling of the multiloop research MR reactor. The MR reactor and its elements from reactor hall were dismantled. At the moment carry out works on decommissioning and dismantling contaminated support facilities and equipment.

The hot chamber is located under the central hall of MR reactor (fig. 1). The hot chamber is a room of square area 17 m² (4.84 m x 3.53 m) with a ceiling height about 4 m. The reactor hall and the hot chamber are connected by 2 technological holes. Under the floor of hot chamber in a monolithic concrete protection (layer ~ 4 m) there is montejus for liquid radioactive waste volume of 3 m³ (diameter -1 m, height 4 m).

The hot chamber and montejus were used from the beginning of the 60's, after the MR reactor start-up. The hot chamber was used for cutting fuel assembly and selection of samples for metallographic and structural analysis. As a result, shavings and particles of fuel assembly fell on the hot chamber floor and then washed into montejus. The control of filling cutting chamber by radioactive waste was not conducted. The cutting chamber was partly filled up by borated granules. Before dismantling work it is necessary determine the amount of radioactive waste, and make radiochemical analysis of sample from montejus.

Due to high exposure dose rate in hot chamber (10 mSv/h) we made sampling from reactor hall. The underwater video camera was passed in montejus through waste pipe. By marking the video cable we can estimate the level of radioactive waste. On the bottom of montejus there are 1 meter layer of solid radioactive waste covered 5 cm of slime and then 1 meter of water. 200 ml water sample were obtained with a specially made teflon sampler. To sample the solid radioactive waste was not be possible from the reactor hall. The water sample had a high radioactive contamination and showed necessities for further research.

After deactivation hot chamber exposure dose rate was 100 μ Sv/h. Sampling of contaminated water and solids radioactive waste from montejus carried out from hot chamber by a pump OMNIA 160/7 with non-return valve. After settling the water pumped from montejus to plastic container were taken water samples and solid samples. Solid radioactive waste sample shown in figure 2 and have a form of metal shavings. Then we made alpha-, and gamma-spectrometric analysis of the samples.

The concentration of gamma-ray radionuclides was estimated by the spectrometric complex InSpector-2000 of the Canberra Company that included a semi-conductor detector made of HP Germanium GC-4018. The analysis of the gamma-spectrum was made by the GENIE 2000 software.

The concentrations of the alpha-emitting radionuclides uranium and plutonium were determined by the alpha spectrum of the targets prepared electrochemically after radiochemical purification and concentration of the investigated samples [1-3]. The alpha-spectra were obtained from the vacuum Alpha Analyst Integrated Alpha Spectrometer of the Canberra company with a semi-conductor passivated implanted planar silicon detector.

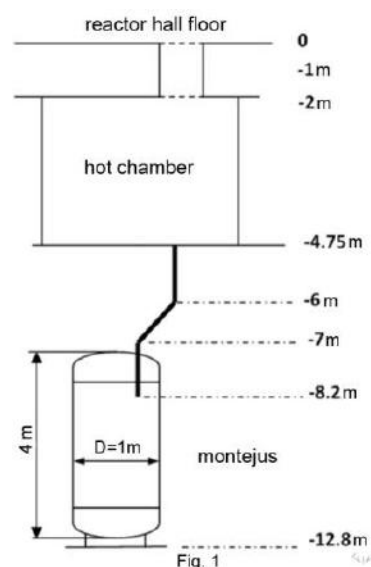


Fig. 1

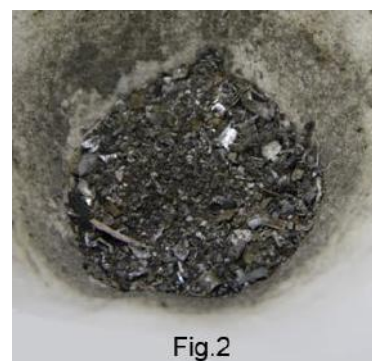


Fig. 2

A 500ml water sample was acidified with nitric acid, and added 1 Bq of ^{232}U and 1 Bq ^{242}Pu as tracers. Then reduced to 50 ml by distillation and evaporated to dryness. To examine the solid sample 50-100 mg with eddied tracers (1 Bq of ^{232}U and 1 Bq ^{242}Pu) was leached with 5ml of hot concentrated nitric acid for 1 hour, then the procedure was repeated using 5 ml of aqua regia. The resulting solutions were combined and evaporated to dryness.

The dry residue was dissolved in 10 ml of 5M nitric acid, and uranium-plutonium fraction was extracted by 30% solution of tributyl phosphate in toluene. Earlier 1 Bq of ^{232}U and 1 Bq ^{242}Pu were added to samples as tracers. Plutonium was reextracted from the organic phase by the equal volume of the mixture of 0.25M nitric acid and 0.025M hydrofluoric acid. Uranium was reextracted by the equal volume of distilled water. Reextraction was repeated twice for 3 minutes. The aqueous phases were combined and evaporated to dryness. Residue was dissolved in 10 ml of 0.5M solution of nitric acid. Then 1 ml of saturated solution of ammonium oxalate and 1 ml of 25% solution of ammonium chloride were added to solution and pH was adjusted to 9 by an ammonia solution. The resulting solution was put in electrolytic cell. Uranium and plutonium were deposited on a stainless steel cathode during 45 minutes under the current density of 0.3 A/cm². During the electrolytic process we kept the pH level at 9 adding the ammonia solution if necessary. The cathode was washed by distilled water and we analyzed alpha-spectra of the prepared target with the vacuum Alpha Analyst Integrated Alpha Spectrometer (fig.3). The examples of alpha-spectra are represented in figure 3. Results of the spectrometric analysis of solid and water sample are shown in Table I. These data are preliminary. Sample has been selected from the upper layer of solid radioactive waste in a montejuis

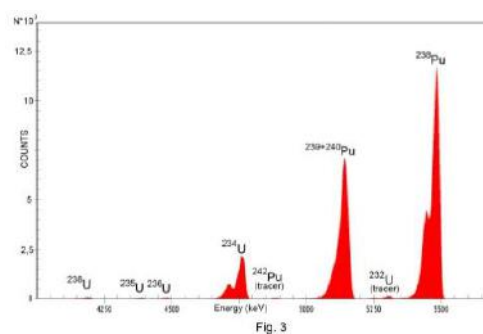


Table I.

	specific activity, KBq/kg						
	^{137}Cs	^{234}U	^{235}U	^{236}U	^{238}U	^{238}Pu	$^{239+240}\text{Pu}$
water	$1.7 \cdot 10^5$	89	2.4	2.4	2.9	1.5	2
solid sample	$1.2 \cdot 10^6$	303	6.3	5.8	9.7	2400	3700

Nevertheless, from this data follows the main dose-forming radionuclide is ^{137}Cs . The total activity of ^{137}Cs in water is approximately 3.5 Ci and total activity ^{137}Cs in solid waste in montejuis is approximately 350 Ci. It is important to understand that these calculations are made using only one sample. The results cannot fully reflect the real activity ^{137}Cs and uranium amount. It is necessary to carry out farther researches for understanding real concentration and distribution of radionuclides.

References

1. A.V. Stepanov, Yu.N. Simirskii, I.A. Semin, A.G. Volkovich // Atomic Energy. 2014. Vol. 117. № 1. P. 57-61.
2. A.V. Stepanov, Yu.N. Simirskii, I.A. Semin, A.G. Volkovich // Atomic Energy. 2015. Vol. 117. № 3. P. 191-195.
3. Alexey Stepanov, Iurii Simirskii, Ilia Semin, Anatoly Volkovich // WM2016 Conference proceedings - 16022, March 6 –10, 2016, Phoenix, Arizona, USA

Modeling molten-salt separation of radionuclides in spent nuclear fuel

Sungyeol Choi^{a,*}, Dokyu Kang^a, Byunggi Park^b

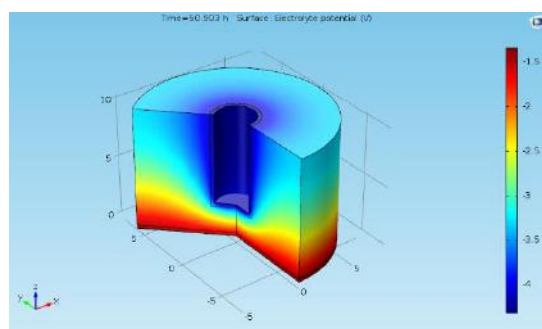
^a Ulsan National Institute of Science and Technology, UNIST-gil 50, Ulsan, 44919, Korea

^b Soon Chun Hyang University, Asan, Chungnam, 31538, Korea

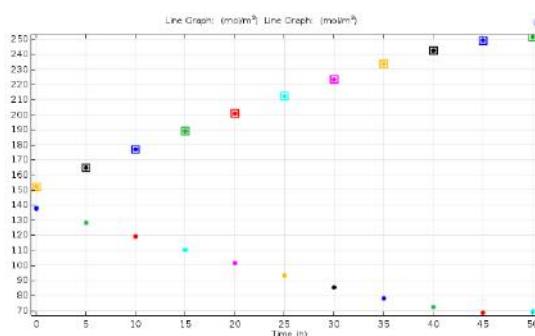
* chois@unist.ac.kr

Molten-salt pyroprocessing has been developed for treating oxide and metal spent nuclear fuels. This process separates long-lived actinide isotopes together as a group from fission products for burning the long-lived isotopes in fast neutron nuclear reactors. Main processes of pyroprocessing (i.e., oxide reduction, electrorefining, and electrowinning) are based on a concept of electrolytic cell consuming energy to proceed electrochemical reactions. To achieve cost effective separation processes, it is significant to compare different unit process designs and find optimum designs and operating conditions. However, this optimization process is very costly if we need to conduct experiments on every case with spent nuclear fuel. Instead, a validated simulation model can help to rapidly calculate and evaluate different cases at significantly reduced costs.

We have developed a COMSOL-based kinetic simulation model for molten-salt pyro-chemical electrolysis systems. This model uses a combined approach of the COMSOL-supplied modules, electrodeposition and species transport modules with a user-defined ordinary differential equation module. The electrodeposition module calculates competitive electrochemical reactions at electrode interfaces while the user-defined module calculates changes of species concentration at the bulk electrolyte. This simulation model is validated by the experimental results of U/Pu electrorefining conducted by and openly published by the Argonne National Laboratory in the early 1990s. Since the experimental setup uses the liquid anode and the solid cathode systems, this benchmark exercise allows us to validate our model for electrowinning using liquid cathode and inert anode and partially electrorefining using solid anode and solid cathode. The benchmark case is a kinetic case for more than 50 hours. As shown in below two figures, U is a main species to be deposited on the cathode surface initially, so it is consumed in the bulk electrolyte. Later, as U in the bulk becomes not enough to meet the applied current and cathode potential becomes more negative, Pu starts to be deposited on the cathode surface. Until that time, Pu is only dissolved from the liquid anode to the bulk with U.



Potential distribution at the last time step (the bottom surface of the cell: liquid anode, the cylinder at the center of the cell: solid cathode) [unit: V]



Change of U (circle) and Pu (square) concentrations at the bulk electrolytes during electrolysis [unit: mol/m³]

Quantifying TBP dimers and trimers in alkane solutions via simulations and experiments

¹VO, Quynh, ¹UNANGST, Jaclynn, ²DANG, Liem, ¹NILSSON, Mikael, ¹NGUYEN, Hung

¹ *University of California, Irvine, CA, USA*

² *Pacific Northwest Laboratory, USA*

Tri-n-butyl phosphate (TBP), a representative of neutral organophosphorous ligands, is an important extractant used in solvent extraction process for the recovery of uranium and plutonium from spent nuclear fuel. This study utilizes molecular dynamics (MD) simulations in conjunction with experimental work to elucidate the self association of TBP in alkane solutions. Microscopic pictures of TBP isomerism and its behavior in n-dodecane diluent were investigated utilizing MD simulations. 2D potential mean force calculations were performed to characterize the conformational criteria for TBP dimers and trimers. For validating our simulations we investigated the self-association behavior of TBPs in various alkane diluents of different chain lengths (8, 12 and 16 carbons) and a branched alkane (iso-octane) by Fourier Transform Infrared Spectroscopic (FTIR) measurements. Our results indicate that TBP does not only self-associate to form dimers, as previous studies showed, but also trimers in the practical concentration range. Using a mathematical fitting procedure, the dimerization and trimerization constants were determined. As expected, these equilibrium constants are dependent on the solvent used. As the alkane chain for linear hydrocarbon solvents becomes longer, dimerization decreases whereas trimerization increases. For the more branched hydrocarbon, we observe a significantly higher dimerization constant. These effects are most likely due the inter-molecular van der Waals interactions between the butyl tails of each TBP molecule and the diluent hydrocarbon chain as all solvents in this study are relatively non-polar. We found that the dimerization and trimerization constants of TBP in n-dodecane determined by MD simulations compared favorably with our FTIR study. These results further confirm the accuracy of our theoretical models for TBP and n-dodecane molecules. The new insights into the conformational behaviors of TBP molecule as a monomer and as part of an aggregate could greatly aid the understanding of the complexation between TBP and metal ions in solvent extraction system.

Sorption of toxic metals by magnetic nanocomposites

KULAKAUSKAITE, Ieva, LUJANIENE, Galina, MAŽEIKA, Kęstutis, DARIUS, Valiulis, SERGEJ, Šemčuk, VIDAS, Pakštas, MARTYNAS, Skapas, SAULIUS, Tume'nas

Center for Physical Sciences and Technology Vilnius, Lithuania

Heavy metals are persistent environmental contaminants since they cannot be degraded or destroyed. Nano-composites possessing magnetic properties can be used for the efficient removal of various toxic elements from contaminated solutions since they can be easily eliminated from the solutions after the treatment procedures. Magnetic nano-materials, apart from having the high surface area to volume ratio, have so many unique properties which make the remediation process economical, efficient and environmentally friendly [1]. This study was carried out to synthesize different magnetic nanocomposites and apply them for the sorption of Cu^{2+} , Co^{2+} , Ni^{2+} , Pb^{2+} from liquid media. The studied sorbents can be used for the removal of radionuclides from contaminated solutions (e.g. ^{59}Ni , ^{63}Ni , ^{58}Co , ^{60}Co radionuclides) and for development of analytical techniques for ^{210}Pb . Magnetite nanoparticles are synthesized by the coprecipitation method, using ferric and ferrous salts in basic medium. Magnetic graphene oxide was synthesized via a chemical deposition of Fe_3O_4 NPs onto GO, followed by reduction of GO to graphene in a hydrazine hydrate solution. [2] Magnetic Prussian blue (PB) and magnetic Prussian blue-graphene oxide composites were prepared by anchoring Fe_3O_4 magnetic nanoparticles (MNPs) onto a large surface area of GO and in situ coating Fe_3O_4 MNPs with PB. [3] The batch technique was used to study the adsorption of elements and three sets were conducted for each experiment. Sorption experiments were performed with the initial concentration of 50-700 $\text{mg}\cdot\text{L}^{-1}$ of Cu, Co, Ni, Pb and 1 $\text{g}\cdot\text{L}^{-1}$ dosage (1:1000 g/ml ratio) of adsorbent. The maximum adsorption capacities of Co(II) , Ni(II) , Cu(II) and Pb(II) on magnetic ferrous oxide based composites varied from 29 to 641 mg g^{-1} .

1. N. Neyaz1, A. W. Siddiqui. IJSR 2014 2319-7064
2. Y. Yunjin, M. Shiding, L. Shizhen, Chemical Engineering Journal 184 2012 326– 332
3. Y. Hongjun, L. Haiyan, Z. Jiali Zhai, Chemical Engineering Journal 246 (2014) 10–19

Degradation mechanism of a novel diglycolamide ligand and its impact on actinide and lanthanide co-extraction efficiency

A. Ossola¹, E. Macerata¹, W. Panzeri², A. Mele², M. Giola¹, M. Mariani¹, A. Casnati³

¹ *Department of Energy, Politecnico di Milano, Piazza L. da Vinci, 32, 20133 Milano, Italy*

² *Department of Chemistry, Materials and Chemical Engineering "G. Natta", Politecnico di Milano, Piazza L. da Vinci, 32, I-20133 Milano (Italy) and CNR-ICRM, Via L. Mancinelli, 7, I-20131 Milano, Italy*

³

Department of Chemistry, University of Parma, Parco Area delle Scienze 17/a, 43124 Parma, Italy

In addition to radiation risk, safety and nuclear proliferation, the management of SNF (Spent Nuclear Fuel) is a major concern for the sustainability and the social acceptance of the nuclear industry.

In order to pursue this challenging vision, it is of fundamental importance to adopt the closed fuel cycle strategy. Whereas processes for the recovery of uranium and plutonium were already developed and implemented, the Partitioning and Transmutation (P&T) strategy, which aims at recovering also minor actinides (MA) from SNF to transmute them in short-lived or stable isotopes, is still under study. Thus several promising multi-cycle hydrometallurgical processes based on the co-extraction of trivalent lanthanides (Ln) and MA, followed by their subsequent separation, have been proposed. In order to reach these goals, numerous molecules have been *ad hoc* designed and studied on a laboratory scale with spiked aqueous feeds or in hot tests on real waste [1, 2].

To date, a solvent based on the lipophilic extractant N,N,N',N'-tetraoctyl-diglycolamide (TODGA) in kerosene/1-octanol 95/5% v/v is considered the reference formulation for hydro-processes devoted to the MA and Ln co-extraction from the raffinate of the PUREX process [3]. Such ligand fulfils the CHON principle and is characterized by a very high extraction efficiency, a fast kinetics and a good affinity for both MA and Ln with respect to other fission and corrosion products (except for Mo and Ru). Moreover, it is hydrolytically and radiolytically stable. Thus, it was tested in multi-stage centrifugal contactor battery with both a spiked synthetic PUREX raffinate at the Forschungszentrum of Jülich and with a genuine fuel waste at the Institute for Transuranium Elements in Karlsruhe, respectively in 2006 and 2007 [4].

Even if TODGA satisfactorily meets the key requirements to implement an industrial process, a valuable alternative, represented by a novel ligand 2,6-bis[(N-methyl-N-docecyl)carboxamide]-4-methoxy-tetrahydro-pyran (DMDCATHP), has been proposed. Its properties were already studied and partially reported in literature: both extraction efficiency and kinetics are high enough to implement a multi-stage process [5, 6]. In particular, DMDCATHP resulted to be a slightly weaker extractant than TODGA, thus enabling an easier cation back-extraction. Interestingly, DMDCATHP is characterized by a similar affinity for MA and Ln resulting in a separation factor closer to 1 with respect to TODGA. Unfortunately, liquid-liquid extraction tests performed with aged or irradiated DMDCATHP-based solvents demonstrated that this formulation is very susceptible to the storage conditions adopted and not enough resistant to radiolysis and ageing [6].

The present research work aims at elucidating which are the main degradation products that lead to a loss of the system extracting capabilities. For this purpose, a series of DMDCATHP solutions, with a different content of 1-octanol, have been prepared and aged under different storage conditions or irradiated at different absorbed doses. The so-obtained samples have been systematically analysed by HPLC coupled with ESI-MS, in order to quantify the ligand degradation and to attempt an identification of the by-products. Furthermore, batch liquid-liquid extractions with a synthetic aqueous feed spiked with ²⁴¹Am and ¹⁵²Eu have been performed to highlight the impact of degradation on the extraction efficiency.

The experimental campaign allowed to explain the worsening of the extraction properties with the formation of the hydrolytic and radiolytic by-products observed by the analytical techniques. On the basis of the main degradation products identified, a feasible solvent clean-up step has been attempted and considerations on the weakest points in the ligand structure susceptible to degrading attack have been made with the aim to improve the long term performance of the system.

References:

- [1] Ansari S. A., Pathak P., Mohapatra P. K., Manchanda V. K. (2012) Chem. Rev. 112, 1751-1772
- [2] Serrano-Purroy D., Baron P., Christiansen B., Glatz J. P., Madic C., Malmbeck R., Modolo G. (2005) Separation and Purification Technology 45, 157-162
- [3] Modolo G., Wilden A., Geist A., Magnusson D., Malmbeck R. (2012) Radiochim. Acta 100, 715-725
- [4] Hill C. (2009) Ion Exchange and Solvent Extraction. A series of Advanced. Vol.19, 119-194
- [5] Macerata E., Ossola A., Giola M., Faroldi F., Tinonin D.A., Casnati A., Mariani M. (2016) *Manuscript in preparation*
- [6] Ossola A., Macerata E., Tinonin D.A., Faroldi F., Giola M., Mariani M., Casnati A. (2015) Radiat. Phys. Chem. DOI: [10.1016/j.radphyschem.2015.12.013](https://doi.org/10.1016/j.radphyschem.2015.12.013)

New method for alpha dose rate profile determination at HLW matrix/water interfaces

M. Tribet, S. Mougnaud, C. Jégou

CEA, DEN, DTCD/SECM/LMPA, 30207 Bagnols-sur-Cèze cedex, France

In the context of deep geological disposal of high level radioactive wastes, irradiation will be governed in the long term by the alpha decay of the actinides. As alpha irradiation exhibits its effects in a short range (micrometric scale), it remains of primary importance to determine the alpha dose rate profiles at the HLW matrix/water interface, with the aim of better characterizing the dose deposition during water-induced leaching mechanisms.

In this study, the MCNPX calculation code [1] was used. This particle transport code is based on the Boltzmann transport equation solver by the repeated random sampling Monte Carlo method. The originality of this approach lied in the ability to focus on dose rate description for both the HLW matrix and the water sides, and in its ergonomics in designing materials, geometrical shapes and radioactive sources, compared to previous studies based on mathematical considerations and limited to water profiles [2-3]. Alpha dose rate profiles were obtained at spent fuel/water and HLW glass/water interfaces by considering different relevant geometries like pellets, powders or water-filled ideal cracks. A general equation was then proposed to fit dose rate profiles in water or in a given HLW matrix from values for dose rate in the matrix bulk, alpha range in water or in the matrix, and linear energy transfer considerations.

References

1. L. S. Waters, G. W. McKinney, J. W. Durkee et al., *AIP Conf. Proc.* 896 (2007) 81-90
2. A. Poulesquen, C. Jegou; S. Peugot, *Scientific Basis for Nuclear Waste Management XXIX* 932 (2006) 505-512
3. F. Nielsen, M. Jonsson, *J. Nucl. Mater.* 359 (1-2) (2006) 1-7

Complexation studies of modified calix[4]arenes with uranium in non-aqueous solution

A. Bauer¹, K. Schmeide¹, J. März¹, A. Jäschke², F. Glasneck², B. Kersting²

¹ Helmholtz-Zentrum Dresden-Rossendorf, Institute of Resource Ecology, Germany

² Leipzig University, Institute of Inorganic Chemistry, Germany

The actinide uranium, well known from nuclear power cycle, plays also a role in rare earth production. The rare earth ores contain, apart from various other components, the actinides uranium and thorium occur as undesired constituents. To facilitate the production of rare earth elements, uranium and thorium have to be removed. Due to their modifiable selectivity and solubility calix[n]arenes are interesting compounds for the extraction of actinides and lanthanides. The chalice-like macrocyclic molecules consist of para-substituted phenolic units. The para-substitution determines the solubility of the molecule and the hydroxyl groups serve either directly as complexation site or can be further functionalized to adjust the selectivity of the calix[n]arene.

Several calix[4]arenes with affinity towards actinides or lanthanides are available. These are to be applied to eliminate uranium (IV)/(VI) and thorium from ore concentrates and subsequently, to separate lanthanides. The separation method based on liquid-liquid extraction utilizing the calix[4]arenes. Thereby metal calix[4]arene complexes are formed in the organic phase. For better process understanding we investigated the mechanisms of uranium interaction with the synthesized calix[4]arenes by UV-Vis spectroscopy, TRLFS, isothermal titration calorimetry, single crystal XRD and extraction experiments. The calix[4]arene modified with 8-hydroxyquinolin derivatives called L₁ is one of the new calix[4]arenes. It achieves a U(VI) extraction yield between 90 to 100 % in the pH range of 4 to 9. It possesses two potential binding sites for U(VI). Stoichiometry determination by the Job's Plot from UV-Vis data indicates a ligand to metal ratio of 1:2 (Fig. 1). The calix[4]arene-L₁ complex absorbs at 280 nm. During spectrophotometric titration of L₁ with U(VI) in acetonitrile the absorption maximum decreases and new peaks at 318, 360 and 525 nm occur. Luminescence signals of L₁ and uranyl nitrate in acetonitrile are weakened by complex formation. First microcalorimetric measurements confirm the binding of two metal ions by L₁. All measurements in solution were carried out at 25°C. In addition to the UV-Vis spectroscopy and isothermal titration calorimetry, the capillary electrophoresis is to be used for determining stability constants.

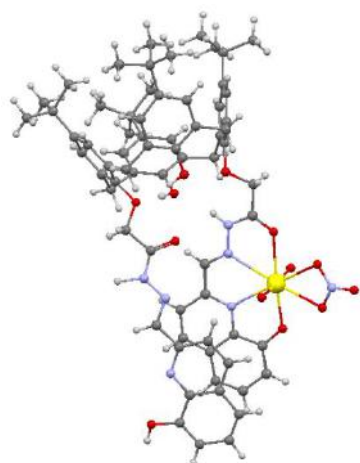


Fig. 2: X-ray crystal structure of a 1:1 U(VI)-L₁ complex

Whereas in solution a stoichiometry of 1:2 is obviously preferred, the single crystal XRD analysis reveals a formation of a 1:1 U(VI)-L₁ complex (Fig. 2). Thereby the hexavalent uranyl ion is coordinated by the singly deprotonated ligand via a N₂O₂ donor set. The charge is compensated by an additional coordinated nitrate ion. To complete the structure information of the formed U(VI)-L₁ complex in solution mass spectrometric and NMR measurements as well as theoretical studies are currently performed. In addition, for better understanding the complexation properties of L₁ the interaction with U(IV) and Th(IV) is studied.

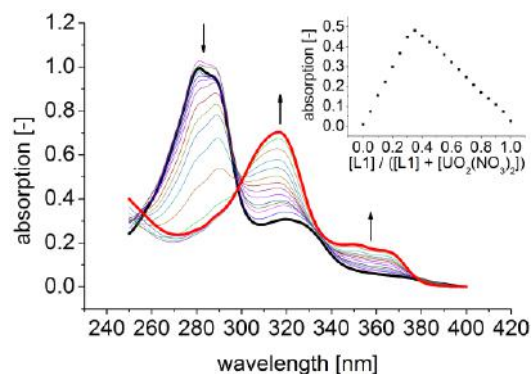


Fig. 1: UV-Vis spectra of 12.5 μM L₁ in MeCN at different UO₂(NO₃)₂ concentrations. Inset: Job's Plot

Local environment of Gd doped actinide oxides ($U_{1-x}Gd_x$)O₂ and (Th_{1-x}Gd_x)O₂ measured by X-ray absorption spectrometry

R. Bès¹, J. Pakarinen², S. Conradson³, A. Baena², M. Verwerft², I. Makkonen¹, F. Tuomisto¹

¹ *Aalto University, Finland*

² *SCK-CEN, Belgium*

³ *MARS beamline, SOLEIL synchrotron, France*

The improve of economic and safety performances of nuclear fuels relies on extend capacities of actual fuels UO₂ and on the development of alternative such as thorium based fuel [1,2]. To this aim, research focused on doped fuels such as ($U_{1-x}Gd_x$)O₂ and (Th_{1-x}Gd_x)O₂ which could allow controlled specific properties along fuel life-time, are of great importance.

Gadolinia doped UO₂ is widely used to reduce the power peaking and excess reactivity during the first reactor cycle of fresh fuel assemblies as ¹⁵⁵Gd and ¹⁵⁷Gd isotope act as burnable neutron absorber. According to the fuel assembly design and the core management constraints, the concentration of Gd varies between 2 wt.% and 10 wt.% (weight fraction of Gd₂O₃). In such concentrations, Gd and UO₂ is expected to form a solid solution ($U_{1-x}Gd_x$)O₂ which keeps the fluorite structure of UO₂ by substituting U⁴⁺ ions by Gd³⁺. The charge balance is usually considered as only modification of the valence state of U⁴⁺ to U⁵⁺ in good agreement with the fact that several phases are only observed for $x > 0.5$ [3]. Nevertheless, the formation of oxygen vacancies could also act as charge balance and would be also possible accordingly to the known stability of the fluorite structure in the presence of vacancies.

Thorium based nuclear fuels represent potential alternatives to uranium based fuels as the fission of thorium isotopes can reduce the long-lived radioactive nuclides. The influence of gadolinium content on doped thorium must be evaluated to ensure future high performance of this alternative fuel. The charge compensation is here awaited to be due to the presence of oxygen vacancies only, as recently demonstrated by molecular dynamics calculations [4]. Indeed, for thorium atoms, valence state modification is not allowed and Th⁴⁺ remains the only possible valence state in the fluorite structure.

The challenging question of the complex interplay between atomic defects and valence state mixing in ($U_{1-x}Gd_x$)O₂ and (Th_{1-x}Gd_x)O₂ will be discussed on the basis of X-ray Absorption Spectroscopy and theoretical calculations.

- [1] O. Lung et al., Nucl. Eng. Design, 180 (1998) 133.
- [2] M. Osaka, et al., J. Nucl. Sci. Technol., 43[4] (2006) 367.
- [3] M. Durazzo, et al., J. Nucl. Mater. 400 (2010) 183.
- [4] M. Osaka, et al., J. Nucl. Sci. Technol. 44[12] (2007) 1543.

Thermochemistry of reactor materials: actinide and fission product compounds

Emily E. Moore, Rudy J.M. Konings

European Commission, Joint Research Centre, Institute for Transuranium Elements, Karlsruhe, Germany

The thermochemistry of the actinide elements is a key component to understanding the behaviour of nuclear fuel components for reactor safety. The most common fuel types are in the form of actinide oxide species, namely UO_2 and a mixed $(\text{U,Pu})\text{O}_2$. Minor actinide inclusion in the form of neptunium and americium are also considered to ease the burden of waste toxicity. These complexes have been the subject of various reviews [1,2] conducted by agencies including the international atomic energy agency (IAEA) and nuclear energy agency (OECD/NEA), who continues to pursue the topic with respect to newly developed data. These reviews present an important basis as the physical properties of reactor materials are determined by their chemical makeup and state. The main focus of these works is to create a comprehensive assessment of available thermodynamic data such as formation enthalpies, standard entropy and heat capacity data, as tabulated and reviewed in [3]. Properties such as the volatile nature of the actinide complexes as well as other fission products (FP's) play a principle role in being able to predict possible outcomes of gaseous release into the atmosphere (i.e. source term) in the case of an accident scenario. Many computational models rely on the chemical thermodynamic descriptions of fuel components and FP's as their behaviour is influenced by variations in temperature, pressure and composition. This work aims to further the current state of assessed data by providing an update and overview of currently available experimental data. A critical review, analysis and assessment of this data provide an important reference bank for these materials. The assessment will be based on fundamental thermodynamic functions including entropy, enthalpy and the Gibbs energy function of the systems. Experimental measurements of incremental enthalpies and heat capacities, equilibrium pressures and constants as well as formation energies and dissociation pressure allow for a complete description at equilibrium for a wide range of temperatures and compositions of the phases of the multicomponent systems considered. The systems under investigation include the fuel components such as UO_2 , PuO_2 , AmO_2 (and their elemental counterparts), in addition to fission products or containment materials (Mo, Pd, Zr, Tc, Se, Te, Ba, Sr) etc. and their oxide compounds. Experimental techniques such as various calorimetric methods (drop, adiabatic, differential scanning and combustion) as well as Knudsen effusion, mass spectrometry and dissociation pressure measurements are considered for their thermodynamic properties and evaluated based on consistency using the third-law method. Gas phase properties are calculated using spectroscopic measurements and molecular constants, at times ab initio techniques are taken into account where data is lacking or completely unavailable.

- [1] J. Fuger, V.B. Parker, W.N. Hubbard and F.L. Oetting. *The Chemical Thermodynamics of Actinide Elements and Compounds*, IAEA, (1983)
- [2] R. Guillaumont, T. Fanghänel, V. Neck, J. Fuger, D.A. Palmer, I. Grenthe and M.H. Rand *Update on the Chemical Thermodynamics of Uranium, Neptunium, Plutonium, Americium and Technetium* (2003) (Elsevier)
- [3] E.H.P. Cordfunke and R.J.M. Konings, *Thermochemical Data for Reactor Materials and Fission Products*, (1990) (North Holland).

Gen IV reactors: fuel, coolant and their interactions

Teodora Retegan, Fredrik Espegren, Erik Karlsson

*Chalmers University of Technology, Department of Chemical and Biological Engineering, Industrial Materials Recycling, Kemivägen 4, 41296 Göteborg, Sweden
tretegan@chalmers.se*

It is clear in most contexts that nuclear fission can be a part of a sustainable energy mix provided that due attention is given to safety aspects and waste. One way to address many of the concerns of today's nuclear power is the so called "Generation IV" reactor systems where thermal reactors are integrated with fast reactors and recycling facilities for the fuel.

The concept "Defense-in-depth" [IAE 96] concerns several levels of protection, like including several successive barriers for preventing the release of radioactive material to the environment.

As well is known that the fuel matrix itself, and the integrity of the fuel rod and the boundary of the primary coolant system are the first physical barriers against the potential release of radionuclides [LIL 02].

The fuel-coolant interaction research is presently addressed at Chalmers by two EURATOM FP7 projects: SEARCH and MAXIMA, where the focus is a Pb/Bi cooled research reactor, in this case MYRRHA reactor.

An extensive work realized for the interaction of an oxide fuel and Pb/Bi eutectic will be presented, where atmosphere (air ingress, Ar) as well as temperature (200⁰ C-1700⁰ C) influence have been the main focus. Also, some structural materials have been tested in similar conditions.

These results constitute a part of the empirical research with regards to reactor safety.

References

[IAE 96] Defence in depth in nuclear safety: INSAG-10 / a report by the International Nuclear Safety Advisory group.- Vienna : International Atomic Energy Agency, (1996), ISBN 92-0-103295-1

[LIL 02] J-O Liljenzin, G. Choppin, J. Rydberg, Radiochemistry and Nuclear Chemistry, Ed. Butterworth-Heinemann, ISBN 0-75606-7463-6, (2002), 3rd Edition.

Accident tolerant fuel: uranium microspheres doped with chromium prepared by modified internal sol gel

Aneta Sajdova, Marcus Hedberg, Teodora Retegan, Christian Ekberg

*Chalmers University of Technology, Department of Chemistry and Chemical Engineering,
Division of Nuclear Chemistry/Industrial Materials Recycling, Göteborg, Sweden*

Uranium nitride (UN) is a possible fuel alternative for uranium dioxide (UO₂). It is studied for use in both Light Water Reactors (LWR) and Generation IV. Reactors. UN has similar melting point but higher thermal conductivity and higher fissile atom density than UO₂. These properties make it an interesting candidate with respect to safe operation, lower central line temperature and economy of nuclear energy production, more fuel in the core. But UN is not stable in hot pressurized water, which is used as a coolant in LWRs, it loses its mechanical integrity, hydrolyses and forms UO₂. Therefore an attempt has been made on developing a material that would have better characteristics against water, e.g. chromium doped uranium nitride, due to known anti-corrosion properties of Cr₂O₃ and CrN.

Internal sol gel and carbothermal reduction was chosen as a production technique. In order to form microspheres with homogeneous distribution of metals and carbon a modification of internal sol gel was done. A glucose was used to complex metals and to serve as a carbon source. A comparative experiment with original urea and *carbon nano powder* was performed. The modified method resulted in production of spheres with homogeneous distribution of uranium chromium and carbon, whereas carbon was not evenly distributed by the original method produced microspheres. Both techniques are promising since metals are well co-precipitated with no cluster formation and therefore more likely to form a solid solution after thermal treatment. A modified technique offers better conditions for carbothermal reduction since carbon is evenly distributed within the material.

ENVIRONMENTAL RADIOACTIVITY

Evaluation of radioactive contamination of alfa emitters in tundra of Western Greenland

Anna Cwanek¹, Jerzy W. Mietelski¹, Edyta Łokas¹, Maria A. Olech²

¹ *Institute of Nuclear Physics, Polish Academy of Sciences, Cracow, Poland*

² *Institute of Botany, Jagiellonian University, Cracow, Poland*

Arctic environment is commonly perceived as a wilderness and exceptionally sensitive to contamination. This vulnerability is connected with relatively short food chains, efficient transfer of contaminants between different organisms forming these chains and close relationship with the terrestrial and marine ecosystems. Moreover, observed warming temperature, changes in precipitation type and amount, may contribute to the increase mobility of radionuclides in the Arctic. On the radioecological point of view quite important is the uptake of pollutants by dominant representatives of Arctic tundra - lichens and mosses. The lack of wax cuticle and root systems causes that lichens and mosses have to uptake of nutrients from the atmosphere and surface water together with inherent contaminants. Furthermore a relatively slow growth rates and long lifespan results in the incorporation of large amounts of impurities in the intracellular structure with time. This is a potential threat for local ecosystems that are exposed to penetration of toxic radioactive elements through the food chain. The main aim of presented study is assessment of contamination of artificial radioisotopes such as: $^{238,239+240}\text{Pu}$, ^{241}Am , comprising the most radiotoxic elements released into environment during nuclear era, in lichens and mosses from coastal zone of Western Greenland. For this purpose activity concentration and isotopic ratios of $^{238}\text{Pu}/^{239+240}\text{Pu}$ and $^{241}\text{Am}/^{239+240}\text{Pu}$ were calculated. The major sources of studied alfa emitters in considered region and characteristic activity ratios were collected in table below.

Type of sources	A $^{238}\text{Pu}/^{239+240}\text{Pu}$	A $^{241}\text{Am}/^{239+240}\text{Pu}$
Global fallout + SNAP 9A (Northern Hemisphere)	0.03 – 0.05	0.3
Chernobyl fallout	0.3 – 0.65	2.4
Thule	0.014	-

Research materials were collected during two French-Canadian-Polish scientific expeditions in 2012 and 2013. Appropriate radiochemistry procedures were used in order to separate isotopes from sample followed by alpha-ray spectrometry measurements. On the basis of initial analysis it can be concluded the global fallout is a dominant source of contamination.

Assessment of ^{210}Pb -contamination in soil

Dag Øistein Eriksen*, Ketil Haarstad**

* *Primus.inter.pares AS, Norway*

** *Norwegian Institute of Bioeconomy Research, Norway,
d.o.eriksen@kjemi.uio.no*

It is well known that oil and gas not only contain hydrocarbons, but also metallic components, in particular those elements capable of making metal-organic compounds. Examples of such metals are mercury (Hg), vanadium (V), chromium (Cr), arsenic (As), and zinc (Zn). Thus, oil may contain also compounds of inorganic origin in addition to the pure organic ones. Such metal-organic compounds are usually very toxic. Radioactive components in the oil and the related aqueous brine are also usually present. The origin of these is, however, different from the ones of the metal organic compounds. Most rocks contain radioactive components (NORM) and uranium and thorium are usually present as oxides or silicates, compounds of minute solubility. In the uranium series, radium (Ra) is the first element to be soluble in brine if the environment is made of oxides. Radon (Rn) being a noble gas will prefer to stay in a non-polar environment like oil and gas, compared to the often very saline aqueous brine found in the oil reservoir. This noble gas, created through the decay of radium, diffuses into the non-polar phase. This is a rather slow process and the only isotope with sufficient half-life is ^{222}Rn . The daughters of ^{222}Rn all have too short half-lives to leave their environment until ^{210}Pb with 22.2 years half-life. This is illustrated in Figure 1 showing the radioactive series from ^{238}U . The main decay-routes and half-lives are indicated.

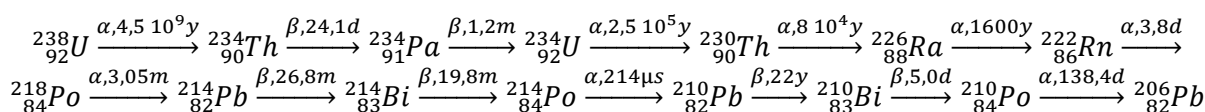


Figure 1. The ^{238}U -serie indicating the main decay routes

At oil and gas handling installations there will always be equipment exposed to oxidation agents and thus corrosion. In the hydrocarbon fluids there may be traces of water vapor, CO_2 and H_2S . These components may attack iron forming what is known as black powder, FeS_x . When ^{210}Pb comes about, it will stick to the sulfide due to the high affinity between lead and sulfide.

In order to assess a possible contamination from a decommissioning plant for old oil installations from the North Sea, Bioforsk¹, a Norwegian research institute, was engaged in a survey of the area surrounding the decommissioning plant. Soil samples were taken in three campaigns. The soil was sampled at three depths, each sample consisting of a bulk sample of four to five subsamples. Radioactivity was included in the measurements of the samples from the last two campaigns. All samples of the soil were taken according to guidelines issued by the Norwegian pollution authorities and all analyses have been performed by the commercial and certified laboratory ALS. The content of radioactive elements has been determined by ALS' laboratory in the Czech Republic by gamma-detection.

A back-ground level for the radioactivity in the area before the decommissioning plant was established was not established, and the geology in the area indicates bedrocks like granite and gneiss as well as mica and rocks of volcanic origin. A small, old and depleted uranium mine is situated some four km NE of the decommissioning site. Thus, there is natural radioactivity in the surrounding area. To determine any

additional radioactivity it was therefore imperative to find a method for establishing the back-ground level of the natural radioactivity in the area.

An additional complication was that the region has a high annual precipitation, 1738 mm rain in a normal year, and the predominating winds are from SE. The topography is also quite steep, so the water fallen as rain soon ends up in the fjord. Potassium, i.e. ^{40}K , can be used as an indication of the mobility of the water soluble elements in the soil. Very little mobility of ^{40}K could be determined from the samples.

The method chosen was to acquire samples in three levels of 100 mm each from randomly selected sites. Then the radioactivity in the samples were compared for the ^{234}Th , ^{226}Ra , and ^{210}Pb . Those samples where radioactive equilibrium between two or more of the nuclides could be established, were then used for calculating an average back-ground level. Still the uncertainty was high. The value determined was $34,2 \pm 12,3$ Bq/kg, i.e. one standard deviation is 36%. Still, there were several samples containing ^{210}Pb at levels well above the back-ground value + three standard deviations (i.e. > 71.1 Bq/kg). These samples were all from the top 100 mm soil sampling level. The analyses of the soil samples together with a geo-statistical analysis of the results shows that the concentration of Hg and As was higher in the two top layers adjacent to the site, but not in the lowest layer, indicating spreading by dust of these metals in measurable amounts. These samples were correlated with the samples with high ^{210}Pb . The conclusion was that ^{210}Pb as well as Hg had been introduced to the soil from dust pollution through air from the decommissioning plant. Plumes of dust have been observed several times entering the surrounding area. ^{210}Pb can thus be regarded as a tracer for pollution from oil and gas handling equipment.

Seasonal variation and chemical property of radioactive cesium released by the FDNPP accident

Nobufumi Fujita¹, Kazuhiko Ninomiya¹, Zijian Zhang¹, Shunsuke Kakitani¹, Takashi Yoshimura², Yoshiaki Yamaguchi², Kazuyuki Kita³, Haruo Tsuruta⁴, Akira Watanabe⁵, Hitoshi Yamamoto⁶, and Atsushi Shinohara¹

Graduate School of Science, Osaka University¹, Radioisotope Research Center, Osaka University², Ibaraki University³, Atmosphere and Ocean Research Institute, the University of Tokyo⁴, Fukushima University⁵, Department for the Administration of Safety and Hygiene, Osaka University⁶

[Introduction]

Tohoku Pacific Ocean Earthquake and tsunami attack on March 11, 2011 caused a severe accident at the Fukushima Daiichi Nuclear Power Plant (FDNPP) in Japan, and a large amount of radioactive nuclides was released into the environment. Radioactive Cs (¹³⁴Cs and ¹³⁷Cs) is one of the most significant radioactive nuclides in the nuclear accident. The total amounts of radioactive Cs released in the FDNPP accident are estimated to be more than 10 PBq [1]. Though over 5 years passed from the accident, the radioactive cesium still has been detected in the atmosphere. Investigation of chemical and/or physical properties of radioactive cesium is important to estimate the influences on human body. Our research group has continuously studied on radioactivities in air samples in the Eastern Japan area near FDNPP just after the accident. In this paper, we will discuss on the time variation in concentration of radioactive cesium and chemical and/or physical properties of radioactive cesium.

[Experiment]

We performed air sample collection in Fukushima, Marumori, and Hitachi areas (Figure 1) using high-volume air samplers. Aerosols were collected on quartz fiber filters. Times for collecting samples were 1 to 21 days and it corresponds to air volume with 700-20000 m³. Radioactivities in the filters were determined by gamma-ray counting using Ge detectors with 10-80 % relative efficiencies for 1 to 7 days duration at Radioisotope Research Center in Osaka University.

[Results and Discussion]

Figure 2 shows seasonal variation of the radioactivity concentration of Cs in the air detected in Fukushima. The obtained activity ratio of ¹³⁴Cs and ¹³⁷Cs was consistent with the ratio derived from the FDNPP accident. In 2011, the radioactivity concentrations of Cs in the air were high, but these were decreased sharply. Direct release process from FDNPP was affected this time variation. In Fukushima, radioactivity concentrations in the air were relatively high in the winter season. On the other hand, such seasonal variation was not identified in Marumori, and Hitachi. This fact suggests that seasonal resuspension origins exist in Fukushima area.

In addition, we found some high concentration events mainly in summer season in 2013. In this period, some resuspension events existed. These events were also found in Marumori and Hitachi, however, the date of high concentration events was different each other. It shows the Cs resuspension process occurs in the local regional scale. We found activity concentrated spot on these filter samples from measurement of radiography using imaging plates. Cs-concentrated insoluble particles [2] [3] are one of the candidates of the resuspension source in 2013. These particles were directly released from the FDNPP, and the influences on human body was grate concern. We also tried to reproduce such insoluble particles in the laboratory [4], and the details will be discussed in the presentation.

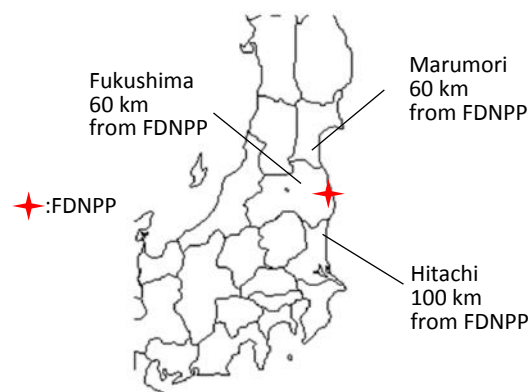


Figure 1. A map of sampling points

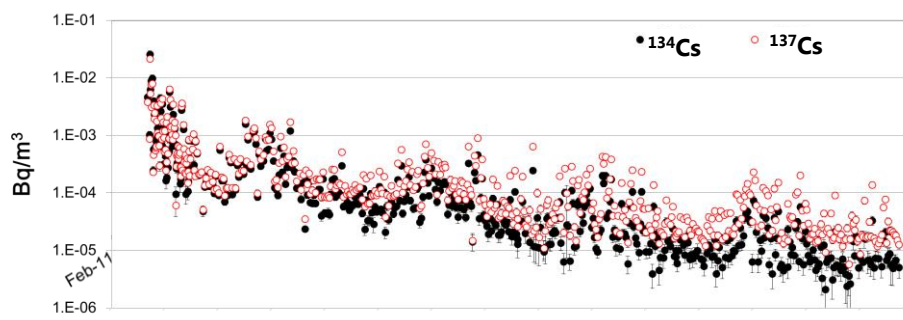


Figure 2. Seasonal variation of radioactivity concentration of ^{134}Cs and ^{137}Cs in the air detected in Fukushima

[References]

- [1] T. Kobayashi *et al.*, J. Nucl. Sci. Technol., 2013, 50, 255-264
- [2] K. Adachi *et al.*, Sci. Rep., 2013, 3, 2554
- [3] Y. Abe *et al.*, Anal. Chem., 2014, 86, 8521–8525
- [4] T. Yoshimura, Proceedings of the 16th Workshop on Environmental Radioactivity, March9 - 11, 2015

Radiation contamination factor (RCF) in marine sediments from Cuba north and south coasts

M. García Batlle, J. M. Navarrete

Faculty of Chemistry, Inorganic and Nuclear Chemistry Department, National University of Mexico

Radiation Contamination Factor (RCF) is a figure obtained as percentage of contaminant radioactivity (^{137}Cs) related to natural one (^{40}K) when some mass of marine sediments are detected during few hours either by a 3x3" NaI or HPGe detector. In this way, RCF have been obtained for samples taken up from Pacific and Gulf of Mexico coasts¹, showing that RCF at global scale produced mainly by more than 2,000 test nuclear explosions performed in time span from 1945 to 1965 in South seas, reaches no more than 1% in these samples. However, same method applied to Cuba's North and South coasts show a significant increment till near 10%, maybe due to some other source, perhaps the cooling water of nuclear power plants evacuated from USA south coast to Gulf of Mexico. Anyhow, this figure might be useful either to measure the radioactive contamination at global scale, which at present seems to be minimal compared with ^{40}K natural one, or to assess its decline or growing up in the future, since ^{137}Cs half life is 30.2 years.

- 1) J. M. Navarrete, G. Müller, J. I. Golzarri, G. Espinosa, Int. J. of Environment and Health, 5/4, 318-323, 2011.

Measuring the NORM in the Oil Fields & Oil Ports in Libya (2)

Ezeddine Hamida

Petroleum Training and Qualifying Institute, Tripoli, Libya

This paper is the second part of a comprehensive research, its goal is to create a database about the existence of the NORM (Naturally Occurring Radioactive Material) in Petroleum Fields, Terminals & Gas Export Stations across Libya, the NORM was measured in two oil ports (Al-Hariqa Port –Tobruk, east of the country, and Zawia Port, west of the country) where oil is exported therefrom, which is coming from two oilfields in which a relatively high proportion of radiation in scales' samples was recorded (the first part of the research, which was presented in -RANC2016- Budapest) in order to try to track the spread of pollution resulting of the Scales' NORM and make sure the possibility of arriving at the ports. The results were as follows:

Table (1)

Activity concentration recorded in the waters of Al-Hariqa port	Activity concentration recorded in the scales sample in the field connected to the Port Al-Hariqa	Activity concentration recorded in the waters of Zawia port	Activity concentration recorded in the scales sample in the field connected to the Zawia Port
26.6± 5.15(Bq / L)	5522.6±74.31 (Bq /kg)	19.9±4.46 (Bq / L)	4017.2±63.38 (kBq / kg)

(P.S.: There was no reference to the name of fields upon the request of officials of these fields)

The NORM was also measured in some commercial ports so as to compare the NORM levels in each of the Petroleum Ports and the Commercial ones. The results were as follows:

Table(2)

The Port	Port Rating	Activity concentration(Bq/L)
Zawia Port	Petroleum	19.9±4.46
Port of Tobruk(Al-Hariqa)	Petroleum	26.6±5.15
Khoms port	commercial	15.9±3.98
Misrata port	commercial	33±5.74
Port of Tripoli	commercial	8±2.8

From the results, it is clear that the NORM levels in oil ports & Commercial ones is within the allowed limits(Exemption level). Samples were of 1.5 liters of water taken from the ports' basins where the oil tankers are shipped in shipping oil ports at the shipping & discharge basins into the commercial ports. Gamma Ray which was emitted from the samples was measured by High pure Germanium Detector –HPGe at the Radiation Prevention Department in Tajura Nuclear Research Center-Tripoli, Libya.

Radon emanation from fresh, altered and disturbed granitic rock characterized by ^{14}C -PMMA impregnation and autoradiography

K-H. Hellmuth¹, M. Siitari-Kauppi², H. Arvela¹, A. Lindberg³

¹ *Radiation and Nuclear Safety Authority (STUK), 00881 Helsinki, Finland*

² *Laboratory of Radiochemistry, Department of Chemistry, University of Helsinki, Finland*

³ *Geological Survey of Finland, Espoo, Finland*

The emanation of radon from the geological substrate leading to enhanced concentrations in houses is a major health problem in Finland. As the overburden in Finland is generally very thin, a large number of houses is founded directly on the rock; it is, therefore, relevant to know more about emanation of radon from intact rock and the possible effects of blasting activities (often called EDZ: excavation disturbed zone).

Radon emanation from overburden, soil and sediment material has been studied widely in the laboratory. But, there is little information available on the radon emanation factor of compact crystalline rock and its dependence on humidity. Suitable, intact, fine-grained, homogeneous granitic rock with sufficient radium content from Kuru, SW-Finland was studied. Samples of (i) fresh, undisturbed rock, (ii) rock adjacent to vertical and horizontal fractures showing weak signs of weathering, including horizontal decompression fractures (unloading by post-glacial unloading) and (iii) rock from blasting zones, all about 15 m below the present rock outcrop, were studied. In addition, weathered rock near the surface (0.5 m below the rock outcrop) was studied.

The pore network of the samples which is determining the fate of the recoiling decay products and the matrix transport properties, was characterized by impregnation with ^{14}C -PMMA and autoradiography. There was a clear influence of the relative humidity of the atmosphere in equilibrium with the rock samples on the radon emanation observed which is linear and within narrow limits has the same slope for fresh, slightly altered and excavation disturbed matrices. Absorption of water in the pores is increasing radon emanation up to about 98% relative humidity (r.H.), but complete saturation is clearly decreasing radon escape.

The increased fracturing of the excavation disturbed zones (EDZ) does not increase radon emanation compared with the undisturbed matrix. Alteration/weathering along fractures has a slightly increasing effect on radon emanation. It seems that on the scale of small samples the escape is not diffusion controlled, but source term controlled by the distribution of radium within the pore system. In the weathered outcrop zone the radioactivity content is significantly lower and primary phases are absent, but the radon emanation coefficient is higher than that of the fresh matrix. ^{14}C -PMMA autoradiography of the weathered and disturbed zones is indicating significant and selective increase of porosity, clear porosity gradients and major changes of the pore network which is influencing rock matrix transport properties.

**Cs-137 source identification and its use as geochronometer in a sediment
of the water reservoir Klingnau, Switzerland**

Jäggi, M. and Eikenberg, J.

Paul Scherrer Institut, Laboratory of Radioanalytics, 5232 Villigen PSI

maya.jaeggi@psi.ch

Major Cs-137 input in waters can either derive from the atmosphere or from releases of radioactive wastewater of nuclear power or reprocessing plants. The aim of this study was to date a sediment of the water reservoir Klingnau. Two Cs-137 peaks could be related to the atmospheric Cs-137 input of the nuclear bomb tests in the 1960'ies with its peak in 1963 and to the nuclear accident of Chernobyl in 1986. Using the sampling date and the dates of the two atmospheric inputs as chronometer, we achieved a sedimentation rate of $1 \text{ cm/a} \pm 0.35 \text{ cm/a}$. This enabled the identification of four additional Cs-137 peaks which may be related to legal Cs-137 wastewater releases from two nuclear power plants in Switzerland. Possible long-distance transport of Cs-137 in a river-lake-river system is discussed.

Transuranic elements in soil samples from Fukushima Prefecture collected in March 2011

R. Kierepko^{1,2} and S.K. Sahoo¹

¹*National Institute for Quantum and Radiological Science and Technology, Anagawa, Inage-ku, Chiba, Japan*

²*H. N. Institute of Nuclear Physics Polish Academy of Sciences, ul. Radzikowskiego 152, Krakow, Poland*

The gigantic tsunami in the northeast Japan region (11 March 2011) caused serious damage to Fukushima Dai-ichi nuclear power plant (FDNPP). As a result, large amount of fission products dispersed across a large area of northern Japan.

This work, focus on the estimation of radioactivity level by determination of transuranic isotopes (Pu, ²⁴¹Am, U) and/or the activity ratios in the surface soil samples collected during a few days after accident (17 – 19 March 2011) from the Fukushima prefecture. All samples were dried at temperature of 105^o C overnight and passed through 2 mm mesh sieve. Subsequently, samples were placed in the polypropylene cylindrical containers for gamma spectrometric measurements. The measurement time was fixed during 1h. Results clearly showed contamination of all samples by aerosols related to FDNPP accident (activity ratio of ¹³⁴Cs/¹³⁷Cs was found almost to unit). After that, samples were homogenized and about 10 g of each powdered samples were ashed at a temperature of 600^o C. The soil samples were decomposed and dissolved by strong acids. Subsequently, radiochemical separation and purification of plutonium, americium and uranium isotopes were measured by α - spectrometry.

Radionuclides and their isotopes ratios have been used as tracer of anthropogenic activity. The relation between them can provide an idea about the source/sources of an investigated contamination. The activity concentration of ²³⁹⁺²⁴⁰Pu in samples ranged between <0.006 Bq kg⁻¹ and 0.216 Bq kg⁻¹ with an average value of 0.052 Bq kg⁻¹. Obtained level was lower than average activity concentration of Pu in soil (0.15 Bq kg⁻¹) from Japan (before FDNPP accident) reported by IAEA . The explanation of that difference could be fact that investigated samples originated from cultivated area (before accident). We could notice ²³⁸Pu only in three samples and the values were usually close to MDC (0.005 Bq kg⁻¹). The activity ratios of ²³⁸Pu/²³⁹⁺²⁴⁰Pu in two samples coincided with global fallout and were comparable with reported value. There was no strong correlation between high activity concentration of volatile radioisotopes (¹³⁴Cs, ¹³⁷Cs) with Pu. Results of Am and U isotopes and their interpretation will be presented at the conference.

Concentrations of radiocesium in wild mushrooms collected in Miyagi prefecture, Japan

¹ KINO, Yasushi, ¹ IRISAWA, Ayumi, ² SEKINE, Tsutomu

*Department of Chemistry, Tohoku University, Japan
IEHE, Tohoku University, Japan*

It has been known that mushrooms accumulate larger amount of radioactive Cs than agricultural products. Since Fukushima Daiichi Nuclear Power Plant accident, we have collected over 800 samples belonging to 120 species of wild mushrooms in Miyagi prefecture that locates on the north of Fukushima prefecture. Radioactive Cs concentrations in the mushrooms were measured with highly pure Ge detectors. The concentrations varied in the ranges of 0.04 to 2,500 Bq/kg wet mass in 2011, 5.8 to 25,000 Bq/kg wet mass in 2012, 4.8 to 150,000 Bq/kg wet mass in 2013, 3.9 to 52,000 Bq/kg wet mass in 2014, and 0.5 to 75,000 Bq/kg wet mass in 2015. These values were decay-corrected to the day when the nuclear reactors were stopped, March 11, 2011. The radioactivity ratio of Cs-134 to Cs-137 was around 1 except for mushrooms collected in lower contaminated areas than 0.1 $\mu\text{Sv/h}$. The values the ratios were from 0.6 to 0.8. The difference from 1 should be ascribed to global fallout due to the atmospheric nuclear weapons testing. Radioactive Cs concentrations of wild mushrooms varied depending on date, place and species. The concentrations showed a positive correlation to the contamination levels of sampling areas. The median of the concentrations increased in 2012. This is related to an annual change in the radioactive Cs distribution in soil. The distribution of mushroom mycelia in soil has different depth profile depending on species. Therefore, varieties of wild mushrooms can be used as indexes of radioactive Cs movement in the environment because of their high ability to accumulate Cs.

Detection of ^{90}Sr in the teeth of cattle contaminated by environmental pollution from the Fukushima-Daiichi Nuclear Power Plant accident

¹ KOARAI, Kazuma, ¹ KINO, Yasushi, ¹ TAKAHASHI, Atsushi, ² SUZUKI, Toshihiko
Dr. SHIMIZU, Yoshinaka, ² CHIBA, Mirei, ^{2,3} OSAKA, Ken, ² SASAKI, Keiichi, ⁴ FUKUDA, Tomokazu, ⁵ ISOGAI,
Emiko, ⁶ YAMASHIRO, Hideaki, ^{1,7,8} OKA, Toshitaka, ^{1,7,8} SEKINE, Tsutomu, ⁹ FUKUMOTO, Manabu, ²
SHINODA, Hisashi

¹ Department of Chemistry, Tohoku University, Japan

² Graduate School of Dentistry, Tohoku University, Japan

³ IRIDS, Tohoku University, Japan

⁴ Faculty of Science and Engineering, Iwate University, Japan

⁵ Graduate School of Agricultural Science, Tohoku University, Japan

⁶ Faculty of Agriculture, Niigata University, Japan

⁷ Tohoku University Hospital, Tohoku University

⁸ IEHE, Tohoku University, Japan

⁹ IDAC, Tohoku University, Japan

[Introduction]

^{90}Sr (half-life of 28.9 y) has a bone-seeking property which may cause internal exposure together with its daughter nuclide, ^{90}Y . The attention has been paid to the determination of ^{90}Sr in the bodies after the past atmospheric nuclear weapons testing and the Chernobyl Nuclear Power Plant accident. The Fukushima Daiichi Nuclear Power Plant (FNPP) accident released ^{90}Sr into the atmosphere and resulted in contamination of the environment. No studies, however, have reported on ^{90}Sr concentrations in teeth or bones because amount of its release was lower than that of ^{134}Cs and ^{137}Cs . Moreover, detection of ^{90}Sr required a great deal of effort. In the present paper, we examined ^{90}Sr concentrations in teeth of cattle caught within a 20-km radius around the FNPP [1]. We had investigated activities of ^{134}Cs , ^{137}Cs , ^{110m}Ag , and ^{129m}Te in organs of the cattle [2], and examined the effect of radioactive Cs on cattle testes after the FNPP accident [3].

[Materials and Method] We selected two young cattle residing in area A (High-contamination area ($10\sim30\ \mu\text{Sv h}^{-1}$)) and area B (Low-contamination area ($0.8\sim1.2\ \mu\text{Sv h}^{-1}$)) from November 2011 to July 2012 (fig 1). Two other cattle from the uncontaminated area C were chosen as controls (fig 1). The teeth were dissected from the mandible. Radioactivity of ^{90}Sr in the teeth was determined by a low background 2π gas flow counter after chemical separations with fuming nitric acid. Concentrations of Ca and stable Sr were determined by ICP-AES.

[Result and discussion] Small amounts of ^{90}Sr (several $20\ \text{mBq (g Ca)}^{-1}$) were detected in the teeth of cattle in Japan at 2008 [4]. The activity concentrations are higher than the ^{90}Sr activity concentrations in the control teeth ($14\sim7\ \text{mBq (g Ca)}^{-1}$, fig 2) of this study. The results show that ^{90}Sr in the control teeth was originated from the atmospheric nuclear weapons testing. The activity concentrations in teeth of cattle from area A and B were higher than those of control cattle (fig 2). The high ^{90}Sr activities in area A and B represent that ^{90}Sr in teeth from the areas should be originated from the FNPP accident. Fig 2 shows activity concentrations of ^{90}Sr in various teeth (DM: deciduous molars, M: molars and P: pre molars) of the young cattle. Judging from the ages of the cattle, M and P were developed after the FNPP accident, while DM were fully developed before the accident. Even within an individual young cattle from area A and B, the activity concentration of ^{90}Sr varied: The M and P exhibited high ^{90}Sr activity concentrations, while the DM exhibited low ^{90}Sr activity concentrations. The difference in ^{90}Sr activity concentration suggests that ^{90}Sr in teeth reflects the contamination from the FNPP accident in development stage. We should note that there were some possibilities of incorporation of ^{90}Sr after the development stage. Thus, we conclude

that we detected the presence of ^{90}Sr from the FNPP accident in teeth of large animals like human beings with statistical significance. Assessment of ^{90}Sr in teeth could allow for the measurement of time-course changes in the degree of environmental ^{90}Sr pollution. We discuss the detail of the time-course changes with Sr specific activity. We determined ^{137}Cs concentrations in and the variation of the ratio of Sr to Ca in biological pathway.

[Summary]

We conclude that we detected the presence of ^{90}Sr from the FNPP accident in teeth of large animals like human beings with statistical significance. Assessment of ^{90}Sr in teeth could allow for the measurement of time-course changes in the degree of environmental ^{90}Sr pollution. We discuss the detail of the time-course changes with ^{90}Sr specific activity. We determined ^{137}Cs concentrations in and the variation of the ratio of Sr to Ca in biological pathway

[1] K. Koara

i, et al., *Sci. Rep.*, **6**, 24077 (2016). [2] T. Fukuda, et al., *Plos One*, **8**, e54312 (2013).

[3] H. Yamashiro, et al., *Sci. Rep.*, **3**, 2850 (2013). [4] Japanese MEXT, (2009).

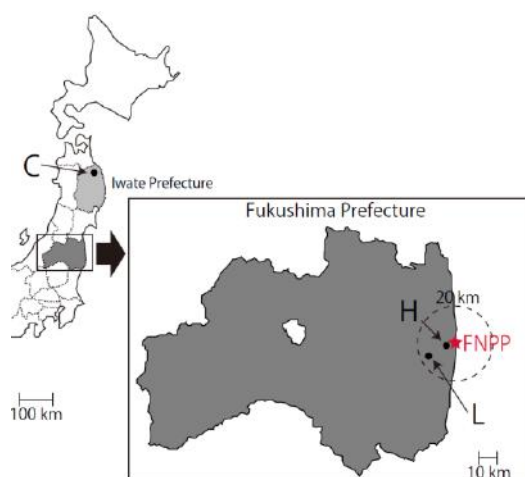


Figure 1. Study Sites.

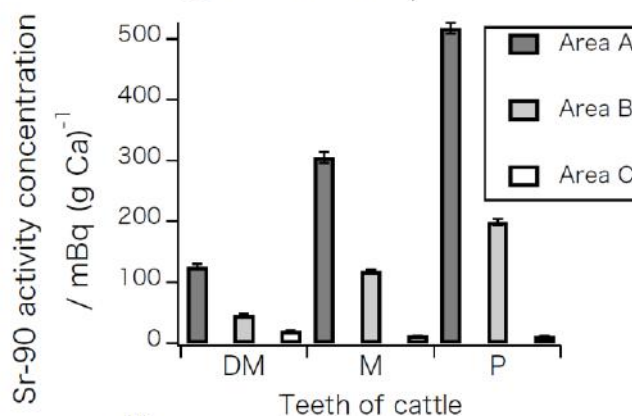


Figure 2. ^{90}Sr activity concentration in teeth.

Diagnostic possibility of digital autoradiography in a study of ^{137}Cs behavior in “soil-plant” system, model experiment

Natalia Kuzmenkova (2), Tatiana Paramonova (1), Maria Godjaeva (1)

Soil Science (1) & Chemistry (2) Faculties of Moscow Lomonosov State University, Russia
kuzmenkova213@gmail.com

Transfer of ^{137}Cs from soil into plants via root uptake and the further radionuclide distribution over food chains is one of the most important problems for radioactively contaminated ecosystems including the long-term period after severe radiation accidents. An accurate understanding of the qualitative and quantitative characteristics of ^{137}Cs behavior in “soil-plant” system is the basis for the elaboration of land use and the prediction of ecological risks. To gain greater insight into the problem how biological features of plants effected ^{137}Cs root uptake a model experiment with simulated wet deposition of ^{137}Cs on pots with undisturbed soil monoliths and subsequent growing of oat (*Avena sativa*, fam. *Gramineae*, typical monocotyledonous) and salad *Lactuca sativa*, fam. *Asteraceae*, typical dicotyledonous) was conducted. Soil monoliths were collected from Plavsky radioactive hotspot (Tula region) and were presented by arable leached chernozems. The soil was chosen because of widespread occurrence throughout the post-Chernobyl radioactively contaminated lands of Russia. Contemporary level of ^{137}Cs in plagued horizon of the soil is 408 ± 19 Bq/kg (154 ± 30 KBq/m²) that exceeds radiation safety standard by 4 times. Plastic pots with soil monoliths were 25 cm in depth and had a surface square 20×20 cm². To simulate a single accident of radiocaesium-containing atmospheric fallout 150 ml of ^{137}Cs solution (CsCl+H₂O) with activity 5 MBq/L were wet deposited on the soil surface as equivalent of a monthly rate of atmospheric precipitation in region (50 mm/month). The 24-h period passed between rain simulation and plant landing to obtain semi-equilibrium distribution of ^{137}Cs in soil monoliths. Six plants for oat and twenty plants for salad were planted per pot in duplicate, and one pot with contaminated soil monolith was used like a blank. Plants were grown at a temperature 20-22°C with additional lighting by fitolamp (regime 12/12 h) and were regularly watered with tap water by sprinkling according to needs of vegetation. After 16 weeks of growing the plants were removed from pots, separated into above- and belowground parts (belowground parts were simultaneously carefully washed out from soil particles), dried at 80°C, weighted and milled to powder for gamma-spectrometry. Two plants from every pot were entirely dried at a room temperature under pressing for subsequent digital autoradiography. As regards soil, two smaller undisturbed soil monoliths (with a square of cross section 4×2.5 cm²) were separated as columns from every basic monolith, air-dried, subjected to digital autoradiography, and afterwards sliced by thin soil layers (0-1 cm, 1-2 cm, 2-3 cm, 3-4 cm, 4-5 cm, 5-6 cm, 6-8 cm, 8-10 cm, 10-20 cm), weighted and subjected to gamma-spectrometry. Digital autoradiography of prepared soil and plant samples was conducted with Cyclone (PerkinElmer). The exposure time was individual and averaged from 8 hours to 24 hours for soil and plants because of different values of ^{137}Cs in the samples. To determine total ^{137}Cs activity samples were analyzed by gamma-spectrometry with the use of HPGe detector Canberra GR 3818. The combination of two analytical techniques reveals the details of ^{137}Cs interaction with soil and the features of the radionuclide fixation by solid phase of arable chernozems (fig.1). In particular, high heterogeneity of ^{137}Cs distribution over soil microprofiles is clearly visible: whereas exponential decreasing of ^{137}Cs activities with soil depth proceeds as a whole, sporadic rise of the measured characteristics at a depth could be attributed with local ^{137}Cs penetration through soil cracks, pores and along root surfaces. Independently of plant species growing in experimental pots (and including blank soil monolith) the ^{137}Cs accumulation occurs in mass just in the top layer up to depth 4-6 cm (max 8 cm), but isolated spots of ^{137}Cs contamination are detectable up to depth 15 cm. Digital autoradiographycal study of the soils indicates very irregular radioactive contamination inside these top layer. Moreover, there is drastic difference in 1.5-4 times between ^{137}Cs activities in soil columns separated from the same monolith as replications for the further analysis. Therefore, the process of ^{137}Cs fixation by the surface of soil aggregates is rather fast and the space of originally radioactive contamination is likely attributed with the wetting depth in the course of ^{137}Cs -containing atmospheric fallout.

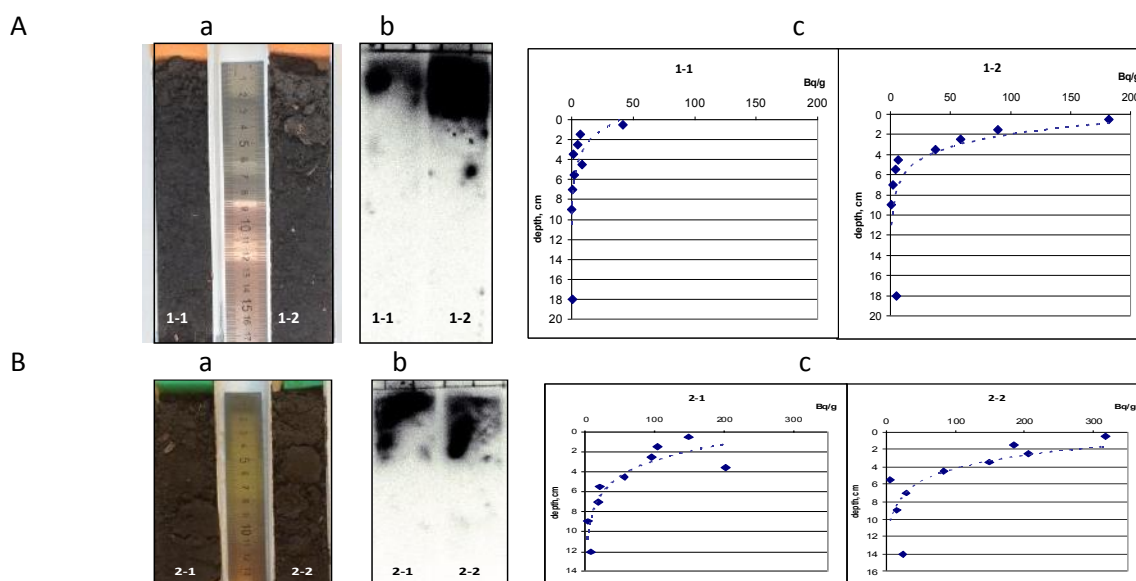


Fig. 1. ^{137}Cs distribution in soil monoliths: A – after growing oat, B – after growing salad; a – photography, b – results of digital autoradiography, c – results of gamma-spectrometry

The less dissimilarity of ^{137}Cs accumulation was noticed between the replications of oat and salad vegetation grown on contaminated soils: the radionuclide activity varied in a range 8-11 Bq/g for oat leaves and stems, 40-121 Bq/g for oat roots, 33-49 Bq/g for salad leaves and stems, 26-55 Bq/g for salad roots. In any event the difference between mono- and dicotyledonous plants is immediately appeared: salad is characterized by relatively evenly ^{137}Cs distribution over the biomass, oat is distinctive by prevailing ^{137}Cs accumulation in roots. Digital autoradiography is unlikely could show this difference for individual plants of oat and salad (fig.2). It is possible to declare that ^{137}Cs is incorporated into all organs of the plants, but visual sites of thickens into darkness are attributed with sample thickening, but not with increasing of ^{137}Cs activity in roots, stems or leaf veins.

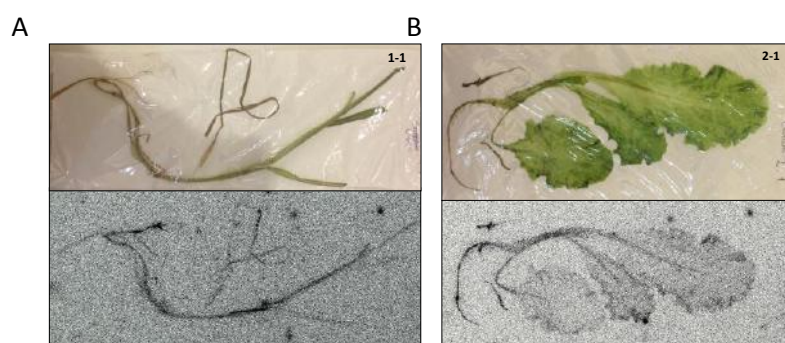


Fig. 2. Photography and digital autoradiography: A – oat, B – salad (dark spots outside of plants are scrapped parts of phosphor layer)

Eventually, the combination of gamma-spectrometry and digital autoradiography techniques is a good advantage for revealing the details of ^{137}Cs behavior in “soil-plant” system and seems perspective for the next development.

The study was conducted with the support from the Russian Foundation for Basic Research (project No. 14-05-00903).

Radionuclide extraction from aqueous solutions by ionic liquids

Raphlin Leyma, Sonja Platzer, Marzieh Habibi, Wolfgang Kandioller, Regina Krachler and Gabriele Wallner*

*Institut für Anorganische Chemie, Universität Wien, Währingerstr. 42, A-1090 Wien, Austria
gabriele.wallner@univie.ac.at*

Ionic liquids (ILs) are salts with a low melting point (below 100 °C) and they are composed of completely dissociated large ions. ILs have many advantages and they are of growing interest in the field of green chemistry. Some of the unique properties of the most widely studied ILs include the large liquid temperature range, high thermal stability, electrical conductivity, and tunable physical properties.¹ Especially the extraction of uranium by using ILs is of enduring interest in the literature as it may also be relevant to spent fuel reprocessing.^{5,6}

The presented work is part of a project dealing with purification processes for drinking water. The aim of our work was the extraction of Uranium, Pb-210 and Po-210 from aqueous solutions with different ILs. Furthermore, a successful back-extraction of the radionuclides from the IL is desirable in order to be able to re-use the IL for several times. Investigations in our laboratory demonstrated that extraction of uranium from water is possible with [A336][TS]^{2,3}, tricaprylmethylammonium thiosalicylate, as well as from maltol-based ILs, namely [A336][Mal] (tricaprylmethylammonium maltolate) and [C101][Mal] (tetradecyltriethylphosphonium maltolate).⁴ The ILs under investigation now are [A336][HNBA] and [A336][Ant] (trioctylmethylammonium 2-hydroxy-5-nitrobenzoate and anthranilate, respectively), as well as [PR4][HNBA] and [PR4][Ant] (triethyltetradecylphosphonium 2-hydroxy-5-nitrobenzoate and anthranilate, respectively).

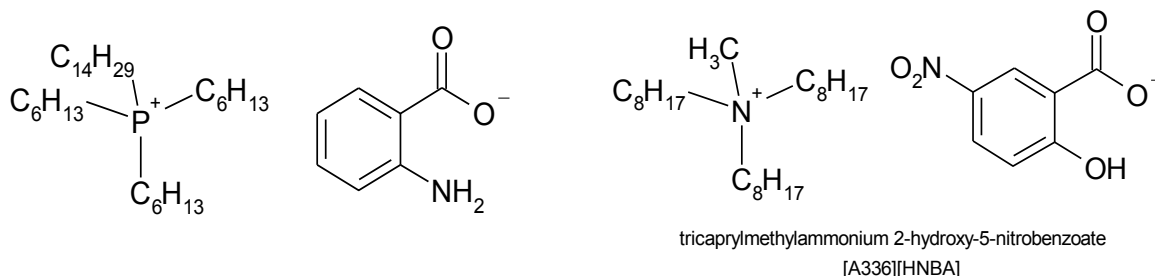


Figure 1: some of the ILs investigated: [PR4][Ant] and [A336][HNBA]

Investigations were performed with artificial water samples: uranyl nitrate solution with known uranium concentration was added to about 10 mL of distilled water, then NaOH was added in order to set a specific pH-value. The resulting uranium content is 27.7 µg U_{nat}. (sum activity 683 mBq or 41 dpm for U-238 and U-234) in 10 ml corresponding to a uranium concentration of 2.8 mg/L. This solution is then mixed with the respective ILs. After centrifugation the phases were separated and an aliquot of the aqueous phase was analysed by liquid scintillation counting (LSC) to ensure that the uranium was removed. For Pb-210 and Po-210 the added activities to the aqueous phase was about 500 mBq, respectively. Afterwards 0.05M HNO₃ was used for back extraction of the radionuclides from the IL phase.

Generally, all investigated ILs showed a high extraction yield for uranium and for Po-210, while Pb-210 was only extracted in very low percentage rates. From the adsorption isotherms we learned that at least one of the investigated ILs was able to take up a rather high quantity of uranium.

- [1] Violina A. Cocalia et al., *Coordination Chemistry Reviews*, 250, 2006, 755- 764.
- [2] Daniel Kogelnig et al., *Tetrahedron Letters* 49, 2008, 2782-2785.
- [3] Michaela Srncik et al., *Applied Radiation and Isotopes* 67, 2009, 2146-2149.
- [4] Sonja Platzer et al., *J. of Radioanal. Nucl. Chemistry* 303, 2015, 2483-2488.
- [5] James E. Quinn et al., *Solvent Extraction and Ion Exchange* 31, 2013, 538-549.
- [6] Dimitrios Tsaoulidis et al., *Chemical Engineering Journal* 227, 2013, 151-157.

The study on sorption process in geological materials of long-lived radioactive isotopes Sr-90 and Cs-137 in model systems with the use of short-lived isotopes Sr-85 and Cs-134

M. Miecznik, J.W. Mielinski, E.Łokas

The Henryk Niewodniczański Institute, Polish Academy of Science, ul. Radzikowskiego 152, 31-342 Cracow, magdalena.miecznik@ifj.edu.pl

This paper presents results of experiments carried out in order to determine adsorption capacity of soil in case of uncontrolled leakage from waste repository of low to medium activity radioactive substances. The adsorption of soil was measured according to pH, ionic strength, time, and concentration of the isotope in the solution. Figure 1 shows determination of the Langmuir adsorption isotherm to data points obtained from ^{134}Cs measurements. These analyzes were carried out for 8 m soil profile taken in the vicinity of National Radioactive Wastes Disposal in Rożan. Based on geological, granulometric and mineralogical analysis, the profile was divided into four layers of depth intervals: 0 - 1.2 m, 1.2 - 2.5 m, 2.5 - 6.5 m, 6.5 - 8 m. The predominant fraction of the tested specimens was sand consisting of quartz. As was shown in the experiment, the importance of recognized fraction cannot be ignored in the adsorption process. Based on the Langmuir isotherm fit to the data points, the adsorption capacity of the soil under the landfill was determined. Hydrogeological conditions in the area of the NRWD in Rózan are discussed. A numerical simulation of radionuclide migration in the vicinity of NRWD in Rózan was performed according to the results of the experiment. The methodology of measuring adsorption on soil samples was set as well as a simple computer program was written for modeling the transport of radionuclides in the environment.

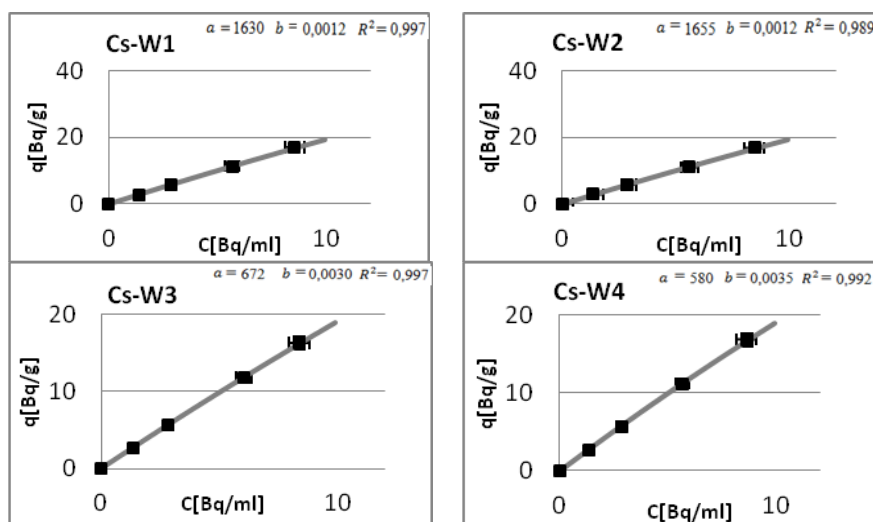


Figure 9 Fit of the Langmuir adsorption isotherm to ^{134}Cs data points for each of the 4 layers of collected soil profile. Langmuir isotherm and matching curve parameters are shown in the upper right corner of each chart.

Variation of ^{210}Pb , ^{210}Po , ^{238}U and ^{232}Th concentrations in atmospheric deposition and aerosol samples collected in Rokkasho, Aomori, Japan

Yoshihito Ohtsuka, Yuichi Takaku, Shun'ichi Hisamatsu

Department of Radioecology, Institute for Environmental Sciences, 1-7 Rokkasho, Aomori 039-3212, Japan

Lead-210 and ^{210}Po are naturally occurring radionuclides in the ^{238}U decay series that are continuously produced as decay products from gaseous ^{222}Rn in the atmosphere. These radionuclides attached to aerosols are transported with air masses from mainly the Asian continent to the Japan Islands, where they are deposited on the ground by wet and dry deposition processes. Because their radioactivities are comparatively high in general atmospheric aerosol samples and can be easily measured, these radionuclides have been used in geochemical studies as tracers of air-mass transport. In contrast, most atmospheric ^{238}U and ^{232}Th are considered to be provided by resuspension from the ground surface. Because the ^{238}U concentration is relatively high in seawater, some atmospheric ^{238}U occurs as sea salt aerosols derived from sea spray.

To evaluate the deposition fluxes and atmospheric concentrations of these radionuclides in Rokkasho, Aomori, which is near the northern tip of Honshu Island, Japan, we collected total (dry and wet) deposition and aerosol samples there from August 2011 to December 2013. Total deposition during 5–12 d was collected as a single sample, and the sampling was continuous throughout the observation period. Aerosol samples were collected during 1 d of each deposition sampling period.

Alpha spectrometry was used to determine ^{210}Po activity in each sample, and ^{210}Pb activity was determined by measuring the activity of its daughter ^{210}Po after a sufficient period of ingrowth. An ICP-MS was used to analyze ^{238}U , ^{232}Th and Al concentrations, and an ICP-AES was used to analyze Na concentrations.

The deposition fluxes of ^{210}Pb and ^{210}Po showed a clear seasonal pattern, being high during November–March and low in June–October. The higher fluxes during November–March were most likely related to the winter monsoon, which brings air masses enriched in these radionuclides from the Asian continent. The overall average of the monthly mean residence time (Figure 1A) in the total deposition was 27 d. The mean residence time was longer in June and September than in other months, though the deposition fluxes in those months were low.

The seasonal ^{210}Pb concentration pattern in aerosols was similar to that of the deposition flux, but the ^{210}Po concentration increased only during February–March. The monthly mean residence time in aerosols (Figure 1B) varied over a smaller range than the residence time in the total deposition. The overall mean residence time was 22 d, slightly shorter than that in the deposition, but within the range of literature values.

The monthly deposition fluxes of both ^{238}U and ^{232}Th also varied seasonally, being high during March–April and low in summer. The deposition fluxes of both ^{238}U and ^{232}Th correlated well with those of Al, indicating that they likely originated from soil particles resuspended from the ground surface. Asian dust is frequently observed in Japan in spring; the high concentrations in March and April may be due to their transport from the Asian continent.

Both the deposition flux (Figure 2B) and atmospheric concentration (Figure 2D) of ^{232}Th correlated well with those of Al. Slopes of regression lines for ^{232}Th on Al in Figure 2B and 2D are quite similar each other, showing the same source and behavior in the atmosphere of ^{232}Th and Al. Although the deposition fluxes of ^{238}U well correlated with those of Al, the correlation between atmospheric concentrations of ^{238}U and Al was not so good. The slope of regression line for deposition flux of ^{238}U on Al (Figure 2A) was also different from that for the atmospheric concentrations (Figure 2C). The dashed line in Figure 2C shows the regression line

for deposition fluxes of ^{238}U on Al for comparison. It is clear that the behaviors of ^{238}U in the atmosphere and in the deposition process are different from those of Al. The reason for the different behaviors is unknown; further study, including detailed measurements of the aerodynamic diameter of ^{238}U and related elements is required.

Acknowledgments

This study was performed under a contract with the Government of Aomori Prefecture, Japan.

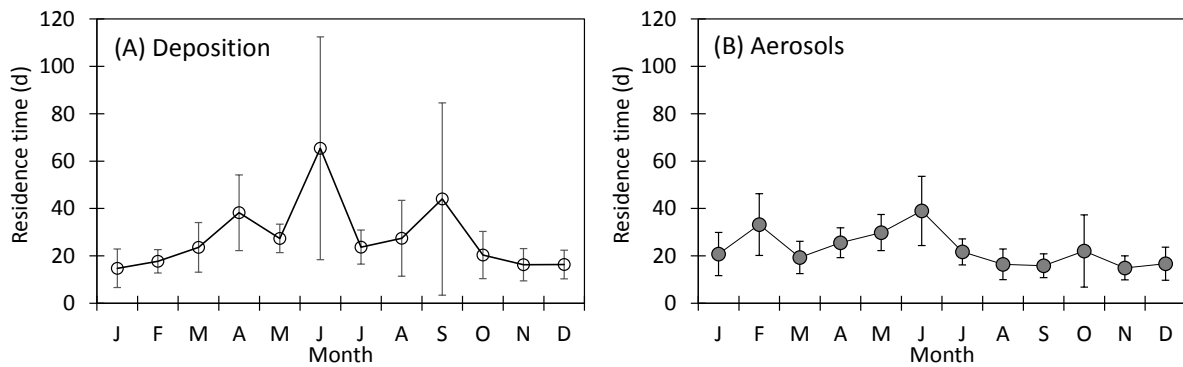


Figure 1 Monthly mean residence times, evaluated from $^{210}\text{Po}/^{210}\text{Pb}$ activity ratios, for (A) total deposition and (B) aerosol samples corrected from August 2011 to December 2013. The error bars indicate standard deviations.

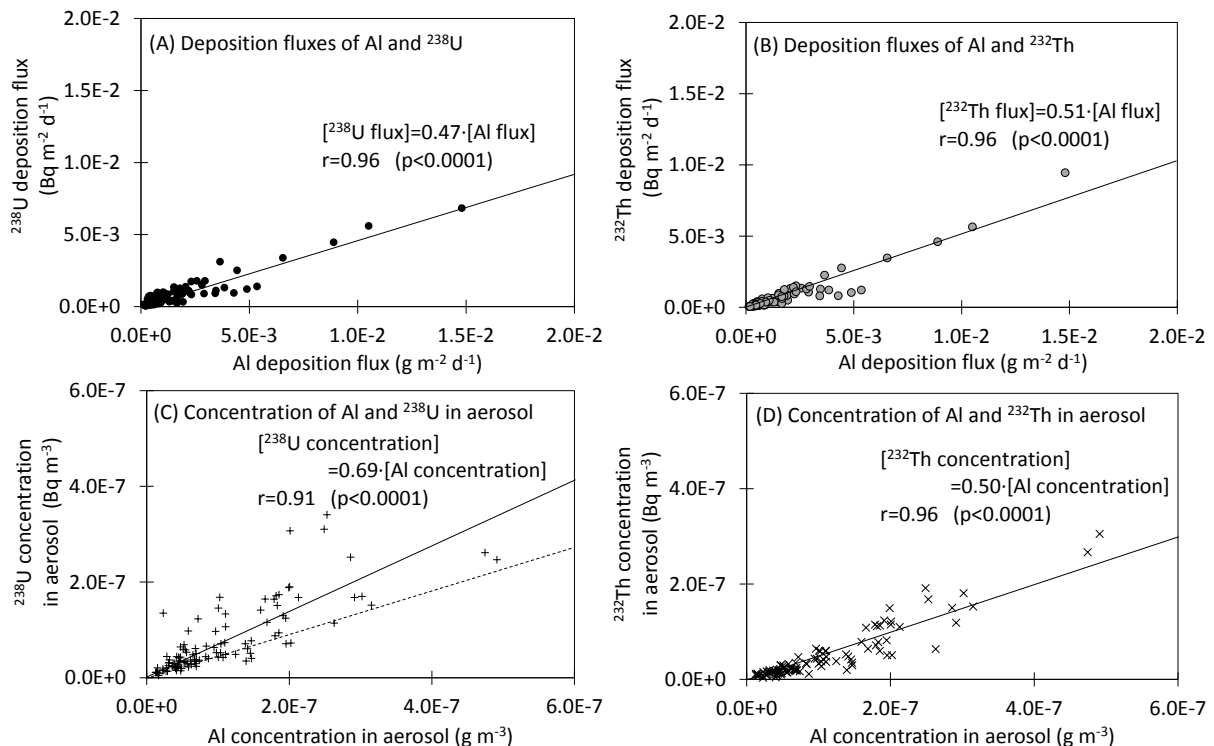


Figure 2 Deposition fluxes of (A) ^{238}U and (B) ^{232}Th versus that of Al, and aerosol concentrations of (C) ^{238}U and (D) ^{232}Th versus that of Al. Solid lines show regression lines. A dash line in (C) shows the regression line for deposition fluxes of ^{238}U on Al for comparison.

Ionizing radiation in the upper atmosphere over Finland

Jussi Paatero, Juha Hatakka and Rigel Kivi

Finnish Meteorological Institute, P.O.Box 503, FI-00101 Helsinki, Finland

Radiosonde is a lightweight instrument which is lifted from the Earth's ground up to the atmospheric pressure level of 10...2 hPa (altitude of 35...40 km) with a balloon filled with hydrogen or helium. During its ascent the radiosonde measures temperature, humidity, and pressure (PTU) of the ambient air. The vertical profiles of wind direction and velocity are obtained by horizontal positioning of the sonde with the GPS satellite positioning system. The radiosonde transmits the measured data to a ground station. The received data is further processed and meteorological values (temperature, humidity, pressure, and wind speed and direction) are calculated in the ground station computer. Radiosondes can be equipped with additional sensors such as ozone or radiation sensors to obtain vertical profiles of these parameters.

The radiation sensor used in this work consists of two Geiger-Müller (GM) tubes and an integrated interface to the radiosonde. It is thus possible to measure the vertical distribution of atmospheric ionizing radiation up to 2 hPa pressure level together with the PTU data. One of the GM tubes measures only gamma radiation while the other measures both beta (>0.25 MeV) and gamma radiation. The wall thickness of the GM tubes is 250 mg/cm^2 and $32\text{--}40 \text{ mg/cm}^2$ for the gamma only tube and gamma and beta tube, respectively. The GM tubes are specially designed for low-temperature environment and they are tested down to the temperature of -70°C . The accuracy of the tubes is $\pm 10\%$. The sensitivity of the GM tubes depends on the energy of radiation. The natural radiation environment in the upper atmosphere differs significantly from the radiation emitted by a single radionuclide. This prevents an accurate conversion from measured pulse rates to absorbed dose rate in the air D (Gy/h) and even further to ion production (ion pairs per unit time and per mass/volume). In this work we used the conversion equations based on the radiation emitted by ^{137}Cs . These equations were provided by the GM tube manufacturer. The conversion equations are for the gamma tube:

$$D (\mu\text{Gy/h}) = 0.23 R^{1.15}, \quad (1)$$

and for the beta and gamma tube:

$$D (\mu\text{Gy/h}) = 1.1 R^{1.02}, \quad (2)$$

where R is the measured count rate [1/s].

The measuring range of the radiation detector is wide, up to $100\,000 \mu\text{Gy/h}$ and $200\,000 \mu\text{Gy/h}$ for the gamma only tube and gamma and beta tube, respectively. For comparison, following the 1986 Chernobyl nuclear accident the maximum absorbed dose rate observed at ground level air in Finland was less than $4 \mu\text{Gy/h}$ (Paatero et al. 2010). For historical reasons these upper air soundings have been called radioactivity soundings even though precisely speaking they should be called count rate or dose rate soundings.

The sounding stations where this work was carried out are the FMI's Arctic Research Centre at Sodankylä and the FMI's meteorological observatory at Jokioinen, Finland. The Sodankylä site is situated 100 km north of the Arctic Circle at 67.368°N , 26.633°E , and 179 m above mean sea level. The geomagnetic coordinates of the station are 63.9°N and 120°E , and the vertical effective cutoff rigidity less than 0.7 GV (Smart and Shea 2008). The Jokioinen site is situated in south-western Finland at 60.814°N , 23.498°E , and 104 m above mean sea level. The geomagnetic coordinates of the station are 58.3°N and 112°E , and the vertical effective cutoff rigidity ~ 1.2 GV. Radioactivity soundings have been made at both sites since the mid 1990s, the number of soundings has varied usually from one to four per year.

It has been known over a half a century that the intensity of cosmic radiation in the atmosphere increases from the magnetic equator towards the magnetic poles but that the intensity levels off above the 50th

latitude (Neher and Stern, 1955). There the shielding effect of the atmosphere becomes more dominant than the cosmic radiation cutoff. This is reflected in the plot of radioactivity soundings in Figure 1. There is only a minor difference in the soundings made at Sodankylä and at Jokioinen. On the contrary there is a marked difference between the Finnish soundings and the sounding of Hong Kong, where the Pfotzer maximum lies between 16000 m and 18000 m, several thousand meters lower than in Finland (Lui and Lee 2009; Li et al. 2007). Also the intensity is clearly lower. In the north even the numerous low-energy particles can penetrate the Earth's magnetic field and reach the stratosphere. But these particles are quickly stopped and thus the maximum intensity of their secondary particles occurs in a relatively high altitude. Close to the magnetic equator, on the other hand, only the few most energetic particles can pass the Earth's magnetic field. But they have more penetration power in the atmosphere and thus the secondary particles formed from them have an intensity maximum deeper in the atmosphere.

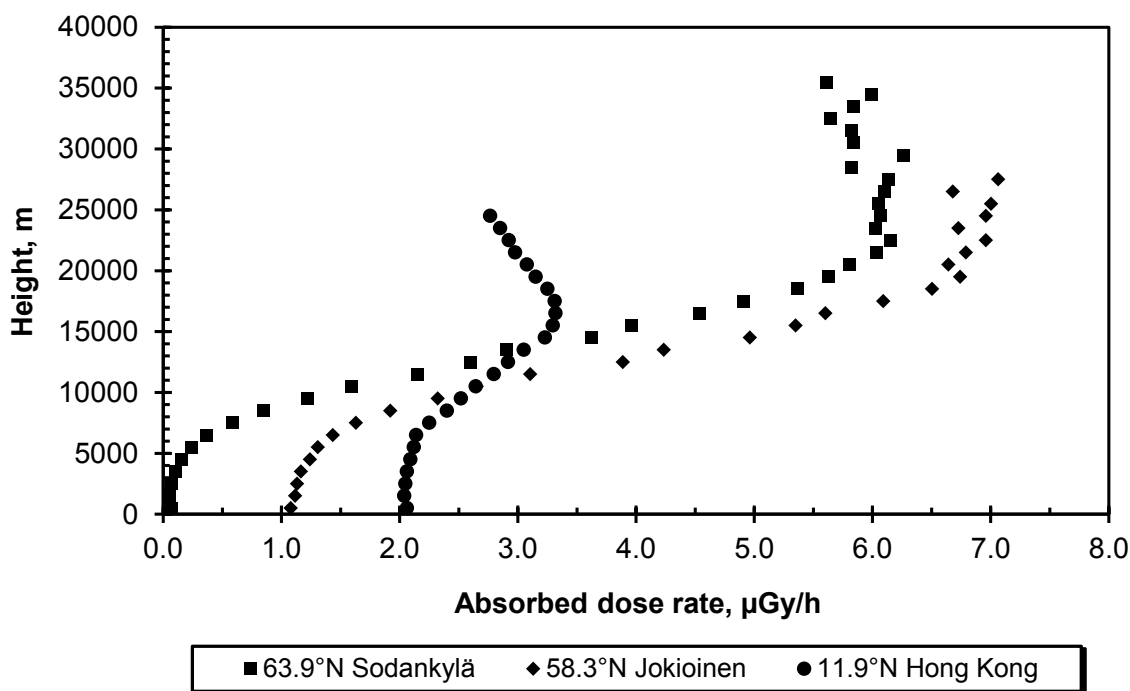


Figure 1. Radioactivity soundings (gamma tubes) made at different geomagnetic latitudes in summer 2008, from left to right: 63.9°N (Sodankylä), 58.3°N (Jokioinen), and 11.9°N (Hong Kong). The leftmost sounding represents absolute values. The next ones have an offset of 1 and 2 µGy/h to separate them from each other. The data for the sounding at Hong Kong (11.9°N) is from the report of Lui and Lee (2009).

References

- H.V. Neher, E.A. Stern. "Knee" of the Cosmic-Ray Latitude Curve. *Physical Review* 98, 845-846 (1955).
 S.W. Li, Y.S. Li, K.C. Tsui. Radioactivity in the atmosphere over Hong Kong. *Journal of Environmental Radioactivity* 94, 98-106 (2007).
 C.M. Lui, C.W. Lee. Summary of Environmental Radiation Monitoring in Hong Kong 2008. Technical Report No. 29. Hong Kong, Hong Kong Observatory (2009).
 J. Paatero, K. Hämeri, T. Jaakkola, M. Jantunen, J. Koivukoski, R. Saxén. Airborne and Deposited Radioactivity from the Chernobyl Accident – A Review of Investigations in Finland. *Boreal Environment Research* 15, 19-33 (2010).

Interaction of radio-metals with microorganisms

Johannes Raff^{1,2}, Manja Vogel¹, Alix Günther¹, Björn Drobot¹, Christine Schmooch³, Henry Moll¹, Hilmar Börnick³, Eckhard Worch³, Thorsten Stumpf¹

¹*Institute of Resource Ecology, Helmholtz-Zentrum Dresden-Rossendorf, Dresden, Germany;*

²*Helmholtz Institute Freiberg for Resource Technology, Helmholtz-Zentrum Dresden-Rossendorf, Dresden, Germany*

³*Institute of Water Chemistry, Technische Universität Dresden, Dresden, Germany*
j.raff@hzdr.de

Metals interact in various ways with living organisms. This affects first of all the behavior of the metals in the environment as different metal species differ in their mobility in the geo- and the biosphere as well as in their bioavailability. Conversely, metals are essential for the vitality of cells. Many metals are an integral part of one or more enzymes involved in metabolic and biochemical processes. Beside essential metals there are also toxic and radioactive metals that can seriously damage an organism at least at higher concentrations. Figure 1 shows possible interaction mechanisms between microorganisms and radio-metals.

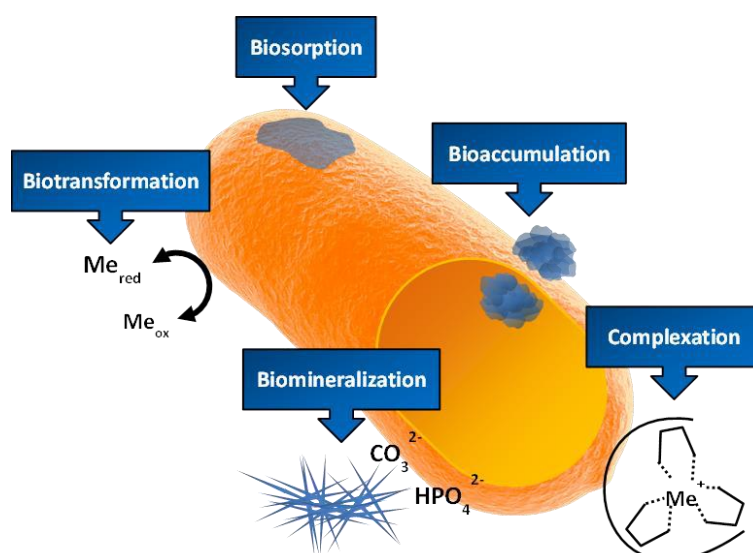


Figure 1: Possible interaction mechanisms of radio-metals with microorganisms (according to [1])

Furthermore, radio-metals may damage or even destroy cells by radiation. The latter excites or ionizes atoms or molecules causing the formation of radicals, changes of biomolecules or even the breakage of chemical bonds. But also for this kind of damage microorganisms have successfully developed effective strategies. Different spectroscopic methods and electron microscopy reveal that different groups of organisms such as bacteria, algae and fungi, differ in their interaction with radio-metals.

In case of bacterial uranium mining waste pile isolates belonging to the genera *Lysinibacillus* and *Bacillus* it was demonstrated that so-called S-layer proteins, forming a latticed protein envelope on many bacteria and almost all archaea, are able to effectively scavenge reactive oxygen species (ROS). The latter can be formed by either radiolysis of water or the Fenton reaction. These ROS react with tyrosine side chains of the proteins forming bityrosines and thereby causing an intramolecular crosslinking. Furthermore, these S-layers possess different functional groups on their surface such as carboxyl, hydroxyl, amino, phosphate, sulfoxide and sulfate groups. These groups mediate selective binding of different metals including uranyl(VI) [2]. As most S-layer proteins are also calcium binding proteins, these S-layers additionally possess at least two different Ca binding sites binding trivalent actinides such as Cu(III) with high affinity [3]. In case of the alga

Chlorella vulgaris U(VI) concentrations up to 5 μM are bound via carboxyl and phosphate groups being located on the cell surface. This process is followed by desorption in which probably the secretion of complexing bio-ligands is involved [4]. At higher uranium concentrations of 100 μM the alga will die and no desorption can be observed. In comparison to this alga, the fungus *Schizophyllum commune* interacts with moderate concentrations of uranium (4.2 μM) via organic phosphates. At higher U(VI) concentrations (420 μM) the fungus stays alive and accumulates uranium additionally inside the cell by forming inorganic uranyl phosphates [5]. Due to their high uranium resistance and high accumulation rates different fungi were selected to be further investigated regarding their application potential for a fungal-based concept for the reliable immobilization of released radionuclides within the so called BioVeStRa project.

References

- [1] Lloyd J.R. and Macaskie L. E. (2002), *In Interactions of Microorganisms with Radionuclides*, Ed. Keith-Roach & Livens, Elsevier, 313-342,
- [2] Merroun M.L. et al. (2005), *Appl. Environ. Microbiol.* 71(9), 5532-5543.
- [3] Moll H. et al. (2011), Curium(III) complexation with surface-layer (S-layer) proteins from a uranium mining waste pile isolate. Poster at Migration 2011, 18.-23.09.2011, Beijing, PR China.
- [4] Vogel M. et al. (2010), *Sci. Total Environ.* 409, 384-395.
- [5] Günther A. et al. (2014), *Biometals* 27,775-785.

Scavenging processes of natural and anthropogenic radionuclides on the continental margin of the East China Sea

Masatoshi Yamada¹ and Jian Zheng²

¹ *Department of Radiation Chemistry, Institute of Radiation Emergency Medicine, Hirosaki University, 66-1 Hon-cho, Hirosaki, Aomori 036-8564, Japan*

² *National Institute of Radiological Sciences, 4-9-1 Anagawa, Chiba 263-8555, Japan*
myamada@hirosaki-u.ac.jp

Anthropogenic radionuclides such as Pu-239 (half-life: 2.411×10^4 years), Pu-240 (half-life: 6.564×10^3 years) and Pu-241 (half-life: 14.325 years) have been released into the environment as the result of atmospheric nuclear weapons testing, disposal of nuclear wastes and nuclear fuel-cycle reprocessing operations, etc. Am-241 (half-life: 432.2 years) originated mainly from the decay of Pu-241. Am-241, Pu isotopes and Pb-210 (half-life: 22.3 years) are highly particle-reactive elements and those are therefore removed from the water column by scavenging onto settling particles. Compared with intensive studies of Pu isotopes and Pb-210, distributions and behavior of Am-241 in the ocean have been poorly investigated. In the North Pacific Ocean, two distinct sources of Pu isotopes can be identified; i.e., the global stratospheric fallout and close-in tropospheric fallout from nuclear weapons testing at the Pacific Proving Grounds (PPG) in the Marshall Islands. The atom ratio of Pu-240/Pu-239 is a powerful fingerprint to identify the sources of Pu in the ocean

The objectives of this study are to measure the concentrations of Am-241, Pu-239+240 and Pb-210 and the atom ratios of Pu-240/Pu-239 in settling particles and surface sediments and to discuss the removal of reactive radionuclides by scavenging on the continental margin of the East China Sea. Settling particle samples were collected at four stations. Two types of sediment traps were used, cylindrical traps and conical time-series traps. Sediment samples were collected with a multiple core sampler. The Pu-239+240 concentrations in settling particles increased with depth from 1.8 mBq/g at 100-m depth to 3.0 mBq/g at 120-m depth on the continental shelf edge and they ranged from 3.0 to 4.0 mBq/g at depths below 120 m. The Pu-240/Pu-239 atom ratios in settling particles ranged from 0.21 to 0.25 and they were higher than the global fallout ratio of 0.18. The Am-241 activities in settling particles ranged from 2.6 to 7.3 mBq/g, indicating that they increased gradually with increasing trap depth. The Am-241/Pu-239+240 activity ratios were 1.5 at 100-m depth and 2.1 at 600-m depth. The Am-241/Pu-239+240 activity ratios were significantly higher than the global fallout ratio of 0.3–0.4. These results showed that Am was more effectively scavenged from seawater than Pu isotopes. The Am-241 fluxes ranged from 1.5 to 170 mBq/m²/day and increased with depth, with an especially large increase near-bottom. The activities and fluxes of Am-241 showed large seasonal variations. There was a tendency for Am-241 activities and Am-241/ Pu-239+240 activity ratios in surface sediments (0–1 cm) to increase almost linearly with depth. This tendency was in good agreement with that of Pb-210. All these results can be attributed to enhanced Am-241 scavenging by particles and removal near the front between the Kuroshio Current and the East China Sea shelf water. It appears that the same removal mechanism occur between Am-241 and Pb-210.

Development of aerosol generation system for simulating dry deposition process of radioactive nuclides released from the Fukushima accident

Z. Zhang*, K. Ninomiya, A. Shinohara

Graduate School of Science, Osaka University, Japan

Introduction

A large amount of radioactive nuclides was discharged in the environment by the accident of the Fukushima Daiichi Nuclear Power Plant. The discharged nuclides were transported in the atmosphere with aerosol form. The chemical and physical properties of the aerosol strongly affected to the transportation and deposition processes. Most of radioactive nuclides released in land deposited to the forests in Fukushima prefecture. Kaneyasu reported that the long half-life radionuclide, ^{137}Cs was transported through the atmosphere mainly as sulfate aerosol form [1]. For evaluating behaviors of ^{137}Cs in forest system, fundamental data of dry deposition and uptake process of aerosol was desired. However, most of foliar uptake experiments performed with solution. The knowledge on dry deposition process with aerosol form was very limited.

The aim of our study is investigation of radioaerosol dry deposition process to vegetation, and observation of foliar uptake behavior of radiocesium. For this purpose, an aerosol generation system that can produce aerosols in any chosen diameter and chemical composition, was needed. In this paper, we will discuss the status of developed aerosol generation system and the results of aerosol deposition experiments using this system.

Development of aerosol generation system

Our method of aerosol generation based on the spray drying of mineral salt solution. Solution was sent to a nozzle by a syringe pump and spraying with a high speed air flow. The mist was generated in a chamber in high temperature condition. The mist was dried quickly, and micro size solid aerosols were generated. The experimental conditions, such as the size of chamber, chamber temperature, solution flow rate, air flow rate and so on, were optimized. The particle size distributions were determined from aerosol collection by a cascade impactor, and

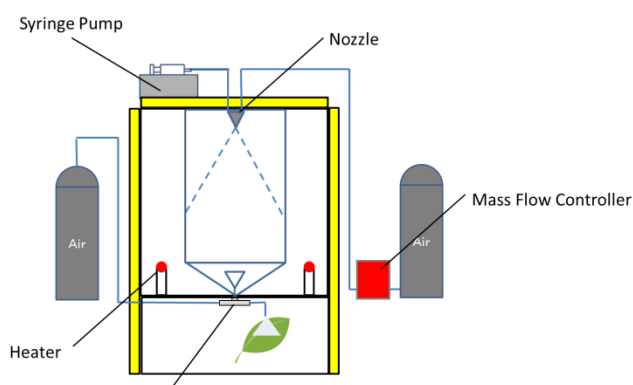


Figure 1. Aerosol generation system

found that the produced aerosols had several micro-meter in diameter. Aerosol was suctioned to inlet of ejector and discharged from outlet of ejector, and deposited to a leaf by impaction with high speed gas flow.

Deposition experiment

We performed experiments for simulating deposition process of FDNPP. Leaves of *Camellia japonica* were used for deposition experiments. For comparing dry and wet deposition, chemical compounds containing ^{137}Cs in aerosol form and droplet form were mounted to upper side of leaf, by a syringe and our aerosol generation system. The leaves were washed by purified water, and the amount of absorbed ^{137}Cs in leaf was measured by germanium detectors and absorption rates were determined in each deposition form. In the presentation, we will discuss about ^{137}Cs absorption rate with time dependence, temperature and humidity dependence and chemical compounds dependence.

[1] N. Kaneyasu et al, Environ. Sci. Technol, 46 (2012) 5720 – 5726

Atmospheric $^{90}\text{Sr}/^{137}\text{Cs}$ activity ratio in eastern Japan after the FDNPP accident

Z. Zhang^{1*}, K. Ninomiya¹, Y. Yamaguchi¹, T. Saito², K. Kita³, H. Tsuruta⁴, Y. Igarashi⁵, A. Shinohara¹

¹ Graduate School of Science, Osaka University, Japan

² Shokei Gakuin University, Japan

³ Ibaraki University, Japan

⁴ University of Tokyo, Japan

⁵ Meteorological Research Institute, Japan

Introduction

A large amount of radioactive nuclides have been released into the environment by the nuclear accident at the Fukushima Daiichi Nuclear Power Plants (FDNPP). Measurement of radionuclides will give us much information about the accident circumstance. Furthermore, radioactivities in air are critical for estimation of internal exposure. There are many measurement results of ^{131}I , ^{134}Cs and ^{137}Cs in environmental samples. However, in other radionuclides, such as the pure beta emitter nuclide, ^{90}Sr , has not been measurement sufficiently. Strontium-90 is different from radiocesium in discharging behaviour from nuclear fuels under reactor accident [1]. Therefore, determining $^{90}\text{Sr}/^{137}\text{Cs}$ activity ratio will give use better understanding about the reactor accident, such as temperature in the reactor.

We developed a new simple and quick strontium isolation method using solid-phase extraction for determination ^{90}Sr in aerosol by liquid scintillation counter (LSC) [2]. In this study, we determined ^{90}Sr activity in aerosol samples collected after the FDNPP accident using this method.

Sampling and Measurement

Our group has been operating aerosol samplings after the accident mainly in eastern Japan. The samples were collected on grass fiber filters using high volume air samplers. Air volume of each sample was 1700 – 4000 m³. Sampling spots are shown in Fig. 1. Cesium-137 activities in aerosol samples were measured by germanium detectors from gamma-ray intensities of 661.6 keV. Strontium-90 in aerosol samples was isolated by a sequential chemical separation method using solid-phase extraction [2]. This method achieved more than 80% of Sr yield and complete elimination of naturally occurring radioactivity; ^{210}Pb .

To determine ^{90}Sr , Cherenkov radiation of ^{90}Y has been measured by a LSC, 1220 QUANTULUS™ Ultra Low Level Liquid Scintillation Spectrometer. The detection efficiency of ^{90}Y was 68.7% and detection limit of ^{90}Sr was 0.004 Bq in our experimental system. With sequential measurement, the growth of ^{90}Y activity was obtained and the shape of growth curve was completely agreed with the growth of ^{90}Y from ^{90}Sr decay.



Results and Discussion

Strontium-90 concentration obtained was in the order of 10^{-3} and 10^{-5} Bq/m³ and had decreased exponentially to the background level until December, 2011. The $^{90}\text{Sr}/^{137}\text{Cs}$ ratios was shown in Fig.2. We found that the ratio was 1.2×10^{-3} at March 2011 and it had risen to 1.3×10^{-1} at August 2011. Such a temporal variation in $^{90}\text{Sr}/^{137}\text{Cs}$ ratios have never been reported. The maximum and minimum $^{90}\text{Sr}/^{137}\text{Cs}$ ratios obtained in this study were well agreed with the simulated radioactivity ratios of the radionuclides discharged from the Unit 2 and the Unit 3 reactors in the FDNPP. Our results clearly show that the main radionuclides discharging source were changed from the Unit 2 to the Unit 3 around June 2011.

- [1] M. Allen et al., Nuclear Technology 92 (1990) 214-227
- [2] Z. Zhang et al., submitted to Applied Radiation and Isotopes

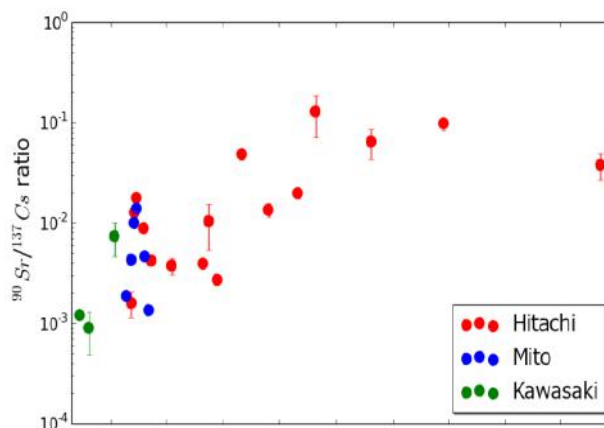


Figure 2. Daily changes of $^{90}\text{Sr}/^{137}\text{Cs}$ activity ratio within 2011

Susanna Salminen-Paatero¹ and Jussi Paatero²

¹ *Laboratory of Radiochemistry, Department of Chemistry, P.O. Box 55, 00014 University of Helsinki*

² *Finnish Meteorological Institute, Observation services, P.O. Box 503, 00101 Helsinki, Finland*

A sample set of human livers, ribs, lungs and lymph nodes was analyzed for estimating concentrations of heavy metals and ²³⁹⁺²⁴⁰Pu in different organs. The samples were collected within autopsies made in Southern Finland and Lapland in 1976-1979. The sampling program was part of investigations concerning enrichment of radionuclides along the food chain lichen-reindeer-man (Jaakkola et al. 1981, Mussalo-Rauhamaa 1981). Furthermore, in this recent study, the enrichment of heavy metals in the food chain lichen-reindeer-man was investigated by determining their concentrations in reindeer and lichen samples.

Over 200 samples were collected from the autopsies of 67 persons during 1976-1979. In this preliminary study, 31 samples were used as test samples, both for

- a) modifying existing analytical methods for biological samples and
- b) to adjust the detection techniques (LSC, ICP-AES) for biological samples with high matrix content and low radioactivity concentration

The samples were ashed and/or wet-ashed with conc. HNO₃ and HCl. A fraction of this solution was taken for the determination of heavy metals by ICP-AES. From rest of the solution, ²³⁹⁺²⁴⁰Pu, ²⁴¹Am and ⁹⁰Sr were separated by ion exchange and extraction chromatography. The activity concentrations of ²³⁹⁺²⁴⁰Pu and ²⁴¹Am were determined with alpha spectrometry and that of ⁹⁰Sr with liquid scintillation counting.

The activity concentration of ²³⁹⁺²⁴⁰Pu per wet weight was 0.5±0.2 – 4.9±0.8 µBq/g in lungs (9 results), 21±5 µBq/g in livers (average of 2 results), 14±7 µBq/g in ribs (one result), and 9±3 µBq/g in collarbone (one result). The activity concentration of ²³⁹⁺²⁴⁰Pu in these human samples is in accordance with a previous study of the same sample collection (Mussalo-Rauhamaa 1981) and with worldwide values summarized by Taylor (1995). In most cases, the activity concentration of ²³⁸Pu was close to or below detection limit and sometimes also ²³⁹⁺²⁴⁰Pu. This is a challenge for analytical method development, as large sample mass is needed and biological samples contain loads of interfering matrix (bone: calcium, lungs: iron, all: organic compounds). The composition of these samples was problematic for heavy metal determination as well, since some organic compounds were not destroyed during ashing+wet ashing procedure: iron-containing precipitation occurred in some final samples soon after diluting for ICP-MS-samples, and ICP-AES had to be used instead of ICP-MS for measuring heavy metal concentrations, due to better tolerance of former against sample impurities.

Heavy metal concentrations varied with orders of magnitudes inside and between sample categories (Table 1). Cobalt was not detected in any of the samples and lead was found only in 9 lung samples (< D_L – 0.99±0.20 µg/kg wet weight). Elevated levels of lead, nickel and cadmium (not determined here) in lungs are typical for tobacco smokers. Average uranium contents for skeleton and soft tissues have been reported to be 3.79±0.45 µg/kg and about 0.5 µg/kg wet weight, respectively, for three Caucasian men (Kathren&Tolmachev 2015), our general uranium concentration being roughly at the same magnitude, but our values for ribs 0.18±0.04 – 0.46±0.09 µg/kg being lower than for the skeleton by Kathren&Tolmachev (2015).

Our highest value for nickel concentration in lungs, 3.74±0.75 µg/kg wet weight, is even higher than that of mine workers in Ontario, 1.84 µg/kg dry weight (Verma 2013). The same lung sample contained also the highest chromium content of lungs (14±3 µg/kg), as well as high amount of uranium (5.9±1.2 µg/kg), but lead content was low (0.28±0.06 µg/kg), indicating smoking as an improbable nickel source of this lung. This lung donor of our study lived 50 years in Sodankylä, Lapland, working as a reindeer herder outdoors most of the time. The lungs of this person might have exposed to pollutants from Kola Peninsula metal smelters via inhalation.

After this preliminary sample set and analytical method adjustment, the work for analyzing the rest of the human samples will continue and a larger data set will be produced.

Table 1. Heavy metal concentration in different human organs determined with ICP-AES ($\mu\text{g/kg}$ wet weight).

Sample type (n)	Zn	As	V	Cu	Ni	U	Cr
lung (16)	< D _L – 52±10	< D _L – 0.11±0.02	1.30±0.26 – 13±3	< D _L – 1.96±0.39	< D _L – 3.74±0.75	0.68±0.14 – 7.3±1.5	< D _L – 14±3
lymph nodes (7)	< D _L – 29±6	< D _L – 0.07±0.01	3.02±0.60 – 45±9	< D _L – 6.8±1.4	< D _L – 1.59±0.32	< D _L – 3.39±0.68	< D _L – 2.59±0.52
rib (3)	< D _L – 15±3	–	3.06±0.61 – 4.12±0.82	–	–	0.18±0.04 – 0.46±0.09	–
flesh (2)	88±18 – 165±33	–	1.51±0.30 – 1.74±0.35	1.63±0.33 – 2.23±0.45	< D _L – 0.48±0.10	0.97±0.19 – 2.21±0.44	< D _L – 0.13±0.03
collar-bone (1)	99±20	0.04±0.01	1.90±0.38	1.88±0.38	1.36±0.27	2.71±0.54	0.24±0.05
liver (2)	79±16 – 141±28	–	2.41±0.48 – 5.2±1.0	6.4±1.3 – 7.9±1.6	1.31±0.26 – 1.61±0.32	2.89±0.58 – 4.52±0.90	–

References

- T. Jaakkola, M. Keinonen, M. Hakanen, J.K. Miettinen. Actinides in Man and Animals. Proceedings of the Snowbird Actinide Workshop (M.E. Wrenn, ed.). RD Press, USA (1981), p. 509.
- Helena Mussalo-Rauhamaa. Accumulation of plutonium from fallout in southern Finns and Lapps. Report Series in Radiochemistry 4/1981. Helsinki 1981.
- D.M. Taylor. Environmental Plutonium in Humans. Applied Radiation and Isotopes 46, 1245-1252 (1995).
- R.L. Kathren, S.Y. Tolmachev. Natural Uranium Tissue Content of Three Caucasian Males. Health Physics 109, 187-197 (2015).
- D.K. Verma. Metals in the Lungs of Ontario Hardrock Miners. Archives of Environmental & Occupational Health 68, 180-183 (2013).

Simulation of the occupational radiation dose caused by contamination of primary circuit media in pressurized water reactor

A. Artmann², G. Bruhn², S. Schneider², E. Strub¹

¹Gesellschaft für Anlagen- und Reaktorsicherheit (GRS) gGmbH, Schwertnergasse 1, 50667 Cologne

²Abteilung Nuklearchemie der Universität zu Köln, Zùlpicher Str. 45, 50674 Cologne, Germany

Introduction

The occupational radiation exposure of workers in Nuclear Power Plants (NPPs) is determined by numerous parameters. An important factor is the radiation exposure caused by contamination of the primary circuit. The aim of this work was to model a generic power plant to understand and simulate the radiation exposure connected to defined jobs and tasks in a nuclear power plant. This simulation comprises 4 steps: (i) Determination of the relevant representative nuclide vectors, (ii) 3D modeling of the PWR primary circuit, (iii) Dose rate calculations, and (iv) Definition of jobs.

Determination of the relevant nuclide vectors

A broad overview of the relevant microscopic processes was derived from Neeb [1], see Figure 1.

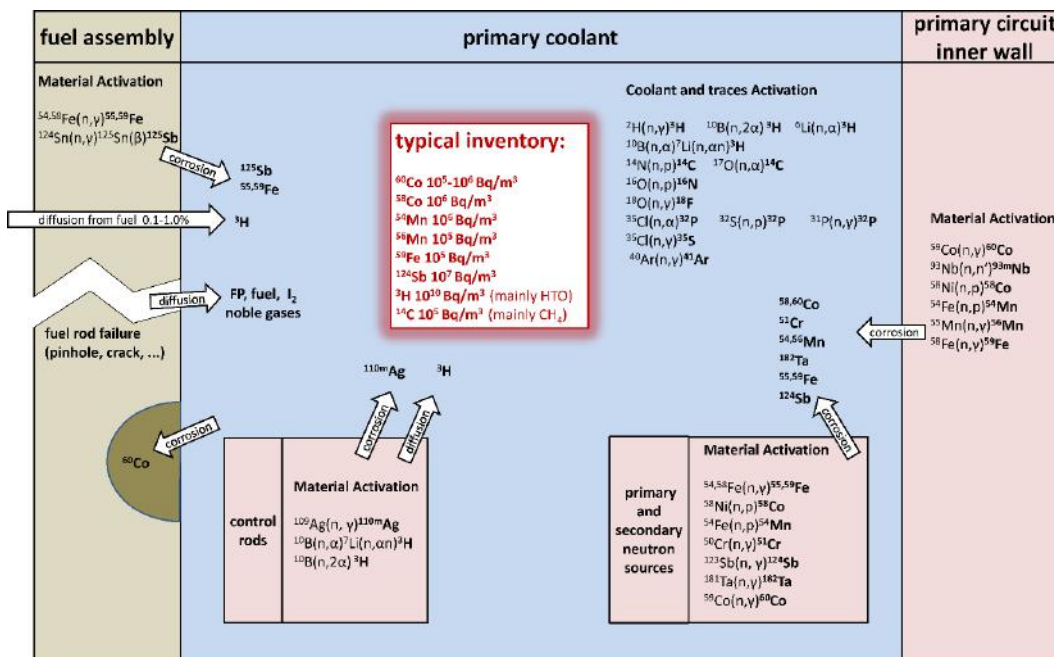


Figure 1: Physico-chemical processes, resulting concentrations of radionuclides in PWR primary loops (adapted from [3]). The typical inventory comprises the radiologically most important nuclides during revision assuming of no fuel defects.

Several attempts have been made to simulate those processes quantitatively [2,3], but this proved challenging due to the complexity of chemical and thermodynamic processes. Therefore, in this work more general scientific considerations were used as a basis to develop plausible nuclide vectors for different scenarios, namely (i) operation, (ii) maintenance and revision, and, (iii) decommissioning of a NPP. The *relative contributions* of the radionuclides were determined by the evaluation of actual radionuclide concentrations in German NPPs of the past 15 years. Finally, the nuclide vectors were scaled using local dose rate measurements from the the ISOE database [4], i.e. by reverse simulation.

The 3D Model

The generic 3D model of the primary circuit was based on the technical documentation of German NPPs. A 3D CAD model was constructed with SketchUp [5]. Within the model, the NPP is represented as a number of elementary radiation sources and elementary shieldings. Each of these construction elements is defined such that it can be fitted to a single MicroShield [6] calculation. An example of the modelling of a steam generator as a set of sources and shielding is shown in Fig. 2 (left). The inner structure is partly modelled as a virtual composite material (consisting of a mixture of metal (Incoloy 800), water and steam).

Dose rate calculations

The NPP generations 2, 3 and 4 of KWU/Siemens PWRs are characterised in MicroShield [4] by the representative nuclide vectors (see above), the thickness of available shielding, and the material composition of the components. The distribution of contamination of about $1 - 2 \cdot 10^{14}$ Bq to the components of the primary circuit is done on one hand based on reverse simulation, starting from the (relatively few) known local dose rates, and on the other hand based on geometrical and physical considerations.

Definition of jobs

Working tasks are modelled as a combination of retention times and related local positions. For these geometrical coordinates, the contribution of any subcomponent and subsystem to the local dose rate is calculated and summarised afterwards. Each job/working task/craft is broken down into several (usually three or four) specific local points. Realistic retention times of the average worker at each of the defined local points is again derived from the ISOE database[5]. With knowledge of dose rates at the specific local points and the respective retention times, a calculation of the occupational dose is possible.

Results and Discussion

Our generic model allows the calculation of the resulting occupational doses generated by definable jobs and working tasks. It could be shown that assuming a nuclide vector and shield arrangement of a KWU/Siemens pre-Konvoi plant, the resulting occupational dose caused by working tasks related to the reactor coolant pump is close to measured data. The calculated dose rates for different jobs are within the range of reported data from the ISOE database (see Fig. 8 and Tab. 1). This shows the validity of this generic model approach in this case.

It could be shown that the described generic NPP model allows the prediction of expected individual and collective doses. The resulting values have been compared with Job/Task dose data from the ISOE database, showing good agreement between the real data and the simulated data. The described model but can be easily adapted to any 4-loop PWR reactor, mainly by adjusting shieldings as well as the ^{60}Co content in nuclide vectors to a specific NPP [7].

References

- [1] *Neeb, K. H.*: The Radiochemistry of Nuclear Power Plants with Light Water Reactors, Walter de Gruyter, Berlin/New York, 1997
- [2] Data processing technologies and diagnostics for water chemistry and corrosion control in nuclear power plants (DAWAC), IAEA TECDOC 1505, June 2006
- [3] Modelling of Transport of Radioactive Substances in the Primary Circuit of Water-Cooled Reactors, IAEA TECDOC 1672, 2012
- [4] Occupational Exposures at Nuclear Power Plants, Nineteenth Annual Report of the ISOE Programme, OECD, 2011
- [5] Trimble Navigation Limited: Sketchup, V. 8.0, 2012
- [6] Microshield, Grove Software Inc., <http://www.radiationsoftware.com/mshield.html>
- [7] *Artmann, A., Bruhn, G., Schneider, S., Strub, E.*, Generische Studie zum Zusammenhang zwischen Kontamination von Primärkreislaufmedien und beruflicher Strahlenexposition bei Kernkraftwerken mit Druckwasserreaktor – Abschlussbericht, GRS gGmbH, 2015

Effect of air radiolysis products on the chemistry of ruthenium during a severe nuclear accident

Ivan Kajan¹, Teemu Kärkelä², Ari Auvinen², Christian Ekberg¹

¹ *Chalmers University of Technology, Nuclear Chemistry, Kemivägen 4, 41296 Göteborg, Sweden*

² *VTT Technical Research Centre of Finland, P.O. Box 1000, FI-02044 VTT, Espoo, Finland*
kajan@chalmers.se

During a nuclear accident the most important chemical elements are those forming volatile compounds that can be released from the irradiated fuel into the environment. For the proper evaluation of a possible source term during an accident, the quantity of the released radioactive nuclides, their transport and further interactions with the structural materials in the nuclear power plant are necessary to be known. Among others ruthenium is one of the critical radiotoxic elements in the case of an accident due to its ability to form volatile oxides. This work was focused on the transport of ruthenium through the reactor cooling system in case of a nuclear accident connected with air ingress. Main objective was to evaluate the effect of air radiolysis products that will be unavoidably formed during an accident and their impact on the quantities and chemical speciation of transported ruthenium. Separate effects of NO₂, N₂O and HNO₃ on the ruthenium transport were studied in the primary circuit simulating facility. Gaseous and aerosol forms of ruthenium were collected at the outlet of the facility and quantified with use of neutron activation analysis. Chemical characterization of the collected samples was performed with use of SEM, XPS, XRD and photospectroscopy. In the experiments nitrogen oxides as well as nitric acid had significant effect on the ruthenium chemistry in the model primary circuit. The fraction of transported gaseous ruthenium was increased when NO₂ or HNO₃ were injected into the airflow with volatile ruthenium oxides. This effect was most prominent in case of NO₂ precursor at temperature of 1300 K. The overall transport of ruthenium was strongly increased at 1500 when N₂ was injected into the gas phase, when compared to the pure humid air atmosphere. The obtained results indicate a strong effect of air radiolysis products on the quantity of transported ruthenium and its partition to gaseous and aerosol compounds.

Retention of organic iodides on charcoal filter material

Emma Aneheim and Mark Foreman

Department of Chemistry and Chemical Engineering, Nuclear Chemistry, Chalmers University of Technology, SE-41296 Gothenburg, Sweden

The threat posed to the general public by a nuclear reactor accident is mainly due to the release of radioactivity from the plant into the environment, where it can cause both external and internal exposure of the population. The progression of a nuclear reactor accident and the form and amount of radioactivity subsequently released are determined by a series of chemical and physical effects. The physical properties of substances released upon a nuclear accident are controlled by their chemistry. Thus, after the nuclear reaction stops, the effect of the entire accident is influenced by chemical effects. Serious nuclear accidents generally include overheating of nuclear fuel. In this type of accident a strong correlation between the volatility of a radioelement and the fraction which is released from the fuel exists. In this work focus therefore revolves around the chemistry of the volatile fission product iodine released upon a loss of cooling accident similar to Three Mile Island or the Fukushima accident.

One of the key chemical phenomena which limits the escape of radioactivity from a damaged nuclear plant is adsorption of radioactive materials onto surfaces present in the plant. An important surface on which adsorption can occur is the charcoal used to treat gases and air leaving the reactor containment. However, a series of questions exist regarding the effectiveness of such charcoal filter materials. One important question is how well the charcoal filters can capture and retain radioactivity in the form of organic iodine compounds. It is known that methyl bromide (and by implication methyl iodide) is able to pass unchanged through an activated charcoal filter.¹ Methyl halides do, however, react with the amines commonly added to charcoals designed to retain these compounds. It has previously been shown that paint² and paint solvents³ are able to form different organic iodine compounds under simulated nuclear accident conditions. While no evidence exists regarding the relative amounts of radioactivity present in the form of different organic iodine compounds released from e.g. Fukushima, it has been shown that nuclear fuel processing plants emit a complex mixture of organic iodine compounds.⁴ It is therefore possible that multiple forms of organic iodine will be released during both normal operation and during a serious nuclear accident.

In this work the retention of radioactive organic iodine on charcoal filter material has been investigated and compared to elemental iodine retention. A flow of gas has been allowed to pass through a pad of charcoal after volatilizing the radioactive iodine compound. Experimental conditions such as the presence of moisture in the carrier gas and different gas flow rates have been investigated. The results have been evaluated using on-line gamma detection with NaI-detectors and autoradiography of the charcoal pads after the end of experiment. Pure radioactive methyl and ethyl iodide was successfully synthesized from the corresponding tosylate and used without any presence of carrier solvent. Both alkyl iodides were found to be retained in the first few centimeters of the charcoal pad (Figure 1) and did not reach the NaI detectors in the experimental setup. The retention was the strongest for elemental iodine followed by ethyl iodide and methyl iodide. Increasing the carrier gas flow-rate, or introducing moisture did not affect the retention to any larger extent.

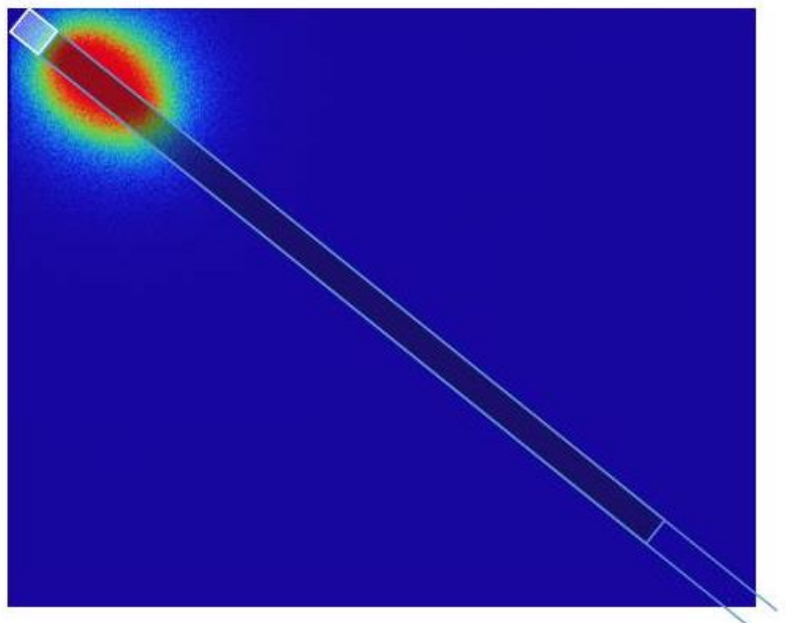


Figure 1. Autoradiography image of one charcoal pad after a flow experiment with methyl iodide. Activity introduction to the top left.

¹ S. Tanaka, S. Abuku, K. Imaizumi, H. Ishizuka, Y. Seki and S. Imamiya, *Industrial Health*, 1989, **27**, 111-120.

² S. Tietze, M.R.S. Foreman, C.H. Ekberg and B.E. VanDongen, *Journal of Radioanalytical and Nuclear Chemistry*, 2013, **295**, 1981-1999.

³ S. Tietze, M.R.S. Foreman and C.H. Ekberg, *Journal of Nuclear Science and Technology*, 2013, **50**, 689-694.

⁴ W.A. Haller and R.W. Perkins, *Health Physics*, 1967, **13**, 733.

Indoor radon (^{222}Rn) concentration level study in child care centers and kindergartens using nuclear track methodology (NTM)

G. Espinosa and J.I. Golzarri

*Instituto de Física, Universidad Nacional Autónoma de México Circuito de la Investigación Científica,
Ciudad Universitaria, Mexico City, 04510, Mexico.*

espinosa@fisica.unam.mx

As it is known, staying for long periods of time in a place with high concentration of radon is a health hazard. This health risk can be increased into the adulthood, if on infant ages the young people grow inside places with important indoor radon levels. Causal associations between exposure level and lung cancer have been demonstrated in epidemiological studies around the world, suggesting that for younger age children groups, the risk coefficient of lung cancer for inhaled radon and their daughters is about a factor of 4 on children from recent born to 10 years old, and 2 for ages between 10 to 20 years old.

The aim of this work is to determine the indoor radon levels where infants from 3 months to 6 years old, remaining long times in Child Care Centers and Kindergartens. Indoor radon (^{222}Rn) concentration levels were measured in the Child Care Centers and Kindergartens of the 16 political administrative regions, covering 5% of the total in Mexico City. This study was conducted over one-year period of time, divided into four three-month periods coinciding with the seasons. Nuclear Track Methodology (NTM) was selected for the measurements. A passive close-end-cup with Poly Allyl Diglycol Carbonate (PADC) as detection material, device designed for children places was used, with one step chemical etching process, following a well-established detection and analysis protocol originally developed by the "Dosimetry Applications Project" (DAP), of the Physics Institute of the National Autonomous University of Mexico.

In this study, the results of measurements of indoor radon concentration in Child Care Centers and Kindergartens in Mexico City are encouraging, finding indoor radon levels between 35 Bq/m^3 and 65 Bq/m^3 with a maximum of 85 Bq/m^3 and a minimum of 20 Bq/m^3 . It can be considered that the indoor radon concentration levels are low in this type of buildings, due the benign climate in the city, and the architecture design of the constructions.

Natural radionuclides in infant formulae (powder milk)

Miha Trdin*, Ljudmila Benedik

Jožef Stefan Institute, Jamova 39, SI-1000 Ljubljana, Slovenia

**miha.trdin@ijs.si*

It is well known that any food and foodstuff contains the naturally occurring radionuclides originating from uranium and thorium decay chains. Since a dose coefficient is always related to a specific radionuclide, it is therefore necessary that the activity concentrations of particular radionuclides are determined when estimating a radiological risk assessment. Dose coefficients, however, are age dependent with the highest values being prescribed for infants; one of the most sensitive parts of the population. Due to the fact that data on particular radionuclides content in infant formula are scarce the aim of our research was their determination in infant formula available on the Slovenian market (Aptamil and Novalac).

The first estimation of activity concentrations was done by gamma-ray spectrometry. For particular radionuclides determination (uranium, polonium, etc. radioisotopes) alpha particle spectrometry and radiochemical nuclear activation analysis were applied. Results obtained by radiochemical neutron activation analysis showed that concentrations of uranium in the samples are in the range of 1 ng per gram of infant formula. When a sample was decomposed by lithium borates fusion and the ^{238}U content was determined by alpha particle spectrometry the activity concentrations were determined to be in the range between 0.03 and 0.06 Bq/kg of infant formula. ^{210}Po content was determined by alpha particle spectrometry and its activity concentrations were in the range between 0,15 - 0.4 Bq/kg. Obtained activity concentration of ^{40}K was determined by gamma-ray spectrometry to be between 150 and 200 Bq/kg. The results obtained enabled us to calculate cumulative annual dose for infants received from infant formula ingestion.

An experimental study on in situ gamma spectrometry using room model

KIM, Chang-jong, JI, Young-yong, JANG, Mee, CHUNG, Kun Ho

Korea Atomic Energy Research Institute, Korea

The problem of building materials with elevated content of natural radioactivity has emerged in recent years and many researches on dose assessment of building materials have been studied. In situ gamma spectrometry can be utilized to determine the radioactivity from building materials containing the natural radionuclide, especially it is useful in a situation that sampling is difficult. In this study, in situ gamma spectrometry is verified to apply existing building using real room model. The room model is made of acrylic and filled with standard material of ^{238}U , ^{232}Th , ^{226}Ra and ^{40}K which are radioactivity range between 200 and 1000 Bq/kg. These natural radionuclides is in normal indoor and outdoor space, so experiment is tested on the lake which background of gamma ray is lower. Gamma spectrometry measurements carried out with HPGe detector which was modeled by MCNP code. And detection efficiency is determined to calculate radioactivity by MCNP simulation. Net count of standard material is calculated by subtracting background on the lake which is less than 10 times compared with land. ^{234}Th , ^{234m}Pa and ^{228}Ac of daughter nuclide of ^{238}U and ^{232}Th is analyzed and ^{226}Ra and ^{40}K is analyzed directly with gamma ray of 186, 1461 keV. In the result, the percentage difference between reference value and analysis value is within about 20%. So, this method will be applicable to assessment radioactivity of existing building without sampling.

EDUCATION

Beta-ray spectrometry for radiation education

Etsuko Furuta¹, Keiji Kusama² and Yasuo Watanabe³

Ochanomizu University¹, Japan, Japan Radioisotope Association² and Saint Gobain³

For radiation education, measurement training is important to understand mechanisms of radiation. Additionally, it is important to be easy training for a learner of radiation. Generally, a liquid scintillation counter (LSC) is used for quantitative analysis of beta-ray emitters. An LSC with 2 or 3 photomultiplier tubes (PMTs) is required to get spectra; however, they always show quenching with liquid scintillator for fluorescence emitting. Using a quenched spectrum is hard to study what kind of radionuclides is measured. When unquenched spectra are able to get, a learner studies a mechanism of radiation measuring and quenching.

We developed a new measurement method for beta-emitters with an LSC and plastic scintillators (PS), which did not generate organic liquid waste and solid waste [1-4]. Additionally, we developed a prototype device of PMTs connected with a multichannel pulse height analyzer (MCA) to measure low energy beta-ray emitters with the PS sheets [5]. By these studies, unquenched spectra were gotten. Since energy calibration of the MCA is only estimated by the energy divided with channels, it is necessary to calibrate energy for identification of beta-emitters with their spectra. Our purposes of this study are to try to calibrate energy using internal conversion electrons, to clarify the calibration is suitable for low energy beta-emitters and to show what kinds of training are possible for radiation education.

This prototype device had 1 PMT and connected with a plug in type MCA. Plastic scintillator of sheets or block was used as fluorescence emitter, which was BC-400 (Saint-Gobain) and cut in 48 mm ϕ with 0.5mm in thickness sheet or 24 mm thickness block. The suitable high voltage and gains for this system was adjusted.

Liquid sources of beta-emitters such as ³H-methionine (maximum beta ray energy; E_{\max} = 18.6 keV), ¹⁴C-arginine (E_{\max} = 156 keV) and ³⁵S-methionine (E_{\max} = 167 keV) (Moravek Biochemicals) were prepared pipetting on each PS-sheet, then dried up in a lab and put another sheet on the source (an assemblage). Beta particle standards such as ¹⁴⁷Pm (E_{\max} = 225 keV), ⁶⁰Co (E_{\max} = 318 keV), ³⁶Cl (E_{\max} = 709 keV) and ²⁰⁴Tl (E_{\max} = 764 keV) (Eckert & Ziegler) were used. The internal conversion electron source was ²⁰⁷Bi (Eckert & Ziegler), which electron energies were 482, 554, 976 and 1048 keV [6].

Peaks of the ²⁰⁷Bi were widened like a Gaussian distribution by PS of BC-400. The 2 peaks of near energies emitted were overlapped. However, each peak top showed each internal conversion electron energy. Additionally, each assemblage of beta-ray emitter showed exemplary continuous beta-ray spectrum and the end-point channel was decided at the cross point with its baseline. Then, using 4 peaks of the internal conversion electrons and some beta-energy end points, the horizontal line energy were decided to each channel. A good linearity was shown between the energy and channel. This technique was applicable to identify ³H, ¹⁴C and ³⁵S on their spectra as shown in Fig.1.

With the device connecting a PMT, a MCA and plastic scintillator sheets or block, estimation of beta energies was possible by using unquenched spectra. For radiation training, it was effective for learner to settle measurement condition and to get spectra by themselves.

References;

1. E. FURUTA et al., 2014, Measurement of tritium with high efficiency by using liquid scintillation counter with plastic scintillator. J Applied Radiation and Isotopes, 93, 13-17.
2. E. Furuta et al., 2014, The effect of atmospheric plasma treatments on plastic scintillator for beta-ray measurement. J Radioanal Nucl Chemis, 299,471-476.
3. Y. Yoshihara et al., 2015, Measurement of tritium with plastic scintillator: Surface improvement. Fusion Science and Technology, 67(3), 654-657.
4. E. Furuta et al., 2015, A new tritiated water measurement method with plastic scintillator pellets. Isotopes in Environmental & Health Studies, (In printing 2015.10)
5. E. Furuta and Takao Kawano, 2015, A plastic scintillation counter prototype. Applied Radiation and Isotopes, 104, 175-180.
6. Table of isotopes 8th Edition, R.B.Firestone et al. Edit., John Wiley & Sons, INC, New York, USA 1996.

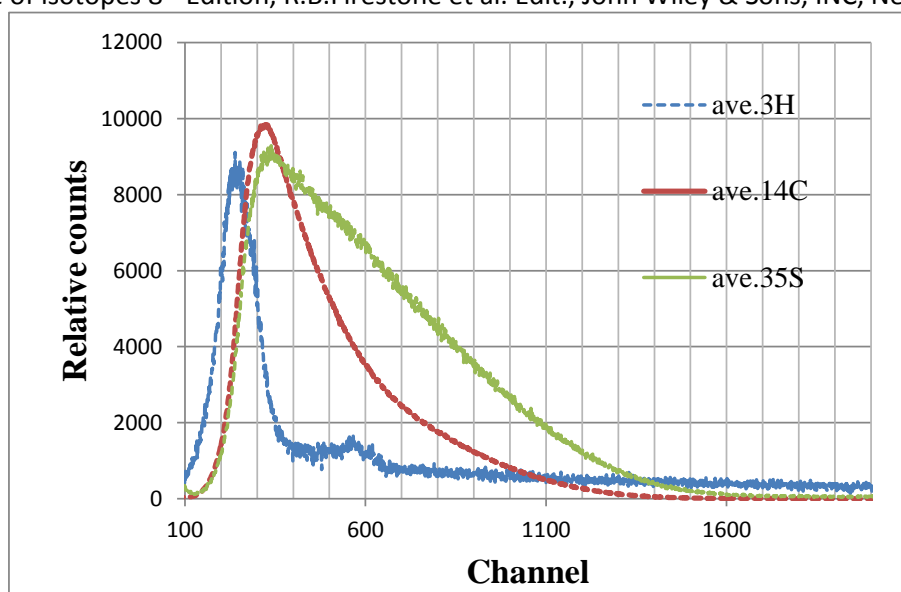


Fig.1 Three kinds of unquenched spectra of beta-emitters; ^3H , ^{14}C and ^{35}S by using plastic scintillator. The condition of this case was HV=920, coarse gain=8, fine gain=5, low level discrimination=5 and base line threshold=5

Undergraduate summer school in radiochemistry at OSU

A. Paulenova

*School of Nuclear Science and Engineering, Radiation Center
Oregon State University, Corvallis, OR 97331, United States*

Oregon State University has a long history of high quality instruction in nuclear and radiochemistry. As one of the few universities in the US where students can gain hands-on experience in working with actinides, we have great capabilities to accommodate a summer undergraduate school in radiochemistry. The School of Nuclear Science and Engineering is housed in the OSU Radiation Center, where also the 1MW TRIGA research reactor, several research laboratories, multiuser counting rooms, research library and computing labs are available for undergraduate student projects in radiochemistry.

This summer the OSU School of Nuclear Science and Engineering was responsible for hosting and conducting a laboratory-intense six week Radiochemistry Summer School focusing on the back-end of the nuclear fuel cycle, funded by the US Department of Energy. The objective of this summer school was to provide undergraduate students with the opportunity of hands-on research experience related to the radiochemistry and chemistry of nuclear fuel cycle, and encourage them to apply for graduate study and support their interest to this field and possible career considerations.

The main focus was training in fundamentals of nuclear science, radioanalytical chemistry and radiodetection, combined with fundamental chemical properties of radionuclides, solution thermodynamics and kinetics, chemical speciation, radiation chemistry, all closely related to the back-end of the fuel cycle. The first week was devoted to introduction to nuclear science: nuclear properties, nuclear forces and nuclear structure, decays and nuclear reactions, fission, fusion and heavy elements, followed by radiodetection lectures and laboratory classes, review of reactor designs and fuels, tour to Hanford (WA) and finally 3 weeks of a full-time work on a research project.

Student projects addresses were related to different aspects of the back-end of the fuel cycle: speciation in the organic phase of the ALSEP separation process, chemistry of zirconium, uranium peroxide particles, oxidation of americium, synthesis of plutonium chloride, U238/234 equilibrium in uranium, detection of gaseous fission products.

The results of the student surveys are so interesting that it is worth to share with wider audience.

Remote controlled radiochemical experiments developed at the Institute for Radioecology and Radiation Protection, Hanover

Wolfgang Schulz

Institute for Radioecology and Radiation Protection, Leibniz Universität Hannover, Hannover, Germany

In order to mitigate the effects caused by the declining number of staff qualified in nuclear chemistry, the CINCH-II project aiming at the Co-ordination of education In Nuclear CHemistry was supported within FP7 Euratom from July 2013 to May 2016. The CINCH-II project is built around the three pillars Education, Vocational Education and Training (VET) and Distance Learning. These main pillars are supported by two cross-cutting activities – Vision, Sustainability and Nuclear Awareness that includes also dissemination, and Management.

One of the goals of this collaboration is the development of six fully remote-controlled experiments, based on the RoboLab concept, spotlighting on different aspects of nuclear chemistry. Three of these automated laboratories have been designed and built at the Institute for Radioecology and Radiation Protection (IRS) of the Leibniz Universität Hannover, Germany, and are presented in this poster:

GammaLab is focused on teaching gamma spectrometry on environmental samples, and on showing the importance of characteristic limits in the evaluation of a gamma spectrum.

AutoDepositionLab demonstrates the potential of electrochemical deposition techniques for the measurement of radionuclides.

IonLab gives the students the possibility to conduct from their own computer a very simple radionuclide separation on a chromatographic column followed by an "on-line" detection of the activity.

Remote controlled radiochemical experiments developed at the University of Oslo

¹ OMTVEDT, Jon Petter, ² FOURNIER, Claudia, ¹ LERUM, Hans Vigeland, ¹ GRØNÅS, Terje, ¹ MATSDAL, Johannes, Ø., ² WALTHER, Clemens

¹ *Department of Chemistry, University of Oslo, Norway*

² *Institut für Radioökologie und Strahlenschutz (IRS), Leibniz Universität Hannover, Germany*

The pilot project “RoboLab”, developed at the University of Oslo in 2004-2007, demonstrated the remote operation of an experiment in a real radiochemical laboratory, by using modern computer controlled hardware. As part of the FP7 CINCH-II project this concept was developed further and expanded as a collaboration between the University of Oslo and the Institute for Radioecology and Radiation Protection of the Leibniz Universität Hannover. On these two sites a total of six remote controlled exercises have been developed. All the exercises can be used either as preparation training before entering a real lab, or as a stand-alone exercise. The three exercises located at the University of Oslo are presented in this poster.

The first one, “Absorption of radiation in matter”, allows the students to measure the attenuation of gamma radiation by lead, copper or aluminum absorbers of various thicknesses. The intended learning outcome of this exercise is to understand the absorption of gamma radiation in matter and to calculate the corresponding absorption coefficient.

A second experiment, “Neutron-activation of silver”, demonstrates the principle of neutron activation and the deconvolution of a decay curve with two components. The intended learning outcome is a good understanding of how radionuclides can be produced using neutrons and how we can deconvolute measured decay data with several radionuclides present.

The third RoboLab, called “Separation and detection of ^{234m}Pa ”, is the most complex one and allows the student to perform real radiochemical manipulations in the (remote) laboratory by loading ^{234}Th on a generator column from a uranyl solution. Once the generator is set up, the student can subsequently milk ^{234m}Pa from it. It illustrates the general concept of making and using a radionuclide generator and provides the opportunity to measure a decay curve for a short-lived radionuclide.

Further information and instructions for how to use the developed e-learning tools can be found on the cinch project-website and the NucWik teaching material wiki-site. These sites has the following web-addresses:

<http://cinch-project.eu/>

<https://nucwik.wikispaces.com/>

Development of self-glowing ceramics based on cubic stabilized zirconia

¹ BOGDANOVA, Oksana, ¹ BURAKOV, Boris and ² KUZNETSOVA, Yana

¹ *V.G.Khlopin Radium Institute, St. Petersburg, Russia*

² *Ioffe Physical-Technical Institute Russian Academy of Sciences, St. Petersburg, Russia*

The main idea of development of self-glowing materials is to combine an optimum amount of phosphor and a relatively small amount of radionuclide in durable crystalline matrices. The first stage of creating self-glowing materials it is necessary to define the optimal concentration of phosphors for non-radioactive samples. The aim of this work was to select the optimal amount of phosphor (Eu and Eu with admixture of Tb for sensibilisation) responsible for the highest intensity of luminescence for ceramics based on cubic zirconia stabilized by yttrium. Monophase ceramics based on cubic zirconia was synthesized. And for the first time several intense peaks of luminescence of cubic zirconia were discovered. The next stage of this research includes synthesis of ceramics and crystals based on cubic zirconia doped with Pu-238 and Am-241.

Selected major, minor and trace elements study of Precambrian outcrops from the south of Eastern Paraguay by XRF and NAA

Peter Kump¹, Julio Cabello² and Juan F Facetti-Masulli^{2*}

1. *Josef Stefan Institut, Ljubljana Slovenia*

2. *Universidad Nacional de Asunción Paraguay, Paraguay*

[*jfafama@rieder.net.py](mailto:jfafama@rieder.net.py)

In Eastern Paraguay the Precambrian is present mainly in two structural highs: the Apa High in the north and Caapucu in the south. The outcrops in the former, distributed along the Apa River, belong to the Brazilian Shield. The latter is constituted by Rio Tebicuary complex; to the north of the Rio Tebicuary is exposed the Caapucu Group.

In relation to its magmatism, the literature is somewhat limited, particularly concerning to trace elements. Some analyses of rock samples were published in 1913 with reliable data on major elements; afterward analyses of Precambrian rocks that included results of minor and trace elements performed by spectrography, were published in 1959. More recently geochemical studies were performed in the Precambrian plug of Fuerte San Carlos, near the Apa River providing analytical data in this regard.

In this work hand specimen of granitoid rocks from the *southern Precambrian* outcrops were studied in some of their major, minor and trace elements aiming to look for relationships with the northern outcrops and their provenance. The analyzed elements were Na, Al, Si, K, Ca, Ti, Mn, Fe, Cu, Zn, Ga, Pb, Rb, Sr, Th, Y, Zr, Nb, Ba, La, Ce, Pr, Nd. Analysis were carried out by EDXRF except for sodium that was analyzed by Neutron Activation. The XRF experiments were carried out using radioisotopic sources of Fe-55, Cd 109 and Am 241 whereas NAA was done with an Am-Be neutron source with a flux of 5×10^7 n/s. The results of analysis allow to establish inter alia indexes, ratios which can be related with crystallization, type granitoid etc. The spidergrams of refractory elements content standardized to primordial mantle show an enrichment of incompatible elements in the samples. Besides, they resemble to those found in Precambrian outcrops from the northern area (Eastern and Western Paraguay) as well as from Brazil.

Determination of proton beam energy with target activation method

V. Jakovlev¹, S. Makkonen-Craig², E. Honkaniemi², V. Jallinoja², J. Järvenpää², M. Keskitalo², M. Matara-aho², S. Muje², A.-E. Pasi², V. Suorsa², K. Helariutta^{2,*}

¹ *Laboratory of NDT Methods, V.G. Khlopin Radium Institute, St. Petersburg, Russia*

² *Laboratory of Radiochemistry, Department of Chemistry, University of Helsinki, Helsinki, Finland
kerttuli.helariutta@helsinki.fi*

The IBA 10/5 Cyclone cyclotron at the University of Helsinki is utilized primarily for producing short-lived positron-emitting radionuclides ^{18}F and ^{11}C in radiopharmaceutical research, but also for other research like nuclear reaction cross-section studies [1] and in the radiation chemistry of polymers [2]. In the research applications it is vital to know the proton or deuteron beam energies accurately for planning experiments optimally or for the reliable interpretation of results. While the proton and deuteron beam energies are rated nominally at 10 and 5 MeV, respectively, the actual energy of an extracted beam at individual target ports can deviate from the nominal value depending on the axial position of the stripper. For example, when a proton beam approaches its extraction energy of 10 MeV, a 5 mm difference in stripper axial position corresponds to a difference of approximately 0.3 MeV in proton beam energy. In this work we determined the actual energy at the proton beam at target exit 5 of our cyclotron, which has been used for radionuclide production cross-section studies.

The beam energy was determined by utilizing charged particle reference cross sections from the IAEA Nuclear Data Services [3]. We used monitor reactions $\text{natCu}(p,x)^{63}\text{Zn}$ and $\text{natCu}(p,x)^{65}\text{Zn}$. The reference data consists of a fit to a cross section data set from 13 (^{63}Zn) and 15 (^{65}Zn) separate measurements in different laboratories. We irradiated a stack of 15 natural copper foils with our proton beam giving a set of 15 different proton energies. After the irradiation, activities of the foils were measured, and they were used in calculating the production cross sections of $^{63,65}\text{Zn}$. Knowing the foil thickness and thus the energy loss in each foil, we were able to compare our data to the reference data. By using χ^2 analysis to overlap our results optimally in energy axis to the reference cross sections, an energy value of 9.34 ± 0.05 MeV was obtained. The position of each beam exit of the cyclotron has been tuned separately for enabling balanced extraction to all exits. In the future, we aim to determine also the extraction energies to the external beam line for both protons and deuterons.

References

- [1] E. Gromova, et al. Study of proton and ^3He induced reactions on ^{235}U at low energies. Nuclear Data Sheets 119 (2014) 237.
- [2] S. Makkonen-Craig et al. Formation of pores in polymer film by UV-assisted etching of overlapped light ion tracks. In prep.
- [3] IAEA Nuclear Data Services: Charged-particle cross section database for medical radioisotope production. <https://www-nds.iaea.org/medical/>

On the identification of titanium-tantalum niobates in «wiikites» from Karelia

Mohammad Hosseinpour Khanmiri, Dmitry K. Goldwirt, Natalia V. Platonova, Svetlana Yu. Janson Yury S. Polekhovski, Roman V. Bogdanov

Saint-Petersburg State University (SPbSU), Universitetskaya emb., 7–9, Saint Petersburg, 199034, Russia

There is no consensus regarding the nature of the Ti-Ta-niobates as a part of mineral assemblages called “wiikites” (outdated). The main difficulty in identifying is associated with their metamict features. In this paper, the authors develop a research methodology, which is based on two approaches: 1) Semiquantitative microanalysis of phases, identified by SEM-EDS method. Based on the data obtained, a hypothesis about the nature of Ti-Ta-niobates in a study sample and mineral composition of the respective paragenetic association is offered. 2) X-ray diffraction analysis of phases formed during isochronal thermal annealing of samples from 200 to 1000 °C with a one-time temperature rise of 200 °C. On the basis of the received data, the previously put hypothesis is accepted or rejected.

Using this methodology, three samples of wiikites from granitic pegmatites of Nuolainiemi peninsula, Ladoga Lake, Karelia were researched. (This area is the site of its initial discovery and description). Formation time for pegmatites is 1780-1800 million years. In confirmation of the prevalent conception of wiikites as pyrochlore group minerals [1,2], Ti-Ta-niobates in two wiikites (№ 2 and № 3) were pre-defined, respectively, as pyrochlore and betafite. In the third sample (laboratory description: wiikite № 7), Ti-Ta-niobate was attributed to polycrase, a euxenite-like mineral. The results of X-ray diffraction analysis of the annealed samples did not contradict the primary hypothesis on betafite and polycrase as the initial minerals in wiikites 3 and 7, respectively. For more reliable statements about polycrase as the initial Ti-Ta-niobate in Wk7, the division of the sample in the gravimetric fractions was performed together with X-ray structural and alpha-spectrometric analysis of each of the fractions separately. Previously made hypothesis of polycrase as the main Ti-Ta-niobate in Wk-7 was confirmed by research results. In contrast, during annealing of wiikite sample №2, Ti-Ta-niobate different from expected, i.e is indicated in the Table. 1 as a pyrochlore, was found.

It allowed the authors to address the issue of chemical conditions necessary for reproduction and identification of the original Ti-Ta-niobate during metamict structures recrystallization. Several possible competing thermochemical processes both favourable to the formation of the original Ti-Ta-niobate and hindering this process, were considered. The former include the release of electrons from (E₁)'- silicate phase centers at 350-400 °C, leading to the reduction of U⁶⁺ atoms to U⁴⁺ and the start of the original Ti-Ta-niobate formation at these temperatures. This process can be probably hindered by the following factors: 1) fixation of U⁶⁺ and niobium in liandratite composition 2) uranium forming its own uranium oxide phase; 3) stabilization of uranium atoms in the form of uranyl ions as a result of autoradiolysis and exposure to natural solutions [3].

References

- [1] Encyclopedia of Earth Sciences, Vol. IV B: The Encyclopedia of Mineralogy/ Edited by Keith Frye. Stroudsburg, Pennsylvania. 1981, 794 p.
- [2] Krivovichev V. G. Glossary of minerals (Mineralogichesky slovar'). Saint-Petersburg, 2008, 556 p. (in Russian).
- [3] Bogdanov, R.V., Batrakov, Yu F., Puchkova, E.V., Sergeev, A.S., and Burakov, B.E. (2002a). Study of natural minerals of U-pyrochlore type structure as analogues of plutonium ceramicwaste form. Materials Research Society, Symposium Proceedings, 713.Ed.: B.P. McGrail, G.A.Cragolino, Boston, USA. 295-301.

Volume reduction technology for treatment of spent uranium catalyst used for production of acrylonitrile

Kwang-Wook Kim*, Keun-Young Lee, Min-Jeong Kim, Maeng-Kyo Oh, Jimin Kim, Dong-Yong Chung, Jei-Kwon Moon, Jong-Won Choi

Korea Atomic Energy Research Institute, 989-111 Daedeok-daero, Yuseong-gu, Daejeon, Republic of Korea,
*e-mail: nkwkim@kaeri.re.kr

A large volume of problematic radioactive waste of spent uranium catalyst, which was used to produce acrylonitrile for fabrication of synthetic fibers, was generated by a private company in Korea until 2004, and has been stored in its production site awaiting a management strategy that will minimize the volume/cost requirements for the final disposal. The spent catalyst consists of not only depleted uranium oxide U (3-6 wt%) but also several metals oxide such as Sb, Fe, Al, V, etc on SiO_2 support occupying about 60-70% of total volume of the catalyst. The uranium waste is to be mandatorily disposed to an underground silo-typed facility for low-intermediate level radioactive waste, which results in a huge disposal cost of the uranium catalyst waste. One drum of 200 liters disposed to such as facility is approximately priced at US\$ 12,500 in Korea. To reduce disposal cost of the uranium catalyst waste and to enhance utilization of the facility as much as possible for radioactive waste generated from commercial nuclear power plants operated in Korea, the volume reduction of such a waste to be disposed is very necessary.

If the environmentally-harmless silicon component occupying much portion of the catalyst is removed from the spent catalyst, and if the radioactivity of the subtracted silicon is low enough to meet appropriate conditional clearance level for release to environment, the waste volume from spent uranium catalyst to be disposed at the expansive underground facility could greatly decrease. Of course, the volume reduction way has to have a high cost competitiveness compared to its direct disposal. For that, KAERI has been developing a process of Fig.1, which consists of several steps including dissolution of spent uranium catalyst in acidic and alkaline solution, Si precipitation followed by its purification, and precipitation of U and Fe ion in the liquid waste generated in the previous steps. The elements in brackets in Fig.1 represent minor elements in the flow. The Si precipitate and the supernatant of U precipitation, which are released to environment, have to meet a radioactivity of about 0.1 Bq/ml (or g) for clearance.

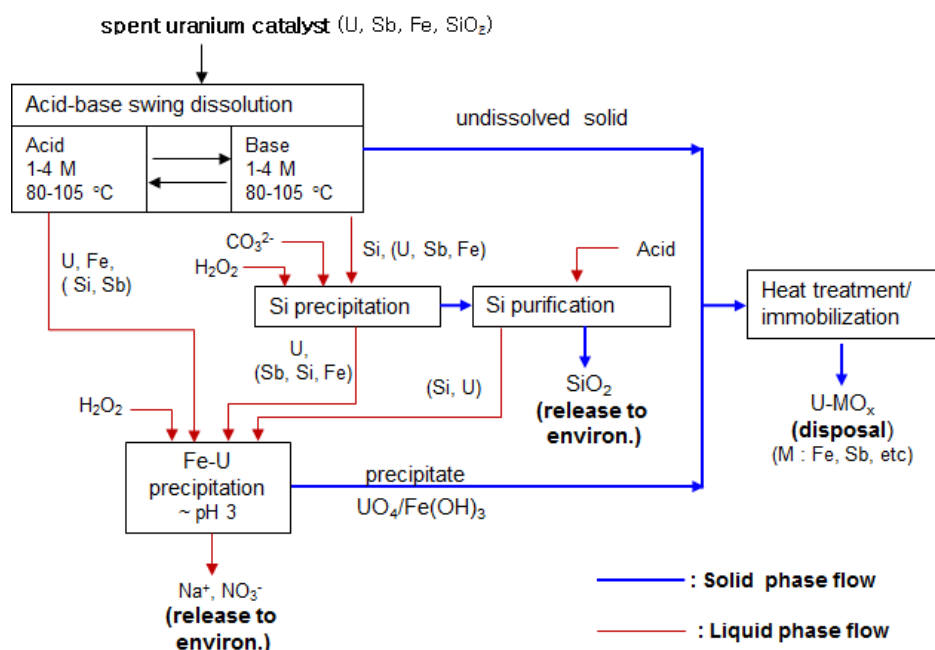


Fig.1. Flow diagram of a treatment process for volume reduction of spent uranium catalyst

A lot of chemical data and knowledge relevant to elements of the spent catalyst are required to embody the process of Fig.1 and to find optimal conditions of unit technologies in the process. Especially, a lot of information on U and Si such as their solubilities with a change of pH, and their chemical forms in solutions are necessary. In the Si precipitation step of Fig.1, the Si-dissolved NaOH solution was adjusted to change to a carbonate solution with hydrogen peroxide in order the uranium ion to remain in the form of uranyl peroxo-carbonate [1] in solution as much as possible when Si is precipitated as silicon oxide around pH 10. A UO_4 precipitation to remove uranium from effluents from the previous steps was done by pH-control and addition hydrogen peroxide, while it supernatant to be released to environment meeting the clearance condition [2]. In this work, various chemical characteristics and uranium complex ion behaviors, and other element behaviors relevant to the process of Fig.1 process will be evaluated and discussed.

References

- [1] Kim K.-W., Jung E.-C., Lee K.-Y., Cho H.-R., Lee E.-H., Chung D.-Y., "Evaluation of the Behavior of Uranium Peroxocarbonate Complexes in $\text{Na-U(VI)-CO}_3\text{-OH-H}_2\text{O}_2$ Solutions by Raman Spectroscopy" *J. Phy. Chem. A.*, 116, 12024-12031 (2012)
- [2] Kim K.-W., Kim Y.-H., Lee S.-Y., Lee J.-W, Joe K.-S., Lee E.-H., Kim J.-S., Song K., Song K.-C., "Precipitation Characteristics of Uranyl Ions at Different pHs Depending on the Presence of Carbonate Ions and Hydrogen Peroxide" *Environ. Sci. Technol.*, 43, 2355-2361 (2009)

Apatite rock digestion with sulfuric acid and phosphoric acid

Pentti Laukkanen

Laboratory of Radiochemistry, Department of Chemistry, University of Helsinki, Helsinki, Finland

Introduction

The lanthanides are becoming more and more important in many areas of high technology. The use of lanthanides is increasing and their technical applications are numerous. The uneven global distribution of their primary resources makes the exploration of new resources as well as the beneficiation of secondary resources (industry by-products, recycling) important.

The Sokli orebody in northeastern Finland is important as a phosphorus resource, and it contains significant concentrations of lanthanide minerals. Apatite is the main phosphate mineral of the ore. Apatite contains more than 20 % calcium and 3-4 % fluorides. The ore also contains a significant amount of iron minerals (ca. 15-25 % Fe). Yttrium and the light lanthanides (La, Ce, Pr, Nd) occur in significant concentrations, while the other occur only in traces. The Sokli ore also contains thorium and uranium in concentrations between 0.005-0,015 per cent. The removal of these radioactive elements before lanthanide separation is of utmost importance.

Procedure

Different digestion procedures have been developed for dissolution of crushed and fine ground ore. Acid digestions are the most common, but concentrated sodium hydroxide solutions in high temperatures have also been used.

Sulfuric and phosphoric acid were selected in this work because they offer possibilities to remove calcium and iron in the first steps of the procedure. The sulfuric acid treatment is worldwide used in the manufacture of phosphoric acid from apatite and is known as the wet process. In this process the insoluble phosphates of the ore are converted to phosphoric acid or soluble monocalcium phosphate. Calcium is removed as calcium sulfate dihydrate or hemihydrate (gypsum).

Phosphoric acid digestion is known as the superphosphate process, with several modifications. This process also converts phosphates to phosphoric acids. The drawback is the coprecipitation of lanthanides with calcium and iron as soon as the pH is increased. The higher concentration of phosphates favors precipitation. Phosphoric acid digestion takes place in higher pH than the sulfuric acid digestion.

Sulfuric acid digestions

The starting idea in the digestions was to keep the acid/rock ratio as low as possible and yet to achieve a complete digestion. In sulfuric acid digestions the finely powdered rock was first digested in a Teflon beaker on a hot plate for 2 h. 40 % sulfuric acid was used. After the digestion the sample was transferred into a distilling flask fitted into a condenser. The sample was then refluxed for 2 h in a boiling water bath. The pH was adjusted by using NH_3 . In this stage a precipitate formed. The sample was filtered and the precipitate was dissolved into acid. The solutions were finally diluted with dilute HNO_3 for ICP-MS analysis.

Phosphoric acid digestions

The finely powdered rock was digested in a Teflon beaker on a hot plate for max. 2 h. Commercial concentrated phosphoric acid diluted with water (1:1) was used. A few drops of acid or water was added when needed to prevent drying. Phosphoric acid is very efficient in digesting this rock. Often the sample was nearly completely dissolved in much shorter time. A very small residue of silicates remains. The sample was

diluted with a small amount of water. The filtering and the following stages were done as in sulfuric acid treatment.

Results and discussion

All digestion procedures where a liquid and a solid phase are included cause some losses of the elements of interest. Both the acids tested are good in keeping the lanthanides in solution at low pH. For sulfuric acid, two different acid/rock ratios were tested. In phosphoric acid digestion the effect of water dilution, an important issue to stabilize the sample with high phosphoric acid concentration, was tested.

The results are presented in the following tables. Table 1 presents the effect of the amount of sulfuric acid in the distribution of calcium, iron yttrium, the lanthanides, thorium and uranium in the filtrate and in the precipitate Table 2 shows the effect of water dilution taking place after phosphoric acid digestion.

Table 1. Percentage distribution of the elements in filtrate and precipitate in sulfuric acid digestion. F = filtrate, P = precipitate.

acid vol., ml	Ca F	Ca P	Fe F	Fe P	Y F	Y P	La F	La P	Ce F	Ce P	Pr F	Pr P	Nd F	Nd P	Sm F	Sm P	Eu F	Eu P
10	44	56	99	1	53	47	81	19	82	18	80	20	80	20	78	22	77	23
15	33	67	99	1	53	47	76	24	77	23	74	26	73	27	70	30	68	32
	Gd F	Gd P	Tb F	Tb P	Dy F	Dy P	Ho F	Ho P	Er F	Er P	Yb F	Yb P	Lu F	Lu P	Th F	Th P	U F	U P
10	78	22	76	24	74	26	74	26	73	27	76	24	77	23	96	4	97	3
15	71	29	69	31	67	33	66	34	67	33	69	31	68	32	94	6	95	5

Table 2. Percentage distribution of the elements in filtrate and precipitate in phosphoric acid digestion. F = filtrate, P = precipitate.

H ₂ O add ml	Ca F	Ca P	Fe F	Fe P	Y F	Y P	La F	La P	Ce F	Ce P	Pr F	Pr P	Nd F	Nd P	Sm F	Sm P	Eu F	Eu P
30	94	6	99	1	98	2	100	0	100	0	100	0	99	1	100	0	98	2
50	94	6	98	2	95	5	81	19	82	18	81	19	81	19	83	17	81	19
80	80	20	96	4	80	20	73	27	71	29	99	1	97	3	67	33	82	18
	Gd F	Gd P	Tb F	Tb P	Dy F	Dy P	Ho F	Ho P	Er F	Er P	Yb F	Yb P	Lu F	Lu P	Th F	Th P	U F	U P
30	99	1	72	28	87	13	97	3	97	3	97	3	91	9	100	0	69	31
50	86	14	88	12	88	12	89	11	77	23	97	3	26	74	92	8	90	10
80	93	7	99	1	99	1	82	18	75	25	90	10	90	10	98	2	86	14

Sulfuric acid is well-known and the reactions predictable. The increase in sulfates in digestion increases gypsum formation and the binding of lanthanides. Phosphoric acid makes digestion easier. On the other hand it makes the subsequent steps more difficult. Solutions of concentrated acid and high concentrations of metals are dynamic, because the acid tends to make oligomers (polyphosphates). The effect of dilution is seen with the largest amount of water added (80 ml). This research continues towards the following steps, i.e. removal of matrix metals and radioactive elements, followed by the precipitations of lanthanides.

On the solubility of radium sulfate and carbonate in sodium chloride media

Artem V. Matyskin,¹ Paul L. Brown,² Christian Ekberg¹

¹ Nuclear Chemistry and Industrial Material Recycling, Department of Chemistry and Chemical Engineering, Chalmers University of Technology, Kemivägen 4, SE-412 96 Göteborg, Sweden

² Rio Tinto Technology and Innovation, 1 Research Avenue, Bundoora VIC 3083, Australia

Radium is a naturally occurring radioactive material (NORM) and can be found in the environment. Due to the long half-life of 1600 years and the relatively high abundance of the parent nuclide (^{238}U) ^{226}Ra is the most abundant radium isotope. Its migration from man-made wastes is of major concern. Modelling of the migration process requires reliable thermochemical data. Such data are limited for radium compounds because of the fact that radium has no stable isotopes and is extremely toxic.

In this work, a radium source, previously used in brachytherapy, was safely disassembled and RaSO_4 was dissolved by three cycles of RaSO_4 heating in 1.5 M Na_2CO_3 up to 85 °C, cooling and subsequent removal of supernatant. The synthesized RaCO_3 was dissolved in HCl and a 0.40 ± 0.02 mM radium solution was prepared. The radium solution was used to investigate the solubility of both RaSO_4 and RaCO_3 from oversaturation using sodium sulfate and sodium carbonate. Sodium chloride was used as a background electrolyte to maintain constant ionic strength. The solubility was determined over a wide range of NaCl concentrations and at 25.1 °C. Samples were centrifuged for 1 hour at 50000 G to separate the solid and aqueous phases. The radium concentration was measured using a High Purity Germanium Detector.

The extended specific ion interaction theory (ESIT) was used. Analysis of the $\text{RaSO}_4(\text{aq})$ and $\text{RaCO}_3(\text{aq})$ ion pair formation and complexation of $\text{NaSO}_4^-(\text{aq})$ and $\text{NaCO}_3^-(\text{aq})$ using the ESIT was also undertaken. The solubility product constants were extrapolated to zero ionic strength ($\log_{10} K_{\text{sp}}^\circ = -10.16 \pm 0.05$ for RaSO_4 and $\log_{10} K_{\text{sp}}^\circ = -7.73 \pm 0.56$ for RaCO_3) as showed in Fig. 1 and Fig. 2, respectively.

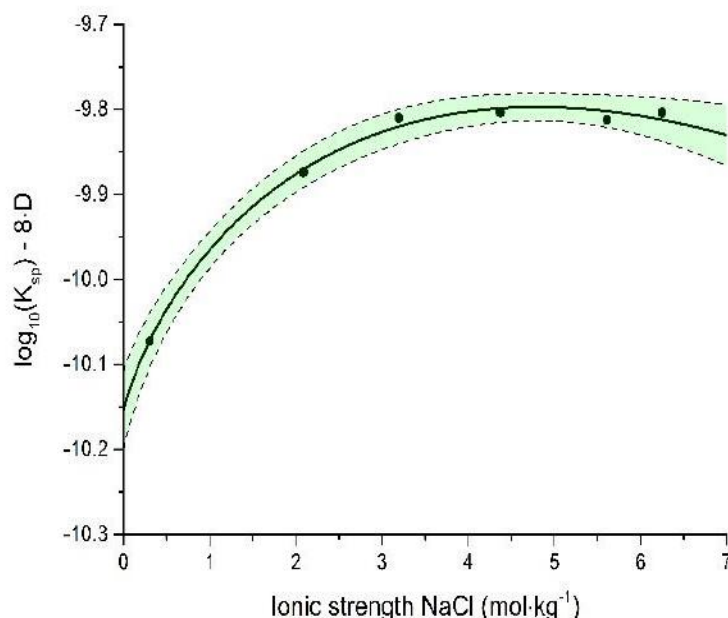


Figure 1. Extrapolation of $\log_{10} K_{\text{sp}}$ of $\text{RaSO}_4(\text{s})$ to zero ionic strength using the ESIT. The dotted lines are the 2-sigma

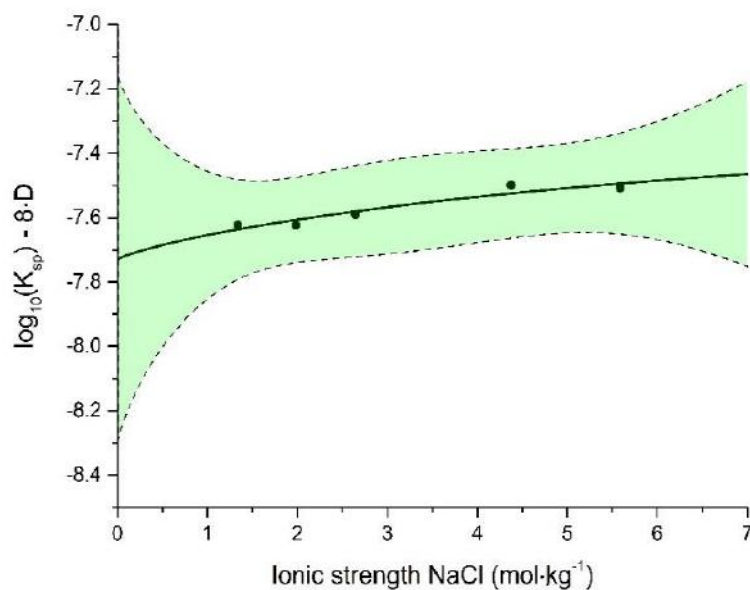


Figure 2. Extrapolation of $\log_{10} K_{sp}$ of $\text{RaCO}_3(\text{s})$ to zero ionic strength using the ESIT. The dotted lines are the 2-sigma

It was found that the solubility curves of RaSO_4 and RaCO_3 have a similar shape as those of BaSO_4 and BaCO_3 , respectively, as shown in Fig. 3. It can be inferred that Ra^{2+} and Ba^{2+} undergo similar specific ion interactions in NaCl media.

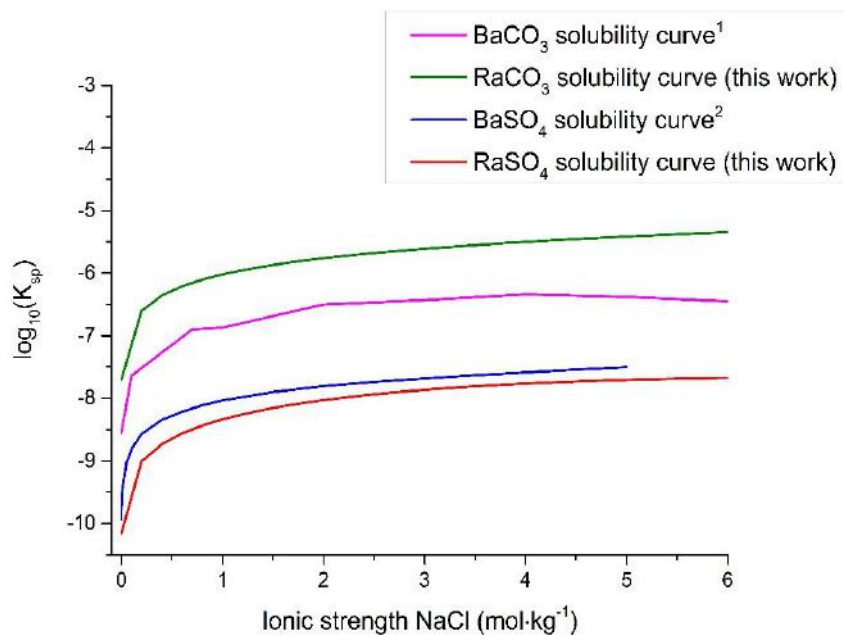


Figure 3. Comparison of logarithm of apparent RaCO_3 - BaCO_3 and RaSO_4 - BaSO_4 solubility product constants at different ionic strengths in NaCl media at 25 °C

References

- Millero, F. J., Milne, P. J. and Thurmond, V. L. (1984). The solubility of calcite, strontianite and witherite in NaCl solutions at 25 C. *Geochimica et Cosmochimica Acta*, 48, 1141-1143.
- Templeton, C. C. (1960). Solubility of barium sulfate in sodium chloride solutions from 25 to 95 °C. *Journal of Chemical and Engineering Data*, 5, 514-516.

K concentration in peel and seeds of coffee and cacao by ^{40}K radioactive detection.

J. M. Navarrete, K. Lüchinger

Faculty of Chemistry, Department of Inorganic and Nuclear Chemistry, National University of Mexico

Since K concentration in foodstuff and beverages is very important for human and animal nutrition, a technique based on ^{40}K radioactive detection has been performed and tested with minimum statistical variation (5%), when some known weight of any nourishing product is conditioned in a Marinelli container to be detected during few hours either by a 3x3" NaI scintillation or HPGe detector. Counts obtained in 1.46 Mev peak are divided by detection time in minutes, sample weight in grams, detector efficiency for 1.46 Mev γ rays emitted, as well as fraction of ^{40}K nucleus decaying by EC and emitting γ rays (11%). When this figure is divided by the specific elementary K γ decaying (31.19 d/m-gK), concentration of K in the sample is obtained (gK/g sample)¹. In this paper, results are given for peel and seeds of some varieties of coffee and cacao, which show significant variations between them and also a major K concentration than other nourishing species.

- 1) J. M. Navarrete, T. Martínez, L. Cabrera, P. Lizárraga, M. A. Zúñiga, M. Camacho, M. Flores, J. of Life Sciences, 5/8, 614-617, 2011.

The force dependent of time and quantity with applications in the Uranium's extraction

M. Răileanu

Alexandru Ioan Cuza University, Iasi, Romania

The force dependent of time and quantity (F_{qt}) discovered and calculated in the present paper, is a combination between the force dependent of time and the electric forces, this meaning the quantity of electric charge represented by the quantity of the organic compound or of metallic compound, in this case the Uranium, which is influencing the chelation (extraction) force. This force dependent of time and quantity is calculated varying the ratio extraction solution's quantity/ the Uranium solution's quantity in the both senses in accordance with the variation of the time of extraction. On a graphic representing the Uranium's extracted quantity/1 ml extracting solution in accordance with the time of extraction and with the ratio the extraction solution's quantity/ the Uranium solution's quantity, the value of the force dependent of time and quantity is given by the ratio between the Uranium's extracted quantity/1 ml extracting solution and the time of extraction extrapolated from the crossing of the linear graphics of evolution of the Uranium's extracted quantity/1 ml extracting solution in accordance with the time of extraction and with the variation of the ratio the extraction solution's quantity/ the Uranium solution's quantity in both senses. In the case of the Uranium's extraction with paraffin $F_{qt}=0,000008853$.

C-14-PMMA porosity analysis of andesite from Petite Anse, Martinique

Juuso Sammaljärvi¹, Charli Delayre², Paul Sardini², Kimmo Kallonen¹, Mikko Voutilainen¹ and Marja Siitari-Kauppi¹

1 Laboratory of Radiochemistry, Department of Chemistry, University of Helsinki, Finland

2 HYDRASA, IC2MP, Université de Poitiers, France

The migration behaviour of elements through water saturated rock matrices is the result of a complex combination of flow, matrix diffusion and chemical interactions determined by mineral-specific compositional and microstructural controls. The ¹⁴C-PMMA autoradiography [1-2] provides information on the connected porosity and microstructure on centimetre scale rock samples needed to evaluate the migration of elements. Combined image analysis of mineral and porosity maps allows quantification of the connected porosity distribution in rocks and their minerals as well as in their alteration products.

Rock samples from Caribbean island of Martinique representing altered volcanic rock (4 cm in diameter and 3 cm in height) were characterised for their porosity and its links to mineralogy. Total porosities were characterised by water gravimetry and by ¹⁴C-PMMA autoradiography performed in University of Helsinki and in University of Poitiers. Dried samples were impregnated with ¹⁴C-MMA and an optimised temperature program was used to polymerise the ¹⁴C-MMA using a thermal initiator. Spatial distribution of porosity could then be characterised via the ¹⁴C-labelled tracer fixed within the sample material by autoradiography techniques. In addition pore structure links to mineralogy of the samples was characterized by SEM. The samples were altered andesite. Minerals such as smectite, calcite and pyrite was found in all samples, indicating an argillic alteration.

The main objective for this work was to compare the two porosity calculation tools developed for 8-bit film autoradiographs and 16-bit digital autoradiographs. These porosity calculation tools were used to convert the grey values of the sample images into local activity values using a set of activity standards and beta correction. Finally, the initial ¹⁴C-PMMA tracer activity was used to obtain local porosity values and in effect, the spatial distribution of porosity. First the ¹⁴C-PMMA impregnated samples were exposed on a photographic X-ray film (Kodak Biomax MR, Kodak) in University of Poitiers and the film was digitized by a scanner. The porosity calculation was performed on 8 bit grey level images from film autoradiography method.

The second method was the digital autoradiography or phosphor screen autoradiography in which the samples were placed on imaging plates which were scanned using FLA 5000 scanner (Fuji) to produce 16-bit digital autoradiographs of the samples. The imaging plates (= phosphor screen plates) contain BaFBr:Eu₂ photostimulable crystals which are excited by the ¹⁴C beta emissions.

The 16-bit digitized images were handled in MATLAB-based porosity analysis program developed in-house in University of Helsinki. The digital autoradiography has larger linear range than film autoradiography by several magnitudes and this advantage can be best utilised in 16-bit images. This translates into more accurate porosity measurements as smaller areas are found in the saturation range. Typical calibration curves for 8-bit and 16-bit autoradiographic images are illustrated in Figure 1. More detailed comparison together with discussion will be provided in the conference presentation.

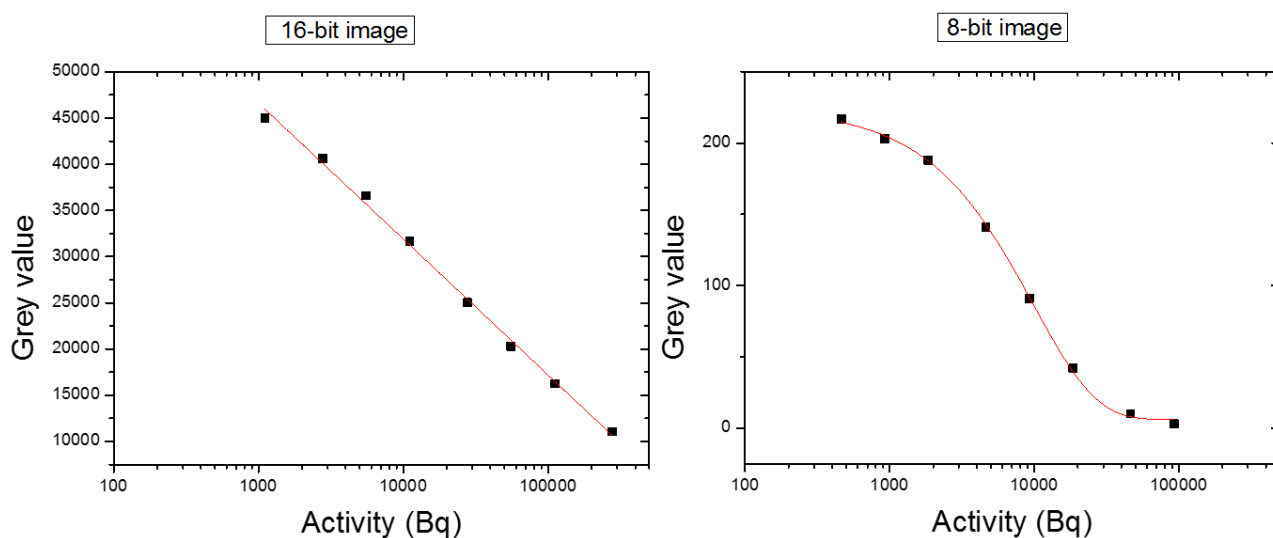


Figure 10 Typical ^{14}C -PMMA calibration curves for 8-bit (right) and 16-bit (left) autoradiographic images. 8-bit image can have grey values between 0-255 and 16-bit image can have grey values between 0-65535.

1. K-H. Hellmuth, S. Lukkarinen, M. Siitari-Kauppi, (1994). Rock matrix studies with carbon-14-polymethylmethacrylate (PMMA): method development and applications. *Isotopenpraxis. Isotopes in Environmental and Health Studies* 30, 47-60.
2. Sardini P. Siitari-Kauppi M. Beaufort D. and Hellmuth K-H (2006) On the connected porosity of mineral aggregates in crystalline rocks, *American Mineralogist* 91, 1069-1080

The investigation of heterogeneous equilibria in the saturated aqueous solutions of rare earth elements uranyl silicates and uranyl germanates

Natalya Zakharycheva

*Research Institute for Chemistry of Lobachevsky State University of Nizhny Novgorod,
Nizhny Novgorod, Russia
nszakh@rambler.ru*

The state of uranyl silicates and uranyl germanates with formula $A^{III}(HB^{IV}UO_6)_3 \cdot nH_2O$ (A^{III} – La-Lu; B^{IV} – Si, Ge) in aqueous solutions in the pH range of 0-14 was investigated. The pH range where compounds save their composition and structure was established, products of conversion and solubility of $A^{III}(HB^{IV}UO_6)_3 \cdot nH_2O$ were defined. The instrument of equilibrium thermodynamic was used to full quantitative description of physic-chemical processes in the system “aqueous solution – solid phase”. This description can to model the behavior of the uranium compounds at the different conditions.

It is shown that the behavior of rare earth elements uranyl silicates and uranyl germanates in the heterogeneous aqueous-salt systems depends on the general laws. Uranyl silicates and uranyl germanates in the aqueous solutions preserve the own structure in the limited pH range. At $pH < 3 \div 4$ the structure of the compounds destructs with the formation of $GeO_2(cr)$ or $SiO_2(am)$, respectively. At $pH \geq 11$ structures of $A^{III}(HB^{IV}UO_6)_3 \cdot nH_2O$ begin to destroy because of $A^{III}(OH)_3$ formation and it destructs full in the strong alkaline media. Under the circumstances uranium (VI) stays in the solid state as polyuranates. The formation of low soluble secondary phases such as SiO_2 , GeO_2 , $A^{III}(OH)_3$ was established by X-ray diffraction.

The solubility of $A^{III}(HB^{IV}UO_6)_3 \cdot nH_2O$ changes on the several order of magnitude in the pH range, where its composition and structure preserve, from 10^{-7} M in the neutral and alkaline media to 10^{-3} M in the acid and more alkaline solutions. At the same conditions, the solubility's value for uranyl silicates is on 1-2 orders of magnitude lower than for uranyl germanates. Generally the stability of studied uranyl silicates and uranyl germanates increases from La compounds to Gd derivative and changes insignificantly to Lu compounds, that is caused by the similarity of investigated compounds structure and A^{III} properties.

The quantitative physic-chemical description was developed. The description characterizes the state of the system “solid phase $A^{III}(HB^{IV}UO_6)_3 \cdot nH_2O$ – aqueous solution” and takes into account both heterogeneous process of solution and homogeneous equilibrium, where U(VI), Si(IV) or Ge(IV) and A(III) are presented as set of the different ion and molecular forms. The constants of equilibrium of heterogeneous dilution reactions were calculated. The values of constants for all studied uranyl silicates are on the some orders of magnitude lower than the same constants for uranyl germanates. It is shown that uranyl silicates are more stable in the aqueous solutions.

The obtained constants of the dilution's reactions were used to calculate Gibbs's functions of $A^{III}(HB^{IV}UO_6)_3 \cdot nH_2O$ formation. Using presented physic-chemical description the solubility's curves were calculated, the diagrams of uranium (VI), silicon (IV), germanium (IV) and rare earth elements state in solutions and solid phases were built.

Modelling an Iso-Breeder Nuclear Programme: Determining optimum cooling time and generating waste inventories

K Dungan^a, G Butler^b, R Gregg^c, S Howell^d, R Patrick^a

^a*School of Earth and Environmental Sciences, University of Manchester, Oxford Road, Manchester, M13 9PL*

^b*Faculty of Science and Engineering, University of Manchester, Oxford Road, Manchester, M13 9PL*

^c*National Nuclear Laboratory, Preston Laboratory, Springfields, Preston, PR4 0XJ*

^d*Alliance Manchester Business School, Booth Street West, Manchester, M15 6PB*

In order to derive and quantify the key drivers in nuclear waste disposal across a range of nuclear power systems, it is essential to first model each programme so that waste inventories may be generated. These inventories may then be assessed to determine if a system offers particular advantages in waste disposal over another, such as reduced heat generation, lower volume or lower actinide content. In this work a model has been built of a nuclear programme which utilises both PWR (pressurised water reactors) and iso-breeder sodium fast reactors (SFR), using the software ORION. An iso-breeder reactor produces as much new fissile material as it uses up, and in this model will use the spent MOX fuel generated by the PWR fleet in order to manage actinides and generate further fissile fuel, which it will then re-use. While longer cooling times will reduce the challenges involved in reprocessing, if they become too lengthy, the amount of spent MOX fuel produced is not enough to sustain the SFR.

ORION has been used to model the effect of varying spent fuel cooling time on radiotoxicity and decay heat, along with the optimum spent fuel cooling time and the quantity of MOX spent fuel stock available to the SFR. Alongside ORION the codes ERANOS, CASMO and FISPIN have been used in order to generate a full waste inventory for the nuclear programme.

The resulting model established that the optimum cooling time was 5 years; a point at which there is little benefit seen in cooling SFR fuel longer however short enough that the fuel stock of PWR spent fuel is not exhausted. The PWR fleet produces enough spent MOX to fuel the SFR fleet for 4 refuelling batches (plus initial core loading), but after this there must be sufficient reprocessed fuel for the SFR to sustain itself. The radiotoxicity and decay heat both decline rapidly over the initial 2 year period of cooling as short lived fission products in the fuel decay away, before levelling off.

Further work will generate a complete set of inventory data from ORION and FISPIN, comprising of spent fuel, as well as cladding and fuel impurities. This data will be quantitatively evaluated alongside a selection of other nuclear programme models, including once-through, thermal and open fuel cycles.

CHEMISTRY OF THE NUCLEAR FUEL CYCLE II

Highly selective inorganic ion exchangers for Fukushima cleanup

Jukka Lehto¹, Risto Koivula¹, Heikki Leinonen², Esko Tusa³ and Risto Harjula¹

¹ *Laboratory of Radiochemistry, Department of Chemistry, University of Helsinki, Finland*

² *Carrum Oy, Finland,* ³ *Fortum Power and Heat Oy, Finland*

Two inorganic ion exchange materials developed at the University of Helsinki and manufactured by Fortum company, Finland, have been used at the Fukushima Daichi nuclear plant in Japan since 2012. These materials are CsTreat®, a transition metal hexacyanoferrate for radiocesium removal and SrTreat®, a sodium titanate for radiostrontium removal. They have been used at ton-scale in the Advanced Liquid Purification System (ALPS) plants purifying liquids generated in the cooling of damaged reactors. They both have exhibited superior performance in comparison to other available materials. SrTreat material, connected with pre-precipitation, has decreased the concentration of ⁹⁰Sr below the detection limit corresponding to a decontamination factor of 165,000,000. In terms of processing capacity, the CsTreat performance in the removal of ¹³⁷Cs from seawater has surpassed those of zeolite and silicotitanate exchangers (Fig. 1) which also have been utilized at Fukushima.

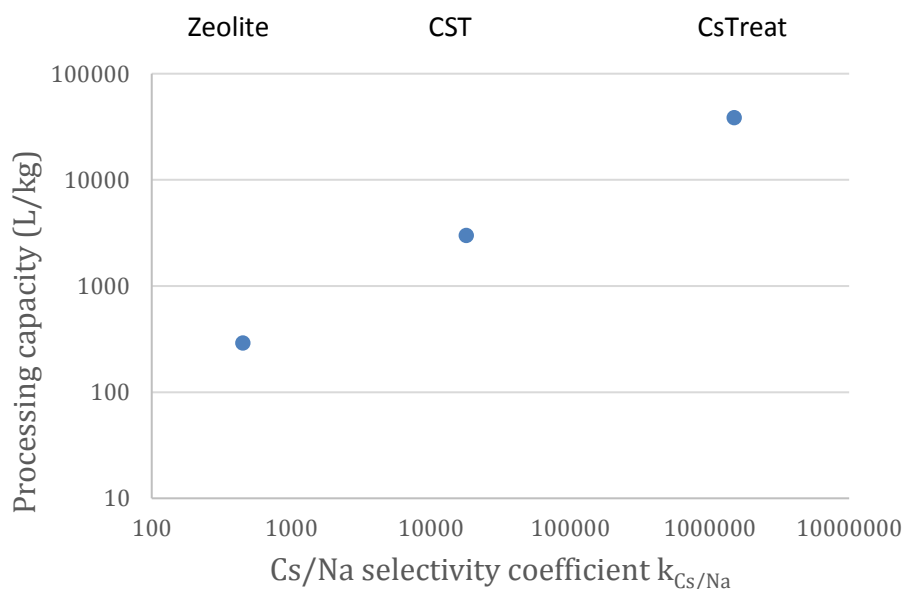


Figure 1. Processing capacity (L/kg) vs. Cs/Na selectivity coefficient of three exchangers used at Fukushima for radiocesium removal, Chabasite zeolite (Kurion), CST silicotitanate (UOP) and CsTreat hexacyanoferrate (Fortum). Processing capacity is the volume (L) of liquid processed up to 50% breakthrough with a unit amount (kg) of exchanger in a column mode.

According to our analysis and as can be seen in Fig. 1, the key factor in determining the processing capacity is the selectivity, in this case the selectivity for cesium over sodium the concentration of which is enormous compared to that of cesium. This applies to all separations, for which the distribution coefficient (K_d), equaling with the processing capacity, can be expressed as:

$$K_d = \frac{Q}{\frac{[Na]_L}{k_{Cs/Na}} + [Cs]_L}$$

where Q is the ion exchange capacity, $[Na]_L$ and $[Cs]_L$ sodium and cesium concentrations in solution, respectively and $k_{Cs/Na}$ is the selectivity coefficient (mass action quotient). Only in highly active solutions the concentration of cesium is so high that it affects the processing capacity. The capacity is a constant to each exchanger and varies only in a rather narrow range from exchanger to another. Instead, the selectivity coefficient may vary dramatically: for example the ratio the Cs/Na selectivity coefficient of CsTreat to those of chabasite and silicotitanate is 3300 and 80, respectively. A major shortcoming of inorganic ion exchangers, limiting their introduction into industrial processes, is their often poor mechanical stability: the granules may not tolerate dynamic column use but disintegrate and clog column. The technology developed by Fortum together with the University of Helsinki, has however offered products suitable for column use as well, when properly managed.

In the Laboratory of Radiochemistry, University of Helsinki, the development of inorganic ion exchangers started in late 1970's. Since then a great number of exchangers have been developed and characterized. Three of the exchangers, SrTreat, CsTreat and CoTreat, are being manufactured by the Fortum company at industrial scale as NURES® products¹. The third one, CoTreat, is a titanate material applicable for radiocobalt removal. The first industrial utilization of these exchangers started in 1991 at the Loviisa nuclear power plant in Finland where ^{137}Cs was removed with one 8 liter column from 253 m³ of highly saline waste effluent with a total decontamination factor of 2000. Ever since, in the last 25 years, these exchangers have been utilized in over 60 nuclear facilities worldwide. Largest of these applications is the Fukushima APLS plant.

Major new developments, in addition to those described above, have been development of technology to use of inorganic ion exchangers as powders, development of inorganic sorbents for the removal anionic radionuclides and development of technology for the separation of minor actinides (Am, Cm) from lanthanides. Use of powders instead of granules considerably improves ion exchange rate and thus enables use of considerably higher processing rates being favorable when large volumes are purified. For this, three kinds of technology has been developed and tested at industrial scale processes. In the first one precoat filter method is used: a filter element is coated with a thin layer of powder-form exchanger. In the second method, the exchanger powder has been incorporated into porous organic matrix. The third method is to produce inorganic exchangers as fibers having optimum contact surface for treated liquids. All methods have yielded high processing rates with high decontamination factors. Development of sorbents for anionic radionuclides, especially for ^{99}Tc (TcO_4^-) and ^{125}Sb (SbO_3^-), has been most challenging since the surface charge of inorganic sorbent materials are mostly anionic in the pH range mostly faced with waste effluents. However, progress in this field has been gained and new products to the NURES product family have been developed, TcTreat and SbTreat, both zirconium oxide materials. For example, in the test run to remove ^{99}Tc from 1M $NaNO_3$ solution with TcTreat exceptionally high decontamination factor of over 2000 was observed and the processing capacity was over 1000 bed volumes. In the separation of minor actinides from lanthanides promising results have been gained with layered zirconium phosphates.

In conclusion, inorganic ion exchangers developed at the University of Helsinki together with the Fortum company offer unique selectivity to key radionuclides present in nuclear waste effluents. The high selectivity results in high processing capacity which in turn yields minimization of volumes of the waste for final disposal and thus may dramatically decrease final disposal costs. In addition, high decontamination factor observed with highly selective exchangers minimizes environmental radioactivity discharges and/or enables releases of purified liquids into the environment.

1. <http://www.fortum.com/en/products-and-services/powersolutions/psnuclear/nures/pages/default.aspx>

Development of a selective americium separation process using TPAEN as a water-soluble stripping agent

C. Marie,^{*,1} V. Vanel,¹ M.-T. Duchesne,¹ E. Russello,¹ P. Kaufholz,² A. Wilden,² G. Modolo,²
M. Miguiditchian¹

¹CEA, Nuclear Energy Division, RadioChemistry & Processes Department, 30207 Bagnols-sur-cèze, France

² Forschungszentrum Jülich GmbH, Institute of Energy and Climate Research, IEK-6: Nuclear Waste Management and Reactor Safety, 52428 Jülich, Germany.

Recycling americium from spent fuels is an important option considered for the future nuclear fuel cycle as americium belongs to the main contributors of the long-term radiotoxicity and heat power of final high active waste. Removing Am would allow to significantly reduce the surface footprint necessary for a geological repository of vitrified waste. In this context, the liquid-liquid extraction process “Euro-EXAm” is under development, to allow the recovery of Am alone from a PUREX raffinate (a nitric acid solution of spent fuel dissolution liquor already cleared from U, Np and Pu). The challenge here is to recover americium (III) with high selectivity towards curium and lanthanide (Ln) trivalent cations which have very similar physico-chemical properties. In this new separation system, two main steps would be necessary (Figure 1):

- first all lanthanide cations are co-extracted together with americium and curium in the organic phase, using a solvent containing 0.2 mol/L of TODGA (*N,N,N',N'*-tetraoctyldiglycolamide) extractant in TPH (Hydrogenated TetraPropylene) diluent with 5%_{vol.} octanol, and are separated from other fission products,
- then americium is stripped in a second step with selectivity towards curium and lanthanides. The water soluble ligand TPAEN (*N,N,N',N'*-tetrakis[(6-carboxypyridin-2-yl)methyl]-ethylenediamine) was studied to selectively strip Am from a loaded organic phase. Used in combination with TODGA as lipophilic extractant, TPAEN shows a quite high Cm/Am selectivity ($SF_{Cm/Am} \approx 4$ at 0.1M HNO₃), which allows to selectively strip Am while Cm and Ln remain extracted in the organic phase.
-

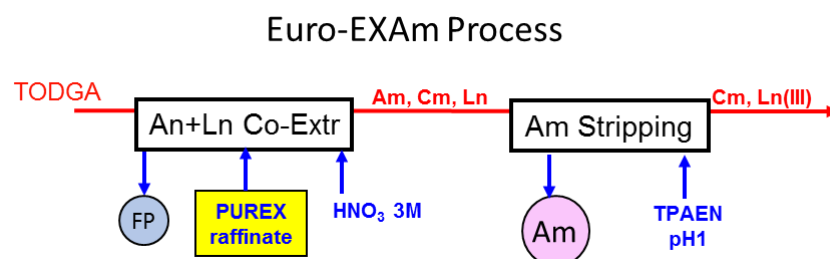


Figure 1: Simplified scheme of the Euro-EXAm process (FP = fission products, An = Am and Cm, Ln = lanthanides)

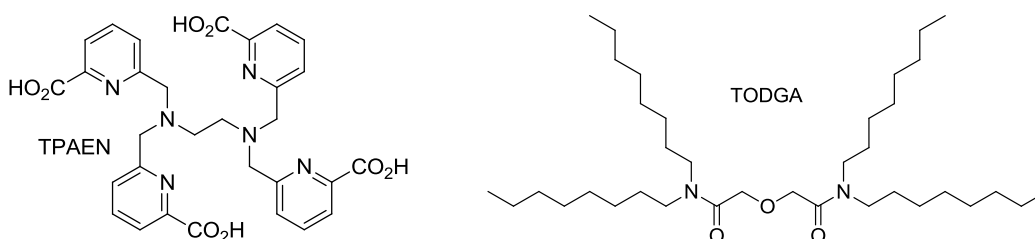


Figure 2: Structure of ligands used in the Euro-EXAm process

Batch extraction data were acquired to evaluate the best conditions to develop a liquid-liquid separation flowsheet with this promising TODGA/TPAEN separation system. It was demonstrated that TPAEN has a strong complexing capacity allowing the back extraction of Am in macro concentration (1 – 2 mM) even with low ligand concentrations (around 1.5 equivalent of ligand is enough). TODGA has a lower affinity for light lanthanides, hence the selectivity between La and Am might become low depending on experimental conditions. The influence of parameters such as temperature, pH, ligand and cations concentrations was studied. Kinetics experiments in batch contactors were also performed to characterize times necessary to reach equilibrium. This set of experimental work data allowed the elaboration of a thermodynamical model which was implemented in the PAREX simulation code in order to propose a flowsheet. The feasibility of this process will be evaluated during spiked tests in centrifugal contactors at Jülich research center, starting from a surrogate feed solution spiked with traces amounts of ^{241}Am , ^{244}Cm and ^{152}Eu .

This work is the result of collaborations in the framework of the SACSESS European Project.

Keywords: americium, curium, liquid-liquid extraction, TPAEN

* Corresponding author. Tel.: +33 4 66 39 70 52

E-mail address: cecile.marie@cea.fr.

Application of Aliquat-336 nitrate ionic liquid based extractants for minor actinide separation

Peter Zsabka^{1,2}, Michiel Van de Voorde^{1,2}, Karen Van Hecke¹, Thomas Cardinaels^{1,2}, Marc Verwerft²,
Giuseppe Modolo³, Koen Binnemans²

1. SCK•CEN Institute for Nuclear Materials Science Boeretang 200, 2400 Mol, Belgium

2. KU Leuven, Molecular Design and Synthesis, Department of Chemistry, Leuven, Belgium,

3. Forschungszentrum Jülich GmbH, Institute for Safety Research and Reactor Technology, Jülich, Germany

The presence of minor actinides in spent nuclear fuel poses a major obstacle for both open and closed fuel cycles. Several long-lived isotopes of Am and Cm are mainly responsible for the heat production, and high radiotoxicity of the nuclear waste after the elements U, Np and Pu are separated in the PUREX process. These make both reprocessing as well as final disposal very difficult and costly. In the framework of the Belgian MYRRHA project, a Gen IV prototype accelerator-driven fast reactor will be built, in which these long-lived minor actinide isotopes can be incorporated in an accelerator target. Upon the irradiation by high-flux fast neutrons, these nuclei can be effectively spallated and the resulting product nuclei shall be shorter lived by several orders of magnitude.

In order to separate a small amount of trivalent actinide elements from such a complex system as a PUREX raffinate remaining after the reprocessing of spent nuclear fuel, several sophisticated methods have been elaborated (TALSPEAK, DIAMEX, SANEX or GANEX etc.), all of which are based on the use of molecular diluents. However, these molecular diluents have a common shortcoming, namely they are volatile, flammable and sensitive to radiation-induced degradation that reduces their process lifetime. In contrast, ionic liquids are non-volatile and non-flammable moreover radiation stability studies show that several ionic liquids are more stable against elevated absorbed radiation doses. By the application of a more radiation-resistant diluent for the separation of minor actinide, secondary waste production can be reduced. An additional task that needs to be solved, is the separation of chemically similar trivalent lanthanides (present in much higher concentration) from the minor actinides in the extraction process. The presence of lanthanides in a reactor target material must be avoided because of their high neutron absorption cross section. In compliance with the approach adopted in subsequent European projects, CHON compounds were selected to address the problem posed by secondary waste.

[Aliquat-336][NO₃] and benzyl-trioctylammonium nitrate ionic liquids as diluents and TODGA as extractant were used for the liquid-liquid extraction of lanthanides and actinides from nitric acid solutions. The present work is an extension of recent work reported by Rout et al. using Am(III) tracers.¹

Batch extractions using stable lanthanide isotopes together with tracers of ¹⁵²Eu, ²⁴¹Am and ²⁴⁴Cm isotopes have been conducted to determine the distribution ratios, separation factors, the kinetics of the extraction and the loading effect on the phase behavior of the ionic liquid. The actinide and lanthanide ions are extracted via a neutral solvation mechanism with TODGA and their extraction kinetics are fast. From a slope analysis of logD_{Am(III)} vs. log [TODGA] plot the number of extracting molecules participating in the metal-ligand complex was determined.

The possibility of separating the chemically similar trivalent actinides from trivalent lanthanides using actinide-selective soft-donor BTBP ligands was also investigated. These initial experiments are complemented by radiation stability studies on the ionic liquids to simulate realistic extraction circumstances. The effects of degradation are being studied by NMR and ESI-MS as well as by extraction experiments.

1. A. Rout, K. A. Venkatesan, M. P. Antony, P. R. Vasudeva Rao, Liquid/liquid extraction of americium(III) using a completely incinerable ionic liquid system, Separation and Purification Technology, 158 (2016) 137-143.

Polonium evaporation from liquid lead-bismuth eutectic coolant and its capture for accelerator driven systems

Borja Gonzalez Prieto¹, Alexander Aerts¹, Jörg Neuhausen², Emilio Andrea Maugeri² and Robert Eichler³

¹ *Chemistry and Conditioning Programme, Belgian Nuclear Research Centre, Boeretang 200, Mol, Belgium*

² *Radwaste Analytics, Laboratory for Radiochemistry, Paul Scherrer Institut, CH-5232 Villigen, Switzerland*

³ *Heavy Elements, Laboratory for Radiochemistry, Paul Scherrer Institut, CH-52325 Villigen, Switzerland*
borja.gonzalez.prieto@sckcen.be

The search of a solution for the disposal of the radioactive waste generated in nuclear power plants is one of the major challenges to face in the near future by the nuclear community. Accelerator driven nuclear systems (ADS), currently under development in several countries, are among the most promising solutions. In these systems the use of lead-bismuth eutectic (LBE) as coolant and spallation target is foreseen owing to its beneficial physico-chemical properties. However, one of the major drawbacks of the use of LBE lies on the formation of several hazardous radionuclides generated as result of spallation and neutron capture reactions. Among the latter, the generation of significant quantities of the highly radiotoxic and relatively volatile element polonium is a major safety concern. Therefore, for the development and licensing of LBE-based ADS accurate predictions of polonium evaporation from LBE and the development of suitable filter systems for its capture are required. However, reliable physicochemical data in the operation temperature range of ADS are fairly scarce.

In the last years extensive work, both experimental and theoretical, has been carried out to gain insight into this subject in the frame of the MYRRHA ADS project. As a result of these studies the evaporation of Po from LBE at temperatures between 600 °C and 1000 °C is currently well understood. However, at lower temperatures, in the temperature range where LBE-based ADS are foreseen to operate (200 °C-400 °C), the results revealed a larger Po release from LBE than anticipated when using the derived high-temperature correlations.

Among the characteristics leading to this enhanced release one could highlight the composition of the carrier gas above the LBE sample. Specifically, when using moist gaseous atmospheres it was found that not only the release of polonium but also the volatility of the formed Po species was enhanced. This result emphasizes the necessity of finding suitable filter systems to capture these more volatile Po species. In the current contribution, we present first the latest results on the evaporation behavior of Po from LBE in humid atmospheres in conditions relevant to LBE-based ADS. In addition, it was found that the construction material of MYRRHA, SS316L, captures all formed Po species, even the most volatile released in moist atmospheres, more effectively than inert materials such as fused silica. The results of detailed thermochromatography studies performed to characterize the interaction between the released Po molecules and SS316L are also discussed.

RADIOPHARMACEUTICAL CHEMISTRY I

Carbon-11 chemistry: Why fighting a 20 minute half-life really makes sense

Albert Windhorst

VU University Medical Center, Amsterdam, Netherlands

Carbon-11 is a powerful positron emitting nuclide for radiotracers that are used in Positron Emission Tomography (PET). All biologically active molecules contain natural carbon, which can in theory be replaced by carbon-11 and thus any of these molecules can be converted into potential PET radiotracers. Proper radiochemistry is required for carbon-11 PET tracer development and nowadays many compounds have been radiolabeled and many more could be. Current drawbacks of carbon-11 from a radiochemistry point of view are its short half-life of 20 minutes and the risks of obtaining low specific activity carbon-11 products (less than 20 GBq.μmol⁻¹). Nevertheless, if these challenges can be controlled, many radiotracers can be obtained and exciting clinical research can be conducted with them. This lecture discusses the characteristics of carbon-11 chemistry and the application of carbon-11 radiotracers.

Production of carbon-11

The production of [¹¹C]CO₂ will be addressed focusing on reliability and specific activity of the radioactive building block. This will be based on the practical experience where [¹¹C]CO₂ is produced using a the (p,α) reaction on Nitrogen-14 utilizing an IBA Cyclone 18/9 cyclotron. This setup resulted in a reliable system, capable of doing >15 irradiations a day obtaining [¹¹C]CO₂ in a high specific activity.

A selection of carbon-11 radiochemistry methodology

Focus will be on recent advances in [¹¹C]CO and [¹¹C]CO₂ chemistry, utilizing these two carbon-11 labelled reagents. Furthermore renewed carbon-11 reagents like carbon-11 labeled *iso*-butyl iodide, *iso*-butanol and benzyl iodide will be discussed. Some new radiotracers will be presented applying the reagents addressed, ranging from enantiomerically pure amino acids to small peptides and enzyme inhibitors.

Production and applications of carbon-11 labelled tracers

In order to demonstrate the clinical value of carbon-11 labelled tracers the cases of [¹¹C]erlotinib and [¹¹C]docetaxel will be discussed. Erlotinib is an approved drug for the treatment of e.g. non-small cell lung cancer. It is a tyrosine kinase inhibitor (TKI) targeting the kinase domain of the epidermal growth factor receptor (EGFR), but only when there is a defined sensitizing mutation present. The EGFR mutation status can be assessed via biopsies, however given the heterogeneity of every tumor these are not always accurate. Assessment of the whole tumor would be better and this can only be achieved by PET with [¹¹C]erlotinib. For this reason we developed [¹¹C]erlotinib and the first clinical study results will be discussed.

Docetaxel is a chemotherapeutic that is frequently used in combination with other chemotherapeutic drugs. It was postulated recently that the combination of the anti-angiogenic drug bevacizumab with docetaxel had positive clinical effect, most likely due to a better drug delivery of docetaxel caused by the anti-angiogenic properties of bevacizumab causing more properly arranged vasculature in the tumor. However, this is not in full compliance to the drug action which is based on reducing the vasculature of a tumor, thus keeping important nutrients for the tumor cells and as a consequence the tumor growth is reduced. Only with PET the effect of bevacizumab on docetaxel uptake in the tumor could be assessed and results of this quantitative [¹¹C]docetaxel PET study will be presented .

Bifunctional tetraamine chelator ^{99m}Tc -SpmTrien (^{99m}Tc -1, 12-diamino-3, 6, 9-triazadodecane) for renal function imaging

Brianda Barrios-Lopez^{1,2*}, Thomas R. Hayes³, Emily Witthuhn³, Jouko Vepsäläinen⁴, Kim Bergström^{2,5,6}, Paul D. Benny³, Anu J. Airaksinen¹

¹Laboratory of Radiochemistry, Department of Chemistry, University of Helsinki, Finland

²Division of Pharmacology and Toxicology, Faculty of Pharmacy, University of Helsinki, Finland

³Washington State University, Department of Chemistry, Pullman, WA, USA

⁴University of Eastern Finland, School of Pharmacy, Biocenter Kuopio, Finland

⁵Center for Drug Research, Faculty of Pharmacy, University of Helsinki, Finland

⁶HUS Medical Imaging Center, Helsinki University Central Hospital, Finland

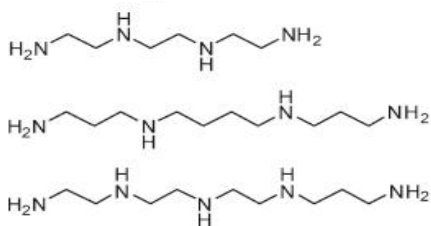
^{99m}Tc is the label of choice in diagnostic Nuclear Medicine. ^{99m}Tc possesses ideal imaging properties ($E_\gamma=140$ keV, and half-life is 6.02 h). ^{99m}Tc is easily accessible at a low cost because of the use of commercial $^{99}\text{Mo}/^{99m}\text{Tc}$ generators.

Bifunctional chelators are one of the key components since the *in vivo* behavior of radiolabeled biomolecule is heavily shaped by the nature of the ^{99m}Tc complex. The bifunctional chelator must reach several requirements such as an efficient and fast complex formation, retention of receptor affinity of the biomolecule and *in vivo* stability, but still show a convenient biodistribution pattern.

There is a necessity to investigate other bifunctional chelates for the making Tc-complexes to be exploitable as platforms for the development of radiopharmaceuticals. One potential group of chelators are polyamines. Some studies have been published using linear polyamine analogs as chelators for ^{99m}Tc complex formation. However, there has not been extensively reports in the literature discussing about the side reactions in the in the radiolabeling procedures with tetraamine chelators even though there has been clinical studies reported. Side reactions in the radiolabeling can produce radiochemical impurities such as bound ^{99m}Tc , ^{99m}Tc colloids, or different ^{99m}Tc -complexes.

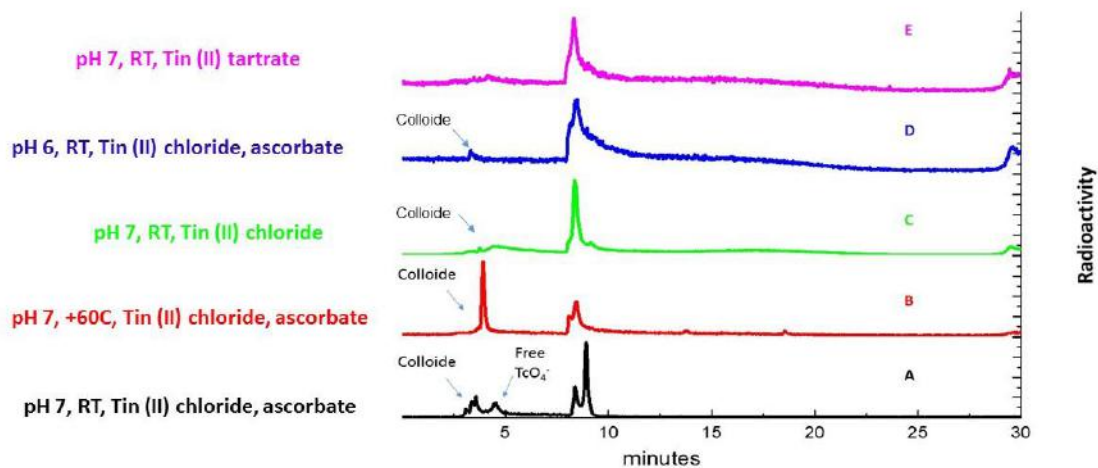
SpmTrien (Figure1, 3) is an analogue of the natural polyamine Spermine (Figure 1, 2-Spm) which exists in all mammalian cells. SpmTrien has very low affinity towards polyamine transporter, although it accumulates into DU145 cells efficiently. We have previously used SpmTrien as a bifunctional chelator in radiolabeling of hexosomes with ^{99m}Tc . However, the method has suffered from some variations in radiochemical yields during ^{99m}Tc chelation. Therefore, we decided to explore the conditions influencing the reaction yields and formation of side products. Here we report influence of reaction conditions (pH and reducing agents) for the radiolabeling of SpmTrien with ^{99m}Tc . Our aim is to avoid formation of any ^{99m}Tc colloids in future formulations when SpmTrien is covalently attached to a nanocarrier or other vector.

We varied different conditions such as pH, temperature of incubation, reducing agent and time of incubation in order to achieve a final complex free of colloids without the necessity of additional clean-up steps. The ^{99m}Tc complex formation was observed by reverse phase HPLC (Figure 2) and paper chromatography. In order to study biodistribution of the ^{99m}Tc -SpmTrien complex alone, it was injected into healthy mice. Intense activity on kidneys was observed (Figure 3). In conclusion, SpmTrien demonstrated to be a stable chelator *in vivo* (results not shown) until 4 hours and targeted kidneys in mice.



1. Trien
2. Spm
3. SpmTrien

Figure 1



Incubation time for A, B, C, D, and E: 30 minutes
HPLC Analytical Column: Phase C18, (250mm X 4.6 mm), Particle size 5 μ m
HPLC Solvent System: A = 2mM Phosphate Buffer pH = 7.4, B = Methanol.

Figure 2

Renal Clearance of SpmTrien-99mTc at 30 min

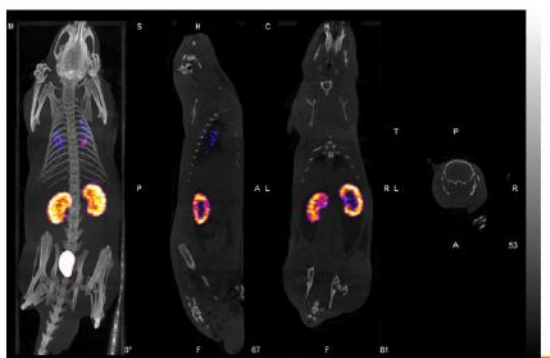


Figure 3

Labelling of DOTA-girentuximab conjugates with therapeutic radionuclides

Tais Basaco Bernabeu^{1,2} – Stefanie Pektor³ – Josue Moreno¹ – Matthias Miederer³ – Andreas Türlér^{1,2}

¹ University of Bern, Switzerland, e-mail:

² Paul Scherrer Institute, Switzerland.

³ University Medical Centre of Johannes Gutenberg Mainz, Germany.
tais.basaco@dcb.unibe.ch

Girentuximab (G250) is a chimeric monoclonal antibody (mAb) reactive with the anti-carbonic anhydrase IX (CAIX) antigen, overexpressed on the cell surface of most (>90%) clear cell renal carcinomas (ccRCC) and not in the normal kidney tissue. This preferential high expression in ccRCC has been used in many preclinical and clinical studies for imaging and therapy of ccRCC. Due to the limited efficacy observed in the first clinical trials using ¹³¹I-girentuximab, the search for more suitable radionuclides was initiated. The goals of this study were: i) label DOTA-conjugates with ¹⁷⁷Lu and ²²⁵Ac using a one-step labelling method in order to increase the radiochemical yield and the specific activity and compare with the two step labelling method; ii) evaluate the stability of the radioconstructs in vitro and in vivo and iii) evaluate the immunoreactivity to CAIX positive cells in vitro and in vivo. First DOTA-G250 conjugates were prepared, purified and characterized by size exclusion chromatography (SE-HPLC/UV), electrophoresis (SDS-PAGE) and mass spectrometry (LC-MS/MS). The ratios of number of DOTA per mAb were calculated and the potential sites modified by DOTA were identified in the light and heavy chains of the antibody. The DOTA-G250 conjugates were labelled with Lu-177 and purified. The radiostability of ¹⁷⁷Lu-DOTA-G250 at high specific activity was increased by addition of sodium ascorbate after the labelling. The stability in vitro of different types of radioconstructs was analysed in human serum, human serum albumin 20% and buffer phosphate saline at 37°C up to 7 days. The radioconstructs with the highest specific activity (13MBq/ug) were not stable in vitro and in vivo. Binding to CAIX positive cells (SK-RC-52) at different specific activities was higher for conjugates with less DOTA content. The immunoreactive fraction of the radioconstructs was calculated. To investigate the optimal protein dose for radioimmunotherapy, mice with subcutaneously growing SK-RC-52 tumours were injected with different amounts of ¹⁷⁷Lu- DOTA-G250. In a further step it is intended to label the DOTA-G250 conjugates with ²²⁵Ac and to evaluate the biological activity.

Macrocyclic bisphosphonates for diagnosis and therapy of bone metastases: Chemistry, *in vivo* evaluation and human application

¹ PFANNKUCHEN, Nina, ¹ MECKEL, Marian, ² BERGMANN, Ralf, ² PIETZSCH, Jens, ² STEINBACH, Jörg, ³ MIEDERER, Matthias, ⁴ MOHNIKE, Wolfgang, ⁵ BAL, C.s, ⁶ SATHEKGE, Mike, ¹ ROESCH, Frank

¹ *Institute of Nuclear Chemistry, Johannes Gutenberg University Mainz, Germany*

² *Institute of Radiopharmaceutical Cancer Research, Helmholtz-Zentrum Dresden-Rossendorf, Dresden, Germany*

³ *Department of Nuclear Medicine, University Medicine Mainz, Germany*

⁴ *Diagnostisch Therapeutisches Zentrum, DTZ am Frankfurter Tor, Berlin, Germany*

⁵ *Department of Nuclear Medicine & PET, AIIMS, New Delhi, India*

⁶ *Department of Nuclear Medicine, University of Pretoria & Steve Biko Academic Hospital, Pretoria, South Africa*

Bisphosphonates (BP) are commonly used for treatment of osteoporosis and other diseases showing increased bone resorption. Due to their high affinity to hydroxyapatite (HAP), radiolabeled BPs can also serve as imaging and therapeutic agents of metabolic active bone tissue, like bone metastases and other skeletal lesions. Conjugation of BPs with macrocyclic chelators offers the possibility of diagnosis and therapy of these painful bone metastases. Chelators like DOTA are able to build stable complexes with various radiometals like ⁶⁸Ga or ¹⁷⁷Lu, which can be used for positron emission tomography or radiotherapy, respectively.

One of the DOTA-BPs established by our group is BPAMD. BPAMD can be easily labeled with ⁶⁸Ga at pH=3–5 and 100 °C for 10 min with a RCY of 90 %. It showed high binding in HAP binding studies (81.5 ± 0.5 %) and only a slight decomposition against apo-transferrin (9.1 ± 0.6 %) and in PBS buffer (4.2 ± 0.8 %) within 3 hours. μ PET small animal studies revealed distinct bone uptake of [⁶⁸Ga]BPAMD, especially in regions with a high remodeling activity like the epiphysis. In a bone metastases rat model [⁶⁸Ga]BPAMD demonstrated significant accumulation in metastases, approximately four times higher than in healthy bone.^[1] Furthermore, BPAMD showed RCY > 98 % with ¹⁷⁷Lu after 30 minutes at 98 °C. In *ex vivo* biodistribution studies in healthy Wistar rats high bone accumulation (SUV_{femur} = 4.84 ± 0.44, 60 min p.i.) and a good target-to-background ratio (e.g. SUV_{kidneys} = 0.35 ± 0.06, 60 min p.i.) were found.^[2]

For better complexation of ⁶⁸Ga a NOTA-based BP, NO2AP^{BP}, was synthesized, radiolabeled and evaluated *in vivo*. As expected, it showed faster kinetics than BPAMD, providing quantitative radiochemical yields in 5 minutes at 98 °C. [⁶⁸Ga]NO2AP^{BP} exhibited a distinct higher binding on HAP (93.8 ± 4.4 %) than [⁶⁸Ga]BPAMD, which was also confirmed in μ PET and *ex vivo* biodistribution studies in healthy Wistar rats. [⁶⁸Ga]NO2AP^{BP} showed high uptake in bone (SUV of 6.19 ± 1.27 %ID/g in femur), which is superior if compared with [⁶⁸Ga]BPAMD or established bone tracers like [^{99m}Tc]MDP and [¹⁸F]NaF, and very low uptake in non-target organs.

Hydroxybisphosphonates (HBP) like risedronate and zoledronate not only show even higher binding to HAP, they are also interacting in the mevalonate pathway and are inhibiting farnesyl diphosphate synthase (FPPS).^[3] Therefore, a new DOTA-conjugated BP based on zoledronic acid was synthesized. Radiochemical yields for labeling of DOTA^{ZOL} (MM.MZ) with ⁶⁸Ga were 80 – 90 % after 15 minutes at 98 °C. With ¹⁷⁷Lu, RCY were > 98 % after 30 minutes at 98 °C. Binding studies on HAP proved the expected high affinity of HBPs (92.7 ± 1.3 %). Biodistribution studies of [⁶⁸Ga]MM.MZ in healthy Wistar rats showed low uptake in soft tissue, fast renal clearance and high bone accumulation (SUV_{femur} = 5.40 ± 0.62, 60 min p.i.) which is superior to [¹⁸F]NaF (SUV_{femur} = 4.87 ± 0.32, 60 min p.i.). [¹⁷⁷Lu]MM.MZ revealed similar distribution in rats (SUV_{femur} = 2.11 ± 0.11), also with a total skeletal retention of almost 50 %ID which is comparable to [¹⁸F]NaF.

Those promising results of μ PET and biodistribution studies led to first applications of various compounds in patients suffering from bone metastases. [^{68}Ga]BPAMD was primarily tested in a prostate cancer patient. It revealed high accumulation in osteoblastic lesions with a SUV_{max} of 77.1 and 62.1 in the 10th thoracic and L2 vertebra compared to 39.1 and 39.2 for [^{18}F]fluoride, respectively, as well as very high target-to-soft tissue ratios and fast clearance.^[4]

[^{68}Ga]NO2AP^{BP} first showed its diagnostic efficiency in a human study in comparison to [$^{99\text{m}}\text{Tc}$]MDP and [^{18}F]NaF. It revealed a similar detection capability as the gold standard [^{18}F]NaF, in selected metastases BP uptake was even higher. In another preliminary study [^{68}Ga]NO2AP^{BP} was compared with [^{68}Ga]HBED-PSMA in the same prostate cancer patients. The BP demonstrated fast uptake at target tissue, fast renal excretion within two hours and low uptake in soft tissue. In most of the metastases uptake of the BP was noticeable higher than that of [^{68}Ga]HBED-PSMA, on average about threefold higher in identical metastases ($\text{SUV}_{\text{max}} = 17 - 46$ for [^{68}Ga]NO2AP^{BP} vs. $\text{SUV}_{\text{max}} = 4 - 21$ for [^{68}Ga]HBED-PSMA), while soft tissue uptake was generally lower.

Furthermore, patient studies were conducted with DOTA^{ZOL} which was developed for theranostics with ^{68}Ga and ^{177}Lu . First applications of [^{177}Lu]MM.MZ in 10 patients were performed using 1.0 – 1.2 GBq per patient with subsequent whole body scintigraphies at different time points for dosimetry issues. [^{177}Lu]MM.MZ already showed bone uptake only a few minutes after injection, a high target-to-background ratio and fast renal clearance.

[^{68}Ga]MM.MZ was used to perform a first human study in a male prostate cancer patient. SUV_{max} values in skeletal lesions and soft tissues were compared to a [^{68}Ga]HBED-PSMA scan. PET results showed an excellent target-to-background ratio. SUV_{max} in bone lesions were on average threefold higher for [^{68}Ga]MM.MZ (e.g. L2 vertebra $\text{SUV}_{\text{max}} = 68.9$) compared to PSMA ($\text{SUV}_{\text{max}} = 8.8$). In an individual application of 5.5 GBq [^{177}Lu]MM.MZ the PSA value of this prostate cancer patient decreased from 478 to 88 ng/mL within two month.

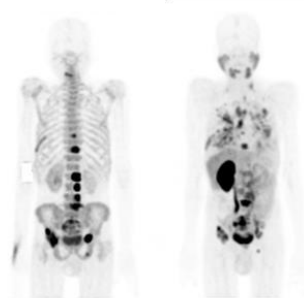


Figure 1: Comparison of maximum intensity projections of [^{68}Ga]MM.MZ (left) and [^{68}Ga]HBED-PSMA (right) in a prostate cancer patient

BPs exhibit a fast and high uptake in bone lesions in connection with a fast blood clearance. They provide better target-to-background ratios than PSMA, what means reduced stress for nontarget tissue. MM.MZ showed promising results in preclinical studies as well as first patient applications and can possibly extend the theranostic concept for a promising bone metastases treatment.

- [1] M. Fellner *et al.*, *Nucl Med Biol* **2012**, 39, 993–999.
- [2] R. Bergmann *et al.*, *EJNMMI research* **2016**, 6, 5.
- [3] Russell *et al.*, *Osteoporos Int* **2008**, 19, 733–759.
- [4] M. Fellner *et al.*, *Eur J Nucl Med Mol Imaging* **2010**, 37, 834.

WEDNESDAY 31ST AUGUST
CHEMISTRY ON THE NUCLEAR FUEL CYCLE III

Study of actinide chemistry in big scientific facilities

Zhifang Chai

*Institute of High Energy Physics, Chinese Academy of Sciences, Beijing 100049, China
School of Radiological & Interdisciplinary Sciences (RAD-X), Soochow University, Suzhou 215123, China*

No actinides, no nuclear fission. Actinide chemistry constitutes one of the key factors of nuclear fission energy, which is strongly relevant to the existing energy security, climate change, resource sustainability and nuclear weapon proliferation, etc. Thus, knowledge of actinide chemistry is fully needed for the maximization of the utilization of uranium resources, the lifetime extension of the existing nuclear power plants, and the minimization of nuclear waste via spent nuclear fuel reprocessing. However, study of actinide chemistry is a tough task, mainly caused by their 5f electronic structures, relativistic effect, spin-orbit coupling and other unknown behaviors, which result in many unusual properties of actinides that even today are not well understood. Furthermore, even surrogating experiments prepared in laboratory are plagued by multiple oxidation states and various coordination patterns of the 5f elements. For example, plutonium can be found as Pu^{3+} , Pu^{4+} , Pu(V)O_2^+ , and Pu(VI)O_2^{2+} under naturally occurring pH conditions. As such, actinide chemistry studies pose extreme challenges to the scientific community in terms of their chemistry, composition, and characterization. In addition, due to the radioactive nature of actinides and the difficulty of safely handling, preparing and measuring, the thorough understanding of the electronic structure, surface chemistry, and interfacial properties of actinide materials lags substantially behind that of other elements.

On the other hand, big scientific facilities such as synchrotron X-ray sources, accelerator-based spallation neutron source and high neutron flux nuclear reactor can offer revolutionary opportunities to the actinide chemistry research. Nowadays synchrotron radiation based techniques have become the key analytical methods in actinide research, due to their advantages: tunable high flux and high-energy beams; highly focused beams for small sample sizes and quantities; the large energy range for the excitation of the O, N, M and L-edges of actinides besides the conventional K-edges; a wide variety of synchronous radiation based spectroscopic and microscopic methods for different scientific objectives. For these reasons, synchronous radiation techniques have been intensively applied in study of actinide chemistry. This presentation is to summarize the latest achievements of various synchronous radiation techniques, mainly X-ray fluorescence spectroscopy, X-ray absorption spectroscopy, and X-ray diffraction and scattering spectroscopy, which are powerful tools to understand the microstructures of actinides, towards the definite scientific aspects of actinide materials, with emphasis on the advances made in our laboratory. In the meantime, the technical needs for synchronous radiation techniques towards sample preparation, radiation protection and other measures will be briefly introduced.

As a complimentary to X-ray techniques, spallation neutron source based on accelerator and nuclear reactors can provide important information about actinides chemistry, which is difficult for synchronous radiation, because neutron is characterized of high penetrability, sensitivity to light elements, like hydrogen, nitrogen and oxygen, etc., ability to detect nuclear-nuclear interaction, and to measure magnetic moment and spin. Its new advances of this nuclear technique for actinide research will be introduced as well.

Finally, future development trends in this area of research will be looked forward.

This work was supported by the National Natural Science Foundation of China and the "Strategic Priority Research Program" of the Chinese Academy of Sciences.

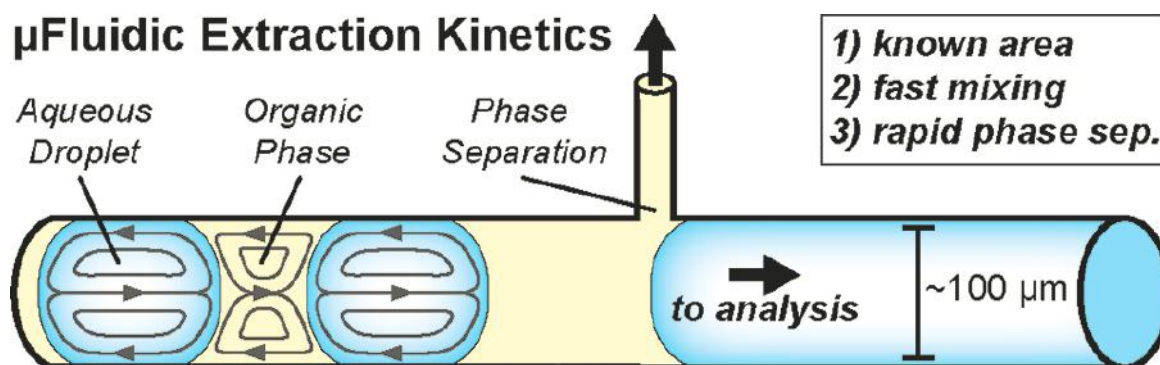
Interfacial mass transfer studies of selected Pu(IV), Am(III), and Pm(III) liquid-liquid extraction systems by microfluidic technique

Pavel Bartl^a, Artem V. Gelis^b, Cari A. Launier^b, Petr Distler^a, Mojmir Nemec^a, Jan John^a

^aCzech Technical University in Prague, Faculty of Nuclear Sciences and Physical Engineering, Brehova 7, Prague 1, 115 19, Czech Republic

^bNuclear Engineering Division, Argonne National Laboratory, 9700 South Cass Avenue, Argonne, IL 60439, USA

Many liquid-liquid extraction schemes have been and still are being designed for separating radionuclides produced in used nuclear fuel. Yet, just one of them, PUREX, has been fully industrialized and implemented in the nuclear fuel cycle, while others are still in development phase. One area of great importance in process development is interfacial mass transfer. Knowing the interfacial mass transfer rate constants and its mechanism can provide important insight in understanding the extraction chemistries involved and allow for modeling and optimization of a particular process for industrial applications.



The main drawbacks affecting conventional techniques for interfacial mass transfer studies are either insufficient mixing velocity or unknown interfacial area. However, an advantageous slug-flow setup of the microfluidic technique allows both rapid mixing and an interfacial area determination. As shown on the scheme above, rapid mixing is provided by a shear force generated by the moving slug itself and measurement of the interfacial area can be performed simply by a microscope snapshot technique. Microfluidics, moreover, allow us to follow strict safeguards and environmental limits due to micro-scale volumes the method utilizes.

In this work, we focus on forward- and backward-extraction steps involving radionuclides of interest and relevant for European project SACSESS (Safety of ACTinide SEparation proceSSes) and US concept ALSEP (Actinide-Lanthanide SEparation). Specifically, interfacial mass transfer rate constants for systems based on TODGA, BTBP/BTPPhen and HEH[EHP] will be presented along with corresponding interfacial processes and kinetic regimes. Pressure pumps along with T-junction droplet generator chip are utilized for generating slug-flow in the flow rate range up to almost 800 μL per minute. Measurement of the specific interfacial area is also of great interest, and microscope snapshot technique measurements were carried out for this purpose.

Key words: Microfluidics, Liquid-liquid extraction, Kinetics, Interfacial mass transfer, Actinide separation

This work was supported by the U.S. Department of Energy, Office of Nuclear Energy, under Contract DE-AC02-06CH11357. Argonne National Laboratory is operated for the U.S. Department of Energy by UChicago Argonne, LLC.

Recent results on the U-Pu-Pb-Bi-O phase relation

Karin Popa^a, Damien Prieur^a, Philippe M. Martin^b, Jean-François Vigier^a, Ondrej Beneš^a, Philippe E. Raison^a, Rudy J.M. Konings^a, Joseph Somers^a

^a European Commission, Joint Research Centre, Institute for Transuranium Elements, Karlsruhe, Germany

^b CEA Marcoule, CEA, DEN, DTEC/SECA/LCC, Bagnols-sur-Ceze Cedex, France

karin.popa@ec.europa.eu .

Liquid Lead–Bismuth Eutectic (LBE) is the coolant considered for the MYRRHA reactor; it has a high boiling point and chemical inertness with respect to air and water. The high boiling point results in a large operational margin, whereas the chemical stability contributes effectively to enhanced safety. The MYRRHA design foresees (U,Pu)O₂ mixed oxide as (initial) fuel and for that reason the compatibility between the fuel and coolant needs to be investigated. Thus, a detailed knowledge of the phase relations in the U-Pu-Pb-Bi-O system is essential. The potential reaction products must be identified, the thermodynamic conditions for their formation must be understood, and their potential effects on the fuel elements have to be investigated. The current extensive studies have concentrated on compounds existing in the Bi-U-O and Pb-U-O ternary systems.

Cubic fluorite-type phases exist in the U^{IV} system, UO_{2+x}-Bi₂O₃, over the entire compositional range, but a non-linear evolution of the lattice parameter with relative stoichiometry has been observed, in contrast to other M^{III}-U^{IV}-O systems. This unusual behaviour was explained previously as a consequence of substitution increasing the amount of anionic vacancies with increasing Bi₂O₃ content. We have confirmed the unusual evolution of the lattice parameter with composition, but have found that, even under an inert atmosphere at 800 °C, U^{IV} is oxidised to U^V/U^{VI} as a function of the substitution degree. Thus, using a combination of methods, we have identified the formation of the BiU^VO₄ and Bi₂U^{VI}O₆ compounds, within this series. Our studies so far using a solid state synthesis route provide no evidence for the formation of corresponding plutonates.

Recent process in pyroprocessing technology development for spent fuel recycling at KAERI

Geun-il Park*, Won Il Ko, Do-hee Ahn, Jeonghoe Ku, Kee Chan Song

*Korea Atomic Energy Research Institute, 989-111 Daedeok-daero, Yuseong-gu, Daejeon, Republic of Korea,
nqipark@kaeri.re.kr

Pyroprocess is non-proliferation technology which is based on a group recovery of reusable elements by electro-chemical reaction in high temperature molten salt electrolytes. It recovers TRU mixture form from the spent fuel for TRU fuel fabrication and it's burning in SFR. Therefore, this process has an intrinsic nonproliferation feature by effectively achieving the concept of "dirty fuel and clean waste". Pyroprocessing was originally developed for the recycling of the metal fuel from a fast reactor. However, it was noted that pyroprocessing can be modified by an oxide reduction process enabling treatment of PWR spent fuels which is in an oxide form. KAERI (Korea Atomic Energy Research Institute)'s pyroprocessing is connecting to a sodium-cooled fast reactor, from the head-end process of spent fuel to electrowinning to obtain TRU metal.

KAERI has full spectrum R&D programs for spent fuel recycling which are the closed fuel cycle system using Pyroprocessing-SFR as well as the transportation/storage of spent fuel and geological disposal system for high-level waste (HLW). Technical issues of pyroprocessing are higher throughput, process efficiency, scalability and waste minimization. The other issue is regarding to the safeguards aspect. Because there have been proliferation concerns on spent fuel recycling technologies and the IAEA has no experience on safeguarding pyroprocessing facility, effective safeguards system for enhancing proliferation-resistance is important. We have been incorporating safeguards R&D along with pyroprocessing technology development. Achievements we got are; Development of safeguards approach for Reference Pyroprocessing Facility in collaboration with IAEA and Test of promising NDA technologies for future IAEA authentication and its performance at JFCS(Joint Fuel Cycle Study).

KAERI has been focusing to develop a viable pyroprocessing system with engineering-related leading-edge technologies using R&D facilities such as PRIDE (PyRpprocess Integrated inactive DEMonstration facility) and DFD/ACPF hot-cell, and to develop an advanced Pyroprocessing Facility by applying 3S (Safeguards, Safety and Security) concept with high proliferation resistance. The R&D status of Pyroprocessing was evaluated based on the Technical Readiness Level. Overall, Pyroprocessing have reached TRL 5 through PRIDE, JFCS, and DFD activities performing engineering scale simfuel tests and laboratory scale active tests. Waste salt treatment and remote operation show relatively slower progresses. But we believe we can expedite the progresses by PRIDE and JFCS activities. We will carried out as future works, the development of Engineering scale off-gas trapping system, Alternative anodes to replace expensive Pt, Engineering scale multi-electrodes system, Advanced drawdown technology to minimize TRU loss, Engineering scale solidification process, remote automation technology, engineering scale safeguards approach. Regarding to safeguards R&D, key technologies test such as NDA benchmark measurement test on pyro-processed hot materials and modelling and simulation for material accountancy of engineering-scale pyroprocessing facility has been implemented with US and IAEA in JFCS. We expect that DA and NDA measurement data from next phase JFCS test will be fed into our safeguards model, so it can validate the safeguards effectiveness for engineering scale safeguards approach.

In addition, the United States and Republic of Korea has been jointly conducting the evaluation of integrated pyroprocess operation in the Phase II-B stage of the Joint Fuel Cycle Study (JFCS) with IAEA cooperation with respect to safeguards and transparency. Objectives of JFCS is to evaluate the technical and economic feasibility and nonproliferation acceptability of pyroprocessing process.

Adopting Advanced Fuel Cycle with SFR is a promising strategy for resolving the issues of spent fuel management and nuclear energy resources.

References

- [1] Hansoo Lee, Geun-II Park and Ho-Dong Kim, "Progress in Pyroprocessing Technology at KAERI" *J. Korea Atomic Industry Forum*, 1-20 (2013)
- [2] Hansoo Lee, Geun-II Park, Kweon-Ho Kang, Jin-Mok Hur, Jeong-guk Kim, Do-Hee Ahn, Yung-Zun Cho and Eung HO Kim, "Pyroprocessing Technology Development at KAERI" *Korea Nuclear Society*, 43, 4, 317-328(2011)

Reversibility of $^{241}\text{Am}^{3+}/^{152}\text{Eu}^{3+}$ during alteration and ageing of 2-line ferrihydrite: implications for radionuclide mobility

Graham Kenyon¹, Sam Shaw¹, Nick Bryan², Katherine Morris¹

¹ *The University of Manchester, School of Earth, Atmospheric and Environmental Sciences, The University of Manchester, Manchester, M13 9PL, UK.*

² *National Nuclear Laboratory, 5th Floor, Chadwick House, Birchwood, Warrington, WA3 6AE, UK.*

Accurately predicting the mobility of radionuclides, including the trivalent actinides (An^{3+}), in the far field of a geological disposal facility requires knowledge of radionuclide reversibility from key reactive minerals such as iron(III) (oxyhydr)oxides. As well as determining whether An^{3+} uptake is reversible/irreversible the rate at which An^{3+} is released from the minerals is also key to their long term mobility. In this study, $^{241}\text{Am}^{3+}$ and $^{152}\text{Eu}^{3+}$ desorption kinetics have been measured from the alteration products of 2-line ferrihydrite during ageing, with particular focus given to the influence of ageing on radionuclide reversibility.

Batch experiments containing 2-line ferrihydrite ($373 \text{ ppm} \pm 1 \text{ ppm} [\text{Fe}]$) at pH 7.8 were aged (up to 6 months) at 75 °C inducing crystallisation into a mixed hematite and goethite (75 : 25 wt%) phase. Additions of $^{241}\text{Am}^{3+}$ ($4 \times 10^{-9} \text{ M}$) or $^{152}\text{Eu}^{3+}$ (10^{-10} M) were made either before or after ageing in order to determine the impact of the ageing process on reversibility. The reversibility of $^{241}\text{Am}^{3+}$ and $^{152}\text{Eu}^{3+}$ from the aged mineral phases was assessed using ethylenediaminetetraacetic acid trisodium salt hydrate (EDTA, 0.05 M) as a chelating agent for the radionuclides in the presence of monobasic potassium phosphate (KH_2PO_4 , 0.1 M) to suppress ligand-radionuclide re-adsorption (Bryce and Clark, 1996; Nowack and Sigg, 1996). This ligand mixture provides a means of removing any surface bound radionuclides from the mineral phase into the solution phase. The subsequent release of $^{241}\text{Am}^{3+}/^{152}\text{Eu}^{3+}$ from the minerals was measured over several months to provide information on the desorption kinetics.

Our results revealed that $^{241}\text{Am}^{3+}$ or $^{152}\text{Eu}^{3+}$ additions made after 2-line ferrihydrite ageing resulted in uptake that was fully reversible (within ~10 days). By contrast, $^{241}\text{Am}^{3+}$ or $^{152}\text{Eu}^{3+}$ additions made before 2-line ferrihydrite ageing resulted in uptake that was partially irreversible requiring several months to reach equilibrium. The size of this irreversible fraction increased with mineral ageing from 48 hrs to 7 days, but showed negligible change upon further ageing up to 6 months. At equilibrium the size of the irreversible fraction was greater for $^{241}\text{Am}^{3+}$ relative to $^{152}\text{Eu}^{3+}$, $35 \% \pm 8 \%$ and $25 \% \pm 5 \%$ respectively. The kinetics data were successfully modelled using two simultaneous first-order desorption rate constants. In addition to the EDTA/ KH_2PO_4 extraction, an acid leaching method with progressively stronger acids used to leach the mineral phases was used to further examine the extent of $^{241}\text{Am}^{3+}$ and $^{152}\text{Eu}^{3+}$ sorption versus irreversible binding in the experimental end products (Doornbusch et al., 2015). The leaching experiments provided evidence that the irreversible fraction was a result of $^{241}\text{Am}^{3+}/^{152}\text{Eu}^{3+}$ incorporation into the hematite and/or goethite crystallisation products.

These findings have potentially important consequences for predicting the mobility of Ln^{3+} and An^{3+} in environments where iron-oxide crystallisation processes are actively occurring. Overall, the observed irreversible binding of Eu^{3+} and Am^{3+} with the bulk mineral phases offers a pathway to potentially long term sequestration of M^{3+} ions in environments where iron-oxide crystallisation is occurring. By contrast, if the bulk mineral phase with incorporated An^{3+} can subsequently form a mobile colloid phase, for example after contact with natural organic matter (Ramos Tejada et al., 2003), it may result in colloid-facilitated transport of An^{3+} .

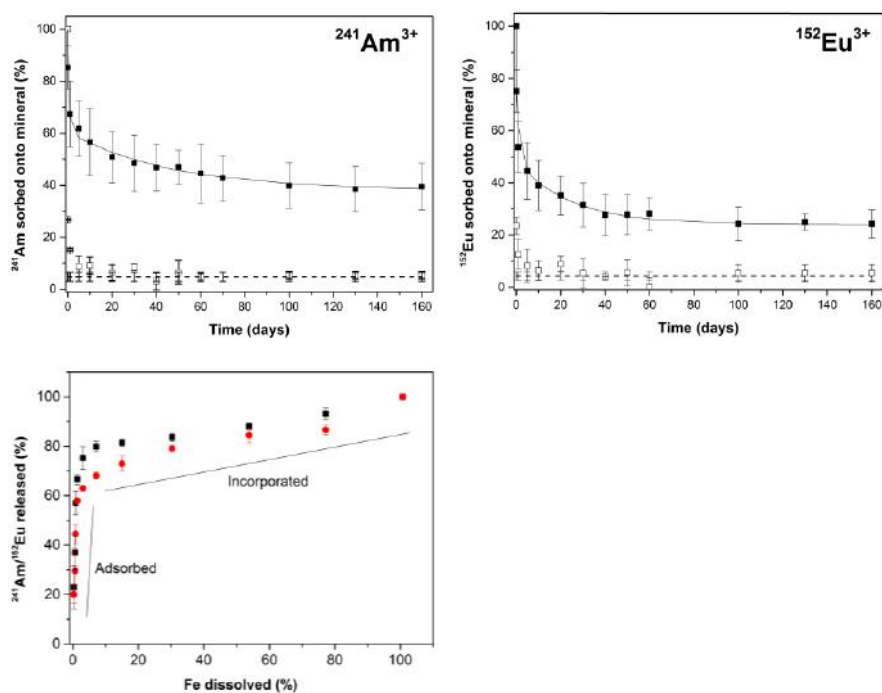


Figure 1. Desorption kinetics for $^{241}\text{Am}^{3+}$ (upper left) and $^{152}\text{Eu}^{3+}$ (upper right) using EDTA/ KH_2PO_4 extraction. Samples where the addition of $^{241}\text{Am}^{3+}/^{152}\text{Eu}^{3+}$ was made before or after 2-line ferrihydrite ageing are represented in the figure as (■), and (□), respectively. The acid extraction results (lower left) for Am^{3+} (●) and Eu^{3+} (■); for samples where the addition of $^{241}\text{Am}^{3+}/^{152}\text{Eu}^{3+}$ was made before 2-line ferrihydrite ageing. All results are from 7 days aged 2-line ferrihydrite samples and error bars are 1σ from triplicate sample measurements.

References.

- Bryce, A. L. & Clark, S. B. (1996) Nickel desorption kinetics from hydrous ferric oxide in the presence of EDTA. *Colloids and Surfaces a-Physicochemical and Engineering Aspects*, **107**, 123-130.
- Doornbusch, B., Bunney, K., Gan, B. K., Jones, F. & Graefe, M. (2015) Iron oxide formation from FeCl_2 solutions in the presence of uranyl (UO_2^{2+}) cations and carbonate rich media. *Geochimica Et Cosmochimica Acta*, **158**, 22-47.
- Nowack, B. & Sigg, L. (1996) Adsorption of EDTA and metal-EDTA complexes onto goethite. *Journal of Colloid and Interface Science*, **177**, 106-121.
- Ramos-Tejada, M. M., Ontiveros, A., Viota, J. L. & Duran, J. D. G. (2003) Interfacial and rheological properties of humic acid/hematite suspensions. *Journal of Colloid and Interface Science*, **268**, 85-95.

Acknowledgement. Funding for this project was provided by EPSRC and Radioactive Waste Management.

ENVIRONMENTAL RADIOACTIVITY II

Chernobyl lava and radioactive particles: 30 years of existence

Irina Vlasova¹, Andrey Shiryayev², Vasilii Yapaskurt¹, Alexey Averin², Yan Zubavichus³, Olga Batuk, Steven Conradson, Boris Ogorodnikov⁴, Boris Burakov⁵, Stepan Kalmykov^{1,3}

¹*Lomonosov Moscow State University, Moscow, Russia*

²*Institute of Physical Chemistry and Electrochemistry RAS, Moscow, Russia*

³*Kurchatov Institute, Moscow, Russia*

⁴*Karpov Physical Chemistry Institute, Moscow, Russia*

⁵*Khlopin Radium Institute, St.Petersburg, Russia*

Thirty years ago severe accident on 26 April 1986 has led to destruction of reactor core of the 4th Unit of the Chernobyl Nuclear Power Plant (ChNPP) and to release of about 3-5% of the total amount of the fuel as dispersed radioactive particles and gaseous radioactive products to the environment. During first days of the active period of the accident (till 6 May 1986) dispersed fuel particles were widely scattered by prevailing winds. Distribution of the radioactive particles was determined by their size. The heaviest and larger particles (more than 50-100 μm) fell down near the ChNPP while the particles less than the first tens μm spread widely. Volatile fission products deposited on the aerosol particles formed so-called “condensation particles” which spread widely throughout Northern hemisphere.

The fate of Chernobyl fuel particles in the environment is of great interest due to their long-term radiological hazard. Morphology features, composition of the fuel particles and speciation of U and Zr in them have been analyzed using SEM-EDX, μ -XAFS, μ -XRF and Raman spectroscopy. XAFS shows that U is predominantly tetravalent [1], though according to Raman spectroscopy some of the particles possess distorted urania structure. The U/Zr ratio varies even within individual particles, which manifests processes of U-Zr-O interaction during the accident.

In November 1986 dedicated cover - “Shelter” – was erected to cover the destroyed part of the 4th Unit. Presumably, major fraction of the fuel (up to 90% from initial 190 tons) remains inside the “Shelter”. A significant fraction of the fuel of the 4th Unit reactor is incorporated in the lava-like fuel-containing materials (LFCM) called Chernobyl “lava”. Melting of UO_2 and zircaloy began in the local part of the reactor core at transient temperatures higher than 2000°C. Fragmented reactor core melted together with construction materials (steel, concrete, serpentinite from biological shield, sand) in sub-reactor room at temperatures about 1660°C. After several days of the melting part of the melt spread from the initial pool into the different rooms of the reactor building forming horizontal and two vertical flows. Large vertical flow reached the lower water-filled level of the building (Bubbler Basin 1) and formed pumice-like material. During the first decade after the accident major efforts have been done to collect samples and to investigate properties of various types of Chernobyl lava. But long-term behavior of LFCM is still poorly understood and their stability estimations vary widely. While at the end of 1986 LFCM were characterized by extremely high mechanical hardness, four years later the formation of soluble U(VI) compounds on the surface of LFCM heaps was observed.

The current state of LFCM samples and aerosol particles collected inside the “Shelter” is reported [2, 3]. Chernobyl lava consists of glassy matrix with numerous inclusions and gaseous bubbles. Glassy matrix of different types of lava is characterized by a high content (up to 10%) of U and Zr. Unpolarised Raman and IR reflectance spectra of the glassy matrix of brown and black lava samples show features typical for

metaluminous depolymerized glass. According to IR data glassy matrix of LFCM is anhydrous and only some inclusions may contain OH-groups. XAFS of the black lava sample showed that, in spite of the numerous inclusions (zircons, urania and zirconia), most of U and Zr are dissolved in the glassy matrix.

Inclusions in the LFCM glassy matrix are of different origin. Most of them have formed during the melting process and subsequent cooling of the melt (uranium with Zr, zirconia, Zr-U-O phase, steel balls and U-rich zircons). Relatively rare inclusions are represented by incompletely dissolved fragments of fuel (UO_2 without Zr). EBSD and Raman spectroscopy proved the presence of high-temperature tetragonal phase of zirconia which was probably stabilized by the U admixture. Interaction with water vapor and self-irradiation of tetragonal zirconia could lead to transition of high-temperature ZrO_2 phase to low-temperature monoclinic phase, which is accompanied by volume expansion and cracking of the lava. U-rich zircon (chernobylite) inclusions are zoned crystals with an unusually high percentage of U for natural and synthesized zircon reaching 15%. According to Raman spectroscopy and EBSD data chernobylite inclusions are well-crystallized. Inclusions of urania have a small amount of Zr and morphologically are represented by dendrites or small inclusions inside zircons. According to Raman spectroscopy, UO_{2+x} inclusions in lava demonstrate almost ideal stoichiometry ($x < 0.7$).

Aerosols inside the construction "Shelter" consist of fuel dust, small UO_2 particles of about 200 nm in size and glassy fragments originated from lava accumulations. The tendency of LFCM to disperse depends on the type of the lava and the room conditions (humidity). At the lower level of the "Shelter" spontaneous detachment of large (up to 100-200 μm) glassy particles with UO_2 inclusions is observed. The analysis of the size distribution and radionuclide composition of the aerosols at the outlet of the ventilation system and in rooms of the "Shelter" continues without interruption for thirty years.

The construction "Shelter" was built in a short time and under extremely high dose rate conditions. It was designed as a temporary shield. At present a new confinement "Arch" which will cover the 4th Unit completely is on the advanced stage. It will protect the environment from the radioactive materials of the 4th Unit ChNPP for at least 100 years. By that time the concept of the removal of the radioactive material and its safe isolation will be developed.

1. Olga N. Batuk et al. Multiscale Speciation of U and Pu at Chernobyl, Hanford, Los Alamos, McGuire AFB, Mayak, and Rocky Flats. *Env. Sci. Technol.*, 2015, 49(11):6474-84
2. Vlasova I. et al. Radioactivity distribution in fuel-containing materials (Chernobyl "lava") and aerosols from the Chernobyl "Shelter". *Radiation Measurements*, 2015, 83, 20-25.
3. Shiryaev A. et al. Physico-chemical properties of Chernobyl "lava" and their destruction products. Submitted.

Marine dispersion of ^{236}U in Danish Straits

Jixin Qiao,^a Peter Steier^b, Sven Nielsen,^a Xiaolin Hou,^a Rer Roos,^a Robin Golser^b

^a Center for Nuclear Technologies, Technical University of Denmark, DTU Risø Campus, Roskilde, Denmark

^b VERA Laboratory, Faculty of Physics – Isotope Research, University of Vienna, Vienna, Austria

In recent years, the potential of ^{236}U as an oceanographic tracer has been promisingly recognized. However, the distribution of anthropogenic ^{236}U in the marine system is not well assessed yet. Danish straits are the connecting area between the North Sea and the Baltic Sea, which provides geographic advantages to study the mixing behaviour of uranium along these two water systems exchange process and the dispersion pattern of ^{236}U in North-Baltic Sea. In the present work, both surface and bottom seawaters collected along the Danish straits were analysed for ^{236}U (as well as ^{238}U and ^{137}Cs) to investigate the distribution characteristics of ^{236}U , thus to better understand the uranium mixing behaviour, source term and transfer of ^{236}U in North-Baltic Sea. Our results indicate that ^{236}U concentrations in both surface and bottom seawaters from Danish straits are distributed within a relatively narrow gradients of, and somewhat independent on the variation of salinity. $^{236}\text{U}/^{238}\text{U}$ atomic ratios vary in the range of $(5-35) \times 10^{-9}$, being > 4 times higher than the estimated global fallout value (1×10^{-9}), with a notable increase trend from northwest Jutland and Zealand (North Sea area) to southeast Zealand (Baltic Sea area). The positive linear correlation between ^{238}U concentration and salinity confirms the conservative mixing character of uranium during the exchange process between the North Sea and the Baltic Sea water. Comparable results obtained in this work to the literature values regarding both ^{236}U concentrations and $^{236}\text{U}/^{238}\text{U}$ atomic ratios for seawaters from the North Sea area demonstrate the Sellafield and La Hague nuclear processing plants related ^{236}U source term in Danish straits. The unexpected high $^{236}\text{U}/^{238}\text{U}$ ratios and ^{236}U concentrations in the Baltic Sea area observed in this work might be a clue indicating another potential ^{236}U input originated from the Baltic Sea. Nevertheless, comprehensive investigation in the Baltic Sea and its surrounding environment are needed to clearly identify the ^{236}U source term in the Baltic Sea.

^{137}Cs , ^{90}Sr , $^{238,239+240}\text{Pu}$ and ^{241}Am in terrestrial Antarctic ecosystem

Katarzyna M. Szufa¹, Jerzy W. Mietelski¹, Maria A. Olech^{2,3}

¹ *The Henryk Niewodniczański Institute of Nuclear Physics, Polish Academy of Sciences, Poland,*

² *Institute of Botany, Jagiellonian University, Zdzisław Czeppe Department of Polar Research and Documentation, Poland.*

³ *Institute of Biochemistry and Biophysics, Polish Academy of Sciences, Department of Antarctic Biology, Poland.*

katarzyna.szufa@ifj.edu.pl

Due to harsh climatic conditions Antarctic ecosystem is not very diverse. In that area most widespread representatives of biota are lichens and mosses. They are pioneering organisms characterized by slow growth, long lifespan, a lack of wax cuticle and root systems. These features make mosses and lichens good biomonitors of air pollution. These pioneer organisms are the most susceptible to accumulation of radioactive contaminants. In Antarctic region such traces originate from nuclear weapons testing and American satellite accident (SNAP-9).

Previous studies conducted by our Laboratory of Radioactivity Analyses of Institute of Nuclear Physics in Cracow revealed some variations of plutonium isotopic ratio between marine and terrestrial Antarctic samples. In the present investigation samples of mosses, lichens and soils have been studied. Research material was collected from the South Shetlands Archipelago (King George Island, Deception Island, Penguin Island) and Antarctic Peninsula by the Polish Antarctic Expeditions during four decades (1980–2015). Caesium concentrations were determined using low background gamma spectrometry with an HPGe detector of high energetic resolution. Subsequently material was dissolved in hot acids, isotopes of plutonium were adjusted to tetravalent oxidation state and separated by anion-exchange with Dowex-1 resin during passing the column. The next stage was strontium extraction using column filled with Sr-Resin. Americium was removed using a conventional methanol-acid standard procedure on Dowex 1x8. Plutonium and americium sources were measured by alpha spectrometers with silicon detectors, strontium concentrations were determined using Liquid Scintillation Counter. Data obtained revealed ^{238}Pu , $^{239+240}\text{Pu}$, ^{90}Sr and ^{241}Am tracers in mosses and lichens samples. At the same time ^{137}Cs was discovered above detection limits predominately in mosses and in few lichen samples. Plutonium activity ratios are various but consistent within uncertainties. In aim to get more data on homogeneity of plutonium measurements of ^{240}Pu to ^{239}Pu atom ratio by ICPMS is our close future plan. This investigation will be performed for terrestrial as well as for marine biological samples.

Environmental ^{129}I : level, distribution and source in Northwestern China

Dongxia Zhang^{1, 2}, Xiaolin Hou^{1, 2, *}

¹ SKLLQG, Shaanxi Key Laboratory of AMS Technology and Application, Xi'an AMS Center, Institute of Earth Environment, CAS, Xi'an 710061, China

² Center for Nuclear Technologies, Technical University of Denmark, Risø Campus, Roskilde, Denmark
[*houlx@ieecas.cn](mailto:houlx@ieecas.cn)

^{129}I is a long-lived radionuclide with a long half-life of 15.7 Ma. ^{129}I in the present environment mainly comes from human activities including nuclear weapons testing, nuclear fuel reprocessing, nuclear accidents and operation of nuclear reactors. Iodine is a volatile element, and chemically active, the radioactive isotopes of iodine released can easily spread in the environment, migrate in the ecosystem and enrich in the thyroid gland in the human body. Due to long half-life, ^{129}I can be used as a tracer to investigate nuclear environment safety, seawater exchange and transport, stable iodine geochemical cycle, etc. In this work, surface soil samples (0-5 cm) collected in Northwest China were analysed for ^{127}I and ^{129}I using an effective chemical separation combined with a high sensitivity AMS measurement, in order to investigate ^{129}I level and distribution in Northwest China, explore its sources in this region. The data is also useful for establishment ^{129}I environmental background in Northwest China, and investigation on the impact of early human nuclear activities on the environment in the region.

The collected soil samples were dried, ground and sieve through a 200 mesh sieve. About 5 g ground soil samples was taken to a quartz boat, 1.0 kBq ^{125}I tracer was spiked for measurement of chemical yield. The boat with sample was put to a quartz working tube in a tube furnace for separation of iodine using combustion. The temperature of the furnace was gradually increased to 800°C and kept for 1.5 hours under oxygen gas flow. The off gas from the working tube passed through a bubbler filled with 0.5 M NaOH-0.02 M NaHSO₃, liberated iodine from the sample was trapped in the solution in the bubbler. The entire combustion took about 3 hours. 3 ml of trap solution was taken to a plastic tube and measured using a gamma detector for ^{125}I , which was compared with the ^{125}I standard (the same amount of ^{125}I spike solution and diluted to 3 ml using the same trapping solution) for measurement of chemical yield of iodine during combustion. Chemical yield of more than 97% were obtained for soil samples. After measurement of ^{125}I , the solution is combined to remained trap solution. 1.0 ml trapped solution was taken and diluted 10 times using deionized water for measurement of ^{127}I using ICP-MS. To the remained solution, NaHSO₃ and 0.5 ml of ^{127}I carrier solution with a concentration of 2.0 mg/ml (prepared from a ^{129}I free iodine provided by Woodward company, USA, with a measured $^{129}\text{I}/^{127}\text{I}$ ratio less than 5×10^{-14}) were added, and pH was adjusted to 1-2 using HNO₃. After mixed, 1 ml of 1.0 mol/L AgNO₃ was added for precipitate iodine as AgI, which was separated by centrifuge. After dried, AgI precipitated was ground and mixed with niobium powder in a mass ratio of 1:5, which was then pressed in copper target holder. $^{129}\text{I}/^{127}\text{I}$ atomic ratio was measured using 3 MV accelerator mass spectrometry in Xi'an AMS Center. I^{5+} ion was selected for ^{129}I measurement. Procedure blanks were prepared using the same procedure as samples, the measured $^{129}\text{I}/^{127}\text{I}$ in the blanks are $(1-2) \times 10^{-13}$, which is 2-3 orders of magnitude lower than that in samples.

More than 200 surface soil samples was analysed, the concentrations of iodine isotope show a significant variation. The concentrations of ^{127}I in Northwest China are 0.43 to 16.8 μg/g (dry mass), with an average of 3.65 μg/g, which agree with the literature values (0.5~40 μg/g); ^{129}I concentration are 1.38×10^6 to 2.62×10^{10} atoms/g, with an average of 4.29×10^8 atoms/g. There is a hotspot, where high ^{129}I level is observed, with ^{129}I concentrations higher than 10^9 atoms/g, this might be attributed to the early nuclear activities in this regional; $^{129}\text{I}/^{127}\text{I}$ atomic ratios in all samples range from 9.1×10^{-11} to 7.38×10^{-6} , with an average of 7.47×10^{-8} ,

which is higher than pre-nuclear level of 10^{-12} by 1-4 orders of magnitude. These data indicating that the surface environment in Northwest region was significantly influenced by human nuclear activities.

Acknowledgement: This work was financially supported by China Ministry of Science and Technology through two projects(2012IM030200 and 2015FY110800). NKS project funding support for the conference.

The author thanks staff in Xi'an AMS center leading by prof. Weijian Zhou for their support in sample measurement, prof. Guangmin Cao from Northwest Plateau Institute of Biology, CAS for provide part of soil samples and Dr. Yukun Fan, Shan Xing and Ning Chen who participated in the sampling campaign.

Chemical effects on production mechanism of fission product aerosols

K. Takamiya, T. Tanaka, S. Nitta, S. Sekimoto, Y. Oki, T. Ohtsuki

Research Reactor Institute, Kyoto University, Japan

The attachment behavior of fission products to aerosol particles has been investigated in order to understand the production mechanism of radioactive aerosols which had been released from the Fukushima Daiichi Nuclear Power Plant after the Great East Japan Earthquake in 2011. The aerosols which contains a radioactive fission product were generated under known conditions and the production ratio of fission product aerosol was measured to reveal principal parameters in the production mechanism of the aerosols in the present work. The radioactive aerosols were produced by passing a primary aerosol through a chamber in which a spontaneous fission source of Cf-252 was installed. Solution and solid aerosols were used as primary aerosols for comparison. The primary solution aerosols were generated from alkali halide solutions using an atomizer, and the primary solid aerosols were prepared by heating alkali halide salt or other solid materials in an electric furnace. The primary aerosol was classified by size using a differential mobility analyzer before the injection to the chamber. Finally, the radioactive aerosol produced in the chamber by attaching fission products to aerosol particles was collected on a filter. The amount of fission products which attaches to aerosol particles were measured by gamma-ray spectrometry for the filter using a Ge detector. On the other hand, fission products emitted in the chamber from the spontaneous fission source was collected by a filter which was placed directly on the source and measured by the Ge detector. The attachment ratio of fission products to aerosol particles, which is equivalent to the production ratio of radioactive aerosol, was estimated from the ratio of photopeak areas for each fission product. It was found that the attachment ratio is proportionate to the surface area of aerosol particles in the small surface area region and the increasing rate of the relationship varies with materials of the aerosol particles. The proportional relation and the variation of increasing rates suggest that the attachment ratio of fission products to aerosol particles depends on both geometric collision rates and chemical effects. On the other hand, the increasing rates decrease and the attachment ratios were saturated in the larger region of surface area of aerosol particles. This trend indicates that the attachment behavior of fission products to aerosol particles could be held in an adsorption-desorption equilibrium. The relationships between the surface area and the attachment ratio were fitted by functions on the basis of the assumption of the adsorption-desorption equilibrium between fission products and aerosol particles. As results of the fitting, equilibrium constants and saturated attachment ratios were obtained for each fission products and aerosol materials. In the comparison among the estimated equilibrium constants of Tc-104 for solution aerosols of sodium chloride, sodium bromide, sodium iodide and cesium chloride, it was found that the equilibrium constant for sodium chloride solution aerosol is smaller than those for other solution aerosols. This difference might be caused by density profiles of the anions in in the fine solution particles that is explained by molecular dynamics simulations.

RADIOPHARMACEUTICAL CHEMISTRY II

Radiolabeling with novel ^{18}F -labeled electrophilic agents

Olof Solin

1. *Turku PET Centre and Department of Chemistry, University of Turku, Turku, Finland*
2. *Accelerator Laboratory, Åbo Akademi University, Turku, Finland*

Positron (β^+) emission tomography (PET) is a non-invasive molecular imaging technique that allows for the in vivo investigation of physiological processes. As a radioisotope, fluorine-18 has an advantageous half-life (109.7 min), a very clean decay process (97% β^+ emission), and a short β^+ trajectory, due to the low energy of the beta particle, which is a property that enables the acquisition of high-resolution PET-images. The widespread use of the radiotracer 2- ^{18}F fluoro-2-deoxy-D-glucose has generated a massive amount of invaluable clinical data and has motivated a worldwide interest in PET and ^{18}F radiochemistry.

For fluorine chemistry other than radiolabelling, nucleophilic and electrophilic fluorinations are complementary processes that are used indiscriminately; the method of choice depends on the reactivity profile of the precursor to be fluorinated. A similar degree of synthetic flexibility would facilitate significantly the production and evaluation of new ^{18}F radiotracers but to date, this is far from the reality because the range of reactions suitable for ^{18}F labelling remains limited in comparison with the number of transformations available to access non-labelled fluorinated material. Electrophilic ^{18}F -fluorination suffers from well-recognized drawbacks. The carrier added method employed for the production of ^{18}F gas gives labelled products with low specific activity. In addition, ^{18}F gas, a reagent that requires specialist equipment for its handling, can react unselectively and lead to a mixture of products. This complication lowers the radiochemical yield and will lead to problematic and time-consuming purification processes.

In order to decrease the reactivity of ^{18}F gas, various fluorinating agents have been synthesized (Fig. 1). Acetyl ^{18}F hypofluorite¹ (^{18}F CH₃COOF) is the most common agent, and other compounds such as xenon ^{18}F difluoride² (^{18}F XeF₂), ^{18}F fluoro-2-pyridone³ and N- ^{18}F fluoro-N-alkylsulfonamides⁴ have been employed but are not widely used. Low yield and poor reproducibility have prevented the use of no carrier added ^{18}F perchloryl fluoride⁵. A novel ^{18}F NF reagent, ^{18}F -N-

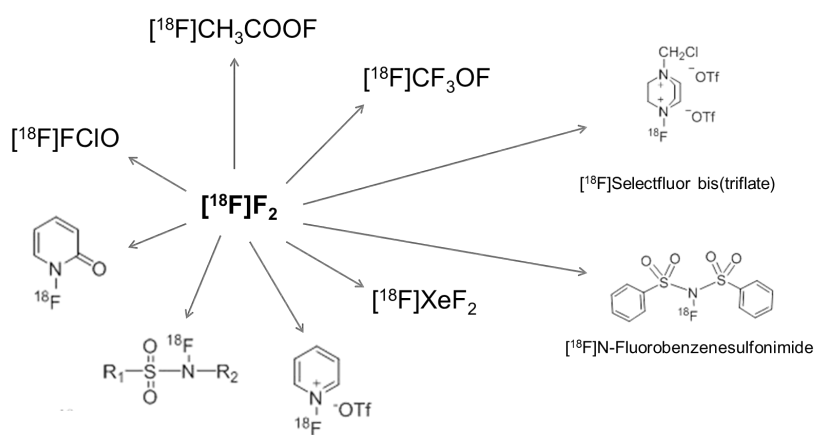


Figure 1. ^{18}F -labeling precursors derived from ^{18}F gas

fluorobenzenesulfonimide⁶, has also been prepared and used for the synthesis of ^{18}F -labeled compounds. More recently, the preparation of ^{18}F selectfluor bis(triflate)⁷ and its usefulness in the preparation of clinically used radiotracers has been demonstrated. The development of stable, reactive, and selective electrophilic ^{18}F -fluorination agents will most likely advance electrophilic ^{18}F -labeling in PET radiopharmaceutical synthesis.

1. Fowler et al., J Label Compd Radiopharm 1982; 19:1634, 2. Chirakal et al., Int Appl Radiat Isot 1984;35:401, 3. Oberdorfer et al. Appl Radiat Isot 1988;39:685, 4. Satyamurthy et al. Appl Radiat Isot 1990; 41:733, 5. Hiller et al. Appl Radiat Isot 2008; 66:152, 6. Teare et al. Chem Comm 2007:2330, 7. Teare et al. Angew Chem Int ed 2010; 49:6821

Preparation of n.c.a. 6-¹⁸F-fluoro-L-tryptophan using copper-mediated radiofluorination

Dominique Schäfer, Philipp Weiß, Johannes Ermert, Johnny Castillo Meleán, Bernd Neumaier

Institut für Neurowissenschaften und Medizin, INM-5: Nuklearchemie, Forschungszentrum Jülich GmbH, Germany

Objectives: The essential amino acid tryptophan is involved in various physiological processes. Besides protein synthesis, tryptophan is the precursor for serotonin and kynurenine. An upregulated utilization of tryptophan in tumor cells was reported (1). The degradation product kynurenine was described as an important factor in tumor growth and immune suppression (2). Accordingly, labelled tryptophan could enable to trace alterations of tryptophan uptake in regions of serotonergic neurons (3). Until now, [¹⁸F]fluorotryptophan was labelled using the Balz-Schiemann reaction (4) providing insufficient radiochemical yields. A recently published isotopic exchange reaction (5) appears to engender challenges in automation that are preventing their routine use. In the last few years, several innovative ¹⁸F-fluorination methods have been published (6-8). The copper-mediated radiofluorination method exhibits several major advantages like sufficient RCYs, bench-stable precursors and mild reaction conditions and was therefore chosen in this study. First, the synthesis of an appropriate aryl boronic ester was developed. The labelling step and hydrolysis were optimized with regard to automation.

Methods: An appropriate precursor for ¹⁸F-labelling was designed starting from bromo-indole. The Schöllkopf's auxiliary (9) was introduced within five steps. The pinacol boronate ester was inserted using a Suzuki-Miyaura coupling reaction.

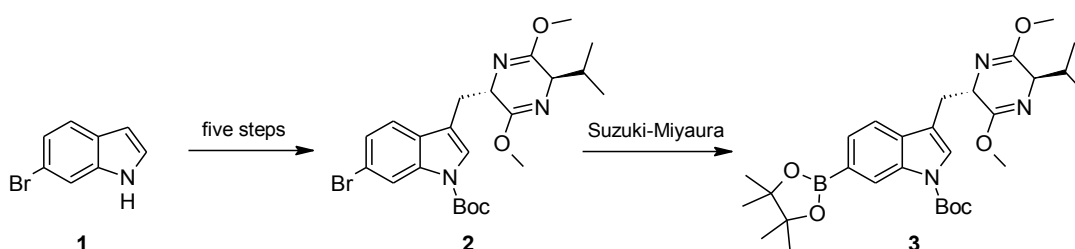


Figure 1: Synthesis scheme for the pinacol ester tryptophan derivative **3**.

In preliminary studies indole derivatives with the pinacol ester in different position were used as model compounds. The highest yields were obtained at 6-position of the indole motif. Besides reaction time and temperature, different reaction conditions like the type of nucleophilicity enhancer, temperature, time and solvents were examined. The subsequent deprotection step was optimized with regard to acid, reaction time and temperature.

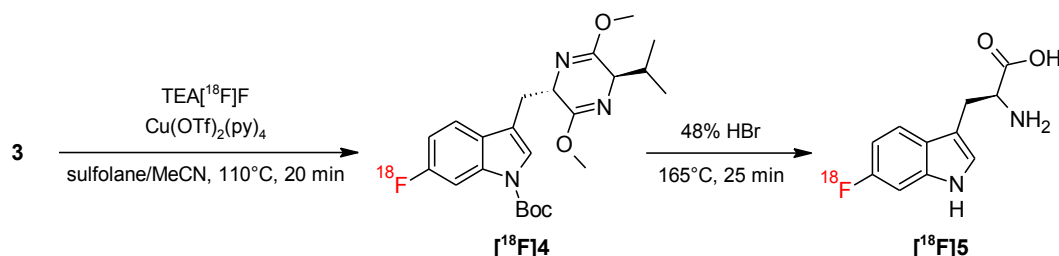


Figure 2: Radiosynthesis of 6-¹⁸F-fluoro-L-tryptophan.

Results: The synthesis of the appropriate precursor for copper-mediated radiofluorination was achieved within six steps and an overall yield of 37 %. The optimized radiofluorination conditions are as follows: precursor and Cu(OTf)₂(py)₄ were solved in sulfolane/acetonitrile were given on dried tetraethylammonium [¹⁸F]fluoride (TEA[¹⁸F]F) and heated for 20 min at 110 °C. The radiochemical conversion (RCC) protected [¹⁸F]4

was 52 ± 10 % determined by radioTLC. Purification of [^{18}F]4 from residual [^{18}F]fluoride and copper was achieved by using a silica cartridge. Highest RCC for deprotection yields were obtained using 48 % hydrobromic acid for 25 min at 165°C giving 36.1 ± 5 % RCC.

The total radio synthesis of 6-[^{18}F]fluoro-L-tryptophan was carried out within 120 min including HPLC purification (Figure 3) with an overall radiochemical yield of 13 ± 4 %. The radiochemical purity was more than 99 %, with an enantiomeric excess of 89 % and a specific activity of 280 GBq/ μmol . Automation of the reaction as well as the biological evaluation of the radiotracer is in progress.

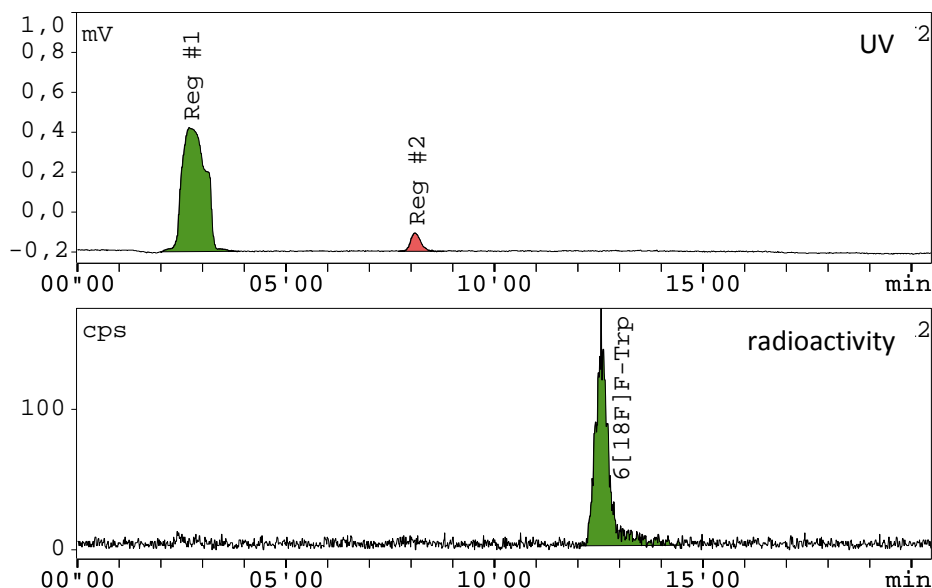


Figure 3: Radioanalysis of HPLC purified 6-[^{18}F]fluoro-L-tryptophan.

Conclusion: The herein reported method allows to obtain n.c.a. 6-[^{18}F]fluoro- L-tryptophan in high RCYs. Accordingly, the potential of this tracer could be evaluated in different applications like tumor detection or psychological disorders. Furthermore, an automated synthesis unit equipped with a two-reactor-system is in progress.

References:

1. Opitz CA, Litzenger UM, Sahm F, Ott M, Tritschler I, Trump S, et al., *Nature*. **2011**; 478: 197-203.
2. Prendergast GC., *Nature*. **2011**; 478: 192-4.
3. Drevets WC, Thase ME, Moses-Kolko EL, Price J, Frank E, Kupfer DJ, et al. *Nucl. med.biol.*, **2007**; 34: 865-77.
4. H. L. Atkins DRC, J. S. Fowler, W. Hauser, R. M. Hoyte, J. F. Kloppe, S. S. Lin, and A. P. Wolf., *J. Nucl. Med.*, **1972**; 13: 713-9.
5. Weiss PS, Erment J, Castillo Melean J, Schafer D, Coenen HH., *Bioorg. med. chem*, **2015**; 23: 5856-69.
6. Lee E, Hooker JM, Ritter T., *J. Am. Chem. Soc.*, **2012**; 134: 17456-8.
7. Ichiishi N, Brooks AF, Topczewski JJ, Rodnick ME, Sanford MS, Scott PJH. *Org. Lett.*, **2014**; 16: 3224-7.
8. Tredwell M, Preshlock SM, Taylor NJ, Gruber S, Huiban M, Passchier J, et al. *Angew. Chem. Int.*, **2014**; 53: 7751-5.
9. Schöllkopf U, Neubauer H-J., *Synthesis*. **1982**; 19: 861-4.

Synthesis of [^{18}F]F-DPA, a novel [^{18}F]DPA-714 analogue for PET imaging of neuroinflammation

Keller Thomas¹, Krzyczmonik Anna¹, Forsback Sarita¹, Kirjavainen Anna¹, Lopez Picon Francisco², Almajidi Rana², Takkinen Jatta², Rajander Johan³, Cacheux Fanny⁴, Damont Annelaure⁴, Dollé Frédéric⁴, Rinne Juha O⁵, Haaparanta-Solin, Merja², Solin Olof^{1,3,6}

1 Radiopharmaceutical Chemistry Laboratory, Turku PET Centre, University of Turku, Finland

2 MediCity/PET Preclinical Imaging Laboratory, Turku PET Centre, University of Turku, Finland

3 Accelerator Laboratory, Turku PET Centre, Åbo Akademi University, Finland

4 CEA, I2BM, Service hospitalier Frédéric Joliot, Orsay, France

5 Turku PET Centre, Turku University Hospital, Finland

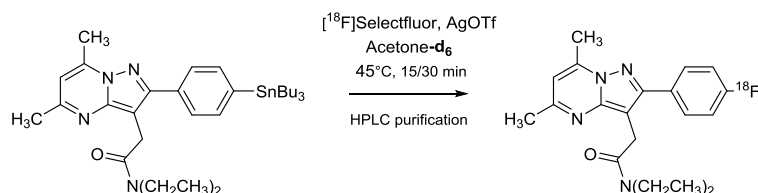
6 Department of Chemistry, University of Turku, Finland

Introduction

Electrophilic ^{18}F -fluorination provides a fast and simple synthetic route to a range of target molecules inaccessible by nucleophilic labelling. Herein we report the electrophilic synthesis of [^{18}F]F-DPA, a novel TSPO-specific radioligand for neuroinflammation imaging, using post-target produced, [^{18}F]F₂-derived, [^{18}F]Selectfluor. The use of [^{18}F]F₂ resulted in the fluorination of the stannylated precursor of labelling but without loss of the tributyl tin moiety, hence [^{18}F]Selectfluor was selected as a milder and more selective ^{18}F -fluorination reagent.

Materials and methods

[^{18}F]F₂ and [^{18}F]Selectfluor were prepared according to previously reported methods^{1,2}. The crude stock of [^{18}F]Selectfluor was used without purification in the labelling of the [^{18}F]F-DPA precursor with the use of silver triflate as an additive (Scheme 1).



Scheme 1: Synthesis of [^{18}F]F-DPA using [^{18}F]Selectfluor

Preclinical evaluation of [^{18}F]F-DPA was carried out in Sprague Dawley rats and APP/PS1-21 and wild type mice. Data was compared to that obtained with another TSPO radioligand, [^{18}F]DPA-714.

Results and discussion

[^{18}F]F-DPA was successfully synthesised by electrophilic substitution. The RCY, decay corrected to EOB and calculated from [^{18}F]Selectfluor, was $15.9 \pm 4.3\%$. Radiochemical purity exceeded 99% and SA was 9.0 ± 2.9 GBq/ μmol . Preclinical results show that the novel [^{18}F]F-DPA can be used to image neuroinflammation *in vivo* and also shows a higher metabolic stability relative to [^{18}F]DPA-714.

Conclusions

The aromatic labelling position does confer a higher degree of metabolic stability relative to [^{18}F]DPA-714. The preclinical study demonstrates the validity of [^{18}F]F-DPA for the detection of neuroinflammation and due to its slower formation of radiolabelled metabolites and superior wash-out kinetics, [^{18}F]F-DPA might be the preferred radiotracer for, at least, small animal imaging.

Acknowledgements

Funding was received from the European Union's 7th Framework Programme for Research, grant numbers 316882 and HEALTH-F2-2011-2788850 (INMiND) and from the Academy of Finland, grant number 266891

References

1. H. Teare et al, *Angew Chem Int Ed*, **2010**, 49, 6821, 2. J. Bergman, O. Solin, *Nucl Med Biol*, **1997**, 24, 677

Synthesis of a tetrazine-based prosthetic group for synthesis of ^{111}In and ^{68}Ga radiopharmaceuticals via biorthogonal click reactions

Dave Lumen¹, Outi Keinänen¹, Brianda Barrios-Lopez¹, Kim A. Bergström², Anu J. Airaksinen¹

¹*Laboratory of Radiochemistry, Faculty of Chemistry, University of Helsinki, Finland*

²*HUS Medical Imaging Centre, Helsinki University Central Hospital, Helsinki, Finland*

Introduction: The aim for this project was to develop new prosthetic groups for synthesis of radiopharmaceuticals for single-photon emission tomography (SPECT) and positron emission tomography (PET) by using ^{111}In and ^{68}Ga nuclides and biorthogonal reactions. These tetrazine-based prosthetic groups could also be used in pretargeting studies. The use of structural imaging modalities such as computer tomography (CT) and magnetic resonance imaging (MRI) in combination with SPECT or PET enables precise anatomical localization of the radioactive signal.

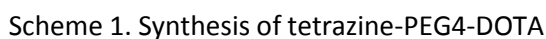
The term bioorthogonal chemistry refers to a chemical reaction that will neither interact nor interfere with biological systems. Bioorthogonal reaction typically involves two steps. A substrate with a bioorthogonal functional group is administered first. The substrate is allowed to find its target e.g. a tumor and then a probe containing the complementary functional group and a suitable label is administered. The probe reacts with the substrate and then location of the substrate can be detected via the label on the probe. Bioorthogonal reaction must fulfill few important rules: it has to be selective, it must function in biological conditions and it has to have fast reaction kinetics at low concentrations. The probe and substrate have to be biologically and chemically inert.

Bioorthogonal reactions have been successfully applied on tumor imaging by using tumor-targeted antibodies and radiolabeled probes. Strain-promoted inverse-electron-demand Diels-Alder cycloadditions has been used in bioorthogonal studies. It has reaction kinetics several orders of magnitude faster than other biorthogonal reactions. Faster reaction kinetics makes the reaction more efficient for in vivo studies when smaller amounts of radiolabeled probe is used.

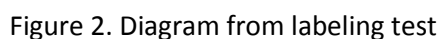
One of the most used counterparts in inverse electron-demand Diels-Alder cycloaddition are electron-deficient tetrazine (Tz) and trans-cyclooctene (TCO). TCO is typically attached to an antibody or nanomaterial because it has better stability than tetrazine in biological systems. Radiolabel is respectively attached to tetrazine. When using metallic radionuclides different chelates can be conjugated to Tz and then coordinate the radionuclide to the chelate.

We decided to synthesize tetrazine molecule with DOTA because then we could label the molecule with ^{111}In or ^{68}Ga depending whether there are SPECT or PET camera available for the studies.

Methods: Tetrazine-PEG4-DOTA was synthesized from tetrazine-PEG4-amine HCl salt (1) and DOTA-NHS ester (2) in mild reaction conditions (Scheme 1). Tetrazine and DOTA molecules were mixed with 2 ml DMF and 200 μl Et_3N and the reaction mixture was mixed over night at room temperature and covered from light. The reaction was monitored by using TLC (1:1 MeOH: DCM). Product (3) was purified by using semi preparative HPLC (gradient flow 2ml/min, 0.1 % TFA in mQ: 0.1 % TFA in ACN). The product was evaporated to dryness resulting a red oil.



Results: Synthesis of Tz-DOTA (3) worked well and it was optimized resulting 78±2 % yields. Synthesized product was used in labeling tests, which showed us that labeling worked well (over 95 %) when mass of Tz-DOTA was over 0,008 mg but dropped significantly when mass was lower than that (Figure 2). All test were made using 2 MBq of $^{111}\text{InCl}_3$.



Acknowledgements: The project was funded by the Academy of Finland (project 260316)

AAZTA-5: a new theranostic chelator with kit-type labeling abilities for ^{68}Ga , ^{44}Sc and ^{177}Lu

J-P. Sinnes, D. Wiebe, S. Böhlend, A. Fuente, F. Roesch

Institute for nuclear chemistry, Johannes Gutenberg-University Mainz, Germany

Objective: Chelators for theranostic application provide access to tracers for imaging and therapy. The main representative is DOTA, whose conjugates like DOTA-TOC however are labeled under harsh conditions. The aim of this work was the development of a chelator and its TOC-derivative, which are capable of kit-type labeling (RT, pH 4.5-5.5). Both should be evaluated with ^{177}Lu as well as ^{44}Sc and ^{68}Ga among kit-type labeling conditions. Furthermore the stability against HS, PBS-buffer, EDTA and DTPA were tested and challenge studies against iron were performed for evaluating *in vivo* applications.

Methods: The bifunctional chelator AAZTA-5 (6-Amino-6-(5-methoxy-5-oxopentyl)-1,4-diazipine-tetraacetate) was synthesized in a 5-step synthesis and further coupled with TOC in 3 steps. Both derivatives were characterized and labeled at room temperature with ^{177}Lu , ^{44}Sc and ^{68}Ga varying pH, time and chelator concentration. Complex stabilities against PBS-buffer, human serum, DTPA and EDTA were tested and challenge studies against iron were performed. For comparison analog labeling experiments were performed for a DOTA analog (5-methoxy-5-oxopentyl-DO3A) with ^{177}Lu and ^{44}Sc .

Results: Labeling studies of AAZTA-5 and AAZTA-5-TOC with all 3 radiometals showed quantitative yields at room temperature within minutes (< 5 min, Figure), whereas the DOTA derivative couldn't reach these results with ^{177}Lu and ^{44}Sc below 90 °C (< 10 min). Increasing stability of the complexes was found in the order Ga < Lu < Sc for the free chelator and Lu < Sc < Ga for the TOC derivative, respectively.

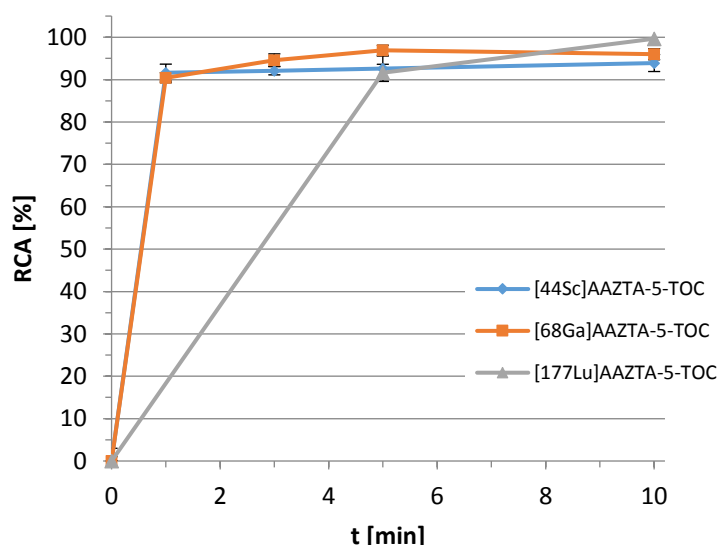


Figure: Labeling of AAZTA-5-TOC at 25 °C, pH 5.5 (Sc pH 4), 10 nmol chelator with ^{68}Ga , ^{44}Sc and ^{177}Lu

Conclusion: The bifunctional chelator AAZTA-5 is able of complexing ^{44}Sc , ^{68}Ga and ^{177}Lu under kit-type conditions. In a proof-of-principle study AAZTA-5 showed the capability of adding a targeting vector to the binding side without losing the ability of kit-type labeling, in fact the stability increased in some cases. AAZTA-5 and AAZTA-5-TOC showed quantitative labeling under mild conditions as well as high complex stabilities. Especially the stability for ^{44}Sc seems to be resilient enough for *in vivo* application.

CHEMISTRY OF THE NUCLEAR FUEL CYCLE IV

Recycling the actinides, a promising pathway for improving the nuclear environmental footprint, and sustainability

Christophe POINSSOT

CEA, French Nuclear And Alternatives Energies Commission, Nuclear Energy Division, Radiochemistry & Processes Department, CEA Marcoule, F-30207 BAGNOLS SUR CEZE, France

In the framework of COP21 agreement, nuclear energy could help mitigating the global climate change together with the renewables, due to its low green-house-gases emissions, its reliability and its high base-load capacity. However, the political uncertainty in many countries about the future of nuclear energy source clearly illustrates that there is a need for a more global approach to assess the relative merit or disadvantage of nuclear energy by comparison with the other energy sources, and draw its potential future improvements. Indeed, beyond the well-known economic aspect, many other criteria are also implicitly considered when choosing a relevant energy mix to be implemented in a given country. This rather recent situation requires extending the classical approach based on the technological and economic optimization to a wider approach also including the overall environmental footprint and the more general social acceptability and social impact. Sustainability approach includes by definition the different criteria describing the environmental, economic and societal fields. It is therefore of prime importance of assessing the relevant and relative sustainability of the different nuclear energy systems and evidence any potential improvement directions.

Worldwide, different types of fuel cycles are nowadays implemented: (i) the so-called once-through cycle (OTC) in which spent nuclear fuel is considered as an ultimate waste to be directly disposed of after an interim storage phase, but also (ii) the so-called twice-through cycle (TTC) in which spent nuclear fuel is treated to recycle the energetic valuable materials (U and Pu) to manufacture the specific MOX fuel to be irradiated in the current LWR reactors. Currently, many countries implicitly chose the so-called once-through cycle driven by short-term perspective, whereas few others like France, UK, Japan reprocess their spent fuel. Although both options can be considered relevant, fitting diverse criteria, they clearly have different figures of merit in terms of sustainability and open the doors to very different long-term perspectives. Indeed, in a long lasting prospective, the once-through cycle sustainability is clearly low since it does not optimize the consumption of natural resource (less than 1% of uranium is actually burnt in reactor) and does not recycle the energetic material (U and Pu) although they still represent more than 95% of the spent nuclear fuel. This question can be seen as a key issue for the intergenerational equity. OTC also leads to larger-volume and longer-term radiotoxic waste to be disposed of and do not optimize the use of the repository, a scarce resource as evidenced by the last 40y research in this area. Reversely, twice-through cycle can be seen as a first step towards sustainability with the once-recycling of major actinides, the reduction of the waste volume and toxicity and the implementation of a more robust final waste confinement, the nuclear glass. It also allow reducing the space required to dispose the ultimate waste in a future repository for the same amount of electricity produced. Furthermore, Life Cycle Assessment (LCA) approach demonstrates that TTC has a lower environmental impact due to the reduction of the front-end activities which have much larger impact than the back-end: most of the environmental indicators are improved by the recycling which hence appears as the most efficient pathway to reduce the overall environmental impact of nuclear energy.

However, TTC is still not sufficient for the very long-term since it only allows consuming a few percent of the natural uranium resource. Protecting future generations rights require implementing a more efficient recycling to preserve uranium natural resource. Future nuclear fuel cycles will therefore have to better consume natural uranium likely by improving the actinides recycling, to still minimize the volume and toxicity of nuclear waste, to ensure their long-term confinement and to prevent any proliferation-risk. Such an evolution calls for implementing appropriate technologies such as fast neutrons reactors (FNR) to increase the ^{238}U conversion in fissile materials and the plutonium recurrent burning. It involves in a first step the Pu-

multi-recycling in FNR with the optimisation of the existing efficient Pu-partitioning processes. For the longer term, minor actinides recycling has to be optionally considered as a mean to decrease the waste burden towards future generations and improve the social acceptance: (i) Am-recycling would allow as a first option to decrease the waste heat-power, and therefore, to increase the repository density and the subsequent repository lifespan, (ii) Cm-recycling would allow as a second option to decrease the waste long-term toxicity down to a few centuries. Ultimate nuclear waste could hence be back within Human History by comparison to the initial hundreds of thousands of years of lifespan.

The stepwise implementation of this different processes defines a path towards nuclear energy with increasing sustainability that could significantly contribute to mitigate the global climate change. As a conclusion, this paper will demonstrate how nuclear energy sustainability can be improved in terms of environment preservation, economic efficiency and societal acceptance by implementing a more and more efficient actinides recycling. By such, Actinides recycling clearly appears to be the cornerstone of any future sustainable fuel cycle, and therefore a key issue for mitigating global climate change.

Sorption of Cs(I), Ra(II), Eu(III), Am(III), Pu(IV), Np(V), U(VI) and Se(-II) on the rocks of the exocontact zone of Nizhnekansky granitoid massif

Vladimir Petrov^a, Irina Vlasova^a, Natalia Kuzmenkova^{a,b}, Artem Kashtanov^a, Tatiana Kuchinskaya^a,
Vladislav Petrov^c, Valery Poluektov^c, Stepan Kalmykov^{a,d}, Jörg Hammer^d

^a*Department of Chemistry, Lomonosov MSU, Moscow, Russia*

^b*Vernadsky Institute of Geochemistry and Analytical Chemistry of Russian Academy of Sciences, Moscow, Russia*

^c*Institute of Geology of Ore Deposits, Petrography, Mineralogy and Geochemistry of RAS, Moscow, Russia*

^d*NRC "Kurchatov Institute", Moscow, Russia*

^e*BGR, Geozentrum Hannover, Hannover, Germany*

The deep geological disposal is the accepted in Russia principal concept of the high level wastes (HLW) final stage. Recently geological and geophysical researches have been performed in the area of the proposed future repository. The main suggested place is the "Eniseysky" area in the exocontact zone Nizhnekansky granitoid massif. Crystalline rocks will be the last geochemical barrier blocking the migration of radionuclides to biosphere in the case of the penetration of ground waters into the repository of high level waste. The backfilling of the canisters with the conditioned HLW by bentonites (Khakassiya) is accepted in Russia. Thus, determination of sorption properties of the host rocks in the presence of the simulated ground water, pre-equilibrated with bentonites, towards long-lived radionuclide is essential for safety assessment of future HLW repository.

In this study we have investigated time-dependence of the Cs(I), Ra(II), Eu(III), Am(III), Pu(IV), Np(V), U(VI) sorption onto five rock samples drilled in the exocontact zone of Nizhnekansky granitoid massif ("Eniseysky" area) in the range of depth 166 m – 477 m. Rock samples were used in two types of sorption experiments: set #1 – determination of distribution coefficients and time-dependencies of radionuclide sorption; set #2 – determination of spatial distribution of sorbed radionuclides depending on mineral composition, structure and/or degree of metasomatic and deformation transformations.

It was found that sorption of metal ions is fast, quantitative and almost independent on rock sample. It reaches 95% within 1 hour for americium and europium, 4 hours – for plutonium, neptunium and cesium. Sorption of selenium is negligible under experimental conditions. The obtained results demonstrate that sorption of metal ions is quantitative onto investigated rock samples from exocontact of Nizhnekansky massif.

According to the radiography data (Cyclone Phosphor Storage system, PerkinElmer, with Imaging Plates) extremely inhomogeneous distribution was established for all of the studied nuclides sorbed on the different types of the rocks of the exocontact zone. While quartz and unaltered feldspars (plagioclase and K-feldspar) show very low sorption activity towards to all radionuclides, the phases of preferential sorption of radionuclides differ significantly. SEM-EDX has indicated the best sorbents among mineral phases of Nizhnekansky massif exocontact zone rocks:

1. magnetite, titanomagnetite, ilmenite and apatite for Pu and Am;
2. biotite, monazite, magnetite for Np;
3. muscovite including sericite and biotite for Ra.

This work was supported by Russian Science Foundation (16-13-00049).

Sorption competition of trivalent metals on corundum ($\alpha\text{-Al}_2\text{O}_3$) studied on the macro- and microscopic scale

S. Virtanen¹, M. Eibl², S. Meriläinen¹, A. Rossberg², J. Lehto¹, T. Rabung³ and N. Huittinen²

1) Laboratory of Radiochemistry, Department of Chemistry, University of Helsinki, Finland

2) Helmholtz-Zentrum Dresden-Rossendorf, Institute of Resource Ecology, Dresden, Germany

3) Institute for Nuclear Waste Disposal, Karlsruhe Institute of Technology, Karlsruhe, Germany

Sorption of trivalent actinides and lanthanides onto the surface of geological materials relevant for nuclear waste disposal is a topic that has been widely studied in recent years. However, the sorption properties of metals are often investigated by studying the sorption behaviour of a single metal at a time. Thus, these experiments do not account for potential effects of sorption competition in the presence of multiple dissolved elements or compounds. Bradbury and Baeyens (2005) performed extensive investigations of the sorption competition between various metal cations on the clay mineral montmorillonite. By investigating the competition of metals with similar and dissimilar chemical behaviour (e.g. tendency to hydrolysis and valence state), the authors concluded that metal cations with dissimilar chemical properties do not affect the uptake of one another by the clay mineral, whereas metals with similar chemistries do. Thus, if the data obtained in single metal sorption experiments are used in the safety assessment of nuclear disposal, careful considerations of the chemical environment in the near- or far-field of nuclear waste repository is needed to avoid the possible overestimation of radionuclide sorption.

In this study, we have combined batch sorption and spectroscopic experiments that were performed with Eu(III), Cm(III) and Am(III) in the absence and presence of Y(III) as competing cation. The objective was to investigate how the sorption behaviour of trivalent actinides and lanthanides is affected by the presence of another trivalent metal. Following the findings of Bradbury and Baeyens (2005) our hypothesis is that the addition of higher concentrations of trivalent Y(III) together with a chemically similar trivalent metal, Eu(III), Cm(III) or Am(III), would affect the sorption behaviour of that metal.

Batch sorption experiments were performed with Eu(III) at different pH (pH-edges) and concentrations (isotherms). The competing metal Y(III) was added before Eu(III) to the mineral suspension in concentrations ranging from 1×10^{-6} M to 1×10^{-4} M. In the Eu(III) pH-edge experiments, the sorption of 1×10^{-5} M Eu(III) was investigated on 0.5 g/l corundum at varying pH, with and without Y(III). In the Eu(III) isotherm experiments, the initial Eu(III) concentration was varied between 1×10^{-9} M – 1×10^{-4} M and Y(III) was used in the competing isotherm samples at a constant pH of 7. Batch experiments showed (Figure 1) that the addition of Y(III) could strongly decrease the sorption of Eu(III) on a macroscopic scale by orders of magnitude (Figure 1, right). Additionally, spectroscopic methods were also employed as the main emphasis of this study was to elucidate the possible changes happening at the molecular level as a result of sorption competition. Time-resolved laser fluorescence spectroscopy (TRLFS) enables the investigations of Cm(III) sorption speciation directly on the mineral surface. We investigated the changes in the speciation of 1×10^{-7} M Cm(III) in 0.5 g/l corundum suspensions at varying pH under non-competing and competing conditions using 1×10^{-4} M Y(III). The results indicate changes in the Cm(III) species distribution, thus, confirming our findings in the batch sorption experiments showing that 1×10^{-4} M Y(III) suppresses Cm sorption complex formation on the mineral surface depending on the solution pH (Figure 2). Cm(III) luminescence spectra of only Cm(III) and of Cm(III) together with Y(III), show that the fraction of aqueous Cm species is substantially greater with high concentrations of Y(III) present. Only when the pH is increased above 7, a clear shift in the emission peak maximum is observed, indicating a change in Cm(III) speciation. X-ray absorption spectroscopy (XAS) was applied to identify the formed trivalent actinide sorption complexes. We investigated the sorption of 6×10^{-6} M or 2×10^{-5} M Am(III) on the corundum surface at pH 8.5 in the absence and presence of 2×10^{-5} or 2×10^{-4} M Y(III). The treatment of the XAS-data is still ongoing and results will be discussed more closely in the conference presentation.

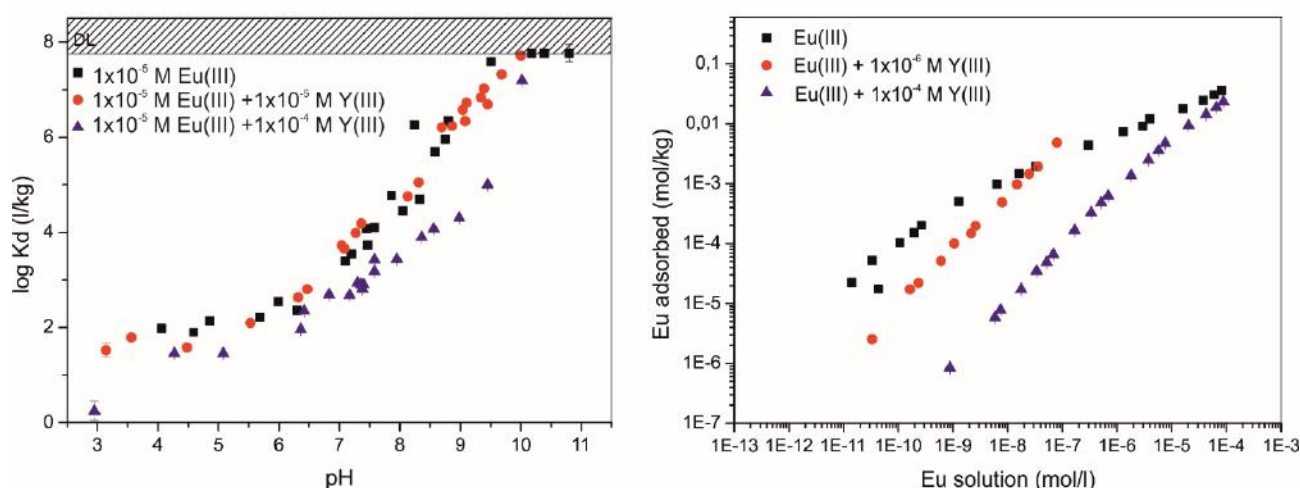


Figure 1. Left: Sorption of 1×10^{-5} M Eu(III) in the absence and presence of 1×10^{-5} M or 1×10^{-4} M Y(III) as a function of pH. Right: Eu(III) sorption isotherms at pH 7 with different initial Eu(III) concentrations and 1×10^{-6} or 1×10^{-4} mol/l Y(III). The corundum and electrolyte (NaClO_4) concentrations were kept constant at 0.5 g/l and 0.01 M, respectively.

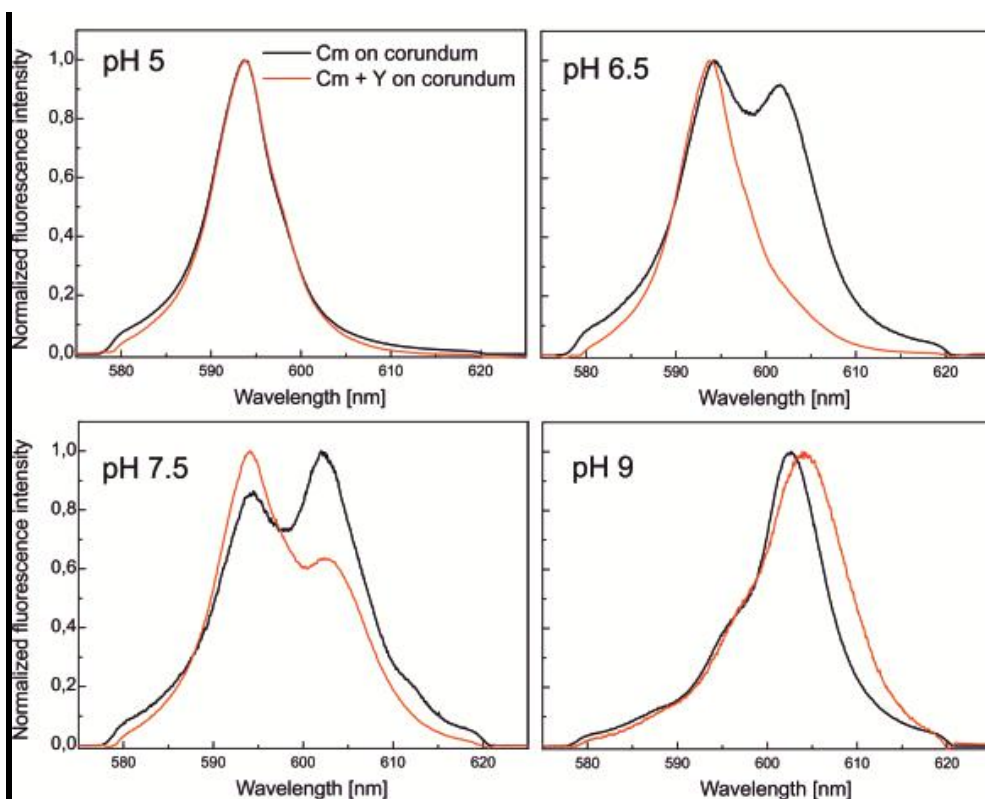


Figure 2. Comparison of 1×10^{-7} M Cm(III) luminescence emission spectra obtained with TRLFS for only Cm(III) on 0.5 g/l corundum (black lines) and for Cm(III) in the presence of 1×10^{-4} M Y(III) (red lines) at various pH between 5 to 9.

References

Bradbury M. H. and Baeyens B. (2005) Experimental measurements and modelling of sorption competition on montmorillonite. *Geochimica et Cosmochimica Acta*, 69, 4187-4197

Comparative study of 3-H, 36-Cl, Se, 99-Tc, and 125-I diffusion through Grimsel rock samples

Eva Hofmanová*, Kateřina Kolomá, Václava Havlová

ÚJV Řež, a. s., Fuel Cycle Chemistry Department, Hlavní 130, 250 68 Husinec-Řež, Czech Republic

*hofmanova. eva@gmail.com

Safety assessments mostly consider anion exclusion as a relevant process within the porous rock matrix which has to be taken into account (Jakob, 2004). Smaller diffusivities for anions as compared to neutral species (HTO) are attributed to electrostatic repulsion of anions from negatively charged mineral surfaces leading to reduced porosity being accessible for anions.

Several laboratory through-diffusion experiments with tritiated water, 36-chloride and selenate were already performed on samples from experimental and monitoring borehole of the Long Term Diffusion Phase III experiment in Grimsel Test Site. Despite the fact that chloride and selenate differ in charge, and thus larger exclusion effect might be expected for bivalent selenate (Van Loon et al., 2007), no significant difference in formation factors F_f of chloride and selenate was determined.

In order to shed more light on diffusion of anions in rock matrix, two experimental approaches might be used. The first one consists of performing diffusion experiments under different groundwater salinity. In low ionic strength waters the effects of anion exclusion are more pronounced than in highly saline waters (Jakob, 2004). Few data are available (e.g. Tachi et al., 2015; Li et al., 2012), not exhibiting significant dependencies on groundwater salinity. The second approach follows the hypotheses that either charge (Van Loon et al., 2007) or charge density (Jakob, 2004) influence the anion exclusion effect. For this study, the second approach was applied. Iodide and pertechnetate were chosen as another conservative tracers having comparable charge density but differing from the charge density of chloride and selenate.

The effective diffusion coefficients D_e were evaluated from the fitting of break-through curves using numerical modelling. Zero sorption on Aare granite under ambient conditions was assumed for studied species. The D_e values that are product of geometrical factor G , porosity ϵ and reference diffusivity D_w were in the sequence of $\text{HTO} > \text{I} > \text{Cl} \sim \text{Tc} > \text{Se}$. Porosities were calculated using following reference diffusivities $D_w \cdot 10^{-9} \text{ m}^2/\text{s}$ for tritiated water, chloride, selenate, iodide, and pertechnetate: 2.27 (Mills, 1973), 2.032, 2.016, 2.045 (Vanýsek, 2010), 1.95 (Sato et al., 1996), respectively; and geometrical factor defined based on HTO experiments $G = 0.621 \pm 0.080$. The values of effective porosity were approx. 1.9 times lower for monovalent tracers and approx. 3.4 times lower for selenate compared to total porosity of 0.24 %. It should be noted that such findings cannot be used for confirmation of anion exclusion effect because they are based on reference diffusivities at infinite dilution.

Therefore, several through-diffusion experiments on glass frits (WINZER, 23-013-41, S3) have been carried out in order to determine D_w for the same conditions as for the diffusion experiments on granite. Present results show that published selenate and pertechnetate reference diffusivities seem to be overestimated. Using D_w values obtained in synthetic Grimsel groundwater by own experiments, the formation factors F_f ($\epsilon \cdot G = D_e/D_w$) were calculated. No significant difference in $F_f(\text{anions})$ was found. On the other hand, $F_f(\text{anions})$ is 1.7 times lower than $F_f(\text{HTO})$ that cannot be explained yet.

Acknowledgments: This research was funded by SÚRAO.

References

Jakob, 2004. Nagra Technical Report 04-07.

Mills, 1973. *Journal of Physical Chemistry*, 77, 685-688.
Van Loon et al., 2007. *Applied Geochemistry*, 22, 2536-2552.
Tachi et al., 2015. *Journal of Contaminant Hydrology*, 179, 10-24.
Li et al., 2012. *Journal of Radioanalytical and Nuclear Chemistry*, 293, 751-756.
Sato et al., 1996. *Journal of Nuclear Science and Technology*, 33, 12, 950-955.
Tachi et al., 2015. *Journal of Contaminant Hydrology*, 179, 10-24.
Vanýsek, 2010. *CRC Handbook of Chemistry*, 90th edition.
Van Loon et al., 2007. *Applied Geochemistry*, 22, 2536-2552.

Selective complexation and separation of pentavalent and hexavalent actinides for nuclear processes

M. Nilsson*, C. G. Bustillos*, R. Copping#, C. Hawkins*, I. May#

**Department of Chemical Engineering and Materials Science, University of California Irvine, Irvine, CA 92697 #Chemistry Division, Los Alamos National Laboratory*

Increased knowledge of actinide coordination chemistry and the development of advanced actinide separation processes are essential to increase the utilization of the fuel and decrease the volume of waste from nuclear power production. Commercial separation techniques for nuclear fuel (i.e. PUREX) selectively remove U(VI) and Pu(IV) from the other components, while the minor actinides, e.g. Np and Am, are not extracted. However, these four mid-actinides (U, Np, Pu, Am) have accessible oxidation states (+V, +VI) at which they exist as linear dioxo actinyl ions $[\text{AnO}_2]^{n+}$. While the stability of these oxidation states can be a challenge for some of the transuranic actinides under acidic conditions, studies suggest that these oxidation states may be stabilized by coordination of ligands to the equatorial plane of the actinyl ion. For example, recent studies indicate that Schiff bases have been able to stabilize U(V). In light of this we are exploring both water soluble and organic phase soluble Schiff bases as actinyl-selective complexation reagents.

Our crystallography studies have shown that the Schiff-bases can complex uranyl, plutonyl and neptunyl in a 1:1 ligand:metal complex. Furthermore, our results of the extraction of Ln(III) and An(V/VI) cations from aqueous nitrate solutions containing the water-soluble Schiff base *N,N'*-bis(5-sulfonato-salicylidene)ethylenediamine ($\text{H}_2\text{salenSO}_3$) by bis(2-ethylhexyl)phosphoric acid in toluene suggest significant holdback of U(VI) and Np(V) and weak retention of Eu(III). The organic soluble Schiff-bases are able to selectively extract U(VI) from Ln(III) indicating that the ligand may be useful for group separation of mid actinides from trivalent lanthanides.

In this presentation, ongoing studies of these ligands in our laboratories as well as future directions will be presented and discussed.

The incorporation of uranium into Fe(II)/Fe(III) (oxyhydr)oxide phases

H. E. Roberts,¹ K. Morris,¹ G. T. W. Law,² P. Bots,¹ J. F. W. Mosselmans,³ and S. Shaw^{1*}

¹*School of Earth, Atmospheric and Environmental Sciences, Univ. of Manchester, M13 9PL, UK.*

²*School of Chemistry, Univ. of Manchester, M13 9PL, UK.*

³*Diamond Light Source Ltd, Didcot, OX11 0DE, UK.*

sam.shaw@manchester.ac.uk

The current policy for the disposal of higher activity radioactive wastes in the UK is within a deep geological disposal facility (GDF). Here, within the engineered environment and over long timescales, the anaerobic corrosion of steel from storage canisters and engineering structures within a GDF will lead to the formation of a number of solid phases, including magnetite ($\text{Fe}^{\text{II}}\text{Fe}^{\text{III}}_2\text{O}_4$) and green rust ($\text{Fe}^{\text{II}}_3\text{Fe}^{\text{III}}(\text{OH})_8\text{Cl}\cdot n\text{H}_2\text{O}$). U(VI) adsorption and reduction to U(IV) can occur on the mineral surfaces limiting its environmental mobility.^{1,2} However, it is also clear that adsorbed U(IV) surface species can be easily remobilised through oxidation. Recently, incorporation of U into iron (oxyhydr)oxide structures has been proposed as a pathway to irreversibly bind U in the mineral structure.^{3,4} Despite the strong potential benefit of limiting U mobility in the environment through incorporation, the mechanism(s) of uranium incorporation into key Fe(II)/Fe(III) (oxyhydr)oxide phases such as magnetite and green rust are poorly understood.

In this study, magnetite and green rust were synthesized at a range of starting Fe(II):Fe(III) ratios (0.5–2.0) via a direct co-precipitation method in the presence of U(VI). X-ray diffraction analysis showed the reaction products consist of magnetite (Fe(II):Fe(III) = 0.5 and 0.6) and green rust (Fe(II):Fe(III) = 0.8 and 2.0). EXAFS spectroscopy confirmed that U was present as a mixture of U(IV)O₂ and uranium directly substituted for octahedrally coordinated U in the magnetite structure with XANES spectroscopy suggesting that incorporated U may be present as U(V). For green rust, U(VI) was also reduced to both U(IV)O₂ and as U incorporated within the Fe(II)/Fe(III) octahedral sites of the layer double hydroxide structure. Again, XANES analysis suggested this incorporated U was present as U(V) in the green rust structure. Acid dissolution experiments provided additional evidence that significant incorporation of U into the iron (oxyhydr)oxide phases was occurring.

Overall, these results confirm that U can be directly incorporated in the structures of both magnetite and green rust, which may offer a significant new pathway for U immobilisation in contaminated land and geological disposal systems.

References

- (1) Latta, D. E.; Gorski, C. A.; Boyanov, M. I.; O’Loughlin, E. J.; Kemner, K. M.; Scherer, M. M. Influence of Magnetite Stoichiometry on U VI Reduction. *Environ. Sci. Technol.* **2012**, *46*, 778–786.
- (2) Latta, D. E.; Mishra, B.; Cook, R. E.; Kemner, K. M.; Boyanov, M. I. Stable U(IV) complexes form at high-affinity mineral surface sites. *Environ. Sci. Technol.* **2014**.
- (3) Marshall, T. A.; Morris, K.; Law, G. T. W.; Livens, F. R.; Mosselmans, J. F. W.; Bots, P.; Shaw, S. Incorporation of uranium into hematite during crystallization from ferrihydrite. *Environ. Sci. Technol.* **2014**.
- (4) Kerisit, S.; Felmy, A. R.; Ilton, E. S. Atomistic simulations of uranium incorporation into iron (hydr)oxides. *Environ. Sci. Technol.* **2011**, *45* (7), 2770–2776.

THURSDAY 1ST SEPTEMBER
ENVIRONMENTAL RADIOACTIVITY III

The characterisation, treatment and disposal of Naturally Occurring Radioactive Material (NORM)

David Read

*Chemistry Department, University of Surrey, Guildford, GU2 7XH, UK
National Physical Laboratory, Hampton Road, Teddington, Middlesex, TW11 0LW, UK*

The exploitation of natural resources is often associated with enhanced levels of radioactivity owing to the large volumes of material processed by modern plants and the propensity of uranium and thorium progeny to concentrate in mineral phases. The term used to describe these deposits, 'Naturally Occurring Radioactive Material' (NORM), is misleading; the isotopes themselves are members of the natural series decay chains but their activity concentrations and relative abundance are entirely due to industrial processing. The presence of NORM has been recognised in many sectors, including oil and gas extraction; water treatment; the recovery of metalliferous ores; production of steel and cement; processing of phosphorites and China Clay and in the burning of fossil fuels. Scales affecting production equipment can contain activity levels in excess of 10 GBq/tonne. The majority are less active but still require careful handling and disposal to limit exposures. Recent revision of the Basic Safety Standards (BSS) Directive has led to a clearer definition of NORM and a more comprehensive framework for treating wastes that are both radioactive and hazardous.

The solid residues removed from contaminated equipment within the oil & gas sector, fall into two main categories, mineral and metallic (Figure 1). In mineral scales, of which the most common is barite-celestite (Ba-SrSO_4), radium isotopes dominate; the relative proportion of ^{226}Ra and ^{228}Ra depending on the source rocks. The second category comprises deposits of metallic lead, often of high purity in which ^{210}Pb occurs by isotopic substitution. The lead may be oxidised to litharge (PbO), reduced to galena (PbS) or altered by reaction with circulating fluids to form, for example, hydroxy-carbonates such as hydrocerussite ($\text{Pb}_3(\text{CO}_3)_2(\text{OH})_2$). Arsenic may be present at levels ≥ 10 wt% and several toxic heavy metals, including mercury, are also common. An unusual lead-mercury amalgam (PbHg_2) containing several kBq g^{-1} ^{210}Pb and ^{210}Po has been recorded from natural gas wells in northern Germany.



Figure 1 Mineral scale, mainly barite (left) and metallic lead (right) on oil tubulars

Almost all metal smelting and refinement processes have the potential to generate NORM, including iron and base metal production. However, the issue is most acute with rare earth, titanium and zirconium ores owing to the naturally high uranium and thorium contents in the source materials. Monazite may contain 15% thorium and was exploited for this metal before the rare earth elements themselves became such a valuable resource. The more soluble bastnäsite, which is the main commercial ore today, also contains substantial amounts of uranium and thorium. Concentrations are lower in the case of rutile and ilmenite (titanium) or zircon, but significant enrichment occurs in process residues. Again, barite is an important phase, often containing $>1 \text{ kBq g}^{-1}$ radium isotopes and, in extreme situations, $>100 \text{ kBq g}^{-1}$. Two key industries in non-metalliferous mineral ore processing are production of phosphate fertilisers and China Clay. A typical 1,000t/day phosphate plant can generate $>200,000\text{t}$ phosphogypsum per annum. These deposits are enriched in radium isotopes whereas uranium itself is found in phosphates, including final products and fluorides.

The legislation sets activity thresholds for notification, exemption and disposal of NORM residues. Ideally, the residues are recycled or re-used; for example contaminated slurry may be re-injected into an oil well or fine blast furnace dusts captured by electrostatic precipitators and added to new feedstock. Where they cannot be recycled as part of the extraction process, solid residues containing lower activity concentrations, typically $<5 \text{ Bq g}^{-1}$, are usually consigned to landfill. However, NORM scales derived from exploitation of mineral deposits can contain much higher levels of radium and its progeny. In such cases, cementation is used for stabilisation of solid wastes, subject to testing to ensure compliance with the relevant limits. Although most attention to date has been focussed on solid residues, NORM can also occur in liquid (e.g. 'flowback') or gaseous form.

Analytical requirements for NORM are demanding. The principal determinands for solid wastes comprise uranium and thorium, their progeny isotopes and hazardous waste acceptance criteria (HazWAC) analysis. With fixed laboratories, uranium and thorium are conventionally determined by ICP-MS. High resolution gamma and alpha spectrometry are then used for shorter-lived progeny and most modern facilities offer the complementary methods (GC-MS etc.) needed for HazWAC. As one would expect, regulated NORM industries are required to comply with very stringent limits when discharging to water courses; in the United Kingdom, the limit for ^{226}Ra is 10 mBq dm^{-3} . However, ^{226}Ra is present naturally in all groundwaters and such a low regulatory target presents a serious challenge when attempting to differentiate natural background from industrial contamination. Currently, only alpha spectrometry offers the required sensitivity and speed for routine analysis, albeit after laborious separation. Recent developments suggest ICP-MS in conjunction with rapid pre-concentration has the potential to rival the sensitivity of radiometric techniques, whilst offering a significant reduction in preparation time.

Controlled co-precipitation of radium with barite may be employed for both sensitive analysis of radium isotopes and decontamination of flowback waters from hydraulic fracturing ('fracking'). The two applications differ in that the first requires deposition of a uniform layer, which should be as thin as practicable, whereas the latter focusses on optimising radium removal from highly saline fluids without concomitant removal of potentially interfering ions (Figure 2).

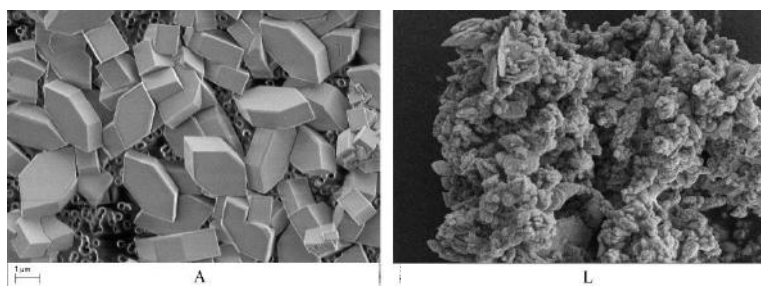


Figure 2 Induced barite precipitation from brackish (left) and saline solutions (right)

This paper summarises the isotopic composition of deposits from a number of NORM industries to illustrate how chemical fractionation of radioactive progeny ($^{226/228}\text{Ra}$, ^{210}Pb and ^{210}Po) arises from industrial processing and the methods used to manage the wastes produced.

The uptake of Se by two strains of *Pseudomonas* sp. isolated from a nutrient-poor boreal bog

M. Lusa⁽¹⁾, J. Knuutinen⁽¹⁾, J. Lehto⁽¹⁾, M. Bomberg⁽²⁾

⁽¹⁾ Laboratory of Radiochemistry, P.O. Box 55, 00014 University of Helsinki, Finland

⁽²⁾ VTT Technical Research Centre of Finland, P.O. Box 1000, 02044 VTT, Finland

⁷⁹Se is one of the high priority radionuclides in the dose calculations for long-term biosphere safety assessment of spent nuclear fuel [1] and therefore knowledge about its behavior and fate in the boreal ecosystems, including nutrient-poor bog environments, is important. In this study, the uptake of selenium (as selenite SeO_3^{2-} and selenate SeO_4^{3-}) by two *Pseudomonas* sp. strains PS-0-L and T5-6-I, previously isolated from a boreal, ombrotrophic bog [2] was examined using batch experiments with $^{75}\text{SeO}_3^{2-}$, transmission electron microscopy (TEM) and energy-dispersive X-ray spectroscopy (EDX).

Although, the reduction of both SeO_3^{2-} and SeO_4^{3-} have been shown to be an environmentally significant process, only a few SeO_3^{2-} respiring bacteria have been isolated. Previously, we found that the two *Pseudomonas* strains examined in this study were able to remove $^{75}\text{SeO}_3^{2-}$ from 1 % Tryptone and 1% Yeast extract broths, with maximum uptake of 6800 L/kg DW for PS-0-L in 1 % Tryptone and of 2200 L/kg DW for T5-6-I in 1 % Yeast extract [3]. There are various hypotheses about the uptake mechanisms of SeO_3^{2-} found in different bacteria, including transport via sulphate ABC transporter complex and reduced selenium (Se^0) formed in the periplasmic compartment as well as use of various enzymes, such as the sulphite reductase and OYE enzyme ("Old Yellow Enzyme", NADPH oxidoreductase [eg. 4]. It is, however, likely that also alternative still unidentified carriers exist, as for example the repression of the sulphate ABC transporter does not completely inhibit SeO_3^{2-} uptake [4]. Therefore, we tested the effect of both glucose (in 0.5% peptone + 0.25% yeast extract) and cysteine (100 μM – 5000 μM in 1 % Tryptone) on the SeO_3^{2-} uptake. The addition of 0.1 % glucose substantially increased the SeO_3^{2-} uptake in both *Pseudomonas* strains; the uptake was 2-fold in PS-0-L and 7-fold in T5-6-I after glucose addition at + 20°C (Fig. 1A). However, as we decreased the incubation temperature to + 4 °C, a slight decrease of 4 % was observed in the SeO_3^{2-} uptake by PS-0-L after glucose addition. The stimulatory effect of glucose on SeO_3^{2-} accumulation indicates active transport by the cells. However, as both bacteria were able to accumulate SeO_3^{2-} also in the absence of glucose, passive (energy-independent) mechanisms (sorption on cell walls, diffusion into the cell) for SeO_3^{2-} uptake should also be considered. If SeO_3^{2-} enters the cells by an active mechanism, it should be affected by various inhibitors. The sulphur-containing amino acid L-cysteine was used to inhibit the SeO_3^{2-} uptake and its addition reduced SeO_3^{2-} uptake in both studied bacteria (Fig. 1B). This observation is similar to the results obtained with the yeast *Saccharomyces cerevisiae*, in which the addition of 100 μM cysteine inhibited active transport of SeO_3^{2-} [5]. The biosynthesis of selenoamino acids by microorganisms has been reported in many cases [eg. 6]. The inhibitory effect of cysteine addition in our study indicates that SeO_3^{2-} uptake is regulated by cellular products formed in the sulphur metabolism.

Both intra- and extracellular reduced Se^0 has been found in phylogenetically and physiologically distinct bacteria [eg. 7], but the generation of intra- and extracellular Se^0 granules is still partly unknown, especially concerning the secretion of Se^0 granules from the cell. In our study, in the cultures containing SeO_3^{2-} and SeO_4^{3-} , formation of brick-red reduced Se^0 was observed, although it was more visible in the case of SeO_3^{2-} (Fig. 2B). In the TEM images, clearly visible intracellular Se^0 granules verified by EDX were found both in *Pseudomonas* PS-0-L and T5-6-I after growing in SeO_3^{2-} -containing media (Fig. 3). Furthermore, in cultures grown with SeO_4^{3-} the number of dividing cells compared to the cultures with no SeO_4^{3-} present, was clearly decreased. As the SeO_3^{2-} carrier concentration in the nutrient broth was increased from 10^{-8} M to 10^{-3} M (Fig. 2A), the uptake of $^{75}\text{SeO}_3^{2-}$ was reduced in the batch experiments and a vast majority of the cells were found lysed in the corresponding TEM images. The number of lysed cells increased with higher SeO_4^{3-} concentrations. It therefore seems that in the bacteria examined in this study, the increase in SeO_3^{2-} concentration results in toxic effects which eventually prevent further SeO_3^{2-} accumulation. This could be caused by continuous accumulation of reduced Se^0 inside the cells to a certain point, which after the cells lyse and Se^0 is released from the cells. However, until now we have been unable to detect extracellular Se^0 in the cultures of lysed cells using TEM to prove this hypothesis.

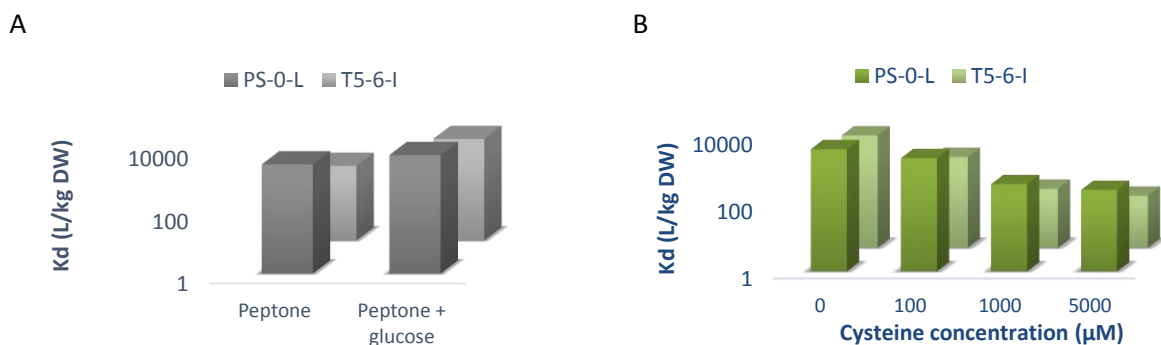


Figure1. The uptake of SeO_3^{2-} (as K_d) after 7 days at $+20^\circ\text{C}$ in *Pseudomonas* PS-0-L and T5-6-I with and without glucose addition to the 0.5 % Peptone broth (A) and after addition of 0 μM – 5000 μM of cysteine to the 1 % Tryptone broth (B).

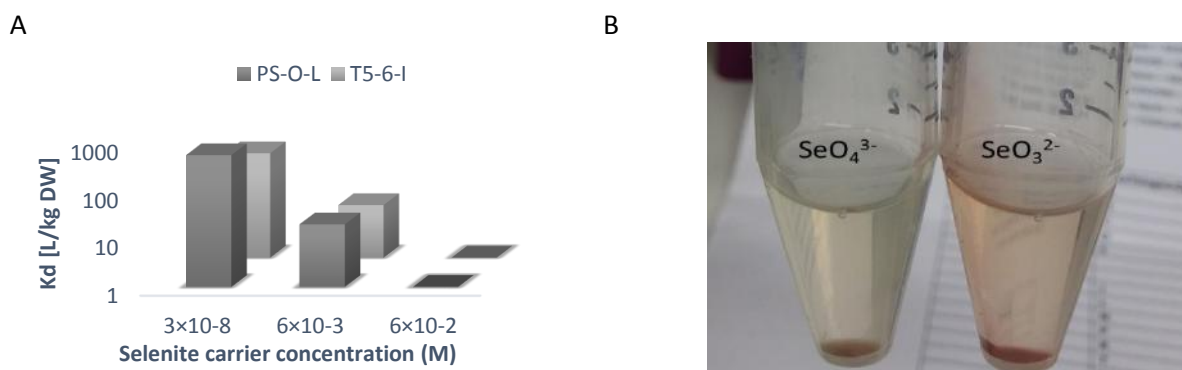


Figure 2. $^{75}\text{SeO}_3^{2-}$ uptake after 1-day incubation by *Pseudomonas* PS-0-L and T5-6-I in different carrier concentrations of SeO_3^{2-} in 1 % Tryptone (A). SeO_4^{3-} and SeO_3^{2-} broths after incubation with *Pseudomonas* T5-6-I.

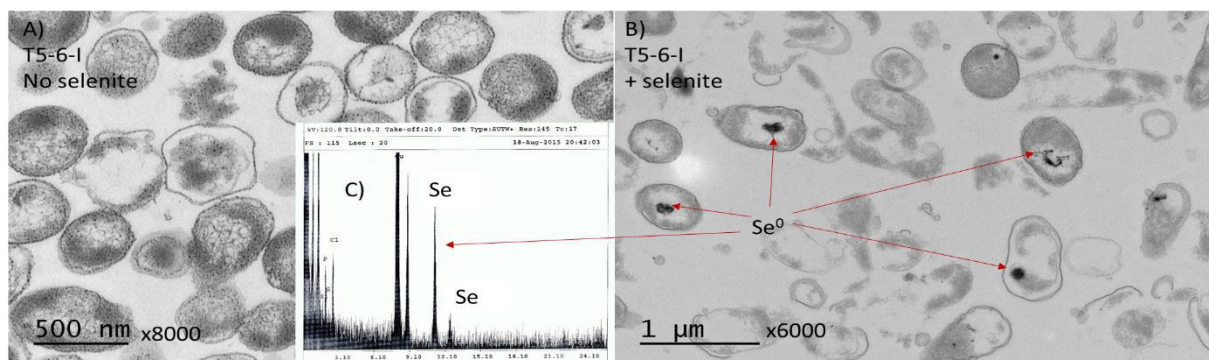


Figure 3. TEM figures of *Pseudomonas* T5-6-I without SeO_3^{2-} (A) and with SeO_3^{2-} (B) and EDX spectrum of selenium, found in *Pseudomonas* T5-6-I incubated with SeO_3^{2-} (C).

[1] Helin J et al. (2010). Working Report 2010-37, Posiva Oy, Eurajoki, Finland. [2] Lusa M et al. (2016). J Environ Sci, <http://dx.doi.org/10.1016/j.jes.2015.08.026>. [3] Lusa M et al. (2015). J Environ Radioactiv 147, 85-96. [4] Turner RJ et al. (2008). Biometals 11, 223-227. [5] Charieb MM and Gadd GM (2004). Mycol Res 108(12), 1415-1422.[6] Stadtman TC (1991). J Biol Chem 266, 16257–16260. [7] Nelson DC et al. (1996). Geochim cosmochim Acta 60(18), 3531-3539.

**Organically Bound Tritium (OBT) activity determination in environmental samples.
How monitoring labs are dealing with it? Feedback of the international OBT working group.**

N. Baglan⁽¹⁾, S. B. Kim⁽²⁾, C. Cossonnet⁽³⁾, I. W. Croudace⁽⁴⁾

¹ CEA/DAM/DIF – F91297 Arpajon - France.

² AECL, Chalk River Laboratories, Chalk River, Ontario, Canada, K0J 1J0.

³ IRSN/PRP-ENV/STEME/LMRE, Bât 501 - Bois des Rames, 91400 Orsay, France.

⁴ GAU-Radioanalytical, University of Southampton, NOC, European Way, SO14 3ZH, UK.

Work to promote the use of validated procedures for tritium fraction determination, including OBT, is ongoing in several countries. However, for almost all inter comparison exercise organisers it is difficult to provide the samples to the participants and to realise the statistical treatment of the results on a yearly basis. Therefore, to overcome these limitations and to improve OBT analytical skills, an international task group devoted to the improvement of OBT analytical procedures was created. The main goal of the OBT working group is to allow each participating country involved in OBT analysis to improve its analytical skills through interlaboratory exercises, as well as scientific and technical discussions.

In the framework of the OBT working group actions, an intercomparison on wheat was prepared. As an ISO Standard (ISO 13528) that discusses the calculation of the consensus value is available, it was used to handle the results obtained from this exercise. It was first used to check the homogeneity of the distributed sample and secondly to determine the consensus value (robust method).

Sample preparation, dispatching and homogeneity testing are briefly described first. Then the characteristics of the exercise are shortly defined; (number of participants, number of countries involved in the exercise, amount of sample, fresh to dry mass ratio). The results were obtained both in Bq.L⁻¹ of combustion water and Bq.kg⁻¹ of dehydrated material were separately taking into account predominant parameters such as combustion procedure, analytical device, amount of sample used to assess OBT activity concentration. In addition, the importance of the hydrogen percentage (mass) value, which is used to convert the activity concentration in combustion water to the one for dehydrated material, is also discussed.

The results obtained by all the labs look rather good for an OBT activity concentration below 100 Bq.L⁻¹ of water combustion, which indicates that with time tritium analysis skills for non-aqueous environmental matrices are improving.

Challenges with naturally occurring radioactive material (NORM) in road- and tunnel construction

Lindis Skipperud

Center for Environmental Radioactivity, Norwegian University of Life Sciences, 1432 Ås, Norway

In 2000 a group of scientists determined that the spread of the natural radioactive substances in Europe contributes to higher radiation dose to humans and the environment compared to the emission of radioactive substances from nuclear industry ¹. All organisms are inevitably exposed to radionuclides that are naturally present in the environment. Primordial radionuclides such as ²³⁸U, ²³⁵U and ²³²Th have been present in rocks and minerals of the earth's crust since its formation. Various anthropogenic activities such as mining, oil and gas production, phosphate industry, etc. use or disturb ores that contain naturally occurring radionuclides (NOR) resulting in elevated levels of NOR in certain (by)products and wastes. Besides enhanced NOR levels, these wastes are complex mixtures of different chemical compounds, minerals and elements, including heavy metals.

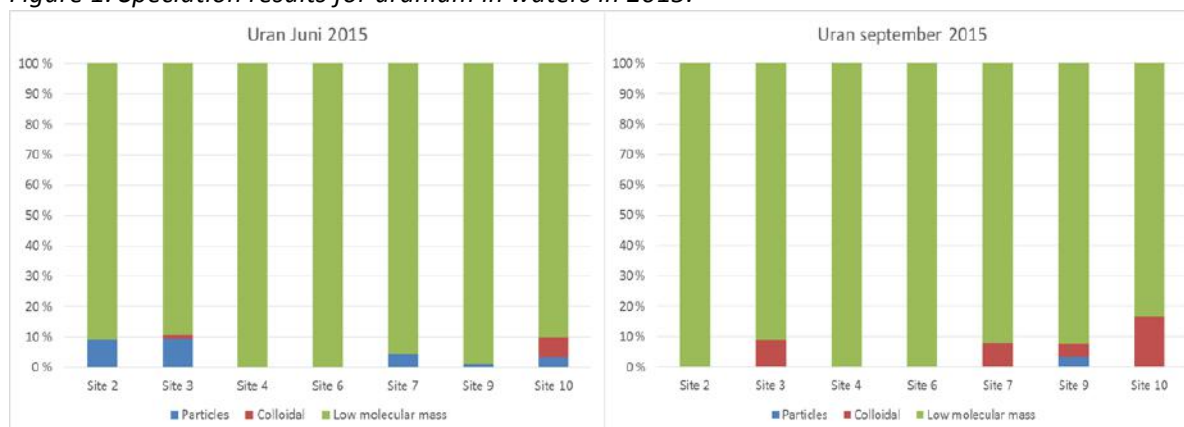
In 2011, the Norwegian Pollution Control Act was amended to include naturally occurring radioactive materials as contaminants, in addition to trace metals and organic compounds ². This amendment implicated that radioactive waste regulations were no longer exclusive to the nuclear industry, but also applied natural radioactive material derived from non-nuclear industries. Naturally occurring radioactive materials can be defined as those materials where human activities have increased the potential for exposure in comparison with the unaltered situation. Concentrations of radionuclides may or may not have been increased.

CERAD/NMBU have been focusing on alum shale leaching from the road- and tunnel construction site in the Gran municipality on Highway Rv4 in Norway as a case for NOR contamination to the environment. The bedrock is rich in U-bearing minerals, giving a high potential for environmental contamination. Through industrial processes involving U-bearing minerals such as alum shale minerals, i.e. road and tunnel construction, it is produced large quantities of waste that may contain a variety of contaminants such as radioactivity and metals. Impact assessment of multiple stressors has been highlighted as one of the major challenges by national and international research and regulatory communities. To assess the effects, consequences and risks to the environment associated with the intervention in alum shale and evaluate relevant measures for the protection of environment, it is important to include both radionuclides and metals in the survey program and researching the effects and assess pollutants overall.

Fieldworks in the area and variety of laboratory experiments have been performed in later years. Industrial processes and storage of alum shale waste could change the chemical and physical properties of radionuclides and metals, compared with its original state form. Weathering processes contributes to environmental pollutants transferred from the solid phase into soluble compound, being more mobile in the environment and can also be more bioavailable to the organisms in the environment and also for man. Runoff of radium, uranium and arsenic from landfill is observed, even at high pH³. When rock is supplied with air / oxygen oxidizes sulphide to sulphate, and upon contact with water forms sulfuric acid. The runoff from weathered alum shale may be very acidic, and the pH of the runoff from pure sulphide rock is estimated to be down to 2 pH down to 4 is measured in runoff from deposited alum-containing masses. Such low pH values is in itself harmful to fish and other aquatic organisms. Alum also contains a number of toxic metals, primarily cadmium, copper, nickel and zinc. Radionuclides and metals in such concentrations are very harmful to aquatic and soil organisms.

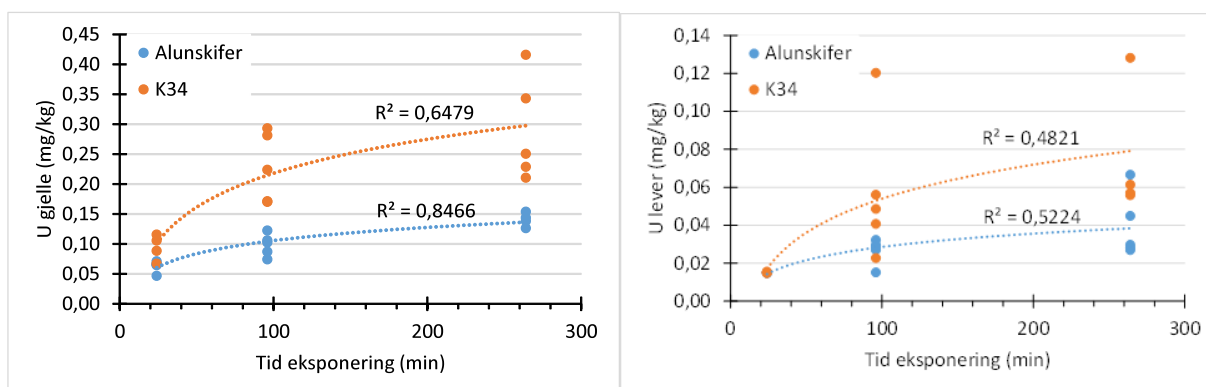
Concentrations of U and other metals are varying but higher than average due to the presence of alum shale in the area. In some waters the concentrations exceeded the WHO's uranium drinking water guideline set for 30 µg/L ⁴, and drinking water limits are often too high to provide sufficient protection of aquatic organisms. Fractionation of the waters showed that uranium is present in the waters as low molecular forms (fig 1), making uranium rather mobile and with high potential bioavailability.

Figure 1. Speciation results for uranium in waters in 2015.



Leaching experiments of U, Al, Cd, Cu, Mn, Mo and Ni and other metals in water in contact with different types of alum shale and lime stone have been done. Uranium concentrations in the leachate water after 7 week of the experiment varied from 17 to 602 $\mu\text{g/L}$, due to the different types of minerals, and the leaching of uranium and metals were still increasing, still not reaching steady state. Further, these elements, U and other metals, is possibly taken up in organisms. Concentration ratios (CR) for some elements in fish studied in field are showing varying values according to fish organs. Experimental uptake studies shows that fish exposed to alum shale leachate water take up rather much uranium over time (fig 2).

Figure 2. Uptake of uranium in fish gills and liver over time.



The studies shows that leaching from U-bearing minerals is of importance for all types of industry (construction, mining), and there is a demand for specially designed waste rock deposits or other countermeasures to hold back possible leaching to aquatic environments.

1. Marina, II *MARINA II: Update of the MARINA project on the radiological exposure of the European community from radioactivity in Northe European marine waters*; 132; European Commision: Luxembourg, 2002.
2. LOVDATA, Forskrift om begrensning av forurensning (forurensningsforskriften). In 9, miljødepartementet, K.-o., Ed. LOVDATA: Oslo, Norway, 2004; Vol. FOR-2004-06-01-931.
3. Skipperud, L.; Strømman, G.; Yunusov, M.; Stegnar, P.; Uralbekov, B.; Tillboev, H.; Zjazjev, G.; Heier, L. S.; Rosseland, B. O.; Salbu, B., Environmental Impact Assessment of radionuclide and metal contamination at the former U sites Taboshar and Digmai, Tajikistan. *Journal of Environmental Radioactivity* **2012**, *In Press*.
4. WHO, *Guidelines for Drinking-water Quality, 4th edition*. World Health Organization: 2011.

RADIOANALYTICAL CHEMISTRY II

In-beam activation analysis at MLZ Garching

Zsolt Revay, Petra Kudejová, Krzysztof Kleszcz, Christian Stieghorst

Technische Universität München, Heinz Maier-Leibnitz Zentrum, 85747 Garching, Germany

Both Prompt Gamma Activation Analysis (PGAA) and Neutron Activation Analysis (NAA) are based on radiative neutron capture, or the (n,g) reaction. While in PGAA, we count the gamma photons emitted during the neutron irradiation, in NAA the rest activity of the sample is counted. Both of them are characteristic, i.e. they provide analytical information on the constituents and their quantities. It has always been a desire to combine the two methods to take an advantage of both. However, the implementation is not so obvious.

Almost all nuclides emit prompt gamma radiation, while delayed radiation from activated isotopes is emitted by the elements practically from the fourth period of the Periodic Table. That is why the total intensity of the emitted gamma radiation is much higher in the prompt case, than when counting the delayed gammas. The difference can be as high as 3-4 orders of magnitude.

Normally, NAA is performed in high-flux neutron fields, typically in an irradiation channel of a nuclear reactor, where the flux of the thermal neutrons is at least $10^{12} \text{ cm}^{-2} \text{ s}^{-1}$. Then the samples up to about a gram can be counted using a regular high-purity germanium (HPGe) detector using typically 5–20 cm as sample-to-detector distances at different times after the irradiation to determine nuclides with all possible half-lives from minutes to years. Because most light elements are not detectable with NAA, it is mainly suitable for the determination of trace elements.

PGAA is best performed in cold (or thermal) neutron beams at large neutron sources, and the beam flux is typically around $10^8 \text{ cm}^{-2} \text{ s}^{-1}$. Due to the double shielding against neutrons and gamma photons, the sample-to-detector distances are typically larger, 20–40 cm for these beam facilities. Thus, the count rates would be comparable to those in the previous case. PGAA is mainly used for the determination of the major and minor components, while just a few trace elements can be detected thanks to their high cross sections, like B, Cd, and certain rare earths. Using Compton suppression is essential in PGAA to reduce the intensity of the spectral background. The most sensitive detection systems are equipped with a bismuth germanate (BGO) scintillator annulus to detect the scattered gamma photons, and thus it lowers the baseline with 90–95% below the characteristic peaks, significantly improving their detection limits.

Both methods can be performed at MLZ [1]. However, the combination of the two is also possible now using the world's strongest neutron beam with the thermal equivalent neutron flux of $6 \times 10^{10} \text{ cm}^{-2} \text{ s}^{-1}$ for the analysis of a large set of chemical elements. The problem, as can be seen above, is that the gamma emission during the irradiation is orders of magnitude more intense than can be properly counted, while it may be still relatively weak when counting the delayed activity.

The latest methodological developments at MLZ, however, offer a solution for this problem. The irradiation facility is equipped with a flexible shielding that can be quickly rearranged for the actual experiment: making a PGAA measurement with reduced detector efficiency: i.e. using a large sample-to-detector distance and a narrow collimation during the irradiation. Then right after the irradiation, the short-lived nuclides can be counted using a smaller distance and thus higher efficiency. Finally the medium- and long-lived nuclides can be counted in the low-background counting chamber next to the beam facility.

The low-background counting facility at MLZ is now also equipped with Compton suppression. The NaI scintillator annulus serves as an active shielding against the cosmic muons and the gamma radiation from natural radioactive nuclides found in the surrounding materials. Together with the passive shielding made of lead, the count rate is less than 0.5 cps in the background spectrum. The reduced baseline enables the counting of low-activity nuclides with significantly better detection limits.

In-beam activation analysis as the combination of PGAA and NAA proved to be a useful analytical tool in the determination of samples where the matrix components, and also the trace element content are interesting. The methodological developments and several applications of the in-beam activation analysis will be presented in the talk.

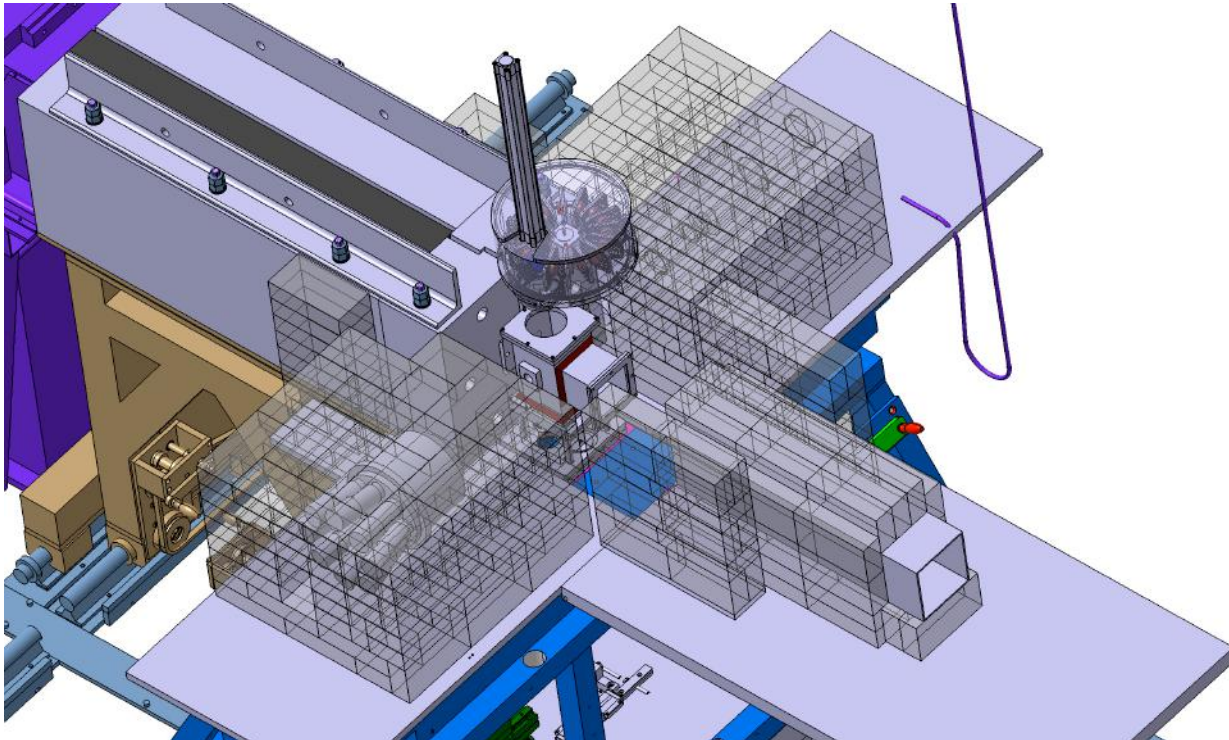


Figure 1. The in-beam activation analysis facility with the sample changer, and the shielded Compton-suppressed detector system. (Stefan Thiel, Institute for Nuclear Physics, University Cologne)

[1] Revay, Z ; Kudejova, P; Kleszcz, K; Sollradl, S; Genreith, C: In-beam activation analysis facility at MLZ, Garching, Nucl Instrum and Meth A799 (2015) 114-123.

Ultra-low level determination of actinides in large-volume urine samples using compact accelerator mass spectrometry

Xiongxin Dai^{1,2}, Marcus Christl³, Sheila Kramer-Tremblay², Hans-Arno Synal³

¹ *China Institute for Radiation Protection, Taiyuan, China*

² *Canadian Nuclear Laboratories, Chalk River, Ontario K0J 1J0, Canada*

³ *Laboratory of Ion Beam Physics, ETH Zurich, 8093 Zurich, Switzerland*

Internal exposure of nuclear workers to actinides could occur during decommissioning activities of nuclear facilities, refurbishment of ageing reactors, handling of spent nuclear fuel, and reprocessing of radioactive wastes. Highly radiotoxic alpha emitting actinides, such as ^{239/240}Pu, ²³⁷Np, ²⁴¹Am and ²⁴⁴Cm, are likely to be the major contributors of the internal dose, as these nuclides are present in significant amounts in spent fuels. Urinalysis is the most commonly used *in vitro* bioassay method for internal dose assessment of actinide exposure. However, this often requires extremely sensitive analytical techniques to detect actinides at low femtogram levels or even less in large-volume urine samples to meet the stringent regulatory requirements for radiation protection.

Due to its high rejection of molecular isobaric interferences and low susceptibility to matrix effects, accelerator mass spectrometry (AMS) is an extremely sensitive and robust technique for the analysis of intermediate- and long-lived radionuclides, which allows for simplification of the sample preparation chemistry with a good potential for high sample analysis throughput. Although AMS has been applied for the precise and accurate determination of Pu at fg-levels in urine bioassay samples for some years, the use of this technique for routine measurements has been limited by lack of availability and high operational costs of the complicated AMS system. In our recent studies, with newly developed actinide urine bioassay procedures and improved AMS target preparation method, the applicability of a compact AMS system at the Swiss Federal Institute of Technology (ETH) has been demonstrated for the determination of actinides (including Pu, Np, Am, Cm and Cf isotopes) at atto- to femtogram per litre levels in urine samples. This compact system, running at ~300kV terminal voltage with a much smaller footprint and low maintenance needs, provides a very competitive and cost effective alternative to conventional mass spectrometers. Details of these actinide bioassay methods, along with the results for method validation, will be presented.

Resonant Laser-SNMS on actinides for spatially resolved ultra-trace analysis

Clemens Walther¹, Hauke Bosco¹, Michael Franzmann^{1,2}, Linda Hamann¹, Mohammad Tanha¹, Klaus Wendt²

¹IRS - Institute for Radioecology and Radiation Protection, Leibniz-Universität Hannover,
Herrenhäuser Straße 2, D-30419 Hannover, Germany

²Institute of Physics, Johannes Gutenberg-Universität Mainz, Staudingerweg 7, D-55128 Mainz, Germany

The transport mechanisms and geochemical behavior of actinides in natural systems is of major importance to evaluate their distribution in geological formations at contaminated areas and storage sites. The composition analysis and spatial imaging of hot particles, sorption on mineral surfaces and migration of trace concentrations of radionuclides requires an excellent suppression of organic background and isobaric contamination in combination with high spatial resolution while maintaining the natural structure of the sample.

The new resonant Laser-SNMS system at the IRS Hannover was developed to cover those specifications by combining the high element selectivity of resonance ionization with the non-destructive analysis of a static TOF-SIMS with spatial resolution down to 70 nm. This system was planned based on a test installation at the nuclear chemistry department of the University Mainz [1]. After the setup of a Ti:Sa laser system and the adaption of an IONTOF TOF.SIMS 5 for laser post-ionization we achieved a platform for a broad range of radioecological measurements.

The laser-ionization of a neutral particle cloud above the sample required a simulation of the expanding particles and a simulation based optimization of the TOF analyzer due to different ionization behavior. The results of this optimization were verified by a gain of laser ion signal and improved measurement conditions during several tests. The sensitivity was increased by almost one order of magnitude to about $1\text{E-}4$ as demonstrated by measuring uranium in a 200 nl droplet of a 1 ppb uranium standard solution and by measuring well defined uranium spheres. The sensitivity will be further improved by a two stage extraction process. First mass spectra of synthetical uranium and plutonium samples demonstrated the expected suppression of interfering elements and molecules, which was confirmed with environmental samples. In MOX fuel Pu-238 and U-238 were successfully discriminated. Furthermore, with the ability to retrace the origin of the resonant laser ions, it was possible to create isotope selective images of environmental sample material (Fig.1). For preselection of sample material, the technique of alpha track analysis is applied and further refined for application on environmental bulk samples with a system capable to ablate few atomic layers and to detect on a single ions level.

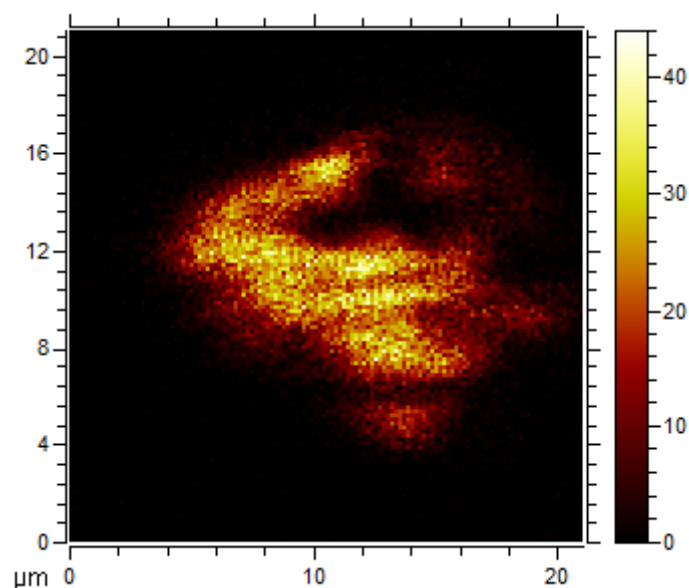


Fig. 1 Spatially resolved resonant SN MS measurement of U-238 of a natural mineral particle from Kabul.

We present first resonant Laser SNMS Measurements on Pu and U samples. Natural minerals from Afghanistan close to Kabul containing enhanced levels of natural radioactivity were characterized. First results on particles from the Chernobyl exclusion zone and from the evacuated zone close to the Fukushima Daichii nuclear power plant are presented.

References:

- [1] N. Erdmann, J.-V. Kratz, N. Trautmann, G. Passler, *Analytical and Bioanalytical Chemistry*, 2009, Volume 395, Number 6, Page 1911

⁴¹Ca in concrete by liquid scintillation and inductively coupled plasma mass spectrometry

M. Garcia Miranda, B. Russell, S. Woods, A. Arinc, P. Ivanov

National Physical Laboratory, Hampton Road, Middlesex, TW11 0LW Teddington, UK

The process of radiological characterisation of radioactive waste (RAW) and suspected materials originating from the decommissioning of nuclear sites is a key stage of the nuclear decommissioning. It requires accurate measurement of a number of difficult to measure, medium and long-lived radionuclides in a range of complex sample matrices due to the importance of such radionuclides for the long term safety assessment of RAW disposal facilities. Calcium-41 has been identified as one such nuclide, because it is a neutron activation product with a half-life of 1.002×10^5 years, with high bioavailability and mobility in the environment.

The aim of the current study is to develop and validate methods for isolation and quantification of ⁴¹Ca in an active concrete sample (³H, ¹⁴C, ⁴¹Ca, ⁵⁵Fe, ⁶⁰Co, ⁶³Ni, ¹³³Ba, ¹³⁴Cs, ¹⁵²Eu and ¹⁵⁴Eu) using a combination of radiochemical separation techniques, mass spectrometry analysis and liquid scintillation counting. The key part of the radiochemistry procedure is the separation of ⁴¹Ca from other radionuclides present in the sample, which could interfere with its quantification by liquid scintillation counting.

Blank concrete spiked with stable calcium is used for the method development work, to determine the amount of calcium carrier needed, and the recoveries at each step of the analysis, with aliquots of the resulting fractions measured by inductively coupled plasma mass spectrometry (ICP-MS).

The concrete digestion is carried out by lithium borate fusion at 1000°C, followed by dissolution in diluted nitric acid and polyethylene glycol precipitation, used as a method to remove silicate that would otherwise hinder the performance of the subsequent radiochemical separation. The fusion of the sample in combination with several radiochemical techniques are used for the removal of the interfering nuclides and purification of ⁴¹Ca prior to liquid scintillation measurement. Volatile nuclides (³H, ¹⁴C and ¹³⁷Cs) are removed during the fusion process. Bivalent and trivalent transition metals and rare earth nuclides (⁵⁵Fe, ⁶⁰Co, ⁶⁵Ni, ¹⁵²Eu and ¹⁵⁴Eu) are removed by co-precipitation with iron hydroxide. Finally, following the ¹³³Ba precipitation as BaCrO₄, Ca-41 is isolated as CaCO₃.

ICP-MS is used for method development to determine the effectiveness of radiochemical separations, and for final quantification of the Ca chemical recovery in the active samples. Liquid scintillation counting is used to for final quantification of Ca-41 in the active samples.

Through the use of radiochemical separation techniques in combination with mass spectrometry and liquid scintillation counting, a robust and reliable procedure will be developed to allow accurate and reproducible measurement of ⁴¹Ca in concrete.

A novel approach for analyzing element composition of large aqueous solution samples with a PGNAA setup

Hei Daqian, Cheng can, Jia Wenbao

*Institute of Nuclear Analysis Techniques, Nanjing University of aeronautics and astronautics, Nanjing, Jiangsu, China
heidq@nuaa.edu.cn*

Prompt gamma ray neutron activation analysis (PGNAA) is a non-destructive technology for determining the concentration of elements in the samples. The most advantageous of PGNAA technique is the applicability for the large volume samples analysis, because both the neutrons and high energy gamma rays can penetrate through the samples easily. However, the non-linearity, which between elements concentrations and the counts of its prompt gamma rays, are often observed when using PGNAA technique for analyzing large samples.

To study the non-linearity, a PGNAA setup (Fig. 1) for determining the elements in the aqueous solutions has been designed. Elements including Cl, B and heavy metals contained in the deionized water were measured. And the neutron self-shielding has been verified as the main effect of the non-linearity. The results showed the non-linearity turn to linearity after neutron self-shielding correction.

So a new spectra analysis approach based on the neutron self-shielding correction has been applied to analyze the full spectrum of complex samples. In this method, a corrected full spectrum can be taken as the linear superposition of the single element standard spectra and background. More effective information can be used to improve the analytic level of PGAA by this novel approach. Series of aqueous solutions with four elements including Cl, B, Cd and Hg were measured with the setup. And four elements standard spectrums, hydrogen spectrum and background were calculated (Fig. 2). Then the method and the standard spectrums have been applied for the aqueous solutions to improve its effectiveness (Fig. 3).

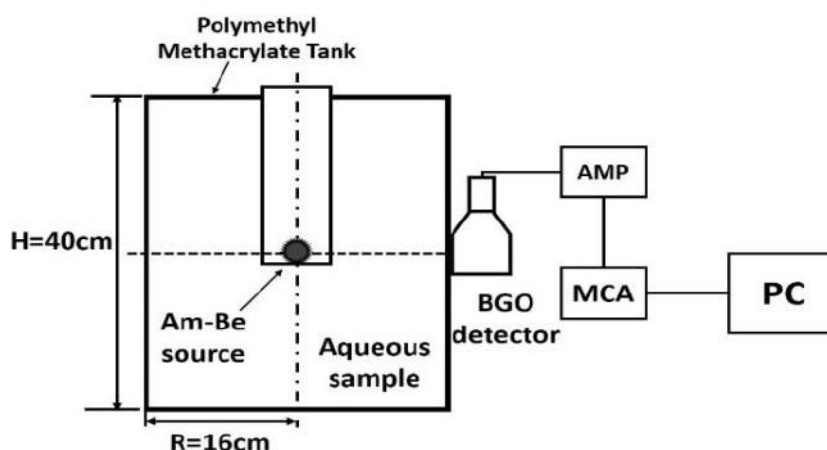
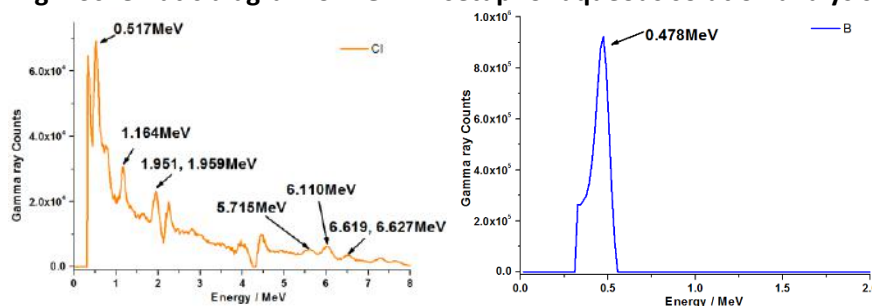


Fig1. Schematic diagram of PGNAA setup for aqueous solution analysis



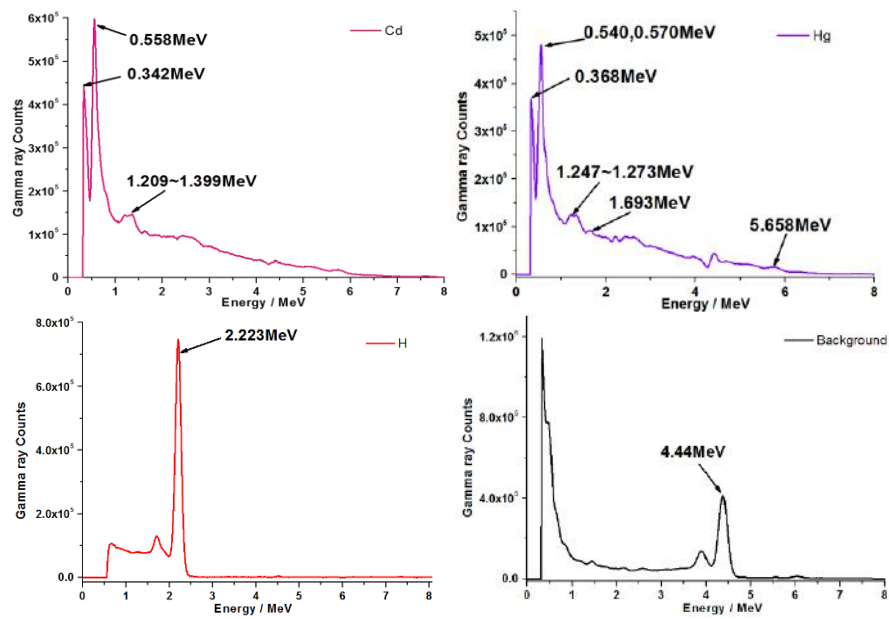


Fig2. The standard spectra of Cl, B, Cd, Hg, H and background

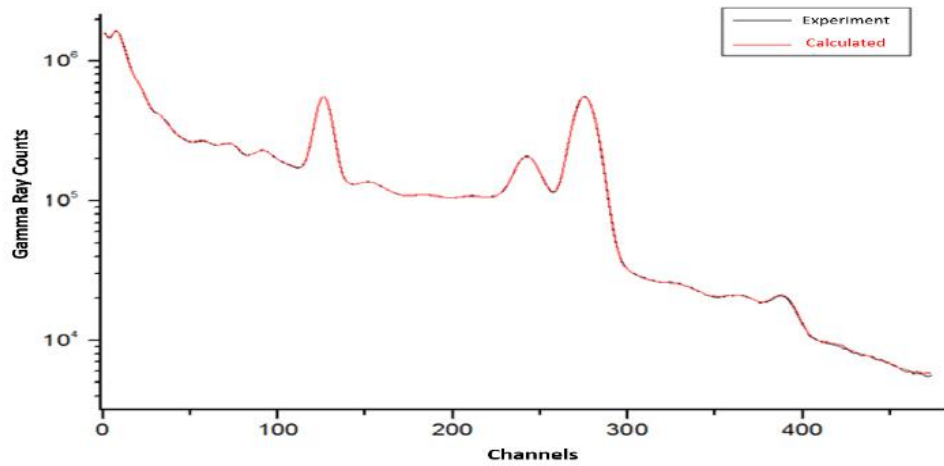


Fig3. The experimental spectrum versus calculated spectrum

POSTER SESSION II
ACTINIDE CHEMISTRY

New extraction systems on the base of polar fluorinated diluent

I. Voronaev^a, V. Babain^{b,c}, M. Alyapyshev^{a,b}, M. Logunov^d

^a *Khlopin Radium Institute, 28, 2nd Murinskiy pr., St. Petersburg, Russia*

^b *ITMO University, 49, Kronverksky pr., St. Petersburg, Russia*

^c *ThreeArc Mining Ltd., 5, Stary Tolmachevskiy per., Moscow, Russia*

^d *FSUE "PA "Mayak", Ozersk, Russia*

Separation of minor actinides from high level wastes generated during spent nuclear fuel reprocessing is one of the most challenging tasks of atomic industry. Many extraction systems for actinides and lanthanides separation were developed and tested. The most of proposed solvents are solutions of polar ligands (like CMPO, dicarboxamides, polynitrogen heterocycles) in hydrocarbon diluents, for example n-dodecane. The main drawback of such extraction systems is low solubility of metal-ligand solvates in organic phase. This causes the low solvent loading capacity and third phase formation.

One of the possible ways to increase the loading capacity of organic phase is using of polar diluents. In Russia the heavy diluents including fluorinated are traditionally in focus. The polar fluorinated diluents as diluents for CMPO, diamides of diglycolic acid and diamides of heterocyclic dicarboxylic acids were proposed.

The main goal of this work was to study a new class of polar fluorinated diluents – esters of fluorinated alcohols – as potential diluents for listed above ligands. The extraction of actinides and lanthanides from nitric acid solutions was investigated. It was shown that new solvents possessed high extraction ability to actinides. The main advantages of new extraction systems are low diluent toxicity, high loading capacity and fire and explosion safety

Interaction and effect of the complexation of actinides by a protein: the Calmodulin

BRULFERT Florian^{a*}, SAFI Samir^a, JEANSON Aurélie^a, BERTHOMIEU Catherine^b, ROQUES Jérôme^a, SAUGE-MERLE Sandrine^b, SIMONI Éric^a

^a *Institut de Physique Nucléaire d'Orsay, CNRS-IN2P3, Univ. Paris-Sud, Université Paris-Saclay, Orsay, France*

^b *CEA/DSV IBEB, Laboratoire des Interactions Protéine-Métal, Saint-Paul-lez-Durance*

brulfert@ipno.in2p3.fr

Considering the environmental impact of the Fukushima nuclear accident, it is fundamental to study the mechanisms governing the effects of the released radionuclides on the biosphere and thus identify the molecular processes generating the transport and deposition of actinides, such as neptunium and uranium. However, the information about the microscopic aspect of the interaction between actinides and biological molecules (peptides, proteins...) is scarce. The data being mostly reported from a physiological point of view, the structure of the coordination sites remains largely unknown. These microscopic data are indeed essential for the understanding of the interdependency between structural aspect, function and affinity.

The Calmodulin (CaM) (abbreviation for CALcium-MODULated proteIN), also known for its affinity towards actinides, acts as a metabolic regulator of calcium. This protein is a Ca carrier, which is present ubiquitously in the human body, may also bind other metals such as actinides. Thus, in case of a contamination, actinides that bind to CaM could avoid the protein to perform properly and lead to repercussions on a large range of vital functions.

The complexation of Np and U was studied by EXAFS spectroscopy which showed that actinides were incorporated in a calcium coordination site. Once the thermodynamical and structural aspects studied, the impact of the coordination site distortion on the biological efficiency was analyzed.

In order to evaluate these consequences, a calorimetric method based on enzyme kinetics was developed. This experiment, which was conducted with both uranium (50 – 500 nM) and neptunium (30 – 250 nM) showed a decrease of the heat produced by the enzymatic reaction with an increasing concentration of actinides in the medium. Our findings showed that the Calmodulin actinide complex works as an enzymatic inhibitor. Furthermore, at higher neptunium (250 nM) and uranium (500 nM) concentration the metals seem to have a poison-like behavior and “kill” completely the enzymatic activity.

The role of mixed solvents on the solvation and complexation of trivalent f-elements

H. M. Felmy⁽¹⁾, Z. Wang⁽²⁾, S. B. Clark⁽¹⁾

⁽¹⁾ Department of Chemistry, Washington State University, Pullman, Washington 99164, USA

⁽²⁾ Pacific Northwest National Laboratory, Richland, Washington 99354, USA

Ion solvation plays a dominant role in the solution chemistry of the trivalent f-elements, impacting the thermodynamics of complexation, chromatographic separation, and the behavior in reprocessing systems. The solvation and thermodynamic data for Eu(III) complexation with α -hydroxyisobutyric acid (HIBA) was determined in mixed aqueous-organic solvents with the goal of understanding the role of solvation on the behavior of the trivalent lanthanides (Ln(III)) and actinides (An(III)). This was accomplished using mixed methanol (MeOH)-water and N,N-dimethylformamide (DMF)-water solvents. This research can be applied to study the behavior of radionuclides in the environment as well as applied in the the nuclear fuel cycle where the separation of the Ln(III)s and An(III)s is an important part of the reprocessing of spent nuclear fuel.

The f-element cations, with their high charge density, impose significant order in polar solvents such as water, resulting in the formation of ordered solvation spheres around the cations.¹ The driving force for the complexation of f-element cations with organic ligands is often due to the entropy gained through the desolvation of the metal cation. Through this complexation, Ln(III) cations are known to form bonds that are more ionic in nature than the An(III)s, which are slightly more covalent in their bonding character.² There is also a slight difference in the radius of the Ln(III) and An(III) cations which will affect the charge density and therefore the extent of the solvation spheres. The goal of this project is to explore these differences in solvation and the energetics of complex formation by first studying the Ln(III)s and then moving on to the study of the An(III)s. The data presented here is for the first metal of interest, Eu(III).

Eu(III) was chosen for this study due to its fluorescent properties. The ligand HIBA has been used extensively in chromatographic separations and the available data in the literature allows for comparisons for Eu(III) complexation with HIBA in aqueous systems. In this study, Eu(III) solvation and complexation thermodynamic data was determined in 0, 10, 30, and 50% (v/v) MeOH-water and DMF-water solvents. The changes in both the fluorescence spectra and the fluorescence lifetime of Eu(III) can be used to determine the composition of the inner solvation sphere of the metal cation in each mixed solvent system. Equation 1 was used to calculate the number of inner-sphere water molecules for the Eu(III) cation before the addition of HIBA and throughout titrations with the ligand in various mixed solvent systems (Figure 1).³

$$N_{\text{H}_2\text{O}} = 1.05 \cdot 10^3 \cdot k_{\text{obs}}(\mu\text{s}^{-1}) - 0.7 \quad (1)$$

The results in Figure 1 show that in MeOH-water solvents there was little difference in the number of inner-sphere water molecules as the concentration of MeOH was varied. This indicates that MeOH did not replace water molecules in the primary solvation sphere of Eu(III) to a significant extent in solutions up to 50% (v/v) MeOH-water. There was, however, a more significant dehydration of the metal center as the ligand concentration was increased. This reduction in the number of inner-sphere water molecules could have been caused by both desolvation of the metal through complexation with HIBA as well as MeOH molecules entering the inner solvation sphere. In DMF-water solvents, there was a greater dehydration of the metal center with added DMF with no ligand present indicating a greater ability for DMF to replace water molecules surrounding Eu(III) when compared to MeOH. There was also a decrease in the number of inner-sphere water molecules with added ligand similar to the MeOH-water solvents.

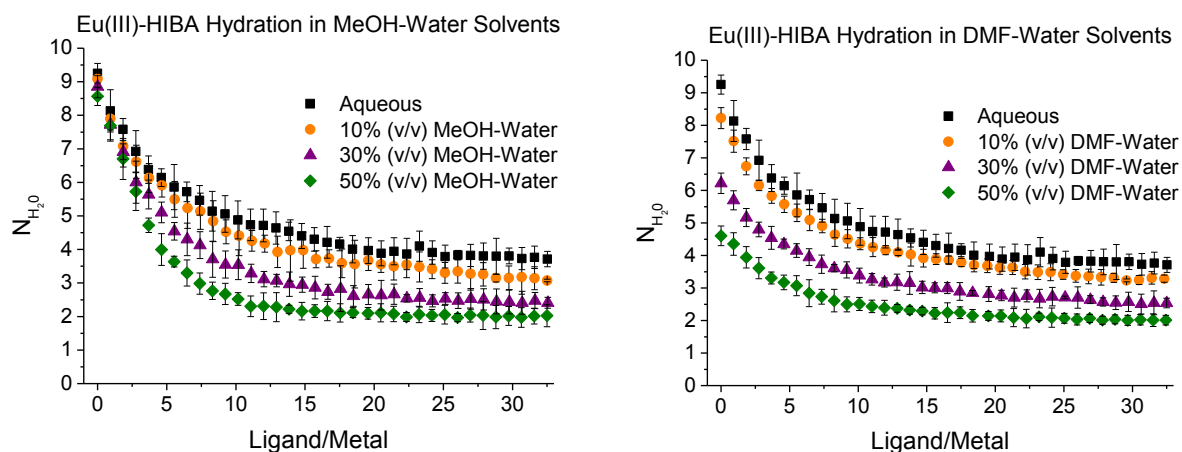


Figure 1. Number of inner-sphere water molecules for Eu(III) calculated from the fluorescence lifetime in MeOH-water solvents (Left) and DMF-water solvents (Right). In each solvent, 5 mM $\text{Eu}(\text{ClO}_4)_3$ was titrated with 0.2 M HIBA (70% neutralized). The uncertainty is represented by 3 standard deviations from 5 spectra, $I = 1.0 \text{ M NaClO}_4$, $T = 25^\circ\text{C}$.

Potentiometric titrations of Eu(III) with HIBA in solutions of 0, 10, 30, and 50% (v/v) MeOH-water and DMF-water solvents showed that the metal-ligand stability constants increased as a function of the concentration of MeOH in solution but did not change significantly with a change in the concentration of DMF in solution.

The results of these experiments show that changing the solvent composition can have a significant impact on the solvation of the Eu(III) cation, and can result in changes in thermodynamic data depending on the solvent chosen. In MeOH-water solvents there was little solvation change but a more significant change in the thermodynamic data and in DMF-water solvents, there was a greater change in the solvation of Eu(III) but little change in thermodynamic data. The next step of this project will be the study of Cm(III) for a direct comparison between a trivalent lanthanide and actinide.

Acknowledgements: A portion of the research was performed using EMSL, a DOE Office of Science User Facility sponsored by the Office of Biological and Environmental Research and located at Pacific Northwest National Laboratory.

- (1) Rizkalla, E. N.; Choppin, G. R. **1994**; pp 529–558.
- (2) Choppin, G. R. *J. Alloys Compd.* **1995**, 223 (2), 174–179.
- (3) Barthelemy, P. P.; Choppin, G. R. *Inorg. Chem.* **1989**, 28 (17), 3354–3357.

Adsorption behavior of Lr on a Ta surface at high temperature

Y. Kaneya,^{1,2} M. Asai,¹ Ch. E. Düllmann,^{3,4,5} K. Eberhardt,^{4,5} R. Eichler,^{6,7} S. Goto,⁸ J. Grund,⁴ K. Hirose,¹ H. Kamada,⁹ Y. Kasamatsu,¹⁰ J. V. Kratz,⁴ H. Makii,¹ A. Mitsukai,^{1,2} S. Miyashita,¹¹ Y. Nagame,^{1,2} R. Naguwa,¹¹ K. Nishio,¹ K. Ooe,⁸ A. Osa,¹ V. Pershina,³ J. Runke,⁴ M. Sakama,¹² D. Sato,⁸ T. K. Sato,¹ M. Schädel,³ M. Shibata,⁹ Y. Shigekawa,¹⁰ K. Shingu,¹¹ K. Shirai,⁸ P. Steinegger,⁷ P. Thörler-Pospiech,^{4,5} T. Tomitsuka,⁸ A. Toyoshima,¹ N. Trautmann,⁴ K. Tsukada,¹ A. Yakushev^{3,5}

¹Japan Atomic Energy Agency, Tokai, Japan; ²Ibaraki University, Japan; ³GSI Helmholtz Centre for Heavy Ion Research, Darmstadt, Germany; ⁴University of Mainz, Germany; ⁵Helmholtz Institute Mainz, Germany; ⁶Paul Scherrer Institute, Villigen, Switzerland; ⁷University of Bern, Switzerland; ⁸Niigata University, Japan; ⁹Nagoya University, Japan; ¹⁰Osaka University, Japan; ¹¹Hiroshima University, Japan; ¹²Tokushima University, Japan

Recently, we determined the 1st ionization potential of the last actinoid, lawrencium (Lr), using an Isotope Separator On-Line (ISOL) at the JAEA tandem accelerator [1]. The obtained result was nicely reproduced by a relativistic calculation [1]. This calculation suggests that the outermost electron of Lr is bound in a 7p_{1/2} orbital, although a 6d orbital is anticipated to be occupied simply from the analogy to its homolog Lu. Thus, the volatility of the elemental Lr atom can be addressed indirectly by determining its adsorption enthalpies on metallic surfaces. The adsorption enthalpies of Lr on various metal surfaces were empirically predicted for the two configurations 7s²7p and 6d7s² [2]. Jost *et al.* investigated the adsorption behavior of Lr on quartz and Pt by an isothermal gas-chromatographic method [3]. However, no conclusive results were obtained. In the present work, the adsorption behavior of Lr was studied by a newly developed method combining vacuum chromatography with the surface ionization in a metallic column/ionizer of the ISOL system.

In vacuum chromatography, the adsorption-desorption processes of single atoms on a column surface depend on the temperature of the chromatographic column and on the adsorption enthalpy of the species under investigation. To observe this adsorption behavior, surface ionization, occurring at high temperatures, was applied. In the course of which, atoms within the ionizer were either ionized during desorption from a heated metal surface or desorbed as neutral atoms. The associated ionization efficiencies are described by the Saha-Langmuir equation [4,5] assuming no adsorption on the ionizer surface, its ionization efficiency fully follows the equation. If there is indeed a sizable adsorption interaction, the ionization efficiency will become lower. In the present study, we first measured ionization efficiencies of short-lived radionuclides of lanthanoid elements at varied temperature conditions in order to establish a relationship between adsorption enthalpies and the ionization efficiencies of these elements. The ionization efficiencies of Lr were then measured under the identical conditions. This contribution will present experimental details and first results obtained in this study.

References

- [1] T. K. Sato *et al.*, *Nature* **520**, 209 (2015).
- [2] B. Eichler *et al.*, *Inorg. Chim. Acta* **146**, 261 (1988).
- [3] D. T. Jost *et al.*, *Inorg. Chim. Acta* **146**, 255 (1988).
- [4] E'. Y. Zandberg & N. I. Ionov, *Sov. Phys. Usp.* **2**, 255 (1959).
- [5] R. Kirchner, *Nucl. Instr. Methods A* **292**, 203 (1990).

Derivatives of phenantroline- and pyridine-dicarboxylic acids as selective extractants for separation of Am(III), Cm(III) and lanthanides(III)

Petr Matveev^a, Vladimir Petrov^a, German Lavrov^b, Ivan Soglasov^a, Stepan Kalmykov^{a,c}, Nickolay Ustynyuk^b, Yuri Ustynyuk^a

^aDepartment of Chemistry, Lomonosov Moscow State University, Leninskie gory, 1 bld.3, Moscow, 119991, Russia

^bA.N.Nesmeyanov Institute of Organoelement Compounds of Russian Academy of Sciences, Vavilova St. 28, Moscow, 119991, Russia

^cNRC "Kurchatov Institute" Akad. Kurchatov sq., 1, Moscow, 123098

New schemes of reprocessing of spent nuclear fuel and high level radioactive wastes require separation of americium, curium and lanthanides that is a complicated chemical and technological task. The most stable oxidation state is the same for these elements (+III) and it determines their very close chemical properties. The liquid-liquid extraction is suggested as the most efficient technological method for their separation.

Here we present the study of the extraction of americium, curium and europium with dilactams of N,N'-diethyl-N,N'-di(para-hexyl-phenyl)-diamide 1,10-phenanthroline-4,7-dichloro-2,9-dicarboxylic acid (marked as L1) and pyridinedicarboxylic acid (L2 and L3) (Fig 1).

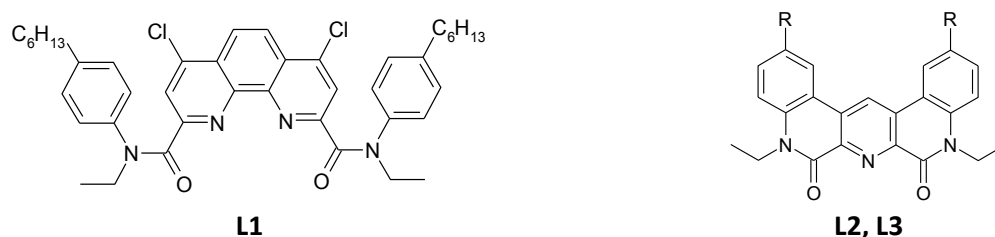


Fig. 1. The structure of the studied extractants: R = -C₆H₁₃ (L2), -C₂H₅ (L3).

Results of quantum mechanical calculations indicate that investigated ligands extract preferentially softer cations (Am). We added N,N,N',N'-tetra-ethyl-diglycolamide (TEDGA) into the aqueous phase to increase the separation factors (SF). This ligand has a tendency to bind harder cations (Cm, Eu). Radionuclides ²⁴¹Am, ²⁴⁴Cm and ¹⁵²Eu were used as tracers in present study. Curium radioactivity was measured by liquid scintillation counting; americium and europium – by gamma spectrometry. Nitrobenzene, meta-nitrobenzotrifluoride (F3) and *n*-octanol-1 were used as diluents for all ligands. Additionally, in case of L1 ligand toluene and decane/octanol mixture were used as well. The concentration of HNO₃ in the aqueous phase in all experiments was 3 M. The concentration of TEDGA was in the range of 0 – 50 mM.

The formation of complexes Metal-TEDGA causes the decrease of the efficiency of extraction with increasing the TEDGA content in aqueous solution. The separation factors (SF_{Am/Cm} and SF_{Am/Eu}) have non-linear dependency on concentration of TEDGA. Based on values of distributions coefficients and separation factors, the optimal concentration of TEDGA was found to be around 5-10 mM.

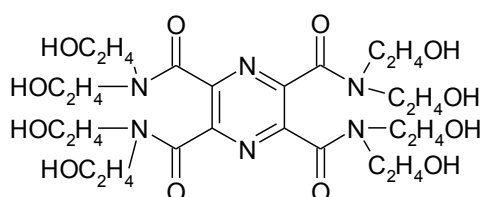


Fig. 2. Structure of A1 ligand.

We also used a novel water-soluble ligand – octahydroxyethyltetraamide of 2,3,5,6-pyrazinetetracarboxylic acid (A1) (Fig. 2) to improve the selectivity of extraction. The constants of protonation and complex formation

were determined using solvent extraction and potentiometric titration. We have determined that ligand A1 forms stronger complexes with heavier lanthanides. In extraction system consisting of 100% TBP – 3M NaNO₃ and A1 the maximum value for SF_{Cm/Am} was reached the value 3.3. The study of A1 influence on extraction of Am(III), Cm(III) and lanthanides in systems containing Aliquat 336 and L1 are ongoing.

This work was supported by Russian Foundation for Basic Research (15-03-99646-a).

Uranyl polyrotaxanes involving cucurbituril: Diversity of topologic structures and uranyl secondary building units

Lei Mei, Wei-qun Shi, Zhi-fang Chai

Key Laboratory of Nuclear Radiation and Nuclear Energy Technology, Institute of High Energy Physics, Chinese Academy of Sciences, Beijing 100049, China. Corresponding author: meil@ihep.ac.cn

Metal-organic materials with dynamic components, such as mechanically-interlocked rotaxane molecules (MIMs), integrate the attractive feature of flexibility into rigid frameworks as well as broad functionalities. Among plenty of rotaxane-based coordination polymers, transition metal ions and lanthanide ions have been intensively studied due to their rich coordination patterns and availabilities. However, polyrotaxanes containing actinide cations, such as uranyl or thorium cations, have been never reported. Hence, we are currently pursuing the preparation of actinide polyrotaxanes from uranyl cation and pseudorotaxanes ligands containing cucurbituril. This effort has finally succeeded to produce a series of uranyl polyrotaxanes with a rich library of structures from one dimension to three dimensions.¹⁻³ Moreover, we found that the diversity of topologic structures is in close relationship with the direction role of different uranyl secondary building units.

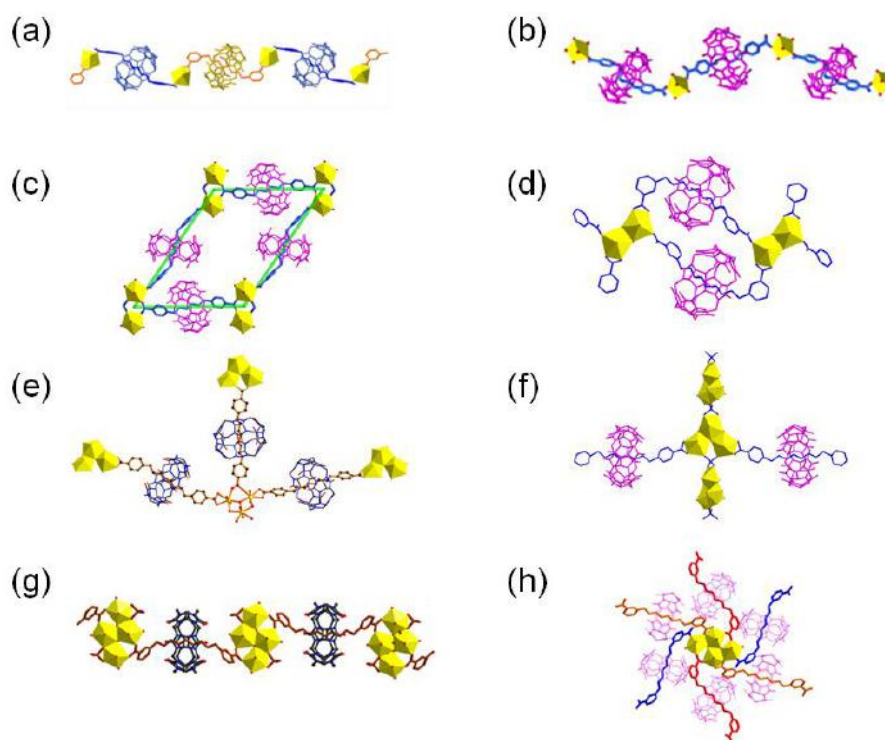


Figure 1. The diversity of topologic structures in close relationship with the direction role of different uranyl secondary building units: (a-b) monomeric uranyl; (c-d) dimeric uranyl; (e-f) trimeric uranyl; (g-h) tetrameric uranyl.

References

- [1] Mei, L.; Wu, Q. Y.; An, S. W.; Gao, Z. Q.; Chai, Z. F.; Shi, W. Q., *Inorg. Chem.* 2015, 10.1021/acs.inorgchem.1025b01988.
- [2] Mei, L.; Wang, L.; Yuan, L. Y.; An, S. W.; Zhao, Y. L.; Chai, Z. F.; Burns, P. C.; Shi, W. Q., *Chem. Commun.* 2015, 51, 11990-11993.
- [3] Mei, L.; Wang, L.; Liu, C. M.; Zhao, Y. L.; Chai, Z. F.; Shi, W. Q., *Chem. Eur. J.* 2015, 21, 10226-10235.

Solid phase alpha spectrometry – application of leached ThO₂ pellets

E. Myllykylä^{1)*}, L. Koivula²⁾, T. Lavonen¹⁾, K. Ollila¹⁾, K. Helariutta²⁾, M. Siitari-Kauppi²⁾

¹⁾VTT Technical Research Centre of Finland Ltd, P.O. Box 1000, FI-02044 VTT, Finland

²⁾Laboratory of Radiochemistry, Department of Chemistry, University of Helsinki, Finland

This study was a part of the project, which aimed for better understanding of the dissolution processes of UO₂ the structure of matrix of spent nuclear fuel. This was studied through the oxides, ThO₂, CeO₂, and UO₂, which are isostructural with fluorite structure of UO₂. The research was mainly performed as a part of the EU project, REDUPP, and was later continued under national program (SAFIR2018).

In this work, the surface of ThO₂ pellets was studied by alpha spectrometry after the leaching experiment. The observations of leaching experiment suggested that thorium precipitation occurred simultaneously with dissolution. The aim of this study was to define the possible precipitation on the ThO₂ pellet surface with alpha spectroscopy and related simulations with AASI program. The sintered ²³²ThO₂ pellets were made to meet an ideal composition and microstructure similar to the fluorite structure of UO₂ fuel [1]. The leaching experiments were conducted in 0.01 M NaCl solution using ²²⁹Th spike (10⁻⁹ mol/L) with single solid ²³²ThO₂ pellet (3.8 mm x 8.7 ø mm) under Ar atmosphere at 25 °C in parallel with similar experiments without ²²⁹Th spike for 534 days. Sector field ICP-MS was used to analyze the concentration of ²³²Th and the isotopic ratio of ²²⁹Th/²³²Th.

Alpha spectra of the pellets after leaching were analysed under vacuum with Canberra 450 PIPS detector using analysis program MAESTRO for Windows Model A65-332. The peaks of the thorium and daughter nuclides were identified from the spectra. The spectra were modelled by AASI (Advanced Alpha Spectrometric Simulation) program, which has been developed by the Radiation and nuclear safety authority of Finland for simulating the propagation of alpha particles in the medium, air and the detector material [2]. It is based on the Monte Carlo methods and derives the spectrum from large number of initial decay incidents. Program can be used for qualitative and quantitative analysis of alpha active sources containing comprehensive repertoire of isotopes. Geometry of the source medium and the distribution of the isotopes inside the matter are possible for investigation. Studying the shape of the energy spectrum with in detail on the tail of the peaks and comparing measurements with the simulations we can examine the prevalence of individual isotopes underneath the surface.

Figure 1 shows the alpha spectrum of leached ThO₂ pellet and it's AASI simulation, which gives valuable information about the distribution of ²²⁹Th tracer on the thorium oxide pellet and additional information about proportions between ²²⁹Th and ²³²Th, and also their daughter nuclei. Most of the alpha particles are absorbed inside the pellets and therefore a well-defined simulation is crucial for correct activity measurement. The alpha analysis confirmed the precipitation of ²²⁹Th layer and concentrated amount of ²²⁸Th, daughter nuclide of ²³²Th, on pellet surface.

Separate simulations were run for the bulk medium and the 0.1 µm thick surface layer. This allowed better scaling for the spectrum for comparing the simulations and measurements as the concentrations in the bulk medium nor surface layer were known. Simulations were run with following equilibrium assumptions. ²²⁹Th and daughter nuclei (²²⁵Ac, ²²¹Fr, ²¹⁷At, ²¹³Bi, ²¹³Po) simulated in equilibrium and taking into account the alpha branching of 2.1 percent for ²¹³Bi. ²³²Th with twice the activity compared to daughter nuclei (²²⁸Th, ²²⁴Ra, ²²⁰Rn, ²¹⁶Po, ²¹²Bi, ²¹²Po) which were simulated in equilibrium among themselves, taking account the alpha branching of ²¹³Bi to be 35.94 percent.

It should be noticed that the dissolution/precipitation sparingly soluble oxides might continue even after the solubility limit of the oxide has been achieved. The continuation of dissolution despite the equilibrium is relevant when considering the disposal of spent nuclear fuel.

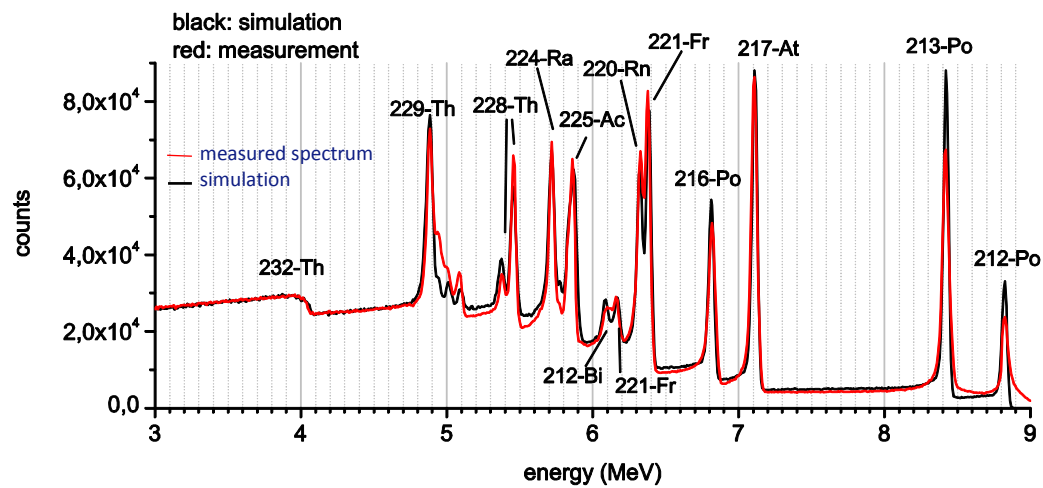


Figure1. Alpha spectra of the solid pellet from the leaching experiment A .

[1] E. Myllykylä, T. Lavonen, M. Stennett, C. Corkhill, K. Ollila and N. Hyatt, (2015), *Radiochim. Acta* 103 (8), 565-576.

[2] Siiskonen, T. and Pöllänen, R, (2005) *Nuclear Instruments and Methods in Physics Research Section A: Accelerators, Spectrometers, Detectors and Associated Equipment*, 550 (1–2), 425–434.

**ThermAc – a joint project on aquatic actinide chemistry and thermodynamics
at elevated temperature conditions**

P.J. Panak³, M. Altmaier¹, F. Brandt⁵, V. Brendler², I. Chiorescu⁶, E. Colàs⁷, H. Curtius⁵, F. Endrizzi¹, C. Franzen², X. Gaona¹, M. Grivé⁷, S. Hagemann⁴, C. Koke³, D.A. Kulik⁸, S. Krüger⁶, J.-Y. Lee¹, M. Maiwald³, A. Skerencak-Frech³, R. Steudtner², T. Thoenen⁸, S. Tsushima²

¹⁾ *Karlsruhe Institute of Technology, Institute for Nuclear Waste Disposal, (KIT-INE), Karlsruhe, Germany*

²⁾ *Helmholtz-Zentrum Dresden-Rossendorf, Institute of Resource Ecology (HZDR-IRE), Dresden, Germany*

³⁾ *University of Heidelberg, Institute of Physical Chemistry, Heidelberg, Germany*

⁴⁾ *Gesellschaft für Reaktor und Anlagensicherheit (GRS), Braunschweig, Germany*

⁵⁾ *Jülich Research Center, Institute of Energy and Climate Research (IEK-6), Jülich, Germany*

⁶⁾ *Technische Universität München, Munich, Germany*

⁷⁾ *Amphos21 Consulting, Barcelona, Spain*

⁸⁾ *Paul Scherrer Institut, Laboratory for Waste Management (PSI-LES), Villigen, Switzerland*

The ThermAc project aims at extending the chemical understanding and available thermodynamic database for actinides, long-lived fission products and relevant matrix elements in aquatic systems at elevated temperatures. To this end, a systematic use of estimation methods, new experimental investigations and quantum-chemistry based information is intended. ThermAc has started in March 2015 and is projected for three years, running until 28.02.2018. The project is funded by the German Federal Ministry for Education and Research (BMBF) and is coordinated by KIT-INE. Within the collaborative project, the following German and international partners and researchers are involved:

Karlsruhe Institute of Technology (KIT-INE, Germany)

Helmholtz-Zentrum Dresden-Rossendorf (HZDR-IRE, Germany)

University of Heidelberg (Germany)

Gesellschaft für Anlagen- und Reaktorsicherheit (GRS)

Jülich Research Center (FZJ-IEK-6, Germany)

Technische Universität München (Germany)

Amphos21 Consulting (Spain)

Paul Scherrer Institut (PSI-LES, Switzerland)

The ThermAc project is developed with the aim of improving the scientific basis for assessing nuclear waste disposal scenarios at elevated temperature conditions. In the case of disposal of highly active heat producing waste, the repository system is expected to feature elevated temperature conditions over a significant period of time, due to the high decay heat of the waste at an early stage of repository operation. If early canister failure occurs, radionuclides therefore may contact aquatic systems at higher temperature conditions. Adequate scientific tools must be available to assess the related chemical effects and their impact upon safety. A clear focus of ThermAc is on long-lived actinides in oxidation states III, V and VI, with selected fission products and important redox controlling matrix elements like Fe also receiving attention. Tetravalent actinides and detailed investigations of redox processes are excluded from the current ThermAc work programme. ThermAc addresses the temperature range from ~5°C up to ~90°C, focusing on systems at low or intermediate ionic strength. Only for selected cases with specific relevance or scientific interest, higher temperatures up to 200°C or highly concentrated salt brine solutions will be investigated. Chemical analogs for the actinide elements will be used, especially in order to gain information on solid phase transformation processes. Ion-interaction processes are treated with the Specific Ion Interaction theory (SIT), in agreement with the approach favored by the NEA-TDB project. Quantum chemical calculations are used to support the interpretation of experimental findings and to establish a fundamental understanding of chemical effects on a molecular level.

Within the scope of ThermAc, a significant impact can be realized within a strong collaborative and integrated concept with the following strategic components:

(1) Systematic use of estimation methods for thermodynamic data and model parameters

Using several different estimation methods both for aqueous species and solid phases, a “working database” will be set up for modeling selected reference systems at elevated temperatures. Focus is on simplified systems at low or intermediate ionic strength. Based upon this newly derived thermodynamic basis, geochemical model calculations are performed and predictions on solubility and speciation are made for selected reference systems at elevated temperature.

(2) Comprehensive experimental validation of the estimations

The estimations made in (1) are validated by new experimental studies using a set of complementary experimental approaches and analytical tools, including quantum chemistry. The ThermAc consortium features partners with a broad set of competences and available experimental techniques. The experimental studies established to validate the estimations focus on both aqueous and solid phases with broad variation of background electrolyte media, pH conditions, and temperature, allowing for a comprehensive picture of radionuclide solubility and speciation.

(3) Fundamental studies for improved process understanding of actinide chemistry at elevated T

Key processes which are likely to influence aquatic chemistry at elevated temperature conditions are investigated, like solid phase characteristics (e.g. changes in particle size), secondary phase formation processes, the relevance of intrinsic colloids, or ion-interaction processes. Following this approach, a qualitative or (semi)-quantitative assessment of relevant processes that are at present exceedingly difficult to be addressed within the explicit chemical/thermodynamic concepts and models used in (1) and (2) is possible, also serving as an anchoring point for the use of estimation methods.

(4) Comprehensive critical evaluation of the work performed within (1-3)

A key result from the comparison of predictions based upon estimation methods with new experimental data derived within ThermAc will be the assessment of the use of estimations methods to set up a workable thermodynamic database for elevated temperatures with high applicability to nuclear waste disposal issues. In this context it will be clarified, to which extent systems will remain critical with regard to available thermodynamic data, and which relevant processes at elevated temperatures are still not sufficiently understood.

ThermAc has a strong commitment to disseminate the outcome of the project to the international research community and interlink with similar R&D efforts and applied programs performed elsewhere. Given the scope and very large intrinsic complexity of investigating systems at elevated temperatures, establishing synergies and exchange with groups having complementary interests and competences at an international level seems mandatory. To this end, ThermAc offers the opportunity of external partners joining the consortium as Associated Groups. Associated Groups will join the ThermAc project at their own costs, receiving no financial support via the ThermAc project. Associated groups will have access to the results generated within ThermAc, are invited to the ThermAc project meetings which serve as main forum to present and discuss new results, have the opportunity to communicate their own expertise and research to the consortium and may join in bi- or multilateral cooperation with ThermAc partner institutions. For further information on Associated Groups to ThermAc, please contact the project coordinator at marcus.altmaier@kit.edu.

Acknowledgement: This project is funded by the German Federal Ministry for Education and Research (BMBF) under the contracts 02NUK039 A-F.

Is the chemistry of lawrencium peculiar?

W-H. Xu¹ and P. Pyykkö²

- ¹⁾ Key Laboratory of Synthetic and Natural Functional Molecule Chemistry of the Ministry of Education, College of Chemistry and Molecular Science, Northwest University, Xi'an, China
²⁾ Department of Chemistry, University of Helsinki, Helsinki, Finland

The Periodic Table (PT) is about chemistry. Lawrencium (Lr, $Z = 103$) is a short-lived man-made element. Its position in the PT had been debated for some time.¹ Recent experimental work² confirmed the theoretical predictions of its ground state,³ which is different from that of its lanthanide counterpart lutetium. Lr is $7s^2(7p_{1/2})^1$, not $7s^26d^1$. In this study, we find that lawrencium atomic ionization potentials and molecular electronic structures are similar to lutetium in various regards. The molecular systems considered include hydrides, trichlorides, monocarbonyls and other organometallic molecules, from zero- to trivalent lawrencium. We conclude that the peculiar atomic ground state of Lr does not lead to special chemistry, thus further supporting the current position of lawrencium in the PT.

References

1. W. B. Jensen, *Found. Chem.*, 2015, **17**, 23-31.
2. T. K. Sato, M. Asai, A. Borschevsky, T. Stora, N. Sato, Y. Kaneya, K. Tsukada, Ch. E. Düllmann, K. Eberhardt, E. Eliav, S. Ichikawa, U. Kaldor, J. V. Kratz, S. Miyashita, Y. Nagame, K. Ooe, A. Osa, D. Renisch, J. Runke, M. Schädel, O. Thörle-Pospiech, A. Toyoshima and N. Trautmann, *Nature*, 2015, **520**, 209-211.
3. J. P. Desclaux and B. Fricke, *J. Physique*, 1980, **41**, 943-946.

Silica-salophen hybrid material for uranium sequestration

Jaclynn Unangst^a, Kenneth J. Shea^b, Mikael Nilsson^{a,b}

^a *Department of Chemical Engineering and Materials Science, University of California Irvine, CA, USA*

^b *Department of Chemistry, University of California Irvine, CA, USA*

Selective uranium ion complexation is an active area of research that has potential in nuclear fuel sourcing, remediation, containment and sensing. In this current research Schiff Base chemistry is the foundation for a nonsymmetrical salophen synthesized in a multistep approach for incorporation into a silica-based hybrid material for uranyl ion, $[\text{UO}_2]^{2+}$ sequestration. The salophen ligand utilizes a (propyl)triethoxysilyl tether for covalent attachment into the hybrid material formed through co-condensation reactions of Stöber silica and the bridged polysilsesquioxane (BPS), bis(trimethoxysilylethyl)benzene. The hybrid material is chosen based on the robustness of silica with enhanced porosity from the bridged polysilsesquioxane. Previous studies using salophen have shown that it can complex uranium in solution. It is the goal of this research to find the optimal balance of salophen ligand, silica and BPS concentrations to give desirable surface area, functionalization and porosity for maximum uptake of the uranyl ion from aqueous environments. Uptake testing will show the efficiency and selectivity of the hybrid material at sequestering uranium.

Theoretical insights into the bonding nature and stabilities of a series of low-oxidation actinide complexes

Qun-Yan Wu,^a Cong-Zhi Wang,^a Jian-Hui Lan,^a Zhi-Fang Chai,^{a,b} and Wei-Qun Shi^{*a}

^aLaboratory of Nuclear Energy Chemistry and Key Laboratory for Biomedical Effects of Nanomaterials and Nanosafety, Institute of High Energy Physics, Chinese Academy of Sciences, Beijing, 100049, China
School of Radiological and Interdisciplinary Sciences (RAD-X), and Collaborative Innovation Center of Radiation Medicine of Jiangsu Higher Education Institutions, Soochow University, Suzhou 215123, China
wuqy@ihep.ac.cn

Recently, +2 formal oxidation state complexes for lanthanides (except Pm) and actinides (Th and U) in solution have been discovered.^{1, 2} These experimental studies significantly enrich the breadth of f-element molecular species and expand our vision about low-valent oxidation states. However, they are highly reactive even at a low temperature, which makes it challenging to experimentally probe their physical and chemical properties because all the actinide elements are radioactive and toxic, especially for protactinium and transuranic elements. Recently we have theoretically studied a series of actinide complexes and found that the covalency dominates the An-N (An=Pa-Pu) and U-E (E=N-Bi) multiple bonds.^{3, 4} To explore the bonding nature and stabilities of the low-valent actinide complexes, a series of divalent actinide species, $[\text{AnCp}'_3]^-$ (An=Th-Am, $\text{Cp}'=[\eta^5\text{-C}_5\text{H}_4(\text{SiMe}_3)]^-$) have been investigated using quasi-relativistic density functional theory in THF solution.⁵ Electronic structures and electron affinity properties were systematically studied to identify the interactions between the +2 actinide ions and Cp' ligands. The ground state electron configurations for the $[\text{AnCp}'_3]^-$ species are obtained according to MO analyses. The total bonding energy decreases from the Th- to Am- complex and the electrostatic interactions mainly dominate the bonding between the actinide atom and ligands. The electron affinity analysis suggests that the reduction reaction of $\text{AnCp}'_3 \rightarrow [\text{AnCp}'_3]^-$ should become increasingly facile across the actinide series from Th to Am, in accordance with the known An(III/II) reduction potentials. In addition, the corresponding properties of series of the +1 oxidation state actinide complexes were also investigated. This work will expand the knowledge on the low oxidation state chemistry of actinides, and further pave the way for the synthesis of related low oxidation state compounds of 5f elements.

References:

- (1) MacDonald, M. R.; Fieser, M. E.; Bates, J. E.; Ziller, J. W.; Furche, F.; Evans, W. J. Identification of the +2 Oxidation State for Uranium in a Crystalline Molecular Complex, $[\text{K}(2.2.2\text{-Cryptand})][(\text{C}_5\text{H}_4\text{SiMe}_3)_3\text{U}]$. *J. Am. Chem. Soc.* **2013**, *135*, 13310-13313.
- (2) Langeslay, R. R.; Fieser, M. E.; Ziller, J. W.; Furche, F.; Evans, W. J. Synthesis, Structure, and Reactivity of Crystalline Molecular Complexes of the $\{[\text{C}_5\text{H}_3(\text{SiMe}_3)_2]_3\text{Th}\}^{1-}$ Anion Containing Thorium in the Formal +2 Oxidation State. *Chem. Sci.* **2015**, *6*, 517-521.
- (3) Wu, Q.-Y.; Wang, C.-Z.; Lan, J.-H.; Xiao, C.-L.; Wang, X.-K.; Zhao, Y.-L.; Chai, Z.-F.; Shi, W.-Q. Theoretical Investigation on Multiple Bonds in Terminal Actinide Nitride Complexes. *Inorg. Chem.* **2014**, *53*, 9607-9614.
- (4) Wu, Q.-Y.; Lan, J.-H.; Wang, C.-Z.; Zhao, Y.-L.; Chai, Z.-F.; Shi, W.-Q. Terminal $\text{U}\equiv\text{E}$ (E = N, P, As, Sb, and Bi) Bonds in Uranium Complexes: A Theoretical Perspective. *J. Phys. Chem. A* **2015**, *119*, 922-930.
- (5) Wu, Q. Y.; Lan, J. H.; Wang, C. Z.; Cheng, Z. P.; Chai, Z. F.; Gibson, J. K.; Shi, W. Q. Paving the Way for the Synthesis of a Series of Divalent Actinide Complexes: A Theoretical Perspective. *Dalton Trans.* **2016**, *45*, 3102-3110.

TRANSACTINIDE CHEMISTRY

Chemical identification and chemistry of transactinide elements at FLNR

N.V. Aksenov, S.N. Dmitriev

Flerov Laboratory of Nuclear Reactions, JINR, 141980 Dubna, Moscow region, Russia

The discovery of relatively long-lived radionuclides of elements with $Z=104-118$ in ^{48}Ca -induced complete nuclear fusion reactions with actinides have stimulated chemistry studies of the heaviest elements and their lighter homologues. In this report chemical studies of Db and group-5 homologues, Nb and Ta in liquid phase and element 113 in gas phase at FLNR are reviewed. The chemical identification of ^{268}Db ($T_{1/2}=26$ h) [1-3] and $^{284}\text{113}$ ($T_{1/2}=1$ s) [4] in the decay chains of the discovered element 115 was used to confirm the discovery. Detailed studies of chemical properties of Db using co-precipitation with LaF_3 , ion-exchange and extraction chromatography from HF and HCl solutions were performed in 2005 [3], and using a DGFRS separator – in 2011 [5]. In this report we will also describe recent results and status of preparation for future gas-phase chemistry experiments with element 113 with physical pre-separation at FLNR.

Currently efficiency of performed experiments is low because of a limited choice of chemical methods and insufficient data due to low yield and short life times of the elements. Progress in the area of study of transactinide elements is only possible if experiment efficiency is increased. In order to increase efficiency we at FLNR JINR have been constructing a Superheavy element Factory based on a new heavy ion cyclotron DC280 [6]. As part of this project we have been developing new high-power heavy ion targets made from actinides [7], a new separator for radiochemical research [8] and new experimental instruments.

References

- [1] S.N. Dmitriev et al., *Mendeleev Commun.* 15, 1 (2005).
- [2] D. Schumann et al., *Radiochim. Acta* 93, 727 (2005).
- [3] N.J. Stoyer et al., *Nuclear Physics A* 787, 388 (2007).
- [4] S.N. Dmitriev et al., *Mendeleev Commun.* 24, 253 (2014).
- [5] N. Aksenov et al., in *Book of abstracts of NRC-8*, Mauro Bonardi – Milano: Università degli Studi di Milano, Dip. Fisica, 72 (2012).
- [6] Yu.Ts. Oganessian, S.N. Dmitriev, M.G. Itkis. in *Proceedings of International Symposium on Exotic Nuclei*, World Scientific, Singapore, 483-490 (2015).
- [7] S.N. Dmitriev, A.G. Popeko. *J. Radioanal. Nucl. Chem.* 305, 927 (2015).
- [8] A.G. Popeko *Nucl. Instr. Meth. B*, in press, (2016), <http://dx.doi.org/10.1016/j.nimb.2016.02.025>

The challenge of target preparation for superheavy element research

G. Bozhikov, A.V. Sabel'nikov, N.V. Aksenov, G.K. Vostokin and S.N. Dmitriev

Flerov Laboratory of Nuclear Reactions, JINR, 141980 Dubna, Moscow region, Russia

The construction of new accelerator complex at FLNR JINR with ion beam intensities 10 times higher than that of today will require to revise the fabrication and irradiation of actinide targets to avoid their destruction [1]. In this report we focus on systematics of targets exposed to ^{48}Ca ion beams at different energy in dependence on target materials. The fabrication method influence on the target resistance will also be taken into consideration.

[1] S.N. Dmitriev, A.G. Popeko. J. Radioanal. Nucl. Chem. 305, 927 (2015).

Towards selenides of the SHE Copernicium and Flerovium: Unexpected Cn-Se bond formation

N.M. Chiera^{1,2}, N. V. Aksenov³, Y. V. Albin³, G. A. Bozhikov³, V. I. Chepigin³, S. N. Dmitriev³, R. Dressler¹, R. Eichler^{1,2}, V. Ya. Lebedev³, A. Madumarov³, O. N. Malyshev³, D. Piguet¹, Y.A. Popov³, A. V. Sabel'nikov³, P. Steinegger^{1,2}, A. I. Svirikhin³, A. Türlér^{1,2}, G. K. Vostokin³, A. Vögele¹, A. V. Yeremin³

¹Paul Scherrer Institute, Villigen, Switzerland, ²University of Bern, Bern, Switzerland, ³Flerov Laboratory of Nuclear Reactions, JINR, Dubna, Russian Federation

In preparation of the chemical characterization of the superheavy elements copernicium (Cn, Z = 112) and flerovium (Fl, Z = 114), the adsorption behaviour of elemental mercury on red amorphous and trigonal selenium surfaces was investigated experimentally by off-line and on-line gas chromatographic methods. Red amorphous selenium surfaces were deposited applying the vapor transport deposition method described in [1]. Trigonal selenium surfaces were obtained through thermal treatment of the deposited red amorphous selenium, as suggested in [2].

Off-line model experiments with the carrier free isotope ¹⁹⁷Hg were performed [3]. Monte-Carlo simulations of a diffusion controlled deposition were in good agreement with the experimental results, assuming as lower interaction limit of mercury on a red amorphous selenium surface of $-\Delta H_{\text{ads}}^{\text{Hg}}(\text{a-Se}) > 85 \text{ kJ/mol}$, while the interaction of mercury on a trigonal selenium surface was estimated as $-\Delta H_{\text{ads}}^{\text{Hg}}(\text{t-Se}) < 60 \text{ kJ/mol}$ [3]. These results indicate a severe kinetic hindrance of the Hg / trigonal Se reaction, taking into account the thermodynamic stability of HgSe. Additionally, the reactivity difference of mercury towards the two selenium allotropes allowed for monitoring at a microscopic level the spontaneous transformation of the red amorphous selenium surface into the thermodynamically most stable trigonal selenium one.

On-line test experiments using the COLD detector array [4] equipped with Se covered detector surfaces were performed and will be described in this contribution. The ¹⁸³⁻¹⁸⁵Hg deposition pattern revealed an advanced crystallization of the thin red amorphous Se surface on the detectors after 3 weeks of storage [4]. Surprisingly, two events attributed to ²⁸³Cn (Fig. 1) were detected on Se-covered detectors. The following Monte Carlo simulations presuming adsorption chromatographic behavior indicates that Cn interacts with trigonal Se with a probability > 95%, with an interaction potential limit of $-\Delta H_{\text{ads}}^{\text{Cn}}(\text{t-Se}) > 48 \text{ kJ/mol}$ (Fig. 2) [5]. Despite the CnSe formation is expected to be thermodynamically less favored, these first results reveal a lower kinetic formation hindrance compared to the interaction of Hg with t-Se. In order to understand the kinetic process of the Hg/Se interaction, useful later on for the interpretation of the CnSe_(s) formation, inverse thermochromatographic (IT) studies with both the amorphous and the crystalline Se surfaces will be performed [5].

Further on-line studies with Hg, Cn and Fl on both trigonal and amorphous selenium surfaces are envisaged for autumn 2016.

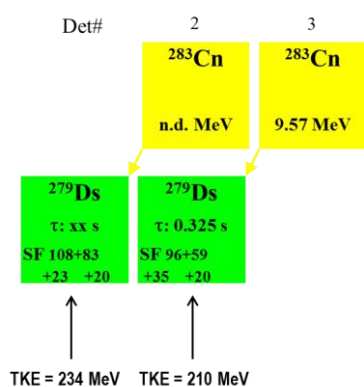


Figure 1. Events attributed to ^{283}Cn observed on the adjacent Se-covered detectors #2 and 3. No other spontaneous fissions signals were observed. Note the high total kinetic energy of the SF, typical of a superheavy element decay.

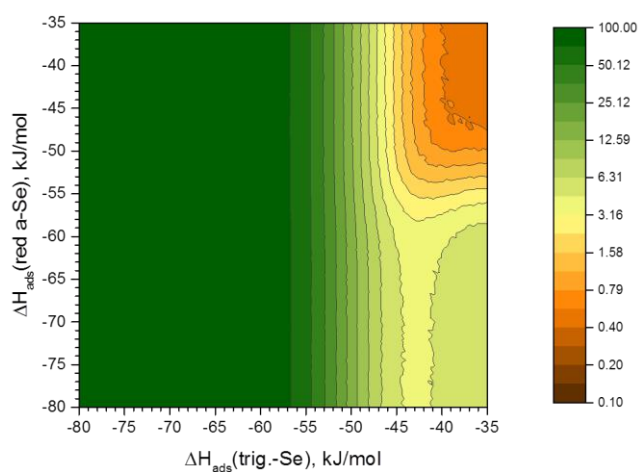


Figure 2. A preliminary analysis of the probability to observe the two ^{283}Cn events on the Se-covered detectors used in the 2015 experimental campaign at the FLNR, Dubna.

References

- [1] N. M. Chiera et al., Thin Solid Films, 592 (2015).
- [2] V.S. Minaev et al., Journal of Optoelectronics and Advanced Materials 7, no. 4 (2005).
- [3] N. M. Chiera et al., PSI LCH Annual Report 2014, p. 5.
- [4] R. Eichler et al., Nature, 447 (2007).
- [5] N. M. Chiera et al., PSI LCH Annual Report 2015, p.3.

Radiochemical investigation of the kinematics of multi-nucleon transfer reactions in $^{48}\text{Ca} + ^{248}\text{Cm}$ collisions 10% above the Coulomb barrier

M. Götz^{1,2,3}, S. Götz^{1,2,3}, J.V. Kratz^{1,3}, Ch.E. Düllmann^{1,2,3}, J. Ballof¹, H. Dorrer¹, J. Grund¹, D. Huber¹, E. Jäger², O. Keller¹, J. Krier², J. Khuyagbaatar^{2,3}, L. Lens^{1,2}, B. Lommel², M. Mendel¹, Ch. Mokry^{1,3}, K.J. Moody⁵, J. Runke^{1,2}, M. Schädel⁴, P. Scharrer³, B. Schausten², D. Shaughnessy⁵, M. Schmitt¹, J. Steiner², P. Thörle-Pospiech^{1,3}, N. Trautmann¹, N. Wiehl^{1,3}, A. Yakushev^{2,3}, V. Yakusheva^{2,3}

¹ Johannes Gutenberg University Mainz, 55099 Mainz, Germany

² GSI Helmholtz Center for Heavy-Ion Research, 64291 Darmstadt, Germany

³ Helmholtz Institute Mainz, 55099 Mainz, Germany

⁴ Advanced Science Research Center, JAEA, Tokai-mura, Ibaraki 319-1195, Japan

⁵ Lawrence Livermore National Laboratory, Livermore, CA, USA

Renewed interest in multi-nucleon transfer reactions as a promising tool for the production of neutron-rich transactinide isotopes [1-4] has motivated us to perform a $^{48}\text{Ca}+^{248}\text{Cm}$ bombardment at an incident energy 10% above the Coulomb barrier to study emission-angle resolved kinetic energies of isotopes of Bk through Fm produced in such reactions. The isotopes of interest implanted into a stack of Ni foils mounted behind the target, see Fig. 1. They were isolated off-line using radiochemical separations and the obtained samples were measured using γ spectroscopy. This way, long-lived isotopes with mass numbers between 246 and 256 were accessible.

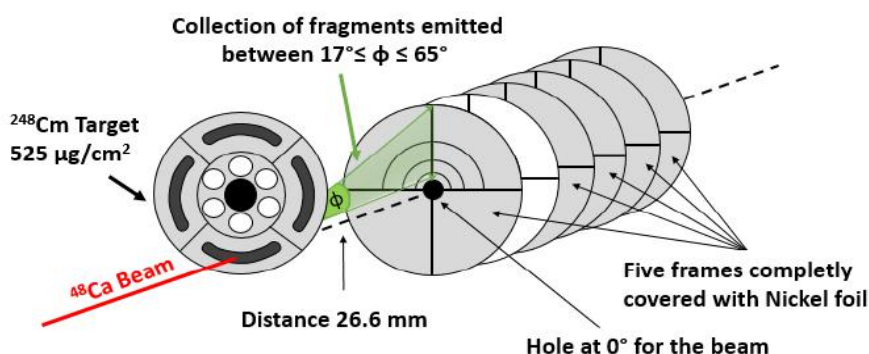


Figure 1: Schematic of the experimental setup: Five frames were completely covered with Ni-catcher foils of different thicknesses ($1 \times 3 \mu\text{m}$, $3 \times 1 \mu\text{m}$ and $1 \times 5 \mu\text{m}$). The first frame was designed to stop sputtered ^{248}Cm target material. On the second frame, only one quadrant was covered with a $5 \mu\text{m}$ nickel foil to catch all transfer products emitted into this quadrant to provide a 100 % reference.

Irradiation of ^{248}Cm with ^{48}Ca ions was performed at the TASCA [5] target position at a beam energy of 5.78 MeV/u, which corresponds to a center of mass energy of 220 MeV in the center of target. At the GSI Helmholtzzentrum für Schwerionenforschung, Darmstadt, the target was irradiated for 10 hours with an average beam intensity of 4.6×10^{12} particles/s. We used the stacked catcher foil technique to obtain information about the ranges of produced actinide isotopes in several few- μm thick Ni-foils, covering laboratory angles from $\phi = 17^\circ - 65^\circ$. Each foil was divided into four arc-segments, which collected reaction products emitted in different angular ranges. This allowed to simultaneously measuring both recoil ranges and angular distributions. After end of bombardment, the foils were dissolved in dilute nitric acid, tracer activities of Lu and Eu were added for chemical yield determination, and the activities were co-precipitated with $\text{Fe}(\text{OH})_3$ using ammonia to remove Ni.

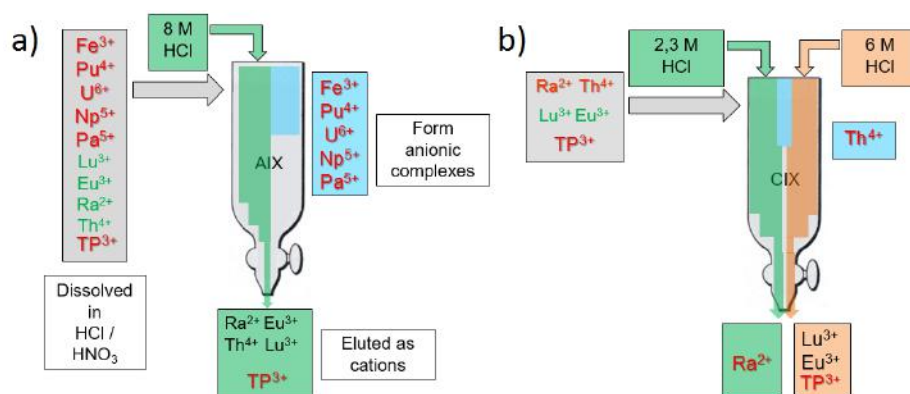


Figure 2: Schematic of the radiochemical separation. In the first step, illustrated in figure 2a, the transfer products are eluted as cations, whereas unintentional by-products in high oxidation states remain on the anionic exchange column under the formation of anionic complexes. Figure 2b indicates the chemical separation of Ra and Th using a cationic resin.

Unintentional by-products of the nuclear reaction which form anionic complexes like Fe, Pa, U, Np, and Pu could be separated on an anion-exchange column in 8 M HCl, Fig. 2a. In the next step of purification, Fig. 2b, the transfer products got separated from Ra and Th on a cation-exchange column in 2.25 M HCl, and were finally separated on a cation-exchange column with 0.12 M α -HiB and 0.14 M α -HiB at pH=4.80 into a Fm(Es) fraction and a Cf(Bk) fraction, respectively. This chemical procedure allowed separating nuclides with adjacent atomic numbers by subsequent column chromatographic treatment. The identification of Bk-, Cf-, Es-, and Fm-isotopes was achieved by detecting α -particles, considering known cross-section ratios [4] for different isotopes of a given element, and their characteristic decay properties as well as precursor effects.

In the data analysis, the most probable number of evaporated neutrons as well as the recoil energies as function of the angular distribution were evaluated for each nuclide. The investigated parameters are the centroids of the post-neutron emission isotope distributions and their displacement from the most probable primary fragment mass numbers. The latter were calculated within Volkov's generalized Q_{gg} systematics [6] including corrections for the breaking of nucleon pairs in the multi-nucleon transfer process. Information of the angular distributions, and the total kinetic energy loss (TKEL) can be used to generate deflection functions for the visualization of the rotational movement through the nucleon-transfer process. Details of the performed experiment, the obtained results and the impact on our understanding of the kinematics of multinucleon-transfer reactions will be discussed at the conference.

References

- [1] V. Zagrebaev *et al.*, *Nucl. Phys. C* **834**, 366c (2010).
- [2] W. Greiner *et al.*, *Nucl. Phys. A* **834**, 323c (2010).
- [3] J.V. Kratz *et al.*, *Phys. Rev. C* **88**, 054615 (2013).
- [4] D.C. Hoffman *et al.*, *Phys. Rev. C* **31**, 1763 (1985)
- [4] J.V. Kratz *et al.*, *Nucl. Phys. A* **944**, 117 (2015).
- [5] C.E. Düllmann, *Nucl. Inst. And Meth. B* **266**, 4123 (2008)
- [6] V.V. Volkov, *Proc. Int. Conf. on Reactions between Complex Nuclei, Nashville 1974*, (North Holland, Amsterdam) Vol. II, 363 (1974).

Speeding up gas-phase chemistry to access elements beyond Fl

S. Götz^{1,2,3}, M. Block^{1,2,3}, Ch.E. Düllmann^{1,2,3}, M. Götz^{1,2,3}, E. Jäger², O. Kaleja^{2,4}, J. Krier², L. Lens^{1,2,3}, A.K. Mistry^{1,2}, S. Raeder^{1,2}, A. Yakushev^{1,2}

¹Helmholtz Institut Mainz, Germany

²GSI, Darmstadt, Germany

³University of Mainz, Germany

⁴Technical University of Darmstadt, Germany

Since the first isothermal gas chromatography studies of rutherfordium (Rf, $Z = 104$), gas-phase separation procedures have grown in importance for studies of the heaviest elements [1, 2]. Currently, time gas-phase chemical techniques allow for elucidating the influence of relativistic effects on the chemical properties of the SuperHeavy Elements (SHE). The heaviest elements, which had their chemical properties reproducibly studied with gas chromatography studies, are copernicium (Cn, $Z = 112$) and flerovium (Fl, $Z = 114$). Due to the low production rates and short half-lives, $T_{1/2}$, only single atoms are available in chemical experiments. Nevertheless, the required sensitivity can be achieved, best by combining chemical setups with electromagnetic preselectors [3]. The gas chromatographic separation system, at which the α -particle spectroscopy and spontaneous-fission detection simultaneously takes place, is connected directly to a Recoil Transfer Chamber (RTC) mounted in the focal plane of the separator, and flushed with rapidly flowing gas. The combination of the chromatography detector COMPACT with the gas-filled separator TASCA could be established at GSI, Darmstadt. The successful gas-chromatography studies of Fl demonstrate the enormous potential of this combination of two-separation techniques for the one-atom-at-time level. A detailed description of the Fl experiments is given in a separate contribution [4]. The extraction of the isotopes of interest with gas flow is the most time-consuming step in the experiments performed with the current TASCA- COMPACT setup. Gas chromatographic techniques, which rely purely on flowing gas to flush the produced isotopes into the chromatography detector, are applicable to isotopes with half-lives that are longer than about 0.5 seconds. Besides Cn and Fl, also element 113 is in reach with this technique, see a separate contribution [5]. Looking at elements beyond Fl, the extraction time of typically 0.5 s is significantly longer than the half-life of the most long-lived isotopes of all elements with $Z > 114$. For element 115, for example, the most long-lived currently known isotope is $^{288}\text{115}$ with $T_{1/2} = 170 \left(\begin{smallmatrix} +40 \\ -30 \end{smallmatrix} \right)$ ms [6]. Thus in a setup using COMPACT coupled to TASCA with an RTC, $^{288}\text{115}$ would predominantly decay in the RTC before reaching COMPACT. No chemical studies with element 115 have been performed to date. To embark on such studies, a faster extraction technique must be established. We have started the development of such an optimized setup. For future experiments with element 115 and beyond, the RTC will be replaced by a gas-catcher, as it is used in many nuclear physics experiments [7, 9], see Fig. 1.

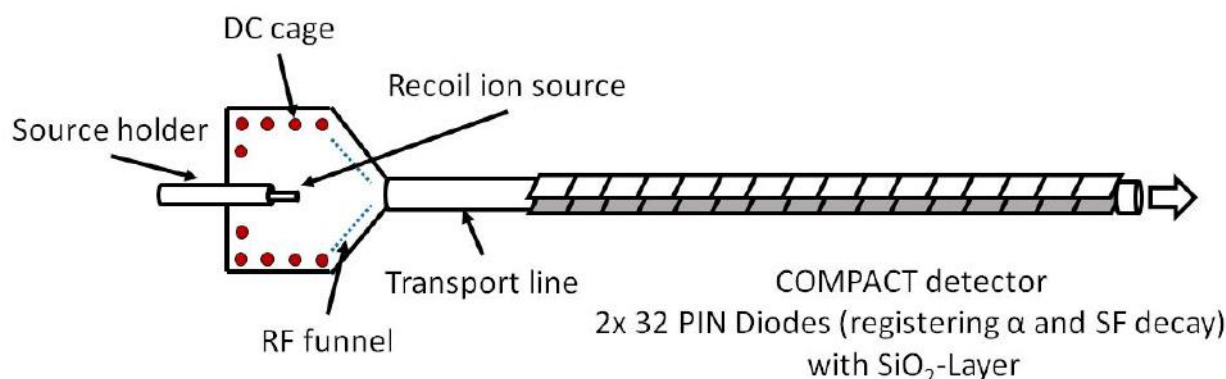


Fig. 1. Gas-catcher-COMPACT setup for future experiments with element 115

At GSI, this type of gas-catcher is used behind the SHIP-separator for thermalization and extraction of charged evaporation residues [9, 10]. The objective of this work is to develop methods suitable to study chemical properties of significantly more short-lived isotopes with $T_{1/2}$ reaching down to tens of milliseconds. A first offline experiment with this new gas-catcher in combination with a COMPACT detector setup, which is shown

in figure 1, was performed in April 2016. For a determination of the extraction efficiency the ^{219}Rn recoil ions from a 8 kBq ^{223}Ra source, were used. This recoil ion source is located at the end of a source holder and through this it is possible to introduce the ^{219}Rn ions into the centre of the DC cage, filled with ultrapure helium gas (He 4.6, flow rate = 0,05 L min⁻¹), kept a pressure of 50 – 100 mbar. The DC-electrode system in the DC cage consists of 5 cylindrical electrodes to achieve a homogeneous electric field gradient for the acceleration of the ions towards the funnel structure. The radio frequency (RF) funnel consists of 40 ring electrodes with decreasing electrode diameter. The principle of the funnel is based on a DC potential gradient dragging the ions to the exit hole in combination with a repulsive RF field to avoid collisions of the ions with the electrodes. After the outlet of the gas-catcher, the ions are transported with the gas flow through a Teflon capillary and a short steel capillary (used for neutralization of the ions) to the COMPACT detector array. This neutralization is needed, because the element of interest has to be present in elemental form for the gas-chromatography. The COMPACT array consisted of 32 positive-intrinsic-negative (PIN) silicon photodiodes ((10 × 10) mm² active area) covered with a SiO₂ surface.

The gas-catcher is characterized and prepared for a future planned online experiment. The main quality factors for the performance of a gas-catcher are the extraction efficiency as well as the extraction time. The emanated ions from the ^{219}Rn recoil ion source are accelerated by the electric fields (10 V/cm) through the segmented DC cage and the funnel structure. The achieved extraction time from the gas cell with this setup is on the order of few tens of milliseconds. Immediately after leaving the gas-catcher, the ions are neutralized by encounters with the steel capillary wall. After the transport line the atoms are directed by a gas flow into the subsequent COMPACT detector, where their radioactive decay is registered.

The experimental details and the results of this first offline experiment with the new gas-catcher-COMPACT setup will be presented.

- [1] M. Schädel (Ed.), The Chemistry of the Superheavy Elements, Kluwer Academic Publishers, Dordrecht, The Netherlands, 2003.
- [2] A. Türler *et al.*, Nucl. Phys. A **944**, 640 (2015)..
- [3] A. Yakushev *et al.*, Inorg. Chem. **53**, 1624 (2014).
- [4] L. Lens *et al.*, contribution to NRC 9.
- [5] A. Yakushev *et al.*, contribution to NRC 9.
- [6] D. Rudolph *et al.*, AIP Conf. Proc. **1681**, 030015-1 (2015).
- [7] M. Wada *et al.*, Nucl. Instrum. Methods B **204**, 570 (2003).
- [8] G. Savard *et al.*, Nucl. Instrum. Methods B **204**, 582 (2003).
- [9] M. Block *et al.*, Eur. Phys. J. D **45**, 39 (2007).
- [10] M. Block *et al.*, Nature **463**, 785 (2010).

Production and decay studies of ^{261}Rf , ^{262}Db , ^{265}Sg , and ^{266}Bh for superheavy element chemistry

H. Haba,¹ F. Fan,² D. Kaji,¹ Y. Kasamatsu,³ H. Kikunaga,⁴ Y. Komori,¹ N. Kondo,³ H. Kudo,⁵ K. Morimoto,¹ K. Morita,^{1,6} M. Murakami,¹ K. Nishio,⁷ K. Ooe,⁵ Z. Qin,² N. Sato,¹ A. Shinohara,³ M. Takeyama,^{1,8} T. Tanaka,^{1,6} A. Toyoshima,⁷ K. Tsukada,⁷ Y. Wakabayashi,¹ Y. Wang,² S. Yamaki,¹ S. Yano,¹ Y. Yasuda,³ T. Yokokita,³ and A. Yoneda¹

¹*Nishina Center for Accelerator-Based Science, RIKEN, Wako, Saitama 351-0198, Japan*

²*Institute of Modern Physics, Chinese Academy of Sciences, Lanzhou 730000, China*

³*Graduate School of Science, Osaka University, Toyonaka, Osaka 560-0043, Japan*

⁴*Research Center for Electron Photon Science, Tohoku University, Sendai, Miyagi 982-0826, Japan*

⁵*Department of Chemistry, Niigata University, Niigata, Niigata 950-2181, Japan*

⁶*Department of Physics, Kyushu University, Fukuoka, Fukuoka 812-8581, Japan*

⁷*Advanced Science Research Center, Japan Atomic Energy Agency, Tokai, Ibaraki 319-1195, Japan*

⁸*Graduate School of Science and Engineering, Yamagata University, Yamagata, Yamagata 990-8560, Japan*

Chemical characterization of superheavy elements (SHEs, atomic number $Z \geq 104$) is an extremely interesting and challenging subject in modern nuclear and radiochemistry [1,2]. We developed a gas-jet transport system coupled to the GAs-filled Recoil Ion Separator (GARIS) at the RIKEN Linear Accelerator (RILAC) as shown in Fig. 1. This system is a promising approach for exploring new frontiers in SHE chemistry; (i) background radioactivities originating from unwanted by-products are strongly suppressed, (ii) an intense primary heavy-ion beam is absent in the gas-jet chamber and hence a stable and high gas-jet transport yield is achieved, and (iii) the beam-free conditions also make it possible to investigate new chemical reactions. The long-lived isotopes of ^{261}Rf ($Z = 104$), ^{262}Db ($Z = 105$), and ^{265}Sg ($Z = 106$) available for chemistry studies were produced in the $^{248}\text{Cm}(^{18}\text{O},5n)$, $^{248}\text{Cm}(^{19}\text{F},5n)$, and $^{248}\text{Cm}(^{22}\text{Ne},5n)$ reactions, respectively [3–6]. The evaporation residues of interest were separated in flight from the beam particles and the majority of the nuclear transfer products by GARIS, and were guided into the gas-jet chamber at the focal plane of GARIS. The evaporation residues were then thermalized in helium gas, attached to potassium chloride aerosol particles, and were extracted through a Teflon capillary to a chemistry laboratory. The production cross sections and decay properties of $^{261}\text{Rf}^{a,b}$, ^{262}Db , and $^{265}\text{Sg}^{a,b}$ were investigated in detail using a rotating wheel apparatus MANON for α and Spontaneous Fission (SF) spectrometry under low background conditions. Using the pre-separated ^{265}Sg atoms, chemical synthesis and gas-chromatographic analysis of the first organometallic compound of SHEs, $\text{Sg}(\text{CO})_6$ were successfully conducted [7]. A rapid solvent extraction apparatus coupled to the GARIS gas-jet system is under development for aqueous chemistry studies of the heaviest SHEs such as Sg and Bh ($Z = 107$) [8]. In the conference, preliminary results on the production of ^{266}Bh in the $^{248}\text{Cm}(^{23}\text{Na},5n)$ reaction will be also presented.

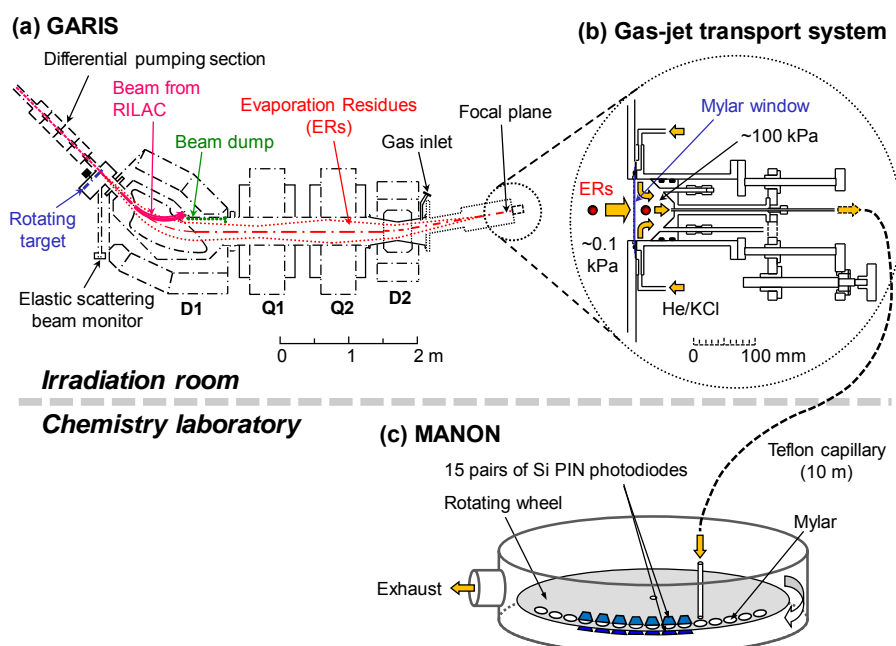


Fig. 1. (a) RIKEN GAs-filled Recoil Ion Separator (GARIS) at the RIKEN Linear Accelerator (RILAC). (b) Gas-jet transport system installed to the focal plane of GARIS. (c) The rotating wheel apparatus MANON for α /SF-spectrometry.

References

- [1] The chemistry of superheavy elements, 2nd ed., edited by M. Schädel and D. Shaughnessy, Springer, Heidelberg, New York, Dordrecht, and London, 2013.
- [2] A. Türler and V. Pershina, Chem. Rev. **113**, 1237 (2013).
- [3] H. Haba et al., Chem. Lett. **38**, 426 (2009).
- [4] H. Haba et al., Phys. Rev. C **83**, 034602 (2011).
- [5] H. Haba et al., Phys. Rev. C **85**, 024611 (2012).
- [6] H. Haba et al., Phys. Rev. C **89**, 024618 (2014).
- [7] J. Even et al., Science **345**, 1491 (2014).
- [8] Y. Komori et al., a contribution to NRC9.

Development of a rapid solvent extraction apparatus for aqueous chemistry of the heaviest elements

Y. Komori¹, H. Haba¹, K. Ooe², A. Toyoshima³, A. Mitsukai³, M. Murakami^{1,2}, D. Sato², R. Motoyama², S. Yano¹, K. Watanabe¹, A. Sakaguchi⁴, J. Inagaki⁴, H. Kikunaga⁵, S. Wulff⁶ and J. P. Omtvedt⁶

¹*Nishina Center for Accelerator-Based Science, RIKEN, Wako, Saitama 351-0198, Japan*

²*Graduate School of Science and Technology, Niigata University, Niigata, Niigata 950-2181, Japan*

³*Japan Atomic Energy Agency, Tokai, Ibaraki 319-1195, Japan*

⁴*Faculty of Pure and Applied Sciences, University of Tsukuba, Tsukuba, Ibaraki 305-8571, Japan*

⁵*Research Center for Electron Photon Science, Tohoku University, Sendai, Miyagi 982-0826, Japan*

⁶*Department of Chemistry, University of Oslo, Blindern, NO-0315 Oslo, Norway*

Aqueous chemistry studies of superheavy elements (SHEs with atomic number $Z \geq 104$) have so far been carried out for element 104, Rf, up to element 106, Sg. However, following the pioneering studies on complexation and hydrolysis of Sg in the 1990s [1], there have been no reports on the aqueous chemistry of Sg and the heavier SHEs. It is extremely difficult to perform aqueous chemistry experiments with SHE nuclides due to their decreasing production yields and half-lives with increasing Z . Furthermore, a huge amount of background radioactivities of by-products become unavoidable in detection of α particles and SF fragments from the SHE nuclei. To overcome these problems, we installed a gas-jet transport system to the RIKEN GAs-filled Recoil Ion Separator (GARIS) as a preseparator for the chemistry experiments of SHEs [2].

Toward the aqueous chemistry of Sg and element 107, Bh, we have been developing a rapid solvent extraction apparatus coupled to the GARIS gas-jet system as shown in Fig. 1. This new chemistry system consists of a continuous dissolution apparatus (Membrane DeGasser: MDG) [3], the Flow Solvent Extractor (FSE) consisting of a Teflon capillary and a phase separator, and a flow liquid scintillation detector for α /SF-spectrometry. We investigated performances of the MDG and the FSE using $^{92,94m}\text{Tc}$ ($T_{1/2} = 4.25, 293$ min) and ^{181}Re ($T_{1/2} = 20$ h) produced in the $^{nat}\text{Mo}(d,xn)$ and $^{nat}\text{W}(d,xn)$ reactions, respectively, at the RIKEN AVF cyclotron. The radionuclides were rapidly transported through a 2.0-mm i.d. \times 10-m long capillary by a carrier gas seeded with KCl aerosol-particles to the MDG placed in a radiochemistry laboratory. In the MDG they were continuously dissolved in 0.5 M and 1 M HNO_3 at a flow rate of 1 mL/min. The liquid output of the MDG was mixed with an organic phase of tri-*n*-octylamine (TOA) in toluene upon entering the FSE. After the phase separation, both aqueous and organic phases from the FSE were subjected to the γ -ray spectrometry in order to determine the distribution ratios (D) in the liquid-liquid extraction. We measured the D values of Tc and Re in 1 M HNO_3 by varying the FSE capillary length from 5 cm to 100 cm to change the extraction time. We also varied the concentration of TOA from 0.005 M to 0.1 M to evaluate an applicable D range with the FSE. These D values were compared with those obtained in the batch extraction under 3-min vigorous shaking.

We found that the extraction equilibrium of Tc and Re in 1 M HNO_3 can be obtained with a 0.5-mm i.d. \times 40-cm capillary at a flow rate of 1 mL/min for both aqueous and organic solutions. The time required for the solutions to pass through such a 40-cm capillary is roughly calculated to be 2.4 s, which is short enough to perform the solvent extraction of ^{266}Bh ($T_{1/2} = \sim 10$ s) produced in the $^{248}\text{Cm}(^{23}\text{Na},5n)$ reaction [4]. We also found that the D values of Tc and Re increase with increasing TOA concentration. The D values with the MDG-FSE were consistent with those in the batch extraction in equilibrium except for the Tc results at TOA concentration of > 0.05 M, where the D values obtained for Tc with the MDG-FSE were slightly smaller than those in the batch extraction. A prototype of the flow liquid scintillation detector is also under development. We plan to perform solvent extraction of ^{174}Re ($T_{1/2} = 2.40$ min) produced in the $^{nat}\text{Gd}(^{23}\text{Na},xn)$ reactions in the HNO_3 -TOA/toluene system by coupling the MDG-FSE to the GARIS gas-jet system. The result of the model experiment for Bh will be also presented in the conference.

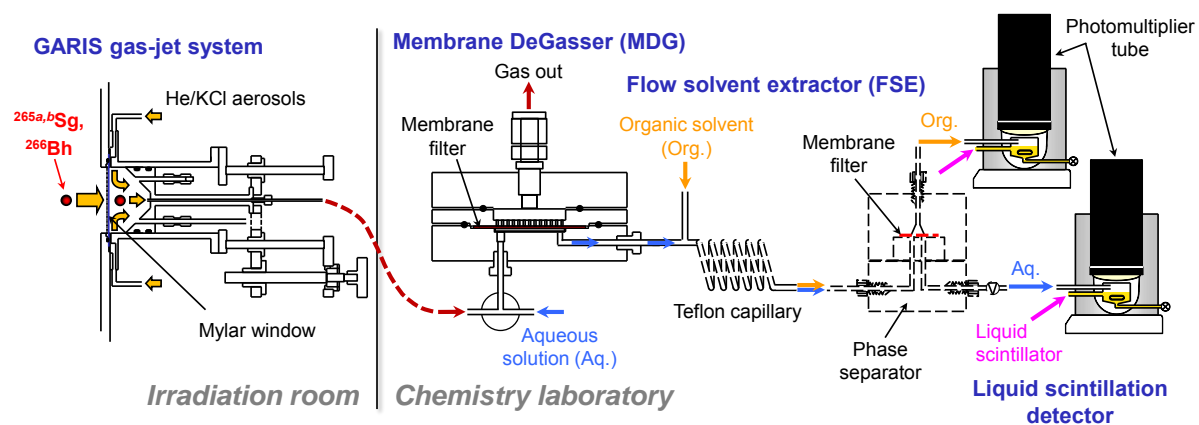


Fig. 1.

Layout of a rapid solvent extraction apparatus coupled to the GARIS gas-jet system.

References

- [1] M. Schädel *et al.*, Radiochim. Acta. **77**, 149 (1997); M. Schädel *et al.*, *ibid.* **83**, 163 (1998).
- [2] H. Haba *et al.*, Chem. Lett. **38**, 426 (2009).
- [3] K. Ooe *et al.*, J. Radioanal. Nucl. Chem. **303**, 1317 (2015).
- [4] H. Haba *et al.*, a contribution to NRC9.

Single-atom flerovium chemistry at TASCA

L. Lens^{1,2}, A. Yakushev^{2,3}, Ch.E. Düllmann^{1,2,3}, M. Asai⁴, M. Block^{1,2,3}, H.M. David², J. Despotopulos⁵, A. Di Nitto^{1,2}, K. Eberhardt^{1,3}, M. Götz^{1,2,3}, S. Götz^{1,2,3}, H. Haba⁶, L. Harkness-Brennan⁷, F.P. Heßberger^{2,3}, R.-D. Herzberg⁷, D. Hinde⁸, J. Hoffmann², A. Hübner², E. Jäger², D. Judson⁷, J. Khuyagbaatar^{2,3}, B. Kindler², Y. Komori⁶, J. Konki⁹, J.V. Kratz¹, J. Krier², N. Kurz², M. Laatiaoui^{2,3}, S. Lahiri¹⁰, B. Lommel², M. Maiti¹¹, A.K. Mistry^{2,3}, C. Mokry^{1,3}, K. Moody⁵, Y. Nagame⁴, J.P. Omtvedt¹², P. Papadakis⁹, V. Pershina², D. Rudolph¹³, J. Runke^{1,2}, M. Schädel^{2,4}, P. Scharrer^{1,2,3}, T. Sato⁴, D. Shaughnessy⁵, B. Schausten², J. Steiner², P. Thörle-Pospiech^{1,3}, N. Trautmann¹, K. Tsukada⁴, J. Uusitalo⁹, A. Ward⁷, M. Wegrzecki¹⁴, E. Williams⁸, N. Wiehl^{1,3}, V. Yakusheva^{2,3}

¹Univ. Mainz, Germany;

²GSI, Darmstadt, Germany;

³Helmholtz-Institut Mainz, Germany;

⁴JAEA, Tokai, Japan; ⁵LLNL Livermore, USA;

⁶RIKEN, Wako-shi, Japan;

⁷Univ. Liverpool, UK;

⁸ANU Canberra, Australia;

⁹Univ. Jyväskylä, Finland;

¹⁰SINP Kolkata, India;

¹¹IITR Uttarakhand, India;

¹²Univ. Oslo, Norway;

¹³Lund Univ., Sweden;

¹⁴ITE, Warsaw, Poland

The chemical and physical properties of transactinide elements are influenced by strong relativistic effects [1]. In current transactinide element research, the determination of chemical properties of element 114 (flerovium, Fl) is a topic of high interest. Early atomic calculations indicated that Fl could be chemically inert [2]. More recent relativistic calculations confirm that it should be more inert than its lighter homolog Pb. Nevertheless, it is predicted to have a distinct metallic character [3]. Experimental studies on Fl are challenging, due to its low production rates and relatively short half-lives. In order to reduce the amount of unwanted background, chemical experiments can be performed behind a physical pre-separator. The method of background reduction will be presented in a separate contribution [4]. The detection setup requires registration of single atoms through their characteristic nuclear decay in a wide volatility range, from the rather reactive and non-volatile metal Pb, up to the inert noble gas Rn.

The first experimental study to measure the properties of Fl was performed by a PSI/FLNR- collaboration without pre-separation [5]. Based on the observation of three radioactive decays attributed to Fl isotopes, a rather weak physisorption on gold, $-\Delta H_{\text{ads}}^{\text{Au}}(\text{Fl}) = 34_{-11}^{+54}$ kJ/mol, was inferred [5]. The first chemical investigation of Fl using a pre-separator was performed at the gas-filled recoil separator TASCA, at GSI, Darmstadt. Two Fl events were detected on gold at room temperature ($-\Delta H_{\text{ads}}^{\text{Au}}(\text{Fl}) > 48$ kJ/mol) with negligible background [6]. Based on this result, the formation of a metal-metal bond of Fl with gold was inferred. Limited statistics and barely consistent results of these two experiments called for advanced experimental studies to clarify this chemical property of Fl. Additional experiments on Fl without pre-separator were conducted by the PSI-FLNR collaboration, but no Fl events were detected [7].

Prior to further investigations on Fl at TASCA, several improvements to the experimental set-up were performed, mainly to optimize the overall efficiency. This was assessed in multiple experiments with short-lived Hg and Pb isotopes. Several Recoil Transfer Chambers (RTC) [8] were developed and operational parameters were optimized to minimize the transportation time of Fl into the detection setup. The detection set-up consisted of multiple COMPACT type detector arrays [9], covered with quartz or gold surfaces, see Fig. 1. Based on the different reactivity of Pb and Hg towards quartz, a separation of these elements was achieved [10]. Pb was retained in the first COMPACT array on quartz, whereas Hg passed through and

deposited on the Au surface at room temperature. The noble gas Rn only deposited at the very cold end of the third Au covered COMPACT detector array, see Fig. 1.

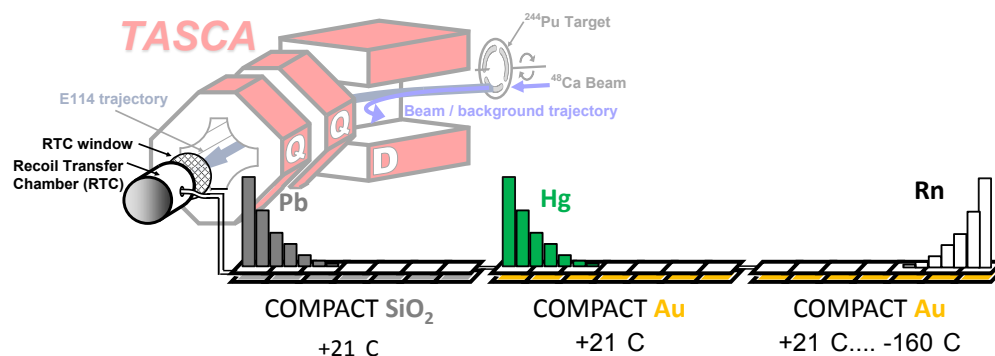


Fig. 1: Deposition of Pb, Hg and Rn in the COMPACT³ setup, used in 2014.

After the preparatory experiments two successful FI studies were performed at TASCA in 2014/2015. Several radioactive decays of FI were observed. The chemical analysis is still ongoing, and will be presented at this conference. With the optimized experimental set-up behind TASCA, the chemical properties of superheavy elements $Z \geq 112$ can be investigated in a very wide volatility and reactivity range.

References

- [1] P. Pyykkö *et al.*, Chem. Rev. 88, 563 (1988)
- [2] K.S. J. Pitzer *et al.*, Chem. Phys. 63, 1032 (1975)
- [3] V. Pershina, Radiochim. Acta. 99, 459 (2011)
- [4] A. Yakushev *et al.*, contribution to NRC 9
- [5] R. Eichler *et al.*, Radiochim. Acta 98, 133 (2010)
- [6] A. Yakushev *et al.*, Inorg. Chem. 53, 1624 (2014)
- [7] A. Türler, R. Eichler, A. Yakushev., Nucl. Phys. A 944, 640 (2015)
- [8] J. Even *et al.*, Nuclear Instruments and Methods in Physics Research A 638, 157 (2011)
- [9] J. Dvorak *et al.*, Phys. Rev. Lett., 97, 242501 (2006)
- [10] L. Lens *et al.*, GSI Sci. Rep. 2014 p. 183 (2015)

Kinetic studies on the mercury – selenium interaction using inverse thermochromatography

A. Madumarov¹, N. M. Chiera^{2,3}, N. Aksenov¹, R. Eichler^{2,3}, D. Piguet², A. Türlér^{2,3}, A. Vögele²

¹Flerov Laboratory of Nuclear Reactions, JINR, Dubna, Russian Federation;

²Paul Scherrer Institute, Villigen, Switzerland

³University of Bern, Bern, Switzerland.

In preparation of chemical experiments with copernicium ($Z = 112$) and flerovium ($Z = 114$), produced in heavy ion induced nuclear fusion reactions, model experiments with mercury - copernicium's lighter homologue - were conducted. For this purpose, trigonal (t-Se, crystalline) and red amorphous selenium (a-Se) have been used as stationary phase in gas chromatographic experiments, allowing for the determination of the adsorption enthalpy limits $\Delta H_{\text{ads}}^{\text{t-Se}}(\text{Hg}) < 60 \text{ kJ/mol}$ and $-\Delta H_{\text{ads}}^{\text{red-Se}}(\text{Hg}) > 85 \text{ kJ/mol}$, respectively [1]. Considering the thermodynamic stability of HgSe , a kinetic hindrance on the adsorption behavior of elemental mercury towards trigonal selenium is observed. Unexpectedly, first on-line experiments with copernicium indicated that Cn reacted with trigonal Se with a lower kinetic formation hindrance compared to the interaction of Hg with t-Se [2]. In order to understand the kinetic process of the Hg/Se interaction towards both red amorphous and trigonal selenium allotropes, useful later on for the interpretation of the $\text{CnSe}_{(\text{s})}$ formation, inverse thermochromatographic (IT) studies will be performed [3]. This approach for the determination of the reaction kinetics is based on a two-step interaction process: 1) a reversible adsorption interaction; eventually followed by 2) an activated complex formation and the final covalent bond formation. For this purpose, an inverse thermochromatographic (IT) setup was developed (Fig.1). The aim of these IT experiments is to derive the lower temperature at which the $\text{HgSe}_{(\text{s})}$ formation is promoted on both allotropic Se surfaces. This temperature will then be used for the estimation of kinetic parameters by means of a Monte Carlo simulation approach. First experimental results will be presented.

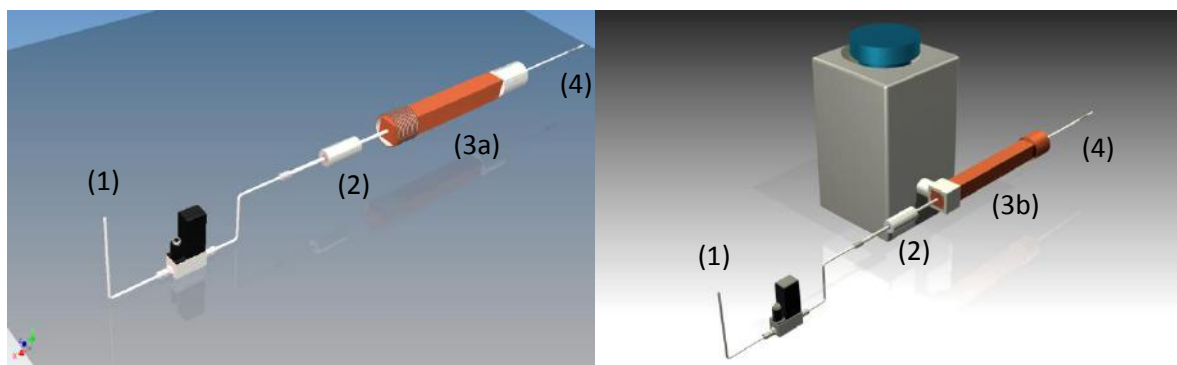


Figure 1. A He gas flow (1) is passed through a source of carrier free ^{197}Hg (2). The evaporated ^{197}Hg is transported to the chromatographic column coated with trigonal Se (3a) or red amorphous Se (3b), inserted in a copper rod where a temperature gradient is applied. The eventually not absorbed ^{197}Hg is captured by a charcoal trap (4).

References

- [1] N. M. Chiera et al., submitted to *The Journal of Radioanalytical and Nuclear Chemistry*
- [2] N. M. Chiera et al., "Towards the selenides of copernicium and flerovium: copernicium - selenium bond formation observed", *LCH Annual Report*, 2015
- [3] N. M. Chiera et al., "Kinetic studies on the mercury – selenium interaction", *LCH Annual Report*, 2015

Extraction behavior of rutherfordium as a cationic fluoride complex with a TTA chelate extractant from HF/HNO₃ acidic solutions

A. Yokoyama¹, Y. Kitayama², Y. Fukuda², H. Kikunaga³, M. Murakami⁴, Y. Komori⁴, S. Yano⁴,
H. Haba⁴, K. Tsukada⁵, and A. Toyoshima⁵

¹*Institute of Science and Engineering, Kanazawa University, Kanazawa, Ishikawa, Japan*

²*Graduate School of Natural Science and Technology, Kanazawa University, Kanazawa, Ishikawa, Japan*

³*Research Center for Electron Photon Science, Tohoku University, Sendai, Miyagi, Japan*

⁴*Nishina Center for Accelerator-Based Science, RIKEN, Wako, Saitama, Japan*

⁵*Advanced Science Research Center, Japan Atomic Energy Agency, Tokai, Ibaraki, Japan*

We have studied a reversed-phase-chromatography technique with TTA (2-thenoyltrifluoroacetone) as a chelate extractant to clarify chemical properties of a cationic fluoride-complex of a superheavy element, rutherfordium (Rf). The resin containing a TTA solution in n-octanol has been newly developed for that purpose. In this study, studied are chemical behaviors of Rf with this technique in various HF/HNO₃ solutions. A nuclide of ²⁶¹Rf with a half-life of 68 s was produced in the ²⁴⁸Cm(¹⁸O, 5n)²⁶¹Rf reaction at the RIKEN K70 AVF cyclotron. Short-lived nuclides of ⁸⁵Zr and ¹⁶⁹Hf were also produced in the ^{nat}Ge(¹⁸O, xn)⁸⁵Zr and ^{nat}Gd(¹⁸O, xn)¹⁶⁹Hf reactions, respectively, to be compared with a result of Rf. The reaction products were rapidly transported with a KCl/He gas-jet system to a chemistry laboratory to investigate the TTA-chromatographic behavior of Rf in HF/0.01 M HNO₃ solutions with an on-line automated chemistry-apparatus (ARCA) and a rapid α /SF detection system for aqueous chemistry of superheavy elements at RIKEN.

The isoto

pe ²⁶¹Rf used in the experiments decays into its daughter ²⁵⁷No. The α -particle energies of ²⁵⁷No ($E_\alpha = 8.22, 8.32$ MeV) are close to that of ²⁶¹Rf ($E_\alpha = 8.28$ MeV). Therefore, these energies are hard to distinguish from each other. In the Rf experiments, two types of ²⁵⁷No α -events are supposed to be observed. One is from ²⁵⁷No produced from α -decay of ²⁶¹Rf after its chemical separation. It reflects the chemical behavior of Rf. The other of ²⁵⁷No, which is deposited during the collection of ²⁶¹Rf, reflects the chemical behavior of No. In order to correct the contribution of ²⁵⁷No, we observed the adsorption behavior of No in the same systems of the Rf experiments.

Similarly to the Rf experiments, the isotope ²⁵⁵No ($T_{1/2} = 3.10$ min) was produced in the ²⁴⁸Cm(¹²C, 5n) reaction with an 84 MeV ¹²C beam at the RIKEN K70 AVF cyclotron and assayed with a rapid α /SF detection system for aqueous chemistry of super-heavy elements at RIKEN. In order to determine the chemical yield, ¹⁶²Yb was simultaneously produced from Gd content in the Cm target and was measured by a Ge detector after measurement of ²⁵⁵No.

We observed 222 α events (8.00–8.40 MeV) including 29 time-correlated α particle pairs from ²⁶¹Rf and its daughter nuclide ²⁵⁷No in 1771 cycles of the column chromatography experiment for Rf. Besides, from 195 cycles of the No experiments, a total of 1042 α -events ²⁵⁵No were registered in the energy range of 7.60–8.20 MeV. In the experiments, the percent adsorptions, %ads with a fixed volume of the effluent were evaluated by using the following equation:

$$\%ads = Fr2 / (Fr1 + Fr2) \times 100, \quad (1)$$

where Fr1 and Fr2 are the radioactivities observed in the fraction 1 and 2, respectively. Decay of the products was taken into account in the correction for the %ads values.

The results for %ads of ²⁵⁵No as a function of $[F^-]_{eq}$ in the range of 1.93×10^{-5} to 1.66×10^{-3} M are shown in Fig. 1. together with the result for ²⁶¹Rf. In the Rf experiments, ¹ the %ads values of Rf are constant at around 60% in the $[F^-]_{eq}$ range up to 5×10^{-4} M and then steeply decreased at $[F^-]_{eq} = 9 \times 10^{-4}$ M. On the other hand, in the No experiments, it was found that the %ads values of ²⁵⁵No are less than 10% in the entire

range of $[F^-]_{eq}$. Based on the present work, it was confirmed that No is adsorbed to TTA to a small extent and the effect to %ads values of ^{261}Rf is negligible.

The adsorption coefficients, K_d values of Rf, Hf and Zr, derived from their %ads by using elution curves of Zr and Hf, are plotted versus the equilibrated F^- concentration ($[F^-]_{eq}$) in Fig. 2. The K_d value of Rf is constant in the $[F^-]_{eq}$ range up to 5×10^{-4} M and then steeply decreases at $[F^-]_{eq} = 9 \times 10^{-4}$ M, while Zr and Hf decrease in the range less than 10^{-4} M. This suggests that the cationic fluoride complexes of Rf are more stable than those of Hf at $[F^-]_{eq} > 1 \times 10^{-4}$ M. The results are consistent with previous results obtained in the cation exchange experiment¹⁾ and the theoretical prediction²⁾.

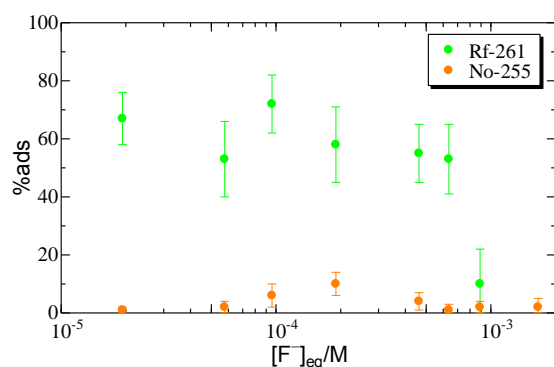


Fig. 1 Percent adsorptions, %ads, of ^{255}No and ^{261}Rf plotted as a function of $[F^-]_{eq}$ in TTA column chromatography.

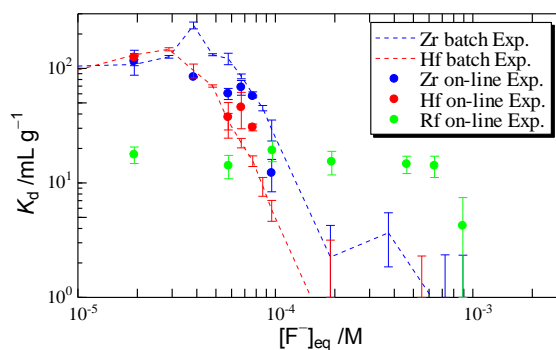


Fig. 2 The K_d values for Zr, Hf and Rf on the TTA resin as a function of the equilibrium concentration of F^- , $[F^-]_{eq}$.

References

- 1) Ishii, A. *et al.*, Chem. Lett. **37**, 288 (2008).
- 2) Pershina, V. *et al.*, Radiochim. Acta **90**, 869 (2002).

RADIONUCLIDE SPECIATION

Thermodynamics of An^{IV}DTPA complexes in biological medium: new brand values and prediction for unknown chemical systems

Lucie Bonin⁽²⁾, Jean Aupiais^{*(1)}, Mohamed Kerbaa⁽¹⁾, Philippe Moisy⁽²⁾, Sylvain Topin⁽¹⁾, Bruno Siberchicot⁽¹⁾

1) CEA, DAM, DIF, F-91297 Arpajon cedex, (2) CEA, DEN, DRCP, F-30207 Bagnols sur Cèze

Diethylenetriaminepentaacetic acid (DTPA) is a versatile polyaminocarboxylic acid used in medicine as actinide chelating agent and in the nuclear industry as component of a synergistic mixture with lactic acid for the separation lanthanide/actinide (TALSPEAK process). Despite common applications in various fields (medicine, nuclear industry, and separation sciences) the available stability constants related to actinides and in particular, the tetravalent actinides are rather scarce and scattered. Reported data for tetravalent actinides consist in a set of values obtained at only 3 ionic strengths ($I = 0.1, 0.5$, and 1 M) and two temperatures ($T = 20$, and 25 °C). They present large discrepancies up to three orders of magnitude. In radiotoxicology, the ligand usually recommended for removing actinide from the human body is DTPA but despite a common use for decorporating plutonium, we have not found the stability constants related to the system $\text{Pu}^{\text{IV}}/\text{DTPA}$, including the potential hydrolyzed form at $I = 0.1\text{ M}$ and basic pH, conditions that approximately correspond to those encountered in the human blood. The aim of this study is to obtain new consistent data for tetravalent actinides at low ionic strength, for which extrapolation down to zero can be done without adjustable parameters. Particular attention will be brought to hydrolyzed species since the pH in blood is enough high for assuming their potential presence. To achieve this goal, a unique technique able to simultaneously compare all tetravalent actinides under the same experimental conditions will be used: the capillary electrophoresis coupled with an inductively coupled plasma mass spectrometry (CE-ICPMS).

Two kinds of experiments have been carried out: at a constant $p_c\text{H}$ with various concentrations of DTPA, and at a constant ligand concentration and various pH. The first experiment allows determining the formation constant of AnDTPA^- . The second experiment was performed to determine the formation constant of $\text{An}(\text{OH})\text{DTPA}^{2-}$. Two behaviors were observed: a continuous variation of the electrophoretic mobility μ (Th, Np) or two distinct peaks as function of ligand concentration or pH (Pu). The first behavior is related to fast formation/dissociation equilibrium whereas the second one refers to the formation of strong complex or slow dissociation kinetics. An example of separation is depicted in the Figure 1 for the system $\text{Pu}/\text{OH}/\text{DTPA}$. The experiments at increasing pH showed two peaks which have been attributed to PuDTPA^- and $\text{Pu}(\text{OH})\text{DTPA}^{2-}$ compounds. The results of two experiments performed for $C_{\text{DTPA}} = 10^{-2}$ and 10^{-4} M are gathered in the Table 1. At the intersection of S-shape curve the concentrations equal and are inversely proportional to the concentration of the free ligand. To our knowledge, no other study detected and quantified the formation the Pu^{IV} hydroxo DTPA complex.

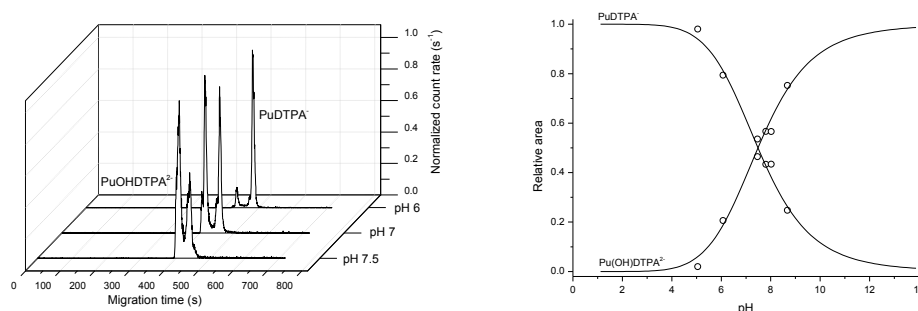


Figure 1: Left. Electropherograms of $\text{Pu}^{\text{IV}}/\text{DTPA}$ compounds as a function of the pH; $C_{\text{DTPA}} = 10^{-2}\text{ M}$, $I = 0.1\text{ M}$ TMAX ($X = \text{MES}$ or HEPES), 25 °C . Right. Relative area variation of $\text{Pu}(\text{OH})\text{DTPA}^{2-}$ and PuDTPA^- for $C_{\text{DTPA}} = 10^{-2}\text{ M}$.

⁴ M. At the inflexion point, $K = \frac{1}{[DTPA^{5-}]}$. The stability constants for the equilibrium $Pu(OH)DTPA^{2-} + H^+ \rightleftharpoons PuDTPA^- + H_2O$ is found to be 7.49 ± 0.15 .

Table 1: Log K stability constants for Pu^{4+} and DTPA at $I = 0.1$ M and $25^\circ C$.

Equilibrium/comments	$I = 0.1$ M
$Pu^{4+} + DTPA^{5-} \rightleftharpoons PuDTPA^-$	36.36 ± 0.36
$PuDTPA^- + OH^- \rightleftharpoons Pu(OH)DTPA^{2-}$	
$[DTPA] = 10^{-2}$ M	$6.44 \pm 0.31^{\#}$
$[DTPA] = 10^{-4}$ M	$6.28 \pm 0.15^{\#}$

[#] recalculated from the equilibrium $An(OH)DTPA^{2-} + H^+ \rightleftharpoons AnDTPA^- + H_2O$ and by using $pK_w = 13.775$ in 0.1 M.

Due to the capability for CE-ICPMS to simultaneously detect all species, it is possible to evaluate the stability constants of $AnDTPA$ species as well as the hydroxo form from linear trend observed along the tetravalent actinide. Two examples are reported in the Figure 2. They show the possibility to calculate the formation constant of $PaDTPA^-$ or $U(OH)DTPA^{2-}$.

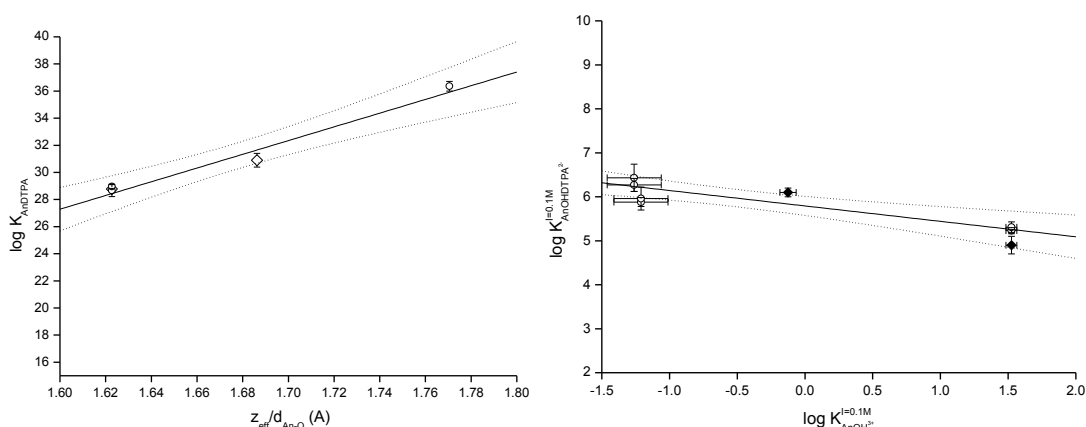


Figure 2: left. Variation of $\log K_{AnDTPA}$ as a function of the distance metal-oxygen ligand calculated by ab initio molecular dynamic (AIMD). \circ data obtained by CE-ICPMS (Th, Pu), \diamond data from literature (Th, U). Interpolated values give for Pa^{IV} and Np^{IV} : $d_{Np-O} = 2.26$ Å, $\log K_{NpDTPA} = 34.8$; $d_{Pa-O} = 2.275$ Å, $\log K_{PaDTPA} = 32.0$. Right. Variation of the formation constant of hydrolysed $AnDTPA$ species as function of the first hydrolysis of An^{IV} recalculated at 0.1 M TMAX (X = MES or HEPES) with Davies equation at $25^\circ C$; \circ data obtained by CE-ICPMS, \blacklozenge data from literature (not considered for the linear regression).

Speciation of trivalent actinides and lanthanides in body fluids

Astrid Barkleit¹, Claudia Wilke¹, Anne Heller^{1,2}, Atsushi Ikeda-Ohno¹, Thorsten Stumpf¹

¹ *Helmholtz-Zentrum Dresden-Rossendorf, Institute of Resource Ecology, Dresden, Germany;*

² *Technische Universität Dresden, Department of Biology, Institute of Zoology, Professorship of Molecular Cell Physiology and Endocrinology, Dresden, Germany*

In case of incorporation into the human body, radionuclides potentially represent serious health risks due to their chemo- and radiotoxicity. In order to assess their toxicological behavior, such as transport, metabolism, deposition, and elimination from the human organisms, the understanding of their *in vivo* chemical speciation on a molecular level is crucial. Due to their high specific radioactivity with very long half-lives, trivalent actinides (An(III)) are considered to be some of the problematic radionuclides particularly in the geological repository of radioactive wastes. The reliable safety and health assessment of the waste repositories requires the information about the behavior of An(III) *in vivo*. Nevertheless, little is known about the speciation of not only An(III) but also trivalent lanthanides (Ln(III)), non-radioactive chemical analogs of An(III), in body fluids.

In order to improve our understanding of the behavior of An(III) and Ln(III) in the human body, the present study focuses on the chemical speciation of An(III) and Ln(III) in the gastrointestinal tract. The human gastrointestinal system was simulated by using an *in vitro* digestion model, which was developed by Oomen et al. [1] and is the basis of an international unified bioaccessibility protocol [2]. To verify the model, natural human saliva samples were included in the speciation investigation. Because An(III) and Ln(III) are excreted mainly by the kidney [3, 4], their speciation in natural human urine was investigated to complete the metabolic pathway from oral ingestion through the digestive system till elimination.

The speciation of curium(III) (Cm(III)) and europium(III) (Eu(III)) in the gastrointestinal tract as well as in human natural saliva and urine has been studied by means of time-resolved laser-induced fluorescence spectroscopy (TRLFS). The standard model body fluids and the natural saliva and urine samples were spiked *in vitro* with Cm(III) and Eu(III) in trace metal concentrations.

The dominant chemical species in the human saliva was identified by a comparison of the natural human sample spectra with reference spectra obtained for synthetic saliva and individual components of the body fluid. Linear combination fitting analysis on the sample spectra indicates the formation of 60-90% inorganic- and 10-40% organic species of Cm(III)/Eu(III) in the salivary media. Ternary M(III) complexes containing phosphate and carbonate anions with the additional counter-cation calcium are formed as the main inorganic species. Complexes with the digestive enzyme α -amylase and the protein mucin (to a minor extent) represent the major part of the organic species (see Figure 1).

When the M(III) reached the stomach, the metal complexes were dissociated due to the high acidic conditions. That is, Cm(III) and Eu(III) are mainly present as the aqua ion, and only a small part (about 20%) is coordinated by the protein pepsin. When entering the intestine the metal ions are strongly bound by the protective protein mucin and inorganic ligands (mainly carbonate and phosphate).

After transporting into the bloodstream and transformation into the urine via the kidney, the speciation of the metal ions strongly depends on the pH of the urine. When the pH is slightly acidic, the formation of Cm(III) and Eu(III) citrate complex dominates, whereas ternary complexes with phosphate and calcium as the main ligands and the additional participation of citrate and/or carbonate occur at around near-neutral pH [5].

These speciation studies in different body fluids pointed out that An(III) and Ln(III) are coordinated by both inorganic and organic molecules in the human body. Proteins (*e.g.* α -amylase, pepsin, mucin) would be the important organic binding partners. Furthermore, ternary inorganic complexes containing phosphate and

carbonate anions with the additional counter-cation calcium are expected to be formed as the main inorganic species in almost all the body fluids.

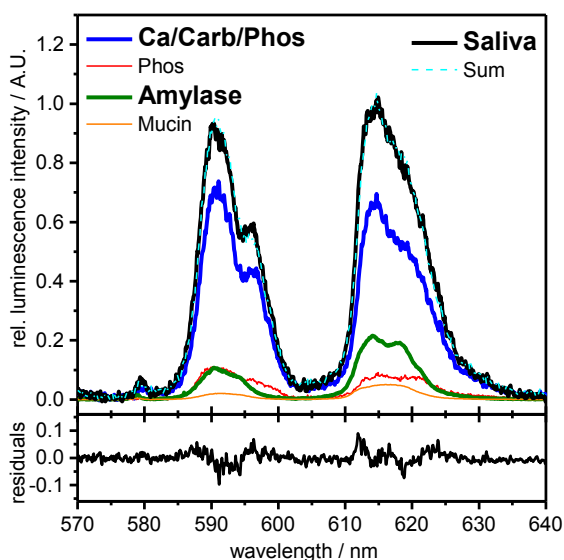


Figure 1. Linear combination fitting of a luminescence spectrum of Eu(III) in natural human saliva based on the reference spectra of the main coordinating individual components of saliva. All samples are spiked with 10 μ M Eu(III).

Acknowledgements

This work was funded by the German Research Council (Deutsche Forschungsgemeinschaft, DFG) under contract number BE 2234/10-1/2 and the Federal Ministry of Education and Research (Bundesministerium für Bildung und Forschung, BMBF) under contract number 02NUK030F.

References

- [1] Oomen, A. G., Rompelberg, C. J. M., Bruil, M. A., Dobbe, C. J. G., Pereboom, D. P. K. H., Sips, A. J. A. M., *Arch. Environ. Contam. Toxicol.* **44**, 281-287 (2003).
- [2] Wragg, J., Cave, M., Taylor, H., Basta, N., Brandon, E., Casteel, S., Gron, C., Oomen, A., van de Wiele, T., British Geological Survey Open Report OR/07/027, Keyworth, Nottingham, 90 pp. (2009).
- [3] Menetrier, F., Taylor, D. M., and Comte, A., *Appl. Radiat. Isot.* **66**, 632-647 (2008).
- [4] Taylor, D. M., Leggett, R. W., *Radiat. Prot. Dosim.* **105**, 193-198 (2003).
- [5] Heller, A., Barkleit, A., Bernhard, G., *Chem. Res. Toxicol.* **24**, 193-203 (2011).

Uranium(VI) speciation in seawater : precision on the role of earth alkali cations

M. R. Beccia¹, M. Matara-Aho^{1,2}, M. Maloubier¹, P.L. Solari³, J. Roques⁴, M. Monfort⁵, C. Moulin⁵,
C. Den Auwer¹

¹University Nice Sophia Antipolis, Institut de Chimie de Nice, UMR7272, 06108 Nice, France

²Laboratory of Radiochemistry, Department of Chemistry, University of Helsinki, FI-00014, Finland

³Synchrotron SOLEIL, MARS beam line, 91192 Gif sur Yvette, France

⁴Institut de Physique Nucléaire d'Orsay, University Paris XI Orsay, UMR8608, 91405 Orsay, France

⁵Commissariat à l'Energie Atomique, DAM/DIF/DASE 91297 Arpajon, France

The fate of radionuclides in the marine environment is a major concern in our societies^[1]. The Fukushima accident in 2011 exemplified that possible dissemination of actinides (although estimated of minor amount) and other radionuclides in seawater may occur and result in non-negligible release of radioactivity into the sea. Among the radionuclides of concern, uranium is one of the most involved elements in nuclear activities. However, very little is known about the speciation of this element in seawater^[2], mostly because it is present at the ultra-trace scale in "normal conditions" but also in accidental conditions due to enormous dilution factors. Improving knowledge on the speciation and reactivity of uranium in seawater is therefore essential to better understand its transfer mechanisms and to evaluate its global impact on the environment. This could also impact the potential industrial mining of uranium from seawater.

In the past we have investigated the chemical speciation of uranium(VI) in doped seawater at $[U(VI)] = 5 \cdot 10^{-5}$ M by coupling EXAFS measurements and theoretical calculation with the JCHESS code. We identified the $Ca_2UO_2(CO_3)_3$ as the main uranium species in these conditions.^[3] The speciation of uranium(VI) in artificial seawater, free of Ca^{2+} and Mg^{2+} ions, was also investigated, in order to get information on the role of Ca^{2+} ions in complex formation. FTIR analysis revealed that, in these conditions, a uranyl carbonate species is formed, with Sr^{2+} ions replacing Ca^{2+} ions. Strontium is structurally and chemically similar to calcium, but unlike calcium, it is detectable by EXAFS in the middle energy range. Therefore, we used Sr^{2+} as a spectroscopic probe to explore the structure of the uranyl carbonate complex. We also showed how the combination of spectroscopic analysis with quantum chemical simulations can unambiguously elucidate the structure of the main uranyl complex in seawater and the role of the earth-alkali counter-ions.

[1] Maher, K., J.R. Bargar, and G.E. Brown, *Inorg. Chem.*, **2013**, 52(7), 3510-3532.

[2] Choppin, G.R., *Mar. Chem.*, **1989**, 28(1-3), 19-26.

[3] Maloubier, M., Solari, P.L., Moisy, P., Monfort, M., Den Auwer, C., Moulin C., *Dalton Trans.* **2015**, 44(12), 5417-5427.

Actinide's valence states determination in materials: benefits and perspectives of high energy resolution fluorescence detected X-ray absorption spectrometry

R. Bès¹, K. Kvashnina^{2,3}, P. Martin⁴, J. Rothe⁵, A. C. Scheinost^{2,3}, P.L. Solari⁶, T. Vitova⁵

¹ *Antimatter and Nuclear Engineering, Department of Applied Physics, Aalto University, Finland*

² *Rossendorf Beamline (ROBL) at the European Synchrotron Radiation Facility (ESRF), France*

³ *Helmholtz Zentrum Dresden-Rossendorf (HZDR), Institute of Resource Ecology, Germany*

⁴ *CEA, DEN, DTEC, Centre d'études nucléaires de Marcoule, France*

⁵ *Karlsruhe Institute of Technology (KIT), Institute for Nuclear Waste Disposal, Germany*

⁶ *MARS beamline at the SOLEIL synchrotron, France*

Since decades, the actinide's chemistry is at the heart of a worldwide research effort due to the complex nature of their 5f electrons which change from delocalized in the early actinides to localized in the later actinides. This attractiveness is not only due to the actinide's high relevance for safety and economic performance of nuclear power plants or the sustainability of the nuclear waste management but also from a fundamental point of view as such materials show exciting interdependence between their properties and their electronic structures which in most cases remain unclear. One of the key knowledge is the correct evaluation of the valence state of actinides. Moreover, the determination of the chemical environment of actinides in natural samples is also a challenge of great importance in environmental and health physics.

To assess such property, X-ray Absorption Near Edge Spectroscopy (XANES) is a suitable element-selective method. Up to now, XANES at the L₃-edge has been the most commonly reported method to determine the oxidation states of U, Pu, Np and Am. However, despite their relative low energy range (3-4 keV) which is now mainly offset by the high photon flux available, experiments at the M_{4,5}-edge are increasingly reported because such edges allow direct probing of the 5f orbitals. Nevertheless, the accuracy is strongly limited by the core-hole broadening of the 2p_{3/2} (> 8 eV) and 3d_{3/2,5/2} (> 3 eV) initial states at the L₃ and M_{4,5}-edges respectively. To overcome the latter difficulty, the XAS experiment can be performed by using one or several crystal analyzers in the X-ray emission spectrometer setup recently developed in beamlines around the world such as MARS (SOLEIL), INE (ANKA) and ROBL (ESRF) dedicated to radioactive materials. These spectrometers are mostly based on the use of silicon and germanium crystals which, by diffracting the emitted X-rays, allows simultaneous focusing and energy discrimination with higher resolution than a conventional solid detector. This is particularly interesting in the case of natural sample where many additional fluorescence lines are present and subsequently very difficult to isolate from the signal of interest. Such method called High Energy Fluorescence Detected XANES (HERFD-XANES) or High energy Resolution XANES (HR-XANES), is situated at the edge of both X-ray Absorption and Emission Spectroscopies (XAS and XES), and allows the collection of spectra with a virtually reduced core-hole. This reduction is from 8-9 eV to 3-4 eV, and from 3-4 eV to roughly 1 eV at the actinide's L₃ and M_{4,5}-edges respectively.

The comparison between high resolution and standard XANES approaches will be discussed in terms of benefits and sensitivity for some typical actinide compounds

Speciation of ruthenium in TBP/TPH organic phases (structure and reactivity)

¹ LEFEBVRE, Claire, ¹ DUMAS, Thomas, CHARBONNEL, Marie-christine, ³ SOLARI, Pier Lorenzo

¹ CEA Marcoule, DEN/DRCP/SMCS/LILA, Bât. 181, BP 17171, 30207 Bagnols-sur-Cèze, France

² CEA Marcoule, DEN/DRCP/SMCS/DIR, Bât. 181, BP 17171, 30207 Bagnols-sur-Cèze, France

³ Synchrotron SOLEIL, L'Orme des Merisiers, BP 48, St Aubin, 91192 Gif-sur-Yvette, France

Ruthenium extraction with uranium and plutonium during the reprocessing of nuclear used fuel draws attention to it because it reduces decontamination factors and causes enhanced radiolysis of the solvent. A study was carried out on the speciation of ruthenium in both aqueous and organic phases by complementary spectroscopic techniques such FTIR and X-ray absorption spectroscopy. By providing a better understanding of ruthenium extraction mechanism, this study helps to support the modeling of the related process.

Ruthenium is one of the major fission products and draws attention to it because of the particular activity of the ¹⁰⁶Rh/¹⁰⁶Ru couple (10% of radioactive waste beta-gamma emissions). In addition ruthenium is partly extracted with uranium and plutonium during the reprocessing of the used nuclear fuel. The decontamination factors of the recoverable materials are impacted by this unwanted transfer from the nitric acid phase to the tributylphosphate (TBP) phase. With the increasing burn up of the fuels and potential use of mixed oxides fuels, the Ru extraction could become a key issue for nuclear waste treatment.

Since the beginning of nuclear waste reprocessing, several authors tried to describe ruthenium behavior in both nitric acid and TBP phases. It appeared that during dissolution, ruthenium forms trivalent nitrosyl complexes with nitrate, nitrite, hydroxo and aquo ligands. The admitted general formula is $\text{RuNO}(\text{NO}_3)_x(\text{NO}_2)_y(\text{OH})_z(\text{H}_2\text{O})_t+$ where x, y, z and t coefficients are such as $x+y+z+t = 5$ and depend on the chemical conditions (pH, concentrations of nitrates or nitrites, temperature, etc.). Apparently only the most nitrated complexes are extracted with a quantitative yield. The study of Ru complexes is made much more difficult by the co-existence of several species with low ligand exchange kinetics. There must be several extracted species, and polydispersity in both aqueous and organic phase.

In this study, different complementary spectroscopic techniques were used to have a better understanding of the ruthenium local environment in simulated reprocessing solutions. It includes mass spectrometry coupled with electrospray ionization source (ESI-MS), vibrational spectroscopy and X-ray absorption spectroscopy. Extraction isotherms of ruthenium by the TBP were also investigated varying ruthenium and nitric acid concentrations. The Ru nitrosyl form was firstly confirmed in aqueous phase, and then the coordination sphere of this core was probed, including an investigation of its hydrolysis as a function of nitric acid concentration. The ruthenium extraction mode by TBP (direct complexation with Ru and/or second sphere coordination) was investigated as a function of initial conditions. Hydrolysis effect was highlighted as well as the ruthenium speciation in the organic phases, depending on acidity of the initial solution. At the end, the aging process of ruthenium in the TBP phase was qualitatively characterized. These collected data would support process simulation codes.

X-ray absorption spectroscopy study the chemical states of U, Th and Cs absorbed in montmorillonite and MX-80

Wey-Tsang Liu², Chih-Hao Lee^{1,2}, Shih-Chin Tsai³, Tsuey-Lin Tsai⁴

1. *Institute of Nuclear Engineering and Science, National Tsing Hua University, Hsinchu, Taiwan*
2. *Department of Engineering and System Science, National Tsing Hua University, Hsinchu, Taiwan.*
3. *Nuclear Science and Technology Development Center, National Tsing Hua University, Hsinchu, Taiwan*
4. *Chemical Division, Institute of Nuclear Energy, Longtan, Taoyuan, Taiwan.*

X-ray absorption spectroscopy is a very useful tool to understand uranium ions and other fission products absorbed on the different soil samples. The chemical state and chemical bonds of the radioactive elements in the environment can be probed even at low concentration and disorder structures. Uranium oxidation states and bond distances are primarily important data for the absorption of uranium in the soil for the long term storage of radwaste.

Montmorillonite and MX80 is a layer structure. The gap of water bonding layers can be revealed by the X-ray diffraction at diffraction angles between 5-8 degrees (wavelength $\text{Cu } \alpha_1$). We find that as the soil samples contained uranium or thorium ions, the 2θ values are shifted to lower angles in comparison to those without uranium or thorium absorption. It means that the samples with uranium or thorium enlarge the distance between molecular layers. But, for other diffraction peaks at higher angles show no change after the ion absorption, which indicates the rigidity of structure within the layer of Montmorillonite.

The X-ray absorption spectroscopy experiments were carried out at 7A beamline of National Synchrotron Radiation Research Center, Taiwan. The samples with different uranium concentrations together with standard samples, UO_3 and UO_2 , were used to identify the oxidation states of uranium on the soil. Observed from the L3 edges of uranium ions, the uranium oxidation states in the Montmorillonite and MX80 sample are close to +6. The EXAFS experiments showed the bond distance of the first shell is around 0.173 nm and 0.243 nm for the second shell around the uranium ion in Montmorillonite.

In the X-ray absorption spectroscopy of Cs in Montmorillonite, we found the chemical state of CS ion is higher than valence state of 1+, which reveals a charge transfer from the Cs ions to the surrounding Montmorillonite molecule. This result implies that the Montmorillonite is a good candidate to fix the Cs ions. We also see the difference of X-ray absorption spectra at higher temperature (50-200 °C) to mimic the environment of storage of the radwaste underground.

Speciation of U in systems relevant for safety assessment of nuclear waste repositories by high-energy resolution X-ray absorption spectroscopy

I. Pidchenko⁽¹⁾, K. O. Kvashnina⁽²⁾, T. Yokosawa⁽¹⁾, N. Finck⁽¹⁾, D. Schild⁽¹⁾, J. Göttlicher^[3],
T. Schäfer⁽¹⁾, J. Rothe⁽¹⁾, H. Geckeis⁽¹⁾, T. Vitova⁽¹⁾

⁽¹⁾ *Institute for Nuclear Waste Disposal (INE), Karlsruhe Institute of Technology, Karlsruhe - Germany*

⁽²⁾ *European Synchrotron Radiation Facility (ESRF), 6 Rue Jules Horowitz, Grenoble Cedex – France*

^[3] *Institute for Photon Science and Synchrotron Radiation (IPS), Karlsruhe Institute of Technology, Karlsruhe, Germany*

In this work, the U M₄ edge high-energy resolution X-ray absorption near edge structure (HR-XANES) and U L₃ edge extended X-ray absorption fine structure (EXAFS) spectroscopic techniques are used in combination with other supplementary techniques to study the uranium (U) redox states and the U speciation in systems relevant for nuclear waste storages and repositories.

Long-term storage of high-level radioactive waste is associated with potential radioecological hazards. One chemical element of high interest is U, which can exist as a mobile U(VI) (oxidizing conditions) and sparingly soluble U(IV) (reducing conditions) species. It is expected that the main inorganic reducing agents for U(VI) in the environment are ferrous species in magnetite, formed on the steel canisters surface as an intermediate iron (Fe) corrosion product^[1]. Results obtained from laboratory experiments for the interaction of U(VI) with magnetite nanoparticles point to partial reduction of U(VI)^[2] or the formation of a few nm size uranium dioxide (UO₂) particles on the surface layer^[3]. The evidence for U(VI) reduction to intermediate U(V) state was found with no direct evidence of U(IV), which is in contradiction with thermodynamic calculations^[4]. Continuous interaction and related phase dissolution/recrystallization processes can also lead to U redox changes and structural U incorporation into Fe oxides, resulting in U immobilization^[5]. U redox state and speciation analyses are still very challenging due to simultaneous formation of several different species in such mineral systems. The main goal of our investigation is to assess the U M₄ edge HR-XANES technique for detection of U(V) possibly co-existing with U(IV) and U(VI) under reducing conditions on/in Fe containing minerals. The U M₄ edge HR-XANES has an advantage compared to the conventionally used U L₃ edge XANES, as the measured spectra are less dominated by core-hole lifetime broadening effects and therefore have narrower spectral features^[6-8]. We have investigated the U redox states and speciation in a set of samples where U co-precipitated with magnetite nanoparticles (15-20 nm) with U concentrations varying in the 1000-10000 ppm range. The studied system models the interaction of U(VI) with magnetite in aqueous solution, important for the understanding of the retarding effect of Fe corrosion products on U in the context of deep geological spent nuclear fuel disposal. These spectroscopic results can be compared with thermodynamic calculations and geochemical models describing this interaction.

After 10 days U interaction with magnetite U M₄ edge HR-XANES results indicate the formation of U(IV), U(V) and U(VI) mixtures in varying ratios, depending on the initial U loading. The U(VI) content decreases continuously with decreasing total U concentration and is no longer found in the 1000 ppm sample, which is at the level of environmentally relevant U concentration. At the same time the U(IV) and U(V) fractions increase. U(V) is stabilized as the main U redox state in the 1000 ppm sample along with a smaller U(IV) contribution. For all samples aged for 240 days U L₃ edge XANES and EXAFS suggest the formation of a non-stoichiometric UO₂ clusters of 4-5 nm size, supported by transmission electron microscopy. The major and minor contributions of U(V) and U(IV), respectively, for the 1000 ppm sample after 240 days confirm the assumption that the U redox kinetics has completed faster than 10 days at this U concentration. EXAFS analyses reveal U(V)-Fe interaction in the second U coordination sphere, which substantially increases from the 10000 to 1000 ppm sample and is the dominant specie in the 1000 ppm sample. Our results confirm that U(V) can be long-term stabilized for at least 373 days when incorporated in magnetite nanoparticles even under ambient conditions.

References

- [1] Jeon, B.H., *et al.*, (2005), EnS&T, 39(15): 5642-5649,
- [2] Missana, T., *et al.*, (2003), GCA, 67(14): 2543-2550,
- [3] Scott, T.B., *et al.*, (2005), GCA, 69(24): 5639-5646,
- [4] Ilton, E.S., *et al.*, (2010), EnS&T, 44(1): 170-176,
- [5] Huber, F., *et al.*, (2012), GCA, 96: 154-173,
- [6] Vitova, T., *et al.*, (2013), J. Phys: Conf. Ser., 430 (1), art. no. 012117,
- [7] Kvashnina, K.O., *et al.*, (2013), PRL, 111(25),
- [8] Vitova, T., *et al.*, (2015), Inorg. Chem., 54(1): 174-182

**X-ray absorption fine structure spectroscopy study of technetium halides
and metal-metal bonded complexes: a review**

Frederic Poineau

*Department of Chemistry, University of Nevada Las Vegas, 4505 Maryland Parkway, NV, USA
poineauf@unlv.nevada.edu*

Transition metal binary halides and compounds with metal-metal multiple bonds play an important role in inorganic, materials, bioinorganic and organometallic chemistry. One element whose metal-metal bond and halide chemistry is not well developed is Technetium, element 43. As of the year 2005, the number of complexes with multiple Tc-Tc bonds was quite limited: 25 dimers, 4 hexanuclear and 6 octanuclear halide clusters had been structurally characterized; no Tc binary halides with multiple Tc-Tc bonds and no complexes with a Tc³⁹⁺ core were reported. For the past 10 years, we have focused on expanding the chemistry of dinuclear complexes and identifying new Tc binary halides. During this time, seven new binary halides and seven dinuclear complexes were prepared and characterized. In our study on Tc binary halides and dinuclear complexes, X-ray absorption fine structure (XAFS) spectroscopy study has been proven a powerful technique for the characterization of metal-metal and metal-ligand separations as well as Tc oxidation states. In this presentation, the role of XAFS spectroscopy in the development of metal-metal bond and halide chemistries of Tc over the past 10 years is reviewed.

Stability of selenate and selenite and their separation using anion exchange chromatography

Keliang Shi^{*}, Run Li, Junqiang Yang, Wangsuo Wu

Radiochemistry Lab, School of Nuclear Science and Technology, Lanzhou University, Lanzhou, China

^{*}shikl@lzu.edu.cn

The present work mainly focused on the stability of selenite (Se(IV)) and selenate (Se(VI)) as well as their separation methods. Our results (Fig.1) show that serious loss of Se happened in HCl solution especially at high concentration of acid when the sample was evaporated to dryness. Compared with HCl media, Se becomes more stable in HNO₃ media. A separation procedure using anion exchange chromatography was optimized and applied for Se(IV) and Se(VI) separation in sample solution. That is the solution can be loaded on an anion exchange column at pH 8~9, and Se(IV) and Se(VI) can be eluted from the column with 0.01 mol/L HNO₃ and 2.5 mol/L HNO₃ respectively.

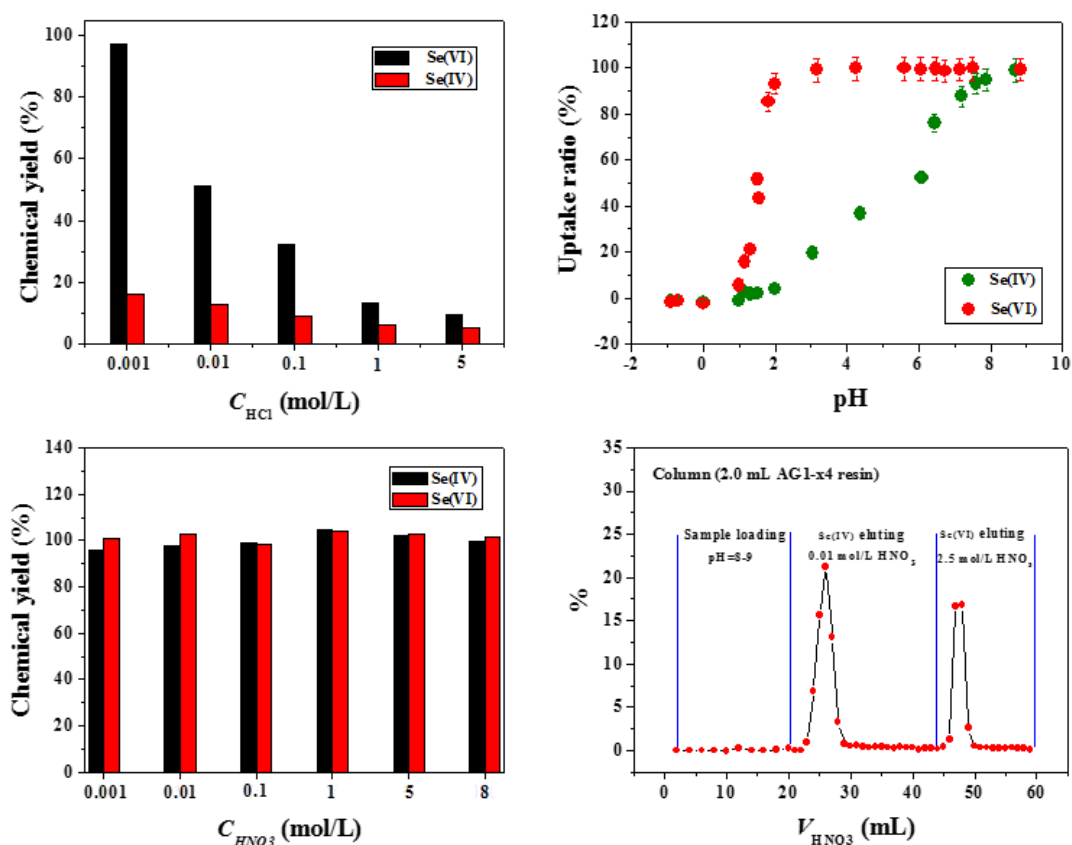


Fig.1 Stability of selenite and selenate in acid solution as well as their uptake and separation using anion exchange resin AG1-x4

This work was supported by the National Natural Science Foundation of China (Grant Nos. 21301083; 41472229).

RADIOANALYTICAL CHEMISTRY

**Determination of ^{126}Sn in intermediate level radioactive waste emerging
from the decommissioning of the NPP A1 Jaslovské Bohunice**

ANDRIS, Boris and BENA, Jozef

VUJE Inc., Slovakia

A recently developed procedure for separation and determination of ^{126}Sn by means of TBP Resin was tested on various liquid and wet RAW samples. Radioactive waste samples were in direct contact with damaged fuel from NPP A1 Jaslovské Bohunice for decades. After ^{137}Cs removal on AMP-PAN column, ^{126}Sn was separated on TBP Resin. ^{126}Sn yield was determined according to the ^{113}Sn tracer recovery. Achieved decontamination factors ($>10^3$) were sufficiently high to determine ^{126}Sn activity (up to $5.0 \times 10^4 \text{ Bq.kg}^{-1}$). Repeatability of the ^{126}Sn determination was studied. Determined activity of ^{126}Sn , or MDA values helped to enhance a waste treatment process, recalculate scaling factors and assess disposal possibility of waste in the national repository Mochovce.

Determination of ^3H , ^{36}Cl , ^{22}Na , ^{134}Cs and ^{133}Ba by means of precipitation and distillation

H. Aromaa⁽¹⁾, K. Helariutta⁽¹⁾, M. Siitari-Kauppi⁽¹⁾ and L. Koskinen⁽²⁾

⁽¹⁾*Department of Chemistry, University of Helsinki, P.O.Box 55, 00014 University of Helsinki, Finland*

⁽²⁾*Posiva Oy, Olkiluoto, 27160 Eurajoki, Finland*

The final disposal of spent nuclear fuel in Finland is planned to take place in a crystalline granitic rock at Olkiluoto island. Behavior of radionuclides has to be calculated for hundreds of thousands of years in the final disposal site for the safety assessment. If released into the bedrock, radionuclides will be transported by advection along water conducting fractures. Retardation may occur by molecular diffusion from the fractures into the stagnant pore water and/or by sorption onto mineral surfaces in the rock matrix. An in-situ Through Diffusion Experiment (TDE) has been launched in autumn 2015 in REPRO niche at Onkalo underground laboratory for studying diffusion and retardation properties of radionuclides [1]. In TDE, concentrated mixture of non-sorbing and sorbing radionuclides ^3H , ^{36}Cl , ^{22}Na , ^{133}Ba and ^{134}Cs is circulated in a meter long packed-off section of a drill hole at a distance of 11–12 m from the niche wall. Breakthrough of the radionuclides is followed in two observation drill holes about 10 cm away from the injection drill hole. Activity decrease in the injection hole is also followed to have more information on retention properties of radionuclides.

The aim of this work was to develop a method to analyze different radionuclides from the ground water samples taken from TDE. ^3H as tritiated water and ^{36}Cl as anion are the non sorbing elements whereas the rest of the radionuclides (cations in the ground water solution) sorb onto the mineral surfaces. ^{22}Na is slightly sorbing (distribution coefficient, $K_d = 1 \times 10^{-6} - 1 \times 10^{-4} \text{ m}^3/\text{kg}$) while ^{133}Ba and ^{134}Cs are known to be strongly sorbing elements ($K_d = 1 \times 10^{-1} - 1 \times 10^{-3} \text{ m}^3/\text{kg}$). ^{22}Na , ^{133}Ba , and ^{134}Cs were analyzed via gamma spectroscopy while liquid scintillation counting (LSC) was used to analyze ^3H and ^{36}Cl . All radionuclides are present in the injection hole and the decrease of their concentration was followed. ^3H and ^{36}Cl are expected to diffuse into the observation holes.

Gamma emitting radionuclides ^{22}Na , ^{133}Ba and ^{134}Cs are measured directly from the ground water solution. In order to measure beta active ^3H and ^{36}Cl they need to be separated from the other nuclides first to ensure beta samples clean from disturbing spectral components. Figure 1 presents the analyses scheme for all five radionuclides. First the gamma active nuclides are measured directly from ground water solution by using a germanium detector. Secondly, ^{36}Cl is separated from the ground water solution by AgNO_3 precipitation and the AgCl precipitate is dissolved to ammonia. Then the ^{36}Cl activity is determined by liquid scintillation counting (LSC) (Part I). After that, ^3H is distilled from the ground water solution and measured by LSC from the distillate (Part II). For ensuring the good quality of the chemical separations, ^3H and ^{36}Cl samples are also measured with a Ge detector.

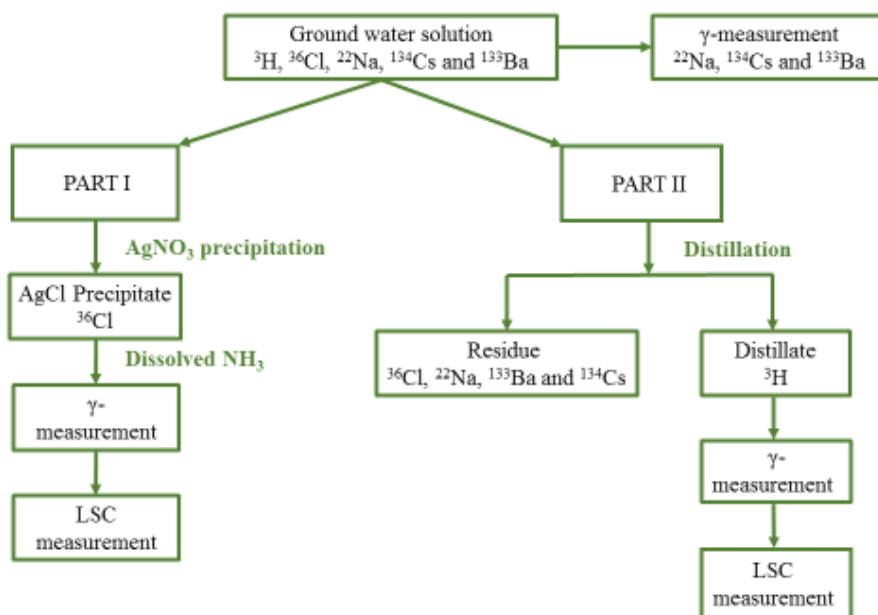


Figure 1. Analysis of ^3H , ^{36}Cl , ^{22}Na , ^{134}Cs and ^{133}Ba from ground water solution in TDE experiment.

Gamma active radionuclides are easily measured with low detection limits. Separation of ^{36}Cl by AgNO_3 precipitation is simple and yield for it is 100 %. Distillation of ^3H is tedious but more reliable than other tested methods. Yield for ^3H separation by distillation is 68 ± 9 %. Since the beta emitters are measured clean from contaminants also their detection limits stay low and depend only on the detector and LSC cocktail background.

References

1. M. Voutilainen, A. Poteri, K. Helariutta, M. Siitari-Kauppi, K. Nilsson, P. Andersson, J. Byegård, M. Skålberg, P. Kekäläinen, J. Timonen, A. Lindberg, P. Pitkänen, K. Kemppainen, J. Liimatainen, A. Hautajärvi, L. Koskinen, *In-situ Experiments for Investigating the Retention Properties of Rock Matrix in ONKALO, Olkiluoto, Finland* – 14258, WM2014 Conference, March 2 – 6, 2014, Phoenix, Arizona, USA

Determination of Zr and Mo isotopes in spent nuclear fuel solution by isotope dilution inductively coupled plasma mass spectrometry for validation of calculated values

Shiho Asai, Yukiko Hanzawa, Miki Konda, Daisuke Suzuki, Masaaki Magara, Takaumi Kimura

Japan Atomic Energy Agency, Tokai, Ibaraki 319-1195, Japan
asai.shiho@jaea.go.jp

Contents of zirconium and molybdenum isotopes in a spent nuclear fuel solution were determined by isotope dilution inductively coupled plasma mass spectrometry (ID-ICP-MS). The sample solution was prepared by dissolving a Japanese PWR irradiated UO₂ fuel with a burnup of 51 GWd/t. The measured contents of ⁹⁰Zr, ⁹¹Zr, ⁹²Zr, ⁹³Zr, ⁹⁴Zr, and ⁹⁶Zr in the sample were agreed well with the predicted values obtained through a burnup calculation code ORIGEN2. For molybdenum, the amounts in the sample were approximately 30% less than the predicted values, indicating that part of molybdenum exists in the insoluble residue.

1. Introduction

Isotopes of zirconium and molybdenum including both radio and stable isotopes can be found in spent nuclear fuel. These isotopes are mainly produced during nuclear fission and activation processes of the constituents in fuel claddings, resulting in the complete difference in the abundances from those found in nature. Of these isotopes, ⁹³Zr and ⁹³Mo which have long half-lives of 1.61×10^6 y and 4×10^3 y, respectively, are of great importance from the viewpoint of managing high-level radioactive wastes (HLW) in a long-term basis. The inventory estimation of such long-lived isotopes using a burnup calculation code is helpful for the safety assessment of HLW disposal. However, the reliability of the predicted values has not been sufficiently validated by experimental values. We have previously determined the contents of long-lived fission products, such as ⁷⁹Se and ¹³⁵Cs, in a spent nuclear fuel by ICP-MS based on isotope dilution technique^[1]. The measured contents of ⁷⁹Se and ¹³⁵Cs coincided with their respective predicted values obtained using a burnup calculation code ORIGEN2 within the uncertainty. In this study, the contents of zirconium and molybdenum isotopes in a spent nuclear fuel were determined with ID-ICP-MS and compared with predicted contents obtained through ORIGEN2 using the nuclear data library JENDL-4.0.

2. Experimental

2.1 Reagents. Natural Zr and Mo standard solutions were obtained from Wako Pure Chemical Industries, Ltd. The HNO₃ and HCl used for the chemical separation and the preparation of solutions for measurements were of ultrapure grade (TAMAPURE AA-10 for HNO₃ and AA-100 for HCl) and supplied by Tama Chemicals.

2.2 Sample preparation. Spent nuclear fuel solution was prepared by dissolving a single fuel pellet that was the part of the UO₂ fuel lattice assembly of a Japanese PWR. The burnup, cooling time, initial enrichment of ²³⁵U of the sampled pellet were 51 GWd/t, 9,228 days, and 3.2wt%, respectively. Approximately 5 g of the pellet excluding the zircaloy cladding was dissolved with 4 M HNO₃ for 2 h at 90 °C, following the procedure detailed in our previous publication^[1]. The concentration of uranium in the

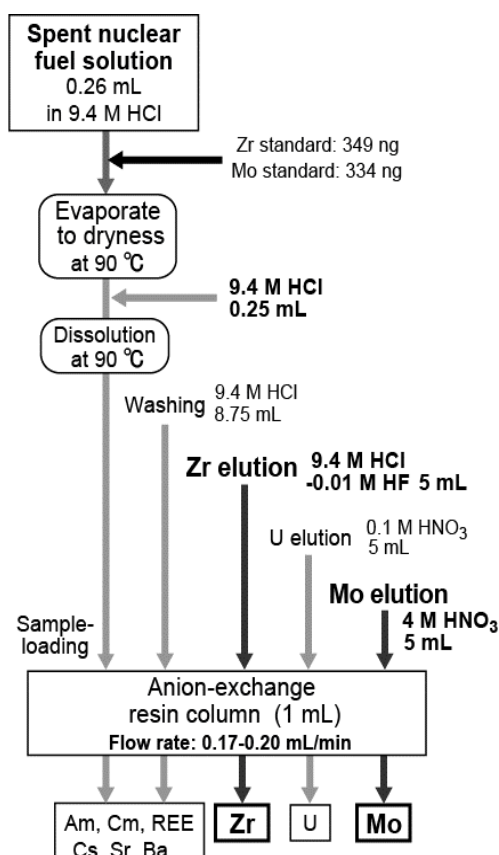


Figure 1. Separation procedure of Zr and Mo in a spent nuclear fuel solution with an anion-exchange resin column.

sample solution was set to 0.32 mg of the initial uranium per g of the prepared solution by diluting with 9.4 M HCl. Zirconium and Molybdenum were separated according to the procedure shown in Figure 1. The elution conditions were selected based on the reported anion-exchange behaviors of zirconium and molybdenum^[2]. The sample solution was evaporated and dissolved with 9.4 M HCl. The resultant solution was divided into two fractions to apply the isotope dilution technique for the determination of each isotope in the sample. Known amounts of zirconium and molybdenum standards were added to the one fraction. Both fractions were processed by the same procedure.

2.3 ICP-MS The concentrations of Zr and Mo isotopes in the sample solution were measured by ICP-MS (Agilent 7700x). The operating conditions are summarized in Table 1. The detection limit at m/z 91 and 95 were 0.0003 and 0.0001 ng/mL, respectively.

3. Results and Discussion

3.1 Separation of zirconium and molybdenum. The Zr-eluted and Mo-eluted fractions were measured with ICP-MS, respectively. In the Zr-eluted fraction, no significant signals attributed to the major constituents, such as strontium, molybdenum, cesium, barium, and lanthanides, was observed. Slight amounts of uranium and plutonium, corresponding to 0.003% and 0.8%, respectively, of the initial amounts in the sample solution were found, causing no clear interference in the determination of zirconium isotopes. Molybdenum which was retained in the anion-exchange column during the zirconium elution, was thoroughly eluted with 5 mL of 4 M HNO₃. In the resulting fraction, no signal originating from almost all of the coexisting elements with the exception of minor ²³⁸U signal was observed. The absence of such signals of coexisting components indicates that the interference-free measurement was achieved for both zirconium and molybdenum isotopes.

3.2 Comparison of measured contents with predicted values. The measured and predicted contents of zirconium and molybdenum isotopes are summarized in Table 2. The contents of all the detected zirconium isotopes, including a long-lived ⁹³Zr, corresponded reasonably with the predicted values, providing the capability to confirm the reliability of the predicted values given by ORIGEN2. That would give helpful information on the long-term safety assessment of HLW disposal. For molybdenum, there was no clear difference in the abundances between measured and predicted values. However, the amounts in the sample were approximately 30% less than those of the predicted values, indicating that part of molybdenum exists in the insoluble residue. In addition, ⁹³Mo, another long-lived isotopes, was not found in the sample. This is mainly because activation of ⁹²Mo in zircaloy cladding is dominant process in producing ⁹³Mo. To evaluate the ⁹³Mo content of HLW, the measurement of the ⁹³Mo contents in fuel rod hulls of fuel elements is necessary.

References

- [1] S. Asai, Y. Hanzawa, K. Okumura, et al. J Nucl. Sci. Technol. 48 (2011) 851-854.
- [2] K. A. Kraus, G. E. Moore, J. Am. Chem. Soc., 73 (1951) 9–13

Table 1 Operating conditions of ICP-MS

RF power	1550 W
Plasma gas flow rate	15.0 L/min
Auxiliary gas flow rate	0.90 L/min
Nebulizer gas flow rate	1.01 L/min
Integration time	0.3 s
No. replicate	5
Measured mass	90-100
	133, 145, 146, 238
Sensitivity [cps/ng mL ⁻¹]	150,000 (⁹¹ Zr)
	150,000 (⁹⁵ Mo)

Table 2 Contents of Zr and Mo isotopes found in spent nuclear fuel sample

Isotope	Measured [g/MTU]	ORIGEN2 [g/MTU]
⁹⁰ Zr	(3.94 ± 0.30) x10 ²	367
⁹¹ Zr	(8.47 ± 0.63) x10 ²	808
⁹² Zr	(9.27 ± 0.64) x10 ²	899
⁹³ Zr	(1.010 ± 0.075) x10 ³	1003
⁹⁴ Zr	(1.087 ± 0.081) x10 ³	1100
⁹⁶ Zr	(1.262 ± 0.097) x10 ³	1181
⁹⁵ Mo	(7.82 ± 1.25) x10 ²	1073
⁹⁶ Mo	(6.1 ± 0.9) x10 ¹	86
⁹⁷ Mo	(8.42 ± 1.17) x10 ²	1206
⁹⁸ Mo	(8.82 ± 1.24) x10 ²	1242
¹⁰⁰ Mo	(9.98 ± 1.56) x10 ²	1466

Ra-226 determination in a certain types of mineral water

N.D. Betenekov, M. Saidzoda, T.I. Mikhailova, D.V. Beresneva

Ural Federal University, Yekaterinburg, Russia

ndbetenekov@urfu.ru

Alpha spectrometry is the most sensitive method for alpha emitting radionuclides determination (the minimal detection limit is 0.001 Bq at counting time of 10^4 s) [1]. The main problem is to obtain a high quality source for measurement. Quality of the source is determined by its thickness and quantity of the alpha emitter. The alpha source should be very thick and the activity should be evenly distributed over the surface of the planchet in order to avoid self-absorption of alpha particles. Usually, thickness of the source should not exceed $50\text{--}100\text{ }\mu\text{g cm}^{-2}$. The evaporation method does not provide enough thickness resulting in unsolved peaks in alpha spectrum. High quality alpha sources are usually prepared via electrodeposition onto a metal planchet after selective extraction separation of the determined radionuclide; in this case, dissolved salts do not interfere with quantitative deposition of the alpha emitter. Many operations and high labor consumption are the disadvantages of this method. The method of sorption separation of a radionuclide using thin films of inorganic compounds impregnated onto a plane support is significantly easier [2]. This method was suggested by authors in 1976 [2]; now it is widely used in radioanalytical practice [3] due to its simplicity as well as to combination of the radionuclide preconcentration, selective separation and preparation of a high quality alpha source with a high resolution into one step.

The data given in the publication [3] show that the Ra-NucFilm disc based on manganese dioxide provides almost complete radium separation (75-90%) from 100 mL sample of drinking water after intensive shaking during 6 hours. It is obvious that sorption degree will strongly depend on a type of water, total salt content and ionic composition. The method for Ra-226 determination in a certain types of mineral water using a MnO_2 -CTA sorbent (produced by the Radiochemistry and Applied chair of Ural Federal University) was tested in this work in order to determine the effect of these factors.

Thin films of manganese dioxide may be deposited onto various supports; particularly, in this work MnO_2 was deposited onto the cellulose triacetate (CTA) film being the basis of a photographic film. Saturation of this support by manganese dioxide in a solution containing potassium permanganate and sulfuric acid was used in this work as a method of MnO_2 deposition onto the surface of the CTA [4].

The study of radium sorption by the thin-layer MnO_2 -CTA sorbent was performed using several types of mineral water that can be found in retail chains of Yekaterinburg city, Russia. Flowing underground, certain types of mineral water may contact uranium-containing rocks resulting in water pollution by radium isotopes [5]. The following natural mineral waters were used in this study: «Nagutskaya-26», «Obukhovskaya-10», «Slavyanovskaya», «Smirnovskaya». The drinking water «Bon Aqua» was also used; this water is not natural mineral one and it contains a low salt concentration. Various salt content in these water samples allows determining the effect of salinity on radium sorption by the MnO_2 -CTA sorbent.

In this study Ra-224 was used as a short-lived radioactive tracer in order to determine quantitative characteristics of radium sorption (sorption degree and distribution coefficient (K_d)) as well as to reveal the effect of various factors (time of phases contact, salinity of the solution, “sorbent weight / solution volume” ratio). For each type of the water, the experimental dependence of sorption on the sorbent quantity in the solution was obtained; in accordance with Henry’s law, radium distribution coefficients were evaluated using these dependences.

The obtained results have shown that the highest values of radium distribution coefficients were typical for water with low salt content, such as «Bon Aqua» and «Obukhovskaya-10»; these values were $(1\text{--}3)\cdot 10^6\text{ L kg}^{-1}$. The values of radium distribution coefficient for other water samples were approximately $(2\text{--}4)\cdot 10^5\text{ L kg}^{-1}$. Taking into the counting error limits, the average K_d value for all water samples seems to be reasonable. The calculated average value was $K_d = (6.8 \pm 2.5)\cdot 10^5\text{ L kg}^{-1}$; this value shows that the MnO_2 -CTA sorbent is very

selective for radium. The results of radiochemical analysis of mineral water samples using various methods are presented in table below.

Water sample	Ra-226 activity, Bq L ⁻¹		
	Emanation method [5]	Sorption by MnO ₂ -CTA + α -spectrometry	Sorption by T-5 + γ -spectrometry
Bon Aqua	-	<0.005	-
Nagutskaya-26	-	0.1 ± 0.1	-
Obukhovskaya-10	-	<0.005	-
Slavyanovskaya	4.1 ± 0.5 (2010)	3.7 ± 0.6 (2013) 2.6 ± 0.7 (2014)	4.5 ± 0.6
Smirnovskaya	2.1 ± 0.3 (2010)	3.7 ± 0.6 (2013)	4.5 ± 0.6

Bibliography

1. Vdovenko V.M., Dubasov Y.V. Analytical chemistry of radium. Nauka, Leningrad, 1973, 190 p.
2. Betenkov N.D., Gubanova A.N., Egorov Yu. V. et al. (1976) Radiochemistry, Vol. 18, N 4, p. 622 – 628 .
3. http://www.triskem-international.com/ru/iso_album/app_note_ra_disc.pdf
4. Ryzhen'kov A.P. Ph.D. thesis / Ural State Technical University. Sverdlovsk, 1981. 150 p.
5. Onishchenko A., Zhukovsky M., Veselinovic N., Zunic Z. S. (2010) Applied Radiation and Isotopes, № 68, p. 825 – 827.

Validation of three laboratory-developed test methods for determination of ^{90}Sr in aqueous samples and milk and ^{99}Tc in aqueous samples

G. Bilancia¹, M. Ferreira¹, L. Fornara¹, A. Ravazzani¹, M. Roveri¹, R. Vasselli¹
N. Bianco², G. Cornara², I. Cydzik², M. Merlo², L. Paolemili², D. Rossi²

¹ JRC European Commission, site Laboratory for Radioactivity Measurements, Via E. Fermi, Ispra, VA, Italy,

² Nucleco Spa, Via E. Fermi, Ispra, VA, Italy

Gianmarco.Bilancia@ec.europa.eu;

In the frame of the Euratom Treaty, the Joint Research Centre (JRC) was created, with sites located in different Member States to contribute to the establishment and growth of nuclear power related industries. The site Laboratory for Radioactivity Measurements (LMR) is in charge of chemical and radiochemical characterisation for the environmental surveillance network and samples from JRC-Ispra's nuclear facilities (Italy). Environmental surveillance is conducted in the framework of JRC-Ispra's nuclear licence for the operation of its nuclear installations. Characterisation of samples is aimed to waste management, facilities characterisation and clearance of materials. LMR activities include: sample collection and transport to LMR (only for environmental network), sample preparation and measurement. LMR works in compliance with the requirements of the international standard ISO/IEC 17025:2005 and has 11 test methods accredited with the Italian accreditation body ACCREDIA. According to JRC LMR's customers' needs and considering the lack of any standard test methods which matches with the specific needs of JRC LMR's customers' needs, it has been decided to validate three laboratory-developed methods for the determination of ^{90}Sr in aqueous samples and milk and ^{99}Tc in aqueous samples. A laboratory-developed (or internal) test method is a not standard-method while validation is the process of confirmation by examination and the provision of objective evidence that the particular requirements for a specific intended use are fulfilled. The validation process has been carried out in conformity to the requirements of the standard ISO/IEC 17025:2005. The separation of ^{90}Sr from the aqueous matrix is based on a pre-concentration of the cations through a generic-cationic resin chromatographic column, followed by Solid Phase Extraction (SPE) of radio-strontium on a crown-ether based resin. The measurement of ^{90}Sr is carried out, without waiting for the establishing of the secular equilibrium, by means of the Liquid Scintillation Counting (LSC) technique. Chemical yield is determined by ICP-MS, measuring total strontium at the beginning and the end of the radiochemical procedure. The separation method of ^{99}Tc from the aqueous matrix is based on the pre-oxidation of Technetium to pertechnetate by means of H_2O_2 , followed by a separation on TEVA resin and final counting by LSC. Chemical yield is measured by ICP-MS determination of the amount the ^{185}Re carrier at the beginning and the end of the radiochemical procedure. In order to validate these three internal methods, the following parameters have been determined, employing "blank" spiked aqueous and milk samples: application field (linearity), accuracy (trueness and precision), decision threshold and detection limit, selectivity and overall uncertainty. The test methods are considered positively validated only if these parameters matches with the JRC LMR's customers' needs. The overall uncertainty has been evaluated in conformity to ISO GUIDE 98-3:2008 and ISO 21748:2010, using the following expression:

$$u^2(y) = s_r^2 + \sum c_i^2 \cdot u^2(x_i)$$

where s_r^2 is the intra-laboratory variance contribution and the other terms refer to the uncertainties of the i quantities which determine the value of the measure and $u(x_i)$, and their associated sensitivity coefficients c_i . The intra-laboratory variance contribution to the overall uncertainty value has been assessed by an ANOVA (Analysis Of Variance) test, in order to determine the homogeneity of intra-laboratory results. In case of confirmation of the homogeneity of intra-laboratory results (ANOVA test with $p\text{-value} \geq 0.05$), the s_r^2 value has been compared with the counting standard deviation by a χ^2 test. If this test gives a positive outcome (that is, s_r^2 follows χ^2 distribution), s_r^2 is set to zero. The presentation will show in more details the methods

in use and the quality parameters' values obtained during the validation processes. Here below in table 1, some of these parameters:

<i>Internal method for determination of ^{90}Sr in aqueous samples</i>		
<i>Interval in which the linearity has been confirmed</i>	<i>Detection Limit ($\alpha = \beta = 0.05$ – counting time 30 min)</i>	<i>Relative Expanded Uncertainty (k=2)</i>
0.1 – 37.0 Bq/L	0.025 Bq/L	5 – 12 %
<i>Internal method for determination of ^{90}Sr in milk</i>		
<i>Interval in which the linearity has been confirmed</i>	<i>Detection Limit ($\alpha = \beta = 0.05$ – counting time 30 min)</i>	<i>Relative Expanded Uncertainty (k=2)</i>
0.1 – 37.0 Bq/L	0.129 Bq/L	5 – 12 %
<i>Internal method for determination of ^{99}Tc in aqueous samples</i>		
<i>Interval in which the linearity has been confirmed</i>	<i>Detection Limit ($\alpha = \beta = 0.05$ – counting time 30 min)</i>	<i>Relative Expanded Uncertainty (k=2)</i>
1 – 50 Bq/L	0.28 Bq/L	3 – 14 %

Table 1: Validation parameters of internally-developed methods in use at LMR

The separation of Th, Ac and Ra using extraction chromatographic material with HDEHP on polyacrylonitrile (PAN)

Buchatskaya Yulia, Nemec Mojmir

Department of Nuclear Chemistry, Faculty of Nuclear Sciences and Physical Engineering, Czech Technical University, 115 19 Prague, Czech Republic

The field of nuclear medicine is strongly developing during last decade with growing interest to radiopharmaceuticals based on α -emitting nuclides. The main advantage of α -emitting isotopes are high energy of particles (5-8 MeV) and short path length in biological tissues (35-100 μm). Several α -emitting nuclides are currently under investigation for potential use in targeted α therapy, including Tb-149, At-211, Bi-212, Ac-225, Ra-224 and Ra-223 [1]. Radium-223 ($T_{1/2} = 11.4$ days) can be produced in a generator form from Ac-227 ($T_{1/2} = 21.8$ years). In its turn Actinium-227 could be produced through thermal neutron irradiation of Ra-226 in a nuclear reactor by the reaction $^{226}\text{Ra}(n,\gamma)^{227}\text{Ra}$ followed by β^- decay of Ra-227 ($T_{1/2}=42.2$ minutes) to Ac-227 [2]. To obtain chemically pure isotope, Ra-223 should be purified from parent isotopes Ac-227 and Th-227. The system chosen as a generator of ^{223}Ra must retain both Ac and Th strongly and provide a highly efficient Ac/Ra separation.

Extraction chromatography using HDEHP-PAN was proposed as method for separation of Ac, Th and Ra. This technique combines the rapidity of chromatographic methods and high separation factors typical for liquid-liquid extraction. The solid extractant HDEHP-PAN was prepared at the CTU in Prague by direct incorporation of di-(2ethylhexyl)phosphoric acid (HDEHP) into modified polyacrylonitrile (PAN) beads [3]. For introductory study the batch experiments were carried out. The isotopes of Th-234, Am-241 and Ba-133 were used as a chemical homologues of Th-227, Ac-227 and Ra-223. The kinetics of cation uptake and dependence of D_g values for these radionuclides on the hydrochloric and nitric acid concentration were obtained. The conditions of following separation using column filled with HDEHP-PAN beads were chosen based on the results of conducted batch experiments. Obtained results showed an effective separation of Ba-133 and Am-241 on column filled with HDEHP-PAN.

To obtain the separation factor and D_g values for Ac-227 and Ra-223 isotopes, the tracer Ac-228 was used for determination of Ac concentrations. Therefore, the procedure of easy separation of Ac-228 and Ra-228 from natural Th-232 was developed. The proposed method includes precipitation of macro-amounts of thorium as a non-soluble thorium peroxide followed by separation of Ra-228 and Ac-228 on the column filled with HDEHP-PAN. Finally the separation procedure of micro-amounts of Ra-228/Ac-228 from macro-amounts of Th-232 nitrate was developed and generator of Ac-228 using HDEHP was prepared. The obtained separation method for Ra and Ac using extraction chromatography with HDEHP-PAN shows promising results for preparation the nuclear medicine generator of Ra-223.

ACKNOWLEDGEMENT: This work was partially supported by the Technology Agency of the Czech Republic and the Grant Agency of the Czech Technical University in Prague, under grant agreements No.: TA03010027 and SGS15/216/OHK4/3T/14 respectively.

References:

1. McDevitt R.M., Sgouros G., Finn D.R., Humm L.J., Jurcic G.J., Larson M.S., Scheinberg A.D., Eur J Nucl Med. **25**, 1341-1351 (1998)
2. Kukleva E., Kozempel J., Vlk M., Mičolová P., Vopálka D., J. Radioanal. Nucl. Chem. **304**, 263-266 (2014)
3. Šebesta F., Kameník J. J. Radioanal. Nucl. Chem. **283**, 845-849 (2010)

Evaluation of ion-exchange and extraction chromatography techniques for the separation of ^{227}Th from its decay products

P.I. Ivanov, E.M. van Es, M.G. Miranda, S.M. Collins, B.C. Russell and S.M. Jerome

National Physical Laboratory, Hampton Road, Middlesex, TW11 0LW Teddington, UK

Thorium-227 is an α -emitting radionuclide with a half-life of 18.697 days, decaying to ^{223}Ra with an average α energy of 5.9 MeV. It is regarded as an emerging radiotherapeutic isotope with potential applications in targeted α -particle cancer therapy. Thorium-227 can be obtained in significant amounts from ^{227}Ac generators and prior to potential use for labelling of therapeutic monoclonal antibodies, or other nuclear medical applications. Its application requires chemical separation from the precursor actinium as well as from the daughter product radium and other decay products.

Various thorium separation approaches have been previously applied, mainly based on ion-exchange and extraction chromatography techniques. Thorium(IV), unlike Ac(III) and Ra(II), shows high affinity towards anion-exchange and extraction chromatography resins from nitric acid solutions over a range of concentrations, with the maximum distribution coefficients for anion exchange resin occurring in the range of 7 to 8M HNO_3 , thus providing the basis for radiochemical separations of thorium from uranium, actinium, radium and other members of the $4n+3$ decay series.

The main objective of the current work is to evaluate the performance of ion-exchange and extraction chromatography separation methods based on AG1, TEVA and UTEVA columns from HNO_3 solutions for the development of a simple and robust separation scheme for the isolation of ^{227}Th . As part of the method development work, Th(IV), Ac(III), Ra(II) and Pb(II) absorption behaviour on anion exchange (Bio Rad AG1-X8) and extraction chromatography (Triskem International TEVA and UTEVA) resins from HNO_3 solutions has been studied. Results show high Th(IV) retention, while the other cations of interest showed no affinity to the resins, thus ensuring efficient ^{227}Th isolation with high separation factors. For the elution of Th(IV), diluted HCl and HNO_3 solutions have been tested, and the highest recoveries have been recorded for 1M HCl in the case of AG1 or UTEVA, and 0.5 M HNO_3 for TEVA resin. The results suggest that both anion exchange and extraction chromatographic techniques can be successfully used for the separation of ^{227}Th from its decay products, however extraction chromatographic resins demonstrates favourable performance in terms of Th recovery and high level of purification from radionuclide impurities. As well as nuclear medicine applications, the procedure developed could form the basis of improved separation of Th in low-level environmental radioanalytical measurements.

Development of strontium-90 pine needle reference material and the labs intercomparison radiochemical analysis

Yanqin Ji*, Fei Chen, Xianzhang Shao, Liangliang Yin

National Institute for Radiological Protection, China CDC. Beijing, China

**jiyanqin@nirp.cn*

Strontium-90 is one of the most important long-lived radionuclide with high-energy β -rays as the fission products of ^{235}U and ^{239}Pu . Its chemical characteristics are very similar with calcium and deposits mainly in the bones, teeth and damaging blood-producing cells of animals by uptake from the soil, food recycle results. Therefore, it is essential to precise detect low-level ^{90}Sr in environmental and biological samples for both environmental protection and emergency preparedness. The measurement of low-level ^{90}Sr normally follows with a long radiochemical separation procedure. The purpose of this work is to prepare strontium-90 pine needle samples, as the higher strontium accumulation plant, reference materials primarily for use in evaluating the reliability of ^{90}Sr analytical methods and the quality control organized nationwide radioactivity monitoring in foodstuffs samples in China.

The sample of pine needles were selected in Changping protected natural forest at the same age located in the north of Beijing, China. After water cleaned, dried at 70°C , jet milled and blended at about $63\mu\text{m}$. Spiked with ^{90}Sr diluted solution and blended uniformly, liquid nitrogen fixed, then freeze-dried directly for one week. Finally it was completely blended again, filled bottles and Gamma ray irradiation sterilized with a total dose of 25kGy using a ^{60}Co source.

A unit of the sample consists of approximately 30 gram of pine needles powder. The batch experiments for the stability and uniformity performed by the Di-(2-ethylhexyl) phosphate (HDEHP) extraction chromatography separation, yttrium-90 precipitated and β counting. The minimum sample amount for the measurement is about 8 gram under the satisfaction uncertainty.

This material was also used as a test material for the interlaboratory comparison exercise between NIRP and Japan Chemical Analysis Center, as well as national-wide in China, for the determination of ^{90}Sr . The main two methods for ^{90}Sr measurement of HDEHP column separation with ^{90}Y β counting, the Sr-spec crown ether separation with liquid scintillation counter. The relative uncertainty of the recommended value is 5.6% of 32.2 Bq/kg ^{90}Sr in pine needle powder. A description of the material collection and preparation, the results of the interlaboratory comparison will be presented and discussed.

Acknowledgments

The authors acknowledge financial support by the Basic Work Project of Chinese Ministry of Science and Technology (No. 2014FY211000).

References

- [1] IAEA, Worldwide open proficiency test on the determination of radionuclides in spinach, soil and water. IAEA/AQ/8, IAEA-CU-2007-03. Vienna, November 2009.
- [2] Elizabeth A., Mackey D. A., Becker R. O. et al., Certification of NIST standard reference material 1575a pine needles and results of an international laboratory comparison. NIST Special Publication 260-156, Department of Commerce, USA. June 2004.

Chemical separation of cadmium and silver from fission products

Jun Jiang, Chris Gilligan, Richard Barfoot

*AWE plc, Aldermaston, Reading, RG6 4PR, UK
jun.jiang@awe.co.uk*

Rapid identification and quantification of fission products are required in Nuclear Forensics. The measurement of Cd-115 and Ag-111 by direct gamma spectrometry in un-purified fission product samples is a challenging and involves complex measurement systems such as Compton suppression. The measurement is complicated by interferences from Cs-136 and La-140. The measurement of Cd-115m is also important, however this has a fission yield an order of magnitude lower than Cd-115 and a long half-life. Therefore cadmium and silver are two elements prioritised for radiochemical separation.

At AWE, cadmium and silver are separated using an anion exchange column. They are eluted in the load fraction with concentrated hydrochloric acid amongst other elements which do not form anion complexes. They are further separated from other fission products by hydroxide and sulphide precipitation. Silver is then separated from cadmium by precipitation of insoluble silver chloride. Cadmium is purified from contaminants by precipitation of insoluble palladium sulphides in 2M hydrochloric acid. Cadmium remains in solution, and any contaminants co-precipitate with palladium. The separation scheme works effectively. However it is complicated and sensitive, requires great care and skill to perform reliably. It also takes long time, usually 3-4 working days.

Based on the fact that cadmium and silver are strongly absorbed on the anion exchange column in diluted hydrochloric acid, improved elution schemes have been developed in order to separate and purify cadmium and silver simply and robustly by using anion exchange chromatography only. A load and rinse solution of 1 M hydrochloric acid removes all Group I and II metals, lanthanides, and actinides, etc. Cadmium and silver are then eluted together using 3 M ammonium hydroxide or separately using 6 M hydrochloric acid for silver and 3 M ammonium hydroxide for cadmium. The obtained solutions can be measured accurately by high resolution gamma spectrometry and the small amount of impurities present do not interfere with the measurement.

The silver purification has also been tested using Triskem CL Resin. CL Resin is an extraction chromatography system that is selective for platinum group metals, gold and silver. Silver is effectively separated from other elements by remaining on the column as an insoluble silver complex, however the elution of silver is challenging.

By using the newly developed methods, results can be available within 1-2 working days. This talk details the method development, its validation, and discusses the results obtained for some samples during recent inter-laboratory comparison exercises.

A rapid method for the determination of radiostrontium in seawater using automated separation system

Yoonhee JUNG, Hyuncheol KIM, Jong-Myoung LIM

*Environmental Radioactivity Assessment Team, Korea Atomic Energy Research Institute, 989-111
Daedeok-daero, Yuseong-gu, Daejeon 305-353, Republic of Korea
wjdehowl89@gmail.com*

Radiostrontium can be released into the ocean by global fallout and nuclear accident. Therefore, the determination of radiostrontium is to be subject to close monitoring of seawater, and it has to be performed within 36 hours in emergency. The fuming nitric acid method is primarily used for separating of radiostrontium but it is a big health hazard, time-consuming and labor intensive work.

Therefore, in this study, Sr in a 2 L seawater sample is pre-concentrated using a cation exchange resin and can be reduced up to 20 mL, having 99% recovery for strontium. After pre-concentration, Some Ca and Mg ion in seawater were precipitated as a form of carbonate precipitate. Sr could be purified using Sr-resin having 90% recovery. An automated separation system used in pre-concentration and purification process. The analytical time for the automated radiochemical process was about 4 hours.

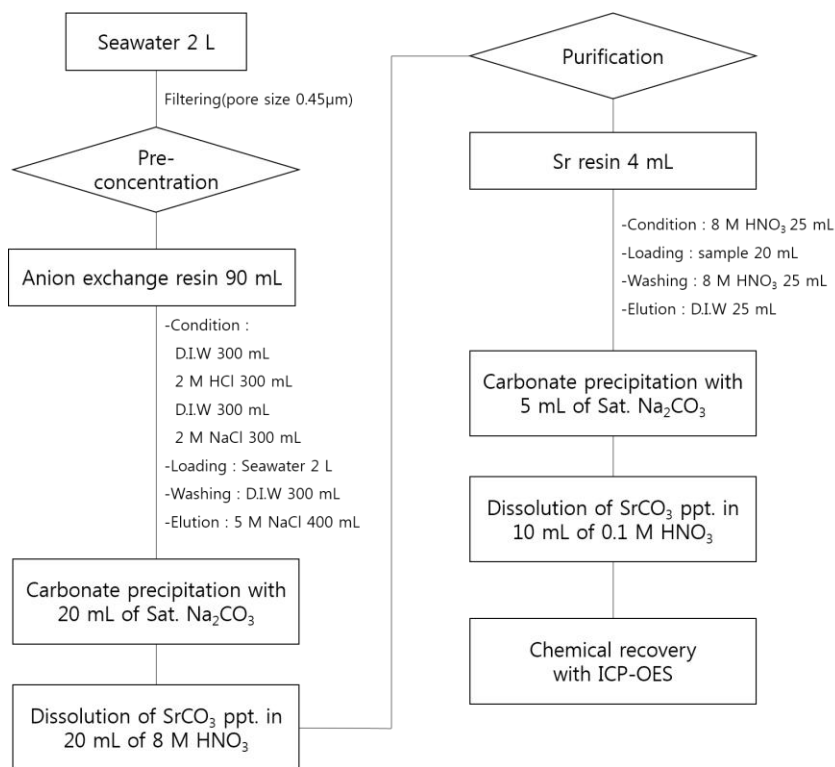


Figure 3 Schematic diagram of the determination of Sr in seawater.

Radiochemical approaches to the measurement of tritium in metallic components

Byungman Kang, Kwang Yong Jee, and Hong-Joo Ahn

*Nuclear Chemistry Research Division, Korea Atomic Energy Research Institute, 989-111 Daedeok-daero,
Yuseong-gu, Daejeon 305-353, Republic of Korea*
bkang@kaeri.re.kr

From the ternary fission of fissile isotopes, tritium, which is produced in irradiated nuclear fuel, exists in the form of HT. A substantial amount of tritium in nuclear fuel is supposed to diffuse out of the fuel into the metallic cladding and supporting components during the operation of the reactor. For this reason, an accurate analysis of the tritium content in metallic components is very critical for both an understanding of the failure mechanism of materials and recovering metallic components for reuse. In addition to nuclear fission, the operation of fusion power plants can also generate radioactive waste of activated metallic materials corresponding to a blanket module and divertor, which require the management of tritium. Among the destructive methods that have been developed for the chemical separation of tritium in radioactive samples, a combination of wet oxidation and acid stripping has been the most common technique owing to a high recovery under mild reaction conditions. To ensure the reliability of the above method for a variety of metallic components, it is essential to analyze a particular sample of a power plant made of steel, tungsten, or copper. In this respect, various sizes of a pressure tube irradiated under CANDU reactor conditions were investigated to assess the tritium activity, and it was confirmed that 99% of tritium was extracted from the sample through the first treatment. Furthermore, to prepare a simulated sample for tritiated metals, hydrogen implantation in metals such as SS316, nickel, and titanium was investigated using an electrochemical method. The resulting study suggests that the amount of hydrogen implanted in metals is strongly influenced by the composition of metal along with the charging potential.

Determination of Cs-137, Sr-90 and plutonium in fish using ion chromatography and extraction chromatography

Claudia Landstetter, Viktoria Damberger, Eva-Maria Lindner, Christian Katzlberger

Austrian Agency for Health and Food Safety, Spargelfeldstrasse 191, 1220 Vienna, Austria

Fish samples from the Pacific Ocean are analyzed by gamma spectrometry in Austria since 2011. In order to attain Cs-137 activity concentrations in fish from other catching areas and to attain also Sr-90 and plutonium activity concentrations additional fish samples from different catching areas were collected. Further shell fish samples were taken. These measurements will be used to get a short overview over different catching areas in the world. The results can be used in the future as background monitoring values to be compared to measured values after a radiological event.

The measurements of Cs-137, Sr-90 and plutonium were conducted with gamma spectrometry, liquid scintillation counting and alpha spectrometry. Sr-90 and plutonium were separated using Dowex 1x8 and Sr-Spec resin. These column separations were optimized to get a combined method analyzing Sr-90 and Plutonium in one sample. As this method will also be used in the future to analyze different environmental samples like soil and vegetation it was tested using different matrices. Hence reference materials and spiked environmental samples were used. Since the method should be as fast as possible the separation of plutonium and strontium by using only the Sr-Spec column was tested. Because of interferences with the matrix and especially the natural radionuclides in the soil this idea had to be discarded. Another problem was the stripping of plutonium using 3 M HNO₃ + 0.05 M oxalic acid solution which was not working properly.

Results of column separation testing and of the activity concentration of Cs-137, Sr-90 and plutonium in fish samples will be presented and discussed.

Study of cadmium extraction from aqueous solutions with high chloride concentration using radiotracer and NMR

Hans Vigeland Lerum¹, Aud Mjærum Bouzga², Sissel Jørgensen^{1,2}, Dirk Petersen¹, Dag Øistein Eriksen², Eddy Walter Hansen¹, Jon Petter Omtvedt¹, Grethe Wibetoe¹

¹ Department of Chemistry, University of Oslo, Norway

²The Foundation for Scientific and Industrial Research (SINTEF) Materials and Chemistry, Oslo, Norway

In the process industry one generally wants to use as pure raw materials as possible in order to simplify the process and hence enhance revenue. However, in many cases the raw materials available contain unwanted impurities which need to be removed because they degrade the final product. In the future it is expected that even more impure raw materials have to be used as the best mineral sources are getting depleted. Therefore, process steps will have to be added to handle this and minerals are selected not only based on purity but also on how easy it will be to handle the impurities. Due to this, the industry needs to enhance their processes and techniques to be prepared for a future where it will be necessary to handle the increased concentration of impurities. In order to find solutions to remove the unwanted elements in the final products, the behaviour of these impurities in the production process needs to be investigated.

Cadmium is a toxic metal and is generally not wanted as a part of the end product. Cadmium occurs in trace amounts in several minerals used for metal production including some raw materials for nickel. In the study presented here the behaviour of cadmium in a chloride environment has been investigated. The concentration level of chloride in the synthetic solution used in the experiments included concentrations in the same level as in the leach solution used for nickel production. In addition to extraction measurements using radiotracers, NMR has been used to investigate the species present in the extraction process.

Cadmium has a high affinity for forming anionic chloride complexes [1]. Therefore, an extractant with anion exchange function was chosen for removing cadmium from an aqueous solution. The quaternary amine Aliquat 336, was selected. In Figure 4 the distribution ratio (log D) of cadmium as a function of extractant activity is shown. Aliquat 336 exchanges a chloride anion with a cadmium complex. The distribution ratio (D-ratio) is defined as:

$$D = \frac{A_{org} V_{aq}}{A_{aq} V_{org}}$$

Here A_{org} and A_{aq} are the chemical activities represented by the count rates in the organic and the aqueous phase, respectively. V_{org} and V_{aq} are the volume of the organic phase and the aqueous phase, respectively. As the chloride activity is increased the D-ratio increases indicating that a more negative species is dominating. The poster will present comparisons of extractions with high ionic strength and low ionic strength.

Extraction of cadmium was traced using the radionuclide ^{109}Cd . ^{109}Cd decays to $^{109\text{m}}\text{Ag}$ ($T_{1/2} = 39.6$ sec) and de-excites by emitting conversion electrons making it suitable for detection by Liquid Scintillation Counting (LSC). The branching for the conversion electrons is 96% [2]. Due to the three-peak structure of the spectrum, standard quench correction methods as implemented by most LSC instruments are not very accurate. A special quench calibration procedure was therefore developed and will be presented at the NRC conference.

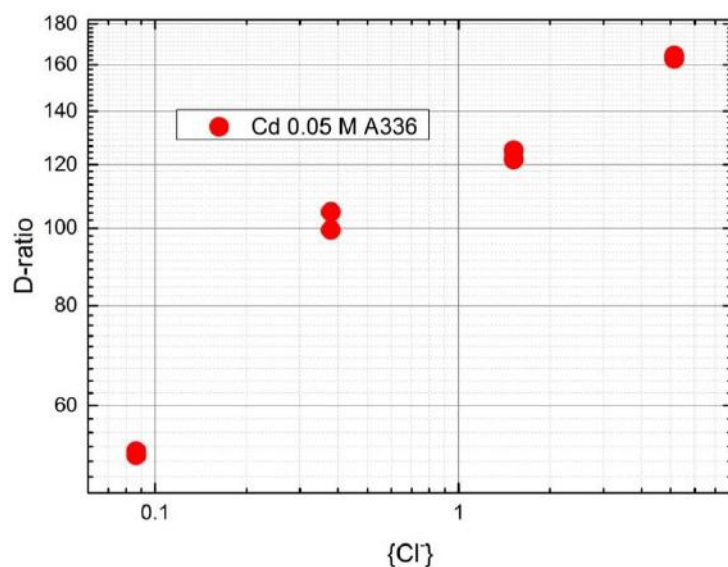


Figure 4 Extraction of cadmium from various chloride activities into 0.05 M Aliquat 336

1. Kipton J. Powell, Paul L. Brown, Robert H. Byrne, Tamas Gajda, Glenn Hefter, Ann-Kathrin Leuz, Staffan Sjöberg, Hans Wanner, *Chemical speciation of environmentally significant metals with inorganic Ligands. Part 4: The $\text{Cd}^{2+} + \text{OH}^-$, Cl^- , CO_3^{2-} , SO_4^{2-} , and PO_4^{3-} systems (IUPAC Technical Report)*. Pure and applied chemistry, 2011. **83**(5): p. 1163-1214.
2. Blachot J., *Nuclear Data Sheet for A = 109*. Nuclear Data Sheets, 2006. **107**: p. 355-506.

Improvement of chemical treatments for ^{32}P analysis in radioisotope wastes

Sang Ho Lim, Dong Je Lee, Se Chul Sohn, Kwang Yong Jee and Hong Joo Ahn

Nuclear Chemistry Research Division, KAERI, Daedeok-daero, Yuseong-gu, Daejeon, Republic of Korea
slim@kaeri.re.kr

Recently, as the use of ^{32}P labeled biomolecules have been dramatically increased for industrial purposes such as in vivo test, gauges, radiation diagnosis and teletherapy, the number of the ^{32}P analysis in RI wastes have been also increased. Therefore adoptions of relatively simple and suitable chemical procedures for separating pure phosphorous with high recovery yield are essentially required for more reliable and effective analysis of ^{32}P in radioisotope (RI) wastes. In general, the chemical procedures can be divided into chemical leaching step in the presence of hot nitric or hydrochloric acids and liquid-liquid extraction by tri-n-octylamine/xylene mixture. The total activity of the separated ^{32}P portion is determined by liquid scintillation counter (LSC). In chemical leaching step adopted in our laboratory, the reflux apparatus consisting of round-bottom flask, condenser, heating mantle, and cooling water circulation system were used to effectively leach out phosphorous portion as a phosphate form from RI wastes. Although this method was well established and regarded as one of the most effective methods, there are some limitations in terms of space, total experiment times per sample, and the amounts of chemical wastes generated during the procedures. In this study, more space-saving and simple chemical leaching process, namely 'pressurized leaching method' using Teflon digestion vessel was introduced to reduce chemical process times and the amounts of chemical wastes during the chemical leaching steps in comparison with the conventional method. To verify this method, recovery yields and analytical results from the chemical leaching step with simulated samples containing ^{32}P standard tracer were estimated. On the other hand, the solution obtained from the chemical leaching step often contain other RI species such as ^3H , ^{14}C , ^{35}S , ^{124}I , and ^{131}I . These other species (mainly ^3H and ^{14}C) with relatively high concentration compared to ^{32}P may lead to interfere with accurate ^{32}P measurement. Herein, we also present improved liquid-liquid extraction procedures to avoid interfering effects by other radioactive species.

Behavior of rare-earth elements and Ac in system UTEVA- acid solution

^{1,2}MARINOV, Genko, ¹MARINOVA, Atanaska, ²MILANOVA, Maria, ³HAPPEL, Steffen, ¹FILOSOFOV, Dmitry

¹ *Joint Institute for Nuclear Research, Dubna, Russia*

² *University of Sofia, Faculty of Chemistry and Pharmacy, Sofia, Bulgaria*

³ *Triskem International, Bruz, France*

Fine purification of rare-earth elements (REE) from actinides (An) like Th and U presents interest, therefore it is an object of growing number of investigations. Showing great retention properties for tetravalent An and U (VI) is the extraction chromatographic resin UTEVA (Uranium and TEtraValent Actinides). In this work, by using different, well-known acids was determined the distribution of some REE on UTEVA resin. In our study we confirm the low sorption of all REE in the range of 1M – 5M HNO₃, which presents the possibility to purify REE from tetravalent An and U (VI). The data we obtained for high concentrations of HNO₃ shows a gradual increase of the distribution coefficients (K_d) with increase of the atomic number of Ln as well as for Y and Sc. Another system examined in this study is the system UTEVA –CCl₃COOH, which showed higher selectivity for Eu. Chromatographic separations were carried out in order to confirm the K_d values we obtained for both systems.

Comparison between two methods of sequential determination of Am, Pu, U isotopes in metallic radioactive waste

ŞANDRU, Adina, TORO, Laszlo, MUŞAT, Aurelia, TEODOROV, Gabriela

MATE-FIN - Cernavoda Site, 79-81 Vulturilor Street, S 3, 030853, Bucharest-ROMANIA

The purpose of this paper is to compare two sequential radiochemical separation methods of Am, Pu, U isotopes from the metallic waste and subsequently to develop and establish the optimal separation method, taking into account the content of the Alpha emitters isotopes. Am, Pu, U isotopes determination is required for radioactive waste characterization and management. Samples which are going to be analyzed have been obtained by scraping the metal surface of the metallic waste parts (pipes from the cooling system, tanks, tools) and then have been decomposed by closed microwave digestion in mixed acid solution (HNO_3 , HCl). Am^{243} , U^{232} , Pu^{242} were used as tracers. The resulting solution was completely evaporated and afterwards dissolved in 8M HNO_3 . Both radiochemical methods (Method A and Method B) use a combination of purifying and separation techniques: anion-exchange resin chromatography, extraction chromatography, coprecipitation and redox techniques. In the first method (method A), the separation of Pu and U isotopes was performed using AG-1X4 100-200 Cl⁻ form anion exchange resin (Bio Rad Laboratories), while Am/Cm isotopes were purified using TRU Eichrom's resin. The second method (method B) uses AG-1X4 100-200 Cl⁻ form anion exchange resin for U isotopes separation and Eichrom's UTEVA and TRU resins for both U and Am/Cm separation. The thin alpha emitters sources were prepared by microprecipitation with CeF_3 . An ORTEC alpha spectrometer was used in order for the measurements to be done. The conclusions generated following the implementation of the two radiochemical separation methods will be presented.

Rapid determination of Radium-224/226 in seawater sample

Lijuan Song^{1,2}, Xiongxin Dai^{1,2}, Maoyi Luo^{1,2}, Yonggang Yang^{1,2}

¹ *China Institute for Radiation Protection, Taiyuan, China*

² *Collaborative Innovation Center of Radiation Medicine of Jiangsu Higher Education Institutions, Suzhou, China*

songlijuan12@yahoo.com

A rapid separation method has been developed, which allows the determination of radium isotopes in seawater samples. In this method, ²²⁴Ra, together with its parents in secular equilibrium in the ²³²U standard solution, is added as a tracer for chemical recovery monitoring and correction for the measurement of ²²⁶Ra. Similarly, ²²⁶Ra can also be used as tracer for the determination of ²²⁴Ra in seawater sample. Radium is first separated from seawater matrix by co-precipitation with hydrous titanium oxide (HTiO) and subsequently purified by combined anion/cation exchange column chromatographic separation. After the co-precipitation with HTiO again, the radium is dissolved in 9M H₂SO₄, followed by a BaSO₄ micro-precipitation step to prepare a thin-layer counting source for counting of Ra-224/226 by alpha spectrometry. Seawater samples spiked with known amounts of Ra-224 or Ra-226 were prepared for method performance testing. The detailed results of method development and validation will be reported and discussed.

Preparation of anhydrous uranium tetrafluoride as a possible matrix material for Accelerator Mass Spectrometry

Irena Špendlíková, Mojmír Němec, Tomáš Prášek

Department of Nuclear Chemistry, Faculty of Nuclear Sciences and Physical Engineering, Czech Technical University, 115 19 Prague, Czech Republic

The detection of ultra-trace concentrations in environmental samples by Accelerator Mass Spectrometry (AMS) is always preceded by sample processing and the final chemical form of the sample is crucial for gaining reliable and repeatable results. For the determination of U-236/U-238 ratios, the most often used final form is uranium oxide from which the UO^+ beam is produced. Uranium fluoride targets containing no oxygen and hydrogen may offer higher molecular isobar suppression together with a higher accuracy and sensitivity of uranium isotope analysis [1]. However, the preparation of anhydrous uranium tetrafluoride targets is more complicated than the preparation of uranium oxide targets.

This work deals with the preparation of anhydrous uranium tetrafluoride at the quality suitable for accelerator mass spectrometry measurements. Our previous research showed that for the initial preparation used uranium dioxide was already partially oxidised to VI+ state which had negatively influenced the results. However, the ion current from only one UF_2^+ sample was in average higher by about 50 % than the UO^+ current from the uranium oxide samples in AMS measurements [2]. Afterwards, our main efforts focused on the quality of reactants and on the improvements of existing preparation methods in accordance with our laboratory equipment and conditions.

Only several methods of anhydrous uranium tetrafluoride preparation without using hydrofluoric gas have been published and three of them were reproduced in our laboratory to find the one which will be the most suitable for the implementation into AMS sample preparation methods. The prepared materials were after thermal treatment as crystalline powder checked for their chemical purity using X-ray powder diffraction which easily analyses the presence of reactants or other unwanted chemicals. Another evaluation criteria is the sort of reactants used in the methods; those based on the U(IV+) state are less preferable due to the employment of necessary step for U(VI+) reduction. Even after minimizing possible oxygen inputs into reactions, the pure anhydrous uranium tetrafluoride has not been prepared. Our following research is focused on finding other possible preparation methods and their connection to the separation procedures in methods of U-236 determination using AMS.

References

1. Wang X.: Nucl. Technol., 2013(182), 235.
2. Povinec et al. J. Radioanal. Nucl. Chem. 2014 (304) 67-73

The evaluation of Ca contents on a radiochemical separation of Sr, Fe, Nb and Ni in DAW

Kyungwon Seon*, Kwang-Soon Choi, Hye Ju Lee, Hyun-Jung Oh and Hong Joo Ahn

Nuclear Chemistry Research Division, KAERI, Daedeok-daero, Yuseong-gu, Daejeon, Republic of Korea

*[*kyungwon0707@kaeri.re.kr](mailto:kyungwon0707@kaeri.re.kr)*

The determination of a radionuclide concentration in low and intermediate-level radioactive wastes is essentially required to meet the waste acceptance criteria of Korean Nuclear Safety and Security Commission (NSSC), which indicates to identify more than 95% radionuclide present in the radioactive waste drums prior to permanent disposal. For a determination of the radionuclide concentration, an individually radiochemical separation process such as precipitation, ion-exchange and/or extraction chromatography from the co-existing radionuclides is preceded in the case of beta-emitting nuclides to prevent the interference with the co-existing radionuclides.

We have established the standard procedure of a radiochemical separation for the following radionuclides, ^{90}Sr , ^{55}Fe , ^{94}Nb and $^{59,63}\text{Ni}$ in dry active wastes. This standard procedure is applied for a radiochemical separation of the above mentioned radionuclides in low and intermediate-level wastes (LILW) from the R&D activity in Korea Atomic Energy Research Institute (KAERI). In details, after preparing oxalate solution by adding oxalic acid to sample solution, the radiochemical separation is processed through following sequential separation steps. Sr is individually separated as Sr(Ca)-oxalate and purified by extraction chromatography using Sr-resin. Fe and Nb are individually separated by ion-exchange chromatography. Ni is separated by ion-exchange chromatography and purified by extraction chromatography using Ni-resin.

Some samples from KAERI R&D wastes containing high concentration of Ca have an effect on a radiochemical yield of each radionuclide in DAW. In this paper, we first show that the evaluation of Ca contents in a radiochemical separation of each radionuclide present in DAW. And we suggest that the fractional precipitation to enhance the radiochemical yield of Sr.

Method development for the analysis of very low-activity ^{226}Ra contaminated environmental water samples by alpha-spectrometry

E. M. van Es^{1, 2}, P. Ivanov², D. Read^{1,2}.

¹ *Chemistry Department, University of Surrey, Guildford, Surrey, GU2 7XH, United Kingdom*

² *National Physical Laboratory, Hampton Road, Teddington, Middlesex, TW11 0LW, United Kingdom*

Exploitation of mineral resources containing Naturally Occurring Radioactive Material (NORM) creates waste in which natural radioactive decay series isotopes, in particular $^{226/228}\text{Ra}$, ^{210}Pb and ^{210}Po , are often concentrated to levels that are hazardous to human health. Consequently, producers are required to comply with very stringent limits when discharging wastes to water courses. In the United Kingdom, the discharge limit for ^{226}Ra is only 10 mBq L^{-1} , however, ^{226}Ra is naturally present in groundwaters at levels close to and above this value; its abundance varying depending on local geology. This regulatory target presents a serious challenge to analysts when attempting to differentiate natural background from industrial contamination. Results are presented for ^{226}Ra determination in environmental groundwater samples prior to unconventional oil extraction, the aim being to determine the baseline ^{226}Ra content in order to assess the impact of future discharges of flowback waters on local aquifers following hydraulic fracturing ('fracking'). A rapid method for ^{226}Ra determination is proposed and verified. Radium-223 was used as a tracer with recovery in the range of 30-50%. Samples ($\sim 1 \text{ L}$, pH 6.5-7.0) were pre-concentrated using a MnO_2 -PAN (polyacrylonitrile) resin (2 mL L^{-1}), the radium was eluted (1.0 mL min^{-1}) with $15 \text{ mL } 10 \text{ M HCl}/1.5\% \text{ H}_2\text{O}_2$ and alpha spectrometry of the Ba(Ra)SO_4 precipitate used for ^{226}Ra determination. It was found that baseline concentrations of ^{226}Ra in the groundwaters ranged from $2\text{-}200 \text{ mBq L}^{-1}$, indicating that in some cases, natural radium activity concentrations already exceed the discharge limit. The practicability of imposing such stringent regulatory limits on industrial discharges is discussed.

Optimization of isolation and mass spectrometric analysis of lanthanides from spent nuclear fuel

Karen Van Hoecke^a, Jakob Bussé^a, Mireille Gysemans^a, Lesley Adriaensen^a, Andrew Dobney^a,
Thomas Cardinaels^a

*Belgian Nuclear Research Center (SCK•CEN), Nuclear Materials Science, Radiochemistry expert group,
BE-2400 Mol, Belgium*

Introduction and objectives

Mass spectrometric techniques are often used to characterize the chemical composition of spent nuclear fuels. Dy, Gd, Eu, Sm, Nd are the main Lanthanide (Ln) analytes of interest. However, in order to prevent erroneous results due to isobaric overlap, separation prior to ICP-MS analysis is necessary. If complete and fast separation can be accomplished using High Pressure Ion Chromatography (HPIC), the latter technique is preferred over gravimetric column separation (e.g. [1],[2]). This work focuses on the implementation and evaluation of HPIC for Ln-Ln separation and sample preparation prior to ICP-MS and TIMS analysis. Initial goals of the work were (1) optimization of the HPIC separation method to achieve complete recovery of pure fractions of Dy, Gd, Eu, Sm and Nd; (2) investigation of the elution behaviour of other elements present in spent nuclear fuel, such as actinides, fission and activation products for the optimized method; (3) removal of the organic matrix from fractions collected after HPIC separation; (4) experimental determination of matrix effects from the sample matrix during ICP-MS and TIMS analyses.

Instrumentation

High Pressure Ion Chromatography instrumentation was supplied by Shimadzu, equipped with a LC-10Ai inert gradient pump. Lanthanides were separated on a Shodex IC-R621 column at 40 °C using double gradient elution with 0.1 M α -hydroxy-isobutyric acid (α -HIBA) pH 4.0 (eluent A) and 0.5 M α -HIBA pH 4.5 (eluent B). Detection of lanthanide elution was performed using a SPD-M20A photo diode array detector, monitoring UV-VIS absorption at 655 nm of lanthanide complexes with ArsenazoIII post-column reagent. Actinides Pu, Am, Cm isolated from a diluted solution of spent nuclear BWR UO₂ fuel were quantified in eluted fractions using α spectrometry. A Thermo XSeriesII ICP-MS instrument was used for elemental analysis. For removal of organic matrix, several digestion methods, involving open and closed vessel acid digestion on a hotplate, UV digestion (Methrohm 705 UV Digestor) and preconcentration of lanthanides on Ziptip[®] pipette tips were tested. Organic carbon concentration in final samples for ICP-MS analysis was quantified using a Hach IL550 total organic carbon (TOC) analyzer.

Results

The optimized double gradient HPIC separation method resulted in completely pure fractions of Dy, Gd, Eu, Sm and Nd, isolated from a 10 mg/l CLMS-1 multi-element certified standard solution, with and without an admixed U concentration up to 500 mg/l. Full elemental recoveries were obtained by means of ICP-MS analysis. Figure 1 shows the chromatogram as detected by means of UV-Vis absorption at 655 nm, indicating the Ln of interest and the percentage of eluent B admixed as a function of time. Examples of activation and fission products with shorter elution times than any Ln elements are Al, Fe, Nb, Mo, Ru, Rh, Sn, Sb and Te. The heavier Ln co-elute with In and U during the first 20 minutes of elution. Rb, Cd, Sr and Cs were the last elements to elute from the column, after all Ln elements. In order to elute Cs from the cation exchange column, an additional 15 minute elution with 1 M α -HIBA at pH 4.5 was required. Although Cs was not included as an analyte in this study, any accumulation of radionuclides on the analytical column had to be prevented.

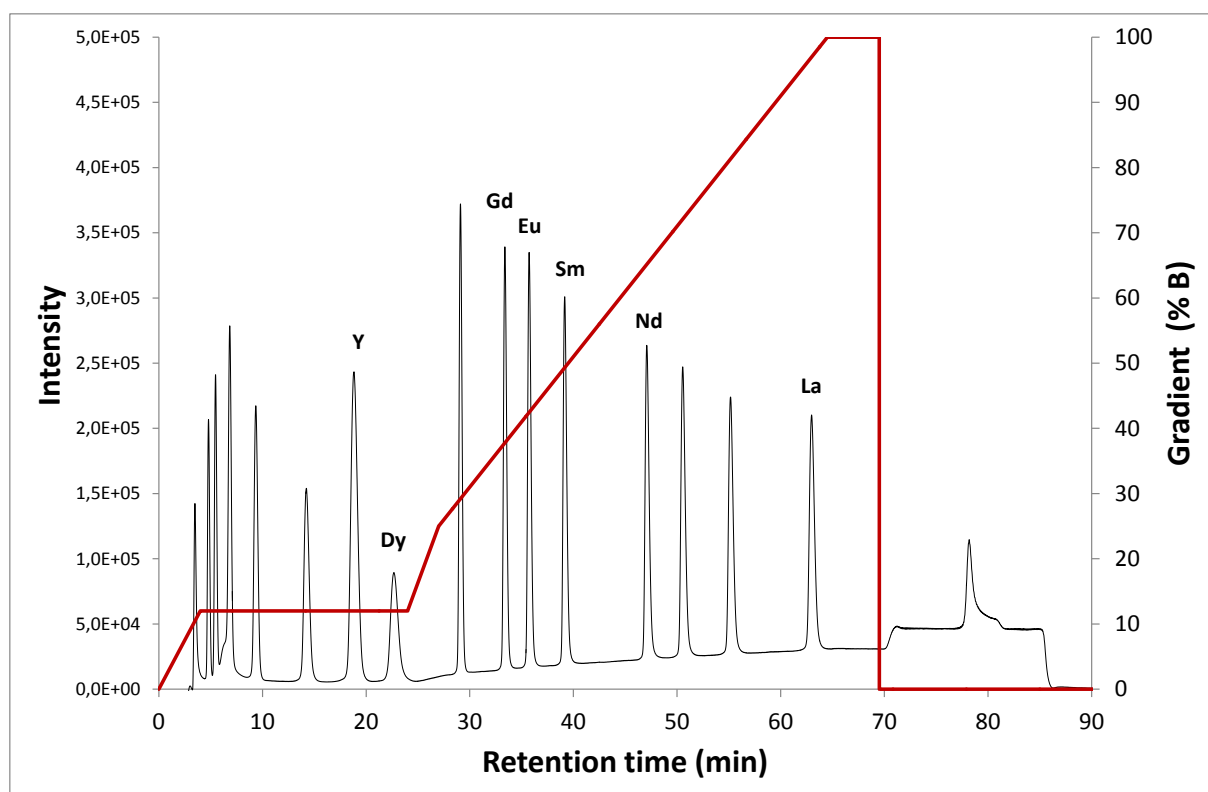


Figure 1 - Chromatogram of optimized Ln-Ln separation method by means of HPIC with UV-Vis absorption spectrophotometric detection (black curve) and % of 0.5 M α -HIBA admixed to the eluent.

Complete removal of the organic matrix of the eluent to a concentration below the TOC-analyzer limit of detection (5 mg/l C) was possible by using a combination of closed vessel acid digestion with aqua regia at 85 °C, evaporation, redissolution in 1 % (v/v) HNO₃ and one hour of UV-digestion, without any loss of Ln analytes. No significant matrix effects were found during ICP-MS analyses of samples prepared using the method described above.

Conclusion

A detailed sample preparation procedure for analysis of Ln from spent nuclear fuel prior to ICP-MS analysis was optimized. Pure lanthanide fractions in α -HIBA medium were obtained after separation via HPIC. Subsequent removal of the organic matrix by means of closed vessel aqua regia digestion followed by UV-digestion resulted in samples that can be readily analyzed by means of ICP-MS.

References

1. Gunther-Leopold, I., et al., *Characterization of nuclear fuels by ICP mass-spectrometric techniques*. Anal Bioanal Chem, 2008. **390**(2): p. 503-10.
2. Kumar, P., et al., *Determination of Lanthanides, Thorium, Uranium and Plutonium in Irradiated (Th, Pu)O₂ by Liquid Chromatography Using α -Hydroxyisobutyric Acid (α -HIBA)*. International Journal of Analytical Mass Spectrometry and Chromatography, 2013. **01**(01): p. 72-80.

Determination of polonium-210 in Lebanese tobacco

Ali Younes ¹, Gilles Montavon², Marcel Mokili ², Cyrille Alliot ³

¹Brookhaven National Laboratory, USA, NY, 11973

²Laboratoire Subatech (UMR 6457), France, Nantes 44307

³INSERM U892, GIP Arronax, France, Nantes 44817

ayounes@bnl.gov

The exposure of human beings to ionizing radiation from natural sources is a continuing and inescapable feature on life earth. For most individuals, this exposure exceeds that from all-made sources combined. The major natural background sources contributors include: Radon gas, high-energy cosmic ray particles which comes from outer space and our own sun (average dose in the U.S.A is 300μSv/year) and the terrestrial sources (30 mSv/year in some areas in Brazil and India). These terrestrial sources present the radioactive nuclides that are originated in the earth's crust and are present everywhere in the environment, such as the radionuclides with half-lives comparable to the age of earth, and their decay products. One of the final long-lived radionuclides which is presents in the terrestrial environments in the decay chain of ²³⁸U is polonium-210 (²¹⁰Po, $t_{1/2}=138.376 \pm 0.002$ days). Although, ²¹⁰Po is present in the environmental at very extremely low concentration, it is considered as one of the highly toxic elements and is estimated to contribute about 7% of the total effective dose equivalent to man from ingested natural internal radiation. This is due to its purely alpha emitter and high specific activity (166 TBq/g), with the main hazard associated with ingestion and inhalation [1]. To illustrate this point, 1 μg of ²¹⁰Po emits as many alpha particles per second as 4.5 mg of ²²⁶Ra, 262 mg of ²³⁸Pu, or 446 kg of ²³⁸U. Polonium-210 enters food chains and it bio-accumulates in tobacco plants. The concentrations of ²¹⁰Po measured in cigarette tobacco in different countries were measured in the range of 2.8–37 mBq/cigarette due to the difference in geological nature. It is known that ²¹⁰Po contained in tobacco is volatile at the temperature of a burning cigarette [2]. Due to the relatively high activity concentrations of ²¹⁰Po that are found in tobacco and its products, cigarette smoking highly increases the internal intake of this radionuclide. Hence a radiation hazard from ²¹⁰Po may arise for a smoker's lung tissues [3]. In the present study, the concentration of polonium was determined in the most frequently sold cigarette produced in Lebanon. Polonium was determined by using alpha spectrometry using a surface barrier detector after radiochemical separation and spontaneous deposition of Po on a copper disk. The results showed the concentration of polonium is equal to 25.98 ± 1.96 mBq per cigarette. The collective committed effective dose resulting from the use of cigarette produced in Lebanon per year is estimated to be 219 ± 16.5 μSv.

References

- [1]. E. Ansoborlo, P. Berard, C. Den Auwer, R. Leggett, F. Menetrier, A. Younes, G. Montavon, and P. Moisy, Chem. Res. Toxicol. 2012, 25, 1551–1564.
- [2]. D. Singh, R. Nikelani. Health Physics. 1976, 31, 393-394.
- [3]. H. Mussalo-Rauhamaa, T. Jaakkola, Health Physics. 1985, 49(2) 296-301.

Assessment and comparison of methods for the fast analysis of alpha and beta emitters in air filters

¹Daniel Zapata-Garcia, ¹Herbert Wershofen, ²Meryem Seferinoğlu, ²Abdullah Dirican, ²Nazife Aslan, ²Gülten Kahraman, ²Ülkü Yucel

¹*Physikalisch-Technische Bundesanstalt, PTB, Bundesallee 100, D-38116 Braunschweig, Germany*

²*Turkish Atomic Energy Authority; TAEK, Sarayköy Nuclear Research and Training Center Saray Mah. Atom Cad. No: 27, 06983 Kazan, Ankara, Turkey*

A reliable determination of radionuclides in air is necessary for regular monitoring of air quality to comply with radiation protection and environmental regulations. Moreover, it is a key factor in order to organise appropriate countermeasures for the protection of the general public against dangers arising both from direct external radiation and from intake of radioactivity from foodstuff and from air in case of a radiological emergency.

The nuclear power plant accident at Fukushima Daiichi showed that the radioactivity monitoring networks in Europe, which were established after the Chernobyl catastrophe, were able to provide the necessary information to evaluate the impact of the accident on the population. But this episode also made it clear that nowadays society demands exchanging information in real-time and at the international level. To make these two features possible, monitoring networks require improvement focused on the development of fast response protocols and harmonisation results.

The work we present deals with adapting traditional radiochemical methods for the determination of alpha and beta emitters in air filters to develop faster alternatives and the difficulties and limitations that it entails. Two rapid methods developed at TAEK (Turkey) and PTB (Germany) are presented. Both methods are based on the extraction chromatography schemes but have differences according to the needs of each laboratory. The harmonisation work in this case consisted in developing an optimisation and validation strategy run by both laboratories in order to grant the comparability of the results.

In this presentation, the chosen strategy, the pitfalls that arose along the work as well as the most significant results of the validation work carried out will be presented and discussed.

NUCLEAR ANALYTICAL METHODS

Emission mossbauer spectroscopy applied for studies on the structure and behavior of amorphous materials under critical conditions

I. Alekseev

V.G. Khlopin Radium Institute, 28, 2nd Murinsky Pr., St. Petersburg, 194021, Russia

^{57}Co diffusion processes have been studied in the classical chalcogenide GeS_x glasses ($x=1.6, 1.8$ and 2.2) at $573\text{--}693\text{ K}$ (the glass vitrification temperature T_g being $666, 701$ and 703 K , respectively). The experimental technique used (the method of sectioning combined with the measurement of emission Mossbauer spectra before and after removing each successive diffusion layer) has enabled the ^{57}Co chemical species to be identified and their contribution into each integral diffusion coefficient to be evaluated. Along the whole depth of the diffusion profiles in the glass matrix there are two different forms of the diffusant present (see Fig.1):

- ^{57}Co atoms in the molecular $^{57}\text{CoCl}_2$ fragment (Doublet I and Singlet II as an aliovalent form of iron resulting from electronic capture of ^{57}Co in the CoCl_2 “molecule”, see Table 1);
- an ionic form of ^{57}Co (Singlet 1).

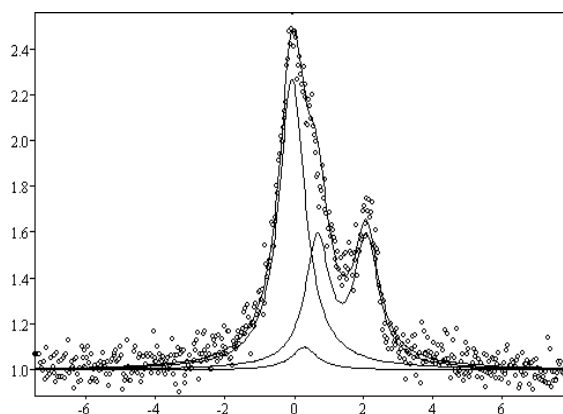


Fig. 1. An Emission spectrum of the $\text{GeS}_{2.2}$ Glass Measured at RT

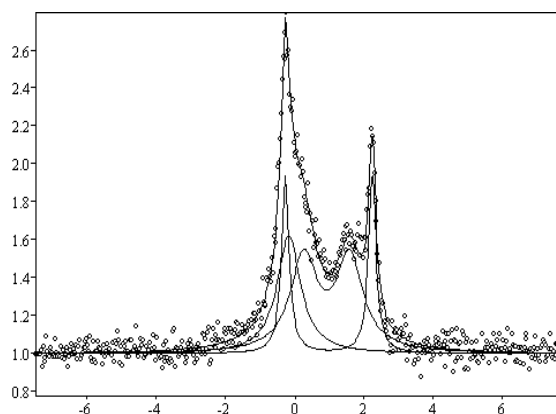


Fig. 3. An Emission Spectrum of the $\text{GeS}_{2.2}$ Glass Measured at 693 K

Table 1

T, K	Singlet I (Fe^{3+})			Singlet II (Fe^{3+})			Doublet I (Fe^{2+})				Doublet II (Fe^{2+})			
	IS	Γ	S	IS	Γ	S	IS	Γ	QS	S	IS	Γ	QS	S
RT	-0.1	0.92	53	0.28	0.90	4	1.37	0.84	1.42	43	-	-	-	-
693	-0.2	0.83	27	-	-	-	0.92	0.94	1.33	48	0.98	0.26	2.52	25

IS - the isomer shift relative to $\alpha\text{-Fe}$, $\pm 0.02\text{ mm}\cdot\text{sec}^{-1}$, QS - quadrupole splitting value, $\pm 0.02\text{ mm}\cdot\text{sec}^{-1}$; Γ - experimental line width, $\pm 0.02\text{ mm}\cdot\text{sec}^{-1}$, S - fraction in the spectrum, $\pm 2\%$

While moving into the depth of samples by sectioning, it is the ^{57}Co ionic form that becomes predominant (Table 2). On the diffusion profiles there is a characteristic bend observed (see Fig.2) testifying to different rates of migration of the “molecular” $^{57}\text{CoCl}_2$ fragment and of the ionic ^{57}Co form in the glass matrix.

Table 2	$^{57}\text{CoCl}_2$, %	^{57}Co -ion, %
Before polishing	50	50
After removal of 430 μm from the glass surface by polishing	25	75

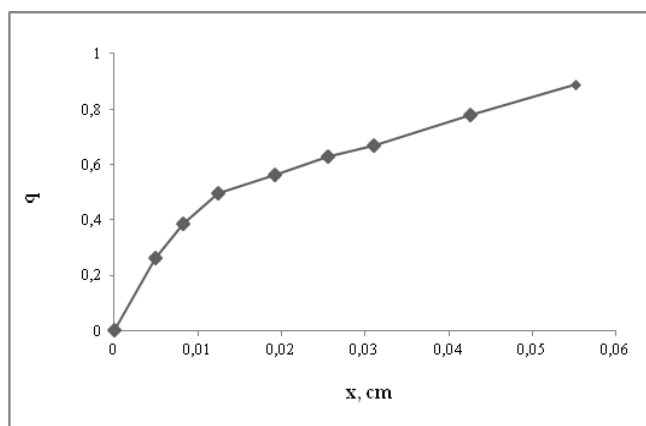


Fig. 3. A Profile of the $\text{GeS}_{1.6}$ Sample after Annealing at 653 K

Taking account of the radius of the $^{57}\text{CoCl}_2$ fragment (~ 0.24 nm), it may be assumed that in the glass matrix there are channels of a larger diameter along which the molecule of such larger size can “freely” move. Evaluative calculations show that diffusion coefficients of the ionic ^{57}Co -species at 573-693 K are 10^{-11} - 10^{-10} $\text{cm}^2\cdot\text{sec}^{-1}$, that of the “molecular” fragment, 10^{-12} - 10^{-11} $\text{cm}^2\cdot\text{sec}^{-1}$. In parallel, there were temperature-dependent measurements conducted of Mossbauer spectra in the RT - 693K temperature range. With the rise of measurement temperature, there is a larger Fe^{2+} fraction observed (see Fig.3). Most probably, the main reason for “quenching” the Fe^{3+} -species is due to the growth of electronic conductance with temperature. Apart from it, at high temperatures (as from 500 K), there is a new Fe^{2+} -species appearing (doublet II in Table 2), with a higher quadruple splitting value, but smaller linewidths that are characteristic for a “crystal-like” environment of Fe. The effect magnitude is practically independent of the measurement temperature: on heating in glasses (more precisely, in the nearest environment of Co/Fe atoms) there are certain transformations occurring that strengthen the structure. On cooling the sample down to RT, the initial picture (see Fig.1) is completely restored. The conducted studies have shown that the emission type of Mossbauer spectroscopy can be a powerful tool in studies on the structure and behavior of amorphous materials under critical conditions (in the vicinity of temperatures of vitrification and crystallization).

The authors would like to express their deep appreciation to Professor E. Bychkov (LPCA, ULCO Univ. Lille Nord de France, Dunkerque, France), who has kindly presented the glass samples for the studies.

Numerical efficiency calibration for environmental gamma spectrometry using a medical imaging software

Tareq Alrefae

*Department of Physics, Kuwait University, Kuwait
tareq@uw.edu*

Gamma spectrometry (GS) is an effective tool for measuring environmental radiation. This technique allows for identification of gamma emitting radionuclides, as well as quantification of the emitted gamma radiation. Like any detection system, GS requires efficiency calibration. Such procedure is typically performed experimentally by the use of standard sources of known radioactivities. Although this experimental application has been proven to give accurate results, it suffers from a number of drawbacks. For example, the constituency and geometry of the standard source has to match those of the investigated sample. This condition is mainly due to the dependence of gamma attenuation on the density and geometry of the absorbing medium. Hence, to cover a wide range of media and geometries, an impractically large inventory of standard sources is needed. Furthermore, with the decay of the radionuclide of interest, the standard source becomes worthless.

An alternative approach is to numerically perform efficiency calibration for GS. In fact, it has been shown that Monte Carlo simulations, coupled with the relevant physics models, can correctly predict the behavior of gamma radiation, thus enabling proper GS efficiency calibration. Consequently, software toolkits were made available for interested users. Aside from the copyrighted commercial software which usually come with the detector for a hefty price, the public domain makes available open-source software. Nonetheless, these free-of-charge software often lack user-friendliness and require a solid knowledge of a major programming language. Such requisites pose major obstacles for interested users.

The GEANT4 Application for Tomographic Emission (GATE), is a Monte Carlo toolkit that was developed for simulating medical imaging and radiotherapy applications. One feature of this software is its simple script syntax which eliminates the need for hard core programming languages. Hence, this advantage was utilized in this work to calibrate the efficiency of GS. Particularly, the medical imaging module was numerically dismantled before computationally reassembling the system as a GS detector. Such numerical manipulation was possible by exploiting the physics similarities between the original medical module and the sought environmental radioactivity application. The output of this approach was validated by comparing its predicted efficiencies to efficiency values obtained experimentally. This comparison revealed close agreement, thus validating the adopted approach.

Study of the disequilibrium of ^{238}U and ^{232}Th decay chains by mapping approach

Axel Angileri¹, Paul Sardini¹, Michael Descostes², Samuel Duval³, Michel Fialin⁴, Tugdual Oger³, Patricia Patrier¹, Marja Siitari-Kauppi⁵, Hervé Toubon², Jérôme Donnard³

1 IC2MP Equipe HydrASA, Poitiers, France.

2 AREVA, Paris, France.

3 Ai4R SAS, Nantes, France.

4 Service Comparis, Paris, France.

5 Laboratory of Radiochemistry, Department of Chemistry, University of Helsinki, Finland.

^{238}U , ^{235}U and ^{232}Th decay chains are naturally occurring. These chains are considered to be at secular equilibrium for a geological sample with an age superior to respectively 2.5 million years, 338 thousand years and 57 years (approximately ten times the half-life of the intermediate radionuclides with the longest half-life). In the industrial cycle of U the selective extraction of U produces tailings with low concentration of U. However, tailings are always highly radioactive due to the presence of daughter radionuclides, such as ^{226}Ra (36.6 GBq/g). No current methods allow to localize these daughter radionuclides.

A new approach was developed and tested in order to spatially localize and determine the equilibrium state of natural decay chains on hand-scale geological samples. This approach is a combination of three techniques: 1) Elementary chemical mapping by microprobe; 2) Digital alpha autoradiography by gaseous detectors (Beaver™) and 3) bulk alpha particle spectrometry.

Elementary chemical mapping of U was calculated into theoretical alpha mapping at equilibrium. The theoretical mapping at equilibrium was compared with the experimental mapping of alpha emission made by the Beaver™, which permitted to identify and localize the equilibrium state on the sample. Bulk alpha spectrometry was used to identify the alpha emitting radionuclides present in the sample and the equilibrium state of the decay chain.

The comparison between the both chemical and numerical autoradiographic methods (techniques 1 and 2) permitted to suppose radioactive equilibrium in two U-rich geological samples. This equilibrium state was confirmed by alpha spectrometry analyses. Moreover, disequilibrium areas were clearly identified on fresh tailing thin section.

Studies of organohalogen species in lipid extracts of northern pink shrimp by neutron activation, chromatographic, nuclear magnetic resonance and mass spectrometric techniques

C.S. Bottaro, J.W. Kiceniuk, A. Chatt*

Trace Analysis Research Centre, Department of Chemistry, Dalhousie University, Halifax, Canada
chatt@dal.ca

A large number of extractable organohalogens (EOX), such as DDT, PCB's, and dioxins, has been well characterized and are routinely analyzed in many environmental samples. Much of this work has been limited to anthropogenic organochlorines (EOCl), organobromines (EOBr) and their metabolites. However, given that a large percentage of total EOX remains unidentified there continues to be a need to find methods to separate and characterize these unknown organohalogens. Much of the EOCl that cannot be accounted for as anthropogenic compounds tends to be found in lipid-containing fractions. In the study reported here a large amount of lipid was extracted from roe of Northern Pink Shrimp (*Pandalus borealis*) using a hexane-acetone mixture. Roe was selected for this study because it was lipid-rich and high in EOX. Various properties of the extracted lipids, such as size, polarity, aromaticity, acidity, etc., were exploited to accomplish further separations followed by their characterization. The techniques used here included dialysis, size exclusion chromatography (SEC), normal-phase chromatography, reversed-phase chromatography, thin layer chromatography, transesterification followed by mass spectrometry and nuclear magnetic resonance spectrometry. We employed a neutron activation analysis (NAA) method using the Dalhousie University SLOWPOKE-2 reactor facility for the determination of low-to-high levels of chlorine, bromine and iodine in various tissues, lipid fractions, and extracts with high precision, accuracy and rapidity. The results indicated that EOCl must be somewhat different than EOI and EOBr and the differences in distribution of the EOCl compared to EOBr illustrated this. This could be related to the origin of EOCl, *i.e.* natural or anthropogenic or to the levels found in the local food source. It can be concluded from the mass spectra of the SEC and Florisil fractions and from the TLC that the majority of the chlorine was a mixture of acylglycerols and fatty acids. This fact combined with the results of the ^1H NMR suggested that much of the chlorinated components found in these fractions were fatty acids. The chlorinated fatty acids could be distributed throughout the various mono-, di-, and triacylglycerols in an extensive number of combinations. The NAA method was found to be extremely useful not only for tracking the halogens during various separation steps but also for independent verification of the existence of the halogens in the fatty acids. Moreover, it gave low overall expanded uncertainties of the halogens compared to other detection techniques. The details of method development and results will be presented.

Analytical applications of nuclear methods at NIST

Pamela M. Chu, R. Gregory Downing, Rabia Oflaz, Rick L. Paul, Danyal Turkoglu, Rolf Zeisler

National Institute of Standards and Technology, Gaithersburg, Maryland 20899, USA

The Nuclear Methods Team of the Chemical Sciences Division develops and applies innovative nuclear methods to solve analytical measurement challenges. NIST's research reactor is one of the world's premier facilities for neutron beam methods and pneumatic tube activation analysis. We routinely probe the composition of a wide range of materials, from human blood to engineered nanoparticles, and develop Standard Reference Materials (SRMs) that establish reliability across most industries and numerous research applications. Our fundamental research programs often engage the collaboration of scientists across NIST, academia, industry, other government agencies, and foreign guest scientists. Recent programs encompass measurements in support of alternative power, environmental and health standards, homeland security, and fundamental measurement science. The poster will highlight a few recent programs and some new instrumentation. For example, the activities in the development of SRMs highlight low-level trace element determinations by radiochemical (RNAA) and instrumental (INAA) neutron activation analysis, as well as the combination of INAA with liquid chromatography and inductively coupled plasma mass spectrometry (ICP-MS) for the determination of arsenic species. The commissioning and further development of the new cold neutron prompt gamma-ray activation analysis instrument as well as the cold neutron beam depth profiling facility offer expanded capabilities for material characterization, including approaches to the quantitative determination of elements in hydrogen containing materials. Further research opportunities are opening up with gamma-gamma coincidence spectrometry employing an array of four high efficiency gamma-ray detectors. We invite guest scientists and talented students to work with us on issues of scientific significance.

Comparison of two autoradiography techniques: Phosphoimager versus The Beaver PIM device on hydrothermally altered andesites from Petite Anse, Martinique.

Charli Delayre¹, Paul Sardini¹, Patricia Patrier¹, Juuso Sammaljärvi², Tugdual Oger³, Jérôme Donnard³ and Marja Siitari-Kauppi²

1 HYDRASA, IC2MP, Université de Poitiers, France

2 Laboratory of Radiochemistry, Department of Chemistry, University of Helsinki, Finland

3 Ai4R SAS, Nantes, France.

Autoradiography technique has been developed since 1970's and is currently used in domains such as neurosciences, biology and geology. This technique allows the determination of spatial distribution of radiolabelled substances as well as radioactive material by placing them on radio-sensitive films. In the 90's, the ¹⁴C-MMA (methylmethacrylate) method has been developed to study distribution of porosity and micro-fractures in hard materials such as granitic rocks¹. The method consists of impregnation of centimetre-scale rock samples with a monomer methylmethacrylate (MMA) labelled with ¹⁴C. ¹⁴C-MMA is then polymerized inside the sample. ¹⁴C-PMMA impregnated samples are then sawed and polished, followed by placing the sample surfaces on imaging plates (IP; phosphor screen plates sensitive to beta radiation) with appropriate exposition time before digitizing the IP plate with a phosphoimager (FLA 5000 scanner, Fuji). Digital photoluminescence process is presented in figure 1. This method produces 16-bits grayscale images called digital autoradiographs (DA).

More recently, a new generation of digital autoradiography i.e. filmless autoradiography system Le Beaver (Ai4r) has been developed using a Parallel Ionization Multiplier (PIM) coupled with a Micro Pattern Gas Detector (MPGD). Structure of the PIM device is presented in figure 2. This new autoradiography technique allows 2D beta and alpha-imaging of samples by placing them directly into a gas chamber. Beta- and alpha particles emitted from the source (sample) induce ionization of the gas molecules contained between the cathode and the anode, with the anode acting as a detector of the PIM system.

In this work, hydrothermally altered andesites showing argillic alteration were impregnated using ¹⁴C-PMMA method for characterization of connected porosity as well as cracks distribution. The samples investigated come from Martinique (Eastern Caribbean) and belong to geothermal system of Petite Anse-Diamant. Influence of hydrothermal alterations on petrophysical properties (e.g. porosity, distribution of cracks, permeability...) is of main interest in understanding reservoir capacity of rocks in geothermal context or diffusion of pollutants in environment. Thus, the work presented here aimed to make comparison of results obtained from analysis of Beta images from the two autoradiography techniques and their adaptability on altered geological samples.

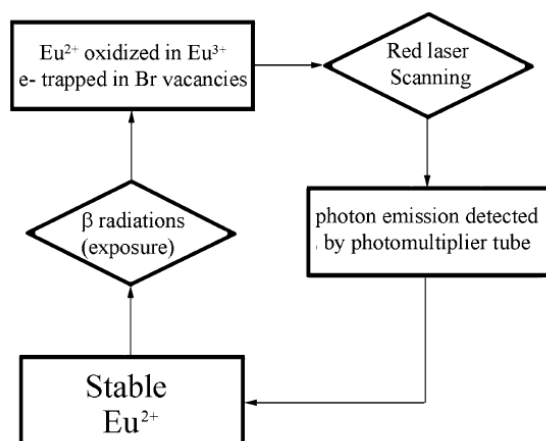


Figure 1: Digital photoluminescence process for digital autoradiographs (DA). From Sardini et al. (2015)

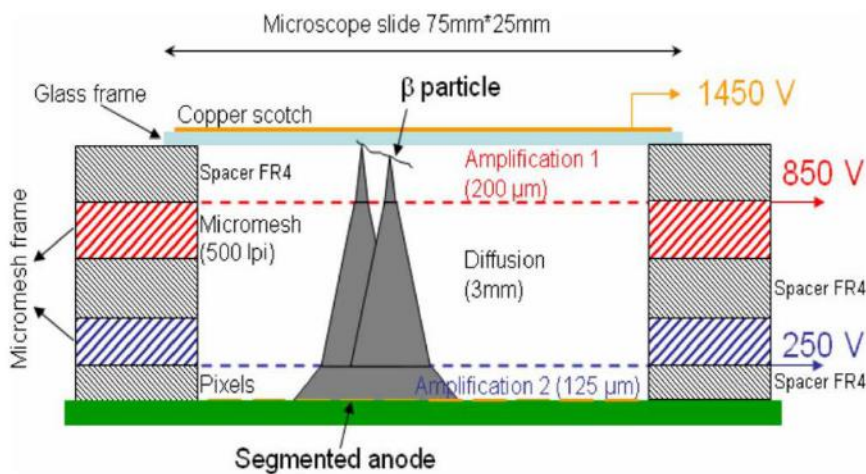


Figure 2: Scheme of the structure of Parallel Ionization Multiplier device (PIM). From Donnard et al. (2009).

References:

- (1) Hellmuth, K.; Siitari-Kauppi, M. Investigation of the porosity of rocks. Impregnation with γ -polymethylmethacrylate (PMMA), a new technique. *Rapp. Finn. Cent. Radiat. Nucl. Saf.* **1990**.
- (2) Sardini, P.; Caner, L.; Mossler, P.; Mazurier, A.; Hellmuth, K.-H.; Graham, R. C.; Rossi, A. M.; Siitari-Kauppi, M. Calibration of digital autoradiograph technique for quantifying rock porosity using ^{14}C -PMMA method. *J. Radioanal. Nucl. Chem.* **2015**, *303* (1), 11–23.
- (3) Donnard, J.; Thers, D.; Servagent, N.; Luquin, L. High Spatial Resolution in-Imaging With a PIM Device. *Nucl. Sci. IEEE Trans. On* **2009**, *56* (1), 197–200.

Hair-selenium concentration in Algerian psoriatics using instrumental neutron activation analysis: relation to gender and age

A. Mansouri^a, B. Beladel^b, L.Baba Ahmed^c, L. Hamidatou Alghem^d, A. Bendaas^e, M. Chohra^f, M.E.A. Benamar^{c,*}.

^a Nuclear Research Centre of Algiers, 02, Frantz Fanon Street, P.O. Box 399, Algiers 16000, Algeria

^b Ziane Achour University, Faculty of Sciences, Djelfa 17000, Algeria

^{c,*} Laboratoire de Physique Fondamentale et Appliquée, Université Saad Dahlab, Blida B.P. 270 Blida (09000) Algérie.

^d Nuclear Research Centre of Birine, P.O. Box 180 Ain Oussera, Djelfa 17000, Algeria

^e Farhat Abbas University, Mabouda City, Setif 19000, Algeria

^f Sub Directorate of Forensic Science and Technology, Châteauneuf – Alger 16000, Algeria

*benamardz64dz@yahoo.fr

Aims: A level of selenium concentrations in hair of Algerian psoriatics is studied. Selenium has a positive impact on psoriasis. The purpose of this study was to evaluate selenium status in psoriasis.

Main methods: 58 hair samples were collected from Algerian psoriatics classified by sex and four age groups and 30 normal subjects. Instrumental Neutron Activation Analysis (INAA) is used to estimate selenium traces.

Key findings: The average selenium concentration for controls and patients were 0.39 ± 0.18 µg/g and 0.28 ± 0.13 µg/g respectively. Se concentration for males and females controls and patients were 0.47 ± 0.20 µg/g, 0.35 ± 0.17 µg/g and 0.28 ± 0.10 µg/g, 0.28 ± 0.14 µg/g respectively.

Significance: There are a significant difference ($p < 0.05$) between selenium level for controls and patients. Selenium concentrations in hair of psoriatic patients can be influenced by physiological conditions such as gender, age and diet. The lower Se status in patients with long-lasting disease might be the result of chronic inflammation with concomitant disturbances in keratinization. It was suggested that Se status is related to the clinical severity of psoriasis.

Impurity measurements in ^{99}Mo solution by means of high resolution gamma spectrometer

Marina Fallone Koskinas*, Denise Simões Moreira, Jamille da Silveira Almeida, Mauro da Silva Dias

*Instituto de Pesquisas Energéticas e Nucleares IPEN- CNEN/SP, Av. Prof. Lineu Prestes,
São Paulo, Brasil
koskinas@ipen.br*

This work aims to investigate the concentration of radioactive impurities gamma emitters in ^{99}Mo provided by commercial producers, for radiopharmaceuticals producer centers. ^{99}Mo is essential to obtain $^{99\text{m}}\text{Tc}$, the main radioisotope used in nuclear medicine, widely applied to diagnosis and therapy purposes. Due to its production method, obtained from the uranium fission, ^{99}Mo carries some other fission products, even after the separation and purifying steps, such as ^{103}Ru , ^{106}Ru , ^{131}I , ^{140}La , ^{95}Nb , ^{125}Sb or some of its daughters. So that this radiopharmaceutical may be properly used, its quality must be evaluated in accordance with the procedures established by quality control agencies, such as “General Requirements for the Competence of Testing and Calibration Laboratories”, ISO/IEC 17025:2005 and the “Good Laboratory Practice” (GLP), controlled by ANVISA (National Agency Health Surveillance), in Brazil, requiring a confirmation of the values of impurities related at the certificates supplied by the manufacturers. The radioactive solutions from four different manufactures were supplied by the Radiopharmaceutical Center of the Nuclear and Energy Research Institute, IPEN, in São Paulo, which is the largest radionuclide supplier to nuclear medicine services in Brazil. The samples were prepared in flame-sealed ampoules. To determine the activity, an HPGe high resolution gamma spectrometer was used. Due to the low activity of the impurities, the assumed distance source-detector was around 1 cm. However, at this distance, the sum coincidence effect is very high, making the measurement of the standard calibration ampoules difficult, so the spectrometer efficiency curve was obtained by a Monte Carlo simulation, with all details of the detection system being modeled and the response curves for X-rays and gamma rays calculated by the MCNPX radiation transport code. The ^{99}Mo gamma spectra were analyzed by Alpino code, which applies the method of numeric peak integration of the area under the photopeaks, previously identified as radionuclide impurities. For gamma emitter impurities, not visually detected, the decision threshold and the detection limits were calculated from the background count rate, under the peak area. The results of impurities ratio for the ^{99}Mo analyzed are in accordance with the manufacturers’ certificate, showing that the outcome is reliable.

Inter-comparison between ML-EM and gold deconvolution algorithms to suppress compton backgrounds in gamma-rays spectroscopy

Sy Minh Tuan Hoang, Gwang Min Sun^{*}, Kiman Lee, Jiseok Kim, and Hani Baek

Korea Atomic Energy Research Institute (KAERI), 111, Daedeok-Daero, 989 Beon-Gil, Yuseong-gu, Deajeon, Republic of KOREA

*[*gmsun@kaeri.re.kr](mailto:gmsun@kaeri.re.kr)*

The suppression of Compton backgrounds is a crucial requirement when applying a gamma-ray spectroscopy to measure gamma-ray spectra for low-background counting. Besides using Compton-Suppression system to reduce the background continuum, the mathematical deconvolution methods have been recently applied in cleanup of the Compton continuum from the measured gamma-ray spectra. In this study, the comparisons of Compton suppression factors and the convergence speeds were carried out in two mathematical deconvolutions, ML-EM and Gold methods, when applied for the gamma-ray spectra of ⁶⁰Co, ¹³⁷Cs and ¹⁵²Eu point sources measuring by HPGe spectroscopy. In the results, the convergence speed of the Gold algorithm is faster than the ML-EM algorithm, and the Peak-to-Total ratio before and after the Gold unfolding is less than that of ML-EM unfolding. In addition, the efficiency of two methods to suppress the Compton background was evaluated by comparing with the experimental Compton-Suppression system, of which used the central detector as ORTEC GMX40-76 HPGe (a PopTop type with relative efficiency 40% and FWHM 1.95 keV at 1.33 MeV peak of ⁶⁰Co).

Self-absorption correction for gamma spectrometry of radioactive environmental reference materials in Taiwan

Huang Ping-Ji, Lee Pi-Fen, Lin Yi-Hsun, Lee and Hsiu-Wei

*Institute of Nuclear Energy Research, Atomic Energy Council
No.1000 Wenhua Rd. Jiaan Village, Longtan District, Taoyuan City 32546, Taiwan (ROC)*

In order to obtain reliable measurement data for gamma-emitting radionuclides in the environment, it has created a need for environmental radioactivity solid reference materials to serve as quality control materials to achieve traceability and instrument calibration. Due to the reference materials offered by established firms are expensive and could hardly be purchased in the necessary quantity and uniformity, we have developed a procedure for preparation of local environmental reference materials using certified mixed-nuclide gamma-ray standard solutions for the proficiency testing program in Taiwan during 2012-2013.

Before measuring the activity of a sample, it is necessary to know the system detection efficiency which is obtained by using known standard sources. The calibration standard source must have physical dimensions, chemical composition and density similar to the samples that will be analyzed, so that the deviation in the measured activity is minimized. Under the conditions of the same physical dimensions and chemical composition, the main source of derivation is the density difference between the sample and the standard source. Therefore, an experiment was undertaken to study the effect of variation of density of the matrix on the efficiency of germanium detectors for two different geometries.

Seven local environmental materials of mushroom, tea leaf, powdered milk, rice, meat, water and soil samples were used as matrices and spiked with certified mixed-nuclide gamma-ray standard solutions, containing ^{60}Co , ^{134}Cs , ^{137}Cs , and ^{85}Sr from Taiwan National Radiation Standard Laboratory, traceable to National Institute of Standards and Technology. The evaluated uncertainties of the spiked activity were all less than $\pm 5\%$ based on the recommendation of ISO Guide 35. The above-mentioned environmental reference materials were then filled into 175 cm³ of cylinders and 1.0 liter of Marinelli beakers to have different densities from 0.45 to 1.64 g/cm³. The detection efficiency curves for two different geometries with various matrix densities were therefore obtained and have been applied for the self-absorption correction of various environment matrices for the 2015 proficiency testing program in Taiwan.

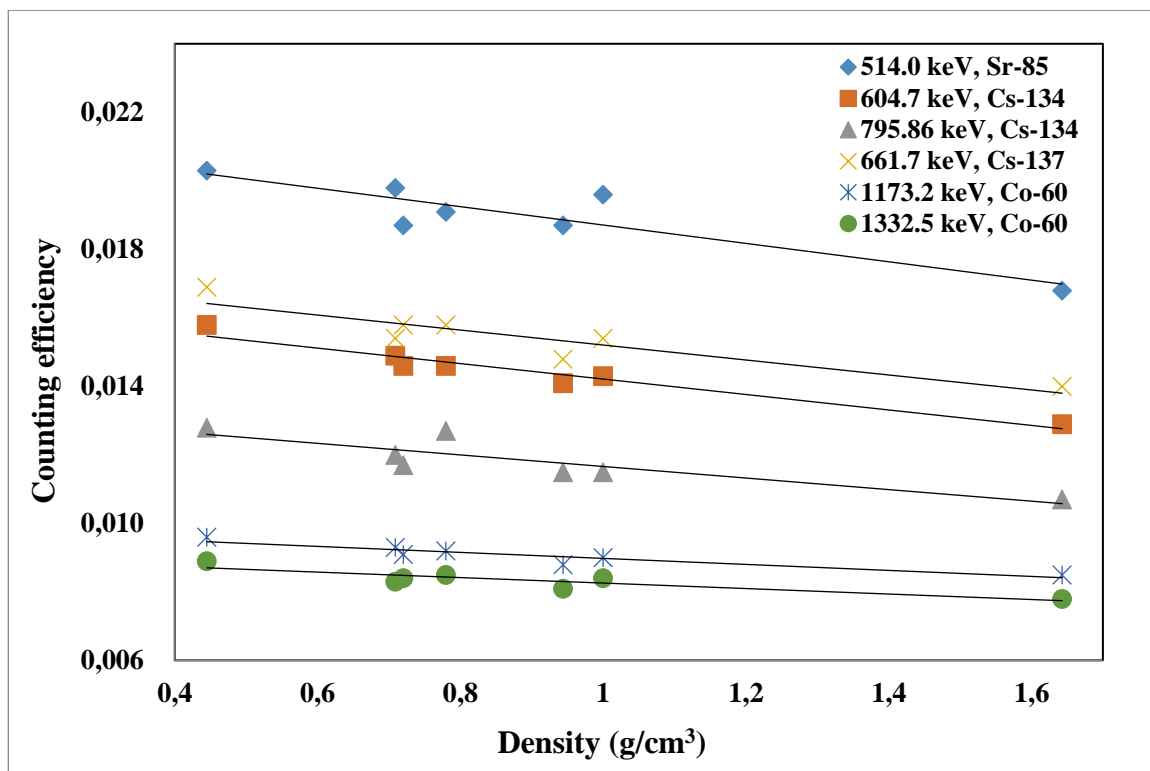


Figure 1. Counting efficiency curve for 175 cm³ of cylinders with various densities of matrices

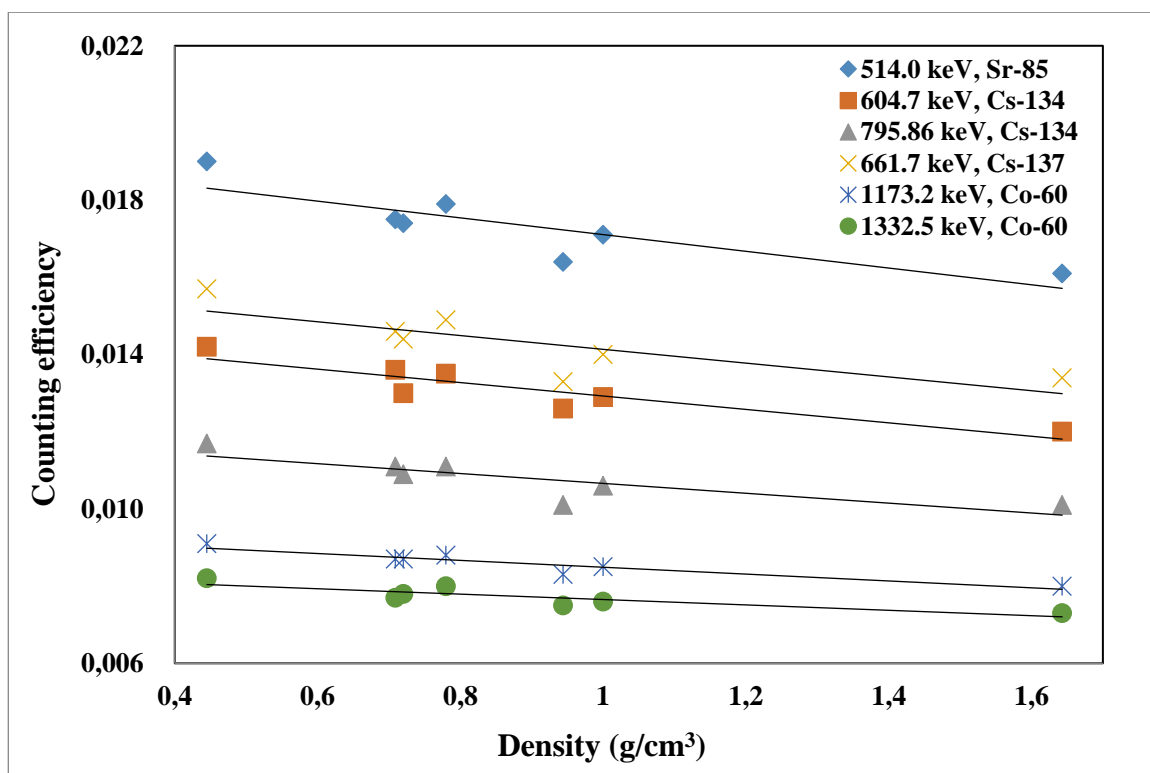


Figure 2. Counting efficiency curve for 1.0 liter of Marinelli beakers with various densities of matrices

The simultaneous determination of ^{235}U and ^{239}Pu using delayed neutron activation analysis

Roger Kapsimalis¹, David Glasgow¹, Brian Anderson¹, Sheldon Landsberger²

¹Oak Ridge National Laboratory, TN, USA

²The University of Texas at Austin, TX, USA

Introduction

For over five decades, delayed neutron activation analysis (DNAA) has been employed as a rapid, nondestructive analytical (NDA) technique for the determination of uranium in a wide range of matrices, provided that the samples contain only a single fissile component. Historically, this has limited many applications of DNAA. This work sought to develop a method to allow for DNAA to be utilized on samples containing multiple fissile components. Work conducted at Oak Ridge National Laboratory and the High Flux Isotope Reactor (HFIR) has shown that using a multivariate linear regression model to describe the time-dependent delayed neutron emission profile of an irradiated sample allows for the concurrent measurement of fissile nuclides in samples, without chemical separation and using only a single counting step.

Analysis

A method was developed to deconvolve the delayed neutron emission rate based on the varying fission product yields, and consequently the varying delayed neutron emission rate, of individual fissile nuclides. Following irradiation of a sample containing fissile material, the time-dependent response of the neutron counting array can be expressed as:

$$c(t) = \varepsilon \sum_{i=1}^N \frac{m_i N_A}{M} \sigma_f \phi (1 - e^{-\lambda_i t_s}) \sum_{k=1}^6 \nu_{d_{ki}} \lambda_{ki} e^{-\lambda_{ki} t_c} \quad (1)$$

where

- ε is the neutron counting efficiency,
- m is the mass of the i^{th} fissile nuclide,
- N_A is Avogadro's number,
- M is the atomic mass number of the i^{th} fissile nuclide,
- σ_f is the fission cross section,
- ϕ is the thermal neutron activation flux.

Equation 1 can be expressed as the count rate per unit mass, $P(t)$, multiplied by the mass of the constituent nuclide (Li, 2004):

$$c(t) = \sum_{i=1}^N P_i(t) \cdot m_i \quad (2)$$

The detector response, $c(t)$, can be thought of as the sum of a series of points given as:

$$c_i = c(t_i \pm \delta/2) \quad (3)$$

where

δ is the detector dwell time.

The detector response at a given point, c_i , is total neutrons from the βn decay of precursor nuclides from the fission of each fissionable nuclide present in the sample:

$$c_i = c_\alpha + c_\beta + c_\gamma \dots + c_\omega \quad (4)$$

where subscripts $\alpha, \beta, \gamma, \dots, \omega$ are contributing fissionable nuclides.

Equation 4 can be expressed in terms of its count rate per unit mass for each nuclide, as was done above.

$$c_i = P_\alpha(t_i \pm \delta) \cdot m_\alpha + P_\beta(t_i \pm \delta) \cdot m_\beta + P_\gamma(t_i \pm \delta) \cdot m_\gamma + \dots + P_\omega(t_i \pm \delta) \cdot m_\omega \quad (5)$$

For a sample containing four fissile nuclides and other contributors to the delayed neutron count rate including background signal (ε), the detector response at point c_i is given by the following expression.

$$c_i = P_\alpha(t_i \pm \delta) \cdot m_\alpha + P_\beta(t_i \pm \delta) \cdot m_\beta + P_\gamma(t_i \pm \delta) \cdot m_\gamma + P_\delta(t_i \pm \delta) \cdot m_\delta + \varepsilon \quad (6)$$

The total count rate of the neutron detector can be expressed as a linear combination of points c_1 to c_i . This is best represented in the following matrix.

$$\begin{bmatrix} c_1 \\ \vdots \\ c_i \\ \vdots \\ c_k \end{bmatrix} = \begin{bmatrix} P_\alpha(t_1 \pm \delta) & P_\beta(t_1 \pm \delta) & P_\gamma(t_1 \pm \delta) & P_\delta(t_1 \pm \delta) \\ \vdots & \vdots & \vdots & \vdots \\ P_\alpha(t_i \pm \delta) & P_\beta(t_i \pm \delta) & P_\gamma(t_i \pm \delta) & P_\delta(t_i \pm \delta) \\ \vdots & \vdots & \vdots & \vdots \\ P_\alpha(t_k \pm \delta) & P_\beta(t_k \pm \delta) & P_\gamma(t_k \pm \delta) & P_\delta(t_k \pm \delta) \end{bmatrix} \cdot \begin{bmatrix} m_\alpha \\ m_\beta \\ m_\gamma \\ m_\delta \end{bmatrix} \quad (7)$$

$$\mathbf{C} = (\mathbf{P}_\alpha, \mathbf{P}_\beta, \mathbf{P}_\gamma, \mathbf{P}_\delta) \cdot \mathbf{M} \quad (8)$$

The parameters \mathbf{P}_i are known from the empirically derived basis functions, which individually contribute to the count spectrum; \mathbf{C} is the neutron intensity-time profile, which will of course be measured experimentally. Using the method of least squares, this system of equations can be solved to determine the masses of each initial fissile nuclide present in the sample.

Results

Experiments were carried out using nanogram quantities of uranium and plutonium mixtures to validate the method. As postulated, the model was capable of concurrently resolving two fissile isotopes at low concentrations. The results showed that DNAA is capable of simultaneously determining ^{235}U and ^{239}Pu within a precision of approximately 5 to 10%.

¹ *Rapid determination of uranium and plutonium content in mixtures through measurement of the intensity-time curve of delayed neutrons.* Li, X., R. Henkelmann, F. Baumgartner. 2004, Nucl. Inst. and Meth. in Phys Res. B, Vol. 215, pp. 246-251.

Determination of ultra-low levels of radium and radon by LSC with pulse shape analysis and delayed coincidence technique

KIM, Hong Joo¹, SONG, Seok Jun¹, PANDEY, Sujita¹

¹Kyungpook National University, Daegu, Republic of Korea
hongjoo@knu.ac.kr

The study has been aimed for development of radium and radon detection in ultra-low levels using both pulse shape discrimination (PSD) between alpha and beta particles and delayed coincidence technique (DCT) of short-lived decay product. Water soluble samples were mixed with liquid scintillation cocktail (LSC) such as Ultima Gold AB or LLT inside the counting vial coated with light reflector. A photomultiplier tube (PMT) was coupled directly to the entrance window of the PMT using index matching optical grease. Signals produced in the PMT were fed into a 400-MHz flash analog-to-digital converter (FADC), this FADC module is fabricated to sample the pulse every 2.5 ns. The FADC output was recorded into a personal computer by using a USB2 connection, and the recorded data are analyzed with a C++ data analysis program. We optimized PSD algorithm for efficient separation between alpha and beta particles. Also DCT was applied using time tagging information of recorded sample.

Using DCT, isotopes having a relatively short half-life could be selected out by their characteristic energy and decay-time distributions for the sample. To estimate activity of ^{222}Rn (^{238}U family), $^{224}\text{Ra}/^{220}\text{Rn}$ (^{232}Th family), and $^{223}\text{Ra}/^{219}\text{Rn}$ (^{235}U family), the sub-chain ^{214}Bi ($Q_{\alpha} = 3.27$ MeV) \rightarrow ^{214}Po ($Q_{\alpha} = 7.83$ MeV, $T_{1/2} = 164$ μs), ^{212}Bi ($Q_{\alpha} = 2.25$ MeV) \rightarrow ^{212}Po ($Q_{\alpha} = 8.95$ MeV, $T_{1/2} = 0.299$ μs) and ^{219}Rn ($Q_{\alpha} = 6.95$ MeV) \rightarrow ^{215}Po ($Q_{\alpha} = 7.53$ MeV, $T_{1/2} = 1.78$ ms) has been analysed in the time and energy interval with beta (alpha) and alpha requirement, respectively.

Using both PSD and DCT method, internal background of LSC was measured to estimate sensitivity of developed method. We applied developed method to drinking water and a $(\text{NH}_4)_6\text{Mo}_7\text{O}_{24} \cdot 4\text{H}_2\text{O}$ samples to measure the radium and radon background level.

Calibration of new RAD-air-water exchanger system for continuous monitoring of radon in water

Kil Yong Lee, Soo Young Cho, Yoon Yeol Yoon, Kyoochul Ha, Kyung-Seok Ko

Groundwater Department, Korea Institute of Geoscience and Mineral Resources, 124 Gwahang-no, Yuseong-gu, Daejeon 305-350, Korea

Air-water exchangers coupled to radon in air detector have been used for continuous monitoring of radon in water at the groundwater and surface water interface. RAD-AQUA system has been widely used in continuous monitoring of radon in water. It is a device to bring the radon concentration in a closed air loop into equilibrium with the radon concentration in a flow through water supply. It consists of a spray chamber, called an “exchanger”, which brings the air and water into equilibrium. The radon in the air is monitored continuously by the RAD7. In RAD-AQUA system, radon concentration in flow through water has been estimated using radon partition coefficient by the temperature at the air-water interface. In the present work, a new RAD-air-water exchanger system (RAD-AWE) was developed to measure sensitively radon concentration variations in a flow through water. The RAD-AWE system consists of a spray chamber with an impeller as well as a nozzle to reach rapidly at steady state of radon in air-water interface. Calibration of radon concentration in water was performed by volume ratio of air-water in the RAD-AWE system, radon in air of the system and radon partition coefficient at given temperature. Radon concentrations by the RAD-AWE system were compared with RAD-AQUA system as well as a liquid scintillation counting (LSC). Sensitivities for variations in radon concentration in flow through water were also compared for both systems of RAD-AQUA and RAD-AWE.

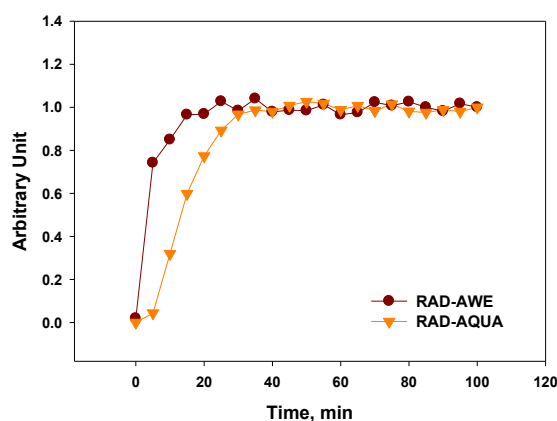


Fig. 1. Time to reach at steady state in the RAD-AQUA and the RAD-AWE systems.

Development of radon generator and radon standards for radon in air and radon in water

Kil Yong Lee¹, Myung-Jin Kim², Soo Young Cho¹, Kyoochul Ha¹, Kyung-Seok Ko¹

¹Korea Institute of Geoscience and Mineral Resources, 124 Gwahang-no, Yuseong-gu, Daejeon, Korea

²Neosiskorea Co. Ltd., Daejeon, Korea

A radon generator was developed using radium standard materials and high radium minerals. Radium free radon standards air and radon standard water were prepared using the radon generator in Korea Institute of Geoscience and Mineral Resources. The radon sources were commercial radium standards as well as high radium minerals. The radon generator consists of a radon source, a radon in air monitor, two dispensing containers and several air-loops. The air-loops were S-loop (source-loop), B-loop (base-loop), A-loop (air container loop) and W-loop (water container-loop). Radon standards were prepared by charging radon rich air in the dispensing bottles after homogenizing radon in each air-loop. Radon activity concentrations were estimated by the radon in air monitor in the air-loop and the volume of each component of the radon generating system. Because the radon in the air-loops have not radium by radium absorbing column, the radon standard air and radon standard water have not radium in their containers. The radon standards were applied to calibrate of radon in air monitor (RAD7) and radon in water counter (LSC).

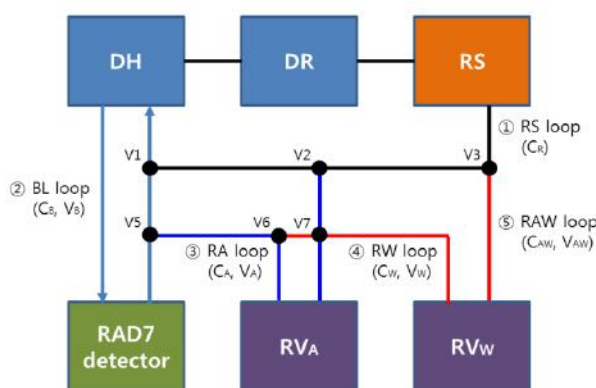


Fig. 1. Schematic diagram of the radon generator in KIGAM.

Simulation of prompt gamma activation analysis for detecting fake tungsten gold bar by using the MCNPX code

LEE, Ki-man, SUN, Gwang-min

Korea Atomic Energy Research Institute, Korea

Introduction

Gold bars have been a target for investment for the following reasons. They are easily transportable because they have a high value to weight ratio, and are fungible with a low margin between the buying and selling prices. However, it is well known that fake gold bars exist on the gold market. They cannot be identified easily without testing because they have the same appearance as a pure gold bar. To avoid the trading of fake gold bars on the market, they should be thoroughly monitored. The purpose of this study is to develop a fake gold bar detection method using a PGAA (Prompt Gamma Activation Analysis) facility at KAERI (Korea Atomic Energy Research Institute). PGAA is an established nuclear analytical technique for a non-destructive determination of elemental and isotopic compositions. As a preliminary study, a Monte Carlo simulation of the prompt neutron-induced γ -ray spectra when a neutron beam is irradiated onto pure and fake gold bars was conducted, and the possibility for detecting fake gold bars was confirmed.

Materials and methods

The HANARO research reactor at KAERI has been operating at 30 MWth since its first criticality in 1995. The HANARO reactor provides thermal neutron beams with a high flux (5×10^{14}) for characterizing the composition and structure of the target substance. To enhance the utilization capacity of the HANARO reactor, a cold neutron research facility has been developed since 2003, and CONAS (Cold Neutron Activation Station) has been constructed for various applications of cold neutrons [1]. CONAS consists of two neutron activation instruments, one of them is the CN-PGAA (Cold Neutron Prompt Gamma Activation Analysis) facility.

The kilo-bar (1000g), which is the most common standard gold bar, measures about $60 \times 110 \times 8 \text{ mm}^3$. The minimum purity of a standard gold bar is 99.5% gold. However, a fake gold bar is commonly made by filling the bar inside with other substances, particularly tungsten, which has a density nearly the same as gold but with a cheaper price [2]. To assume the case of a fake gold bar, tungsten was selected as a representative fake candidate.

The neutron-induced prompt γ -ray spectra were calculated after a thermal and cold neutron beam was irradiated onto pure and fake gold bars using the Monte Carlo N-particle extended code package, MCNPX, which enables one to simulate the transport of neutrons, photons, and electrons in a medium, and to define the three-dimensional geometries in an arbitrary way [3]. An MCNPX simulation was conducted in two separate files. The neutron transport and prompt γ -ray production in the gold bar were first calculated. Second, the photon transport for the detection of prompt γ -rays emitted from the gold bar was simulated. The fake gold bar was assumed to be a 6-mm-thick tungsten bar plated with 1mm of gold. The thermal and cold neutron beams from the HANARO reactor were adopted as a source in the simulation. In particular, the source data for the cold neutron were made based on the energy distributions of a cold neutron in CONAS simulated using a Monte Carlo Simulation of a Triple-Axis Spectrometer (McStas) by Hoang et al. [4]. The simple geometry of the neutron irradiation system in the MCNPX simulation was modeled after the CONAS CN-PGAA facility. The neutron beam is transported to an analytical sample inside the sample mounting box using a tube. The beam tube is used to collimate neutrons from the end of the cold neutron guide line. The sample mounting box is $20 \times 20 \times 20 \text{ cm}^3$ in size, and is suitable for accommodating a gold bar. All calculations were carried out using 107 particle histories resulting in a target relative

error R of less than 1 %. The relative error R is usually used as a parameter to stop the run, and an R of less than 1 % signifies that the calculation is reliable.

Results and discussion

Transmission rate of neutron beams in pure and fake gold bars: The mean free path of a thermal neutron in tungsten is about five-times larger than that in gold. The mean free path of a cold neutron also shows the same tendency as the target substances. This result indicates that the number of neutrons interact with the tungsten is fewer than that interacting with gold. To a depth of 4 mm corresponding to half the thickness of a pure gold bar, 10 percent of the initial incident thermal neutrons can be penetrated. For a cold neutron, only 0.64 percent of the initial number can be penetrated. However, in a fake gold bar, 39 percent of thermal neutrons, and 8 percent of cold neutrons, can penetrate to a depth of 4 mm. Although the transmission rate of a cold neutron is low compared to that of a thermal neutron, a slower neutron is more apt to be absorbed in a target, and can increase the neutron-induced prompt γ -ray emission rate. In addition, the flux of both thermal and cold neutron beams is high enough to activate a thick target. If a neutron beam is irradiated on the front and reverse sides of a gold bar, the entire inside can be detected. Prompt γ -rays emitted from pure and fake gold bars: The neutron-induced prompt γ -ray spectrum of a fake gold bar is obviously different from that of a pure gold bar. Overall, the flux of prompt γ -rays emitted from the gold of a fake gold bar is lower than that of a pure gold bar. In the 3 to 6 MeV γ -ray energy region, the prompt γ -rays emitted from the tungsten of a fake gold bar are observed independently, and in particular, two γ -ray peaks with a high flux (5.26 and 5.32 MeV) appeared very clearly. From these result, the fake gold bar can be distinguished.

References

1. G. M. Sun, Development of HANARO Cold Neutron Activation Station, in: Transactions of the 13th International Conference on Modern Trends in Activation Analysis, Mars.13-18 2011, Texas, USA.
2. I. Prasetyo, I. Sihar, K. Agusta and I. Handayani, A Gold Bar Purity Testing Method Based on Vibration Characteristics, In Applied Mechanics and Materials, 771, pp. 223-226, 2015.
3. D. B. Pelowitz, MCNPX User's Manual Version 2.7. 0, LA-CP-11-00438, Los Alamos National Laboratory, 2011.
4. S. M. T. Hoang, G. M. Sun, J. H. Moon, Y. S. Chung and B. G. Park, Optimization of HANARO cold neutron induced prompt gamma activation analysis system by using Monte Carlo code, Journal of Radioanalytical and Nuclear Chemistry, 296(2), pp. 967-973, 2013.

High-resolution alpha-particle spectrometry of ^{226}Ra

M. Marouli¹, S. Pommé¹, R. Van Ammel¹, E. García-Toraño², T. Crespo², S. Pierre³

¹ *European Commission, Joint Research Centre, Retieseweg 111, Geel, Belgium*

² *Laboratorio de Metrología de Radiaciones Ionizantes, CIEMAT, Avenida Complutense 40, Madrid, Spain*

³ *CEA, LIST, Laboratoire National Henri Becquerel, CEA Saclay, Gif-sur-Yvette, France*

Naturally Occurring Radioactive Materials (NORM) are radionuclides present in natural resources which when processed by industry or when their natural state has been altered may lead to enhanced radiation levels and potentially increased human exposure. ^{226}Ra is present as NORM waste in many activities such as in the phosphate industry, oil and gas production, geothermal energy production, drinking water treatment and rare-earth and coal extraction. ^{226}Ra can be found also in building materials contributing to internal exposure by the inhalation of its decay product, ^{222}Rn . Applications of ^{226}Ra include its use as a tracer to study geochemical and physical transport processes. Radioanalytical procedures involved in the identification of ^{226}Ra and its activity concentrations are in need of decay data. In this context [1], improvement or validation of the already existing decay data of ^{226}Ra is of importance for metrology.

Radium-226 is an alpha-emitter with a half-life of 1600 (7) y [2]. It decays to the stable ^{206}Pb through a series of thirteen short lived alpha and beta emitters. The alpha-particle emission probabilities have been measured only twice in the past: by Bastin-Scoffier et al. [3] and La Mont et al. [4]. Their results differ by more than 0,5 %, which causes the need for re-measurement of the alpha-emission probabilities. In this work the three major alpha-particle emission probabilities have been determined by means of high-resolution alpha-particle spectrometry in the radionuclide metrology laboratories of CIEMAT, LNH and IRMM. The project was conducted within the JRP IND57 MetroNORM project under the auspices of the European Metrology Research Project.

At CIEMAT, two thin, homogeneous sources of pure ^{226}Ra were prepared by electrodeposition, following the method by Crespo and Jiménez [5]. The alpha spectrometry set-ups used at JRC and CIEMAT are based on the same design, comprising of a cuboid source chamber with sliding mount and a cylindrical distance tube with a planar silicon detector on top, both operated under vacuum. To reduce peak shift of the spectrum during long measurements, the preamplifier housing is stabilised in temperature using water from a thermostatic bath. The two main excited states of ^{222}Rn fed by ^{226}Ra alpha decay have a significant probability for de-excitation through the emission of conversion electrons, which gives rise to summing

effects when alpha-particles and conversion electrons are detected simultaneously. These coincidences can be avoided by increasing the source-detector distance and/or by applying a magnet system to deflect the electrons. The latter was applied by JRC and CIEMAT. LNHB also used a set-up with planar silicon detector, lacking however temperature stabilisation, mathematical corrections for peak shift and a magnet system. The acquired energy spectra were deconvoluted with the least-squares fitting software BEST at JRC, ALPACA at CIEMAT and Colegram at LNHB.

The measurements at LNHB, performed at short source-detector distance, exemplified the detrimental effect of coincidence summing between conversion electrons and alpha particles on the determination of alpha emission probabilities, even when mathematical corrections are applied [6]. The LNHB results for the alpha emission intensities for the major peaks were 94,55(4)%, 5,44(4)% and 0,007(6)%, but since the measuring conditions were not optimum they were not included in the final results presented in Table 1.

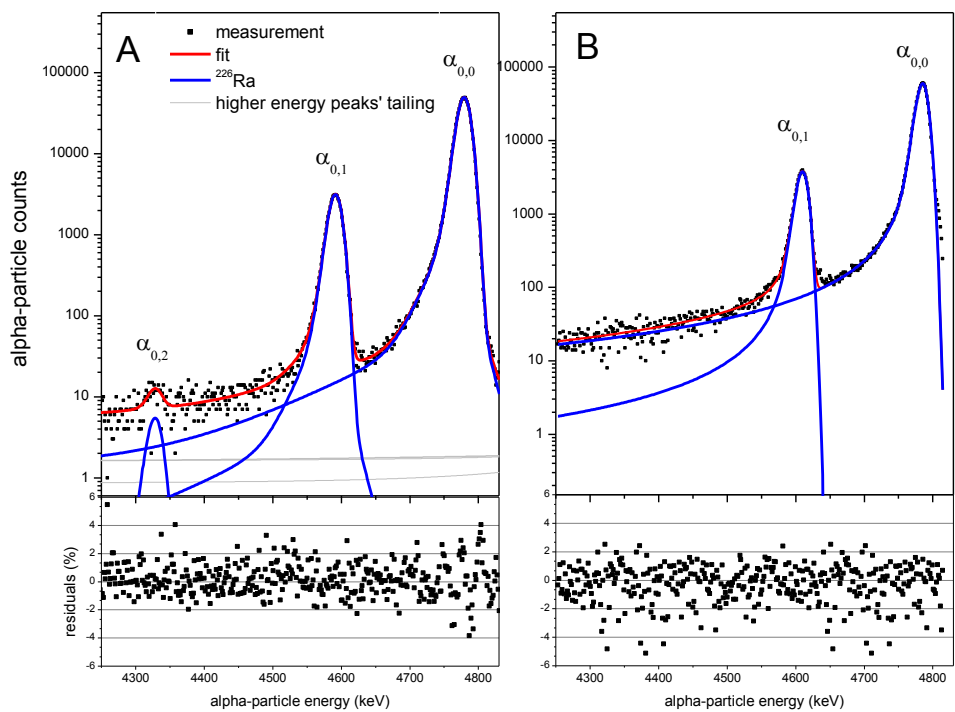


Figure 5. Measured (dots) and fitted (lines) alpha-particle spectra emitted in the decay of ²²⁶Ra: (A) for JRC showing also the fitted contributions from tailing of the daughter nuclides, whereas (B) for CIEMAT the contributions from tailing of the daughter nuclides have already been subtracted. The residuals show the difference between measurement and fit in units of one standard deviation of the channel contents.

Table 2. Measured and evaluated alpha-particle emission probabilities (P_{α}) in the decay of ²²⁶Ra.

Reference	$\alpha_{0,0}$	$\alpha_{0,1}$	$\alpha_{0,2}$
²²⁶ Ra - P_{α} (%)			
G.Batin-Scoffier (1963)[3]	94,45(5)	5,55(5)	0.0065(3)
S. LaMont (2001)[4]	93,84(11)	6,16(3)	
Recommended value (DDEP)[2]	94,038(40)	5,95(40)	0,0066(22)
This work CIEMAT	94,05(1)	5,94(1)	0,0052(15)

This work JRC	94,08(1)	5,93(1)	0,008(3)
New value (JRC and CIEMAT)	94,06(1)	5,93(1)	0,0065(16)

References

- [1] International Atomic Energy Agency, Assessing the Need for Radiation Protection Measures in Work Involving Minerals and Raw Materials, Safety Reports, Series No. 49, IAEA, Vienna (2006).
- [2] Mini Table of Radionuclides 2015. Laboratoire National Henri Becquerel, ISBN: 978-2-7598-1198-4.
- [3] Bastin-Scoffier, G., Leanf C.F., Walen R.J., Spectrographie α de ^{226}Ra et niveaux des Rn de a pair, Le J. de Ph. 24(1963) 854-856.
- [4] La Mont, S.P., Gehrke R.J., Glover S. E., Filby R.H., Precise determination of the intensity of ^{226}Ra alpha decay to the 186 keV excited state, J. Rad. Nucl. Ch. 248 (2001) 247-253.
- [5] Crespo, M.T. , Jiménez, A.S., On the determination of ^{226}Ra by alpha spectrometry, J. Rad. Nucl. Ch. 221 (1997) 149-152.
- [6] Pommé S., Typical uncertainties in alpha-particle spectrometry, Metrologia 52 (2015) S146-S155.

Quantitative autoradiography of alpha particle emission in geo-materials using the Beaver™ system

Paul Sardini¹, Axel Angileri¹, Michael Descostes², Samuel Duval³, Tugdual Oger³, Patricia Patrier¹, Nicolas Rividi⁴,
Marja Siitari-Kauppi⁵, Hervé Toubon², Jérôme Donnard³

1 IC2MP Equipe HydrASA, Poitiers, France.

2 AREVA Mines, R&D Dpt, Paris, France.

3 Ai4R SAS, Nantes, France.

4 Service Camparis, Paris, France.

5 Laboratory of Radiochemistry, University of Helsinki, Finland.

In rocks or artificial geo-materials, radioactive isotopes emitting alpha particles are dispersed according to the mineralogy. At the hand scale specimen, achievement of quantitative chemical mapping of these isotopes takes on a specific importance. Knowledge of the distribution of the uranium and thorium series radionuclides is of prime interest to several disciplines including geochemistry of uranium deposits, and dispersion of uranium mill tailing in biosphere. The disequilibrium of these disintegration chains are also commonly used for dating. Besides, some prime importance isotopes, such as ²²⁶Ra are complicated to localize in geo-material because, in usual conditions, it is found in very low contents, preventing its accurate localization in rock forming minerals.

At the hand scale specimen, how to quantitatively map alpha emitters in geo-materials? We test a new digital autoradiographic method (called the Beaver™) based on a Micro Patterned Gaseous Detectors (MPGD) in order to quantitatively map alpha emission at the centimetre scale rock section. First, for two thin sections containing U-bearing minerals at secular equilibrium, we compared the experimental and theoretical alpha counting rate, measured by the Beaver™ and calculated from U (wt%), respectively. We found that the experimental and theoretical counting rate are very similar. Second, for a set of eight samples made of a mixture of inactive sand and lowly radioactive mud, we compared the counting rate obtained by the Beaver™ and by an alpha spectrometer. The results indicate (i) a linearity between both counting rates, and (ii) that the counting obtained by the Beaver™ can be estimated from the counting obtained by the alpha spectrometry using a factor of 0.82.

Zinc and tellurium contents in tellurite glass materials

¹SEKIMOTO, Shun, ²SHIKANO, Kouji, ¹FUKUTANI, Satoshi, ¹OHTSUKI, Tsutomu

¹*Kyoto University, Japan*

²*National Institute of Technology, Hakodate College, Japan*

Tellurite glass materials are new candidates for optical fiber devices and the source materials of this tellurite glass are tellurium dioxide, zinc oxide, bismuth([U+2162]) oxide, lithium carbonate, and so on. To shorten the time for melting those source materials in production of tellurite glass, there is an advantage of choosing zinc tellurite instead of zinc oxide (having a high melting point of 1975 K). However, the tellurite glass material where zinc tellurite is used as a source material has never been produced, and capabilities of that glass material have not been evaluated. Recently, the tellurite glass materials were produced with zinc tellurite at various melting temperature. To evaluate the capability of those glasses, zinc (Zn) and tellurium (Te) were determined in those tellurite glass materials by instrumental neutron activation analysis (INAA) using Kyoto University Reactor. In this study, contents of Zn and Te in those tellurite glass materials are also determined by atomic absorption spectrometry (AAS) and inductively coupled plasma mass spectrometry (ICP-MS). The suitability of each analytical method for glass materials will be discussed. It has become apparent that the concentration ratio of Te to Zn in those tellurite glass materials do not depend on the melting temperature, suggesting that zinc tellurite can be available as a source material of tellurite glass.

Artificial neural networks in spectroscopy of ionizing radiations: current state

R.K. Spirau, A.N. Nikitin

Institute of Radiobiology of the National Academy of Sciences of Belarus, Gomel, Belarus

Qualitative and quantitative analysis of radioactive isotopes is required in describing and assessing the radiation for environmental monitoring in radioecology, radiation medicine and other related disciplines, as well as for the organization of protection against ionizing radiation in radiation safety. Today to measure nuclear radiation everywhere widely used spectrometric methods of analysis. However, radiation spectrometry was a challenging task. Despite the fact that every year we see improving in the methods of preparation of samples for analysis (sample preparation, radiochemical separation, making the counting of targets), and also increase the sensitivity and resolution of detectors and other hardware components of modern spectrometers, the processing of spectrometric information is impossible without human intervention.

The definition of quality spectrum. Active study of the question of possibility of application of neural networks for processing spectrometric information began in the mid-90s of the XX century after the publication of "Nuclear Spectral Analysis via Artificial Neural Networks for Waste Handling" researchers from the USA P. E. Keller, L. J. Kangas et al [1]. The authors experiencing the problem of fast and qualitative determination of radioactive isotopes in the huge mass of toxic waste generated as a result of forty years (at the time of writing the publication) production of plutonium at Hanford's complex. The researchers aim to demonstrate the application of the paradigm of neural networks to process information in real time, namely, for automated identification of isotopes of pollutants. They considered two problems: first, the use of artificial neural network for determining the quality of alpha spectra and, secondly, the identification of isotopes on the basis of data of gamma-ray spectra. The authors proved the possibility to transfer knowledge about the quality of the alpha-spectrum from the operator to artificial neural networks. Scientists from Japan [2], the UK [3] and Indonesia [4] made same conclusion, they are emphasizing qualitative performance of assigned tasks.

Identification of isotopes. Another application of neural networks, as noted by M. K. Alam, S. L. Stanton and other researchers [5], is automated identification of radioactive isotopes in real-time spectra of gamma radiation. The traditional approach to the identification of the desired isotope on the spectrum of gamma radiation is reduced to the search of the peak and the suitable curves. This approach initiates an iterative process of decomposition and reconstruction of the spectrum until the spectrum generated by the mathematical methods will not match true. Often this process requires a large amount of computation, and often also manual intervention. The neural network in turn uses pattern recognition on the entire spectrum.

Another important problem which successfully cope artificial neural network in the processing of spectrometric information is the analysis of **the ratio of activities** one isotope to another. This problem often occurs in radioecology in relation to the need to determine the type of pollution source: is it natural or anthropogenic origin. But it can help to solve some problems in nuclear engineering, in management of radioactive waste, health physics, geology, geochronology [6] and other natural science disciplines, as well as for screening at international borders [7]. A good example of successful solution of such problems by neural networks is a recent study concerned with activity ratio of uranium-234 to uranium-238 conducted by Iranian scientists Einian M. R., S. M. R. Aghamiri, R. and Ghaderi [8]. It should be noted that the problem of accessing activities ratio can be attributed both to the classification problems and to particular case problems of **quantitative analysis**. The last type of the tasks is devoted to the works of researchers from Spain [9], France [10], Russia [11], etc. In the work of the M. E. Medhat [12] examines not only the qualitative detection of isotopes, but evaluation of their activities within the sources of natural origin.

Conclusions

Implementation of artificial neural networks in the processing of spectrometric information remains an important problem, whose solution will improve the efficiency and accuracy of radiation measurements. The main tasks that can successfully solved by the neural network are follows: assessment of the quality of the obtained spectrum, qualitative analysis (identification of nuclides, the problem of classification), the analysis of activity of isotopes (special case of quantitative analysis, classification) and quantitative analysis (determination of the specific activity of the isotopes).

The advantages of neural networks compared with classical approaches is possibility to reject complicated mathematical model, acceleration processing of a large amount of data, prevent the human influence at this stage. Many conventional statistical criteria allow to evaluate the quality of the network. However, the analysis of literature data showed that it is require more in-depth study of the following issues: network with the whole spectrum instead of individual peaks of radiation, the automated search of zones of interest, the use of stage training model and real spectra, the samples of different nature. In particular, the analysis of biological samples is more complicated due to the large quantity of organic substances that cannot be fully separated by radiochemistry and have an impact on the quality of the spectra. In addition, it is not studied the ability of neural networks to analyze the samples with weak activity. However, despite the number of poorly-studied aspects, the use of artificial neural networks in the processing of the radiation spectrometric information has a number of undeniable advantages in comparison with classical approaches.

References

1. Nuclear Spectral Analysis via Artificial Neural Networks for Waste Handling / P.E. Keller, L.J. Kangas, G.L. Troyer, Sh. Hashem, R.T. Kouzes, IEEE Transactions on Nuclear Science –1995. – Vol. 42, – P. 709–715.
2. Application of neural networks for the analysis of gamma-ray spectra measured with a Ge spectrometer / E. Yoshidaa, K. Shizumaa, S. Endoa, T. Okab // Nuclear Instruments and Methods in Physics Research – 2002. – P. 557–563.
3. Application of artificial neural networks for water quality prediction / A. Najah, A. El-Shafie, O.A. Karim, Amr H. El-Shafie // Neural Comput & Applic – 2013. – № 22. – P. S187–S201.
4. Pengembangan spektrometer sinar-gamma dengan sistem identifikasi isotop radioaktif menggunakan metode jaringan syaraf tiruan / M. Syamsa Ardisasmitta // Risalah Pertemuan Penelitian dan Pengembangan Aplikasi Isotop dan Radiasi – 2001. – P. 117–124.
5. Near-Infrared Spectroscopy and Neural Networks for Resin Identification / M.K. Alam, S.L. Stanton, G.A. Hebner // Spectroscopy – 1994. – P. 30–40.
6. Difficulties in using $^{234}\text{U}/^{238}\text{U}$ ratios to detected enriched or depleted uranium / R.L. Fleischer // Health Phys. – 2008. – № 94 (3). – P. 292–293.
7. The use of artificial neural networks in PVT-based radiation portal monitors / L.J. Kangas, P.E. Keller, Ed.R. Siciliano, R.T. Kouzes, J.H. Ely, Nuclear Instruments and Methods in Physics Research – 2008. – P. 398–412.
8. Application of neural network method to detect type of uranium contamination by estimation of activity ratio in environmental alpha spectra / M.R. Einian, S.M.R. Aghamiri, R. Ghaderi // Journal of Environmental Radioactivity – 2016. – № 151. P. 75–81.
9. A new approach to the analysis of alpha spectra based on neural network techniques / A.Baeza [et al.] // Nucl. Instrum. Methods Phys. Res. – 2011. – P. 450–453.
10. Application of neural networks to quantitative spectrometry analysis / V. Pilato, F. Tola, J.M. Martinez, M. Huver // Nucl. Instrum. Methods Phys. Res. –1999. – P. 423–427.
11. Преобразование спектров с использованием искусственных нейронных сетей / С.В. Малиновский, И.А. Каширин, В.А. Тихомиров // Проблемы прикладной спектрометрии и радиометрии – 2011. – С. 21.
12. Artificial intelligence methods applied for quantitative analysis of natural radioactive source / M.E. Medhat // Ann. Nucl. Energy – 2012. – № 45. P. 73–79.

Investigation on Fire Gilding using XRF and NAA

R. Margreiter, K. Eberhardt, B. Niemeyer, M. Radtke, E. Strub*

Abteilung Nuklearchemie der Universität zu Köln, Zùlpicher Str. 45, 50674 Cologne, Germany

[*erik.strub@uni-koeln.de](mailto:erik.strub@uni-koeln.de)

Fire-gilding or amalgam gilding is a historical technique for the gilding of objects. The object to be gilded is coated with an amalgam (a solution of gold (Au) in mercury (Hg)). By heating, the largest part of the Hg is subsequently evaporated and there remains a gold layer, containing still detectable amounts of Hg.

The information on the used gilding technique might be crucial for the conservation and preservation of archaeological objects. Therefore, the main objective of this work is the detailed understanding of the behaviour of Hg under conditions of fire gilding. I.e. the understanding of the diffusion and evaporating behaviour of Hg, depending on parameters like substrate material (silver, copper, bronze, brass...), heating temperature and duration, and the resulting Hg depth profiles under these conditions. Secondary objective is the establishment of a measurement protocol for the unambiguous identification of different types of gilding, based solely on non-destructive methods, which can be applied to historical samples.

In a first step, fire-gilded samples have been prepared on Cu and Ag sheet metal, respectively. Some of the gildings were produced by a professional goldsmith; another set of samples was produced under laboratory conditions. These samples have been examined with NAA (neutron activation analysis) and SR-XRF (synchrotron radiation induced X-ray fluorescence). First results of these measurements will be presented and discussed (see figure).

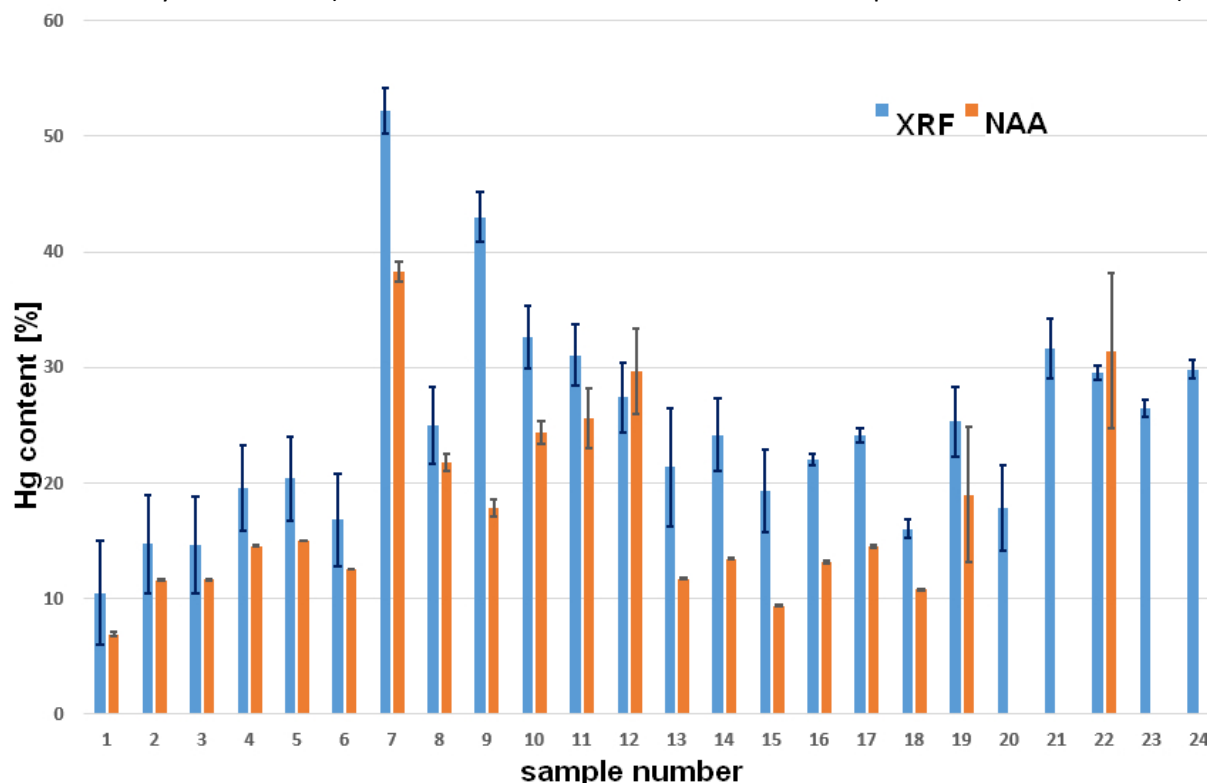


Fig: Hg content of fire gilded samples, determined with both NAA and XRF (preliminary)

Nondestructive analysis of difficult-to-measure radionuclides by TOF-PGA

TOH, Yosuke, *EBIHARA, Mitsuru, HUANG, Minghui, KIMURA, Atsushi, NAKAMURA, Shoji, HARADA, Hideo

Japan Atomic Energy Agency, Tokai-mura, Ibaraki, Japan

**Tokyo Metropolitan University, Tokyo, Japan*

Recently, interest in a spent fuel management has been increased. The determination of radioactivity is needed for each radioactive nuclide before nuclear waste is accepted for storage and disposal or is recycled. The gamma-ray measurement usually makes it possible to determine these of radioactive nuclides, because energies of gamma rays are characteristic for each nuclide. However, the gamma-ray measurement cannot apply to the pure alpha or beta emitters, which are called as Difficult-to-Measure (DTM) nuclides.

Japan Atomic Energy Agency has developed group partitioning process for the treatment of nuclear waste. Elements in a high-level liquid waste are separated into several groups; transuranium elements, platinum group metals (PGM), Sr-Cs and the others by the partitioning process. Among them, the PGM are required in wide variety of industrial applications such as catalysts, medical implants and electronics; however, PGM generated from the partitioning process includes DTM radioisotopes Tc-99 and Pd-107. In order to improve the accuracy and sensitivity, we developed a non-destructive multi-elemental analytical technique which combines prompt gamma-ray analysis with time-of-flight technique (TOF-PGA) by using the intense pulsed neutron beam and Ge detector system in J-PARC ANNRI [1]. The feasibility study was conducted using non-destructive analytical method TOF-PGA for analysis of DTM nuclide in PGM samples. The results indicate that TOF-PGA offers significant advantages of the determination of DTM nuclides.

This work was supported in part by Grants-in-Aid for Scientific Research (25246038).

[1] Y. Toh et al., Anal. Chem. 86, 12030-12036 (2014).

Characterisation of activity content of ^{226}Ra in spiked metallurgical slag using an interlaboratory comparison

F. Tzika¹, E. Garcia-Toraño², M. Hult¹, D. Arnold³, O. Burda³, T. Branger⁵, P. Carconi⁴, B. Caro², P. Dryak⁹, A. Fazio⁴, L. Ferreux⁵, S. Klemola⁶, A. Luca⁷, V. Peyrés², M. Reis⁸, M. Sahagia⁷, M. Santos⁸, J. Šolc⁹, Z. Tyminski¹⁰, B. Vodenik¹¹

¹ EC, JRC-Geel, Joint Research Centre, Retieseweg 111, Geel, Belgium;

² CIEMAT, Metrología de Radiaciones Ionizantes, Avda. Complutense 40, Madrid, Spain;

³ PTB, Physikalisch-Technische Bundesanstalt, Bundesallee 100, Braunschweig, Germany;

⁴ ENEA-INMRI, Via Anguillarese, 301 Santa Maria di Galeria, Roma, Italy;

⁵ CEA, LIST, Laboratoire National Henri Becquerel (LNE-LNHB), CEA-Saclay Gif-sur-Yvette Cedex, France;

⁶ STUK, Radiation and Nuclear Safety Authority, P.O.Box 14, Helsinki, Finland;

⁷ IFIN-HH, 30 Reactorului Street, 077125 Magurele, Ilfov, Romania;

⁸ IST/CTN, Estrada Nacional 10 (km 139,7), Bobadela LRS - Portugal;

⁹ CMI, Czech Metrology Institute, Okružní 31, Brno, Czech Republic;

¹⁰ NCBJ, Narodowe Centrum Badań Jądrowych OR POLATOM, Otwock, Świerk, Poland;

¹¹ IJS, Institute Jožef Stefan, Jamova 39, Ljubljana, Slovenia

faidra.tzika@ec.europa.eu

Introduction

More than half of yearly steel production in EU comes from recycling. The metal foundries pass the metal scrap through radiation portal monitors at the entrance of the foundry; nevertheless an orphan radioactive source may still remain undetected e.g. due to the shielding from the scrap load itself. In such case the source may enter the smelting route ending in contaminated steel products and by-products of the process. The European metal foundries are aware of the problem and increasingly apply radioactivity monitoring of the steel products. It is of outmost importance to perform accurate measurements, in order to prove compliance with respect to legal radioactivity limits, and metrologically challenging to ensure the quality of such measurements. In the light of a global steel market it is obvious that harmonisation of the analytical methodologies is critical. In the EURAMET's EMRP joint research project, 'MetroMetal' (Ionising radiation metrology for the metallurgical industry), existing radioactivity measurement methods were studied and new optimized methods, systems and standards were proposed for the radioactivity control of steel and by-products in steel mills. In this context, reference activity standards, including the most frequently occurring radionuclides in melting incidents in suitable geometries and matrices, have been developed. Amongst these standards were two series of sources of ^{60}Co in cast steel, one of ^{137}Cs in fume dust and one of ^{226}Ra in furnace slag. The common feature in all four standards was that Interlaboratory comparisons (ILCs) were used to characterise the activity concentrations. In the particular case of ^{226}Ra in slag the material was prepared by spiking and an ILC was conducted amongst 9 European National Metrology Laboratories and JRC, with the aim to verify the activity concentration of the spiked material and to validate the calibration and correction methods proposed by MetroMetal. In the present work, the organization and the results of the ILC on ^{226}Ra activity concentration in metallurgical slag standards are presented.

Method

The raw slag material was obtained from a steel foundry located in Spain and was characterised for its natural radioactivity content and for its mineralogical, chemical and radiological features (1, 2). The natural radioactivity concentration of ^{226}Ra in the raw slag was found to be of (14.0 ± 0.6) Bq/kg in average over different measurements and laboratories (2). The ILC samples were prepared by spiking the samples with a known amount of certified solution containing ^{226}Ra . The initial characterisation of the raw slag and the preparation of the ILC samples, including homogeneity testing of the spiked sources, were realized at CIEMAT (2). JRC coordinated the intercomparison and provided each of the 10 participants with one sample, previously prepared by CIEMAT, and associated detailed information (sample and container masses, dimensions and elemental composition). To determine the activity concentration the participants used gamma ray spectrometry, based on HPGe detectors, and

different calibration methods, including experimental, Monte Carlo, and/or numerical ones. Seven out of ten participants measured the sample in the supplied geometry while three prepared their own sample geometries using own containers. All participants reported their activity concentration result, with the combined standard uncertainty, using a standard template which accommodated all relevant information on used detectors, analytical methods and procedures, and decay data. Independency of JRC's participation in the ILC was ensured.

Results

The reported activity concentrations, and combined standard uncertainties ($k=1$), for ^{226}Ra in the ILC materials are shown in Table 1. The ILC's consensus value was calculated as a Power Moderated Mean from the reported activity concentrations and was of (9.08 ± 0.21) Bq/g. All reported results were included in the calculation of the consensus value as no outlier had been identified. The ILC consensus value represented the total (spiked + natural) activity concentration of ^{226}Ra in the slag samples obtained by gamma-ray spectrometry measurements. The individual laboratory performance was evaluated with reference to the ILC's consensus value, and was expressed in terms of relative deviations and En numbers. Six out of ten results deviated by less than 5 %, two between 5 and 10 % and two by more than 10 %, from the reference value. Moreover, eight out of ten results showed satisfactory compatibility, expressed by En numbers, with the ILC's reference activity concentration for ^{226}Ra .

Table 1. Reported activity concentrations for ^{226}Ra in the ILC slag samples¹.

no	Laboratory	Sample ¹ ID	$A'_{rep,i}$ Bq/g	$u(A'_{rep,i})^2$ Bq/g
1	CEA	HSslag-12	10.0	0.5
2	CMI	HSslag-11	9.06	0.46
3	ENEA	HSslag-10	8.27	0.31
4	IFIN-HH	HSslag-09	8.0	0.8
5	IJS	HSslag-08	9.14	0.27
6	IST/CTN	HSslag-06	9.09	0.46
7	JRC	HSslag-05	8.82	0.26
8	POLATOM	HSslag-03	9.90	0.35
9	PTB	HSslag-02	8.86	0.33
10	STUK	HSslag-01	9.39	0.40

¹ The term 'Sample' refers to original slag sample in CIEMAT container which was provided for ILC_2

² Reported combined standard uncertainty ($k=1$)

After completion of the ILC reporting, the mean spiked activity in the ILC samples was provided to JRC by CIEMAT. The nominal activity concentration for the spiked sources was calculated as the sum of the mean spiked activity concentration in the samples and the natural radioactivity concentration measured in the raw slag, and was found to be of (8.84 ± 0.12) Bq/g. Comparing the ILC consensus value of (9.08 ± 0.21) Bq/g with the above nominal value an agreement within 1s is observed. This ILC did not aim at testing the proficiency of the participants, but at assisting the development of a reference procedure and standards for radioactivity monitoring in metal foundries. The ILC results demonstrated the validity of the proposed methods for the measurement of ^{226}Ra in furnace slag. The availability of tested methods and of the new slag activity standard will contribute in ensuring reliable measurements of radioactivity in the EU metal industry.

References

1. Sahagia M, et al., (2013) J Radioanal Nucl Chem 298(3):2037–2042
2. Mejuto M, et al., (2014) Appl. Radiat. Isot. 94:166–174

Activation analysis methods - an analytical toolkit for silicon solar cell developments

B. Karches¹, C. Stieghorst¹, K. Welter¹, H. Gerstenberg³, G. Hampel¹, J.V. Kratz¹, P. Krenckel², P. Kudejova³, C. Plonka¹, B. Ponsard⁴, T. Reich¹, S. Riepe², J. Schön², N. Wiehl¹

¹*Johannes Gutenberg University Mainz Institute of Nuclear Chemistry, Mainz, Germany;*

²*Fraunhofer Institute for Solar Energy Systems, Freiburg, Germany;*

³*Heinz-Maier-Leibniz Zentrum, Technische Universität München, Garching, Germany,*

⁴*Belgian Nuclear Research Centre (SCK•CEN), BR2 reactor, Mol, Belgium*

The efficiency of solar cells made from crystalline silicon is strongly influenced by the impurity level of the silicon. Especially, the 3d-transition elements like manganese, chromium, iron, cobalt, or nickel reduce the cell efficiency because they form recombination centers for the charge carriers. But the well-established Siemens process [1] to purify raw silicon is energy and cost intensive. Therefore, new techniques with optimal performance for both high cleaning efficiency and low energy consumption are investigated. In addition, controlled doping of the silicon with boron and/or phosphorus is necessary for the further solar cell production. One technique to produce multi-crystalline silicon (mc-Si) with the right properties is the directional solidification. In this method, different feedstock materials can be used, for example so called upgraded metallurgical silicon (UMG). UMG is pre-cleaned or under clean conditions produced raw silicon [2]. The purity level of raw silicon (MG silicon) is in the range of 99% - 99.9% whereas the purity level of UMG silicon is in the range of 99.9% - 99.999%. The purity level needed for solar cell production, so called solar grade silicon (SoG), is in the range of 99.99% up to 99.99999%.

In a joint project of the Institute of Nuclear Chemistry at the University of Mainz and the Institute for Solar Energy Systems (ISE) of the Fraunhofer Gesellschaft in Freiburg, the technique of directional solidification of mc-Si was investigated. During the crystallization from bottom to top in a crucible the impurities are enriched in the liquid phase because of their segregation coefficients. But the 3d-transition metals have a high mobility in silicon and can diffuse from the crucible and the top of the ingot during solidification and cooling into the inner part of the ingot. One goal of this project was to establish fast and reliable analytical procedures to measure impurity and dopant contents of feedstock silicon, of crucible materials, and especially to determine their distribution in the produced ingots under different crystallization conditions. Compared to other analytical methods, purely instrumental methods have the advantage that the results are not distorted by possible contaminations during the sample preparation. Here we present how this could be achieved with different activation analysis methods:

3d-transition metals: The concentration of these metals in the samples was expected to be in the range of some 10 ppb up to several ppm. At this impurity level in silicon, standard instrumental neutron activation analysis (INAA) is one of the most reliable methods. Most of the 3d-transition metals have high neutron capture cross sections and the half-life is much longer than that of the silicon matrix. This method was especially used to determine impurity concentration profiles of vertical and horizontal cuts of ingots from a series of crystallization experiments. In these experiments, the influence of the feedstock material, the crucible system, and crystallization parameters on the impurity distribution was investigated. The impurity profiles were compared with measurements of electrical properties of the silicon like the charge carrier lifetime and theoretical simulations of the diffusion of impurities from the crucible system into the ingots. The irradiations were performed at the research reactors TRIGA in Mainz, FRM II in Munich, and BR2 in Mol. To assure measurements of the bulk concentration of the samples, special attention was paid to possible surface contamination.

Boron: For the determination of boron in p-type silicon and crucible material, the prompt gamma activation analysis (PGAA) facility at FRM II in Munich was used. Because of the high neutron capture cross section of 760 b this method is applicable even at low boron concentrations. The determination of the peak area needs some special treatment

because the gamma peak is Doppler broadened and is superimposed by a prompt gamma emission from the silicon. With the fit function suggested by Magara and Yonezawa [3], a combination of error- and gauss functions, good results were achieved. A detection limit of 17 ppb was determined. In addition to boron also the hydrogen content of feedstock material could be measured by PGAA.

Phosphorus: The only activation product of phosphorus, P-32, is a pure beta emitter. Therefore, the determination of the phosphorus content to a level of 0.1 ppm and below by instrumental activation analysis is challenging. First of all, the beta spectrum could be distorted by the beta emission from the impurities in the silicon. Secondly, beta particles are partially absorbed in the silicon which makes an absolute calibration difficult. And finally, P-32 is also produced from the silicon matrix by second order reactions [4]. A beta-gamma anticoincidence setup was constructed and tested to overcome the first difficulty because all other impurities present in the silicon are beta and gamma emitters. To correct for differences of the beta absorption in the samples and the standards, we created a Monte Carlo simulation of the whole setup with Geant4 [5] which was experimentally validated. Finally, the P-32 activity created from the silicon matrix was determined from the irradiation of high purity silicon together with the samples. With this setup, first quantitative determinations of phosphorus in n-type silicon was possible. The results were in agreement with resistivity measurements of these samples. The detection limit was below 0.1 ppm phosphorus in silicon. With an improved setup, a detection limit in the range of 0.01 ppm should be possible as was shown by Geant4 simulations.

Results of different crystallization experiments in comparison with electrical properties and theoretical calculations will be shown.

Acknowledgement

This work was funded by the Deutsche Forschungsgemeinschaft (DFG) under contracts HA5471/4-1 and BO3498/1.

References

1. H. A. Aulich, F.-W. Schulze, J. G. Grabmaier, *Verfahren zur Herstellung von Solarsilicium*, Chemie Ingenieur Technik, 56(9), 667—673 (1984)
2. M. Heuer, *UMG Silicon*, Proceedings of the 19th Workshop on Crystalline Silicon & Modules: Materials and Processes, Vail, Colorado, (2009)
3. M. Magara, C. Yonezawa, *Decomposition of prompt gamma-ray spectra including Doppler-broadened peak for boron determination*, Nuclear Instruments and Methods A, 411 (1998) 130—136
4. W. Maenhout, J.P. Op de Beek, *Interference by second order reactions in activation analysis*, Journal of Radioanalytical Chemistry 5 (1970) 115—121
5. S. Agostinelli et. al., *Geant4 – a simulation toolkit*, Nuclear Instruments and Methods A, 506 (2003), 250—303

Clearance-level radioactive waste measurement comparisons of two gamma-ray counting systems

Chin-Hsien Yeh, Ming-Chen Yuan, Ping-Ji Huang

*Institute of Nuclear Energy Research, Atomic Energy Council
No.1000 Wenhua Rd. Jiaan Village, Longtan District, Taoyuan City 32546, Taiwan (ROC)*

In the past three decades, the routine operation and maintenance of nuclear facilities produced over a thousand tons of low activity (around clearance level) solid radioactive waste in Taiwan. Management and storage of significant quantities of radioactive waste on operating nuclear sites is not recommended and dispatch to an appropriate disposal site is the usual way of dealing with such material. Based on local regulations, the radioactivity and the composition of the nuclides of the waste should be identified before being released or put away in long term storage. Here, issues of the needs of traceability, calibration and evaluation of the measurement systems were raised.

Two counting system containing plastic scintillators (SWAM 2) or three HPGe detectors (AQ2) with 4π shielded counting geometry has been operated to measure low activity waste in 208 L drums at INER for about 10 years. The detection efficiency of these two detectors for specific gamma-emitters such as ^{60}Co and ^{137}Cs was verified through a proficiency testing program held by the National Radiation Standard Laboratory in Taiwan during 2009 and 2011. All the results were acceptable for bias and traceable to the national standards.

In this study, the measurement performance of these two counting systems were evaluated by measuring the activities of four plastic-filled drums with various filling rate (25%, 50%, 75% and 100%) and five metal-filled drums with different source position types to study the hot spot effect. It was found that the measurement bias is getting lower while increasing the filling rate of plastic-filled drums in both two counting systems and the plastic scintillator counting system had larger measurement bias when counting the activities of five hot spot simulated drums.

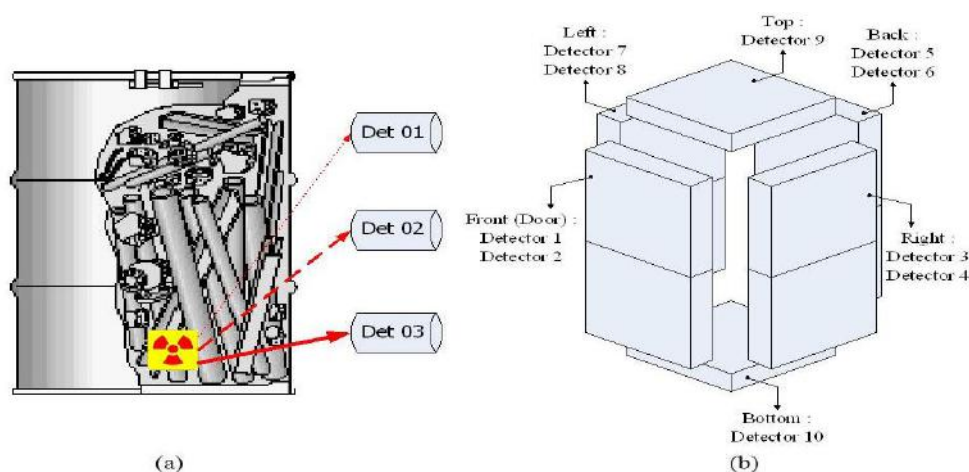


Figure 1. Counting system geometry for (a) AQ2 and (b) SWAM2.

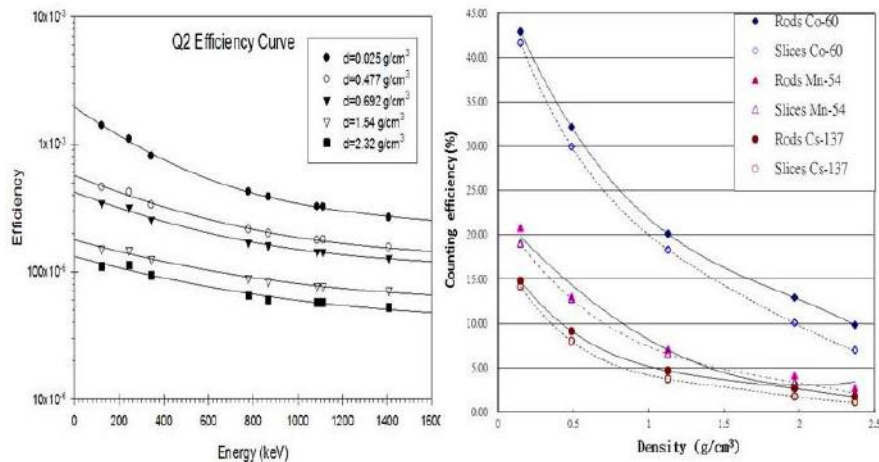


Figure 2. Density vs efficiency calibration curves for (a) AQ2 and (b) SWAM2.

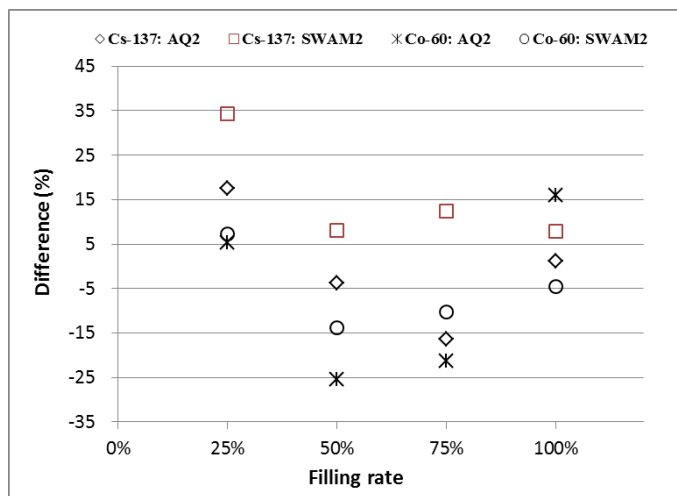


Figure 3. Measurement results for four plastic-filled drums with various filling rate.

Table 1. Measurement results for metal-filled drums with different source position types.

Source position type	Nuclide	Activity (Bq)	Bias (%)	
			AQ2	SWAM2
Horizontal/upper	¹³⁷ Cs	89,295	-20.8	-51.4
	⁶⁰ Co	33,117	23.1	90.0
Horizontal/center	¹³⁷ Cs	89,295	-3.9	-69.0
	⁶⁰ Co	33,117	-1.6	29.4
Horizontal/lower	¹³⁷ Cs	89,295	-15.2	-68.9
	⁶⁰ Co	33,117	-17.9	25.2
Vertical/center	¹³⁷ Cs	86,667	-61.8	-83.6
	⁶⁰ Co	77,778	-56.0	-31.0
Vertical/side	¹³⁷ Cs	86,667	-14.0	-63.5
	⁶⁰ Co	77,778	-18.6	33.7

Calibration of elemental sensitivities in PGAA of hydrogen-containing samples

Rolf Zeisler, Maria Vega Martinez*, Rick Paul, Danyal Turkoglu

Chemical Sciences Division, National Institute of Standards and Technology (NIST), Gaithersburg, MD, USA *Guest
Researcher, Centro de Energia Nuclear na Agricultura, 13400-970 Piracicaba, São Paulo, Brazil

In neutron-induced prompt gamma-ray activation analysis (PGAA), sensitivity changes depending on the hydrogen content of the investigated samples have been reported in applications using both thermal- and cold-neutron beams. Scattering of neutrons has been identified as the major cause. Increased path length in the sample due to scattering leads to higher reaction rates, while scattering of neutrons out of the sample and thermalization of cold neutrons decreases reaction rates. However, the establishment of quantitative relationships between hydrogen content and these multiple effects has proven difficult. Therefore, we explored the feasibility of calibration with standards of matrix composition, mass, and geometry comparable to the unknown samples. The study involved standards for key elements deposited on cellulose filter papers and vegetation-based reference materials, as well as titanium-foil flux monitors placed anterior and posterior to the samples and standards in the neutron beam. Measurements were carried out at both the thermal- and cold-neutron PGAA stations at NIST in order to compare the effects of neutron scattering. The accurate calibration with the comparator standards was demonstrated for several mineral elements in Standard Reference Materials (SRMs) and a candidate sugarcane-leaf reference material; the composition of all had been determined via instrumental neutron activation analysis (INAA). The flux monitors were used to monitor average neutron fluxes in samples and standards and contributed to the comparability of the specific reaction rates for the elements in standards and samples. This allows the determination of trace elements by this comparator method solely by cold-neutron PGAA. Boron, nitrogen, and silicon were determined in the SRMs and the candidate reference material. An extension of this calibration technique to INAA with a cold neutron beam is possible and eliminates epithermal and fast neutron interfering reactions.

RADIOPHARMACEUTICAL CHEMISTRY

Automatic production of astatinated radiopharmaceuticals – from target material to labeled product

Emma Aneheim¹, Sture Lindegren¹, Holger Jensen²

¹Targeted Alpha Therapy group, Department of Radiation Physics, Sahlgrenska Academy at University of Gothenburg, SE41345 Gothenburg, Sweden

²PET and Cyclotron Unit, KF-3982, Copenhagen University Hospital, Copenhagen, Denmark

Targeted radiotherapy of cancer tumors is an area of nuclear medicine that is increasing in interest due to the promising treatment options. For microscopic tumors or single cancer cells, alpha therapy is especially interesting due to the high LET of the alpha particles. One of the more promising nuclides for targeted alpha therapy is ^{211}At . ^{211}At decays with 100% alpha-emission along two different branches and has a half-life of 7.2 hours. The Targeted Alpha Therapy group at Sahlgrenska Academy in Sweden has been performing research regarding alpha therapy using astatine and monoclonal antibodies for intraperitoneal treatment of disseminated ovarian cancer for over fifteen years. The research has been taken from bench to bedside including several preclinical studies and a phase I clinical trial on nine patients with recurrent ovarian cancer. However, to be able to move forward towards future phase II/III studies, the current manual synthesis of the radiolabeled antibodies would benefit from being automated. In this work such an automation has been performed and evaluated.

The automation has been performed by adapting a commercially available radiopharmaceutical module from Scintomics GmbH (Hot Box III) to not only perform labeling but to also automatically produce astatine from irradiated target material (*Figure 1*). The ^{211}At used is produced in a cyclotron (at Copenhagen University Hospital) by alpha particle activation of ^{209}Bi through the reaction $^{209}\text{Bi}(\alpha, 2n)^{211}\text{At}$. This is facilitated using ca 30 MeV alpha particles. The commercially available monoclonal antibody Trastuzumab has been used for labeling and a SKOV3 cell line to investigate maintained immunoreactivity after the automatic labeling procedure.



Figure 1. The automatic equipment for astatine recovery from target material and subsequent carrier labeling

Purified monoclonal antibodies labeled with astatine have been automatically produced from irradiated target material with reasonable yields using the novel equipment. The automatic astatine distillation procedure has been found to be able to deliver astatine to the synthesis with high yield. This has also been demonstrated to be possible using different types of chemical astatine delivery systems. The product has been shown to be radiochemically pure and to maintain its immunoreactivity throughout the process. These results have been obtained after modifications of the manual synthesis and distillation processes as well as an extensive equipment development.

This work has shown that it is possible to produce astatinated radiopharmaceuticals such as labeled monoclonal antibodies from irradiated target material using a custom made automatic system integrating labeling with a commercial module and astatine distillation.

Study of the dissociation kinetics of DOTA derivatives by immobilization on solid supports

R. Bhardwaj^{1,2}, J. Gascon², H. T. Wolterbeek¹, A. G. Denkova¹ and P. Serra-Crespo¹

¹*Radiation and Isotopes for Health, Radiation Science & Technology, Delft University of Technology, Netherlands*

²*Catalysis Engineering, Chemical Engineering, Delft University of Technology, Netherlands*

DOTA (1,4,7,10-tetraazacyclododecane-1,4,7,10-tetraacetic acid) is a molecule derived from the macrocycle cyclen, which is modified on the N-H centers with CH₂CO₂H groups. As a result of the incorporation of the carboxylic acid groups, a high affinity chelating agent for divalent and trivalent cations is formed.

The use of peptide-based targeting agents has become very popular in the last years for diagnosis and therapy. DOTA-peptide conjugates have become widely applied due to their extraordinary thermodynamic and kinetic stability with radionuclides like ⁹⁰Y, ¹⁷⁷Lu and ¹⁵³Sm. Furthermore, the vast number of design possibilities makes the use of DOTA conjugates to be expected to grow in the coming years.

Despite the successful application of these complexes, there is still a lack of reliable data on the kinetic parameters for association and dissociation rates. Common experimental approaches used in different studies leads to varying and not so accurate values of these parameters. The main reason behind these erroneous results is the high kinetic inertness of these complexes.

With the goal of measuring accurately dissociation kinetics of DOTA-conjugates with different metals of medical interest, we have developed a method that combines the immobilization of the DOTA derivatives on different solid supports and the use of radioactive tracers (see figure 1). By immobilizing the complex on a solid support the separation from the metal after dissociation is automatic. In addition, the use of a radioactive tracer together with cold metal in the mobile phase provides the measurement of the dissociation process completely decoupled of re-association. In this way reliable kinetic dissociation measurements can be carry out even for extremely inert DOTA based complexes.

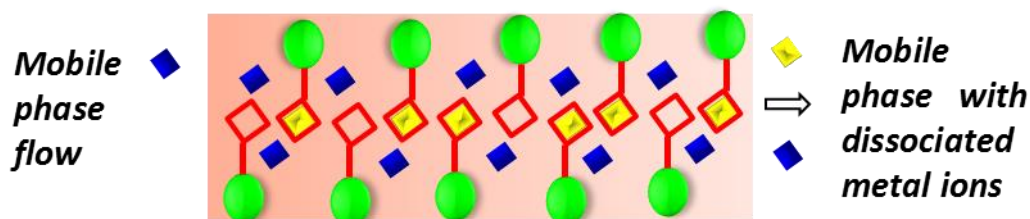


Figure 6. Schematic representation of the experimental approach to measure dissociation kinetics of DOTA-conjugates complexes. (◻●) represents immobilized DOTA conjugate on a solid and (◼ and ◼) represent the cold metal ions and the corresponding radioactive tracer, respectively.

Two different supports have been selected for this purpose, an amine functionalized silica and a carboxy-polystyrene. The immobilization of DOTA on the silica support is done in a one step process using DCC as the coupling catalyst (see figure 2). It leads to silica with an immobilized DOTA complex with three free pending arms (like in many of the DOTA derivatives).

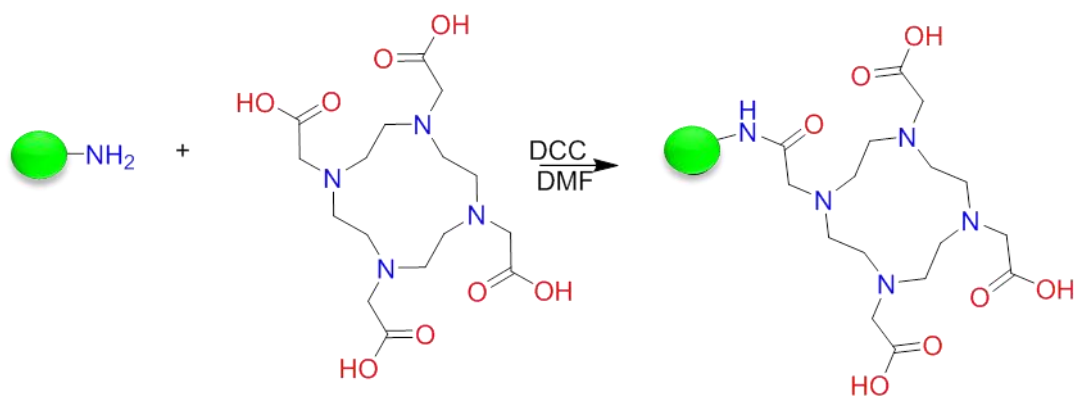


Figure 7. One step immobilization of DOTA on amino modified silica

In contrast, for the immobilization of p-aminoDOTA on a carboxy-polystyrene resin a two-step reaction scheme is followed. In the first step, the carboxyl groups of carboxy-polystyrene resin are converted to more reactive acyl halide using oxalyl chloride. Next they are coupled with amino benzyl DOTA in the presence of DIEPA leading to an DOTA immobilized styrene with four free pending arms (see figure 3)

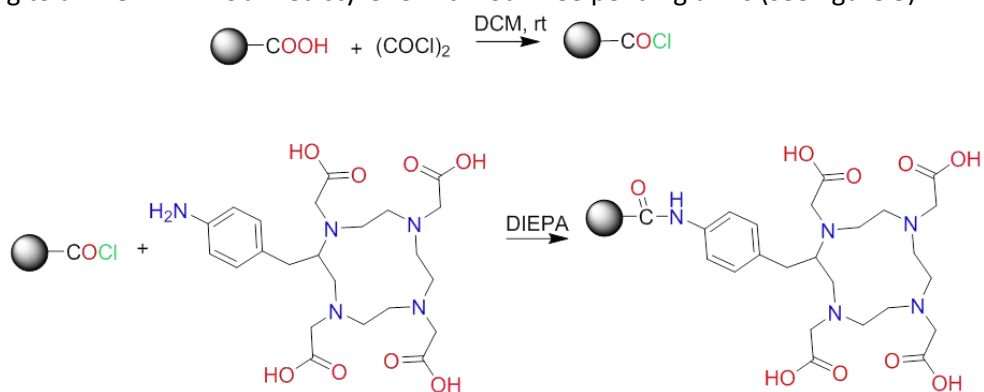


Figure 8. Reaction scheme for the immobilization of p-amino benzyl DOTA on carboxy-polystyrene.

Once the DOTA groups are immobilized, the complexation of different metal ions on both supports will be carried out and the dissociation kinetics will be measured under different conditions. Moreover, the effect of the number of free carboxylic groups involved in the complexation will be studied.

3D cell culture evaluation of polymer vesicles designed for alpha radionuclide therapy

R.M. De Kruijff¹, A. van der Meer¹, K.G.A. Drost¹, D. Lathouwers¹, A. Morgenstern², F. Bruchertseifer², P. Sminia³, H.T. Wolterbeek¹, A.G. Denkova¹

¹*Radiation Science and Technology, Delft University of Technology, Mekelweg 15, 2629 JB Delft, The Netherlands*

²*European Commission, Joint Research Centre, Institute for Transuranium Elements, P.O. Box 2340, 76125 Karlsruhe, Germany*

³*VUmc Cancer Centre Amsterdam, De Boelelaan 1118, 1081 Amsterdam*

Alpha particles have for long been considered to have much better radiotherapeutic effects than beta particles, but their application has only increased in the last decade. Currently ^{225}Ac is considered one of the most important alpha emitting radionuclide, due to its half-life (9.9 d) and the fact that it can serve as an *in vivo* generator, providing four alpha particles with a total energy of 28 MeV. However, a major challenge should be overcome before ^{225}Ac can be used safely in the clinic, i.e. due to the recoil effects the daughter recoil atoms, most of which are alpha emitters as well, receive energies that are much higher (> 100 keV) than the energies of chemical bonds (typically around 2- 8 eV), enabling them to escape from any targeting agents such as antibodies and distribute freely in the body.¹

Previously we have shown that GEANT4 can be used to theoretically design nano-carriers that would be able to retain the recoiling daughters of ^{225}Ac .^{2,3} Here, we present experimental results on the recoil retention of ^{221}Fr and ^{213}Bi when encapsulating ^{225}Ac in polymer vesicles of varying sizes. Two designs have been tested and compared with simulation results. In the first design ^{225}Ac coupled to DTPA is enclosed in a polymer vesicle and in the second design ^{225}Ac is precipitated into phosphate nano-particles on the inside of the same vesicle. For sizes of 100 nm the second design (nano-particles in vesicles) has much better retention of ^{221}Fr ($57 \pm 5\%$) than the first one (37 ± 4). Similarly, the retention of ^{213}Bi has also improved; it increases from $22 \pm 1\%$ for normal vesicles to $40 \pm 2\%$ for vesicles containing nano-particles, but this positive effect seems to be valid only for small nano-carriers.

The ^{225}Ac loaded nano-carriers have been subsequently tested in 3D tumour cell cultures and have proven to be much more effective than ^{225}Ac coupled to DTPA. The tumour spheroids are completely destroyed within a few days when exposed to activities of just 1 kBq (see Figure 1). The better killing efficiency of the nano-carriers containing ^{225}Ac has been ascribed to their accumulation around the cell nucleus.

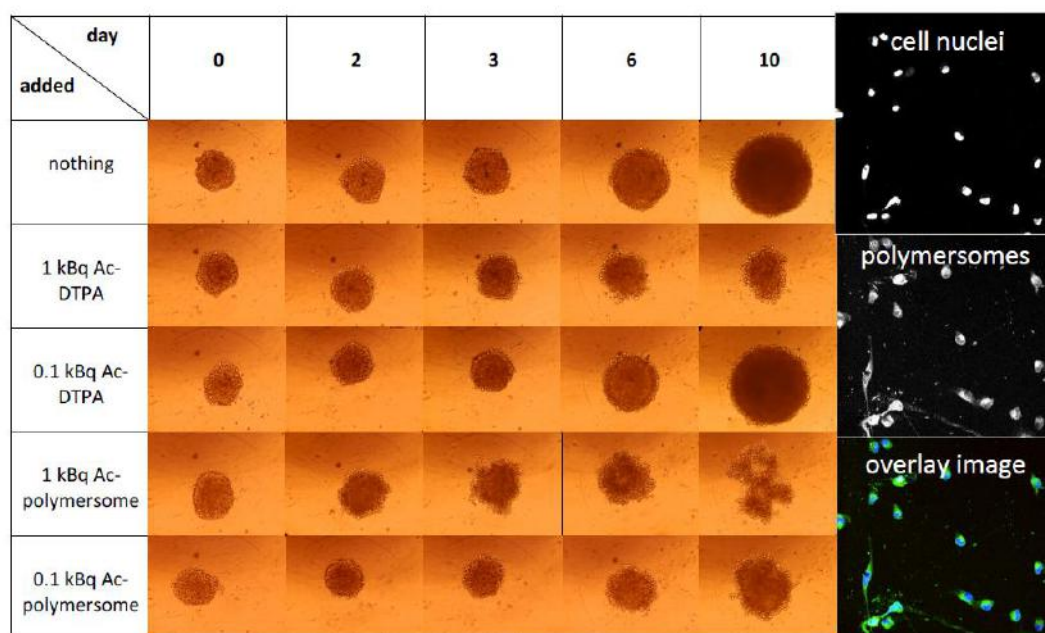


Figure 1 The effect of ^{225}Ac loaded polymersomes on spheroidal tumours in comparison to ^{225}Ac -DTPA at different time points (left) and uptake of the polymersomes in cells (right)

References

1. Kruijff, R.M. de; H.T. Wolterbeek, H.T.; Denkova, A.G. A Critical Review of Alpha Radionuclide Therapy—How to Deal with Recoiling Daughters? *Pharmaceuticals* 2015, 8 (2), 321-336.
2. Thijssen, L.; Schaart, D. R.; deVries, D.; Morgenstern, A.; Brucherseifer, F.; Denkova, A. G. Polymersomes as nano-carriers to retain harmful recoil nuclides in alpha radionuclide therapy: a feasibility study, *Radiochim. Acta* 2012, 100, 473-481.
3. Wang, G., de Kruijff, R.M., Rol, A., Thijssen, L., Mendes, E., Morgenstern, A., Bruchertseifer, F., Stuart, M.C.A., Wolterbeek, H.T., Denkova, A.G. Retention studies of recoiling daughter nuclides of ^{225}Ac in polymer vesicles, *Appl. Radiat. Isot.*, 2014, 85, 45-53.

Acknowledgements

We greatly appreciate the financial help of the STOP HERSEN TUMOUREN, Zabwas and SK foundations.

Pyridine containing azacrown ligands as possible chelators for Bi³⁺, Y³⁺, Pb²⁺ and Cu²⁺ in aqueous solutions

B.V. Egorova¹, M.S. Oshchepkov², A.D. Zubenko², Yu.V. Fedorov², O.A. Fedorova^{1,2}, G.S. Budylin¹, E.A. Shirshin¹, S.N. Kalmykov^{1,3}

¹Lomonosov Moscow state university, Moscow, Russia

²A.N. Nesmeyanov Institute of Organoelement Compounds of Russian Academy of Sciences, Moscow, Russia

³NRC "Kurchatov Institute", Moscow, Russia

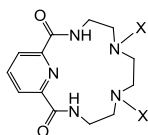
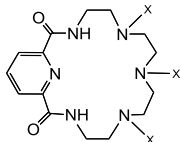
bayirta.egorova@gmail.com

Polyaminopolycarboxylates are attractive ligands as linkers in radiopharmaceuticals for target delivery of specific radionuclides to the tumor cells. Nowadays beta emitting radionuclides of rare earth elements, i.e. Y-90 and Lu-177, are used as therapeutic agents, Ac-225/ Bi-213, Pb-212/ Bi-212 and Cu-67 are considered as perspective for alpha and beta therapy and Cu-64 is a radionuclide for positron emission tomography. In the present work new data on possibilities of azacrown moieties to complex several tri- and divalent cations are studied.

Considered azacrown compounds form complexes with cations within first minutes that confirmed by UV-vis spectroscopy. For ligands' and complexes' characterization potentiometric titration and competitive technique were used. Potentiometric titration data were treated using HYPERQUAD software, as competitive processes liquid extraction and precipitation were performed. Azacrown ethers possess different acidity that affects by the presence of carbamide groups, macrocyclic ring size and addition of carboxylic arms or pyridine fragments. It was found that binding of such "hard" cations as Y³⁺ requires availability of carboxylic groups in ligand but calculated constants (table) are still less than the values required for in vivo applications.

The highest values of stability constants were determined for Bi³⁺ (table). It is bound quantitatively even at pH3. It is shown that L1a and L2a form complexes with Bi³⁺ with two stoichiometries 1:1 and 1:2. L1b, L1c and L2b form ternary complexes with Bi:L=1:1 and presence of OH⁻ depending on pH. Bi³⁺ as extremely hydrolysable cation possesses affinity to different ligands as OH⁻ and different polyaminopolycarboxylates, so constants of respective complexes are usually higher than analogous complexes with trivalent REE. Therefore even without carboxylates strong water soluble complexes with Bi³⁺ could be formed.

Table. Calculated logK_{ML}, μ=0.1M NaClO₄

M	L1			L2	
					
	a) X=H	b) X=CH ₂ COOH	c) X=CH ₂ PO ₃ H ₂	a) X=H	b) X=CH ₂ COOH
ΣpK _a	11.8(2)	15.1(1)	11.4(1)	15.4(1)	22.4(2)
Y ³⁺	-	5.5(4)	-	-	6.9(3)
Bi ³⁺	12.5(1)	16.3(2)	11.8(4)	14.4(1)	21.3(2)
Pb ²⁺	-	8.7(1)	4.9(1)	4.9(1)	14.1(1)
Cu ²⁺	8.8(2)	11.2(1)	8.9(1)	10.8(6)	15.8(1)

Among studied divalent cations azacrown-ethers demonstrate preference to Cu²⁺ in comparison to Pb²⁺. The same tendency as for Bi³⁺: constants increasing with addition of carboxylic arms and no influence of pyridine pendant groups.

It is important to note that all calculated constants correlate with determined acidity constants of ligands (table) and in line with literature data for complexes with other polyaminopolycarboxilates.

To evaluate structure of formed complexes time resolved laser induced fluorescence spectroscopy (TRLIFs) on Eu^{3+} cation as Y^{3+} and Lu^{3+} chemical analog was performed. It was shown that despite the presence of larger number of donor atoms in L2b it does not correspond to the higher stability of Y-L2b in comparison with Y-L1b. For both complexes the number of water molecules in Eu^{3+} environment was determined to be 2.4 ± 0.5 .

Furthermore the best of considered ligands L2b was tested for cytotoxicity by MTT assay for leukemia cell lines and healthy blood cells. It was shown that for cancer cells $\text{LC}_{50} = (5 \pm 2) \cdot 10^{-4} \text{M}$ and for healthy white blood cells $\text{LC}_{50} = (4 \pm 3) \cdot 10^{-3} \text{M}$. Obtained concentrations are suggested not to be ever achieved in the cell during the treatment of disease, so we suppose that pyridine-containing azacrown compounds themselves are not toxic for any cells.

This work was supported by RFBR project 16-33-00642.

Bulk production and evaluation of high specific activity ^{186}Re for cancer therapy using enriched $^{186}\text{WO}_3$ targets in a proton beam

M.E. Fassbender^{1*}, V. Radchenko¹, H.T. Bach¹, E. Balkin², E.R. Birnbaum¹, M. Brugh¹, J.W. Engle¹, M. D. Gott^{1,3}, J. Guthrie⁴, H.M. Hennkens⁴, K.D. John¹, A.R. Ketrin⁴, M. Kuchuk⁴, J.R. Maassen¹, C.M. Naranjo¹, F.M. Nortier¹, T.E. Phelps³, D.S. Wilbur² and S.S. Jurisson³

¹Chemistry Division, Los Alamos National Laboratory, Los Alamos, NM; ²Department of Radiation Oncology, University of Washington, Seattle, WA; ³Department of Chemistry, University of Missouri-Columbia, Columbia, MO; ⁴Missouri University Research Reactor Center, University of Missouri-Columbia, Columbia, MO

* email mifa@lanl.gov

Introduction

Rhenium-186g is a β/γ -emitter with a half-life of 89.2 h and a β - end-point energy of 1.07 MeV. The isotope is suitable to treat cancers of small dimensions (mm range). Moreover, its γ -emission at 137.15 keV is in the energy range favorable for both γ -camera and SPECT imaging. Current production methods rely on the neutron capture reaction $^{185}\text{Re}(n,\gamma)$ in a reactor and are associated with low specific activities ($0.6 \text{ kCi}\cdot\text{mmol}^{-1}$), which limit the application of the isotope to palliative treatments. Production via charged particle interaction with enriched ^{186}W results in a ^{186}Re product with a much higher specific activity; allowing its use in therapeutic nuclear medicine.

Materials and Methods

^{186}Re production and chemical recovery

Test targets of both sintered and pressed $^{186}\text{WO}_3$ powder were proton irradiated in the low-energy slot (15.6 MeV incident energy) of a production target stack at the Los Alamos Isotope Production Facility (LANL-IPF, 100MeV mode) to evaluate radionuclide product yields, impurities, irradiation parameters and wet chemical Re recovery for a bulk production. We demonstrated that rhenium can be isolated in 97% yield from irradiated $^{186}\text{WO}_3$ targets within 12 h of end of bombardment (EOB) via an alkaline dissolution followed by anion exchange sorption and mineral acidic desorption. Tungsten (VI) oxide could easily be recovered from the eluted tungstate solution via acidification and filtration. A ^{186}Re bulk production run was conducted at LANL-IPF using a target consisting of Nb encapsulated pressed, enriched $^{186}\text{WO}_3$ powder (ISOFLEX, USA) in a proton beam (40 MeV dedicated mode). ^{186}Re was recovered wet-chemically as reported previously^{1,2} with a slight modification: the anion exchanger column was eluted with 100 mL of 8M HNO_3 for Re desorption.

^{186}Re SPECT phantom study

Using LANL produced ^{186}Re , a SPECT phantom study was conducted with a Mediso NanoSPECT/CT (Mediso Medical Imaging Systems, Budapest, Hungary) preclinical imaging camera. A collimator consisting of nine pinholes per head with a pinhole size of 0.8 mm and a 1.6 cm field of view and a sensitivity $>2200 \text{ cps/MBq}$ ($27 \mu\text{Ci}$) was used. A micro Derenzo phantom (rod sizes: 0.25 -0.6 mm) was filled with $^{99\text{m}}\text{Tc}$ in 70% EtOH (5mL, 2.85mCi or 105 MBq total activity) and ^{186}Re to the same specifications. The radioactivity present in each phantom was measured by dose-calibrator. Circular CT scans were acquired in 180 projections, at 45 kVp with 1000 ms exposure time and 3 minute scan duration. The scan range was 26 mm. Helical SPECT scans were acquired with acquisition times of 60 minutes.

¹⁸⁶Re radiolabeling studies

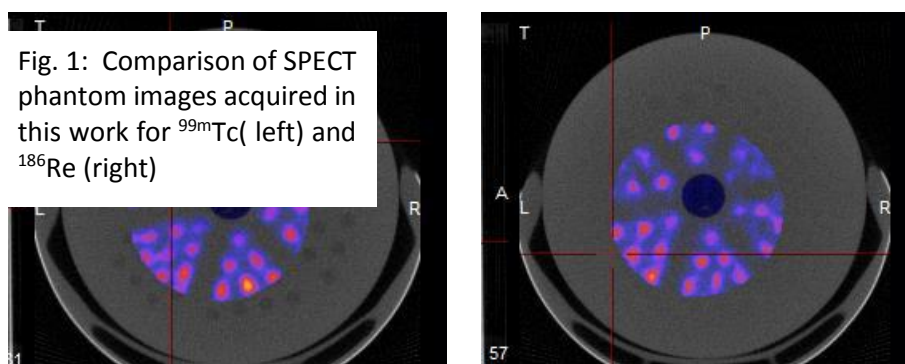
High specific activity ¹⁸⁶ReO₄⁻ from LANL was also used to prepare ¹⁸⁶ReOCl₃(PPh₃)₂ using the method of Wagner et al.³ Briefly, ¹⁸⁶ReO₄⁻ was added to PPh₃ in HCl to obtain a 9 M acidic solution. Dichloromethane was added, and the resulting biphasic mixture was vortexed for 5 minutes before removal of the organic layer, which contained the ReOCl₃(PPh₃)₂ product. A similar Re labeling method was employed in an earlier Los Alamos study⁴.

Results

Table 1 shows the ¹⁸⁶Re bulk production parameters obtained from the LANL-IPF irradiation. Rhenium-186 activity in the form of ¹⁸⁶Re₂O₇ had partially sublimed on the inside beam window during irradiation. The irradiation yielded roughly two therapeutic doses of ¹⁸⁶Re with a specific activity exceeding that of a ¹⁸⁵Re(n,γ) reactor product by a factor of 6-7. Figure 1 depicts acquired SPECT phantom images.

Table 1: Rhenium-186 bulk production parameters

Target material:	¹⁸⁶ WO ₃ , 9.68 ± .02 g, pressed at 111.21 kN for 1 min; ¹⁸⁶ W enrichment 99.90 ± 0.10 % isotopic impurities: ¹⁸⁴ W (0.10 ± 0.05 m-%), ^{180,182,183} W (<0.01 m-%)
Target cylinder dimensions:	5.08 cm x .11 cm
Max. beam current, duration:	230 μA, 16.5 h
Beam window entrance energy:	41.38 ± 0.15 MeV (TOF)
Production energy interval (nominal):	20.7 → 13.3 MeV
¹⁸⁶ Re physical yield (EOB):	126.9 ± 9.0 mCi (37.4 μCi/μAh ; 81.4 % TTY)
¹⁸⁶ Re chemical recovery (EOB):	118.0 ± 4.1 mCi (93 %, ¹⁸⁶ ReO ₄ ⁻ in 0.1 M HCl)
¹⁸⁶ Re specific activity (ICP-AES, EOB):	21.30 ± 2.41 kCi/g (3.96 ± 0.45 kCi/mmol)
¹⁸⁶ Re specific activity (ICP-MS, EOB):	20.30 ± 1.96 kCi/g (3.78 ± 0.37 kCi/mmol)
Radioisotopic impurities (EOB):	¹⁸⁴ Re (0.04 %), ¹⁸³ Re (0.05 %); ¹⁸⁵ Re (6.4 nmol)
Final ¹⁸⁶ ReO ₄ ⁻ solution stables [ppm; ICP-AES]:	Cr 0.7, Cu 3.8, Fe 0.2, Mo 0.3, Ni 1.0, W 0.27, Zn 4.4; Re 0.24; ICP-MS: ¹⁸⁵ Re 0.26, ¹⁸⁷ Re 0.01



The RCY reported in the Wagner paper was 82.7 ± 4.3 %, while our attempts resulted in RCYs that ranged from 60-80%. Low specific activity ¹⁸⁶Re, produced at MURR via a ¹⁸⁵Re(n, γ)¹⁸⁶Re reaction, typically resulted in somewhat higher yields (70-85%).

¹Fassbender, M., et al. Radiochim Acta vol. 101, no. 5, pp. 339–346, 2013.

²Gott, M, et al. Radiochim Acta vol. 102, no. 4, pp. 325-332, 2014.

³Wagner, T. et al. J. Label. Compd. Radiopharm. 57:441-447, 2014.

⁴Fassbender, M., et al. J. Label. Compd. Radiopharm. 44, Suppl (2001) 657.

Radiochemistry of short-lived positron emitters at Turku PET Centre

Forsback Sarita^{1,2} Kirjavainen Anna¹, Lahdenpohja Salla¹, Helin Semi¹, Bin-Yim Cheng¹, Solin Olof^{1,2}

¹Radiopharmaceutical Chemistry Laboratory, Turku PET Centre, University of Turku, Finland

²Department of Chemistry, University of Turku, Finland

The focus of radiochemistry in Positron emission tomography (PET) is to label various biologically interesting molecules with positron emitting radionuclides such as oxygen-15 (half-life, $T_{1/2}$ = 2.03 min), carbon-11 (C-11, $T_{1/2}$ = 20.4 min), gallium-68 ($T_{1/2}$ = 67.7 min), fluorine-18 (F-18, $T_{1/2}$ = 109.8 min) or copper-64 (Cu-64, $T_{1/2}$ = 12.1 h). The radionuclides are typically produced using a cyclotron. Labelled molecules, radiopharmaceuticals, are used to study biological processes. These include concentration and function of transporters and enzymes or energy metabolism in living subjects. This can be carried out without disturbing these processes. Due to the short half-lives, large amounts of starting radioactivity are needed and the labeling procedures must be as fast as possible. Thus, the synthesis and other manipulations must be automated or at least remote controlled and performed in closed lead shielded cabinets. If the final product is intended for clinical studies, good manufacturing procedures (GMP) must be followed. This means that all the methods and procedures are validated, all equipment qualified and the production takes place in clean rooms with controlled environment.

F-18 is the most used radionuclide in PET, due to its almost favorable chemo-physical properties. The half-life is short enough to avoid a high radiation dose to the patients but long enough for most biological processes. Its maximum endpoint β -energy is amongst the lowest of all radionuclides used in PET, thus the PET images acquired with F-18 labeled molecules can achieve high resolution. In fluorine chemistry, nucleophilic and electrophilic substitution are complementary methods. In radiochemistry, however, nucleophilic substitution is preferred. The production of nucleophilic [¹⁸F] fluoride is more effective than the production of electrophilic [¹⁸F]F₂-gas. [¹⁸F]F₂ is very reactive and F₂ carrier is needed in the production. The use of carrier decreases the specific activity (SA), the amount of radioactivity per molar amount of the molecule, which is one of the most important features of a radiopharmaceutical. We have developed a post-target production method for [¹⁸F]F₂ (Fig. 1) [1].

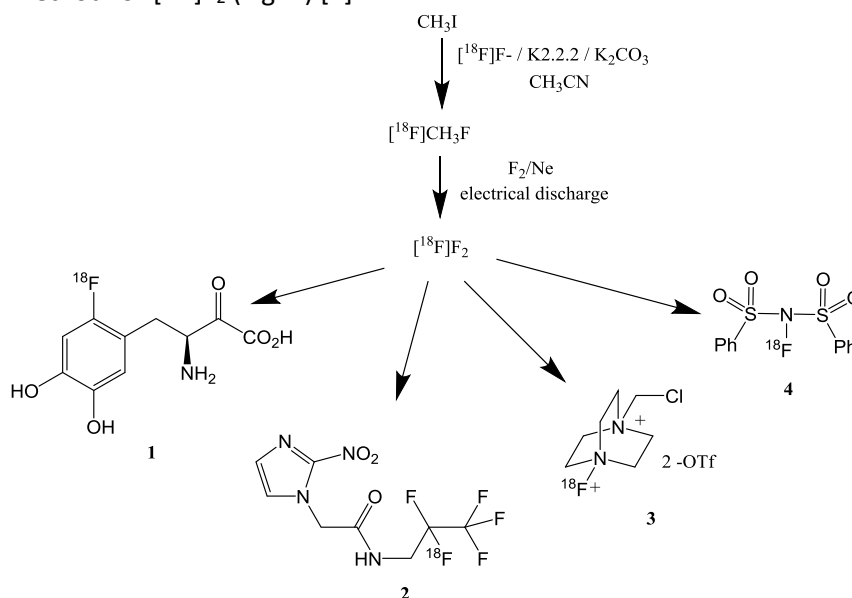


Figure 1. Post-target production and application of [¹⁸F]F₂.

Using this method the SA is significantly higher than with conventional methods, thereby making the electrophilic method a useful option for radiofluorination. This method has been utilized for instance in the production of [¹⁸F]FDOPA by fluorodestannylation (**1**) [2] and [¹⁸F]EF5 by electrophilic addition (**2**) [3] for

clinical studies. We have also, together with prof. Gouverneur from the University of Oxford, developed two new electrophilic labeling reagents, [^{18}F]Selectfluor (**3**) [4] and [^{18}F]NFSi (**4**) [5].

The F-18 half-life provides PET-practitioners with ample time for tracing various *in vivo* processes, whereas the faster decay of ^{11}C -radiotracers enables study protocols using multiple injections for the same patient during the same day. Another important aspect of using C-11 radionuclide arises from carbon being the most common element in biosphere molecules. Carbon is always available for truly isotopic labelling, ensuring that biochemical properties of the labelled compound are not affected. The downsides of abundant environmental carbon are the inevitable isotopic dilution and subsequent lower SA of [^{11}C]radiopharmaceuticals. The majority of [^{11}C]radiopharmaceuticals are synthesized by methylations via the $\text{S}_{\text{N}}2$ reaction mechanism. For this purpose [^{11}C]CH $_4$ is converted into the [^{11}C]CH $_3\text{I}$ electrophile by gas-phase halogenation using either commercial or in-house designed and constructed synthesis devices. The nucleophilic labelling site of the precursor compound is typically a hydroxyl, amine or thiol function.

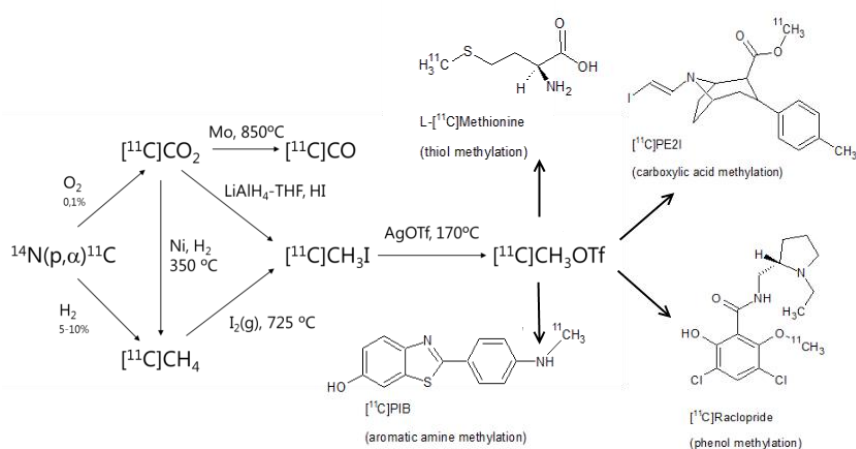


Figure 2. Production pathways for ^{11}C -methylation agents and typical applications.

The nuclear properties of Cu-64 include low positron emission energy, negatron emission and an intermediate half-life. These enable high resolution PET acquisition, monitoring of slower biological processes, distribution of Cu-64 to distant PET facilities without a cyclotron, and offers the potential for both PET and radiotherapy. These interesting properties of Cu-64 have prompted many research groups, as well as the Turku PET Centre, to explore Cu-64-based radiopharmaceuticals.

References: [1]Bergman and Solin Nucl Med Biol 1997; 24:677 [2]Forsback et al J Label Compd Radiopharm 2009; 52:286 [3]Eskola et al Mol Imaging Biol 2012; 14(2): 205; [4]Teare et al Angew Chem Int ed 2010; 49:6821; [5]Teare et al Chem Commun 2007:2330

Metal-implanted mesoporous silicon nanoparticles as a novel drug carrier for radiation theranostics

U. Jakobsson¹, A. Airaksinen¹, A. Etile¹, J. Ikonen¹, E. Mäkilä², J. Salonen² and K. Helariutta¹

¹*Laboratory of Radiochemistry, Department of Chemistry, FI-00014, University of Helsinki*

²*Laboratory of Industrial Physics, Department of Physics and Astronomy, FI-20014, University of Turku*
ulrika.jakobsson@helsinki.fi

The study of porous nanoparticles as drug carriers is a growing field in cancer-therapy research. The porous properties of the particle enable the anti-cancer drugs to be loaded inside the particles and the surface of the particle can be modified with targeting moieties. The nanoparticles are then injected into the bloodstream and with the penetrative capabilities of the nanoparticle the carried drugs can be targeted precisely to the tumour. This enables a high treatment efficiency together with a low strain on the surrounding tissue. Furthermore, as multiple drugs can be simultaneously loaded into the nanoparticle, a lower amount of pharmaceuticals could be needed.

Our project uses mesoporous silicon nanoparticles (PSi) which are biodegradable, and thus suitable for use in a living body [1]. As the PSi particles are loaded with drugs for cancer treatment, they can also be loaded with radioactive nuclides. These nuclides can be used for tracing the migration of the particles inside the living body using nuclear imaging such as PET or SPECT tomography. This allows the control of the proper targeting of the drug during the treatment. On the other hand, the radionuclides themselves can also be used for tumour treatment. As the PSi particles reach the tumour cells, the radioactivity of the nuclide can provide radiation treatment on a very local level. The nuclide implanted into the PSi particle can be chosen so that its specific radiative properties allow for both imaging and therapy at the same time [2].

To load the radioactivity in the PSi particle, the silicon is implanted with stable metallic ions. The metallic nuclei are then activated through a neutron flux at a nuclear reactor or alternatively through an accelerator-produced proton beam. A novel technique that we employ is the direct implantation of the metallic radionuclides into a silicon wafer that is then processed into nanoparticles. The radionuclides are provided by a radioactive ion beam at the HIE-ISOLDE facility located at CERN, and the post-processing of the active nanoparticles takes place at the Department of Chemistry, University of Helsinki. In-vivo stability tests are then performed on tumour xenografts in mice with in-vitro stability tests in bio-compatible buffer solutions.

In this contribution we want to give an overview of the project and present preliminary results from our recent activities.

References

- [1] H. Santos et al., *Nanomedicine* 9, 535 (2014)
- [2] Emerging isotopes, https://www-nds.iaea.org/radionuclides/list_emerg_nuclides.htm, date 13.04.2016

Efficient method for locating nanoparticles with pretargeted PET imaging

Outi Keinänen,¹ Ermei Mäkilä,² Rici Lindgren,² Helena Virtanen,³ Heidi Liljenbäck,^{3,4} Mirkka Sarparanta,^{1,5} Carla Molthoff,⁶ Albert D. Windhorst,⁶ Anne Roivainen,^{3,4} Jarno Salonen,² Anu J. Airaksinen¹

¹Laboratory of Radiochemistry, Department of Chemistry, University of Helsinki, Finland; ²Department of Physics and Astronomy, University of Turku, Finland; ³Turku PET Centre, University of Turku, Turku, Finland; ⁴Turku Center for Disease Modeling, University of Turku, Turku, Finland; ⁵Department of Radiology, Memorial Sloan Kettering Cancer Center, New York, New York, USA; ⁶Department of Radiology and Nuclear Medicine, VU University Medical Center, Amsterdam, The Netherlands

Introduction: Traditionally, targeting moieties with slow pharmacokinetics, like nanoparticles (NP) and antibodies (Ab), are radiolabeled with isotopes with half-lives ranging from several hours to days in order to image their biodistribution and target site accumulation. Pretargeted methodology allows the use of short-lived radioisotopes like fluorine-18 ($T_{1/2}=109.8$ min) to locate these targeting moieties. It is based on first administering the targeting moiety (NP or Ab), and when most of the moiety has reached its target tissue and the unbound fraction has cleared from the body, the radiotracer is given. The use of short-lived radioisotopes greatly reduces the radiation burden of the subject compared to longer-living isotopes applied in non-pretargeting approaches. Bioorthogonal reactions are highly suited for pretargeting since they occur inside living biological system without interfering with or being interfered by any of the system's native biochemical processes and have been proven to be efficient in pretargeting Positron Emission Tomography (PET) imaging.¹ The fastest known bioorthogonal reaction is inverse electron-demand Diels-Alder cycloaddition (IEDDA) between a tetrazine (Tz) and *trans*-cyclooctene (TCO). We have developed a promising fluorine-18 labeled tetrazine (5-¹⁸F]fluoro-5-deoxy-ribose-tetrazine, [¹⁸F]TAF) for pretargeted PET imaging.² Here, we have explored the sensitivity of [¹⁸F]TAF to locate predosed mesoporous silicon nanoparticles (NPs) using non-targeted NPs in healthy mice as a model for these investigations.

Methods: NPs were functionalized with TCO groups (7.1 nmol TCO/mg NPs). TCO-NPs (0.2 mg in 5.4% glucose) were administered intravenously at 15 min prior to the i.v. administration of [¹⁸F]TAF (6.2±2.5 MBq in 0.9% NaCl) in healthy male BALB/c mice (Fig. 1 A). The control animals received only [¹⁸F]TAF (3.4±1.4 MBq in 0.9% NaCl). *Ex vivo* biodistribution was studied at four time points (15, 30, 60, and 120 minutes) after injection of [¹⁸F]TAF. PET imaging with Mediso nanoScan® PET-CT was performed with TCO-NPs until 60 min (n=3). PET imaging with Inveon Multimodality PET/CT was performed with TCO-NPs until 120 min (n=2).

Results: The *in vivo* IEDDA reaction between [¹⁸F]TAF and TCO-NPs was fast and occurred within the first 10 minutes. *Ex vivo* biodistribution results are presented in Fig. 1 B. [¹⁸F]TAF was able to trace the NPs in spleen, liver and lungs. Highest target-to-background-ratio was achieved at 120 min after the tracer injection. A summed PET/CT image (110-120 min) is represented in Fig. 1 C. The *in vivo* reaction yield was approx. 25% as determined in spleen.

Conclusions: [¹⁸F]TAF was used successfully for tracing TCO-functionalized NPs *in vivo*. The *in vivo* IEDDA reaction rate was sufficient for pretargeted PET imaging in tracer conditions. Our study suggests that pretargeted imaging has excellent potential in nanotheranostic PET imaging.

Acknowledgements: Supported by the Academy of Finland (272908, 278056), and CHEMS Doctoral Program

References:

1. Knight J et al. *Am J Nucl Med Mol Imaging*, 2014; 4:96-113
2. Keinänen O et al. *ACS Med Chem Lett.* 2016; 7:62-66

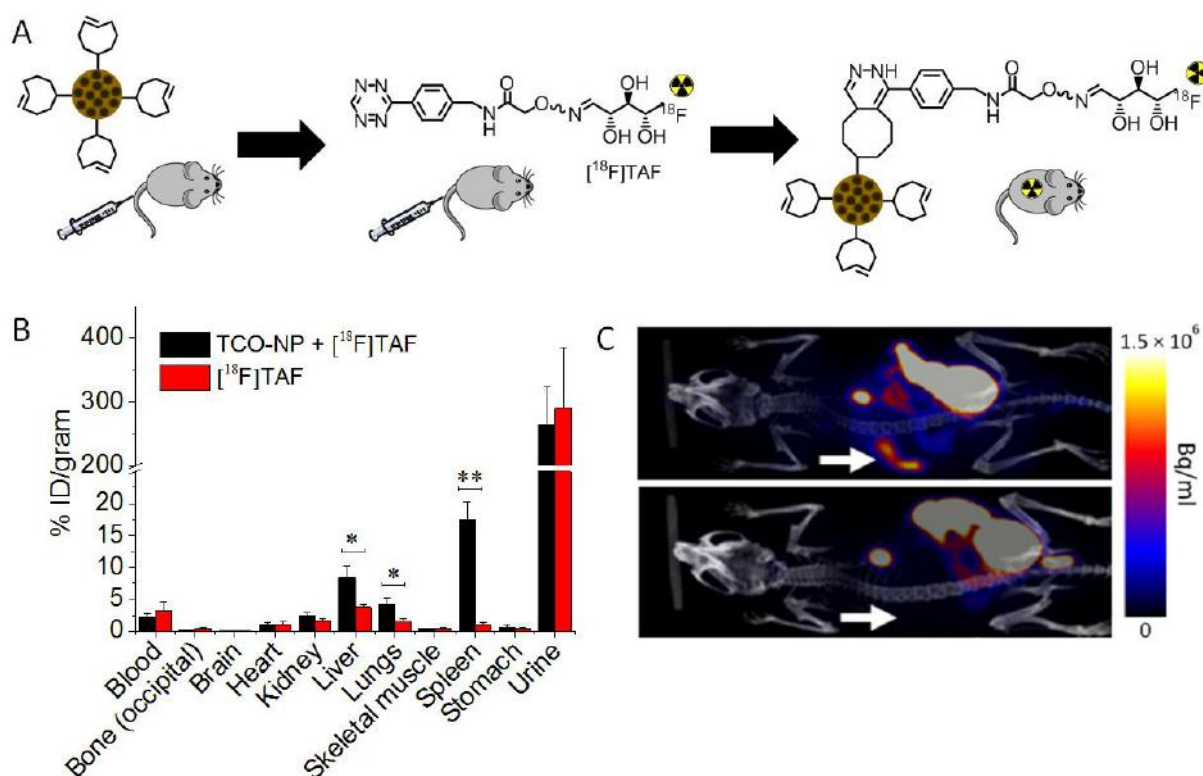


Figure 1. (A) Description of the pretargeted methodology for locating the TCO-NPs in healthy mice by using [¹⁸F]TAF. (B) *Ex vivo* biodistribution of radioactivity after i.v. injection of pretargeted TCO-NPs (black), and [¹⁸F]TAF (red) 60 min after the injection of [¹⁸F]TAF in male 12-week old BALB/c mice. Values represent mean \pm s.d. (n=3). [¹⁸F]TAF was able to trace the NPs in spleen, liver and lungs, based on *in vivo* IEDDA ligation. *p < 0.05 **p < 0.001 (C) Representative summed (110-120 min) PET/CT images. Up: TCO-NPs administered 15 min prior [¹⁸F]TAF. Down: Control, only [¹⁸F]TAF was injected. The arrow indicates location of the spleen.

Fully automated synthesis of [^{18}F]FTHA

Kirjavainen Anna¹, Nina Sarja¹, Olof Solin^{1,2}

¹Radiopharmaceutical Chemistry Laboratory, Turku PET Centre, University of Turku, Finland

²Department of Chemistry, University of Turku, Finland

Aim

14(*R,S*)-[^{18}F]Fluoro-6-thia-heptadecanoic acid ([^{18}F]FTHA) is a fatty acid tracer that has been produced in our laboratory for several years (Fig 1). A growing need for this tracer at our centre brought on the transfer of the [^{18}F]FTHA synthesis to our new GMP facilities. We then developed a fully automated synthesis device suitable for multistep radiotracer synthesis. All production processes and quality control (QC) procedures were validated to be in compliance with GMP.

Materials and Methods

A fully automated in-house built synthesis device is used in the production of [^{18}F]FTHA. This device is combined with an automatic sterile filtration unit. Both are situated in a hot cell placed in a validated clean room and they are controlled from a touch screen (Fig 1). No user intervention is needed during the synthesis. The product fraction eluting from the HPLC was collected automatically, based on radioactivity response from a detector at the outlet of the HPLC column. The solvent exchange of the final product was performed with an automated solid phase extraction (SPE) procedure, using a tC18 cartridge. The product was formulated in a phosphate-ethanol-ascorbic acid solution, instead of the human serum albumin used earlier, as this had caused false positives in sterility analyses. The optimised process was validated in three consecutive runs. All analytical methods were validated prior to the process validation.

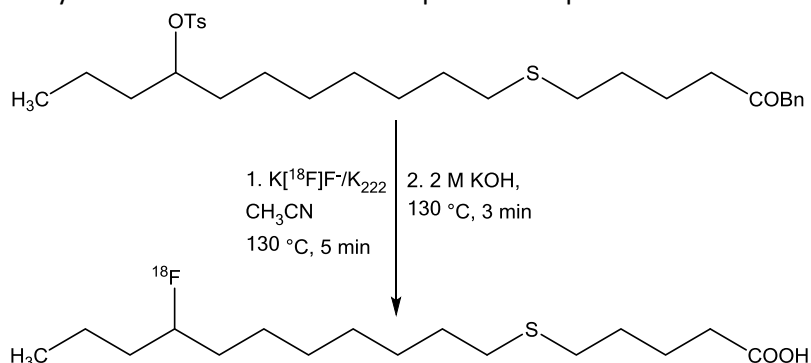


Figure 1. Synthesis route of [^{18}F]FTHA.

Results

The synthesis was done with a modified method from that previously reported [1]. The labelling synthesis was carried out at higher temperature and using a shorter reaction time. The radiochemical yield calculated from initial ^{18}F -fluoride was 12 ± 4 %. The shelf-life of the product was determined as 4 hours. The radiochemical purity of the formulated final product was >95 %. The specific activity was in the order of 1 TBq/ μmol . The amounts of residual solvents were low. The only significant radioactive impurity was identified as [^{18}F]FTHA sulfoxide.

Conclusion

We have developed the [^{18}F]FTHA synthesis according to GMP guidelines. The synthesis is repeatable and we have ample yield for routine clinical production.

Reference

[1] DeGrado T. (1991) J. Labelled Compd. Radiopharm. 29:989-995.

⁹⁰Y microspheres prepared by sol-gel method, promising material for medical application

Marcin Konior¹, Edward Iller¹, Wiesława Łada², Danuta Wawszczak²

¹ *National Centre for Nuclear Research , Radioisotope Centre POLATOM
05-400 Otwock, Andrzej Sołtan 7, Poland*

² *Institute of Nuclear Chemistry and Technology , 03-195 Warsaw, Dorodna 16, Poland*

Selective internal radiation therapy (SIRT) with ⁹⁰Y microspheres into the hepatic artery is a novel method for palliative treatment of primary and metastatic liver cancer. A new technology for the production of radiopharmaceutical ⁹⁰Y microspheres in the form of spherical yttrium oxide particles obtained by sol-gel method has been described. The authors present and discuss the results of investigations performed in the development of new method of production of yttrium microspheres and determination their physic-chemical properties. In accordance with nuclear reaction ⁸⁹Y(n, γ)⁹⁰Y, irradiation of the yttrium oxide microspheres fraction of grains with diameters of 20-50 μm in the thermal neutron flux of 1.7x10¹⁴ cm⁻²s⁻¹ at core of research nuclear reactor MARIA allowed to obtain microspheres labelled with isotope ⁹⁰Y. For every million decays β⁻ occurring in the isotope Y-90, 32 nuclear transformations occur in the form of internal creation of electron-positron pairs, which following the process of annihilation gives rise to two gamma quanta with an energy of 511 keV, which are used in medical diagnosis using PET tomography. The absolute triple to double coincidence method has been adopted for the determination of specific activity of irradiated microspheres. ⁹⁰Y microspheres prepared by proposed technique can be estimated as promising medical material for SIRT.

Utilization of VUV-photons for synthesis of high specific activity [^{18}F]F $_2$ gas

Krzyszmonik Anna¹, Keller Thomas¹, Kirjavainen Anna¹, Forsback Sarita¹, Solin Olof^{1,2,3}

1. Radiopharmaceutical Chemistry Laboratory, Turku PET Centre, University of Turku, Finland

2. Department of Chemistry, University of Turku, Finland

3. Accelerator Laboratory, Turku PET Centre, Åbo Akademi University, Finland

Introduction

Electrophilic fluorination is a fast and effective method for the synthesis of tracers for positron emission tomography (PET). [^{18}F]F $_2$ gas can be used directly for radiosynthesis or it can easily be converted into one of its more selective derivatives such as [^{18}F]Selectfluor or [^{18}F]NFSi [1,2]. [^{18}F]F $_2$ can be produced by cyclotron bombardment of gas targets: $^{20}\text{Ne}(\text{d},\alpha)^{18}\text{F}$ and $^{18}\text{O}(\text{p},\text{n})^{18}\text{F}$ [3,4]. Since both of these traditional production methods require addition of carrier F $_2$ gas, the biggest disadvantage is the low specific activity (SA) of the resulting [^{18}F]F $_2$ (0.1 and 1.3 GBq/ μmol respectively).

[^{18}F]F $_2$ can be also produced post-target from [^{18}F]MeF by using a high voltage discharge to promote the $^{19}\text{F}/^{18}\text{F}$ isotope exchange reaction [5]. This method allows for a higher SA of 55 GBq/ μmol to be obtained. However it suffers from the drawback that a portion of the fluorine gas is consumed by the discharge electrodes.

Herein we report a modification to this procedure, the replacement of excitation by a high voltage discharge with excitation by a laser beam of vacuum ultraviolet (VUV) photons.

Materials and methods

[^{18}F]MeF was produced from MeI and dry [^{18}F]KF/K $_{222}$ complex, purified by gas chromatography and transferred to the illumination chamber. 0.1-1.8 μmol of carrier F $_2$ gas (0.5% F $_2$ in Ne) was added to chamber and illuminated with 193 nm photons (ArF excimer laser). The resulting [^{18}F]F $_2$ gas was used for synthesis of [^{18}F]NFSi which could be analysed by radioHPLC.

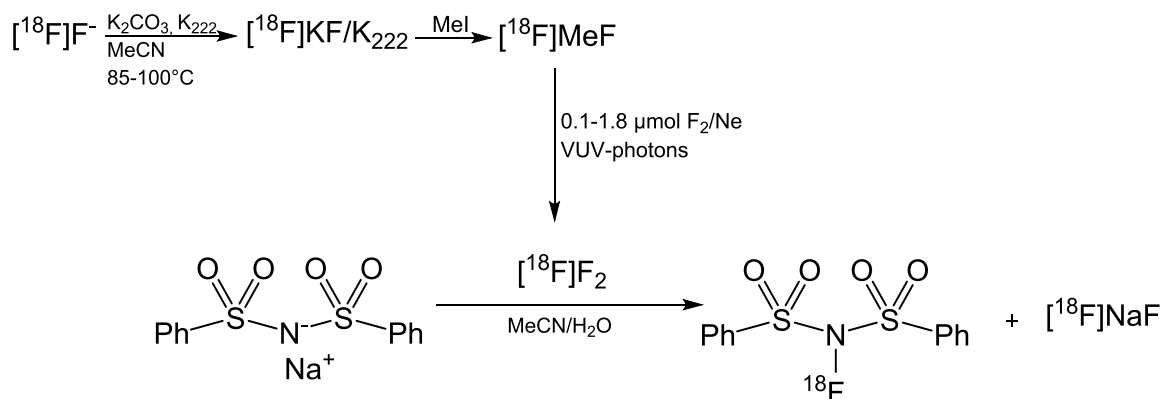


Figure 1. Production of [^{18}F]F $_2$ gas and labelling of [^{18}F]NFSi

Results and discussion

[^{18}F]F $_2$ gas was successfully produced by using laser illumination. Reactions were carried out with low initial activities (2-4 GBq) to optimize the amount of carrier F $_2$ gas used and the number of laser pulses, with regard to yield and SA.

The SA obtained with the initial conditions was 1.2 ± 0.6 GBq/ μmol and the [^{18}F]NFSi radiochemical yield was 13 ± 6 % (incorporation yield calculated from the radioHPLC chromatogram). Experiments are now underway

to test the optimal conditions with a high [^{18}F]fluoride starting activity with the intention of achieving high SA.

Conclusion

First studies demonstrated that presented method can be used for production [^{18}F]F₂ gas for electrophilic labelling.

Acknowledgement

Funding was received from the European Union's 7th Framework Programme for Research, grant number 316882 and from the Academy of Finland, grant number 266891.

References

[1] Teare H. et al. *Angew Chem*, **2010**, 49, 6821 [2] Teare H. et al. *Chem. Commun.*, **2007**, 23, 2330 [3] Blessing G. et al. *Appl. Radiat. Isot.*, **1986**, 37, 1135 [4] Hess E. et al. *Appl. Radiat. Isot.*, **2000**, 52, 1431 [5] Bergman J., Solin O. *Nucl. Med. Biol.*, **1997**, 24, 677

The use of [^{18}F]selectfluor bis(triflate) in electrophilic fluorination

Lahdenpohja Salla¹, Kirjavainen Anna¹, Forsback Sarita¹, Solin Olof^{1,2}

¹Radiopharmaceutical Chemistry Laboratory, Turku PET Centre, University of Turku, Finland

²Department of Chemistry, University of Turku, Finland

Aim Various aryl molecules can be labelled with reasonable reaction times and reaction conditions only by electrophilic ^{18}F -fluorination. In electrophilic ^{18}F -labelling with [^{18}F]F₂-gas the major problems are low specific activity (SA) of the final product and also formation of numerous by-products. Less reactive labelling reagents have been developed in order to control the reactions. One novel “mild” ^{18}F -labelling reagent is [^{18}F]Selectfluor bis(triflate). It has been successfully used in synthesis of several radiotracers.

Materials and Methods [^{18}F]Selectfluor bis(triflate) was produced from [^{18}F]F₂ [1], which was produced from [^{18}F]F⁻ [2] (Fig 1). [^{18}F]Selectfluor bis(triflate) was used directly in subsequent labelling reactions (Fig 2) without purification. 6-[^{18}F]FDOPA, [^{18}F]NS12137 and [^{18}F]6-fluoro-marsanidine were produced by fluorodestannylation of suitable stannylated precursors [3-5]. [^{18}F]Selectfluor bis(triflate) was used in fluorodesilylation reactions to produce ^{18}F -labelled ketones and allylic fluorides [1]. ^{18}F -labelled tri- and difluoromethylarenes were produced by fluorodecarboxylation using [^{18}F]Selectfluor bis(triflate) [6]. After labelling reactions with [^{18}F]Selectfluor bis(triflate) protecting groups were removed if needed and the obtained radiotracers were purified by HPLC. The reaction time to produce [^{18}F]Selectfluor bis(triflate) from [^{18}F]F⁻ was ~30 minutes. Subsequent labelling reactions with [^{18}F]Selectfluor bis(triflate) were 15 – 30 minutes and deprotection reactions were fast, ~5 minutes.

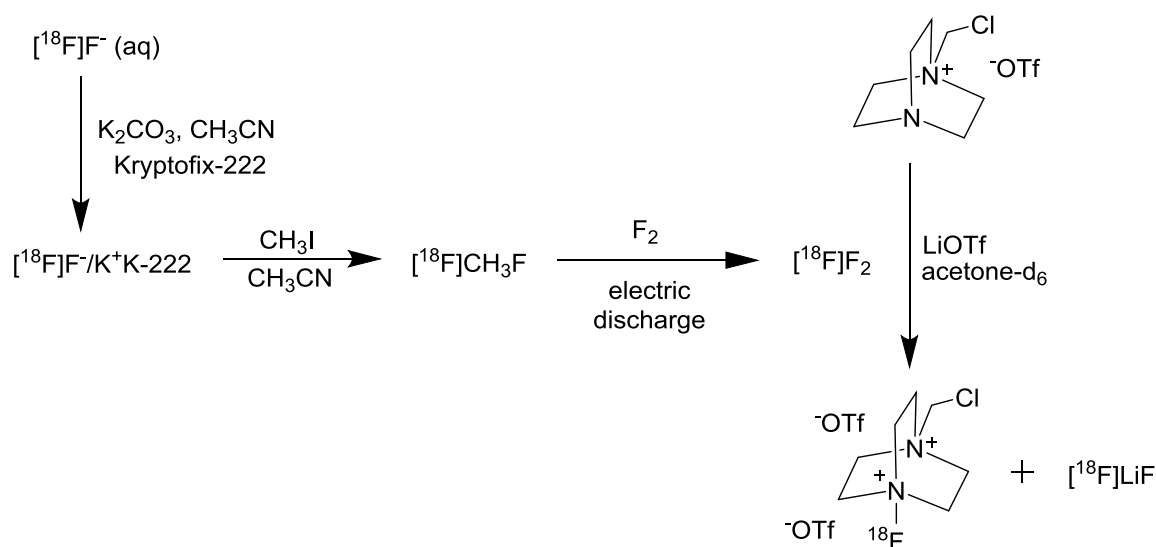


Figure 9. Production of [^{18}F]Selectfluor bis(triflate) starting from [^{18}F]F⁻.

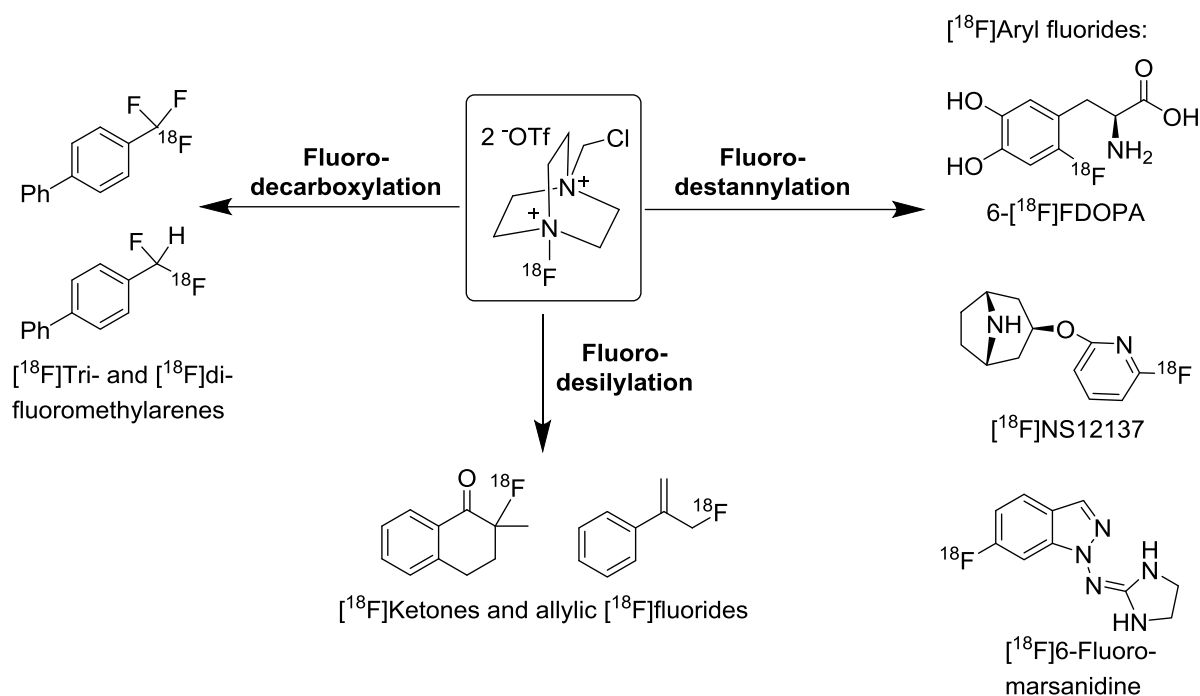


Figure 10. ^{18}F -labelling reactions and products with ^{18}F Selectfluor bis(triflate)

Results ^{18}F Aryl fluorides were obtained with >95 % radiochemical purity, radiochemical yields varied from 2 to 20 % and SAs were 1 - 6 GBq/ μmol [1,3-5]. In addition, the quality of 6- ^{18}F FDOPA produced from ^{18}F Selectfluor bis(triflate) is comparable to the one produced from $^{18}\text{F}\text{F}_2$ for clinical use. ^{18}F -labelled ketones and allylic fluorides were obtained with approximately 15 % radiochemical yields [1]. ^{18}F -labelled tri- and difluoromethylarenes were obtained with radiochemical yields up to 18 % and SAs up to 2,5 GBq/ μmol [6].

Conclusions ^{18}F Selectfluor bis(triflate) is very promising labelling reagent in electrophilic ^{18}F -fluorination. It is a milder reagent than $^{18}\text{F}\text{F}_2$. It can be used to label almost all the same molecules as $^{18}\text{F}\text{F}_2$ without high amount of by-products. With ^{18}F Selectfluor bis(triflate) it is possible to label tracers which could not be labelled selectively with $^{18}\text{F}\text{F}_2$, like ^{18}F -labelled tri- and difluoromethylarenes. Additionally ^{18}F Selectfluor bis(triflate) is easy to handle and storable within the limits of the fluorine-18's half-life. There is ongoing work in our laboratory to explore further ^{18}F Selectfluor bis(triflate) and its applicability in the preparation of clinically useful radiotracers.

Acknowledgments This work was supported by the Academy of Finland (grant no. 266891).

References [1] Teare H. *et al.* (2010) *Angew. Chem. Int. Ed.* 49:6821-6824 [2] Bergman J, Solin O. (1997) *Nucl. Med. Biol.* 24:677-833 [3] Stenhagen I. *et al.* (2013) *Chem. Commun.* 49:1386-1388 [4] Kirjavainen A. (2014) Thesis, University of Turku [5] Krzyczmonik A. *et al.* (2015) *J. Label. Compd. Radiopharm.* 58:S208 [6] Mizuta *et al.* (2013) *Org. Lett.* 15:2648-2651.

Complex of europium with azacrown-ether: stability in aqueous solutions and fetal bovine serum

E.V. Matazova¹, B.V. Egorova¹, M.S. Oshchepkov², A.D. Zubenko², Yu.V. Fedorov², O.A. Fedorova^{1,2}, S.N. Kalmykov^{1,3}

¹*Lomonosov Moscow state university, Moscow, Russia,*

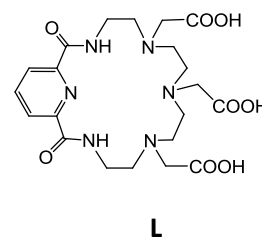
²*A.N. Nesmeyanov Institute of Organoelement Compounds of Russian Academy of Sciences, Moscow, Russia*

³*NRC "Kurchatov Institute", Moscow, Russia*

bayirta.egorova@gmail.com

Bioconjugates composed of radionuclide with peptide bound by linker-chelator are actively developed systems for target delivery of diagnostic or therapeutic emission to cancer cells in nuclear medicine. As chelators polyaminopolycarboxylates are the mostly used and studied class. Among them macrocyclic H₄DOTA and acyclic H₅DTPA have already found their application in radiopharmaceuticals with such radionuclides like Y-90 and Lu-177. However complexes with acyclic DTPA derivatives are not stable in vivo and kinetics of cations binding by H₄DOTA at room temperature is comparable with half-lives of some radionuclides (e.g. Bi-213). Therefore the search for new ligands with fast complexation kinetics and high stability remains an important task. Present work considers complexation of Eu³⁺ as representative of rare earth elements (REE) cations by pyridine containing azacrown-ether.

The fast rate of Eu³⁺ complexation by L was demonstrated by competitive spectrophotometry with Arsenazo III: complex forms during first minute similar to DTPA and by 2 orders faster than with DOTA at the same conditions. Constants of ligand's protonation and complexation with Eu³⁺ were determined by potentiometric titration with consequent data treatment in Hyperquad and by competitive sorption on SiO₂. The values calculated by different methods are in line with each other and equal to $\log K(\text{EuL})=8.2\pm0.2$, $\log K(\text{EuLOH}^-)=2.3\pm0.1$, $\log K(\text{EuL}(\text{OH}^-)_2)=-5.9\pm0.1$, $\log K(\text{EuL}(\text{OH}^-)_3)=-16.9\pm0.1$ in 0.1M NaClO₄.



For evaluation of stability of complex EuL in different media thin layer chromatography on SiO₂ plates was used. Eluents with varied composition were tested for complex with azacrown ligand L (table), Eu-152 was used as tracer. For estimation of behavior of cation bound by serum peptides we used Eu-DOTATATE complex as a reference. All resulting TLC plates were counted on autoradiographic system and associated software (Cyclone, Perkin Elmer).

Table. Retention factors for europium species with using of different eluents in TLC.

Eluent	0.1M (H,Na) ₃ cit pH5.2	CH ₃ CN(CH ₃ OH):H ₂ O: NH ₄ OH (1:1:2)	Py:H ₂ O:C ₂ H ₅ OH (1:4:2)	CH ₃ OH:10% NaOAc (1:1)
Eu-DOTATATE	R _f = 0-0.2	R _f = 1.0	R _f = 0.5-0.6	R _f = 0.5
Eu-L	R _f = 0.6-0.9	R _f = 0-0.4	R _f = 0.7-1.0	R _f = 0.6-1.0
Eu ³⁺	R _f = 0.6-0.9	R _f = 0	R _f = 0	R _f = 0

According to the obtained results for fetal bovine serum experiments 0.1M (H,Na)₃cit was used since it provides better separation of Eu-L and Eu bound with high molecular weight compounds like DOTATATE and serum proteins. For study of stability in physiological solution Py:H₂O:C₂H₅OH (1:4:2) was selected as optimal with better separation of spots of Eu³⁺ and Eu-L and fast and flat eluent development. By these techniques stability of EuL during 3 days in physiological solution and serum was shown.

Since the constant of EuL complex formation is not high enough for complete labeling separation from unbound cation is required. In this work we carried out this separation by HPLC on C₁₈ column in gradient

mode using H₂O and CH₃OH as eluents. In this regime free Eu³⁺ elutes during first minute when flow is H₂O/CH₃OH=0.9/0.1 and consequent monotonous increase of CH₃OH part in the flow extracts Eu-L on 6-8 minutes upon H₂O/CH₃OH=0.4/0.6-0.6/0.4. Eu³⁺ in fractions was measured by gamma spectrometry of Eu-152 and ligand was detected by UV-vis absorption spectroscopy at wavelengths 226 and 275 nm.

This work was supported by RFBR project 16-33-00642.

Synthesis of ^{177}Lu DOTATATE in a microchannel

Elisabeth Oehlke

*Radiation Science and Technology, Delft University of Technology, Mekelweg 15, JB Delft, The Netherlands
e.oehlke@tudelft.nl*

Syntheses of radiopharmaceuticals (mostly ^{18}F and ^{11}C , but also ^{68}Ga , ^{64}Cu and ^{89}Zr) on microfluidic chips have shown that reactions done in microchannels can offer improvement to the usual batch syntheses [1-3]. For instance, the use of microfluidics can result in better reaction control, higher yields, and shorter reaction times. However, one drawback is the fact that most of the reported microsystems are based on microchips, which require special manufacturing. Herein, the synthesis of ^{177}Lu DOTATATE in capillary tubing is reported, which is readily available from common lab-suppliers. The batch synthesis of ^{177}Lu DOTATATE has been studied extensively before [4], which simplifies comparison to the new synthesis method. The experimental set-up consisted of two 1 mL syringes that were connected with capillary tubing to a static mixing tee. A third capillary was connected to the mixing tee, and used as reaction channel. The two syringes were controlled with syringe pumps using flowrates between 3 and 150 $\mu\text{L}/\text{min}$. Two reaction solutions were used: $^{177}\text{LuCl}_3$ solution (0.14mM, $A_s = \sim 16\text{GBq/g}$) and a DOTATATE kit (0.28mM) obtained from ErasmusMC (120 μg [$\text{DOTA}^0, \text{Tyr}^3$]octreotate, 37.8 mg sodium ascorbate and 7.5 mg gentisic acid per 300 μL 0.05 M HCl). The solutions were used in a ratio 1:2, respectively, giving a final pH of ~ 4 . The radiochemical yield was determined by TLC (acetonitrile/water 1:1) [5].

The obtained radiochemical yield showed a clear dependence on the residence time in the microchannel and only slight variation for different capillary diameters. Reactions at 80°C were done within 2 min, which is significantly faster than those done with conventional methods where reaction times of over 10 min have been reported [4]. At ErasmusMC, clinical preparations of ^{177}Lu DOTATATE are currently heated for 30 min using the same conditions as this study. Reactions done in a microchannel at different temperatures showed that the synthesis of ^{177}Lu DOTATATE is highly temperature dependent. By fitting the measured data to the rate equation for second order reactions, it was possible to determine kinetic association constants, e.g. $2.4 \text{ M}^{-1}\text{s}^{-1}$ for 54°C , and $76.1 \text{ M}^{-1}\text{s}^{-1}$ for 80°C . Since the temperature dependence of the obtained association constants follows the Arrhenius equation, the activation energy of the reaction ($E_A = 128 \text{ kJ/mol}$) and kinetic association constants for other temperatures could be estimated. Calculated residence times based on these constants show that radiolabelling at low temperatures ($<50^\circ\text{C}$) is not feasible, for instance 13 hours are needed at 37°C to achieve 98% radiochemical yield.

In conclusion, the synthesis of ^{177}Lu DOTATATE can be done at higher temperatures significantly faster in capillaries than under conventional conditions. The current setup allows for fast screening of reaction conditions using minimal amounts of reactants (5-10 μL reaction volume) and offers high reproducibility (uncertainties of 1-2%).

- [1] G. Pascali et al., Nucl. Med. Biol. 2013, 40, 776.
- [2] D. Zeng et al., Nucl Med. Biol. 2013, 40, 42.
- [3] B.D. Wright et al., J. Nucl. Med. 2016, doi: 10.2967/jnumed.115.166140.
- [4] W.A.P. Breeman et al., Eur. J. Nucl. Med. Mol. Imaging, 2003, 30, 6, 917.
- [5] T. Das et al., Appl. Rad. Isot. 2007, 65, 301.

Acknowledgement: I would like to thank Wouter Breeman and Erik de Blois from ErasmusMC for their support and the supply of DOTATATE kits.

Evaluation of ¹¹¹In-labelled peptide functionalized silicon nanoparticles in a rat model of myocardial infarction

Sanjeev Ranjan^{1,2,*}, Mónica P.A. Ferreira¹, Sini M. Kinnunen¹, Vimalkumar Balasubramanian¹, Brianda Barrios-Lopez², Alexandra M. Correia¹, Ermei Mäkilä⁴, Virpi Talman¹, Jarno Salonen³, Jouni T. Hirvonen¹, Heikki J. Ruskoaho¹, Hélder A. Santos¹, Anu J. Airaksinen²

¹*Division of Pharmaceutical Chemistry and Technology, University of Helsinki, Helsinki, Finland*

²*Laboratory of Radiochemistry, University of Helsinki, Helsinki, Finland*

³*Division of Pharmacology and Pharmacotherapy, University of Helsinki, Helsinki, Finland*

⁴*Laboratory of Industrial Physics, University of Turku, Turku, Finland*

**sanjeev.ranjan@helsinki.fi*

Porous silicon nanoparticles (PSiNP) are promising carriers for targeted drug delivery. Various targeting ligands have been conjugated to these nanoparticles (NPs), resulting to successful *in vitro* cell targeting. However, limited progress has been achieved so far in extending such success into *in vivo* setting in animal models, and the knowledge on their biodistribution is still very limited. The present study aims to investigate the behaviour of several heart-targeted PSiNP *in vivo* and to compare their targetability, biodistribution and pharmacokinetics. The PSiNP were modified with PEG for improving their stealth properties and DOTA for radiolabeling, and further conjugated with heart targeting peptides (Pep-1-4). As controls, PSiNP without any targeting peptides and PSiNP with scrambled sequence were used.

Functionalized PSiNPs were radiolabeled with ¹¹¹In with yield above 70%, and their stabilities were studied in buffers covering a physiologically relevant pH range 2.3 to 8.7, and in 50% human plasma up to 4 h. Isoprenaline injected myocardial infarction model male Wistar rats were intravenously administrated with [¹¹¹In]PSiNPs in order to study the success of their targetability towards the heart tissue, monitored by SPECT/CT imaging, *ex vivo* biodistribution studies and autoradiography.

All tested peptide-modified PSiNPs improved their accumulation in the heart, up to 4.5% of the injected dose (%ID) as quantified by SPECT/CT images (**Fig. 1**). The particles had the highest accumulation at 10 min. The *ex vivo* biodistribution studies revealed that at 4 h, the [¹¹¹In]PSiNP were mainly accumulated in liver and spleen. Further, autoradiographic quantification of heart cryosections was done for Pep-1 modified SiNPs, which exhibited the highest heart accumulation based on the SPECT image quantification. The autoradiographic analysis was performed in order to investigate a regional differences on the NP accumulation within the myocardium. Autoradiographic quantification of myocardium shows that the ratio of activity between endocardium and epicardium (Endo/Epi) is significantly higher compared to control NPs without any targeting peptide and to pure radionuclide Indium chloride solution (InCl₃) (**Fig. 1**).

Functionalized PSiNP were successfully labelled with ¹¹¹In for *in vivo* studies. Peptide modified [¹¹¹In]PSiNP get markedly enhanced accumulation into the heart with differential selectivity between endocardium and epicardium.

Financial support from the Academy of Finland, TEKES 3iRegeneration project (40395/13), University of Helsinki Research Funds, Academy of Finland, and European Research Council are gratefully acknowledged. M.P.A. Ferreira acknowledges the Drug Research Doctoral Programme of the Faculty of Pharmacy, University of Helsinki, for a PhD grant.

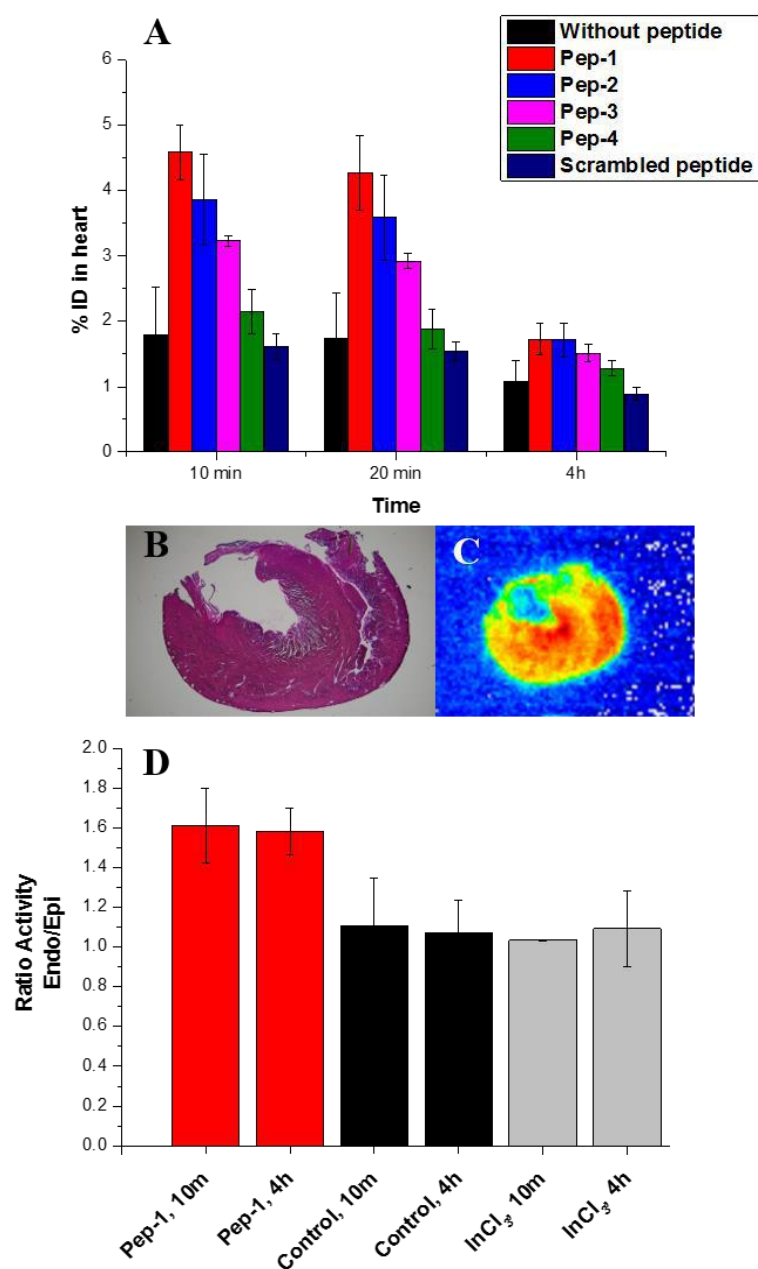


Figure 1: SPECT/CT image quantification of the heart showing the biodistribution of the intravenously administered Porous silicon nanoparticles radiolabeled with ^{111}In (^{111}In]PSiNP) and modified with different heart targeting peptides at 10 min, 20 min, and 4h time points. All tested peptide-modified PSiNPs improved their accumulation in the heart and up to 4.5% of the injected dose (%ID) for Pep-1 modified PSiNP. Values represent mean \pm s.d., $n = 4/5$ (A). Hematoxylin and eosin staining (B) and autoradiography (C) of rat heart. Autoradiographic quantification of heart muscle to show the difference of NPs distribution between endocardium and epicardium at 10 m and 4 h (D). For Pep-1 modified PSiNP the ratio of activity between endocardium and epicardium (Endo/Epi) is significantly higher compared with controls, NPs without any targeting peptide and pure radionuclide (^{111}In) indium chloride solution injected to rat tail vein.

Production and separation of platinum-191 and astatine-211 and their medical applications

A. Kanda¹, A. Toyoshima^{1,2}, Y. Hayashi¹, N. Takahashi¹, Y. Manabe¹, A. Shimoyama¹, K. Kabayama¹, K. Ogawa³, H. Ikeda⁴, S. Watanabe⁴, E. Shimosegawa⁴, T. Kamiya⁴, G. Horitsugi⁴, A. Odani³, T. Yoshimura⁵, K. Fukase¹, J. Hatazawa⁴ and A. Shinohara¹

¹Graduate School of Science, Osaka University, Japan; ²Advanced Science Research Center, Japan Atomic Energy Agency, Tokai, Japan; ³School of Pharmacy, Kanazawa University, Japan; ⁴Graduate School of Medicine, Osaka University, Japan; ⁵Radioisotope Research Center, Osaka University, Japan

[Introduction]

In recent decades, medical research of therapy, diagnosis, and drug development using various radioisotopes has been vigorously conducted. For the development of radiopharmaceuticals, each step of radioisotope production with an accelerator, chemical purification of the produced radioisotopes, their labeling, and clinical trials with prepared radiopharmaceuticals is mandated to be investigated. At Osaka University, we have been investigating these steps in the collaboration among Research Center of Nuclear Physics (RCNP), Graduate School of Science, and Graduate School of Medicine as well as with Graduate School of Pharmacy of another university. Recently, we, nuclear chemistry group, started studying ¹⁹¹Pt for a radiotracer of new platinum-complex anticancer drugs and ²¹¹At for alpha targeted therapy. In this conference, we present production, purification, and application of these radioisotopes to pharmaceutical uses.

[Production and purification]

¹⁹¹Pt (half-life, $T_{1/2} = 2.8$ d) was generated from ¹⁹¹Au ($T_{1/2} = 3.2$ h), which was produced in the reaction of ^{nat}Pt(p, xn)¹⁹¹Au with a 40-MeV proton beam delivered from the AVF cyclotron of RCNP, via the EC or β^+ decay. Beam current was 1.0 particle μ A on Average. A Pt foil with 40-45 mg/cm² thickness was used as a target. Irradiated Pt target was dissolved in an aqua regia immediately after the irradiation. After the evaporation to dryness, it was dissolved in 2 M HCl and a gold carrier was added to the solution. Then, the solution was mixed with ethyl acetate and Au was extracted to the organic phase. After phase separation, the organic phase was stood for 12 hours for the radioactive growth of ¹⁹¹Pt, while the aqueous phase was discarded. After growth, the organic phase was evaporated to dryness and was dissolved in 4M HCl. Then, it was purified by removing the Au carrier by extracting it with Diethylene Glycol Dibutyl Ether, an extraction agent for Au. Radiochemical yield was about 60 %.

²¹¹At ($T_{1/2} = 7.2$ h) was produced in the ²⁰⁹Bi(α ,2n)²¹¹At reaction with 28-MeV ⁴He²⁺ beam at the AVF cyclotron. Beam current was 0.5 particle μ A on average. A vacuum evaporated bismuth metal target of 10-25 mg/cm² thickness as well as a Bi₂O₃ pellet of 200-300 mg/cm² was used as a target. After the irradiation, the target was dissolved with conc. HNO₃. The aqueous solution was mixed with carbon tetrachloride or diisopropylether for extracting ²¹¹At into the organic phase. Then, back-extraction was carried out with NaOH. After neutralization, the aqueous solution containing ²¹¹At were finally obtained. The separation was completed in less than 30 min.

[Attempt for ²¹¹At separation/labeling with resin-supported compounds]

An attempt with ²¹¹At was also made to prepare ²¹¹At-labeled compounds in a simple and convenient way where separation of ²¹¹At from the Bi target and its labeling could be simultaneously performed. A resin holding aromatic carboxylic acid containing an organostannyl group was newly synthesized as an active ester form. An organostannyl group can be substituted for ²¹¹At, and an active ester can combine the astatinated carboxylic acid to an amino group such as in antibody. In the experiment, irradiated Bi₂O₃ target was dissolved in conc. HCl and was then neutralized. Then, under an oxidative condition, the resin was added to substitute the organostannyl group for ²¹¹At. After washing the resin, n-butylamine which is corresponding to a lysine residue of antibody was added in weak-alkaline solution to form an amide bond between the astatinated aromatic carboxyl acid and n-butylamine. After removing the resin by filtration, the filtrate was analyzed by HPLC with UV and gamma counters. As a result, ²¹¹At-labeling in an aromatic ring was successful, while the

combination with the amine was not clearly observed. We need further investigation for the labeling of the amine.

[Application of ^{191}Pt : Pharmacodynamics study of new anticancer drugs by Pt labelling]

4N coordinated Pt(II) complexes was synthesized as model complexes of cisplatin-binding DNA-HMG adduct, Pt(R-phen)(AtX), where R-phen : substituted phenanthroline, AtX : anthracene (At) containing diamine, and found the excellent antitumor effect of Pt(MP)(AtC3) (MP=5-methyl-1,10-phenanthroline, AtC3=N-9-anthracenyl-trimethylenediamine). To explore the excellent anticancer drug, the pharmacological study by using ^{191}Pt -labeled complexes are now going.

[Application of ^{211}At -1: Difference in thyroid uptake between Astatine-211 and Iodine-123 in normal rats: a comparative study between oral and intravenous administration]

To replace ^{131}I β -emitting targeting therapy for thyroid cancer by ^{211}At , difference of biodistribution between ^{211}At and ^{123}I was investigated. Rats received NaAt/NaI either of orally or intravenously. Then, they were imaged by a gamma camera. As a result, lower uptake ratio of ^{211}At than ^{123}I was observed for thyroid gland. But, in oral administration, continuous supply of alpha-emitter to thyroid gland was also observed.

[Application of ^{211}At -2: Targeted Radionuclide Therapy using ^{211}At combined antibody]

It is necessary to make cancer targeting elements of an antibody medicine combine the radionuclide to lead the produced alpha-particle radionuclide to radiation medical supplies. Antibody which targeted CD20 had been developed as an anticancer drug to a malignant lymphoma as business method of treatment in the beta ray, so it was considered using an anti CD20 antibody first. When ^{211}At was introduced into DECABORAN part under the oxidation condition after a preparation, and made a DECABORAN introduction anti CD20 antibody act on a lymphoma origin cell, a cytotoxic case action stronger than ^{131}I introduction antibody was indicated. A cytotoxic case action as well as reproducibility are being considered aiming at an analysis quantitatively at present.

Production and application of copper-64 at Turku PET Centre

Yim Cheng-Bin¹, Elomaa Viki-Veikko¹, Mikkola Kirsi², van Dijk Laura³, Rajander Johan⁴, Nuutila Pirjo^{5,6}, Solin Olof^{1,4,7}

1 Radiopharmaceutical Chemistry Laboratory, Turku PET Centre, University of Turku, Finland

2 MediCity/PET Preclinical Imaging Laboratory, Turku PET Centre, University of Turku, Finland

3 Department of Radiation Oncology, Radboud University Medical Center, Nijmegen, Netherlands

4 Accelerator Laboratory, Turku PET Centre, Åbo Akademi University, Finland

5 Turku PET Centre, University of Turku, Finland

6 Department of Endocrinology, Turku University Hospital, Finland

7 Department of Chemistry, University of Turku, Finland

Background. The nuclear decay characteristics of ⁶⁴Cu includes low positron emission energy (E_{\max} : 660 keV), which exert short average range in tissue, enabling improved spatial resolution in modern PET scanners. Furthermore, its relatively long half-life of 12.7 h provides a feasible time-window for radiosynthesis and enables tracking of fast clearing peptides and larger targeting agents (proteins) with slower accumulation kinetics.

Production. To advance the utility of ⁶⁴Cu for the development of novel PET agents, a dedicated semi-automated production facility was established at Turku PET Centre, for the production of ⁶⁴Cu with high specific radioactivity [1-2]. ⁶⁴Cu in the form of ⁶⁴CuCl₂ is produced via the ⁶⁴Ni(p,n)⁶⁴Cu nuclear reaction by bombarding 13 MeV protons on an electroplated enriched ⁶⁴Ni target. After bombardment, ⁶⁴Cu is isolated by firstly dissolving the irradiated target material in an HCl bath, and then directing the solution through an ion exchange column where ⁶⁴Cu and ⁶⁴Ni are fractionated using HCl solution of different molarities. The collected ⁶⁴CuCl₂-HCl fraction is evaporated to dryness and reconstituted for subsequent radiolabelling. To ensure high purity ⁶⁴Cu, very stringent measures are enforced in all steps from production, separation, to radiolabelling, in order to limit/eliminate metal contaminants.

Application. As an example of ⁶⁴Cu-labelled tracer development, recent preclinical studies using ⁶⁴Cu-labelled NODAGA-exendin-4 showed high and specific uptake in rat pancreatic islets (Figure 1) [3]. This is an important achievement, because efforts to develop sensitive noninvasive methods to quantify beta cell mass, which underlies the development of diabetes, have been challenged by the low abundance (1-2 %) and high dispersion of beta cells in the pancreas. It was concluded that the higher achievable specific activity and lower positron energy of ⁶⁴Cu compared to ⁶⁸Ga favors the application of [⁶⁴Cu]NODAGA-exendin-4 for beta cell imaging. However, the high radiation burden accrued in the kidneys limits its use as a clinical tracer.

In another feasibility study, ⁶⁴Cu-labeled cetuximab-F(ab')₂ demonstrated high and specific uptake in EGFR expressing tumors (Figure 2) [4]. A significant correlation was found between the intratumoral localization of [⁶⁴Cu]NODAGA-cetuximab-F(ab')₂ as determined by autoradiography and EGFR expression as determined by immunohistochemistry. This ability to determine EGFR expression with superior image quality in heterogeneous tumours at a relatively early time interval, provides clinical promise in determining intratumoral EGFR distribution.

References. [1] Elomaa VV, Jurttila J, et al. *Appl Radiat Isot.* **2014**, 89, 74. [2] Rajander J, Schlesinger J, et al. *J Labelled Comp Radiopharm* **2009**, 52, S234. [3] Mikkola K, Yim CB, et al. *Mol Imaging Biol.* **2014**, 16, 255. [4] van Dijk LK, Yim CB, et al. *Contrast Media Mol Imaging.* **2016**, 11, 65.

Funding. Part of this study was conducted within the Finnish Centre of Excellence in Molecular Imaging in Cardiovascular and Metabolic Research, financially supported by the Academy of Finland, University of Turku, Turku University Hospital and Åbo Akademi University. The research has received funding from the European

Community's Seventh Framework Programme (FP7/2007-2013) under grant agreement 222980, the Finnish Diabetes Research Foundation, and from the Dutch Cancer Society, grant no NKB-KUN 2010-4688.

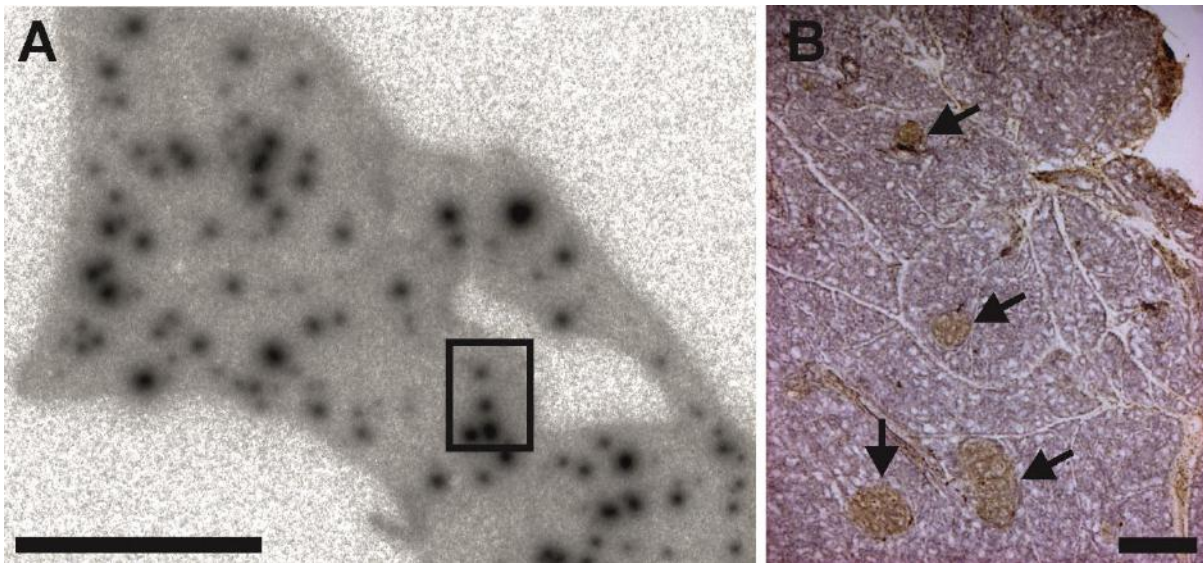


Figure 1. (a) Labelling of islets in rat pancreatic tissue sections at 1 h after the injection of [^{64}Cu]NODAGA-exendin-4, and (b) close-up of the boxed region in (a) after insulin staining of the islets (arrows).

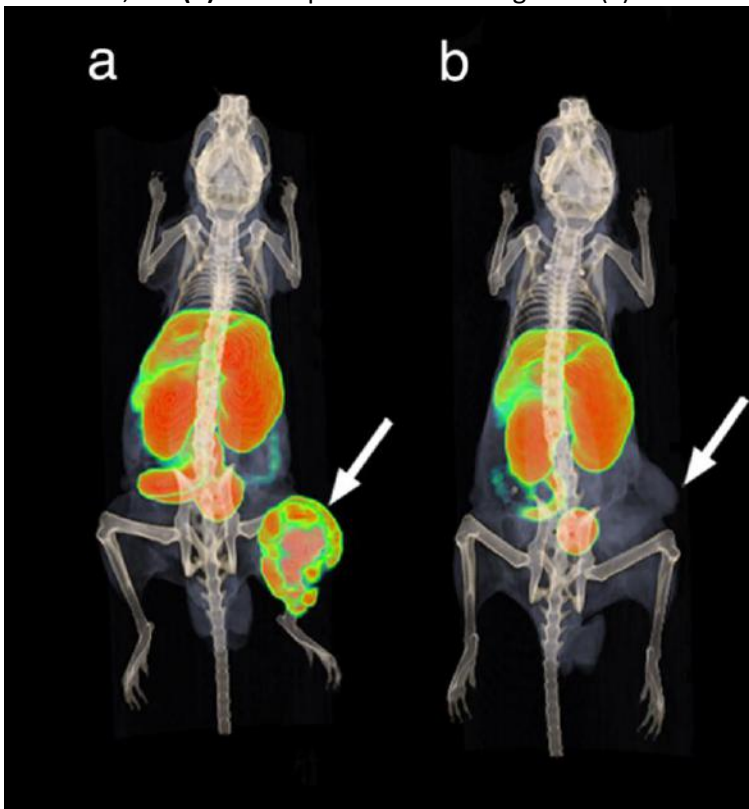


Figure 2. PET/CT images of ^{64}Cu -cetuximab- $\text{F}(\text{ab}')_2$ distribution at 24 h p.i. in mice with UT-SCC tumors. (a,b) Tumors are located subcutaneously on the right hind leg (arrow). (b) Pre-injected with excess cetuximab. Background uptake visible in PET images is liver, kidneys and bladder.

RADIONUCLIDE PRODUCTION

Complexation studies of Po(IV) with a novel hexadentate chelating agent “N₂S₂O₂/N₄O₂”

A. Younes,¹ D. Deniaud,² S. Gouin,² G. Montavon,¹ C. Alliot,^{3,4} M. Mokili,^{1,3} J. Champion¹

1. Laboratoire SUBATECH, UMR 6457, Ecole des Mines de Nantes / CNRS/IN2P3 / Université de Nantes, 4 rue A. Kastler, BP 20722, 44307 Nantes cedex 03, France.
2. CEISAM, UMR CNRS 6230, UFR des Sciences et des Techniques, 2, rue de la Houssinière, BP 92208, 44322 NANTES Cedex 3, France.
3. ARRONAX, 1 rue Arronax - CS 10112 - 44817 Saint Herblain cedex, France.
4. INSERM U892, CRCNA, Nantes 44007, France.

Polonium is a highly radiotoxic element, with the main hazard from ingestion or inhalation. One of polonium's isotopes, polonium-210 (Po-210) occurs naturally in the uranium-238 decay. 20% of the annual effective dose from inhalation of uranium and thorium series radionuclides is composed by Po-210 and 60 % for ingestion. To illustrate this point, 1 µg of Po-210 emits as many alpha particles as 446 kg of uranium-238. Although Pierre and Marie Curie made the discovery of the element polonium (Po) more than a century ago, physical chemistry properties of this element and its complexes are still barely known. This can be explained by two main reasons: first, polonium is very rare in nature, being found in uranium ores at approximately 100 µg/ton. Thus, an adapted cyclotron or a reactor is necessary to produce its isotopes. Second, polonium has thirty five known isotopes, all of which are radioactive. However, a better understanding of polonium's affinity is essential to improve techniques of biological decorporation or environmental remediation.

To carry it, several tasks are presented including, developing a methodology for the production and extraction of polonium's isotopes from a bismuth target to insure its availability,² followed by studying the complexation constants between polonium with complexing agent. There is a need in designing specific decorporating agent for polonium. A novel water soluble multidentate “N₂S₂O₂/N₄O₂” ligand complexing agent was designed and synthesized, as a new water soluble - selective chelating agent for possible polonium decorporation. This ligand presents *a priori* the good characteristics for polonium complexation, *i.e.* a platform presenting four soft heteroatoms (N/S) and additional two pendant carboxylic groups to complete the octahedral coordination shell suitable for polonium (IV) complexation. Its affinity for polonium was studied at pH=7.4 using a liquid-liquid extraction methodology.

References

1. Ansoborlo, E.; Berard, P.; Den Auwer, C.; Leggett, R.; Menetrier, F.; Younes, A.; Montavon, G.; Moisy, P., Review of Chemical and Radiotoxicological Properties of Polonium for Internal Contamination Purposes. *Chemical Research in Toxicology* 2012, 25, (8), 1551-1564.
2. Younes, A.; Montavon, G.; Alliot, C.; Mokili, M.; Haddad, F.; Deniaud, D.; Champion, J., A route for polonium 210 production from alpha-particle irradiated bismuth-209 target. *Radiochimica Acta* 2014, 102, (8), 681-689.

Comparison of microfluidic and conventional extraction for ^{99}Mo produced by Szilard-Chalmers reaction

Dalmázio, Ilza^{1,2}, van Dorp, Jan Willem²; Oehlke, Elisabeth²

1 Nuclear Technology Development Center, CDTN, Brazil

*2 Delft University of Technology, TU Delft, The Netherlands
id@cdtn.br*

Technetium-99m ($^{99\text{m}}\text{Tc}$), a decay product of ^{99}Mo , is the worldwide most applied radionuclide in medical imaging. In the past years, disruptions in the ^{99}Mo supply chain have occurred due to the ageing of production facilities and a limited number of suppliers. These facts have motivated the examination of new strategies for supplying ^{99}Mo in the short, medium and long term, such as research and development of alternative routes for ^{99}Mo production using accelerators or nuclear research reactors [1]. In this scenario, TU Delft researchers have evaluated methods for ^{99}Mo production [2], using, for instance, the Szilard-Chalmers effect to isolate ^{99}Mo with higher specific activity from the $^{98}\text{Mo}(n,\gamma)^{99}\text{Mo}$ nuclear reaction. The purification of ^{99}Mo occurs via liquid-liquid extraction [3]. In order to increase the efficiency of the purification process and offer an option for automation, we translated this separation into a microfluidic channel. Microfluidic separation has been shown to be advantageous for several extraction processes, including radiochemistry applications, due to the effective control of liquid-liquid contacting, the large surface-to-volume ratio and short molecular diffusion distances [4]. Here, we present the first results for microfluidic liquid-liquid extraction of ^{99}Mo produced via Szilard-Chalmers reaction.

For the experiments molybdenum hexacarbonyl was used as target compound based on previous work done at the TU Delft [5]. The compound was exposed to a thermal neutron flux of $3.1 \times 10^{16} \text{ n cm}^{-2} \text{ s}^{-1}$ for 1 hour at the Hoger Onderwijs Reactor Delft (HOR, Delft, The Netherlands). This was followed by dissolving the activated target in dichloromethane and subsequent extraction into an aqueous phase. For the conventional process we used an organic to aqueous volume ratio of 1:1 and a contact time of 30 min. The microfluidic extraction was done in a glass microchannel (dimensions: $46\mu\text{m} \times 160\mu\text{m} \times 120 \text{ mm}$, $6\mu\text{m}$ guide, ICC-DY15G, IMT Co., Japan) in triplicate at different flow rates (10 to $60 \mu\text{L/min}$, org./aq. ratio 1:0.54).

We observed no significant difference in extraction behaviour for different flow rates. Overall specific activities of around 265 kBq/mg were achieved by microfluidic extraction (original solution: 7.5 kBq/mg). The comparison of both conventional and microfluidic results showed that the activity of ^{99}Mo that could be extracted was by a factor of 7 higher in the conventional process. However, also the amount of total molybdenum (all isotopes) transferred was increased in the conventional process (factor 35), which means that overall a higher specific activity and enrichment factor could be achieved in the microfluidic process (by a factor of 5).

In conclusion, our first experiments indicate that the purification of ^{99}Mo that was produced by Szilard-Chalmers reaction can be enhanced by using microfluidic extraction. Nevertheless, more experiments are needed to explore different extraction conditions, and to further improve the separation efficiency.

- [1] International Atomic Energy Agency (2013). *Non-HEU Production Technologies for Molybdenum-99 and Technetium-99m*; IAEA Nuclear Energy Series No. NF-T-5.4; International Atomic Energy Agency: Vienna, Austria.
- [2] Wolterbeek, H.T., Bode, P. (2009). *A process for the production of no-carrier added ^{99}Mo* . European Patent Office. EP, 2131369 (A1).
- [3] Tomar, B.S., Steinebach, O.M., Terpstra, B.E., Bode, P., Wolterbeek, H.T. (2010). Studies on production of high specific activity ^{99}Mo and ^{90}Y by Szilard Chalmers reaction. *Radiochimica Acta*, 98(8), 499-506.
- [4] Ciceri, D., Perera, J.M., Stevens, G.W. (2014). The use of microfluidic devices in solvent extraction. *Journal of Chemical Technology and Biotechnology*, 89(6), 771-786.

[5] van Dorp, J.W., Mahes, D.S., Serra-Crespo, P., Steinebach, O.M, Bode, P., Wolterbeek, H.T., Denkova, A.G. (2016) Towards the Production of Carrier-free ^{99}Mo by Neutron Activation of ^{98}Mo in Molybdenum Hexacarbonyl. Part I. Szilard-Chalmers revisited. *Unpublished manuscript*. Delft University of Technology, Delft, The Netherlands.

Production of radiochemically pure ^{163}Ho for the ECHo experiment

Holger Dorrer^{1,2,3}, Katerina Chrysalidis¹, Thomas Day Goodacre⁴, Christoph E. Düllmann^{1,5}, Klaus Eberhardt¹, Christian Enss⁶, Loredana Gastaldo⁶, Raphael Haas¹, Clemens Hassel⁶, Karl Johnston⁴, Tom Kieck¹, Ulli Köster⁷, Bruce Marsh⁴, Christoph Mokry¹, Sebastian Rothe⁴, Jörg Runke⁵, Fabian Schneider¹, Thierry Stora⁴, Andreas Türler^{2,3}, Klaus Wendt for the ECHo collaboration.

¹ University of Mainz, Mainz, Germany.

² Paul Scherrer Institut, Villigen, Switzerland.

³ University of Bern, Bern, Switzerland.

⁴ CERN, Geneva, Switzerland.

⁵ GSI Helmholtzzentrum für Schwerionenforschung, Darmstadt, Germany.

⁶ Kirchhoff Institute for Physics, Heidelberg University, Heidelberg, Germany.

⁷ Institut Laue-Langevin, Grenoble, France.

The electron neutrino mass is known to be different from zero (Physics Nobel prize 2015: “For the discovery of neutrino oscillations, which shows that neutrinos have mass”), but is very small. Its value is still unknown. The “Electron Capture in Ho-163” (ECHo) experiment [1] aims at investigating the electron neutrino mass in the sub-eV/c² range by means of the analysis of calorimetrically measured energy spectra following the electron capture process of ^{163}Ho . For performing this, the availability of about 10^{19} atoms of the long-lived Ho-radioisotope ^{163}Ho ($T_{1/2} = 4570$ a) in radiochemically pure form is required. Different pathways are available to produce ^{163}Ho either at accelerator or reactor facilities [2]. In all the cases the production of ^{163}Ho is inevitably accompanied by the co-formation of undesired byproducts. We present the production routes, expected byproducts in the different pathways as well as their removal applying chemical (for removal of non-isotopic impurities) and subsequent physical (mainly for exclusion of the Ho-radioisotope $^{166\text{m}}\text{Ho}$) separation methods.

In particular we focus on the production using neutron activation of enriched ^{162}Er , which has been performed during the first stage of the ECHo experiment. The enriched ^{162}Er target was chemically purified by cation exchange chromatography to remove all lanthanides lighter than Er present as impurities before the neutron irradiation. Subsequently, the material was irradiated in the high-flux reactor at ILL in Grenoble for 54 days. The Ho produced during the irradiation was chemically isolated from milligram amounts of Er and GBq amounts of $^{170/171}\text{Tm}$ applying extraction chromatography with decontamination factors of > 500 for Er and $> 10^5$ for Tm. $^{166\text{m}}\text{Ho}$ was the only detectable radiochemical impurity in the obtained Ho-fraction.

This radioisotope can be eliminated by use of the RISIKO mass separator, which is located at the Institute of Physics at Johannes Gutenberg University Mainz. It suppresses neighboring masses by about 5 orders of magnitude and provides excellent ionization and transmission efficiency of $(32 \pm 5) \%$ for Ho [3] from the sample in the ion source to the focal plane thanks to laser resonance ionization. By positioning the detectors that are used for the calorimetric measurements of the electron capture spectrum in the RISIKO focal plane, it is possible to combine the mass separation with the implantation of ^{163}Ho ions directly into the detectors. Samples of the chemically isolated ^{163}Ho have been already used for a high-precision measurement of the electron capture decay Q-value of this radionuclide [4, 5] by means of Penning-trap mass spectrometry as well as for the mass separation and ion-implantation of ^{163}Ho at the GPS mass separator at ISOLDE/CERN. This detector shows perfect performance and absence of any detectable radioactive contamination.

[1] L. Gastaldo et al., J. Low Temp. Phys. **2014**, **176**, 876. [2] J. Engle et al., Nucl. Instrum. Methods B **2013**, **311**, 131. [3] F. Schneider et al., Nucl. Instr. Meth. B **2016**, <http://dx.doi.org/10.1016/j.nimb.2015.12.012>. [4] F. Schneider et al., Eur. Phys. J. A **2015**, **51**, 89. [5] S. Eliseev et al., Phys. Rev. Lett. **2015**, **115**, 062501.

^{47}Sc separation from $^{\text{nat}}\text{Ti}$ irradiated by 55 MeV photons

Furkina E.B., Aliev R.A., Aleshin G.Yu., Priselkova A.B., Kalmykov S.N.

*Lomonosov Moscow State University
National Research Center "Kurchatov Institute"*
Furkina-k@yandex.ru

^{47}Sc is one of the most promising radionuclide for radioimmunotherapy [1] because of its favorable decay characteristics ($T_{1/2}=3.35$ d; average beta particle energy, 162 keV; $E_{\gamma}=159$ keV) and relatively simple chemical properties. It could be used for SPECT imaging [2] as well. Possible production methods of ^{47}Sc include irradiation of $^{\text{nat}}\text{Ti}$ by protons of medium energies [3], neutron irradiation of ^{46}Ca in high-flux reactors via $^{46}\text{Ca}(n,\gamma)^{47}\text{Ca}\rightarrow^{47}\text{Sc}$ reaction [2] and $^{\text{nat}}\text{Ti}$ irradiation using electron linacs [4].

In this work we focus on the photonuclear production of ^{47}Sc via $^{\text{nat}}\text{Ti}(\gamma,p)^{47}\text{Sc}$ reaction. Metallic Ti target was irradiated by 55 MeV photons in race-track microtron of Lomonosov Moscow State University. Yields of Ti and Sc radionuclides in this experiment were reported earlier [5].

Irradiated target (0,5 g) was dissolved in aqua regia. The solution was evaporated near dryness and residue was dissolved in 3M HNO_3 . TiO_2 precipitate was separated by centrifugation; the losses of Sc were less than 3%. Then Sc was separated from residual Ti by extraction chromatography using DGA Resin (Triskem). The sorption of Sc was carried out in 3M HNO_3 , Ti did not retain on the column under this conditions. Then Sc was eluted from the column with 0,4M HCl (Fig.1). ^{47}Sc was determined by gamma spectrometry, stable Ti by spectrophotometry.

Therefore, ^{47}Sc can be produced by photonuclear method from natural Ti. The technique of ^{47}Sc separation from irradiated Ti target was developed. Chemical yield of scandium-47 was more than 95%.

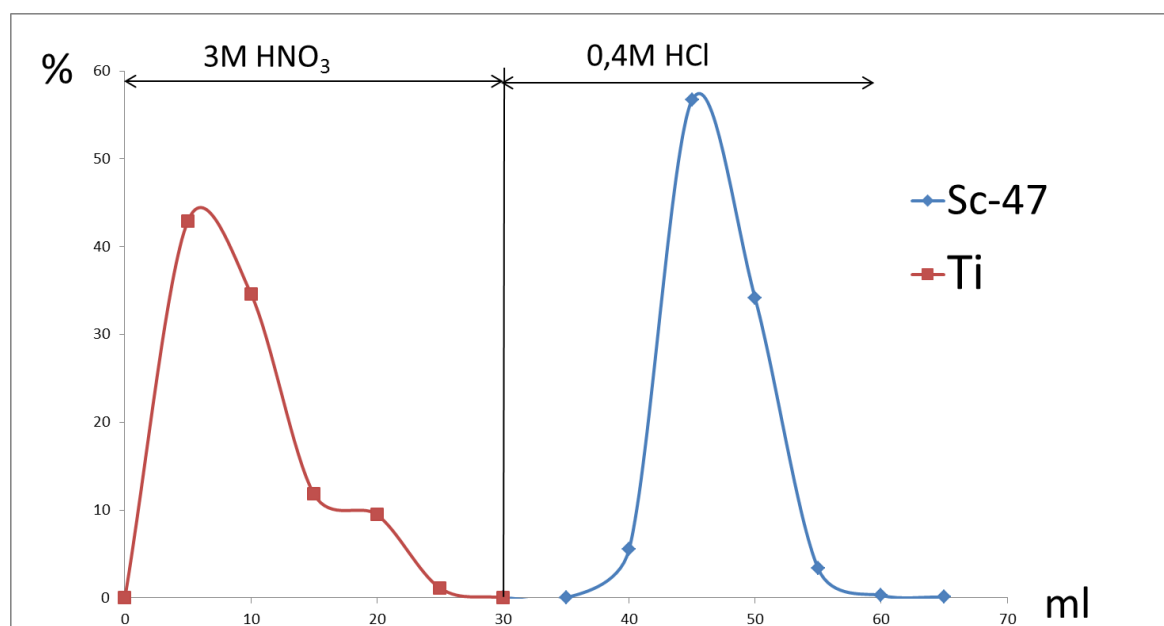


Рис. 1. Elution curve of Ti and Sc

[1] Masuner, L.F., Kolsky K.L., Joshi V., Srivastava, S.C., 1998. Radionuclide development at BNL for nuclear medicine therapy. *Applied Radiation and Isotopes* 49 (4), 285-294

- [2] Müller C., Bunka M., Haller S., Köster U., Groehn V., Bernhardt P., van der Meulen N., Türlér A., Schibli R., 2014. Promising Prospects for ^{44}Sc -/ ^{47}Sc -Based Theragnostics: Application of ^{47}Sc for Radionuclide Tumor Therapy in Mice. *J Nucl Med* 2014; 55:1658–1664
- [3] Khandaker M.U., Kim K., Lee M.V., Kim K.S., Kim G.N., Cho Y.S., Lee Y.O., 2009. Investigation of the $^{nat}\text{Ti}(p,x)^{43,44m,44g,46,47,48}\text{Sc}$, ^{48}V nuclear processes up to 40 MeV. *Applied Radiation and Isotopes* 67, 1348–1354
- [4] Mamtimin, M., Harmon, F., & Starovoitova, V. N. (2015). Sc-47 production from titanium targets using electron linacs. *Applied Radiation and Isotopes*, 102, 1–4.
- [5] Belyshev S.S., Dzhilavyan L.Z., Ishkhanov B.S., Kapitonov I.M., Kuznetsov A.A., Orlin V.N., Stopani K.A., 2015. Photonuclear reactions on titanium isotopes. *Physics of Atomic Nuclei*, 78(2):220–229.

⁹⁹Mo generation by accelerator-driven neutrons and thermo-separation of ^{99m}Tc

M. Kawabata^{1,2}, S. Motoishi^{1,2}, K. Hashimoto², Y. Hatsukawa², A. Ohta¹, T. Shiina¹, H. Saeki^{1,2}, N. Takeuchi¹, and Y. Nagai²

¹ Oarai Research Center, Chiyoda Technol Corporation, Japan

²Quantum Beam Science Research Directorate, National Institutes for Quantum and Radiological Science and Technology, Japan

Technetium-99m ($T_{1/2} = 6$ h) is the most commonly used radioisotope in nuclear medicine accounting for over 80% of diagnostic procedures worldwide. This level of usage and the variety of ^{99m}Tc radiopharmaceuticals come from the availability of parent nuclide ⁹⁹Mo ($T_{1/2} = 66$ h) which is abundantly generated in nuclear reactor using a highly enriched uranium, and so is called “fission ⁹⁹Mo”. A series of unexpected nuclear reactor shutdown since 2007 however, caused a global shortage of ⁹⁹Mo and was recognized as an urgent need to develop an alternative ⁹⁹Mo production method to ensure a secured supply long into the future [1]. Alternative production methods are available, but these rely on the development of appropriate processing technology to accept the specific activity of ⁹⁹Mo much lower than that of fission ⁹⁹Mo.

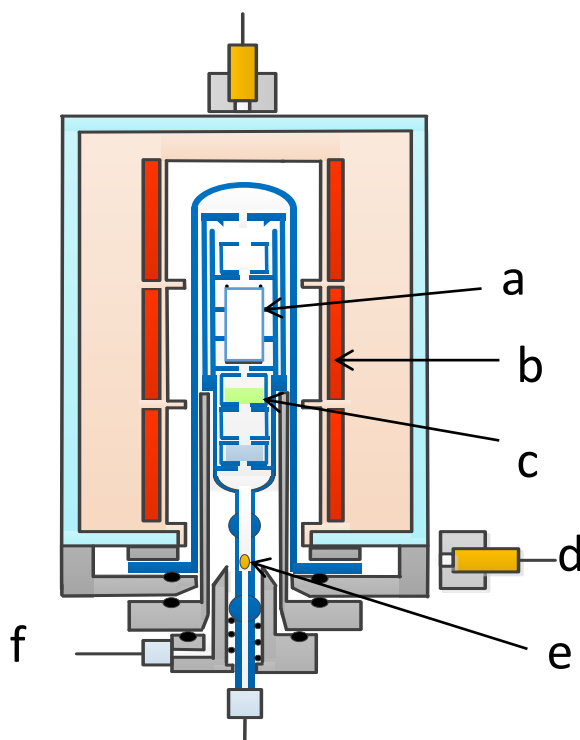


Figure 1. Schematic diagram of thermos-separation system including a: MoO₃ samples, b: heater, c: MoO₃ crystal, d: Cadmium Zinc Telluride detector, e: ^{99m}Tc deposition and f: moist oxygen inlet.

The current approach uses accelerator generated neutrons to produce ⁹⁹Mo via the ¹⁰⁰Mo($n,2n$)⁹⁹Mo reaction where fast neutrons are generated by 40 MeV deuterons bombarded to the carbon converter [2]. A 106g sample of ¹⁰⁰MoO₃ one third of which was irradiated 14 MeV neutron at the Fission Neutronics Source (FNS; a D-T neutron source) of the Japan Atomic Energy Agency (JAEA), was divided into platinum crucibles to be vertically fitted within the high temperature area of a tubular electric furnace (a in Fig. 1). The furnace is heated beyond 800 °C in the sample area with moist O₂ as a carrier gas. ^{99m}Tc generated from ⁹⁹Mo in the molten ¹⁰⁰MoO₃ in the crucibles is rapidly released from the sample as a gaseous species which is then transported and concentrated in the downstream quartz tube at low temperature around 300 °C (e in Fig. 1). The principle behind the methodology is described elsewhere [3]. Concentrated ^{99m}Tc was washed with 18 mL of 0.1 M NaOH and passed through a cation exchange column and alumina column to adjust pH and

adsorb ^{99m}Tc , respectively. The columns were washed with 20 mL of ultrapure water and ^{99m}Tc was eluted with a few mL of saline solution from the alumina column. Overall, the separation efficiency was more than 85% on average. Same thermo-separation procedure was repeated using over 100 g of $^{100}\text{MoO}_3$ sample to assess the recovery yield of $^{100}\text{MoO}_3$. Several grams of sublimated $^{100}\text{MoO}_3$ were lost from the crucibles and recrystallized at a temperature under melting point of MoO_3 during the separation. Most of them were recrystallized in the quartz holder (c in Fig. 1). The $^{100}\text{MoO}_3$ crystals were collected by washing with pure water from the holder and the other quartz glassware containing MoO_3 . The collected crystal was evaporated to dryness to measure its mass. $^{100}\text{MoO}_3$ remaining in the crucibles were inverted and heated in the same electric furnace. Molten $^{100}\text{MoO}_3$ was collected into a quartz tube with a 30 mm diameter to mold a sample for the next neutron irradiation. $^{100}\text{MoO}_3$ was successfully collected with the recovery yield > 95%.

References

- 1) T. Ruth, Nature 457, 29 (2009)
- 2) Y. Nagai and Y. Hatsukawa, J. Phys. Soc. Jpn. 78, 033201 (2009).
- 3) Y. Nagai, M. Kawabata, N. Sato, K. Hashimoto, H. Saeki, and S. Motoishi, J. Phys. Soc. Jpn. 83, 083201 (2014).

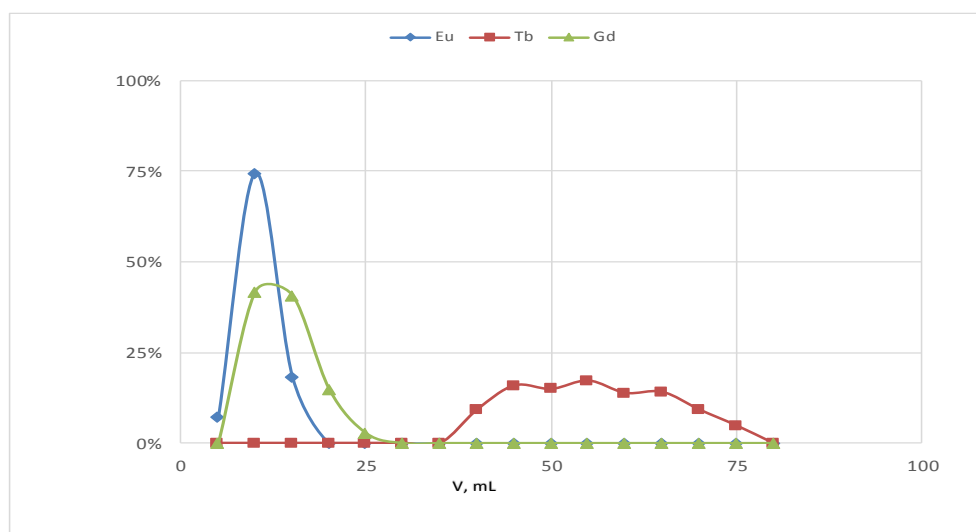
Separation of terbium radionuclides from europium target irradiated by alpha particles

Kazakov A. G.¹, Aliev R. A.^{1,2}, Bodrov A. Yu.², Priselkova A. B.², Kalmykov S. N.^{1,2}

*National Research Center "Kurchatov Institute", Moscow, Russia
Lomonosov Moscow State University, Moscow, Russia*

Terbium isotopes are considered as a perspective for nuclear medicine [1]. The aim of this work was to develop technique of isolation of radioactive terbium isotopes from europium target irradiated by 28 MeV alpha-particles. The method should be effective for separation of Tb from hundreds of mg of Eu and trace amounts of Gd formed during irradiation by $^{151}\text{Eu}(\alpha, \text{pn})^{153}\text{Gd}$ reaction. Several radioactive isotopes of Tb are formed during irradiation of Eu target by 28 MeV alpha particles on cyclotron according to nuclear reactions $^{153}\text{Eu}(\alpha, \text{n})^{156}\text{Tb}$, $^{153}\text{Eu}(\alpha, 2\text{n})^{155}\text{Tb}$, $^{151}\text{Eu}(\alpha, \text{n})^{154}\text{Tb}$, $^{151}\text{Eu}(\alpha, 2\text{n})^{153}\text{Tb}$. Also, in model experiments we used terbium radionuclides mixture obtained by irradiation of natural Tb with 55 MeV gamma quanta by reactions $^{159}\text{Tb}(\gamma, 3\text{n})^{156}\text{Tb}$, $^{159}\text{Tb}(\gamma, 4\text{n})^{155}\text{Tb}$, $^{159}\text{Tb}(\gamma, 5\text{n})^{154}\text{Tb}$, $^{159}\text{Tb}(\gamma, 6\text{n})^{153}\text{Tb}$ on a race-track microtron.

In order to separate terbium from bulk europium we used reduction to Eu(II) by zinc in concentrated HCl and subsequent precipitation of EuSO_4 by ammonia sulphate. The optimal conditions for separation (the kinetics of the process and the concentration of reagents) were determined. Further separation of terbium from europium and traces of gadolinium was done by extraction chromatography. Sorbent LN-Resin [2] (TrisKem) was selected for separation. The chromatographic behavior of Tb, Eu, Gd, in HNO_3 solutions was studied. Thus, the possibility of production of carrier-free terbium radionuclides $^{154,155,156}\text{Tb}$ by alpha-particles irradiation of europium target was shown. The method of terbium separation from macro quantities of europium and trace amounts of gadolinium is developed.



Pict.1 Eu, Tb, Gd separation on Ln-Resin, 0,7 M HNO_3 .

- 1) Cristina Müller, Josefine Reber, Stephanie Haller, Holger Dorrer, Ulli Köster, Karl Johnston, Konstantin Zhernosekov, Andreas Türler and Roger Schibli. Receptor Targeted Alpha-Therapy Using Terbium-149. // Pharmaceuticals. 2014. V.7. P. 353-365.
- 2) Horwitz E.P. and Bloomquist C.A.A. Chemical separations for super-heavy element searches in irradiated uranium targets. // J. inorg, nucl. Chem.. 1975. V. 37. P. 425-434.

Measurement of production cross sections of Tc isotopes in deuteron-induced reactions on ^{nat}Mo up to 24 MeV

Y. Komori, M. Murakami, and H. Haba

Nishina Center for Accelerator-Based Science, RIKEN, Wako, Saitama 351-0198, Japan

^{99m}Tc ($T_{1/2} = 6.0067$ h) is one of the most important radionuclides in the field of nuclear medicine. Recently the production of ^{99}Mo ($T_{1/2} = 65.9496$ h)/ ^{99m}Tc using accelerators has attracted much attention because the expected shutdowns of nuclear reactors for ^{99}Mo production would cause global supply shortage of ^{99}Mo [1]. On the other hand, relatively long-lived isotopes such as ^{96g}Tc ($T_{1/2} = 4.28$ d) and ^{95m}Tc ($T_{1/2} = 61$ d) are useful for tracer experiments of Tc. We plan to study chemical properties of element 107, bohrium (Bh) in aqueous solutions [2]. Since Tc is a lighter homolog of Bh in the periodic table, the long-lived Tc isotopes are useful for model experiments for Bh. The Tc isotopes can be produced by deuteron-induced reactions on ^{nat}Mo (nat: natural isotopic abundance). In this work, we have measured production cross sections in the $^{nat}\text{Mo}(d,x)$ reactions up to 24 MeV for the quantitative production of the Tc isotopes.

The target stack consisted of 16 sets of ^{nat}Mo (99.95% purity, 20.9 mg/cm² thickness), ^{nat}Ti (99.5%, 9.2 mg/cm²), and ^{nat}Ta (99.95%, 16.1 mg/cm²) metallic foils with the size of 15 × 15 mm². The target stack of Mo/Ti/Ta was irradiated for 1 h with a 24-MeV deuteron beam supplied from the RIKEN AVF cyclotron. After the irradiation, each foil was subjected to γ -ray spectrometry. The average beam current of 0.17 μA was determined by the monitor reaction $^{nat}\text{Ti}(d,x)^{48}\text{V}$ [3]. The excitation functions were measured for the $^{nat}\text{Mo}(d,x)^{93m,93g,94m,94g,95m,95g,96m,96g,97m,99m}\text{Tc}$, $^{93m,99,101}\text{Mo}$, $^{90g,92m,95m,95g,96}\text{Nb}$, and ^{89g}Zr reactions. Thick-target yields for the investigated isotopes were deduced from the measured production cross sections. The present results will be discussed by referring to the previously reported data [4–10] and to the theoretical model code TALYS (TENDL-2015 [11]). In addition, we performed precision measurements of half-lives of ^{95g}Tc ($T_{1/2} = 20.0$ h) and ^{96g}Tc using a reference source method [12] because their half-lives were suggested to be slightly shorter than those adopted in the literature [13,14].

References

- [1] IAEA, Non-HEU Production Technologies for Molybdenum-99 and Technetium-99m, Nuclear Energy Series No. NF-T-5.4, IAEA, Vienna (2013).
- [2] Y. Komori *et al.*, a contribution to NRC9.
- [3] IAEA, IAEA-TECDOC-2011, Charged-particle cross section database for medical radioisotope production., International Atomic Energy Agency, Vienna (2007). Data available online <http://www-nds.iaea.org/medical/monitor_reactions.html>.
- [4] Z. Ránda and K. Svoboda, J. Inorg. Nucl. Chem. **38**, 2289 (1976).
- [5] Z. Ránda and K. Svoboda, J. Inorg. Nucl. Chem. **39**, 2121 (1977).
- [6] Z. Ránda and K. Svoboda, Int. J. Appl. Radiat. Isot. **28**, 555 (1977).
- [7] W. Sheng *et al.*, Inst. Nucl. Sci. Technol. Sichuan Univ. Rep., NST-004 (1990).
- [8] O. Lebeda and M. Fikrle, Appl. Radiat. Isot. **68**, 2425 (2010).
- [9] P. Chodash *et al.*, Appl. Radiat. Isot. **69**, 1447 (2011).
- [10] F. Tárkányi *et al.*, Nucl. Instrum. Meth. B **274**, 1 (2012).
- [11] A.J. Koning *et al.*, TENDL-2015: TALYS-based Evaluated Nuclear Data Library (2016). Data available online <https://tendl.web.psi.ch/tendl_2015/tendl2015.html>.
- [12] M.A. Silva *et al.*, J. Radioanal. Nucl. Chem. **264**, 571 (2005).
- [13] S.K. Basu *et al.*, Nucl. Data Sheets **111**, 2555 (2010).
- [14] D. Abriola and A.A. Sonzogni, Nucl. Data Sheets **109**, 2501 (2008).

Production of $^{223}\text{RaCl}_2$ and $^{224}\text{RaCl}_2$ preparations from neutron irradiated ^{226}Ra

Rostislav Kuznetsov, Pavel Butkalyuk, Valery Tarasov, Evgeny Romanov, Alexander Baranov, Irina Butkalyuk

*JSC "SSC RIAR", Ulyanovsk region, Dimitrovgrad, Russian Federation
orip@niiar.ru*

First results of the $^{223}\text{RaCl}_2$ and $^{224}\text{RaCl}_2$ production technology development at SSC RIAR are reported. Short-lived ^{223}Ra and ^{224}Ra are generated from long-lived parents ^{227}Ac and ^{228}Th , that can be produced by neutron irradiation of radium.

The target to be irradiated in the reactor is produced by co-precipitation of radium and lead nitrate from concentrated nitric acid. The precipitate is calcined at 700°C to yield radium metaplumbate (RaPbO_3), which is irradiated in the SM high-flux research reactor for $20\div 30$ days. Thermal neutron flux density in the irradiation position is $1.5\cdot 10^{15}\text{ cm}^{-2}\text{s}^{-1}$. The irradiated material is dissolved, radium is separated by co-precipitation with lead nitrate from concentrated nitric acid. The radium-lead nitrate precipitate is recycled to fabricate reactor targets. Separation procedure for ^{228}Th and ^{227}Ac produced in the target is as follows.

The $^{228}\text{Th}(\text{NO}_3)_4$ is extracted from a filtrate by anion-exchange chromatography using BioRad AG-1x8(NO_3^-) resin. $^{227}\text{Ac}(\text{NO}_3)_3$ is isolated from the solution and purified from impurities of radium, thorium, lead and capsule materials activation products by the extraction chromatography using sorbent Ln-Resin.

The short-lived radionuclides ^{223}Ra and ^{224}Ra , generated from the parent ^{227}Ac and ^{228}Th , are separated by the dual-column method. The first column adsorbs the parent radionuclides, that is Ln-Resin in case of ^{227}Ac , and BioRad AG-1x8 (NO_3^-) in case of ^{228}Th . The second column (AG-50x8(NH_4^+)) in both cases adsorbs radium from the acetate buffer solution ($\text{pH}=4.5$) containing 0.02 M of EDTA. Both ^{223}Ra and ^{224}Ra are eluted from the column with 8 M HNO_3 , and the solution is converted into chloride form by evaporation to dryness followed by dissolution of a dry residue in $0.01\div 0.5$ M of HCl .

In 2015, three targets, each containing $40\div 50$ mg of radium, were fabricated, irradiated and reprocessed to extract ~ 3 Ci of ^{228}Th and ~ 0.2 Ci of ^{227}Ac . Trial batches of $^{224}\text{RaCl}_2$ and $^{223}\text{RaCl}_2$ are periodically produced for experimental needs. Further, the technology will be gradually scaled up to increase amount of radium irradiated in the reactor thus increasing activity of ^{223}Ra and ^{224}Ra production capacity.

Production and purification of no-carrier-added ^{139}Ce at the Leipzig cyclotron CYCLONE® 18/9

Alexander Mansel and Karsten Franke

*Helmholtz-Zentrum Dresden-Rossendorf; Institute of Resource Ecology; Reactive Transport Division;
Research Site Leipzig; Permoserstrasse 15; D-04318 Leipzig; Germany; phone: +49 341 234179 4671;
a.mansel@hzdr.de*

The global demand for the lanthanides has dramatically increased. Therefore, a detailed understanding of ore chemistry and separation methods is needed. To study these processes, the use of the radiotracer technique is a marvellous method to observe the chemical behaviour of such elements. ^{139}Ce ($T_{1/2} = 137.6$ d, $E_{\beta} = 166$ keV, $I_{\beta} = 80\%$) was chosen as a representative element (radionuclide) for the lanthanide elements. We produced ^{139}Ce using the nuclear reaction $^{139}\text{La}(p,n)^{139}\text{Ce}$ by means of irradiation of a few tens mg $[\text{natLa}]\text{La}_2\text{O}_3$ at the Leipzig cyclotron CYCLONE® 18/9^[1]. At an irradiation time of 3 h, an effective proton current of 2.9 μA and a maximal proton energy of 12.5 MeV, an activity of ~ 0.5 MBq ^{139}Ce was achieved. The irradiated La_2O_3 was dissolved in conc. nitric acid and fumed to dryness. For the separation of the radionuclide from the target material, we used the tetravalent oxidation state of cerium by means of an oxidative application with a mixture of dichromate/sulfate in 9 M nitric acid. For the first time, UTEVA® Resin was used to separate the tetravalent cerium (Ce^{4+}) in no-carrier-added (n.c.a.) form from the trivalent lanthanum (La^{3+}) by ion exchange chromatography in column technique, as used for plutonium (Pu^{4+}) separations from trivalent actinides (e.g. Am^{3+})^[2]. The $^{139}\text{Ce}^{4+}$ ions were washed from the column by 1 mM nitric acid. After evaporation of the combined cerium fractions, the ^{139}Ce was dissolved in 1 mM nitric acid to give a stock solution with an activity concentration of ~ 1 MBq/ml. The radiochemical yield of n.c.a. ^{139}Ce was $94\% \pm 5\%$. With a detection limit of 10 Bq/ml, a concentration range down to ~ 0.3 pmol/l n.c.a. ^{139}Ce can be achieved. From the dissolution of the irradiated target until preparation of the stock solution, only 5 h are necessary. The chemical purity of the stock solution was evaluated by ICP-MS. By a weekly in-house production of n.c.a. ^{139}Ce , we can use this radionuclide in our institute (or cooperation partners) for actual studies in liquid-liquid extraction by means of calixarenes or radiolabelling of CeO_2 -nanoparticles.

References:

[1] C. Vermeulen et al. (2007) Nucl. Instr. Meth. B **255**, 331. [2] E. P. Horwitz et al. (1992) Anal. Chim. Acta **266**, 25.

Acknowledgement:

We like to thank the German Federal Ministry of Education and Research (BMBF) for financial support (contract number 033R132A).

Preparation of enriched nickel-63 for nuclear β -voltaic batteries and coatings on its base

A. Kostylev, V. Mazgunova, M. Alyapyshev

*Khlopin Radium Institute JSC, Saint-Petersburg, 2nd Murinsky av., 26, Russia
radium@khlopin.ru*

Radionuclide Nickel-63 is an ideal source of energy for the long-lived (≥ 30 years) and miniature atomic batteries (AB). For their production, it is desirable to use Nickel-63 with enrichment of at least 80%. Currently, only commercial product with enrichment of 18-20% is available. Given report sets out a new concept of preparing Ni-63 with enrichment of 80-90%, thus increasing the efficiency of Nickel-63 containing AB by dozens of times. According to this concept at the first stage corresponding raw material Nickel-62 with enrichment of 70-80% is irradiated with neutrons in conventional nuclear power plants with the thermal neutron flux of $5 \cdot 10^{13}$ - $1 \cdot 10^{14}$ n/cm²s. This approach allows irradiation of the large amount of Nickel-62 without disturbing the planned modes of the nuclear power plants. After irradiation cycle (2-3 years) the Nickel-62 target undergoes corresponding radiochemical purification to remove γ -emitting isotopes, and then the targets are subjected to centrifugal separation for preparing Ni-63 of the required concentration. The material remaining after centrifugal enrichment of Ni-63 can be reused in production of the next batch of Nickel-63. As a result, almost waste-free closed production cycle is realized.

The experience gained in Russia in the enrichment of some other radionuclides, such as iron-55, tin-119, and krypton-85 is very important for the development of the production of highly enriched Nickel-63. For plating of nickel-63 on the semiconductor substrate a method of chemical vapor deposition of nickel-63 (CVD method) is proposed. This method allows to receive homogeneous dense coating with good adhesion to the substrate. Additionally the losses of initial material are minimal. The samples of nickel-63 coatings on semiconductor substrates by chemical vapor deposition at various substrate temperatures in the range 200 - 450 °C were obtained.

Evaluation a radionuclide purity of ^{226}Th formed from the decay of ^{230}U for Targeted Alpha Therapy

R. Misiak¹, M. Bartyzel¹, B. Wąs¹, J.W. Mietelski¹, A. Bilewicz²

1. *Institute of Nuclear Physics Polish Academy of Sciences, Krakow, Poland*

2. *Institute of Nuclear Chemistry and Technology, Warszawa, Poland*

Targeted Alpha Therapy (TAT) is a promising approach for cancer treatment because curative doses of radiation potentially can be selectively delivered not only to the primary tumor but also to metastatic lesions spread throughout the body. Morgenstern and others[1, 2] proposed a new alpha cascade emitter system U-230/Th-226, as a new option for TAT. U-230 ($T_{1/2} = 20.8$ d) can be obtained by the direct and indirect method. In order to produce U-230 by the direct method, a target of natural Th-232 is bombardment with alpha particles of energy range 50-70 MeV where the reaction $^{232}\text{Th}(\alpha, 6n)^{230}\text{U}$ takes place. In the indirect method, target of natural Th-232 is irradiated by protons[2, 3] or deuterons[4]. First, Pa-230 ($T_{1/2} = 17.4$ days) is obtained and transformed to U-230 by β^- decay. Nuclear reaction $^{232}\text{Th}(p, 3n)^{230}\text{Pa}$ allows the production of carrier-free U-230 in clinically relevant level [2]. In order to obtain Pa-230 an irradiation of natural thorium targets using a protons beam of 30 MeV at cyclotron AIC-144 of the Institute of Nuclear Physics in Krakow was carried out.

In the first stage, the alpha emitter system Pa-230/U-230 was prepared. Immediately after the irradiation of the target, a separation of the target material and Pa-230 from the fission products of thorium and the products of the Th-232 decay serie was performed. The separation was done on Dowex 50X8 resin (200-400 mesh, Fluka) used two eluents: mixture of 0,1M HCl - 0,001M HF and 1M HCl. The target material and Pa-230 were retained on chromatography column. Next the Dowex 50X8 resin was washed with mixture of 0,1M HCl - 0,01M HF. After reaching a radioactivity maximum of U-230 from beta-minus decay of Pa-230 (27-28 days from the end of the irradiation) U-230 was eluted from Dowex 50X8 resin with hydrochloric acid at a concentration of 1M.

In order to prepare the U-230/Th-226 generator the eluate of U-230 was evaporated to dryness. 8M HCl was added and repeated evaporation process. Then the radionuclides were transferred to Dowex 1X8 resin (100-200 mesh, Sigma-Aldrich) with a solution of 8M HCl. Under these conditions U-230 was retained on the resin, and radioinuclides of Th and Ra-226 (resulting from the alpha decay of Th-230) passed to the eluate, if they are present in the fraction of U-230 eluted from Dowex 50X8. At this stage, additional purification of U-230 from potential trace quantities of fission products of thorium as well as Pb-212 and Ac-228 from the thorium-232 decay series occurs.

To determination of the radionuclide purity of Th-226, several elution of Th-226 from the U-230/Th-226 generator with 8M HCl solution after reaching radioactivity equilibrium between the parent radionuclide U-230 and the decay product Th-226 (after 5 hours Th-226 reaches its maximum radioactivity) were carried out. Solutions of eluate containing Th-226 were used for the preparation of thin sources for measurements of alpha radiation. Sources were performed by coprecipitation of Th-226 on trifluoride neodymium(III) in a hydrofluoric acid medium and then filtering through a polypropylene filters (diameter 25 mm) of Triskem International Company according to the procedure presented by Silla[5]. The filter after washing was mounted on the steel discs of 25 mm in diameter. To check present alpha radiation contamination of reagents used in the seperation and coprecipitate procedure a blank was performed. All measurements of alpha radiation were conducted on alpha spectrometer -SOLOIST 450 of ORTEC Company.

The alpha spectra of Th-226 source of the second elution measured again after five months, Th-226 source of fifth elution measured again after 5 months, the blank source and clean steel discs as well as a set of clean steel disc with the pure polypropylene filter used in the filtration were similar. By comparing the spectra

significant changes in their shape not observed. The measurement time of the spectra was comparable and the geometry of the measurement was the same. A slight statistical dispersion of pulses for the selected channel for all the analyzed spectra was evident. Therefore, it was assumed that these spectra correspond to the background spectrum of alpha spectrometer. In the alpha spectra of Th-226 source of the second and fifth elution measured again after one year Po-210, a product of decay Th-226, was present.

In the spectra of alpha radioactive sources measured after the decay of the Th-226 radionuclide the presence of long-lived radionuclides Th-230 and Th-232 was not found. A preliminary study on the evaluation of the purity of Th-226 radionuclide, obtained from the decay chain of Pa-230/U-230/Th-226 by ion exchange chromatography, indicates its potential utilization in the TAT treatment. Ultimately, the same procedure for the evaluation of the purity of Th-226 radionuclide should be carried out for radioactivity of U-230 at the level of a few hundred of MBq, which is required for clinical trials.

Acknowledgement: The work was partly supported by Polish Governmental Strategic Project: Supporting technologies for the development of safe nuclear power, Action 4: Development of techniques and technologies supporting management of spent nuclear fuel and radioactive waste (No SP/J/4/143321/11)

- [1] A. Morgenstern, Ch. Apostolidis, R. Molinet, K. Luetzenkirchen, "Radionuclides for medical use." Joint Research Centre, Institute for Transuranium Elements, Patent pending: PCT/EP2005/052966 (2005) (www.jrc.ec.europa.eu)
- [2] A. Morgenstern, Ch. Apostolidis, F. Bruchertseifer, R. Capote, Th. Gouder, F. Simonelli, M. Sin, K. Abbas, "Cross-sections of the reaction Th-232(p,3n)Pa-230 for production of U-230 for targeted alpha therapy" *Applied Radiation and Isotopes* 66 (2008) 1275-1280
- [3] A. Roshchin, S. Yavshits, V. Jakovlev, E. Karttunen, J. Aaltonen, S. Heselius, "Cross sections of nonfission reactions induced in Th-232 by low-energy proton.", *Yadernaya Fizika* 60 (1997) 2121
- [4] C. Duchemin, A. Guertin, F. Haddad, N. Michel, V. M  t  vier "Th-232(d,4n)Pa-230 cross-section measurements at ARRONAX facility for the production of U-230" *Nucl Med Biol.* 41 (2014) 19-22
- [5] C.W. Sill "Precipitation of actinides as fluorides or hydroxides for high resolution alpha spectrometry" *Nucl. Chem. Waste Management* 7 (1987) 201–215

Cross section measurements for cosmochemical important elements with 80-400 MeV monoenergetic neutrons

A. Nanbu¹, K. Ninomiya¹, K. Fujihara¹, R. Yasui¹, T. Omoto¹, S. Sekimoto², H. Yashima², T. Shima³, Y. Iwamoto⁴, D. Satoh⁴, M. Hagiwara⁵, H. Matsumura⁵, S. Shibata⁶, Y. Kasamatsu¹, N. Takahashi¹, A. Shinohara¹, M. W. Caffee⁷, K. Nishiizumi⁸

¹Graduate School of Science, Osaka University, ²Kyoto University Research Reactor Institute, ³Research Center for Nuclear Physics, Osaka University, ⁴Japan Atomic Energy Agency, ⁵High Energy Accelerator Research Organization, ⁶RIKEN Nishina Center, ⁷Department of Physics, Purdue University, ⁸Space Sciences Laboratory, University of California

Introduction

Abundance ratio of isotopes, including long-life radioactive nuclides, provides us very important information in the fields of earth and planetary sciences. For example, solar activity in past can be estimated from ¹⁰Be/²⁶Al ratio in meteorites [1]. In the space, nuclear reactions by high-energy cosmic rays cause variation of isotope abundance ratios in meteorites, and high-energy neutron strongly contributed to this process. When the primary cosmic rays are irradiated to the meteorites, secondary neutrons are generated, and the neutrons can reach deeply inside of the meteorites. To advance such researches, precise knowledge on nuclear reactions by high-energy neutron are strongly desired. However, the experimental data for high-energy neutrons above 50 MeV are very limited due to difficulty to obtain high-energy monoenergetic neutron flux.

We have been studying on nuclear reactions by neutron in high energy region [2–4], by extracting monoenergetic neutron components from two neutron irradiation experiments with different angles to the incident proton direction [5]. In this work, we will report the results for determination of nuclear cross sections by 80-400 MeV neutrons.

Experiments

Beam experiments were carried out at N0 beam line in RCNP (Research Center for Nuclear Physics, Osaka University), Japan. We performed proton irradiation experiments on Li target by 80-400 MeV incident energies, and measured neutron energy spectra with two different angles to the incident proton beam direction. Fig.1 (a) shows neutron spectra with 80 MeV proton condition. By subtraction high angle component from low angle component, quasi-monoenergetic neutron component can be extracted as shown in Fig.1 (b). In the same way, we performed two neutron irradiation experiments with different angles and determined nuclear cross section by monoenergetic neutron. In this study, we selected cosmochemical important elements (C, N, O, Al, Mg,

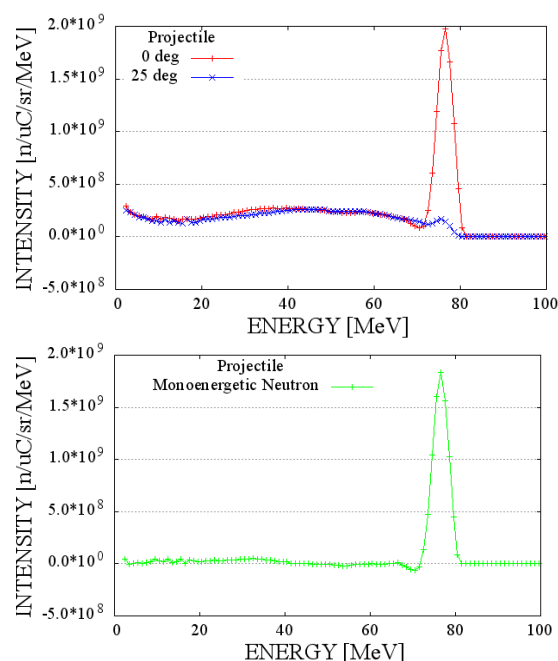


Fig. 1 Neutron energy spectra by (a) Li(p,n) reaction and (b) extracted monoenergetic neutron component.

Si, K, Ca, Fe, and Ni) as neutron irradiation targets. We identified gamma-ray activities using Ge semiconductor detectors, and determined the production rate. The details of the experimental procedures were shown in our previous literature [2–4].

Results and Discussion

Fig.2 shows examples of excitation functions by neutron irradiations for (a) ^{55}Co and (b) ^{60}Co from $^{\text{nat}}\text{Ni}$ target together with these by proton irradiation reactions. Production of neutron-rich nuclide (^{60}Co) is predominant in neutron irradiation experiment compared to proton irradiation experiment [6]. On the other hand, neutron-deficient nuclide (^{55}Co) by proton irradiation is relatively superior [7-8]. These differences are caused by the difference between the nuclear reaction mechanisms by proton and neutron irradiations. For quantitative discussion, we applied semi-empirical equation for nuclear spallation reaction proposed by Rudstam [9]. As a result, we found clear difference between proton and neutron irradiation experiment on most probable atomic charge with the same mass number. Details will be discussed in the presentation.

References

- [1] R. Michel and S. Neumann, Proc. Indian Acad. Sci. Planet. Sci. **107**, 441 (1998).
- [2] K. Ninomiya *et al.*, Proc. Radiochim. Acta **1**, 123 (2011).
- [3] S. Sekimoto *et al.*, Nucl. Data Sheets **119**, 197 (2014).
- [4] H. Yashima *et al.*, Radiat. Prot. Dosimetry **161**, 139 (2014).
- [5] J. M. Sisterson *et al.*, Nucl. Instr. Meth. B **240**, 617 (2005).
- [6] Y. E. Titarenko *et al.*, Phys. At. Nucl. **74**, 573 (2011).
- [7] J. E. Cline and E. B. Nieschmidt, Nucl. Phys. **A169**, 437 (1971).
- [8] R. Stueck, INIS Repository, 'INIS-MF--9214' (1983)
- [9] G. Rudstam, Zeitschrift Fur Naturforsch. - Sect. A J. Phys. Sci. **21**, 1027 (1966).

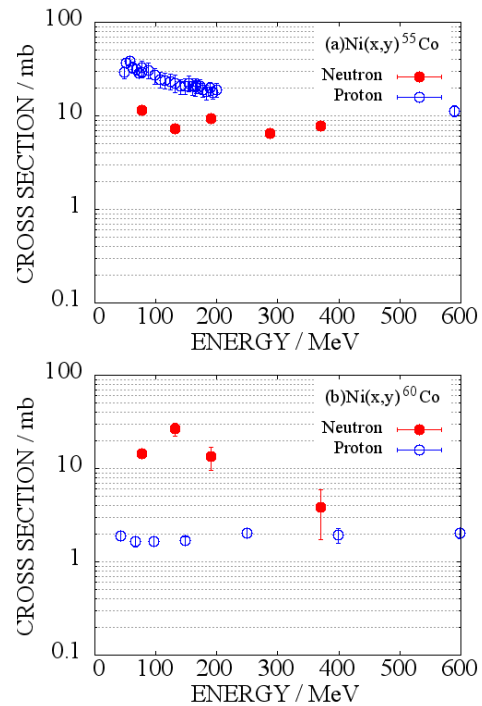


Fig. 2 Neutron excitation functions in (a) $\text{Ni}(n,x)^{55}\text{Co}$ and (b) $\text{Ni}(n,x)^{60}\text{Co}$ reaction. Excitation functions by proton reaction were obtained from the literature [6-8].

Measurements of production cross sections of Be-10 and Al-26 by 120 GeV proton bombardment of Ni-nat., Co-59, and Au-197 targets

S. Sekimoto, S. Okumura, H. Yashima, T. Ohtsuki

Kyoto University Research Reactor Institute, Japan

When a proton strikes a target nucleus with high energy, the nucleus disintegrates into smaller fragments via not only fission, but also spallation and/or fragmentation. Spallation is normally defined as an observation of a small number of light fragments accompanied with numerous individual nucleons after a reaction. A relatively high-energy process where nuclides with heavier masses than mass of the above fragments are split from a heavier target nucleus can be called fragmentation. The processes for nuclear disintegration may lead to a variety of final states, characterized by different sizes of fragments. Though the study of the processes and their applications are important in nuclear physics and nuclear chemistry, the production cross sections of light and middle-mass nuclides have been rarely reported due to difficulty in measurements. The mechanism that causes these processes is not yet clear, even with the data accumulated by experimental and theoretical studies conducted so far [1-3]. To study experimentally and theoretically the processes in detail, the production cross sections of light and middle-mass nuclides in several targets and at various proton energies are required. Recently in our laboratory, the production cross sections of light nuclides, such as the long-lived nuclides Be-10 and Al-26, have been measured, by using high-energy protons on several targets, and some results have been published [4, 5].

In this work, we measured the production cross sections of Be-10 and Al-26 for Ni-nat, Co-59 and Au-197 targets using a proton energy of 120 GeV. The results were compared to the production cross sections of the light nuclides that were produced by targets of various mass numbers when protons of various kinds of energy were used. The dependence of the production cross sections of those nuclides on the incident energy and on the target mass number will be discussed.

[1]Shibata et al., PRC 48(1993)2617. [2]Michel et al., NIMB 103(1995)183. [3]Shibata et al., Radiochim. Acta, 80(1998)181. [4]Sekimoto et al., NIMB 294(2013)475. [5]Sekimoto et al., NIMB 361(2015)685.

Quality of accelerator produced ^{99m}Tc based on $^{100}\text{Mo}(\text{p},2\text{n})$ reaction

S. Takács

Institute for Nuclear Research, Hungarian Academy of Sciences, 4026 Debrecen, Hungary

The ^{99m}Tc is the most frequently used radionuclide in nuclear medicine. It is produced in nuclear reactors and available in a $^{99}\text{Mo}/^{99m}\text{Tc}$ generator technology. As an alternative to the reactor production of ^{99}Mo and the $^{99}\text{Mo}/^{99m}\text{Tc}$ generator technology is the direct production of ^{99m}Tc on accelerators. Among the accelerator approaches the production route based on the $^{100}\text{Mo}(\text{p},2\text{n})^{99m}\text{Tc}$ reaction is one of the most promising one. To provide reasonable prediction by calculation on the quality, (chemical purity, isotopic purity, radionuclidic purity, and specific activity) of the ^{99m}Tc product, one should have well established nuclear decay data and cross section data for all the reactions and radio nuclides potentially involved in the production process. Most of the required data are available. Regarding the cross section data of the $^{100}\text{Mo}(\text{p},2\text{n})^{99m}\text{Tc}$ main reaction there are large discrepancies. There were efforts to determine the amplitude of the excitation function of the $^{100}\text{Mo}(\text{p},2\text{n})^{99m}\text{Tc}$ reaction, by several laboratories, but the data are still not satisfactory. The shape for most of the published excitation functions for the $^{100}\text{Mo}(\text{p},2\text{n})^{99m}\text{Tc}$ reaction is similar but the amplitude of the excitation functions are different by a factor of two. The results of the latest measurements by different laboratories tend to approach a common value but there is still question: what is the proper amplitude. To answer this question dedicated experiments were performed using the latest decay data and optimizing the experiment for determination of the cross section of the $^{100}\text{Mo}(\text{p},2\text{n})^{99m}\text{Tc}$ reaction. Three independent experiments were performed using the standard activation method, the stacked foil target technique and off line high resolution gamma spectrometry to measure the cross sections [1]. Although in the three independent experiments the same values were deduced for the cross section of the $^{100}\text{Mo}(\text{p},2\text{n})^{99m}\text{Tc}$ and $^{100}\text{Mo}(\text{p,pn})^{99}\text{Mo}$ reactions an additional thick target yield experiment were also performed to prove the deduced cross section data and confirm their quality [2]. Results on cross section measurements in comparison with the available experimental data and TALYS calculation is presented as well as the confirming results of the thick target yield experiment will be shown.

The quality of the accelerator produced ^{99m}Tc is very much depends on the cross section of the $^{100}\text{Mo}(\text{p},2\text{n})^{99m}\text{Tc}$ reaction, the composition of the ^{100}Mo enriched target material, the bombarding proton energy, irradiation time, cooling time, post processing time. Due to the composition of the target material a series of other Tc radionuclides are produced which should be minimized by keeping the bombarding energy low and applying the shortest irradiation time. Dependence of the unwanted Tc radionuclides on the production parameters will be presented. Effect on the isotopic composition of the recovered highly enriched target material by successive irradiation is estimated.

[1] S. Takács, A. Hermanne, F. Ditrói, F. Tárkányi, M. Aikawa; Reexamination of cross sections of the $^{100}\text{Mo}(\text{p},2\text{n})^{99m}\text{Tc}$ reaction, Nucl. Instrum. Methods in Phys. Res. 347(2015)26-38

[2] S. Takács, F. Ditrói, M. Aikawa, H. Haba, N. Otuka, Benchmark experiment for the cross section of the $^{100}\text{Mo}(\text{p},2\text{n})^{99m}\text{Tc}$ and $^{100}\text{Mo}(\text{p,pn})^{99}\text{Mo}$ reactions, Nucl. Instrum. Methods in Phys. Res. 375(2016)60-66

R&D on $^{99}\text{Mo}/^{99\text{m}}\text{Tc}$ separation-concentration apparatus based on solvent extraction and column chromatography

Kunihiko TSUCHIYA¹, Yoshitaka SUZUKI¹, Kaori NISHIKATA¹, Akira SHIBATA¹, Natsuki NAKAMURA¹, Masakazu TANASE², Takayuki SHIINA², Akio OHTA², Masako KAWABATA², Nobuhiro TAKEUCHI²

1: Japan Atomic Energy Agency, 4002, Oarai, Higashi-Ibaraki, Ibaraki 311-1393, Japan

2: Chiyoda Technol Corporation, 3681, Oarai, Higashi-Ibaraki, Ibaraki 311-1313, Japan

Technetium-99m ($^{99\text{m}}\text{Tc}$), a daughter nuclide of ^{99}Mo , is the most commonly used medical radioisotope. In case of Japan, all of ^{99}Mo are imported from foreign countries, and the domestic demand of ^{99}Mo is estimated to be 1,000 6-day Ci/week.

Japan Atomic Energy Agency (JAEA) and Chiyoda Technol Corporation (CTC) therefore have a plan to stably produce $^{99\text{m}}\text{Tc}$ from ^{99}Mo , by ^{98}Mo (n, γ) reaction using Japan Materials Testing Reactor (JMTR) under Tsukuba International Strategic Zone. Under the system, our project has been carried out as “Domestic Production of Medical Radioisotope (Technetium-99m) in Japan” in order to create new industries with a global vision since October 2013. We proposed a solvent extraction method followed by a column chromatography, which was confirmed to be very effective in order to recover a large quantity of $^{99\text{m}}\text{Tc}$ at once [1].

In this study, we developed a new $^{99}\text{Mo}/^{99\text{m}}\text{Tc}$ separation-concentration apparatus for domestic production of $^{99\text{m}}\text{Tc}$, and performed the efficiency tests of the apparatus in the dissolution and extraction processes using non-radioactive materials.

Figure 1 shows schematic diagram of the $^{99}\text{Mo}/^{99\text{m}}\text{Tc}$ separation-concentration apparatus. This apparatus consists of a MoO_3 -pellet dissolver, an extraction & separation vessel, and two alumina columns. The advantage of all parts is that it is made of radiation-resistant stainless steel (304SS) for processing more than 200 Ci of ^{99}Mo with a capacity of using natural MoO_3 pellets of up to 500 g in a large quantity. The MoO_3 -pellet dissolver is furnished with an electric heater and a rotating textile-form basket for the dissolution of the pellets. The extraction & separation vessel is furnished with the rotor for extracting $^{99\text{m}}\text{Tc}$ into MEK and with a conductivity detector for separating the Mo solution and MEK containing $^{99\text{m}}\text{Tc}$. After the extraction and separation processes, $^{99\text{m}}\text{Tc}$ is purified with a basic alumina column, adsorbed and concentrated on an acidic alumina column, and eluted with saline.

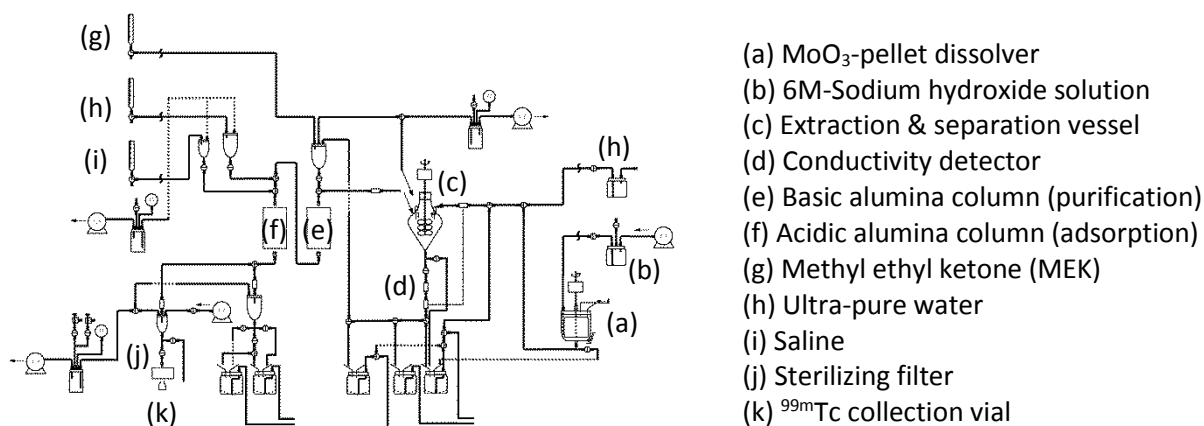


Figure 1. Schematic diagram of $^{99}\text{Mo}/^{99\text{m}}\text{Tc}$ separation-concentration apparatus

The efficiency tests of the apparatus were performed with non-radioactive MoO_3 and rhenium (Re) which was used as a substitute of $^{99\text{m}}\text{Tc}$.

The MoO_3 pellet (12.8 g) with over 90% theoretical density and the MoO_3 powder (287.2g) were used in the dissolution test. The materials of 300 g were dissolved with 6M- NaOH solution (750mL) under the conditions of heating the solution at about 50 degree and stirring it at 250 rpm. Figure 2 shows the photograph of the MoO_3 pellet in the dissolution test. From the result, it was confirmed that the high- density MoO_3 pellet could be dissolved for 2 hours.

To the Mo solution prepared above, 426-580 μg of Re, which are equivalent to 12.4-16.9 TBq (336-457 Ci) of $^{99\text{m}}\text{Tc}$ [2], was added. The Mo/Re solution was used in the extraction test. The Mo/Re solution and 90 ml of MEK were mixed and stirred at 350 to 600 rpm of the rotor speed for 5 and 10 minutes in order to extract Re into MEK. After standing for 5 minutes, the Mo solution and the MEK containing Re were separated by the conductivity detector. The amounts of Re extracted with MEK were measured by ICP-MS device. Figure 3 shows the result of Re extraction rates in the extraction test. The result suggests that the extraction rates were affected by the extraction time and the rotor speed, and reached to our target value of 90 %.

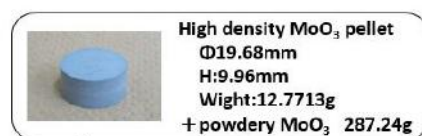
In future, the further efficiency tests in the purification & concentration processes by column chromatography using two kinds of alumina will be performed with non-radioactive materials, and will carry out empirical studies for the commercial production of $^{99\text{m}}\text{Tc}$ in JMTR Hot Laboratory.

Acknowledgement

This study has been carried out for the project 6 (Domestic Production of Medical Radioisotope (Technetium-99m) in Japan under the “Tsukuba International Strategic Zone”. The authors wish to thank the project members (Ibaraki Prefectural officials and Tsukuba Global Innovation Promotion Agency personnel) for his helpful comments in the preparation of this paper.

References

- [1] T. ISHIDA, T. SHIINA et al., “Establishment of Experimental System for $^{99}\text{Mo}/^{99\text{m}}\text{Tc}$ Production by Neutron Activation Method”, JAEA-Technology 2015-030, (2015), (in Japanese).
- [2] M. TANASE, T. SHIINA, et al., “Development of $^{99\text{m}}\text{Tc}$ Production from $(n, \gamma)^{99}\text{Mo}$ ”, Proceedings of the 5th International Symposium on Material Testing Reactors (ISMTR-5), Columbia, MO, USA, October, 22-25, 2012, <http://www.murr.missouri.edu/ismtr/papercall/index.shtml>.



Dissolution with 6M- sodium hydroxide solution




Mixing Time (min)	30	60	90
Photograph of MoO_3 pellet			
Liquid Temperature	46°C	46°C	47°C

Figure 2. Photograph of MoO_3 pellet in the dissolution test.

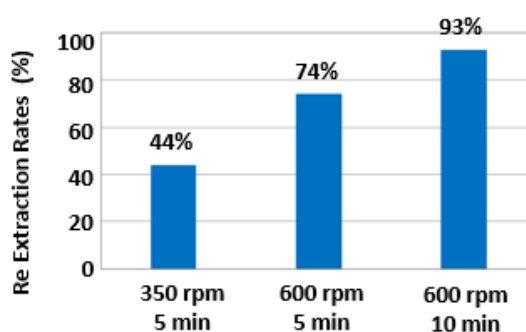


Figure 3. Result of Re extraction rate in the extraction tests.

Separation of the samarium-europium radiolanthanide couple for the production of medical samarium-153 using radiation-resistant supported ionic liquid phases

Michiel Van de Voorde^{1,2}, Peter Zsabka^{1,2}, Karen Van Hecke¹, Simone Cagno¹, Thomas Cardinaels^{1,2}, Koen Binnemans²

¹ SCK•CEN, Radiochemical Analyses and Processes, Institute for Nuclear Materials Science, Mol, Belgium

² KU Leuven, Department of Chemistry, Heverlee, Belgium

Several radioisotopes of elements of the lanthanide series, like ^{153}Sm , are being applied in the field of therapeutic radiopharmaceuticals. These radiolanthanides are mainly being used for treatment of different types of bone cancer because of their favorable physical decay properties since they consist of β^- emitting radioisotopes. Moreover, they can also be used for bone imaging with the use of γ -ray detectors because of the emission of γ -photons during decay. The ^{153}Sm radionuclide is produced via neutron irradiation of a target of enriched ^{152}Sm , i.e. $^{152}\text{Sm}(n,\gamma)^{153}\text{Sm}$ ($t_{1/2} = 46.284$ h). The stable ^{153}Eu isotope is formed via subsequent β^- decay of ^{153}Sm , which can be excreted by the human body without causing additional problems. The ^{153}Sm radioisotope can be produced in the BR2 reactor, considered as a major facility for routine supply of radioisotopes, available at the Belgian Nuclear Research Institute (SCK•CEN). This production is characterized by high specific activities, i.e. 4500 Ci ^{153}Sm per gram of ^{152}Sm . Enriched samarium targets are irradiated during 4 days in a thermal neutron flux of 3.5×10^{14} n/cm²s, being carried out in dedicated in-core devices within standard irradiation cycles of 3-4 weeks. BR2's current annual operating regime is based on five irradiation cycles.^[1] This high neutron flux is needed to ascertain the specific activity of the ^{153}Sm radioisotope. ^{154}Eu ($t_{1/2} = 4.761$ y) is also formed in the targets by neutron capture of ^{153}Eu (decay product of ^{153}Sm). By keeping the irradiation time rather short, the amounts of this impurity can be kept relatively low compared to the ^{153}Sm activity, allowing the ^{153}Sm to be used without purification from Eu. This is, however, associated with the drawback of a rather short shelf-life of the ^{153}Sm product since the ratio of $^{153}\text{Sm}/^{154}\text{Eu}$ decreases significantly with time. To increase the availability of the product, it would be beneficial if the shelf-life could be increased and/or the irradiation time could be prolonged. Therefore, the ^{154}Eu has to be removed from the ^{153}Sm . This, however, is not straightforward since trace amounts of europium have to be removed from large amounts of samarium. Since both are neighbouring lanthanides, the very similar chemical properties have to be taken into account. Moreover, one has to deal with the issues related to the handling of radioactive materials. To minimize the dose rate for the operators, a separation method that could be automatized would be beneficial. Furthermore, the radiation resistance of chemicals and materials that are used in the separation processes is important.

The irradiated solid target is usually first dissolved in highly acidic environment. Afterwards the unwanted by-products can be removed by different separation methods. In this study, the use of *supported ionic liquid phases* (SILPs) for the separation of the aforementioned radiolanthanide pair is investigated. Ionic liquids (ILs) are solvents that consist entirely of ions and they are very interesting alternative for the molecular organic phase in solvent extraction processes. Since bulk ionic liquids are often highly viscous, the kinetics of solvent extraction mechanisms might be rather slow. In SILPs, however, a thin layer of the ionic liquid is immobilized on a high-surface area solid support, leading to faster solvent extraction kinetics. In this study, immobilization of the IL was done physically by impregnation to preserve the properties of the bulk IL. This way, performance of the immobilized and bulk IL can be compared. To prevent high losses of the IL, the hydrophobicity of the IL cation is very important. Since fluorinated ILs have to be prevented, both for radiolysis and waste treatment reasons, hydrophobicity was achieved by using a cation with long alkyl chains. An aromatic group

was added to increase the radiation resistivity. To meet the requirements, the IL cation benzyltriocetylammmonium was chosen in combination with a chloride or nitrate anion.

Europium has the ability of being relatively stable for a short period of time when being reduced to its divalent state by a strong reducing agent, e.g. by Zn(0). This reduction changes the chemical properties of europium, leading to the possibility to separate europium from the other lanthanides, including neighbouring samarium. Since the properties of Eu(II) are similar to the ones of Sr(II), the latter ion can be used to simulate the behaviour of Eu(II) in the development of the Sm(III)-Eu(II) separation. Therefore, in this investigation the extractability of Sm(III) is compared to the extractability of Sr(II). It was been reported in the literature that Sr(II) can be extracted by crown ethers.^[2] Therefore, the use of a crown ether dissolved in the IL phase is studied here for the separation of the Sm(III)-Sr(II) couple. Dicyclohexano-18crown6 (DCH18C6) was chosen because of its high radiation resistivity, good extractability for alkali and alkaline earth ions and a low solubility in water.^[2] Sm(III) is hardly extracted, both in bulk and supported IL phases, whilst Sr(II) (and Eu(II)) are partially removed from the aqueous phase, together with Zn(II) in case chemical reduction of europium with Zn(0) was used. When applying this extractant in a SILP using a column setup, it should be possible to separate the Sm(III)-Sr(II) couple, and thus the Sm(III)-Eu(II) couple, eluting Sm(III) first. Sr(II) (and Eu(II)) can be eluted by changing the nitric acid concentration in the mobile phase. Via this method the pure ¹⁵³Sm radioisotope might be obtained in a faster way compared to separation techniques currently used, where Eu(II) and other possible impurities are eluted first.^[3, 4] Moreover, the separation can be performed without the use of any volatile organic solvents.

Since europium has to be reduced during the initial stage of the procedure, it is important that europium stays in its reduced form until separation is achieved. This has the consequence that oxidizing agents, including nitrate, must be avoided in the first part of the separation procedure. Therefore, different extraction conditions were investigated, where mainly the anions in the aqueous and ionic liquid phases are changed. Extraction experiments using stable isotopes, i.e. Sm(III), Eu(III) and Sr(II) as a simulant for Eu(II), have been conducted from chloride-to-chloride, nitrate-to-nitrate, chloride-to-nitrate and nitrate-to-chloride media to determine the distribution ratios, percentage extraction, separation factors and the kinetics of the extraction. This way, different conditions can be compared to each other to find the optimal extraction parameters.

Complementing radiation stability studies on the ionic liquid phase, both bulk and supported, and the crown ether will provide information about the influence of irradiation on the extraction performance of the investigated system. Other immobilization techniques to create SILPs that eliminates any IL losses (e.g. by chemical immobilization) and the influence of different solid supports will be part of future investigations.

1. Ponsard, B., *Production of radioisotopes in the BR2 high-flux reactor for applications in nuclear medicine and industry*. Journal of Labelled Compounds & Radiopharmaceuticals, 2007. **50**(5-6): p. 333-337.
2. Ao, Y.Y., et al., *Radiolysis of crown ether-ionic liquid systems: identification of radiolytic products and their effect on the removal of Sr²⁺ from nitric acid*. Physical Chemistry Chemical Physics, 2015. **17**(5): p. 3457-3462.
3. Bourgeois, M., et al., *Sm isotope composition and Sm/Eu ratio determination in an irradiated Eu-153 sample by ion exchange chromatography-quadrupole inductively coupled plasma mass spectrometry combined with double spike isotope dilution technique*. Journal of Analytical Atomic Spectrometry, 2011. **26**(8): p. 1660-1666.
4. Islami-Rad, S.Z., et al., *Reactor production and purification of ¹⁵³Sm radioisotope via ^{nat}Sm target irradiation*. Radiochemistry, 2011. **53**(6): p. 642-645.

Synthesis and evaluation of inorganic ion-exchangers for separation of medically relevant radioisotopes

YOUNES, Ali; FITZSIMMONS, Jonathan; ABRAHAM, Alyson; BONICH, Lindsay; MEDVEDEV, Dmitri

Brookhaven National Laboratory, USA, NY, 11973

dmedvede@bnl.gov

While off-the-shelf organic based ion exchange resins have been used extensively for purification of medical isotopes, under certain circumstances their use results in somewhat cumbersome separation processes. It is especially common in high energy accelerator isotope production, where cross sections are somewhat low and massive (tens of grams) targets are used to produce Curie quantities of the radionuclide. Commercially available ion-exchange resins often exhibit appreciable selectivity both for the target material and radionuclide of interest in most media. This results in the need to use large columns and lengthy processes. We synthesized a number of ion-exchange materials to evaluate their potential to aid in separation of medically relevant isotopes. Among processes of interest were separations of ^{225}Ac from gram amounts of $^{\text{nat}}\text{Th}$, ^{44}Ti from gram amounts of $^{\text{nat}}\text{Sc}$, ^{225}Ac from ^{140}La , ^{72}Se from gram quantities of $^{\text{nat}}\text{As}$, ^{82}Sr from gram quantities of $^{\text{nat}}\text{Rb}$. We focused on the materials with two types of structural frameworks: layered and tunnel type. Layered Sodium nonatitanate (SNT), and α -Zirconium phosphate (α -ZrP) as well as tunnel type crystalline silicotitanate (CST)* of different crystallinities and potassium titanate silicate pharmacosiderite (TSP) were synthesized using hydrothermal methods. Once the phase was confirmed by X-Ray powder diffraction**, the ion-exchange properties of the synthesized materials were evaluated by the batch technique in the solutions with pH ranging from 0 to 4. Analyses of initial and final solution were conducted either by ICP-OES or gamma spectroscopy. The distribution coefficients (K_d) were calculated, compared, and the best conditions for separations were determined. The results showed the following: (i) $^{\text{nat}}\text{Th}/^{225}\text{Ac}$: higher selectivity for actinium over thorium was observed by SNT and ZrP at pH of 4.5, (ii) $^{72}\text{Se}/^{72}\text{As}$: TSP was found to be more selective for arsenic than for selenium at pH 1.5 (iii) $^{82}\text{Rb}/^{82}\text{Sr}$: CST and TSP showed selectivity for rubidium over Sr. Results of these experiments along with others mentioned above will be detailed in the talk.

This work is supported by Brookhaven Science Associates, LLC under Contract No. DE-SC0012704 with the U.S. Department of Energy (DOE). The research was funded by U.S. DOE office of Nuclear Physics Isotope Program (ST-50-01-02).

* CST samples for preliminary testing were provided by Dr. Aaron Celestian of Western Kentucky University, Bowling Green, KY, USA.

** X-ray diffraction measurements were carried out at the BNL Center for Functional Nanomaterials.

Radiometric determination of thyrotoxic effects of exogenous bromide

S. Pavelka^{1,2*}

¹*Institute of Physiology, Czech Academy of Sciences, Prague*

²*Institute of Biochemistry, Faculty of Science, Masaryk University, Brno, Czech Republic*

*Stanislav.Pavelka@fgu.cas.cz

INTRODUCTION

Recently, we have shown (Pavelka, 2012) in the isolated rat thyroids marked effects of excessive exogenous bromide and perchlorate ions on the activity of the key enzyme in thyroid hormones metabolism, on thyroid peroxidase (TPO). In contrast to iodine, which forms an irreplaceable part of thyroid hormones (TH) and is one of the essential substances, inevitable for the proper development of young mammals, in case of similar halogen bromine, there is not enough information available on its biological function. This ubiquitous trace element has not been conclusively shown to perform any essential function in animals, plants or microorganisms (for review see Pavelka, 2004a, 2004b, and Pavelka, 2009a, 2009b). Using several radioanalytical methods, including an improved radiometric enzyme assay for TPO, we followed here in more details effects of an enhanced bromide and/or perchlorate ions intake on various aspects of iodine metabolism and, consequently, on metabolism of TH in the rat.

EXPERIMENTAL

Presumed goitrogenic and thyrotoxic effects of excessive bromide and perchlorate ions were followed in adult male Wistar rats, as well as in lactating rat dams and their breast-fed pups. The animals were maintained on diets with various iodine content, ensuring either sufficient iodine supply (on a standard diet B) or mild to severe iodine deficiency (on a very low-iodine diet R). The rats were administered subchronically (for 7 up to 56 days, in drinking water) either with bromide alone (in solutions of Br⁻ with concentrations of 1, 2, 3 and 5 g L⁻¹) or Br⁻ in combination with perchlorate (in solution with concentration of 10 g L⁻¹). The influence of an extremely high bromide intake (> 160 mg bromide per animal per day), and also of lower intakes, on the uptake of [¹³¹I]-iodide by the rat thyroids was determined by in vivo gamma-spectrometry (using Pb collimator). At the end of each experiment, after decapitation of the animals, relative weights of the isolated thyroids were measured. In blood sera of the rats, concentrations of total thyroxine (tT₄) were determined with the use of commercial radioimmunoassay (RIA) kits.

For studies at the molecular level, we adapted the radiometric enzyme assay for TPO (Nakashima and Taurog, 1978). The procedure for radiometric determination of TPO in isolated microsomal fractions of the rat thyroids was based on the ability of TPO to oxidize [¹²⁵I]-iodide in the presence of H₂O₂, which was the immediate oxidant for this reaction and was generated in situ by glucose oxidase. TPO further catalyzed subsequent iodination of specific tyrosyl residues bound in a large glycoprotein thyroglobulin, added in the incubated reaction mixtures.

RESULTS AND DISCUSSION

Van Leeuwen et al. (1988) stated that excessive exogenous bromide inhibited the TPO activity in the rat thyroid glands. With the aid of our improved radiometric assay for TPO, we found that the influence of exogenous bromide on the TPO activity in the rat thyroids was in fact biphasic, in relation to the extent of bromide intake in the animals. An increase (up to 3-fold) in TPO activity was measured in rats with a low or moderate bromide intake (below ca. 50 mg per animal per day), while in animals with very high bromide intake (over ca. 160 mg per animal per day) its thyrotoxic effects prevailed and TPO activity was reduced. This goitrogenic effect of bromide was much more pronounced in rats maintained on very low-iodine diet R (Fig. 1).

We measured a sharp reduction of the 24-h uptake of [¹³¹I]-iodide by the thyroids of rats administered with bromide and perchlorate ions. The suppressive effect of perchlorate on the uptake of radioiodide was much more pronounced (not shown). A consistent increase in relative weight of the rats' thyroid glands with

increasing time and concentration of applied bromide was observed (Fig. 2). In all these animals, we also determined a steady decline in serum total thyroxine concentration.

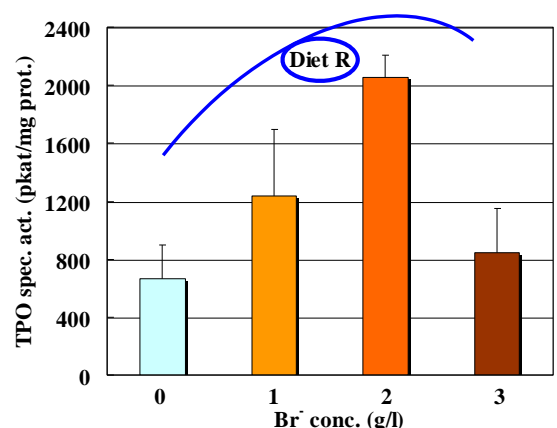


Fig. 1 Thyroid peroxidase (TPO) specific enzyme activity (pkat/mg prot.), determined in microsomal fractions of the thyroid glands of rats maintained for up to 56 days on very low-iodine diet R, in dependence on the extent of bromide intake. The results are means \pm SD for n = 6–8 male rats.

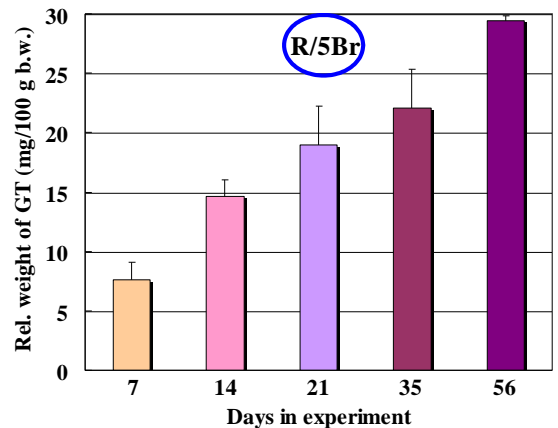


Fig. 2 Relative weight (mg/100 g b.w.) of the thyroid glands of rats maintained for up to 56 days on very low-iodine diet R, in dependence on duration of the treatment. The rats drank permanently water containing bromide 5 g L⁻¹. The results are means \pm SD for n = 8 male rats.

CONCLUSIONS

The presumed thyrotoxic effects of xenobiotics bromide and perchlorate ions have been confirmed and quantified. Excessive bromide exerted a biphasic effect on the enzyme activity of TPO, in dependence on the extent of bromide intake in the animals, and also of iodine content in their diet.

REFERENCES

- Pavelka S. (2012) Radioiodine tracers as useful tools in studies of thyrotoxic effects of exogenous bromide and perchlorate ions. *Journal of Radioanalytical and Nuclear Chemistry* 291: 405-408.
- Pavelka S. (2004a) Bromine (Chapter 9.3), in: *Elements and Their Compounds in the Environment. Occurrence, Analysis and Biological Relevance*, 2nd ed., vol. III (Merian E., Anke M., Ihnat M. and Stoeppeler M., Eds.). Weinheim: Wiley-VCH Verlag, pp. 1445-1455.
- Pavelka S. (2004b) Metabolism of bromide and its interference with the metabolism of iodine. *Physiol. Res.* 53 (Suppl. 1): S81-S90.
- Pavelka S. (2009a) Iodine transfer through mother's milk: The influence of bromide (Chapter 20), in: *Comprehensive Handbook of Iodine* (Preedy V.R., Burrow G.N. and Watson R., Eds.). Oxford: Academic Press, pp. 199-206.
- Pavelka S. (2009b) Bromide interference with iodine metabolism: Goitrogenic and whole-body effects of excessive inorganic bromide in the rat (Chapter 61), in: *Comprehensive Handbook of Iodine* (Preedy V.R., Burrow G.N. and Watson R., Eds.) Oxford: Academic Press, pp. 587-595.
- Nakashima T., Taurog A. (1978) Improved assay procedures for thyroid peroxidase: application to normal and adenomatous human thyroid tissue. *Clin. Chim. Acta* 83: 129-140.
- Van Leeuwen F.X.R., Hanemaaijer R., Loeber J.G. (1988) The effect of sodium bromide on thyroid function. *Arch. Toxicol.* 12 (Suppl.): 93-97.

Improved radiometric enzyme assays for extremely sensitive determination of iodothyronine deiodinases

S. Pavelka^{1,2*}

¹*Institute of Physiology, Czech Academy of Sciences, Prague*

²*Institute of Biochemistry, Faculty of Science, Masaryk University, Brno, Czech Republic*

*E-mail: Stanislav.Pavelka@fqu.cas.cz

INTRODUCTION

Recently, we have elaborated radiometric methods for sensitive determination of iodothyronine deiodinases enzyme activities in homogenates of cultured mammalian cells (Pavelka, 2010). Selenoproteins iodothyronine deiodinases (IDs) are the key enzymes in the metabolism of thyroid hormones (TH) (Bianco *et al.*, 2002). Three distinct types of IDs have been defined on the basis of substrate specificity, selectivity of the reactions they catalyze, sensitivity to inhibition by propyl-thiouracil, and response in activity that occurs in vivo with a change of thyroid status. All the three IDs of types 1, 2 and 3 (D1, D2 and D3, respectively) are integral membrane proteins which require thiols as a cofactor (Köhrle, 2002).

Radiometric enzyme assays, in general, are based on the enzymatically catalyzed conversion of radioactively labeled substrates to labeled products, and on the measurement of radioactivity of either product(s) or residual substrate after their quantitative separation. The availability of a simple and rapid method for quantitative separation of substrate and product(s) is one of the two major requirements of a radiometric enzyme assay. The other requirement is the availability of a suitable labeled substrate of known specific radioactivity.

Most of the previous studies, performed by other authors, examining IDs in different tissues and species did not perform the measurement of enzyme activity under the optimum conditions. In the present study, our objectives were, therefore, to find out proper assay conditions for measuring D1, D2 and D3 deiodinase activities in various subcellular fractions of rat and human tissues, including the concentrations of radioactively labeled substrates and thiol cofactor, the amount of total protein and enzyme concentration in the incubation mixtures, and appropriate incubation times.

EXPERIMENTAL

Our previous radiometric assays for IDs (Pavelka, 2010) were further elaborated and modified – adapted for other types of samples of biological materials (post-mitochondrial supernatants and microsomal fractions of various rat and human tissues). These radiometric enzyme assays were based on the use of high specific-radioactivity ¹²⁵I-labeled iodothyronines (NEN Radiochemicals) as substrates; sophisticated thin layer chromatography (TLC) separation of radioactive products from the unconsumed substrates; film-less autoradiography of radiochromatograms using storage phosphor screens (BAS-IP MS 2025, Fuji Photo Film Co., Japan); and quantification of the separated compounds with a BAS-5000 laser scanner (Fujifilm Life Science Co., Japan), using AIDA software (Raytest Isotopen-messgeräte, GmbH, Germany).

RESULTS

Fig. 1 shows an example of electronic image of radiochromatogram, which was prepared in the course of carrying out the radiometric enzyme assay for D1 deiodinase. The arrangement of the assays for D2 and D3 was similar. Duplicates of appropriate amounts of post-mitochondrial supernatants or microsomal fractions, isolated from samples of various rat tissues (usually 2–200 µg of protein in a volume of 20 µl, in dependence on types of tissue and ID measured) were incubated for appropriate time (usually 30 minutes) under optimum concentration conditions in the presence of the respective labeled substrate; a part at 37 °C (samples) and a part at 0 °C (corresponding blanks). The reaction was stopped on ice by adding 10 µl of a solution containing 10 µM triiodothyronine (T₃) and 10 µM thyroxine (T₄) in concentrated ammonium hydroxide (stop mix), followed by 30 µl of methanol, vortexing and centrifugation. Aliquots (4 x 2 µl) of supernatant extracts were analyzed by TLC on a silica gel plate using an optimized solvent system. Separated products of the reactions containing ≥ 0.5% of the total radioactivity applied (corresponding to ≥ 25

cpm/spot) could be detected in this way. It means that our methodology enabled determination of IDs enzyme activities, in absolute terms, as low as 10^{-18} katal. On the other hand, the same system used under proper concentration conditions (e.g., a thousand-fold pre-dilution of samples of biological materials) enabled measurement of IDs activities as high as 10^{-12} katal.

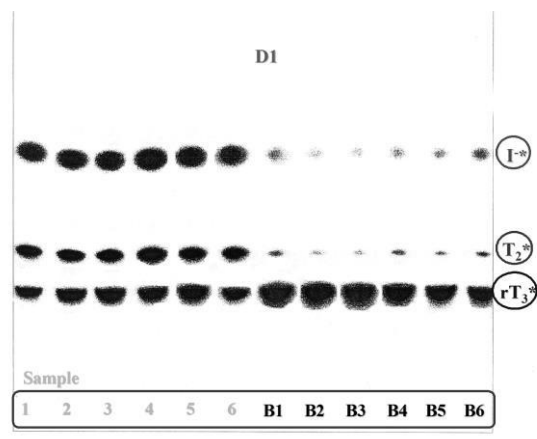


Fig. 1 Electronic image (made with BAS-5000 laser scanner) of radiochromatogram of incubation mixtures in D1 enzyme assay in kidney microsomes (Samples 1–6 and corresponding Blanks B1–B6). The radioactively labeled substrate was [^{125}I]-rT₃ and labeled products of its enzymatic conversion were [^{125}I]-3,3'-T₂ and [^{125}I]-I⁻.

CONCLUSIONS

We elaborated improved radiometric methods for extremely sensitive determination of D1, D2 and D3 iodothyronine deiodinases enzyme activities in post-mitochondrial supernatants and microsomal fractions of various rat and human tissues, as well as in homogenates of cultured mammalian cells. The assays proved to be very sensitive and rapid and, at the same time, reliable and robust.

REFERENCES

- Bianco A.C., Salvatore D., Gereben B., Berry M.J., Larsen P.R. (2002) Biochemistry, cellular and molecular biology, and physiological roles of the iodothyronine selenodeiodinases. *Endocrine Reviews* 23: 38-89.
- Köhrle J. (2002) Iodothyronine deiodinases. *Methods in Enzymology* 347: 125-167.
- Pavelka S. (2010) Radiometric enzyme assays: development of methods for extremely sensitive determination of types 1, 2 and 3 iodothyronine deiodinase enzyme activities. *Journal of Radioanalytical and Nuclear Chemistry* 286: 861-865.

The influence of foodstuff grouping on doses in safety assessments

Jari Pohjola¹, Jari Turunen¹, Tarmo Lipping¹ and Ari T. K. Ikonen²

¹ Tampere University of Technology, Pori, Finland

² Environmental Research and Assessment EnviroCase Ltd., Pori, Finland

Modelling of radionuclide transport in the environment is an important subject in assessing the safety of repositories for radioactive waste. The exposure pathways leading to the annual radiation doses for the most exposed group of people due to radionuclide releases from the repositories have to be assessed (*e.g.*, ICRP, 2013; STUK, 2014). In this paper, a scenario where a radionuclide release enters a lake with a rate of 1 Bq/year is analysed for ³⁶Cl, ¹³⁵Cs, ¹²⁹I, ²³⁷Np, ⁹⁰Sr, ⁹⁹Tc and ²³⁸U in respect of the uncertainty associated with how the foodstuff are grouped in the assessment. The biosphere system analysed consists of a lake receiving the releases and a small farm using the contaminated lake water for drinking and irrigation. The lake is based on a geomorphic landscape development model of the Olkiluoto repository site, in Finland, for the next 10,000 years (Pohjola, 2014). The landscape is changing due to coastline retreat caused by the post-glacial land uplift. This results also in the formation of several lakes near the present Olkiluoto Island. The largest of these lakes (water volume $1.8 \times 10^7 \text{ m}^3$, mean annual discharge $2.1 \times 10^7 \text{ m}^3/\text{year}$), situated southwest from the present island, was selected for this study. The assessment model is based on the agricultural well scenario presented in (Hjerpe & Broed, 2010). However, instead of using well water for human and livestock drinking water and irrigation water for crops in their scenario, here the water source is the local lake. The dose calculations have been stylised to consider only the doses through ingestion (the contribution of the inhalation and the external irradiation were found negligible in this case, *i.e.* more than 2000-fold smaller than the doses from the ingestion). The objective of the study is to find out if the model can be stylised further in respect of the soil-to-plant concentration ratios (CR) and the intake-to-animal product transfer factors (TF) by grouping the foodstuff into broader categories.

The foodstuff in the original model formulation have been divided into drinking water, fish, milk, beef, pork, mutton, eggs and poultry meat, cereals, berries, potatoes, root vegetables, leguminous vegetables, and other vegetables. The soil-to-plant concentration ratios were taken from (IAEA, 2009), consumption rates of the foodstuff from (Helldán *et al.*, 2012; for adult men) and the other parameters from (Hjerpe & Broed, 2010). In this study, nine alternative foodstuff groupings (no. 2–10 in Table 1) were formulated in addition to the original grouping (no. 1). In cases no. 2–5 the animal products were combined one by one into a broader group so that the most pessimistic ratio, taking into notice the transfer factor, the intake rates of water and fodder of the animal in question and the concentration in water and fodder, was chosen to represent the whole group. In cases no. 6–10 a similar procedure was performed for the crop plants: the most pessimistic ratio, taking into account the soil-to-plant concentration ratio and the amount of irrigation water applied, was selected for the whole group meaning that the highest concentration of radionuclides in soil and on the plant surfaces will be transferred to the plant with the highest rate.

Figure 1 shows the effect of these groupings to the dose resulting from the 1 Bq/y release of each nuclide (*i.e.*, the dose conversion factor). The overall trend is, as expected, that the doses increase with coarser grouping as a consequence of choosing the most pessimistic CR or TL. In cases no. 2–5 the increase in the doses is quite subtle. The smallest change in the dose is for ¹³⁵Cs, resulting from the CRs and the TLs having coarsely the same values. The largest changes take place at cases no. 8 (leguminous vegetables) and 10 (berries). Especially with the berries, the effect is largely due to the likely rather conservative CRs values due to the relatively weak data basis. However, in most of the cases this kind of stylised representation of dietary doses seems useful to reduce the number of variables for example in sensitivity and uncertainty analyses of broader systems.

Table 1. The foodstuff grouping cases analysed in this study.

	1	2	3	4	5	6	7	8	9	10
Eggs	X	X								
Poultry meat	X		X	X						
Pork	X	X			X	X	X	X	X	X
Beef	X	X	X							
Mutton	X	X	X	X						
Potatoes	X	X	X	X	X					
Root vegetables	X	X	X	X	X	X				
Other vegetables	X	X	X	X	X	X	X		X	
Leguminous vegetables	X	X	X	X	X	X	X			
Cereals	X	X	X	X	X	X	X	X		
Berries	X	X	X	X	X	X	X	X	X	
Drinking water	X	X	X	X	X	X	X	X	X	X
Fish	X	X	X	X	X	X	X	X	X	X
Milk	X	X	X	X	X	X	X	X	X	X

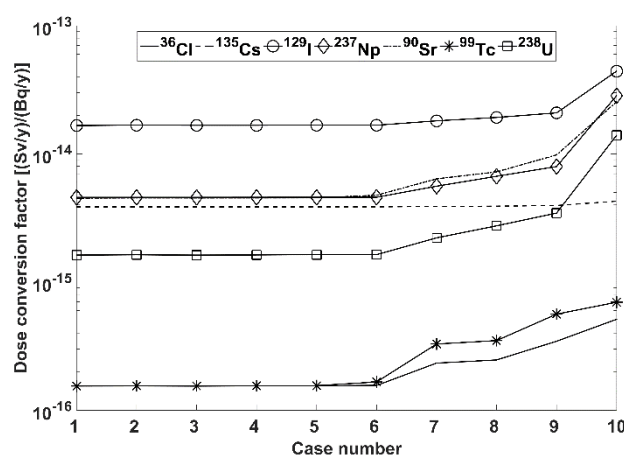


Figure 1. The dose conversion factors (doses after 10 000 years of constant release of 1 Bq/y of each nuclide) calculated for the foodstuff grouping cases outlined in Table 1.

References

- Helldán, A., Raulio, S., Kosola, M., Tapanainen, H., Ovaskainen, M.-L., Virtanen, S., 2013. The National FINDIET 2012 Survey. THL Report 16/2013, National Institute for Health and Welfare, Helsinki, Finland.
- Hjerpe, T., Broed, R., 2010. Radionuclide Transport and Dose Assessment Modelling in Biosphere Assessment 2009. Working Report 2010-79, Posiva Oy, Olkiluoto, Finland.
- IAEA, 2009. Quantification of Radionuclide Transfer in Terrestrial and Freshwater Environments for Radiological Assessments. Report IAEA-TECDOC-1616, International Atomic Energy Agency, Vienna, Austria.
- ICRP, 2013. Radiological protection in geological disposal of long-lived solid radioactive waste. ICRP Publication 122, International Commission on Radiological Protection.
- Pohjola, J., 2014. Probabilistic Modeling of Landscape Development and Surface Water Body Formation. Doctoral dissertation, Tampere University of Technology - Pori Department, Pori, Finland.
- STUK, 2014. Disposal of Nuclear Waste. Guide YVL D.5, Säteilyturvakeskus, Helsinki, Finland.

Preliminary investigation of radioactive emissions from incinerators of municipal solid waste

Fernando P. Carvalho, J. M. Oliveira, M. Malta

*Laboratório de Protecção e Segurança Radiológica
Instituto Superior Técnico/Campus Tecnológico e Nuclear, Universidade de Lisboa
Estrada Nacional 10, km 139; 2695-066 Bobadela LRS, Portugal
carvalho@itn.pt*

Incineration became a common procedure of elimination of municipal solid wastes. Residues from incineration include bottom ash from furnaces (slag) and gas and particles (fly ash) emissions into the atmosphere. Samples of these materials were analyzed for naturally occurring radionuclides, in particular alpha emitters. Materials contained in municipal solid waste, such as domestic organic waste, papers, etc., fed into incinerators are all of very low radioactivity, but mass reduction by combustion change radionuclide concentrations on a mass basis in ash produced. Fly ash displayed concentrations of 28 ± 1 Bq/kg of ^{238}U , 110 ± 8 Bq/kg, ^{226}Ra and 71 ± 5 of ^{210}Po respectively, while bottom ash displayed 121 ± 4 Bq/kg, 88 ± 18 Bq/kg and 123 ± 8 Bq/kg for the same radionuclides, respectively. However, aerosols sampled in surface air in the vicinity of the incineration plant displayed concentrations of 174 ± 5 , 435 ± 50 and 1180 ± 70 Bq/kg of ^{238}U , ^{226}Ra , and ^{210}Po respectively. The main pathways of radionuclide re concentration and release into the environment seem to be 1) volatilization of ^{210}Po and ^{226}Ra which may be released as gases followed by condensation onto and concentration in atmospheric particles, and 2) release of fly ash particles containing enhanced activities of ^{226}Ra and ^{210}Po . This preliminary work suggests that a deeper attention shall be paid to assess the radiological impact of municipal waste incineration procedures.

Distribution of radionuclides in a uranium mine pond

Fernando P. Carvalho, J. M. Oliveira, M. Malta

*Laboratório de Protecção e Segurança Radiológica
Instituto Superior Técnico/Campus Tecnológico e Nuclear, Universidade de Lisboa
Estrada Nacional 10, km 139; 2695-066 Bobadela LRS, Portugal
carvalho@itn.pt*

An abandoned uranium mine open pit abandoned in the 80s became a permanent 20 m deep pond and with about 0.34 hm³ water volume. Over the last 30 years, a freshwater ecosystem stabilized in this pond, comprising aquatic plants and introduced freshwater fish. The pond was sampled and water, bottom sediment, suspended particulate matter, phytoplankton, macrophytes, aquatic insects and fish (carps) were analyzed for naturally occurring radionuclides. Dissolved radionuclide concentrations in surface water, with 20180±530 mBq/L of ²³⁸U, 50±14 mBq/L ²²⁶Ra, 1.06±0.05 mBq/L ²¹⁰Pb, and 28±1 ²¹⁰Po were high and originate in the dissolution of low grade uranium ore in the rock from the pit. Those concentrations varied with water depth and were very different in the water deep layer, close to anoxic sediments. All uranium series radionuclides displayed high concentrations in phytoplankton, viz, 47 MBq/kg (dry weight) ²³⁸U, 50 MBq/kg ²³⁰Th, 23 MBq/kg ²²⁶Ra, 77 MBq/kg ²¹⁰Pb, and 71 MBq/kg ²¹⁰Po. Radionuclides were accumulated in all biota sampled in the lake and concentration factors were computed. These add relevant information to the data base of natural radionuclides in freshwater ecosystems. Furthermore, analysis of radionuclides in the water column and in the soft sediment accumulated on the pit bottom gave additional information about radionuclide cycling in this freshwater system.

Radon removal from groundwater using an aeration-ventilation system in a small community water supply system

Kil Yong Lee, Kyung-Seok Ko, Soo Young Cho, Dong-Hun Kim, Kyoochul Ha

Groundwater Department, Korea Institute of Geoscience and Mineral Resources, 124 Gwahang-no,
Yuseong-gu, Daejeon 305-350, Korea

kylee@kigam.re.kr

Groundwater is the important water source in many little rural communities in Korea. In the community water supply systems that use groundwater, groundwater has been stored in a holding tank after pumping from groundwater well and finally distributed to households. Based on data from a national survey on radon concentrations in groundwater wells (2,788 wells: 1,808 public water supply systems, 980 private water wells) in Korea during 1999 – 2012, 15 % of which were found to be above the US EPA's Alternative Maximum Contaminant Level (AMCL) of 148 Bq/L. Radon can be released into the indoor air when water is used for showering, washing dishes and other household uses. The objective of this study was to reduce radon from the groundwater using an aeration–ventilation system installed in the holding tank. The community water supply system examined in this study was in a little rural village located in Sangju-city, Gyeongbook-do Province, Korea. There were 50 people in 33 households and groundwater was used about 28 m³ in a day. Radon concentration in well groundwater was around 650 Bq/L which was 4.4 times higher than the US-EPA's AMCL. The aeration–ventilation system was installed in the holding tank and estimated radon removal efficiencies by using radon concentration difference between well and tank water. The system consisted of a nozzle to spray groundwater, a blower to produce air bubbles, two exhaust fan to vent radon to the atmosphere and a time controller to adjust operation conditions. The temperature of tank water was around 13°C during examination period. Thus the equilibrium partition coefficient of radon ($k=C_w/C_a$) was measured to 0.304. Flow rate of pumping water was around 65 L/min during pumping from groundwater well. Air flow rate of the blower should be at least 850 L/min to remove 90 % of radon in the well groundwater. Using the time controller, aeration-ventilation system was adjusted to operate for 5 minutes in every 10 minutes. Radon removal efficiency was estimated using radon activities of well groundwater and the tank water. The removal efficiency was ranged in 75 – 98 %.

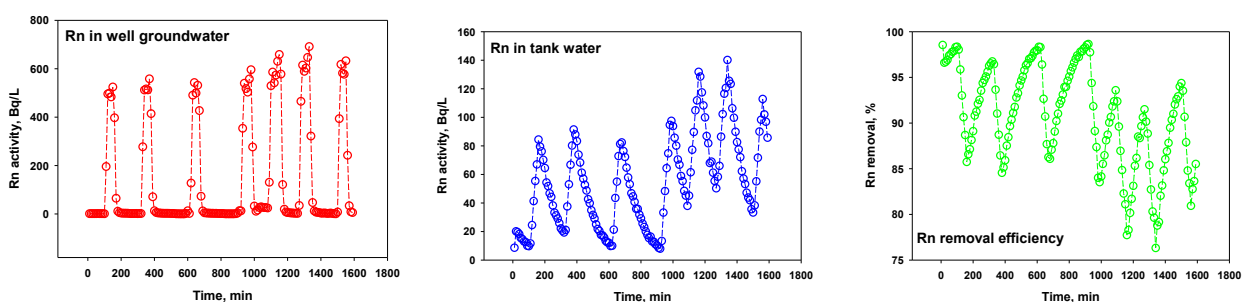


Fig. 1. Radon activities of well groundwater and holding tank water and the removal efficiencies.

Study of radium nitrate solubility in nitric acid solution

Pavel Butkalyuk, Irina Butkalyuk, Alexander Baranov, Alexander Kuprianov, Rafael Abdullov,
Rostislav Kuznetsov

*JSC "SSC RIAR", Ulyanovsk region, Dimitrovgrad, Russian Federation
orip@niiar.ru*

The solubility of radium nitrate in 61÷96 % nitric acid have been studied in two series of experiments reaching equilibria state by adding fuming nitric acid to radium nitrate solution or by partial dissolution of pre-precipitated radium nitrate. The correctness of the procedure, applied to study the solubility, was confirmed by measuring the barium nitrate solubility under the same conditions as well as by comparing the obtained values with the referenced ones.

$\text{Ra}(\text{NO}_3)_2$ precipitate was separated from the solution by centrifugation. ^{226}Ra content in solutions was measured by alpha-spectrometry; the nitric acid concentration was measured by the potentiometric titration using standard solutions of either sodium tetraborate or sodium carbonate. The measurement error of the radium concentration in the solution made up 5-10%; the one of nitric acid did not exceed 3%.

It has been found for barium nitrate solutions that depending on experimental approach (from above or from below) equilibria state is reached during 20 or 4 hours, respectively. Radium nitrate solubility has been found to decrease from ~0.025 to ~0.0004 g/100 g of solution while the nitric acid concentrations increase from 62 to 95 %. The radium nitrate solubility is higher than the barium nitrate one in the whole HNO_3 concentration range under study. Both, radium nitrate and barium nitrate solubility dependencies from nitric acid concentration can be approximated by the following empirical equation:

$$\omega(\text{Me}(\text{NO}_3)_2) = A \cdot (\omega(\text{HNO}_3))^B$$

where $A = 3.0 \cdot 10^{-6}$, $B = -9.0$ and $A = 1.6 \cdot 10^{-7}$, $B = -12.3$ with correlation factors $k=0.941$ and $k=0.977$, for radium and barium, respectively.

Radiolytic decomposition of zinc stearate in presence of PuO₂ powders

J. Gracia¹, L. Venault², J. Vermeulen², M. Guigue², J. Maurin², F. Audubert³, X. Colin⁴

¹CEA/DEN/DTEC/SECA/LFC Marcoule, BP 17171, 30207 Bagnols-sur-Cèze, France

²CEA/DEN/DRCP/SERA/LCAR Marcoule, BP 17171, 30207 Bagnols-sur-Cèze, France

³CEA/DEN/DEC/SA3C/LAMIR Cadarache, 13108 Saint-Paul-les-Durance, France

⁴PIMM, ENSAM ParisTech, 151 Boulevard de l'Hôpital, 75013 Paris, France

Zinc stearate is a metal salt of fatty acid used as lubricant in nuclear industry. The lubricant is added for the manufacturing of the oxide powder as fuel pellet. In 4th generation nuclear reactors, fuels will probably contain increasing amount of plutonium with a higher percentage of ²³⁸Pu isotope. This latter is an alpha emitter with a quite high specific activity (17.12 Ci.g⁻¹). Then, this will enhance the radiolysis phenomena induced by plutonium. The radiolytic decomposition of zinc stearate was mostly studied through radiolysis gas analysis. To carry these experiments, zinc stearate powder was put in close contact with plutonium oxide according to two configurations :

- Zinc stearate and plutonium oxide powders are pressed separately as pellets, which are piled alternately.
- Zinc stearate and plutonium oxide powders are directly mixed with a weight content of zinc stearate between 1 and 2%.

The first kind of experiments was carried out placing on top of each other several zinc stearate pellets and plutonium dioxide discs to increase the contact surface between the materials and to control it. The second configuration aims to reproduce representative conditions of manufacturing process of nuclear fuel. These two configurations are compared in order to determine as much as possible the impact of radiolysis during pelletizing of nuclear fuel and green pellet storage.

Powders are placed in an airtight cell connected to a micro gas chromatograph in order to determine the nature and the quantity of the gases produced in the cell.

Many experiments are made using plutonium oxides with different isotopic vectors, i.e. by varying quantity of ²³⁸Pu. Five gases (H₂, CO, CO₂, CH₄ and C₂H₆) have been analyzed; the major one being H₂ (Fig 1). Based on the kinetics of gases evolution, the radiolytic yields have been estimated and it appears that they do not depend on the isotopy of plutonium. By contrast, changing configuration shows that the release of carbonated species is more important when powders are mixed. Zinc stearate pellets have also been irradiated externally thanks to Cyclotron of CEMHTI laboratory. Alpha radiations are simulated using helium particles. Different energies of incident particles are employed to vary dose rate. Other particles were used – protons, deuterons – to compare impact of radiations with very different linear energy transfer (LET). Gas production was studied in the same way that during first experiments with plutonium oxide. In this way, external and internal (with PuO₂) irradiations can be compared based on radiolytic yields. The major advantage of using external irradiations is that they allow a solid study more accurate than in glove box, and a better understanding of irradiation of zinc stearate, thanks to the non-contamination of the samples. Based on the results acquired through these experiments, radiolytic decomposition mechanisms of zinc stearate are proposed.

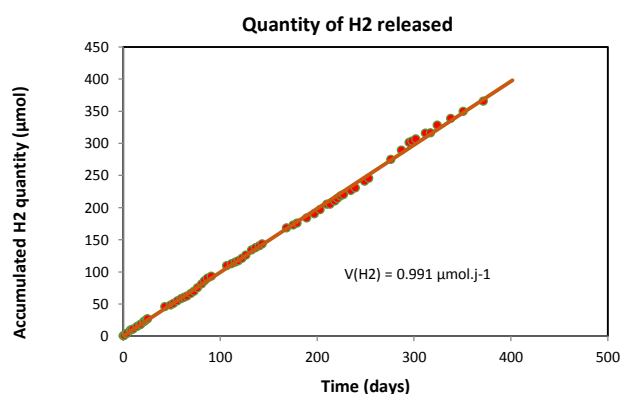


Fig.1: H₂ release kinetic during zinc stearate radiolysis

Optimization of Hauser-Feshbach statistical calculation and evolution of p nuclei with mass numbers of 130–150 in stellar environments

Norikazu Kinoshita

Institute of Technology, Shimizu Corporation, Japan

The p nuclei, which are not produced by neutron capture reactions in stars, are present at a low abundance in the solar system. The nuclides are synthesized in explosive environments such as supernovae through capture reactions of proton and alpha particles, emission reactions of neutron and alpha by photonuclear reactions, and interaction with neutrinos. Isotopic abundances of the p nuclei are smaller in heavier atoms than lighter atoms. Exceptionally, the neutron-magic p nuclei of ^{92}Mo and ^{144}Sm have greater abundances. Generally, cross sections for the capture reactions of proton and alpha particles are smaller with an increase of atom number because of the coulomb barrier. On the contrary, thresholds of neutron emission reactions are lower with an increase of atom number. The neutrino-induced reactions are hard to produce the great abundance of the neutron-magic nuclei. Our group has attempted to simulate the abundances in mass numbers of 130–150 with combination of the proton capture reactions and photonuclear reactions. In the stellar environments, the p nuclei are produced in complicated network of these nuclear reactions. Reaction rates in the nucleosynthesis can be expressed as a product of cross section and spectra of proton or photon. The Maxwell-Boltzmann distribution is used for the proton spectrum and Planck's black body spectrum for photon spectrum. Hence, cross sections of (p,g), (p,n), (g,n), (g,a) reactions at low energies are more important for the nucleosynthesis.

In the calculation for production of the p nuclei in the explosive environments, rates of numerous reaction reactions depend on theoretical predictions using the Hauser-Feshbach (HF) statistical model. Temporal variation of the abundances of the products can be numerically calculated from a balance between reaction rates of production and destruction. Evaluated cross section data give more accurate abundance. In the theoretical prediction, interaction of incoming and outgoing particle inside nuclei is controlled by an optical model potential. In addition, probability that the projectile inside the target fuses together is controlled by a level density of the compound nucleus. Cross sections of (p,g), (p,n), (a,g), (a,n), (g,n), (n,a), (n,g) reactions at low energies in mass numbers of 130–150 have been reported so far. On the contrary, no (g,a) reactions have been reported because reaction products of the (g,a) reactions are stable nuclei in the most of case. The (p,g), (p,n), (g,n), and (n,g) reactions directly contribute to the nucleosynthesis. The (a,g), (a,n), and (n,a) reactions can constrain parameters in the theoretical prediction for the (g,a) reactions. We optimized the level density model and optical model potential used in the HF statistical code of TALYS to fit experimental cross sections of (p,g), (p,n), (a,g), (a,n), (g,n), (n,a) in mass numbers of 130–150. In addition, we computed temporal variations of p nuclei, ^{136}Ce , ^{138}Ce , ^{138}La , and ^{144}Sm , in the explosive environment under temperatures of 1–2 GK (1 GK = 10^9 K).

The selections of the Back-shifted Fermi gas model [1] for the level density and optical model potential of alpha particles described by McFadden and Satchler [2] showed the best fit in the nuclear reactions at astrophysically relevant energies. The calculation using the TALYS with the best input parameters showed that the (g,a) and (g,n) reactions are more dominant than the proton capture reactions with an increase of temperature. All of the nuclei in mass numbers of 130–150 including stable nuclei decompose quickly at temperatures higher than approximately 2 GK by the (g,n) and (g,a) reactions; no nuclei are present after the nucleosynthesis. Hence, the theoretical prediction implies that the p nuclei with mass numbers of 130–150 present in the solar system had been synthesized at temperatures lower than 2 GK. In supernovae, temperature and density drastically change in a short period of time [3]. Temporal variations of p nuclei in the explosive environments are simulated using the TALYS with the optimized inputs. The present abundance of the p nuclei in the Solar System can be produced in a few seconds in the explosive environments with temperatures of 1.5–2.0 GK.

References

- [1] W. Dilg, W. Schantl, H. Vonach, and M. Uhl, Nucl. Phys. A217, 269 (1973).
- [2] L. McFadden, G.R. Satchler, Nucl. Phys. 84, 177 (1966).
- [3] M. Kusakabe, N. Iwamoto, K. Nomoto, Astrophys. J. 726, 25 (2011).

Atmosphere dependence of formation process of oxygen vacancy in zinc oxide

S. Komatsuda¹, W. Sato² and Y. Ohkubo³

¹*Department of General Education, National Institute of Technology, Ichinoseki College*

²*Institute of Science and Engineering, Kanazawa University*

³*Research Reactor Institute, Kyoto University*

Defect-induced properties of zinc oxide (ZnO) have been attracting much attention toward their application to functional materials in a wide field of industry. Especially, physical properties brought about by Al ions and/or oxygen vacancies in ZnO are one of the most intriguing topics for the development of future electronic devices. Extrinsic-semiconductor devices such as of Al-doped ZnO are expected to be in use under various ambient conditions; the states of being of impurity ions in the matrix are susceptible to change depending on the condition. For a practical use of Al-doped ZnO device, therefore, we have investigated the local structures in Al-doped ZnO under various ambient conditions by means of the time-differential perturbed angular correlation (TDPAC) method. In one of our previous TDPAC studies, we observed contrasting atmosphere dependence of the stability of aggregations of ¹¹¹In and Al impurities doped in 100 ppm Al-doped ZnO: (i) Al and In impurities associate with each other by their thermal diffusion in air, and (ii) the ¹¹¹In probe is detrapped from the Al aggregations in high-temperature vacuum, resulting in substitution at defect-free Zn sites[1,2]. Detailed investigation of the thermal behavior of the impurities has revealed that the dissociation reaction is triggered by the formation of oxygen vacancies. In the present work, in order to extend quantitative discussion on the kinetics of the formation process of oxygen vacancy, we evaluated the formation energy of oxygen vacancy from the temperature variation of the detrapping process during heat treatment in vacuum.

It was found from TDPAC spectra of the ¹¹¹In(\rightarrow ¹¹¹Cd) in 100 ppm Al-doped ZnO heat-treated at various temperature that ¹¹¹In probes come to detrapp from the Al aggregations in high-temperature vacuum by degrees. Additional TDPAC experiments have revealed that this detrapping process is controlled by the first-order rate law. For the first-order reaction of the dissociation process, the rate constant, k , can be estimated from the component of TDPAC spectra at various temperature. Figure 1 shows the temperature dependence of the rate constants. A least-squares fit to the k values was then carried out with the Arrhenius equation and the activation energy, E_a , was evaluated to be 0.72 (6) eV. Because the dissociation process of the ¹¹¹In probe and Al would be induced by the formation of oxygen vacancies as discussed above, we suggest that the observed E_a is closely related to the formation energy of oxygen vacancies in Al-doped ZnO sample. This interpretation is supported by the fact that the present E_a value shows good agreement with the theoretical ones calculated for the formation energy of oxygen vacancies in ZnO (0.8 and 1.0 eV)[3,4]. In the session, based on the further investigation of TDPAC spectra for Al-doped ZnO obtained by isochronal annealings in Ar gas atmosphere, we discuss the atmosphere dependence of the formation process of oxygen vacancy.

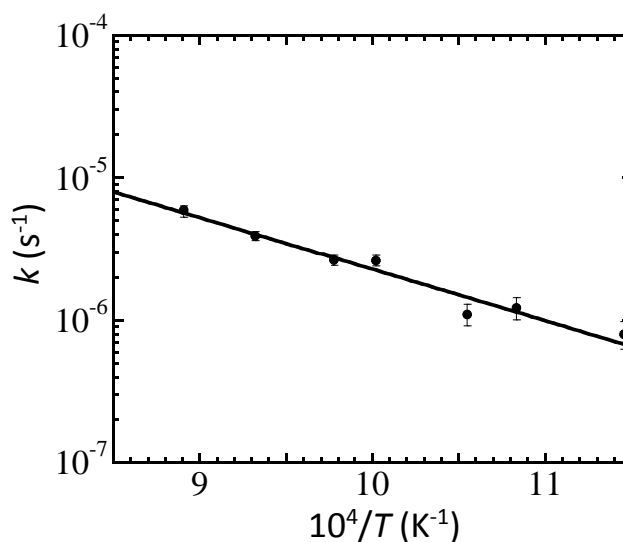


Fig. 1. Temperature dependence of the rate constant, k . An Arrhenius equation was used for the fit.

- [1] S. Komatsuda, W. Sato, and Y. Ohkubo: J. Appl. Phys. **116**, (2014) 183502
- [2] S. Komatsuda, W. Sato, and Y. Ohkubo: J. Radioanal. Nucl. Chem. **303**, (2015) 1249
- [3] S. Lany and A. Zunger: Phys. Rev. Lett. **98**, (2007) 045501
- [4] F. Oba, A. Togo, and T. Isao: Phys. Rev. B **77**, (2008) 245202

New experimental methods for light ion track etched pores in polymer films

Stewart Makkonen-Craig ^{1,2}, Avinash Bhandari ², Ksenia Yashina ², Natalia Bassein ² and Kerttuli Helariutta ¹

¹ *Laboratory of Radiochemistry, Department of Chemistry, University of Helsinki, Finland*

² *Department of Energy and Materials Technology, Arcada University of Applied Sciences, Jan-Magnus Janssonin aukio 1, Helsinki, Finland*

Membranes with precisely controlled pore sizes, morphologies and densities are commonly achieved by chemical etching of ion tracks in thin polymer films. They attract much interest due to their high selectivity in separation and sensing processes. The lower LET thresholds for creating continuous etchable latent ion tracks in such materials, e.g. PC, PET and PI, are reported as 720-900 eV nm⁻¹ [1,2]. Such dense radiolytic damage necessitates irradiation with medium to heavy ions. We have investigated new experimental strategies to test whether ion track etching thresholds can be extended down to lower LET irradiation with light ions.

8 µm thick polyarylate films were irradiated with 1.4 MeV D⁺ ions from an IBA Cyclone 10/5 cyclotron. SRIM simulations indicated that LET values were approximately 40 eV nm⁻¹. Screening conventional post-irradiation treatment and etching methods confirmed that such low radiolytic damage was insufficient for the etching of individual tracks. When the ion fluence was increased to 5·10¹² cm⁻² and irradiated films were etched in a NaOH-ethanol solution with simultaneous irradiation of UV light, continuous non-cylindrical pores were achieved (Figure 1). The physical and chemical mechanisms that permit etching of these multiply-overlapped ion tracks is under investigation. Of particular interest are the degree of ion track overlap, inter-track reactions and the influence of UV on etching.

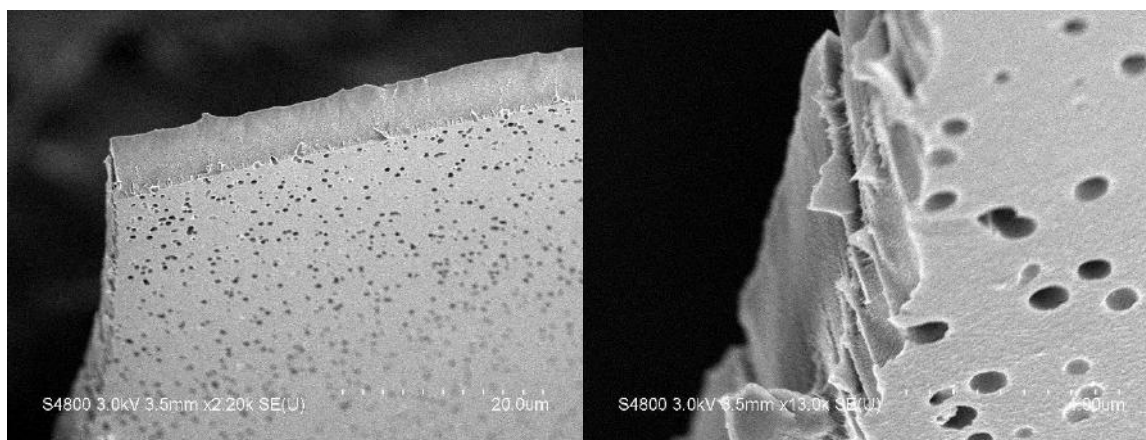


Figure 1 SEM images of pores achieved by etching low LET 1.4 MeV D⁺ ion tracks in polyarylate.

References

- [1] R.G. Musket, J. Appl. Phys. 99 (2006) 114314.
- [2] P.Yu. Apel, D. Fink, Springer Series in Materials Science 65 (2004) 147.

Development of muonic atom beam extraction system for chemical reaction studies of muonic atoms

Go Yoshida¹, Kazuhiko Ninomiya¹, Makoto Inagaki¹, Jun Aoki¹, Michisato Toyoda¹, Naritoshi Kawamura² and Atsushi Shinohara¹

¹*Graduate School of Science, Osaka University, Toyonaka, Osaka 560-0043, Japan*

²*High Energy Accelerator Research Organization (KEK), Tsukuba, Ibaraki 305-0801, Japan*

Exotic atom is an atomic system that contains charged particles except for proton and/or electron. Alike radioactive nuclides, exotic atom can be used as a probe for investigating character of various materials. Muonic atom is one of the exotic atoms that has a negatively charged muon instead of an atomic electron. Because the muon has 200 times heavier mass than that of an electron, atomic muon orbit is 200 times smaller than electronic orbit. As a result the atomic muon shields nuclear charge strongly, and from the view point of orbital electron, center charge of nucleus Z can be seemed as $Z-1$. The purpose of our study is investigation detail chemical properties of muonic Z atom; the difference between muonic Z atom and ordinal $Z-1$ atom.

Muonic atom is formed when muon is stopped in a substance. The captured muon immediately de-excites to muonic ground state by emitting Auger electrons and characteristic X-rays (muonic X-ray). By analyzing Auger electrons and muonic X-rays intensities, we can obtain the information about muon capture process; such as muon capture probability of each atom and initial quantum state of captured muon [1]. In the view point of chemical properties of muonic atoms, it is reported that the energies of characteristic X-rays of muonic Z atom are similar to ordinal $Z-1$ atom [2]. Kinetic isotope effect in muonic helium and muonium (regarded as a light hydrogen isotope) is also reported [3]. However, chemical properties of muonic atom still have been hardly investigated. We aim to investigate chemical properties of muonic atom from luminous radical reaction with muonic atom. In this study, we will report present status on development of muonic atom extraction system as atomic beam form.

Figure 1 shows the photo of the experimental system for muonic atom extraction. In this work, we applied time of flight technique to isolate and detection of muonic atoms. The experimental apparatus consists of vacuum chamber, muonic atom source (PTFE film), electrodes and detector (micro channel plate). In this study, we irradiate muon beam to PTFE film and form muonic fluorine atoms. Shortly after muonic atom formation, muonic atom takes on highly positive charged due to Auger electron emission, and evaporated from the target. Electric fields generated by electrodes accelerate and guide muonic atom to the detector. We are planning to muonic atom extraction experiment at J-PARC MUSE; the world's highest intense pulsed muon beam source [4].

For pilot study, we performed various ions acceleration and detection experiments using LASER ablation method by Nd-YAG pulsed LASER, and optimized ion beam yield and mass resolution. The mass resolution of this apparatus is determined as 300 and this is sufficient to distinguish muonic fluorine ion from ordinal fluorine ion and other back ground events. In our presentation, we will discuss experimental setup of muonic atom extraction, optimization studies of this system and preliminary results for muon irradiation experiment.

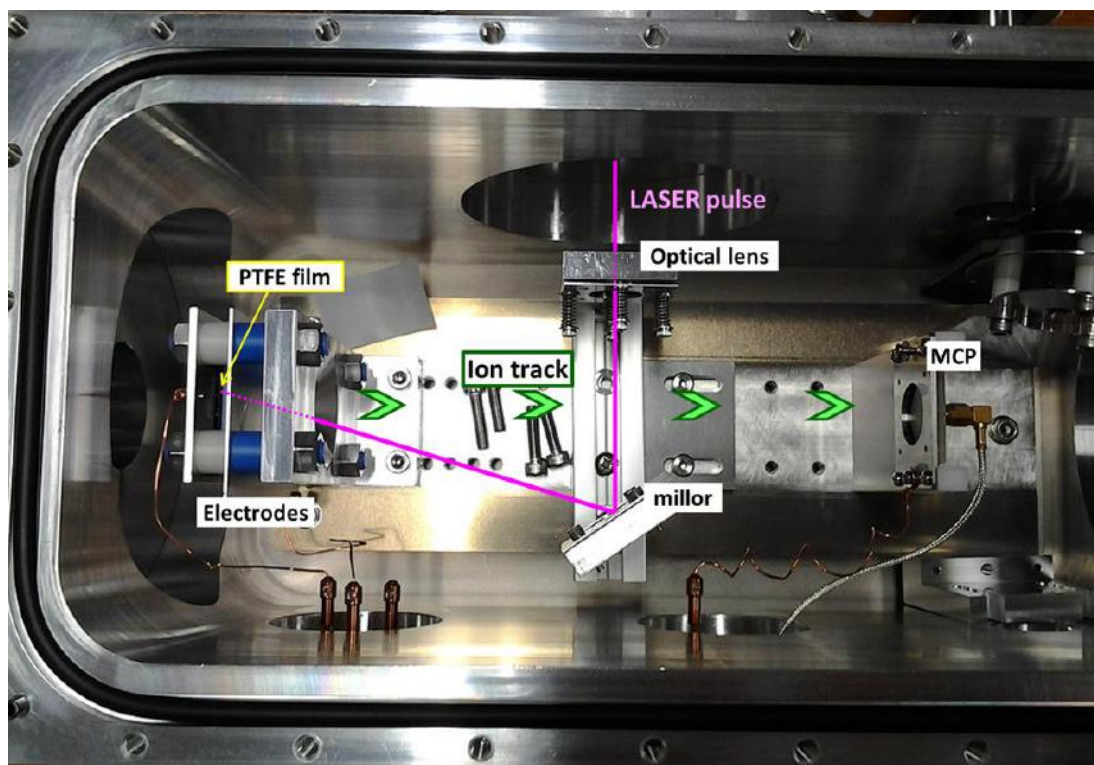


Figure 1 Overview of muonic atom extraction apparatus; it consists of vacuum chamber, muonic atom source (PTFE film), electrodes and detector (micro channel plate). For optimization of the experimental system, we performed various ions acceleration and detection experiment using ablation ions emitted from the film by Nd-YAG pulsed LASER.

References

- [1] G. Yoshida, et al., J Radioanal Nucl Chem. **303** (2015) 1277
- [2] H. Schneuwly et al., Physical Review A **22** (1980) 2081
- [3] D. J. Arseneau et al., Physica B 404 (2009) 946
- [4] R. Kadono et al., Rep Prog Phys **75** (2012) 026032

On the development of a method for the isolation of molybdenum

Bombard, A., Dirks, C., Happel, S.

Triskem International, France

Mo is of importance in nuclear industry both on the nuclear medicine side with Mo-99 as Tc-99m generator and in decommissioning with Mo-99 as burn-up determination of nuclear fuel and Mo-93 as long-lived activation product. In mixtures of radionuclides containing Mo-99 (β^- , $T_{1/2}$ 65.97h) and/or Mo-93 (EC, $T_{1/2}$ 4000 y) [1] need to be isolated to allow for their measurement. In case of Mo-93 determination, isolation of Mo is of importance as Nb-93 and/or Zr-93 can also be present in the matrix and constitute isobaric interferences for determination by ICP-MS. Different methods with multiple stages for Mo isolation from initial matrix exist [2]. The aim of this research work is to develop a fast and easy solid phase separation method selective for molybdenum. First results of this study are presented here.

[1] <http://www.nndc.bnl.gov/nudat2/chartNuc.jsp> (last accessed 16/04/2016)

[2] Bombard A., Determination of long-lived radionuclides Zr-93, Mo-93, Nb-94 in samples from the nuclear industry (2005) – PhD thesis – Nantes University, France

Comparative study for determination of naturally occurring radioactive materials by ED-XRF, ICP-MS, and gamma spectrometry

Jong-Myoung Lim, Young-Yong Ji, Ji-Young Park, Chang-Jong Kim, Kun-Ho Chung, and Mun-Ja Kang

Environmental Radioactivity Assessment Team, Korea Atomic Energy Research Institute, 111, Daedeok-daero 989, Yuseong, Daejeon, 305-353, Korea, e-mail: jmlim@kaeri.re.kr

As an attempt to reduce the social costs and apprehension arising from radioactivity in the environment, an accurate and rapid assessment of radioactivity is highly desirable. Naturally occurring radioactive materials (NORM) are widely spread throughout the environment. The concern regarding the radioactivity of these materials has therefore been growing over the last decade. In particular, radiation exposure in the industry when handling raw materials (e.g., coal mining and combustion, oil and gas production, metal mining and smelting, mineral sands (REE, Ti, Zr), fertilizer (phosphate), and building materials) has been brought to the public's attention. To decide the proper handling options, a rapid and accurate analytical method that can be used to evaluate the radioactivity of radionuclides (e.g., ^{238}U , ^{232}Th , and ^{40}K) should be developed and validated. A measurement technique using ICP-MS allows radioactivity in many samples to be measured within a short time period with a high degree of accuracy and precision. This method, however, encounters the most significant difficulties during pretreatment (e.g., purification, speciation, and dilution/enrichment). Since the pretreatment process consequently plays an important role in the measurement uncertainty, the development and validation of the method should be performed. Contrary to the ICP-MS technique, energy dispersive X-ray fluorescence and gamma spectrometry have the main advantage of non-destruction.

In this study, a series of experiments were conducted to test the compatibilities of three different techniques to determine concentrations of NORM (e.g., ^{238}U , ^{232}Th , and ^{40}K) using gamma spectrometry, ED-XRF and ICP-MS for raw materials (e.g., bauxite, bentonite, ceramic, clay, and zirconium sand) and by-products (e.g., fly/bottom ash from coal fired power plant and air dust in the zirconia production process). A sample digestion process for ICP-MS was used for LiBO_2 fusion and $\text{Fe}(\text{OH})_3$ co-precipitation. For an evaluation of the accuracy and precision of each method, various certified reference materials (CRMs) were analyzed using an established process. The comparative data set for NORM samples showed that the mean of the concentration ratio, derived for the three different methods, was between 0.8 and 1.2 for all target nuclides except for zirconia based samples. For an in-depth study, analytical results obtained from three methods were evaluated through a regression analysis, paired t-test, and Wilcoxon signed-rank test.

RADIONUCLIDE SPECIATION II

Actinide isotopic analysis in nuclear materials without chemical preparation by resonance ionization mass spectrometry

B.H. Isselhardt, M.R. Savina, A. Kucher

Lawrence Livermore National Laboratory, Livermore, CA 94550, USA

Traditionally, the quantification of isotope ratios in mixed actinide samples, such as spent fuel, requires dissolution and chemical separation prior to analysis in a mass spectrometer. Resonance Ionization Mass Spectrometry (RIMS) is a high efficiency, elementally-selective form of mass spectrometry that can provide rapid quantification of actinide isotope ratios even in the presence of isobaric interferences. Recent work at Lawrence Livermore National Laboratory has focused on developing a novel high-sensitivity RIMS instrument capable of rapid analyses of actinide isotope ratios in solids with minimal sample consumption and no or minimum sample preparation. The new instrument, named LION (Laser Ionization of Neutrals), is a vertically-oriented time-of-flight mass spectrometer coupled to six tunable Ti:Sapphire lasers to enable the analysis of multiple elements simultaneously.

We will present the first results from the new instrument showing how it employs atomic spectroscopy to realize very high detection efficiency (20-30%) and excellent elemental selectivity in order to discriminate against isobars. We will discuss results demonstrating the capability of RIMS to quantify both major and minor isotope ratios in U and Pu. The major isotope ratios, $^{235}\text{U}/^{238}\text{U}$ and $^{240}\text{Pu}/^{239}\text{Pu}$, are measured in unpurified reference materials to an accuracy and precision of about 0.3%, while the minor isotopes present are also reported to statistically limited accuracies and precision. We will also discuss active research areas to improve the measurement efficiency of oxide samples using femtosecond laser desorption and *in situ* reduction using a reactive gas ion gun.

This work was performed under the auspices of the U.S. Department of Energy by Lawrence Livermore National Laboratory under Contract DE-AC52-07NA27344. LLNL-ABS-689517.

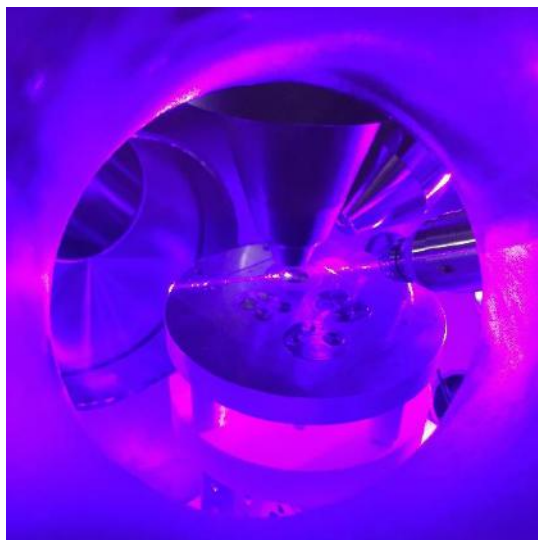


Figure 1. A look into the LION's mouth: RIMS analysis of a U metal sample in the new LION instrument to determine the detection efficiency. The resonance ionization laser beams are creating the stripe on the sample surface to ionize neutral atoms.

Speciation of tetravalent uranium with inorganic ligands in aqueous solution investigated by UV/vis and time-resolved laser-fluorescence measurements.

Lehmann, Susanne, Steudtner, Robin, Brendler, Vinzenz

*Helmholtz-Zentrum Dresden-Rossendorf, Institute of Resource Ecology, Germany
s.lehmann@hzdr.de*

This work is focused on uranium as the major component of spent nuclear fuel. For safety assessment of a future repository it is important to predict the environmental behavior of uranium in diluted to highly saline aquifer systems. Currently most reports are related to the hexavalent oxidation state which is stable under oxidizing conditions. However, reducing conditions are expected in the near field of high level nuclear waste repository after sealing the repository. Therefore, the major purpose of this study is to improve the knowledge of the physico-chemical properties of the tetravalent uranium and to provide thermodynamic data to enable a better prediction of speciation and solubility limits under reducing conditions.

The aim of this study is to examine the potential of U(IV) fluorescence for speciation studies. Kirishima et al. described in 2004 for the first time the luminescence spectra of the free U(IV) ion [1, 2]. Since then, only a few studies on U(IV) fluorescence properties have been published [3, 4]. However, spectroscopic data of U(IV) are necessary to provide a basic understanding of the U(IV) speciation under environmental conditions. We used in our study a combination of UV/vis spectroscopy with long path flow cell and time-resolved laser-induced fluorescence spectroscopy (TRLFS).

First, a U(IV) stock solution was produced by reduction in an electrochemical cell and was monitored by UV/vis spectroscopy. The residual content of U(VI) was determined by TRLFS to be lower than 1%. After that, we studied the aqueous speciation in presence of various inorganic ligands (ClO_4^- , Cl^- , SO_4^{2-} , PO_4^{3-} , CO_3^{2-}). To perform TRLFS measurements of U(IV) a laser system employing a Nd/YAG driven OPO system as excitation source with $\lambda_{\text{exc}} = 245 \text{ nm}$ were installed including a cryogenic unit for measurements at liquid nitrogen temperature (77 K). We detected the luminescence of the free U(IV) ion in acidic aqueous solution at room temperature (rt) and in frozen state at 77 K. At rt we observe the typical fluorescence properties of U(IV) with the peak maxima at 321, 410 and 523 nm and a fluorescence decay time of $2.6 \pm 0.3 \text{ ns}$ in perchloric and chloric acid. The detection limit of 10^{-5} M at rt was determined. By using cryo-TRLFS at 77 K the detection limit was lowered to $5 \times 10^{-6} \text{ M}$ and the fluorescence lifetime increases up to $148.4 \pm 6.5 \text{ ns}$. The spectroscopic results are in good agreement with earlier reports for rt [3] and cryo measurements [2]. In contrast to U(VI), which is often quenched by chloride, a well resolved luminescence spectrum of U(IV) was obtained in 0.1 as well as in 1 M HCl.

The potential of U(IV) fluorescence for speciation analysis was assessed in this study. With our setup we could study aqueous U(IV) systems with concentrations lower than 10^{-5} M and this corresponds to uranium concentrations occurring in the environment [5, 6]. This work was supported by the BMWI (contract number 02E11334B).

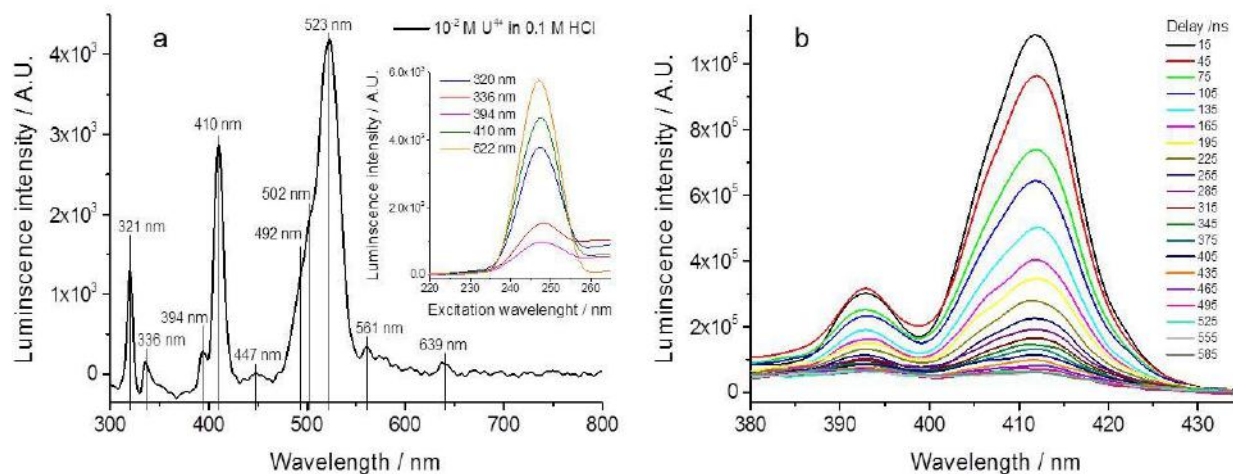


Fig. 1: a) Fluorescence spectrum of 10^{-2} M U^{4+} in 1 M HCl excited by $\lambda = 247$ nm measured at 1°C with fluorometer. The optimum excitation wavelength of the main peaks is shown on the right site. b) TRLFS spectra of 5×10^{-5} M U^{4+} in 1 M HCl between 380 nm and 430 nm excited by $\lambda = 245$ nm measured at 77 K.

References

- [1] A. Kirishima, Chem. Commun., 2003, (7), 910-911.
- [2] A. Kirishima, Radiochim. Acta, 2004, 92, 705-710.
- [3] S. Lehmann, J. Radioanal. Nucl. Chem., 2010 283(2), 395-401.
- [4] N. Aoyagi, N., J. Radioanal. Nucl. Chem., 2015, 303(2), 1095-1098.
- [5] T. Arnold, Geochim. Cosmochim. Acta, 2011, 75(8), 2200-221.
- [6] G. Bernhard, J. Alloys Compd., 1998, 271, 201-205.

The composition and stability of uranium (IV)-silicate colloids in alkaline systems

THOMAS S. NEILL^{1,2}, KATHERINE MORRIS^{1,2}, CAROLYN I. PEARCE³, NICHOLAS K. SHERRIFF⁴ AND SAMUEL SHAW^{1,2*}

¹*School of Earth, Atmospheric and Environmental Sciences, University of Manchester, Manchester, UK.*

²*Research Centre for Radwaste and Disposal, Williamson Research Centre, University of Manchester, Manchester, UK,*

³*Pacific Northwest National Laboratory, Richland, USA*

⁴*National Nuclear Laboratory, Warrington, UK*

sam.shaw@manchester.ac.uk

U(IV) colloids formed via various pathways including corrosion of spent nuclear fuel and have the potential to greatly enhance the mobility of otherwise immobile U(IV) [1]. This is particularly relevant in decommissioning and clean-up of nuclear facilities, such as legacy ponds and silos at the Sellafield site, UK, and in long-term radioactive waste disposal. Previous work [2] has indicated that silicate can stabilise U(IV) colloids at alkaline to near neutral pH and that these colloids could be significant environmental transport vectors for uranium. This study investigates the chemical conditions under which U(IV) silicate colloids can form, and their composition and long-term stability.

U(IV) silicate colloids produced under varying silicate/uranium concentrations (0 - 4 mM silicate, 0.01 - 1 mM U(IV)) and pH (9-12) were analysed using ultrafiltration, scanning transmission electron microscopy (STEM), synchrotron based small angle x-ray scattering (SAXS) and extended x-ray absorption fine structure (EXAFS) spectroscopy. SAXS, STEM and ultrafiltration results indicate that colloids are formed under a range of conditions with a primary particle size typically 1-5 nm. At higher silicate concentrations (4 mM), these primary particles are stable for several months. At lower silicate concentrations (2 mM), stable colloidal aggregates below ~220 nm in size are dominant. EXAFS and STEM data suggest a local U(IV) coordination environment similar to coffinite (USiO₄), but with little or no long range structure within the particles.

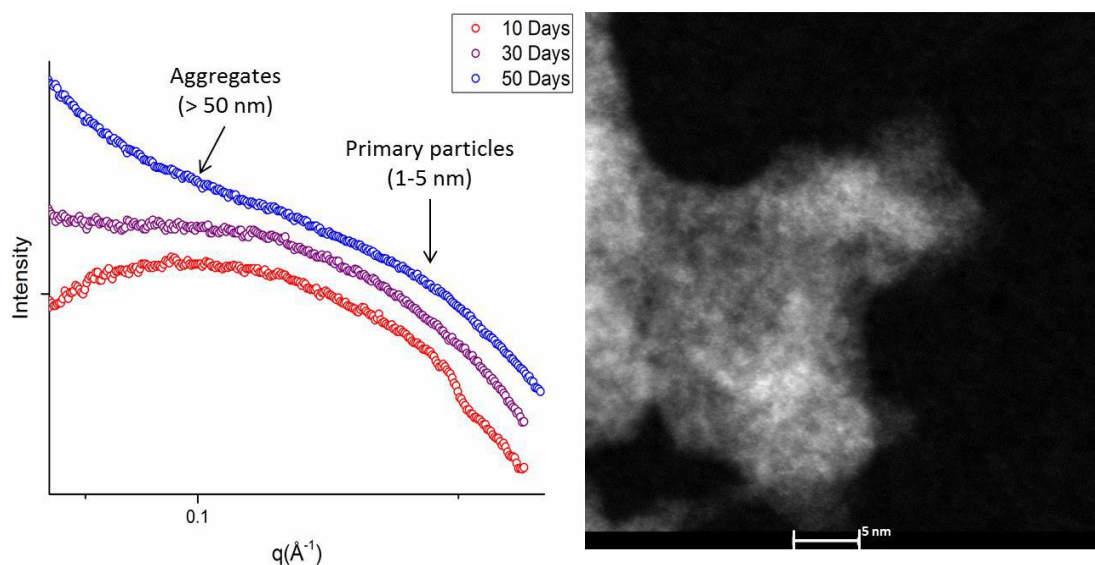


Figure 4: (Left) SAXS patterns of U(IV) silicate colloidal systems aged for 10, 30 and 50 days showing the scattering due to aggregates (> 50 nm) and primary particles (approximately 1-5 nm). (Right) High-resolution HAADF STEM image of a U(IV) silicate aggregate.

Our investigations into uranium (IV) silicate colloids have shown they are stable under alkaline conditions over significant periods of time (up to 6 months), and do not show any structural changes over the time frame analysed. These colloidal phases must be considered in the context of clean-up of nuclear facilities and the long-term storage and disposal of uranium-containing radioactive waste.

Research was sponsored by Sellafield Ltd and the University of Manchester.

References

- [1] Kaminski, et al. (2005). Colloids from the aqueous corrosion of uranium nuclear fuel. *Journal of Nuclear Materials*, 347(1-2), 77-87.
- [2] Dreissig, et al. (2011). Formation of uranium(IV)-silica colloids at near-neutral pH. *Geochimica et Cosmochimica Acta*, 75(2), 352-367.

Impact of electrospray ionization on trivalent f-element: ligand solution equilibria

M. P. Kelley, A. E. Clark, S. B. Clark

Department of Chemistry, Washington State University, Pullman, Washington 99164, USA

Electrospray ionization mass spectrometry (ESI-MS) is a promising technique for the study of f-element solution speciation^{1,2} that may prove to be a valuable supplement to current safeguards techniques within a nuclear reprocessing setting. It may also serve as an effective process control monitoring tool for the production of radiopharmaceuticals. In an ideal case, ESI-MS can provide unambiguous and simultaneous identification of metal ions, organic complexants, and their complexes in a variety of solution media. However, previous work has shown that in some systems, particularly labile complexes,³ the electrospray ionization process may alter speciation during transfer of species from solution to the gas phase. For example, the use of co-solvents such as methanol to enhance ionization likely shifts complexation equilibria, ionization efficiencies of various species are not necessarily the same making quantification challenging, and ionization may also shift complexation kinetics compared to rates of reaction in solution. In this presentation, we describe recent work to address the issues of methanol perturbations to f-element speciation during ionization, and a new approach for correcting ionization efficiencies to obtain stability constants for lanthanide complexes with aminopolycarboxylate ligands.

Although methanol is routinely used as a sheath liquid to improve ionization during electrospray, it likely alters solution equilibria involving complexation of the f-elements. In the absence of a complexant, the high charge density of f-ions results in the organization of polar solvents, e.g. both water and methanol, into ordered solvation spheres⁴. The kinetics and thermodynamics of f-element cation complexation are often dependent on the energy required for ion desolvation, which changes as water is replaced by methanol in the solvation sphere. Using second order Møller–Plesset perturbation theory (MP2) calculations, we have demonstrated that increasing the amount of methanol within the 1st solvation shell of the Cm³⁺ ion decreases the ion-solvent dissociation energy for both methanol and water (Figure 1); Ln³⁺ ions (La³⁺, Gd³⁺, and Lu³⁺) demonstrate a similar trend. Additionally, ESI experiments using ¹⁸O labeled water show that methanol is more likely than water to solvate trivalent f-elements (in this case, Nd³⁺) during ESI (Figure 2).

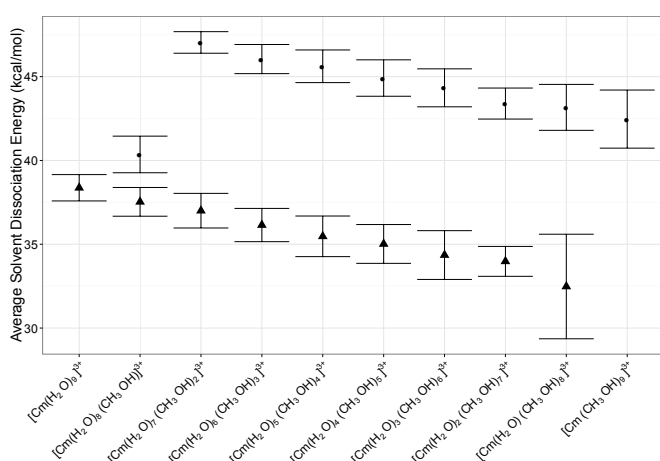


Figure 16. Ion-solvent dissociation energy for water (p) and methanol (l) from the 1st solvation shell of the Cm³⁺ ion.

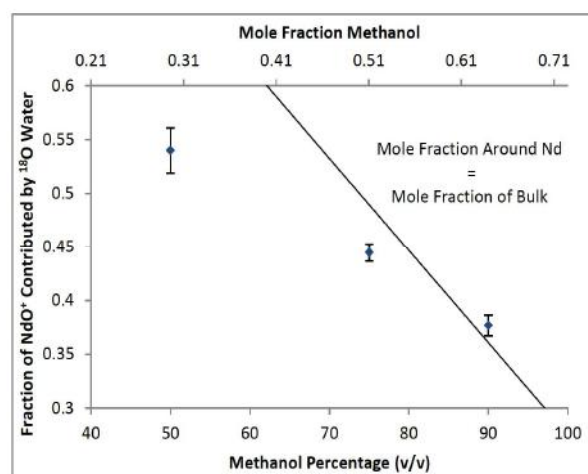
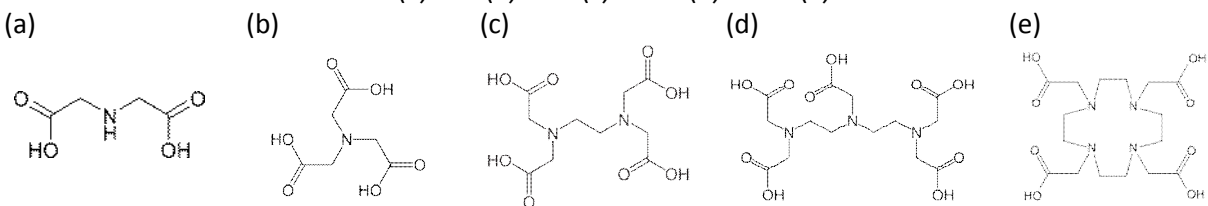


Figure 17. The fraction of NdO⁺ ions resulting from Nd(H₂O)³⁺ versus methanol concentration in solution. NdO⁺ is the primary Nd species observed during ESI at high fragmentation potentials (400 V here). The expected fraction of NdO⁺ resulting from water (based on bulk solution composition) is plotted on the solid line.

Table 3. Molecular structures of: (a) IDA (b) NTA (c) EDTA (d) DTPA (e) DOTA.



Another significant obstacle in the use of ESI-MS in the measurement of metal:ligand systems is the differing ionization efficiencies of different complexes. Unlike results obtained for complexes involving labile carboxylate ligands³, we have observed that ionization of f-elements complexed with strong chelators such as 1,4,7,10-tetraazacyclododecane-1,4,7,10-tetraacetic acid (DOTA; Table 1) is consistent and quantitative. Lanthanide complexes with DOTA have very large equilibrium constants (Reaction 1; $\log(\beta)=23.7$), and are used in applications such as contrast agents for medical imaging.



By using the DOTA complex as an internal standard, we are able to calculate the relative ionization efficiencies of complexes with other ligands of interest. This provides a response factor for ionization of the non-DOTA metal:ligand complex. In this paper, we demonstrate our approach using the family of aminopolycarboxylate ligands: Iminodiacetic acid (IDA), Nitrilotriacetic acid (NTA), Ethylenediaminetetraacetic acid (EDTA), and diethylenetriaminepentaacetic acid (DTPA) (see Table 1).

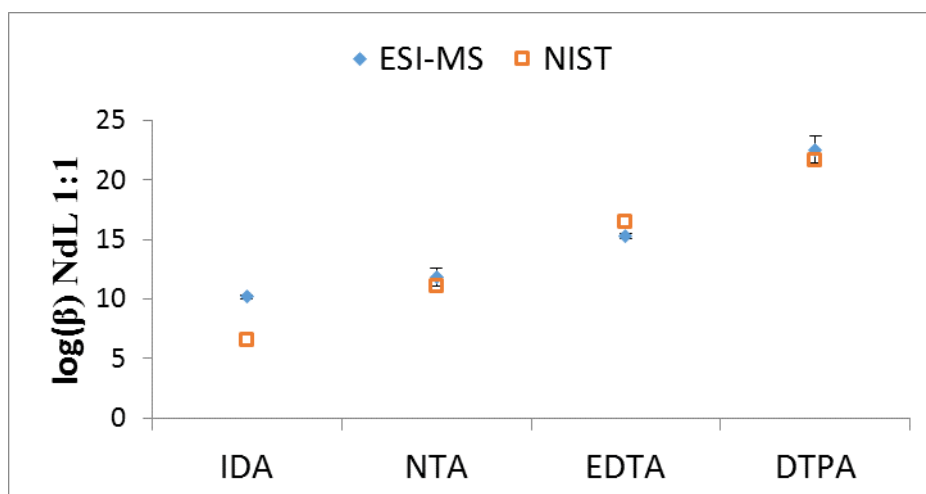


Figure 18. Estimated gas-phase stability constants for Nd^{3+} with aminocarboxylate ligands versus their solution phase NIST values.

Our results for the aminopolycarboxylate ligands are generally consistent with accepted data from the literature. By identifying potential solution perturbations occurring during the electrospray process, as we have done here for methanol, and correcting for differing ionization efficiencies, ESI-MS can be a powerful supplemental tool for solution chemistry.

- (1) McDonald, L. W.; Campbell, J. A.; Vercouter, T.; Clark, S. B. *Anal. Chem.* **2016**, *88* (5), 2614–2621.
- (2) Keith-Roach, M. J. *Anal. Chim. Acta* **2010**, *678* (2), 140–148.
- (3) McDonald IV, L. W.; Campbell, J.; Clark, S. *Anal. Chem.* **2014**, *86*, 1023–1029.
- (4) Rizkalla, E. N.; Choppin, G. R. In *Handbook on the Physics and Chemistry of Rare Earths*; Gschneidner, K. A. J., Eyring, L., Choppin, G. R., Lander, G. H., Eds.; Elsevier Science B.V., 1994; Vol. 18, pp 529–558.

EDUCATION SESSION

**CINCH-II Project – A milestone in the coordination of education and training
in nuclear- and radiochemistry in Europe**

Jan John
on behalf of the CINCH-II consortium

*Czech Technical University in Prague, Department of Nuclear Chemistry, Brehova 7, 115 19 Prague 1, Czech
Republic*

Significant demand for nuclear and/or radiochemists has been identified in repeated surveys to exist both in nuclear energy field and in non-energy fields, such as environmental protection, radiopharmacy, nuclear medicine, biology, authorities, etc. Since the numbers of staff in teaching and the number of universities with facilities licensed for the work with open sources of ionizing radiation has decreased close to the critical level, coordination and collaboration are required to maintain the necessary teaching and training capabilities.

The CINCH-II project, aiming at the Coordination of education and training In Nuclear CHemistry in Europe, was a direct continuation of the CINCH-I project which, among others, identified the EuroMaster in Nuclear Chemistry quality label as an optimum common mutual recognition system in the field of education in Nuclear Chemistry in Europe, surveyed the status of Nuclear Chemistry in industry / the needs of the end-users, developed an efficient system of education/training compact modular courses, or initiated development of the first electronic tools for a future efficient distance learning system.

In this presentation, the outcomes of the follow-on CINCH-II project will be described in detail. The CINCH-II project was built around three pillars - Education, Vocational Education and Training (VET), and Distance Learning - supported by two cross-cutting activities – Vision, Sustainability and Nuclear Awareness that included also dissemination, and Management. Its main objectives, with the broadest impact to the target groups, were further development and implementation of the EuroMaster in Nuclear Chemistry, completion of a pan-European offer of modular training courses for the customers from the end users, development of a Training Passport in Nuclear Chemistry and preparing the grounds for the European Credit system for Vocational Education and Training (ECVET) application in nuclear chemistry, implementation of modern e-learning tools developed in CINCH-I and further development of new tools for the distance learning such as the RoboLab experiments, laying the foundations of NRC Network – a Nuclear Chemistry Education and Training Platform – as a future sustainable Euratom Fission Training Scheme (EFTS) in Nuclear Chemistry, development of a Sustainable System for Mobility within this NRC Network, or development of methods of raising awareness of the possible options for nuclear chemistry in potential students, academia and industry. An important part of the CINCH-II activities were the updates of the detailed survey of the universities and curricula in nuclear- and radiochemistry in Europe performed originally in CINCH-I project and of a similar survey of the training and education needs of the industrial end users.

The CINCH-II project aimed at mobilizing the identified existing fragmented capabilities to form the critical mass required to implement the courses and meet the nuclear chemistry postgraduate education and training needs, including the high-level training of research workers, of the European Union. Networking on the national level and with existing European as well as international platforms was an important feature of the project.

Educational opportunities within the UNLV radiochemistry program

JOHNS, Wendee

University of Nevada, Las Vegas, NV, USA

The Radiochemistry Ph.D. program at UNLV was founded as a joint program by the Department of Chemistry and the Health Physics Department in 2004. It is a student-driven, research intensive program that stresses the fundamental aspects of radiochemistry science. Its curriculum consists of a series of core courses that are complemented by elective classes offered by several different colleges, making it a truly interdisciplinary program. The program offers various research opportunities to undergraduate and graduate students, providing them with unique training and educational opportunities. In particular, it allows students to gain hands-on experience in handling, manipulating and detecting unsealed radioactive material early in their career. UNLV has the resources and capabilities to perform novel experiments that aid in exploring, understanding and utilizing the fundamental properties of radioisotopes. Given Nevada's unique relationship with nuclear activities, UNLV has emerged as a premier location for studying the chemistry of the actinides, technetium and other radionuclides. The curriculum and research provide a comprehensive and interdisciplinary examination of topics and experiences necessary to produce graduates who are ready to secure employment and participate in radiochemistry research. The program has over 7500 square feet of radiochemistry laboratories capable of handling a range of activities. These facilities contain a host of experimental equipment for use in research including radionuclide counting facilities, spectroscopy, microscopy and x-ray diffraction. Student opportunities in research and education are expanded through interactions with national and international collaborators. The program focuses on student development in the areas of technical competency, communication skills, analytical and critical thinking skills and expertise in the field of radiochemistry. The student experience at UNLV's Radiochemistry program is further enhanced by collaboration with the Australian Nuclear Science and Technology Organisation (ANSTO) where education into the nuclear fuel cycle, the characterization of nuclear materials with an emphasis on Technetium, Mo-99 production, actinide chemistry and the chemistry of the nuclear fuel cycle is coupled with exchange visits thus taking advantage of our complementary expertise. Future collaborations will include mentoring undergraduate students in radiochemistry research that is relevant to UNLV graduate student thesis pursuits. Department of Energy researchers and staff scientists from national laboratories hold seminars and lecture series as part of the program which further expands education opportunities for UNLV students. A Ph.D. degree from UNLV in the field of radiochemistry, provides a wide variety of career opportunities performing forefront research in areas as diverse as radiochemistry, nuclear chemistry, materials research, renewable energy studies, nuclear forensics, and environmental studies to name a few.

Webinar-based education and training

Paulenova

*School of Nuclear Science and Engineering, Radiation Center
Oregon State University, Corvallis, OR 97331, United States*

The National Analytical Management Program (NAMP) is a centralized hub for radiological analytical resources within of the US Department of Energy and with collaboration with the US Environmental Protection Agency (EPA) not only provides analytical needs during large-scale responses to emergency situations, but also intends to educate both the public and radiological workers in the related areas. A few years ago, with the aim to liven up this effort and exploit modern internet technologies and reach interest and educate a broad audience, the NAMP has organized an education subcommittee, partnering with university professors and addressing the goal to foster the exchange of scientific and technical information in radiochemistry programs at different universities in United States and deliver a several series of webinars focused on radiochemistry and its application in environmental and other related areas. Each of the topics in the webinar series is designed to strengthen the knowledge of participants in application of actinide and fission products chemistry to mobility of radionuclides, sample preparation, detection, dosimetry and risk assessment. The topical lectures are delivered as live webinars, each representing a comprehensive overview of different subjects of interest and concern and providing an understanding of the advances and challenges faced today. These, about 90 minutes long webinars are advertised at national and international level at https://inlportal.inl.gov/portal/server.pt/community/namp/745/training_and_education/9247 and they are indented to be of interest not only to students currently pursuing formal education in universities but also to everybody who may need refreshing or a better understanding of specific topics. These webinars will address needs of health physicists, environmentalist, quality assurance officers, data validators, managers, regulators, chemists and laboratory technicians. The next goal of this effort is also to identify other training courses, engaging collaboration between universities, national laboratories, governmental and private sectors, including the hybrid courses when the webinar lecture will be combined with the practical laboratory classes at selected university laboratories. The details and examples of the NAMP webinar education modules will be presented in our contribution.

Finally, it is important to point out that the webinars became a desired didactic tool. Besides opening the classroom to everybody in the world, the webinars offer the unpredicted earlier opportunities for interdisciplinary crosslinking, and education and research collaboration. Besides our webinars, there is a growing list of webinars in our field; e.g., graduate student research webinar series organized by Nuclear Science and Security Consortium or research call webinars by the Nuclear Energy University Program of the US DOE.

So far, four series were published: Chemistry of Actinides, Environmental Radiochemistry-Bioassay, Nuclear Fuel Cycle and Nuclear Forensics Series. The details and examples of the webinar education modules will be presented in our contribution.

FRIDAY 2ND SEPTEMBER
PRODUCTION OF RADIONUCLIDES

Non-conventional radionuclides for therapy: looking for new production routes

Ramiz A. Aliev

²Lomonosov Moscow State University, Moscow, Russia

¹National Research Center "Kurchatov Institute", Moscow, Russia

Currently, the nuclear medicine uses the limited number of radionuclides, and the most widely used nuclides are often not optimal in their nuclear and chemical properties. This is especially true for the most high-tech field of nuclear medicine such as targeted radiotherapy. The development of innovative delivery systems (monoclonal antibodies, modular transporters, nanoparticles, etc.) also changes the requirements for medical radionuclides. Analysis reveals that the availability of the radionuclides and the existence of simple methods of their production are the limiting factors in the development of new radiopharmaceuticals. The aim of this study is to expand the range of medical radionuclides, as well as to find new pathways for routine production of already used radionuclides.

In this work we focus on production of nca radionuclides that emit low energy electrons with high LET – alpha, low energy beta particles, conversion and Auger electrons (see table 1). In terms of the joint MSU and INR project possibility of production of ²²⁵Ac by irradiation of natural thorium by medium energy protons (about 100 MeV) was studied. Irradiation was done on INR proton linac. The cross-sections of formation of ²²⁵Ac and side product ²²⁷Ac were published earlier. The radiochemical separation of ²²⁵Ac from Th and fission products was developed. It was shown that this method may be applied for large-scale production of ²²⁵Ac of acceptable quality for Ac/Bi-generators production. Possibility of separation of medical alpha-emitters ²²³Ra and ²³⁰Pa from the same thorium target was studied.

A number of radioisotopes of rare earth elements may be applied in nuclear medicine. Therefore, we studied methods of production and radiochemical separation of radioisotopes of Tb and Ho. The quick and easy method of radiochemical separation of Tb from Eu and Gd was developed. The Eu targets of natural isotopic composition were irradiated by 30 MeV alpha particles. Tb was separated by extraction chromatography using Ln-Resin. For Auger-emitting ¹⁶¹Ho we suggested photonuclear route of production.

⁴⁷Sc and ⁶⁷Cu are of great importance for nuclear medicine because of favorable nuclear and chemical properties. Unfortunately, application of these radionuclides is limited because of difficulties associated with their production. We developed photonuclear techniques for production of ⁴⁷Sc and ⁶⁷Cu. Irradiation was performed on bremsstrahlung beam of MSU 55 MeV race-track microtron. Production yields were determined and radiochemical methods of separation from irradiated targets were developed.

Table 1. Production of several medically relevant radionuclides

Nuclide	T _{1/2}	Decay mode	Production route
²²⁵ Ac	10 d	α	²³² Th(p,x)
²³⁰ U	20.8 d	α	²³² Th(p,3n) ²³⁰ Pa→ ²³⁰ U
²²³ Ra	11.4 d	α	²³² Th(p,p5n) ²²⁷ Th→ ²²³ Ra ²³² Th(p,6n) ²²⁷ Pa→ ²²⁷ Th→ ²²³ Ra
^{153,154,155,156} Tb		EC, β+	^{nat} Eu(α,xn)
⁴⁷ Sc	3.35 d	β-	⁴⁸ Ti(γ,p) ⁴⁷ Sc
⁶⁴ Cu	12.70 h	EC, β+, β-	⁶⁶ Zn(γ,np) ⁶⁴ Cu
⁶⁷ Cu	2.58 d	β-	⁶⁸ Zn(γ,p) ⁶⁷ Cu
¹⁶¹ Ho	2.48 h	EC	¹⁶² Er(γ,p) ¹⁶¹ Ho ¹⁶² Er(γ,n) ¹⁶¹ Er→ ¹⁶¹ Ho
^{195m} Pt	4.02 d	IT	¹⁹⁷ Au(γ,np) ^{195m} Pt

^{43}Sc production development by cyclotron irradiation of ^{43}Ca and ^{46}Ti

Katharina A. Domnanich^{1,2}, Cristina Müller³, Andreas Türler^{1,2}, Nicholas P. van der Meulen²

¹ *Department of Chemistry and Biochemistry, University of Bern, Freiestrasse 3, 3012 Bern, Switzerland*

² *Laboratory of Radiochemistry, Paul Scherrer Institute, 5232 Villigen PSI, Switzerland*

³ *Center of Radiopharmaceutical Sciences, Paul Scherrer Institute, 5232 Villigen PSI, Switzerland*

Introduction

The positron emitter ^{43}Sc is considered to be an attractive PET radionuclide alternative to ^{44}Sc . With a similar half-life and positron energy ($t_{1/2} = 3.89$ h, $E_{\beta^+} = 476$ keV, $I = 88\%$, $E_{\gamma} = 372$ keV, $I = 23\%$) to ^{44}Sc ($t_{1/2} = 3.97$ h, $E_{\beta^+} = 1475.4$ keV, $I = 94.34\%$, $E_{\gamma} = 1157$ keV, $I = 100\%$) but without the accompanying high-energy γ -ray, its decay properties are clearly advantageous regarding the dose burden to patients. Together with ^{47}Sc , which demonstrates therapeutic effect by emitting soft β^- -particles, it can be considered as part of the “matched pair” principle, enabling tumour imaging and, following that, optimal therapy planning. The production of ^{43}Sc is described by different nuclear reactions in literature, however, production of ^{43}Sc in sufficient quantities and radionuclidic purity encompasses several challenges, a low cross section for proton induced reactions, co-production of ^{44}Sc and scarce availability of deuteron providing cyclotrons [1-3]. Within the scope of the current work the focus was laid on the investigation of the $^{46}\text{Ti}(p,\alpha)^{43}\text{Sc}$ and $^{43}\text{Ca}(p,n)^{43}\text{Sc}$ production pathways at the PSI Injector II facility.

Experimental

^{43}Ca and ^{46}Ti targets were prepared by mixing enriched $^{43}\text{CaCO}_3$ or ^{46}Ti powder with graphite powder, pressed and encapsulated in aluminium. Since enriched Ti is only available in the hardly soluble oxide form, the reduction of 97% $^{46}\text{TiO}_2$ to elemental ^{46}Ti powder was performed prior to target preparation [4]. The $^{43}\text{CaCO}_3$ and ^{46}Ti targets were irradiated with protons at different energies.

Chemical separation of both target materials was performed with DGA extraction chromatographic resin. Isolation of $^{43}\text{Sc(III)}$ from the Ca(II) and Ti(III) matrix was achieved by using different molarities of HCl solution. To obtain $^{43}\text{Sc(III)}$ in a small volume, a second column, consisting of SCX cation exchange resin, was used. The product was concentrated in 700 μL 4.8M NaCl/ 0.13M HCl eluent.

Results and Discussion

The $^{43}\text{Ca}(p,n)^{43}\text{Sc}$ production route yielded ^{43}Sc with a radionuclidic purity of 66.1%, with ^{44}Sc being co-produced with 33.9% of the total activity at the end of separation (EOS). This ratio is influenced by the enrichment of the ^{43}Ca target material and by the proton beam energy. The produced ^{43}Sc was used to perform a PET phantom study (Figure 1), indicating promising preliminary results with regard to ^{43}Sc being a superior imaging radionuclide to its ^{44}Sc counterpart. The labelling of the obtained ^{43}Sc with DOTANOC could be performed at a maximum specificity of 7 MBq $^{43}\text{Sc}/\text{nmol}$ DOTANOC with a radiochemical purity of 97 %.

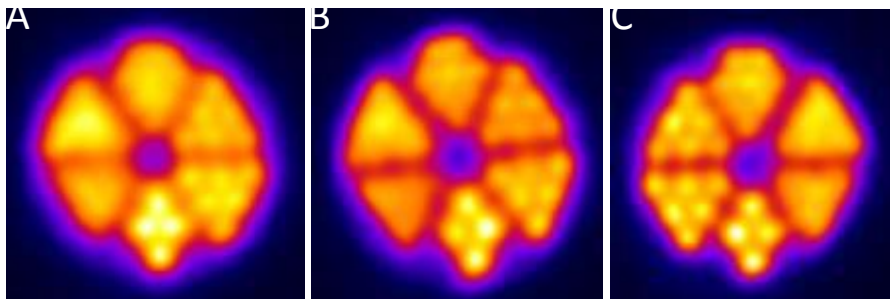


Figure 1: PET-Phantom Images of ^{44}Sc (A), ^{43}Sc produced from ^{43}Ca (B) and ^{43}Sc produced from ^{46}Ti (C).

The $^{46}\text{Ti}(p,\alpha)^{43}\text{Sc}$ production route ^{43}Sc of 98.3% radionuclidic purity at EOS. The percentage of ^{44}Sc in the final product did not exceed 1.5%. The longer-lived impurities $^{44\text{m}}\text{Sc}$, ^{46}Sc and ^{48}Sc were less than 0.04%. To obtain enriched ^{46}Ti target material of higher purity, the $^{46}\text{TiO}_2$ reduction process was performed in high vacuum, simultaneously optimising several parameters, like the amount of reducing agent, temperature profile and reaction time. Initial difficulties with the processing of the irradiated ^{46}Ti target were addressed by changing the irradiation parameters to lower beam intensity and prolonged irradiation time.

References

- [1] R. Walczak et al., EJNMMI Physics, 2:33 (2015).
- [2] P. Kopecky et al., Appl. Radiat. Isotope, 44 (1993)
- [3] EXFOR- database, version from 06.01.2016
- [4] B. Lommel et al., J Radioanal Nucl Chem, 299 (2013)

Why proton or deuteron induced reactions are not relevant for clinically used ^{201}Tl production

A. Hermanne¹, F. Tárkányi², S. Takács², F. Ditrói², Z. Szücs², K. Brezovcsik²

¹ *Cyclotron Laboratory, Vrije Universiteit Brussel (VUB), Brussels, Belgium*

² *Institute of Nuclear Research, Hungarian Academy of Sciences (ATOMKI), Debrecen, Hungary*

Due to its now known detrimental health effects, liquid metal mercury (freezing point $-38,83^\circ\text{C}$) and most of its compounds are extremely toxic and must be handled with care. Industrial and commercial uses are regulated or even banned in many countries. Nevertheless in modern nuclear medicine several mercury radioisotopes, or radionuclides that can be obtained from irradiation of mercury, are of interest and/or clinically used. The isomers $^{197\text{m,g}}\text{Hg}$ appear to be new potential candidates for therapy, while longer lived ^{203}Hg has applications in monitoring the distribution and the accumulation of mercury in different parts of the body and to study mercury transformations in environmental systems. From the point of view of production targets, some early studies for production of the clinically widely used potassium analogue ^{201}Tl , proposed proton induced reactions on mercury [1]. But studies of activation of mercury by charged particles remain scarce. Thick target yields (especially for ^{201}Tl and its contaminants) were studied by several authors. Literature values for cross-sections of deuteron induced activation are totally absent. We hence decided to initiate a study for activation of mercury by deuterons (up to 50 MeV) and protons (up to 65 MeV). The seven stable isotopes of Hg result in a wide mass region of activation products. From direct (d,xn) and (p,xn) reactions we find radionuclides from Tl with masses between 195 and 204. Emission of one proton, together with one or more neutrons results in direct formation of Hg radionuclides (195 to 205 mass numbers). Emission of two protons and one or multiple neutrons (or alpha particle clusters) will result in Au nuclides. Also isobaric parent decay plays a role in formation of some of the Hg and Au nuclides.

The experimental results were obtained by using the activation method with stacked foil irradiation technique, followed by off-line high resolution gamma-ray spectroscopy. Cross-section data were deduced relative to monitor reactions, re-measured simultaneously over the whole covered energy range. The Hg-targets were obtained by deposition of HgS using a sedimentation method. Actual thickness of the layer was determined by measuring of the area and weighing of the HgS deposited on the Al backing. The measured thickness of each foil was used for the cross-section calculations.

Two stacks) were irradiated with deuterons: at the Cyclone 90 cyclotron of the Université Catholique in Louvain la Neuve (LLN) (nominal incident energy 50 MeV) and at the CGR560 of the VUB in Brussels (nominal incident energy 21 MeV). Formation of $^{195\text{g}}(\text{cum}), ^{196\text{m}}, ^{196\text{g}}, ^{197}, ^{198\text{m}}, ^{198\text{g}}, ^{199}, ^{200}, ^{201}, ^{202}\text{Tl}$, $^{194}, ^{195\text{g}}(\text{cum}), ^{196\text{m}}, ^{196\text{g}}(\text{cum}), ^{198\text{m}}, ^{199}, ^{195\text{m}}, ^{197\text{m}}, ^{203}\text{Hg}$ were measured up to 50 MeV incident particle energy for the first time. Three stacks were irradiated with protons: at external beam lines of the CGR560 cyclotron at VUB-Brussels with nominal incident energy of 15 and 34 MeV and the Cyclone 90 cyclotron of the Université Catholique in Louvain la Neuve (LLN) (nominal incident energy 65 MeV). Results for $^{196\text{m}}, ^{196\text{g}}, ^{197\text{g}}(\text{cum}), ^{198\text{m}}, ^{198\text{g}}, ^{199\text{g}}(\text{cum}), ^{200\text{g}}(\text{cum}), ^{201}, ^{202}\text{Tl}$; $^{194\text{g}}(\text{cum}), ^{195\text{g}}(\text{cum}), ^{196\text{g}}(\text{cum}), ^{198\text{m}}, ^{199\text{g}}(\text{cum})$ Au and $^{195\text{m}}, ^{197\text{m}}, ^{203}\text{Hg}$ are obtained up to 65 MeV incident energy, many for the first time.

No chemical separation was performed. Gamma-spectra were measured with HpGe detectors at the VUB premises. To allow quantification of short and longer lived radionuclides, four to five series of gamma-spectra were measured from shortly after EOB (1 h cooling time for VUB irradiation, at least 5 h cooling time for LLN irradiation: transfer to VUB needed) to two or three months after the irradiation. Gamma-spectra were evaluated by using the codes included in the Genie 2000-V1.6 package. The used decay data were taken from online version of NUDAT2. The median beam energies in the individual targets were preliminary determined by a degradation calculation and were corrected on the basis of the fitted monitor reaction. Uncertainty on the

median energies was obtained taking into account cumulative effects of possible uncertainties (primary energy, target thickness, energy straggling, correction to monitor reaction) and is 0.2 MeV on the first foil of each stack increasing to 1.1 MeV, respectively 1.0 MeV, for the last foil. Uncertainty of cross-sections was determined by considering the sum in quadrature of all independent contributions following the ISO recommendations and amounts to 12 -17%.

As natural Hg has six stable isotopes (^{196}Hg with abundance of 0,15%; ^{198}Hg : 9,97 %; ^{199}Hg : 16,87%; ^{200}Hg : 23,1%; ^{201}Hg : 13,18%; ^{202}Hg : 29,8%; ^{204}Hg : 6,87%), elemental cross-sections were determined.

The cross-sections were compared with results in the on-line TENDL-2014 and TENDL-2015 libraries (based on default and adjusted TALYS (1.6) calculations) by calculating weighted sums of the contributions of reactions on all stable Hg isotopes (weighted by isotope abundance). The differences in the cross-sections between the two libraries versions are less than 1%. For some Tl-radioproducts a comparison is made with data derived from the figures published by [1] both for the results on $^{\text{nat}}\text{Hg}$ as for the values obtained on enriched ^{202}Hg . The six stable isotopes of Hg make that in most of the excitation functions more or less pronounced local maxima occur due to the different contributing reactions. For formation of Tl radionuclides (reactions of (d,xn) and (p,xn) type) the shape of the excitation function is mostly well predicted by the theoretical calculations but in general an underestimation of the experimental cross-section values exist. For formation of Hg isotopes (only 3 activation products, emission of one proton and several neutrons) the agreement in shape is unexpectedly good, but the formation of ^{203}Hg is strongly underestimated. For reaction formation of Au radionuclides (emission of α -particles) the discrepancy can reach a factor of five.

From excitation functions obtained by a spline fit to our experimental data, integral thick target yields (TTY) were calculated as function of incident energy. Experimental TTY were determined for deuterons some Tl-radionuclides (for $^{199,200,201,202}\text{Tl}$) by two authors in the energy range 22.5-10.1 MeV and are a factor of 2 lower than our values. For protons measurements for $^{199,200,201,202}\text{Tl}$ were and differences of a factor two to five between our data and published values exist. From the TTY curves it can be seen that both for proton and deuteron irradiations of Hg, batch production of ^{201}Tl could be interesting. In thick targets (degradation to exit energies below the formation threshold) for 30 MeV incident deuterons yields of 25.5 GBq/C could be obtained. In an irradiation of 9 h - 100 μA on target with 30 MeV deuterons (typical values for production of ^{201}Tl through the conventional $^{203}\text{Tl}(p,3n)^{201}\text{Pb} \rightarrow ^{201}\text{Tl}$ route with 30 MeV protons) in principle a batch yield of 82.5GBq (or 2.25 Ci) could be obtained. This is more than double of the practical yield of the above mentioned proton induced route (typically 37 GBq or 1 Ci of ^{201}Tl after the double chemical Tl-Pb-Tl separation-purification and optimal 30 h in-growth process).

In thick targets at 30 MeV proton energy integrated yields of 17.9 GBq/C (respectively 27.8 GBq/C for 40 MeV incident energy) and batch yields of 57.3 GBq (or 1.55 Ci) with typical irradiation characteristics mentioned above could be obtained (50% more than the conventional proton route). It is however clear from the yield curves that no energy window can be found that ensures that contaminations with ^{200}Tl and ^{202}Tl are below 1%, as required by the pharmacopoeia, even with highly enriched target. This will also be demonstrated on by analyzing the most contributing reactions for the different radioisotopes as predicted by the TALYS code. Proton or deuteron irradiation on mercury targets for direct production of ^{201}Tl is hence not an alternative to the indirect production on Tl targets, where the double Tl-Pb-Tl purification chemistry allows drastically reducing isotopic contamination levels

[1] M. Bonardi, C. Birratari, A. Salomone, ^{201}Tl production by (pxn) nuclear reactions on Tl and Hg natural and enriched targets Proc. Conf. Nucl. Data Sci. And Technol., Antwerp 1981, Bockhof K.H. editor, (1982) 916-918.

Medical use radioisotope production with accelerator neutrons by deuterons

K. Tsukada¹, S. Watanabe², N. S. Ishioka², Y. Hatsukawa², K. Hashimoto², Y. Sugo², N. Sato³, T. Kin⁴, M. Kawabata⁵, H. Saeki⁵, Y. Nagai²

¹Japan Atomic Energy Agency, Japan

²National Institutes for Quantum and Radiological Science and Technology (QST), Japan

³RIKEN, Japan

⁴Kyushu University, Japan

⁵Chiyoda Technol corporation, Japan

A new system has been proposed for the generation of medical radioisotopes with ~14 MeV neutrons (accelerator neutrons) by deuterons, especially the production of ⁹⁹Mo ($T_{1/2} = 66$ h), ⁶⁷Cu ($T_{1/2} = 61.8$ h), ⁶⁴Cu ($T_{1/2} = 12.7$ h), and ⁹⁰Y ($T_{1/2} = 64$ h) [1,2,3]. The most common diagnostic radioisotope, ^{99m}Tc ($T_{1/2} = 6$ h), has been obtained from ⁹⁹Mo ($T_{1/2} = 66$ h) which has been produced mostly by the fission reaction of highly enriched ²³⁵U in research reactors around the world. A recent shortage of ⁹⁹Mo worldwide triggered discussions on the supply of ⁹⁹Mo, and a number of ⁹⁹Mo and ^{99m}Tc production methods with reactors and accelerators have been investigated. The specific activity of ⁹⁹Mo, however, is quite low compared to the fission ⁹⁹Mo. The positron emitting radioisotope ⁶⁴Cu and β^- -ray emitting radioisotope ⁶⁷Cu are promising radionuclides suitable for labeling many radiopharmaceuticals for PET imaging and for treating small distant metastases in radioimmunotherapy, respectively. Their generally adopted production routes are ⁶⁴Ni(p,n)⁶⁴Cu and ⁶⁸Zn($p,2p$)⁶⁷Cu, respectively. However the use of ⁶⁷Cu for clinical researches has been limited due to the difficulty in obtaining sufficient quantities. A therapeutic radioisotope ⁹⁰Y, a pure β^- -ray emitter, is obtained from ⁹⁰Sr ($T_{1/2} = 28.8$ y), which is produced by the fission reaction of ²³⁵U. In our study, we investigated a potential of accelerator neutrons to produce ⁹⁹Mo, ⁶⁷Cu, ⁶⁴Cu and ⁹⁰Y [4,5].

Enriched ¹⁰⁰Mo, ⁹⁰Zr, ⁶⁸Zn, and ⁶⁴Zn oxide samples were irradiated with neutrons, which were obtained by the ^{nat}C(d,n) and Be(d,n) using 40 and 50 MeV deuterons provided from the QST TIARA cyclotron. After a bombardment we measured a γ -ray spectrum of the reaction products with a Ge detector. ⁹⁹Mo was successfully produced via the ¹⁰⁰Mo($n,2n$) reaction, and we clearly observed the γ -rays from the internal transition of ^{99m}Tc [4]. The radionuclides of ⁹⁷Zr, and its decay product ⁹⁷Nb, were impurity radionuclides. However, their yields were much smaller than that of ⁹⁹Mo, and therefore radioactive waste produced during chemical processing would be reduced. ⁶⁷Cu was produced via the ⁶⁸Zn(n,pn) and ⁶⁸Zn(n,d) reactions [5]. Relative production yields of impurity radionuclides of ^{69m}Zn, ⁶⁵Zn, ⁶⁴Cu, and ⁶⁵Ni to ⁶⁷Cu are extremely low, which allow us to chemically separate ⁶⁷Cu with a few steps and to reuse high cost of an enriched ⁶⁸Zn sample. The present results strongly suggest that the ⁶⁸Zn(n,x)⁶⁷Cu reaction is the most promising route to produce high quality ⁶⁷Cu and could solve a longstanding problem of establishing an appropriate production method of ⁶⁷Cu. ⁶⁴Cu, ⁶²Zn, and ⁶³Zn were found to be produced by the ⁶⁴Zn(n,x) reaction. Five hours after bombarding, however, the activity of the ⁶³Zn became negligible and the activity of ⁶²Zn was low. We also measured a γ -ray spectrum of the reaction product produced by the ⁹⁰Zr(n,x) reaction. Since the activity of ⁹⁰Y was found to be comparable to that of impurity nuclide ⁸⁹Zr, ⁹⁰Y will be separated from ⁸⁹Zr by using an ion-exchange separation method and purified. The present results demonstrate that the medical radioisotopes, ⁹⁹Mo, ⁹⁰Y, ⁶⁷Cu, and ⁶⁴Cu, can be produced with a minimum level of radioactive waste by using fast neutrons.

References

- [1] Y. Nagai and Y. Hatsukawa, J. Phys. Soc. Jpn. 78 (2009) 033201.
- [2] T. Kin et al., J. Phys. Soc. Jpn. 82 (2013) 034201.
- [3] Y. Nagai et al., J. Phys. Soc. Jpn. 78 (2009) 113201.
- [4] Y. Nagai et al., J. Phys. Soc. Jpn. 82 (2013) 064201.
- [5] N. Sato et al., J. Phys. Soc. Jpn. 83 (2014) 073201.

Nano-structured materials as possible sorbents for radionuclide generators

J.L.T.M. Moret^{1,2}, J. Alkemade¹, E. Oehlke¹, H.T. Wolterbeek¹, J.R. van Ommen², A.G. Denkova¹

¹ *Radiation and Isotopes for Health, Radiation Science and Technology, Applied sciences, TU Delft*

² *Process and Product Design, Chemical Engineering, Applied Sciences, TU Delft*

Radionuclide generators are used to supply hospitals with short-lived medical isotopes, such as ^{99m}Tc. Due to increasing demand of ^{99m}Tc and changes in the production process of its mother isotope ⁹⁹Mo new sorbent materials having high adsorption capacities are needed to replace aluminium oxide that is currently used in generators[1]. Instead of using a pure Al₂O₃ sorbent, we determine the feasibility of using the high surface material SBA-15 as a support on which a layer of Al₂O₃ is deposited, aiming at creating aluminium based materials having high adsorption capacity. SBA-15 itself is not an appropriate sorbent for ⁹⁹Mo, because it is negatively charged above pH 2 (iso-electric point ≈ 2). The molybdate ions itself are also negatively charged, hence limited adsorption. The addition of an Al₂O₃ layer increases the iso-electric point of the sorbent, and therefore also its the adsorption capacity. In this study atomic layer deposition (ALD) is used to deposit several layers of Al₂O₃ on SBA-15. ALD is a gas-phase coating technique with nano-scale precision, mostly used in the semi-conductor industry[2]. Large surface areas can easily be coated with this technique, allowing sorbents with high surface area to be created and hence with high adsorption capacity. Alternating exposures to trimethyl aluminium and water at both ambient conditions and 170°C are used to create the necessary Al₂O₃ coating.

In this work the amount of aluminium deposited on SBA-15 (540m²/g) and the final surface area of the new material is determined using ICP-OES and N₂ adsorption, respectively. In addition to this the stability of the created sorbents is evaluated at different pH values as well as their adsorption capacity for molybdenum. The results show that, although the surface area of SBA-15 is found to decrease almost by a factor of 2 after deposition of aluminium, this material is shown to be suitable for the adsorption of ⁹⁹Mo, i.e. for the preparation of a ⁹⁹Mo/^{99m}Tc generator. The Mo adsorption capacity of this material is determined to be 85 – 95 mg/g at pH 4 which is considerably higher when compared to the adsorption capacity of native SBA-15 (≈ 10 mg/g). The Mo adsorption capacity of the coated material is close to the minimum required capacity of 100 mg/g necessary to make a 2 Ci generator using ⁹⁹Mo with a specific activity of 10 Ci/g. Furthermore, the results show that the developed sorbents do not lose a detectable amount of Al between pH 4 and 6, but the use of buffered solutions decreased the adsorption capacity and increased the release of Al. To decrease the release of Al at low pH values, which might be more favourable for adsorption, the sorbent material needs to be calcined to change the as-deposited amorphous Al₂O₃ layer to a more stable crystalline structure. Unfortunately, so far the calcinations results have been inconclusive and further studies of its effect are needed.

In summary, we show that ALD can be used to create sorbents suitable for the preparation of generators but in order to further improve the adsorption capacity of these materials, SBA-15 having higher surface area should be used as carrier material and the effect of calcinations needs to be determined.

Acknowledgements

This project is funded by STW under the project number 13306 and IDB-Holland.

References

- [1] M.A. El-Absy, M.A. El-Amir, T.W. Fasih, H.E. Ramadan, M.F. El-Shahat, Preparation of ⁹⁹Mo/^{99m}Tc generator based on alumina ⁹⁹Mo-molybdate (VI) gel, J Radioanal Nucl Chem 299 (2014) 1859-1864.
- [2] V. Mikkiläinen, M. Leskelä, M. Ritala, R.L. Puurunen, Crystallinity of inorganic films grown by atomic layer deposition: overview and general trends, Applied Physics Reviews (2012).

RADIATION CHEMISTRY

Irradiation effects of extraction agents used for An/Ln partitioning

C. Ekberg², B. Gruner³, J. Halleröd², G. Modolo¹, H. Schmidt¹, J. Svehla³

¹ *Forschungszentrum Jülich, Germany*

² *Chalmers University of Technology, Gothenburg, Sweden*

³ *Institute of Inorganic Chemistry, Rež, Czech Republic*

Today the use of nuclear power is debated in many industrialised countries in e.g. Europe. The Fukushima accident had very different effects in different countries with Germany deciding to shut down while e.g. UK and Finland continue their plans for more nuclear power. Regardless of these accident related awareness another point often raised in the nuclear energy debate is the sustainability of the power production. Today about 1% of the energy content of the nuclear fuel is actually utilised before it is supposedly deposited in a repository. In society as a whole works like “circular economy” and “recycling” have become more and more important as it becomes rather evident that mankind's current use of the earth resources is not sustainable at all for any length of time. If nuclear power is to remain this thinking will sooner or later have to penetrate also into this field.

The technique for considerable more sustainable use of nuclear energy exist under different names where the most popular are “separation and transmutation” and “Gen IV nuclear power systems”. Essentially the practical working is the same: recover the useful elements from the used fuel, make new fuel and fission in a suitable reactor. The elements in question is typically uranium and plutonium but also the so called minor actinides neptunium, americium and curium. The use of the latter is today debated due to the complexity of incorporating it in new fuels.

Historically there are already working industrial processes for the recovery of uranium and plutonium (and to some extent neptunium) from the used fuel. The challenge was for many years how to separate the remaining trivalent actinides from the also trivalent lanthanides with similar size and same charge but directly unsuitable to keep in the new fuel. As research has advanced the current concept GANEX (Grouped Actinide Extraction) aims at extraction all the useful elements in one process thus avoiding pure streams of e.g. plutonium thus minimising proliferation issues.

Several ligands were developed for the separation of the trivalent actinides from the lanthanides and in Europe the dominating one is the so called BTP and BTBP family. In the well known PUREX process the extractant used, TBP, degrades during use and its now well known degradation products could affect the extraction process so cleaning steps are needed. In a similar way it was shown that the BTP and BTBP families (and others) are also degrading but the degradation products and their behavior is not so well known.

In this presentation the behavior under irradiation as well as identification of degradation products and some of their chemistry will be given.

Electronic irradiation stability of alteration layer formed during nuclear glass leaching by water: comparison with initial glass behavior

¹MOUGNAUD, Sarah, ²TRIBET, Magaly, ¹RENAULT, Jean-philippe, ²JEGOU, Christophe, ³BOIZOT, ⁴Bruno, PANCZER, Gérard, ¹CHARPENTIER, Thibault

¹ CEA, DSM, IRAMIS, NIMBE, UMR 3685 CEA/CNRS, Gif sur-Yvette, France

² CEA, DEN, DTCD, SECM, Laboratoire des Matériaux et Procédés Actifs, Bagnols-sur-Cèze, France

³ LSI, CEA-CNRS-Ecole Polytechnique, Palaiseau, France

⁴ Institut Lumière Matière, UMR 5306 Université Lyon 1-CNRS, Villeurbanne cedex, France

High level radioactive wastes (HLW) produced during spent fuel reprocessing are designed for long-term disposal in a deep geological repository as glass packages. In the event of water intrusion, expected after several thousand years, leaching mechanisms will result in a passivating layer at the glass/water interface[1]. As HLW glasses confine fission products and minor actinides, it is necessary to study the impact of irradiation on these mechanisms [2,3]. This work focuses on the evolution under external irradiation with electrons of the alteration layer formed during the residual alteration rate regime.

Simple glass powder doped with Eu is entirely leached into initially pure water, at 90°C and at high glass-surface-area-to-solution-volume ratio ($S/V = 200 \text{ cm}^{-1}$) in static conditions. The alteration rate is monitored by regular leachate samplings analyzed by ICP-AES. Under these conditions the system quickly reaches the residual alteration rate regime. The altered glass is then externally irradiated, in or out of its leachate, at different doses (up to 1 GGy) with electrons. Two linear accelerators are used: ALIENOR (CEA/DSM/IRAMIS, Saclay, France), providing 10 ns pulses of

10 MeV electrons (30 Hz) and SIRIUS (LSI, Palaiseau, France, supported by the French Network EMIR), providing a continuous beam of 2.5 MeV electrons. Samples are then characterized by continuous and time-resolved luminescence, Raman, ²⁹Si NMR and EPR spectroscopies. Alteration layer and initial glass appear to have different behavior under irradiation. The defect creation efficiency in altered glass is lower than for initial glass: this can be explained by the protective role of pore water contained in the altered material. A slight depolymerization of the altered glass is evidenced, whereas the initial glass typically repolymerizes under electronic irradiation. This is likely related to chemical composition: Na and Ca content could modify the alkaline migration responsible for the repolymerization process occurring on borosilicate glasses. Nevertheless, no strong modification of the structure of alteration layer is evidenced and altered glass, as initial glass, shows good stability under irradiation with electrons up to the GGy dose.

[1] J.D. Vienna, J.V. Ryan, S. Gin, Y. Inagaki, Int. J. Appl. Glass Sci. 4 (2013) 283.

[2] M. Tribet, S. Rolland, S. Peugeot, V. Broudic, M. Magnin, T. Wiss, C. Jégou, Procedia Materials Science 7 (2014) 209.

[3] W.J. Weber, Procedia Materials Science 7 (2014) 237.

Evaluation of the impacts of gamma radiolysis on an *i*-SANEX process solvent

Dean R. Peterman

Idaho National Laboratory, Idaho Falls, ID 83415, USA

dean.peterman@inl.gov

The development of a solvent extraction system capable of partitioning trivalent actinides from trivalent lanthanides is probably the highest aspiration of the fuel cycle separations community. Active research programs are working to solve this problem in Europe, North America and Asia. The most common approach uses soft donor compounds, mainly with N-donor functional groups, to selectively complex the actinides. A bewildering series of acronyms has evolved as incremental improvements have been made on a series of solvent formulations at the various research institutions. Avoiding the acronyms, early multi-cycle approaches extracted the lanthanides and actinides from the fuel dissolution using a non-selective O-donor as a group *f*-element complexing agent dissolved in an aliphatic diluent. Examples of such group extraction ligands include malonamides, diglycolamides and organo-phosphine oxides. The actinides and lanthanides were then back extracted (stripped) to a new, mildly acidic aqueous phase. The resulting aqueous phase containing the actinides and lanthanides then underwent further separations to realize the desired An/Ln separation. Simplification of such multi-cycle processes to one or two unit operations leads to simpler, more cost-effective processes.

In such a simplified process, the actinide/lanthanide differentiation is generally accomplished by employing an aqueous soluble complexant which either inhibits the extraction of the actinide species to the organic phase or selectively strips the actinide ions away from a loaded organic phase. A classic example of this type of chemistry is the use of polyaminocarboxylates as aqueous soluble holdback reagents in the TALSPEAK process. Although the TALSPEAK process has been successfully demonstrated at the laboratory scale, the tight pH control necessary for adequate An/Ln differentiation would likely be very difficult to implement on an industrial scale.

Several processes have been developed which rely upon N-donor heterocycle ligands such as BTPs and BTBPs. However, a very recent development conceived at Karlsruhe Institute of Technology (KIT), Germany, is the functionalization of a BTP with sulfonyl groups, to make it soluble in the aqueous phase. The aqueous phase N-donor is (2,6-bis-(5,6-di(sulfophenyl)-1,2,4-triazin-3-yl)-pyridine, or SO₃-Ph-BTP, shown in Figure 1. In combination with an organic phase diglycolamide O-donor actinide/lanthanide group extraction ligand (tetra-*n*-octyl-*N,N,N',N'*-diglycolamide (TODGA) shown in Figure 1, separation of the actinide species from the loaded organic phase would be accomplished in a single step.

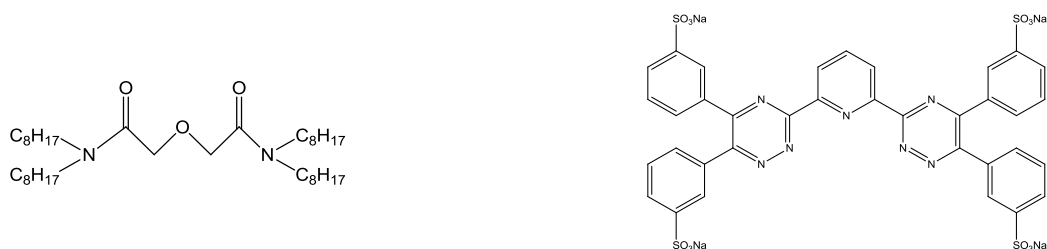


Figure 1. Structures of TODGA (left) and SO₃-Ph-BTP (right).

This innovative Selective ActiNide Extraction process (*i*-SANEX) has been successfully tested at the laboratory scale at Forschungszentrum Jülich (FZJ), Germany and resulted in a 99.8% recovery of Am and Cm from a synthetic, high active dissolved nuclear fuel solution. While this result is promising, in addition to adequate solvent extraction performance any solvent system used in the processing of dissolved nuclear fuel must be robust in a high radiation environment. Unfortunately, the water soluble BTP was recently reported to be sensitive to γ -radiolysis when the aqueous phase was batch irradiated using a ^{60}Co source. However, in that preliminary work, only the BTP-containing aqueous phase was irradiated. In the actual biphasic process, multiple competing free radical reactions occur to either degrade or protect the solvent extraction ligands. Similarly, the rapid depletion of dissolved oxygen in irradiated sealed samples may alter the rate of ligand degradation or ligand radiolysis products generated as compared to the aerated process system.

Therefore, in this study the biphasic *i*-SANEX solvent system was irradiated with continuous mixing and recirculation in a test loop based on a ^{60}Co self-contained irradiator, constructed at the Idaho National Laboratory, USA. The loop was designed to irradiate mixed phases with recirculation under process-like conditions. This *i*-SANEX irradiation was a collaborative experiment between the United States Department of Energy-Nuclear Energy Material Recovery and Waste Form Development (MRWFD) and the European Union Safety of Actinide Separation Processes (SACSESS) programs. The results presented here indicate that the radiolytic performance of the TODGA/ $\text{SO}_3\text{-Ph-BTP}$, *i*-SANEX process under test loop radiolysis is much better than expected based on single-phase batch irradiation experiments.

The *i*-SANEX solvent formulation consisting of 0.2 M TODGA/5% 1-octanol/dodecane was γ -irradiated under realistic process conditions in the INL irradiator test loop, in contact with both extraction and stripping aqueous phases. The extraction aqueous phase was 4.5 M HNO_3 , and the stripping aqueous phase was 0.35 M $\text{SO}_3\text{-Ph-BTP}$ /0.35 M HNO_3 . When irradiated in contact with only the 4.5 M HNO_3 phase, the TODGA solvent maintained excellent extraction performance for americium, cerium, europium and neodymium to a maximum absorbed dose of nearly 0.9 MGy. The results for preliminary static, batch irradiations were consistent with test loop findings. When the aqueous phase was changed to that containing the aqueous soluble $\text{SO}_3\text{-Ph-BTP}$, the irradiated aqueous phase showed a dramatic color change, but this does not appear to have had adverse effects on solvent extraction performance. The distribution ratios for both the lanthanides and actinide were invariant with absorbed dose, and the separation factors were essentially unchanged to a maximum absorbed dose of 174 kGy. The results to be discussed indicate that the performance of the TODGA/ $\text{SO}_3\text{-Ph-BTP}$, *i*-SANEX process under test loop radiolysis is much better than expected based on a literature report using single-phase batch irradiation experiments.

CLOSING LECTURE

Nuclear and radiochemical methods in nuclear non-proliferation

Olli Heinonen

Belfer Center for Science and International Affairs, Harvard Kennedy School, 79 JFK Street, Cambridge, MA, USA

Nuclear safeguards are a fundamental element in working against the spread of nuclear weapons. Safeguards are applied to verify the commitments given by states through international agreements to use nuclear materials and facilities for exclusively peaceful purposes. The verification system of the International Atomic Energy Agency (IAEA), is aimed to ensure that states' declarations are not only *correct*, but also that these declarations are *complete* as well; i.e. all nuclear materials and facilities in the territory of a state has been submitted under the IAEA safeguards.

The IAEA uses non-destructive and destructive analysis to verify nuclear materials and to monitor operation of nuclear installations. During five decades of IAEA safeguards, destructive analysis – nuclear and radiochemical - methods have evolved to meet new challenges.

Destructive analysis are used for inspections for instance:

1. to analyze nuclear material (uranium, plutonium, thorium) as well as in certain cases neptunium, americium, curium and deuterium,
2. in environmental sampling, and
3. in nuclear forensics to establish the origin of nuclear material e.g. in cases of illicit trafficking.

While these methods are precise and well established, new challenges lie ahead. Sample sizes need to be reduced to minimize the amount of radioactive wastes generated in laboratories, calling for more sensitive and increasingly automated analytical techniques to be introduced. Environmental sample analysis is not static and as such needs to be further developed to be more sensitive. At the same time, it is also important to develop techniques which can be used for timely *in-situ* analysis of samples. Increasing restrictions for radioactive sample shipment calls for additional reliance on on-site laboratories, and in developing of techniques, which allow minimization of sizes of samples taken and shipped. Such techniques could also be useful in verification of undertakings under the future Fissile Material Cut-off Treaty, which samples may contain sensitive information not to be disclosed to other parties.



SARL ETUDES-RECHERCHES-MATERIAUX

4 rue Carol Heitz

F-86000 POITIERS FRANCE

www.erm-poitiers.fr

ETUDES-RECHERCHES-MATERIAUX (ERM)

Private Independent Company working in the Earth Sciences since 1989

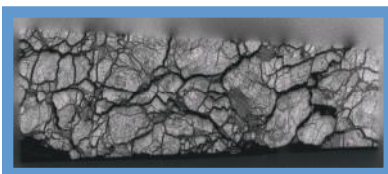
How to obtain realistic 3D models of natural and artificial materials including the porosity distribution from micrometre to centimetre?

The characterization of transport, retardation and storage properties of geological and artificial solid mineral matrices requires investigation of the connected pore space and its relation to composition and structure of the material either in geological context or in artificial matrices. Parameters to be acquired are: porosity, hydraulic conductivity, diffusion and retardation coefficient.

These parameters can be obtained in a laboratory Issued from the POSINAM European Project, and built in Poitiers (France) for industrial use of the ^{14}C -PMMA impregnation method where the radio labeled material as well as hazardous organic liquids can be handled safely.



Different imaging techniques are applied and compared: porosity quantification is investigated by PMMA autoradiographic method but also possibly with XRCT microtomography. Petrographic observations (optical microscope, SEM), and XRD analysis of mineralogy can also be conducted.



Example of application: Development of a fracture network in crystalline rocks during weathering: Study of Bishop Creek chronosequence using X-ray computed tomography and ^{14}C -PMMA impregnation method (A. Mazurier et al., Geological Society of America Bulletin, May 2016).

ERM is able to meet requests from industrial companies or public bodies to characterize porosity of materials (rocks, cement, etc...)

For any information please contact: jean-claude.parneix@erm-poitiers.fr

CLAYS



INDUSTRIAL
EXPERTISES



HISTORICAL
MONUMENTS



NATURAL
RESOURCES





Fortum Nures®

Purifies your
radioactive liquids



WELL-BEING WITH NUCLEAR ELECTRICITY

Teollisuuden Voima Oyj is a nuclear power company founded in 1969 for safe and reliable electricity production for its shareholders, Finnish industrial and energy companies. Nuclear electricity generated at TVO's Olkiluoto plant covers approximately one sixth of the annual electricity consumption in Finland.

Climate-friendly nuclear electricity not only benefits the Finnish society but also reduces the environmental impact of energy production.



**We feel safe
about the footprint
we leave.**

Safety is a prerequisite for final disposal.

As an expert organisation owned by Teollisuuden Voima and Fortum, Posiva has been tasked with the design and construction of a final disposal solution for spent nuclear fuel. Work continues until all of the spent nuclear fuel from the power plants in Olkiluoto and Loviisa has been emplaced deep in Olkiluoto bedrock and the tunnels have been backfilled and sealed.

Read more at [**www.posiva.fi**](http://www.posiva.fi)





Fennovoima will build its Hanhikivi 1 nuclear power plant in Northern Finland

Fennovoima is constructing new nuclear power in order to produce electricity at a stable price to its owners, increase Finland's energy self-sufficiency and increase competition in the electricity markets.

Read more about Fennovoima's project
at our website www.fennovoima.fi

FENNOVOIMA